

Effect of phytase supplementation on tissue inositol phosphate levels in broiler chickens

Colleen Mary Sprigg

A thesis submitted to the University of East Anglia for the
degree of Doctor of Philosophy

University of East Anglia
School of Biological Sciences
Norwich

December 2022

This copy of the thesis has been supplied on condition that anyone who consults it is understood to recognise that its copyright rests with the author and that use of any information derived therefrom must be in accordance with current UK Copyright Law. In addition, any quotation or extract must include full attribution.

Publications arising from this thesis:

Sprigg, C., Whitfield, H., Burton, E., Scholey, D., Bedford, M.R., Brearley, C.A. (2022) Phytase dose-dependent response of kidney inositol phosphate levels in poultry. PLOS ONE 17(10): e0275742.
<https://doi.org/10.1371/journal.pone.0275742>

Sprigg, C., Leftwich, P.T., Burton, E., Scholey, D., Bedford, M.R., Brearley, C.A. (Accepted) Accentuating the positive and eliminating the negative: efficacy of TiO₂ as a digestibility index marker for poultry nutrition studies. PLOS ONE.

Abstract

Phytate, *myo*-inositol hexakisphosphate, serves as an essential phosphorus store in plant seeds, but has antinutritive properties in the animals that consume it. Phytases, enzymes that degrade phytate, are added to the diets of monogastric animals. Many studies have correlated the addition of phytase with improved animal performance, with a subset of these seeking to correlate animal performance with phytase-mediated release of inositol or phosphate.

This study aimed to develop methods to measure inositol phosphates in poultry tissues and to determine the effect of phytase supplementation on poultry tissues, as the effect of dietary phytase on tissue inositol and inositol phosphates and phytase mediated release of inositol and phosphate had not been studied. The study comprised wheat/soy-based diets containing one of three levels of phytase and one level of d30‰ inositol equivalent to the inositol released from total dietary phytate hydrolysis (0, 500 and 6000 FTU/kg of modified *E. coli* 6-phytase and 2 g/kg inositol). Diets were provided for 21 days and on day 21, digesta were collected from the gizzard and ileum, and tissues were harvested from brain, liver, kidney, breast and leg muscle, and intestinal segments. *Myo*-inositol and inositol phosphates were measured in diet, digesta and tissues.

Gizzard and ileal content inositol increased and total inositol phosphates reduced progressively by phytase supplementation. The predominant higher inositol phosphates detected in tissues, D- and/or L-Ins(3,4,5,6)P₄ and Ins(1,3,4,5,6)P₅ different from those generated by phytate degradation by *E. coli* 6-phytase or endogenous feed phytase, suggesting tissue inositol phosphates are not the result of direct absorption. Kidney inositol phosphates were reduced progressively with increasing phytase supplementation. These data suggest that tissue inositol phosphate concentrations can be influenced by dietary phytase inclusion rates, and that such effects are tissue specific, though the consequences of this for animal physiology and performance are yet to be elucidated.

Access Condition and Agreement

Each deposit in UEA Digital Repository is protected by copyright and other intellectual property rights, and duplication or sale of all or part of any of the Data Collections is not permitted, except that material may be duplicated by you for your research use or for educational purposes in electronic or print form. You must obtain permission from the copyright holder, usually the author, for any other use. Exceptions only apply where a deposit may be explicitly provided under a stated licence, such as a Creative Commons licence or Open Government licence.

Electronic or print copies may not be offered, whether for sale or otherwise to anyone, unless explicitly stated under a Creative Commons or Open Government license. Unauthorised reproduction, editing or reformatting for resale purposes is explicitly prohibited (except where approved by the copyright holder themselves) and UEA reserves the right to take immediate 'take down' action on behalf of the copyright and/or rights holder if this Access condition of the UEA Digital Repository is breached. Any material in this database has been supplied on the understanding that it is copyright material and that no quotation from the material may be published without proper acknowledgement.

Table of Contents

Abstract	3
Table of Contents	5
Index of Tables	10
Index of Figures	12
Appendices	15
Acknowledgements	18
Chapter 1	
Introduction	
1.1 Inositol and inositol phosphates	20
1.1.1 Inositol stereoisomers	20
1.1.2 Inositol polyphosphates and pyrophosphates	21
1.1.3 Overview of pathways for inositol biosynthesis	22
1.2 Functions of inositol and inositol phosphates	23
1.2.1 Diverse functions of inositol	23
1.2.2 Link between myo-inositol and glucose metabolism	25
1.2.3 Inositol phosphates in plants	26
1.2.4 Inositol phosphates in human health and disease	27
1.2.5 Role of myo-inositol in poultry	28
1.2.6 Importance of inositol and inositol phosphates in agriculture	29
1.2.7 Environmental implications	30
1.3 Phytases	32
1.3.1 Background to phytases	32
1.3.2 Phytases in plants	35
1.3.3 Use of phytases in agriculture	36
1.3.4 Phytase use in poultry production	38
1.3.5 Superdosing	39
1.4 Aims	40
Chapter 2	
Producing stable isotope labelled <i>myo</i>-inositol from glucose	
2.1 The biosynthetic pathway for the production of <i>myo</i>-inositol	42
2.2 Methods and materials	45
2.2.1 Materials	45
2.2.1.1 Media and reagents	45
2.2.1.1.1 Standard reagents	45
2.2.1.1.2 Antibiotic stocks	47
2.2.1.1.3 Protein purification buffers	47

2.2.1.1.4 SDS PAGE	47
2.2.1.2 Yeast strains	48
2.2.1.3 Gateway cloning materials	49
2.2.1.3.1 Bacterial vectors	50
2.2.1.3.2 Yeast expression vectors	51
2.2.2 Methods	52
2.2.2.1 Arabidopsis plating	52
2.2.2.2 Arabidopsis stress treatment	52
2.2.2.3 RNA extraction	52
2.2.2.4 DNase treatment for RNA	52
2.2.2.5 cDNA synthesis protocol	53
2.2.2.6 PCR cloning of genes of interest	53
2.2.2.7 Gel electrophoresis	55
2.2.2.8 Preparation of competent cells	56
2.2.2.9 Transformation	56
2.2.2.9.1 BP Reaction	56
2.2.2.9.2 Ligation reaction	58
2.2.2.9.3 Transformation of <i>E. coli</i>	58
2.2.2.9.4 Transformation of <i>S. cerevisiae</i>	59
2.2.2.10 Expression and purification of <i>A. fulgidus</i> <i>myo</i> -inositol-1-phosphate synthase	59
2.2.2.11 Purification of <i>A. fulgidus myo</i> -inositol-1- phosphate synthase using the ÄKTA Pure system by immobilised metal ion affinity chromatography	60
2.2.2.12 Glucose and <i>myo</i> -inositol measurement	61
2.2.2.13 Yeast crude total protein extraction	61
2.2.2.14 Optimised method for the production of <i>myo</i> -inositol from glucose	63
2.2.2.15 Isotope ratio mass spectrometry measurement of $\delta^{13}\text{C}_6$ - <i>myo</i> -inositol in poultry tissues and digesta	64
2.3 Results	65
2.3.1 Cloning and expression of <i>myo</i> -inositol phosphate synthase proteins	65
2.3.2 Purification of IPS	76
2.3.3 Function and activity of <i>Archaeoglobus fulgidus</i> IPS	80
2.3.4 Enzyme coupled assays	84
2.3.4.1 Experiments using commercial hexokinase for conversion of glucose to G6P	84
2.3.4.2 ATP regeneration coupled hexokinase assays for conversion of glucose to G6P	87
2.3.4.3 Hexokinase and <i>myo</i> -inositol phosphate synthase coupled assay	90
2.3.4.4 Using titanium dioxide beads for inositol monophosphate purification	95

2.3.5 Three step coupled enzymatic assay from glucose to <i>myo</i> -inositol	97
2.3.6 Chemoenzymatic synthesis of ¹³ C(U)- <i>myo</i> -inositol	102
2.3.6.1 Use of ¹³ C Inositol in Animal Feeding Experiments	105
2.4 Discussion	106

Chapter 3

Improving the efficiency of inositol phosphate extraction from biological tissues

3.1 Introduction	108
3.2 Methods and materials	111
3.2.1 Materials	111
3.2.1.1 Animal tissues	111
3.2.2 Methods	111
3.2.2.1 Tissue disruption	111
3.2.2.2 Titanium dioxide bead extraction	112
3.2.2.3 HPLC Separation of inositol phosphates	113
3.3 Results	113
3.3.1 Whole organ extractions	113
3.3.2 Technical replicability of extraction	117
3.3.3 Standardised extraction procedure as applied to multiple tissue types	125
3.3.4 Comparative capacity of feed grade titanium dioxide to extract inositol phosphates	127
3.4 Discussion	130
3.4.1 Chromatographic resolution of tissue inositol phosphate species	130
3.4.2 Potential implications for the suitability of titanium dioxide as a digestibility index marker	131

Chapter 4

The effect of phytase supplementation on the appearance of lower inositol phosphate esters in the broiler digestive tract

4.1 Introduction	134
4.2 Materials and methods	136
4.2.1 Animals and management	136
4.2.2 Test diet and digesta sampling	140
4.2.3 Diet and digesta extraction	142
4.2.4 HPLC analysis for inositol and inositol phosphates	143
4.2.5 Statistical analysis	144
4.3 Results	144
4.3.1 Diets and bird performance	144
4.3.2 Gizzard digesta	150

4.3.3 Ileal digesta	159
4.4 Discussion	168
4.4.1 Influence of phytase dose on weight gain and feed conversion ratio	168
4.4.2 The impact of endogenous plant phytases on phytate digestibility	172
4.4.3 Phytase supplementation improves phytate digestibility in the gizzard and ileum	173
Chapter 5	
Inositol phosphate species in tissues of broiler chickens	
5.1 Introduction	177
5.2 Materials and methods	177
5.2.1 Animal tissue sampling	179
5.2.2 Tissue extraction	180
5.2.3 HPLC analysis of inositol and inositol phosphates	181
5.2.4 Statistical analysis	181
5.3 Results and Discussion	182
5.3.1 Digestive tissue inositol phosphates	182
5.3.2 Liver tissue inositol phosphates	191
5.3.3 Kidney tissue inositol phosphates	196
5.3.4 Breast and leg muscle inositol phosphates	203
5.3.5 Brain tissue inositol phosphates	209
5.3.6 Inositol phosphate identities in poultry tissues	217
5.4 Conclusions	219
5.4.1 Inositol phosphates in poultry tissues	219
5.4.2 Kidney inositol phosphate levels are responsive to dietary phytase dose	220
5.4.3 Liver inositol phosphate levels are impacted by inositol supplementation	222
5.4.4 Inclusion of titanium dioxide as a digestibility index marker does not impact extractable inositol phosphates in tissues	223
Chapter 6	
The effect of phytase supplementation on circulating metabolites implicated in phosphate homeostasis	
6.1 Introduction	225
6.2 Materials and methods	229
6.2.1 Animals, Diet and Experimental Design	230
6.2.2 Plasma hormones	231
6.2.3 Plasma minerals	231
6.2.4 Plasma inositol	231
6.2.5 Statistical analysis	231
6.3 Results	232

6.3.1 Plasma inositol and metabolites	232
6.3.2 Effect of phytase treatments on vitamin D metabolites	233
6.4 Discussion	235
Chapter 7	
Final Discussion and Future Work	
7.1 Producing stable isotope labelled <i>myo</i> -inositol from glucose	239
7.2 Improving the efficiency of inositol phosphate extraction from biological tissues	240
7.3 The effect of phytase supplementation on the appearance of lower inositol phosphate esters in the broiler digestive tract	241
7.4 Inositol phosphate species in tissues of broiler chickens	243
7.5 The effect of phytase supplementation on circulating metabolites implicated in phosphate homeostasis	244
7.6 Limitations	245
Appendices	247
References	351

Index of Tables

Table 1.1	Phytase classification based on catalytic mechanism.	33
Table 1.2	Classification of phytases based on carbon position for first dephosphorylation.	34
Table 2.1	12% SDS PAGE resolving gel recipe	48
Table 2.2	Bacterial vectors for Gateway cloning	50
Table 2.3	Yeast vectors for Gateway cloning	51
Table 2.4	Reaction mix for Phusion PCR amplification	53
Table 2.5	PCR cycling conditions for amplification of ScINO1 from <i>S. cerevisiae</i> DNA	54
Table 2.6	PCR conditions for amplification of AtMIPS1 and AtMIPS2 genes from <i>A. thaliana</i> cDNA	54
Table 2.7	Primer sequences for the addition of c-terminal histidine tags.	55
Table 2.8	PCR conditions for the addition of 3' 6xHIS to ScINO1 purified gene fragment.	55
Table 2.9	PCR conditions for the addition of 3' 6xHIS to AtMIPS2 purified gene fragment.	55
Table 2.10	Reaction mixture for BP Clonase II reaction.	56
Table 2.11	Reaction mix for the Gateway Ligation Reaction using LR Clonase II.	58
Table 2.12	Recipe for Transformation buffer (TB) for <i>S. cerevisiae</i> transformation	59
Table 2.13	Components of extraction Buffer A for Yeast crude total protein extraction.	62
Table 2.14	Components of extraction Buffer B for Yeast crude total protein extraction.	62
Table 2.15	<i>Myo</i> -inositol phosphate synthase genes selected for cloning and transformation.	65
Table 2.16	Michaelis-Menten constants of selected <i>myo</i> -inositol phosphate synthases for D-G6P.	66
Table 2.17	Reaction mix for the ATP-regenerating hexokinase-coupled IPS assay for the conversion of glucose-6-phosphate to inositol monophosphate	92
Table 2.18	Assay mixture for the 3-step enzymatic coupled assay for the generation of <i>myo</i> -inositol from glucose.	99
Table 2.19	Hexokinase and IPS coupled assay mixture for ¹³ C(U) D-glucose conversion to <i>myo</i> -inositol monophosphate.	103
Table 4.1	Animal feeding trial study design	137
Table 4.2	Animal feeding trial study parameters	138
Table 4.3	Pen layout and assigned blocks	139
Table 4.4	Dietary treatments and Test Substance inclusion rates	141
Table 4.5	Ingredient composition and calculated nutrient concentrations of the basal diet	142

Table 4.6	Measured inositol and inositol phosphate levels of basal diets	148
Table 4.7	Influence of diet on growth of broilers from day 0 to day 21	149
Table 4.8	Growth performance of broilers from day 0 to day 21 calculated feed conversion ratios	149
Table 4.9	Inositol and inositol phosphate (InsP ₃₋₆) levels (nmol/g dwt) in acid extracted gizzard digesta of day 21 broilers	157
Table 4.10	Inositol and inositol phosphate (InsP ₂₋₆) levels (nmol/g dwt) in NaF extracted gizzard digesta of day 21 broilers	158
Table 4.11	Inositol and inositol phosphate (InsP ₃₋₆) levels (nmol/g dwt) in ileal digesta of day 21 broilers (0.5M HCl extracted)	165
Table 4.12	Inositol and inositol phosphate (InsP ₃₋₆) levels (nmol/g dwt) in ileal digesta of day 21 broilers (NaF-EDTA extracted)	167
Table 5.1	Inositol and inositol phosphate (InsP ₃₋₆) levels (nmol/g wwt) in duodenal segments of day 21 broilers	186
Table 5.2	Inositol and inositol phosphate (InsP ₃₋₆) levels (nmol/g wwt) in jejunum segments of day 21 broilers	188
Table 5.3	Inositol and inositol phosphate (InsP ₃₋₆) levels (nmol/g wwt) in ileum segments of day 21 broilers	190
Table 5.4	Inositol and inositol phosphate (InsP ₃₋₆) levels (nmol/g wwt) in liver of day 21 broilers	194
Table 5.5	Inositol and inositol phosphate (InsP ₂₋₆) levels (nmol/g wwt) in kidney of day 21 broilers	199
Table 5.6	Inositol and inositol phosphate (InsP ₃₋₆) levels (nmol/g wwt) in breast muscle of day 21 broilers	206
Table 5.7	Inositol and inositol phosphate (InsP ₃₋₆) levels (nmol/g wwt) in leg muscle of day 21 broilers	207
Table 5.8	Inositol and inositol phosphate (InsP ₃₋₆) levels (nmol/g wwt) in brains of day 21 broilers	215
Table 6.1	Plasma parameters in day 21 broilers	233
Table 6.2	Plasma concentration of vitamin D metabolites (nmol/L) in day 21 broilers	234

Index of Figures

Figure 1.1	The 9 possible isomers of inositol, of which <i>myo</i> -inositol is the most abundant naturally occurring.	21
Figure 1.2	Structures of <i>myo</i> -inositol and phytate, <i>myo</i> -inositol hexakisphosphate.	22
Figure 2.1	<i>De novo</i> biosynthesis pathway of <i>myo</i> -inositol from glucose.	44
Figure 2.2	Agarose gel electrophoresis from Touchdown PCR of ScINO1 and AtMIPS1.	68
Figure 2.3	Agarose gel electrophoresis of AtMIPS2 gene cloned using Touchdown PCR.	69
Figure 2.4	Agarose gel electrophoresis of PCR products resulting from Colony PCR of ScINO1 in pDONR207 Gateway Entry Vector.	71
Figure 2.5	Agarose gel electrophoresis of PCR products of colony PCR conditions for c-terminal 6xHIS tagged ScINO1.	72
Figure 2.6	SDS PAGE analysis of crude total protein extraction of the ScINO1 overexpression line of <i>S. cerevisiae</i> NCYC3466 HIS-tag stained.	73
Figure 2.7	SDS PAGE analysis of crude total protein extraction of the ScINO1 overexpression line of <i>S. cerevisiae</i> NCYC3466 total protein stained.	74
Figure 2.8	SDS PAGE analysis following HisTrap HP Affinity IMAC enrichment of HIS tagged proteins.	75
Figure 2.9	SDS PAGE gel electrophoresis of total expressed protein from expression trials of pET23a:IPS in Rosetta™ 2 (DE3)pLysS.	76
Figure 2.10	UV trace from ÄKTA Pure system of IMAC HiTrap purification of IPS.	77
Figure 2.11	SDS PAGE of unconcentrated fractions from ÄKTA Pure purification of IPS protein following IMAC purification.	78
Figure 2.12	SDS PAGE of concentrated IPS fractions prior to Sepharose gel filtration.	78
Figure 2.13	Size exclusion chromatography (Gel filtration) of IMAC purified IPS fractions.	79
Figure 2.14	SDS PAGE of Sepharose purified IPS protein.	80
Figure 2.15	Scheme for the isomerization reaction for the conversion of G6P to inositol monophosphate by inositol phosphate synthase (IPS), requiring NAD ⁺ as a co-factor.	81
Figure 2.16	Separations of G6P and Ins3P by Ion Exchange Chromatography of IPS assay for conversion of G6P to inositol monophosphate.	83
Figure 2.17	Reaction scheme for the phosphorylation of glucose to G6P by hexokinase, with ATP as a phosphate donor.	85

Figure 2.18	Chromatographic separation on a Dionex AS18 IC column of hexokinase reaction products and standards, measured by suppressed ion conductivity.	86
Figure 2.19	Reaction scheme of the conversion of glucose to G6P by hexokinase, using ATP as a phosphate source. Coupled to this is the regeneration of ATP from ADP by creatine kinase, using phosphocreatine to regenerate ATP and producing creatine as a by-product of this regeneration.	88
Figure 2.20	Separation of ATP-regeneration coupled hexokinase assay products by Ion Exchange Chromatography for 6GP, D-Ins3P, 2 hour and 4 hour coupled assay products.	89
Figure 2.21	Reaction scheme for the conversion of glucose to Ins3P by hexokinase and inositol phosphate synthase, with G6P as an intermediate.	91
Figure 2.22	Separation of Ins3P and G6P by Ion Exchange Chromatography of Hexokinase-IPS coupled assay products with glucose as the starting material.	93
Figure 2.23	Suppressed ion chromatography separation of Ins3P and G6P in IPS reaction products from TiO ₂ clean up.	96
Figure 2.24	Reaction scheme for the stepwise conversion of glucose to inositol by hexokinase, inositol phosphate synthase and alkaline phosphatase enzymes, with G6P and Ins3P as reaction intermediates.	98
Figure 2.25	Calibration of detector response (integrated peak area) for <i>myo</i> -inositol derived from 2D HPLC-PAD of inositol standards.	100
Figure 2.26	Overlay of inositol standards separated by 2D HPLC-PAD with a gradient of 150 mM NaOH used to generate calibration curve in figure 2.25.	100
Figure 2.27	Separation of <i>myo</i> -inositol from glucose and glycerol as a buffer component by 2D HPLC-PAD with a gradient of 150 mM NaOH.	101
Figure 2.28	Suppressed ion chromatography separation of D-Ins3P in IPS reaction from G6P synthesised using hexokinase from D-Glucose- ¹³ C ₆ .	104
Figure 3.1	Profile of inositol phosphates in whole broiler kidneys.	114
Figure 3.2	Profile of inositol phosphates in whole broiler kidneys on 0.8 M HCl gradient.	116
Figure 3.3	Reproducibility of broiler brain tissue extractions.	118
Figure 3.4	Reproducibility of broiler kidney tissue extractions.	120
Figure 3.5	Reproducibility of broiler breast muscle extractions.	121
Figure 3.6	Reproducibility of broiler leg muscle extractions.	123
Figure 3.7	Inositol phosphates in broiler tissue.	123
Figure 3.8	Chromatograms for comparative purification of acid-hydrolysed InsP ₆	129
Figure 4.1	Inositol phosphate (InsP ₂₋₆) levels (nmol/g dwt) in diets fed to broilers from 0-21 days.	145

Figure 4.2	Total inositol phosphate (InsP ₂₋₆) levels (nmol/g dwt) in diets fed to broilers from 0-21 days.	147
Figure 4.3	Inositol levels (nmol/g dwt) in gizzard digesta of day 21 broilers	151
Figure 4.4	Inositol phosphate (InsP ₃₋₆) levels (nmol/g dwt) in acid-extracted gizzard digesta samples and NaF-EDTA-extracted gizzard digesta samples of day 21 broilers	152
Figure 4.5	Inositol phosphates in broiler gizzard digesta with inositol phosphate classes and individual isomers identified.	154
Figure 4.6	Inositol phosphates in broiler ileum digesta with inositol phosphate classes and individual isomers identified.	162
Figure 4.7	Inositol levels (nmol/g dwt) in ileal digesta of day 21 broilers	163
Figure 4.8	Inositol phosphate (InsP ₃₋₆) levels (nmol/g dwt) in acid-extracted ileal digesta samples and NaF-EDTA-extracted ileal digesta samples of day 21 broilers	164
Figure 5.1	Inositol phosphate (InsP ₃₋₆) levels (nmol/g wwt) in duodenum, jejunum and ileum tissue of day 21 broilers.	185
Figure 5.2	Inositol phosphate (InsP ₃₋₆) levels (nmol/g wwt) in livers of day 21 broilers.	193
Figure 5.3	Inositol phosphate (InsP ₂₋₆) levels (nmol/g wwt) in kidneys of day 21 broilers.	198
Figure 5.4	Inositol phosphate (InsP ₃₋₆) levels (nmol/g wwt) in breast and leg muscles of day 21 broilers.	204
Figure 5.5	Model of the dual effects of valproic acid and lithium on inositol depletion and GSK3 inhibition to contribute to mood stabilisation	212
Figure 5.6	Inositol phosphate (InsP ₃₋₆) levels (nmol/g wwt) in brain tissue of day 21 broilers	214
Figure 5.7	Figure previously published in Sprigg <i>et al.</i> 2022.	218
Figure 6.1	Inositol phosphates in broiler digesta and tissue.	
	Metabolic pathway of Vitamin D3 to its metabolites	228

Abbreviations

AC	Acetate
AIA	Acid Insoluble Ash
AME	Apparent metabolizable energy
ANOVA	Analysis of Variance
APS	Ammonium Persulfate
AMP	Adenosine monophosphate
ADP	Adenosine diphosphate
ATP	Adenosine triphosphate
ANOVA	Analysis of Variance
ARRIVE	Animal Research: Reporting <i>In Vivo</i> Experiments
BASF	Badische Anilin und Sodafabrik
BW	Bird weight
cDNA	complementary DNA
DAG	Diacylglycerol
DMSO	Dimethylsulfoxide
DNA	Deoxyribonucleic acid
DTT	Dithiothreitol
DWT	Dry Weight
EDTA	Ethylenediaminetetraacetic acid
ELISA	Enzyme-linked immunosorbent assay
ESI	Electrospray ionisation
FCR	Feed Conversion Ratio
FGF23	Fibroblast growth factor 23
FI	Feed Intake
FTU	Phytase Unit
G6P	Glucose-6-phosphate
GC	Gas Chromatography
HAPhy	Histidine Acid Phytase
HCl	Hydrochloric acid
HIV	Human immunodeficiency virus
HPLC	High performance liquid chromatography
IBH120	Attenuated infection bronchitis toxin H120 vaccine
ICS	Ion Conductivity System
IMAC	Immobilised metal affinity chromatography
IMC	International Minerals and Chemicals
IMP	<i>Myo</i> -inositol monophosphate
InsP	Inositol phosphate
Ins3P	Inositol-3-monophosphate
InsP ₁	Inositol monophosphate
InsP ₂	Inositol bisphosphate
InsP ₃	Inositol triphosphate
InsP ₄	Inositol tetrakisphosphate
InsP ₅	Inositol pentakisphosphate
InsP ₆	Inositol hexakisphosphate
InsP ₇	Diphosphoinositol pentakisphosphate
InsP ₈	Triphosphoinositol pentakisphosphate
IPS	Inositol Phosphate Synthase
IPTG	Isopropyl β -D-1-thiogalactopyranoside
IRMS	Isotope Ratio Mass Spectrometer

IRS	Isotope Ratio Spectrometry
IUPAC	International Union of Pure and Applied Chemistry
K_{cat}	Enzymatic catalytic rate constant
kg	Kilogram
K_m	Michaelis constant
KOH	Potassium hydroxide
LB broth	Luria-Bertani broth
LB	Lohman Brown
LC-MS	Liquid Chromatography – Mass Spectrometry
LR	Ligation Reaction
LSL	Lohman Selected Leghorn
ME	Metabolisable Energy
MeSA	Methanesulfonic Acid
MINPP	Multiple inositol polyphosphate phosphatase
MIPS	<i>Myo</i> -inositol phosphate synthase
MOPS	3-(N-morpholino)propanesulfonic acid
mRNA	Messenger RNA
MS	Murashige & Skoog medium
MW	Molecular weight
n/a	Not applicable
n.d.	Not detectable
NaCl	Sodium chloride
NADP	Nicotinamide adenine dinucleotide phosphate
NADPH	Nicotinamide adenine dinucleotide phosphate hydrogen
NaF	Sodium Fluoride
NaOH	Sodium hydroxide
NE	Net Energy
NC3R	National Centre for the Replacement Refinement & Reduction of Animals in Research
NCYC	National Collection of Yeast Cultures
NMR	Nuclear Magnetic Resonance
NTU	Nottingham Trent University
OD ₆₀₀	Optical density measured at 600 nm
PAGE	Polyacrylamide gel electrophoresis
PAPhy	Purple acid phytase
PCR	Polymerase chain reaction
PIP ₂	Phosphatidylinositol-4,5-bisphosphate
PIPES	Piperazine-N,N'-bis(2-ethanesulfonic acid)
PLC	Phospholipase C
PP	Polyphosphate
PPM	Parts Per Million
PSI	Pounds per square inch
PTFE	Polytetrafluoroethylene
PTH	Parathyroid Hormone
QB	Quantum Blue
RNA	Ribonucleic Acid
RPM	Revolutions per minute
RT	Reverse Transcription
SAX	Strong Anion Exchange
SDS	Sodium dodecyl sulfate

SEM	Standard Error of the Mean
SLC	Solute Carrier
SOB	Super Optimal Broth
SOC	Super Optimal broth with Catabolite repression
TAE	Tris-Acetic Acid-EDTA buffer
TE buffer	Tris-EDTA buffer
TEMED	Tetramethylethylenediamine
T _m	Melting temperature
Tris	2-Amino-2-hydroxymethyl-propane-1,3-diol
UV	Ultraviolet
V _{max}	Maximum rate of catalysis
VPA	Valproic Acid
WT	Wild type
WWT	Wet Weight
YPD	Yeast Peptone Dextrose medium

Acknowledgements

I've never understood the meaning of "it takes a village" more than in the last four years culminating in the production of this thesis. Reaching this point in my PhD has been in no small part due to being surrounded by so many incredible people, a few of which I take this opportunity to thank.

I'd like to begin by thanking my family for all their love and support, and for being my greatest encouragers. I'd like to thank my partner, Dan, for keeping me grounded through it all, even if it sometimes meant having literal pebbles from beaches in my pockets to do so. I'd like to thank Hannah, from day 1 of undergrad, to moving to Norwich to do our PhDs, here's to finishing it out we started – together.

I'd like to thank the BIO inhabitants, current and former. Thanks to Graham, for always being the first smiling face I see in a morning. To Glen, you crazy cat, for making sure I've never left a chat not feeling like Wonder Woman. To Elaine, for there never being too weird a question I could turn up at your door with; and to Jordan, for making sure I'm okay in every literal and metaphorical situation that's come up over the last four years. To Joe and Tim, for making sure I never coffee alone. To Greg, for all the gels we've raced to load, and for attempting the high parts in every lab ABBA duet, for no day being boring. To Libby, for letting me overshare without complaint.

I'd like to thank my supervisory team: with thanks to Professor Jonathon Todd and Dr. Mike Bedford for their support and guidance throughout my project. With special thanks to Dr. Hayley Whitfield, for support beyond standard supervision – for homemade brownies, positive posted notes, alpaca walks, and evening lab chats – thank you for keeping me sane through it all.

Lastly, I'd like to extend my thanks to my supervisor Professor Charles Brearley, from whom I have learnt so much in these past four years, but no lesson has been more important than this: graded grains make finer flour.

Dedication

As I'm unlikely to ever write a novel, I dedicate this thesis to Imogen. When its finally done, finished and bound, a copy will likely sit in the cupboard under nanny and grandad's telly. You'll likely never read it – its big, heavy, and fairly boring compared to most books, so I wouldn't blame you. But if you get this far into it at least, I want you to know this is for you. I still struggle with my 8 times tables, I never learnt to ride a bike, I couldn't tie my shoelaces properly until embarrassingly late in my teens (and I still avoid it now if I can, you can just do them loose enough to slip them on, trust me), but I hope this stands as proof that you can do anything, even the difficult things.

“Our deepest fear is not that we are inadequate, it's that we are powerful beyond measure. It is our light, not our darkness, that most frightens us. Your playing small does not serve the world. There is nothing enlightened about shrinking so that other people won't feel insecure around you. We are all meant to shine as children do. It's not just in some of us, it's in everyone. And, as we let our own light shine, we consciously give other people permission to do the same. As we are liberated from our fear, our presence automatically liberates other.”

- Marianne Williamson

1. Introduction

1.1 Inositol and inositol phosphates

1.1.1 Inositol stereoisomers

Inositol, first characterized as a hexahydroxycyclohexane extracted from a meat sample (Scherer, 1850), was fully purified in 1887 (Maquenne, 1887a, 1887b). A carbocyclic sugar, inositol forms the scaffold of a number of secondary messenger molecules in eukaryotic cells in the form of inositol phosphates (Agranoff and Fisher, 2001; Parthasarathy *et al.*, 2006).

Unique combinations of axial and equatorial hydroxyl groups result in 9 possible stereoisomers of inositol (Figure 1.1), of which only six have been proven to exist in nature. No evidence of the remaining three predicted structures (*epi*-inositol, *cis*-inositol and *allo*-inositol) have been found in nature (Parthasarathy and Eisenberg, 1991). The *myo*- isoform is the most stable and most abundant inositol in nature. It is particularly abundant in the brain and other mammalian tissues (Vadnal and Parthasarathy, 1995; Majumder, Johnson and Henry, 1997). Its phosphorylated derivatives which are products of cellular metabolism are intensely studied but are also abundant in soils (Turner *et al.*, 2002).

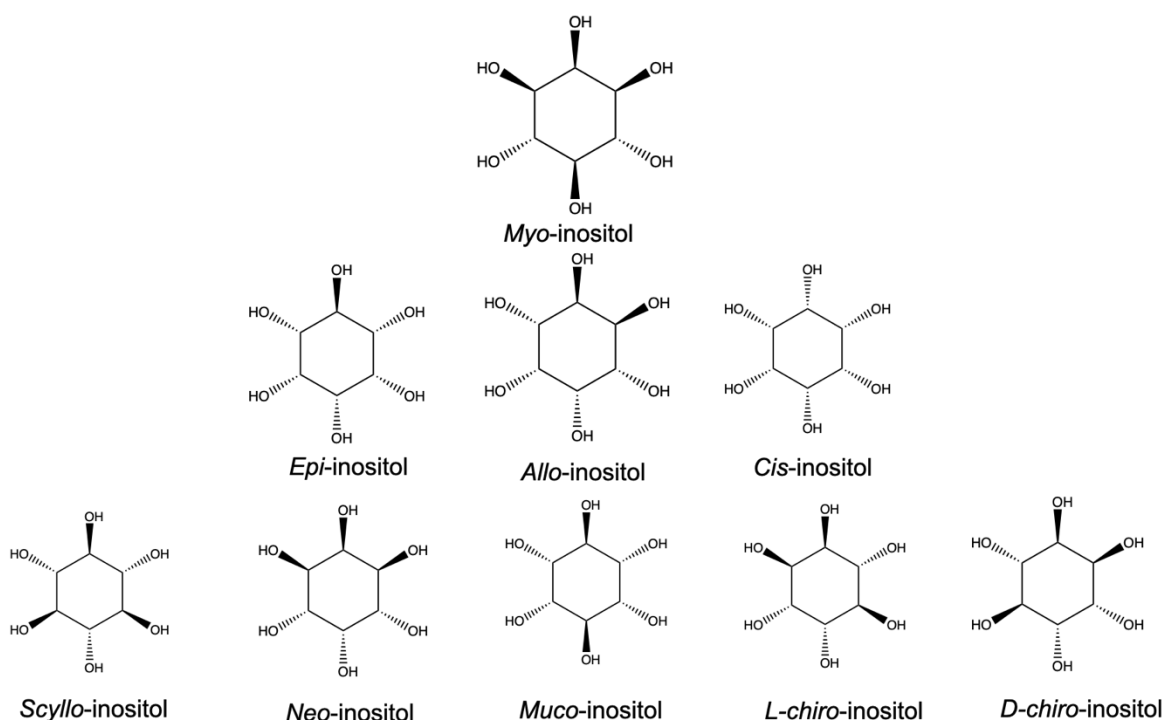


Figure 1.1: The 9 possible isomers of inositol, of which *myo*-inositol is the most abundant naturally occurring. Figure generated using ChemDraw v. 19.0.

1.1.2 Inositol polyphosphates and pyrophosphates

When synthesised *de novo*, *myo*-inositol serves as a precursor for the inositol phosphates and inositol pyrophosphates, which have a number of biological functions within the nucleus and cytosol. The inositol phosphate family is comprised of molecules Ins1P through InsP₆, the inositol pyrophosphates, PP-InsPs such as 5PP-InsP₄, InsP₇ and InsP₈ containing diphosphate moieties, and the lipid-bound phosphatidylinositols (Wilson, Livermore and Saiardi, 2013).

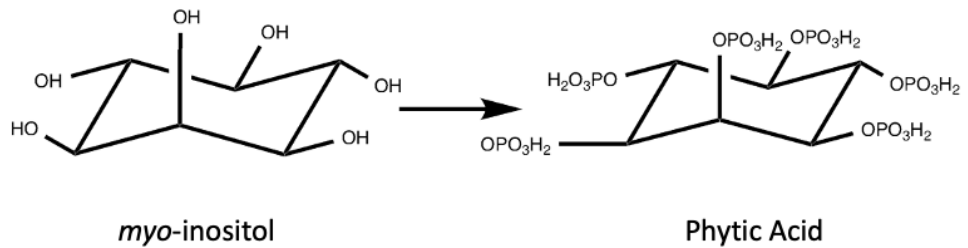


Figure 1.2: Structures of *myo*-inositol and phytic acid *myo*-inositol hexakisphosphate. Figure generated using ChemDraw v. 20.0.

InsP₆, the hexakisphosphate of *myo*-inositol, also known as phytic acid (Figure 1.2) or in salt form as phytate, is the most abundant naturally occurring of the inositol phosphates (Cosgrove and Irving, 1980; Stephens and Irvine, 1990). A number of potential routes for its synthesis *in vivo* have been described in the literature. These include the sequential phosphorylation from *myo*-inositol described in the eukaryotic slime mould *Dictyostelium discoideum* (Stephens and Irvine, 1990), or more commonly a pathway 'starting' from a soluble pool of InsP₃ generated as a cleavage product from the membrane phospholipid phosphatidylinositol 4,5-bisphosphate, the InsP₃ product can be dephosphorylated to *myo*-inositol or phosphorylated to the 'higher' InsP₄, InsP₅ and InsP₆ molecules.

1.1.3 Overview of pathways for inositol biosynthesis

Inositol and inositol-containing phospholipids are found ubiquitously throughout the Eukaryote domain, with a range of diverse functions described in section 1.2.1., though inositol is also found in archaea and bacteria. In bacteria, phosphorylated inositol is used most notably as an intermediate in the production of mycothiol in the Actinomycetales order (Roberts, 2006). Due to the diverse nature of use of inositol and its phosphates across orders and indeed between different species, a number of pathways have been characterised for the synthesis of higher inositol phosphates, divided into the lipid dependent and lipid independent pathways.

At the inositol level however, as a precursor to these abundant molecules, synthesis occurs through an enzymatic cyclization of glucose to *myo*-inositol (Loewus and Loewus, 1983) and a single pathway for this synthesis *de novo* has been characterised in all three kingdoms of life (Michell, 2008). This pathway requires two enzymatic steps, with the *myo*-inositol-3-phosphate synthase catalysing the cyclisation of D-glucose-6-phosphate to D-*myo*-inositol-3-phosphate (Ins3P) in an NAD⁺ dependent reaction, following which Ins3P is dephosphorylated to free *myo*-inositol by an inositol monophosphatase, described in detail in Chapter 2.

A second pathway for the liberation of free *myo*-inositol and soluble inositol phosphates has been described within eukaryotic cells, derived from the lipid phosphatidylinositol-4,5-bisphosphate (PIP₂), whereby PIP₂ is cleaved by phospholipase C (PLC) to form diacylglycerol and inositol-1,4,5-trisphosphate (InsP₃) (Berridge and Irvine, 1989; York and Hatch, 2010).

1.2 Functions of inositol and inositol phosphates

1.2.1 Diverse functions of inositol

Inositol and the compounds it is incorporated in – phosphatidylinositol, phosphatidylinositol phosphates (phosphoinositides) and the inositol phosphates (inositides) – play a key role in a number of signal transduction pathways, including but not limited to insulin signal transduction, with early correlations drawn between increased urinary *myo*-inositol and decreased D-chiro inositol linked to insulin resistance in diabetic patients, with D-Chiro inositol originally discovered as a component of a putative mediator of intracellular insulin action, in that it accelerates the dephosphorylation of glycogen synthase and pyruvate dehydrogenase, the rate limiting enzymes of oxidative and non-oxidative glucose disposal (Ortmeyer *et al.*, 1993; Suzuki *et al.*, 1994; Larner & Craig, 1996; reviewed in Larner, 2002). Additionally, inositol has been implicated in calcium ion signalling, with a complex mechanism described across several papers dating back to 1983,

where InsP_3 was noted to release Ca^{2+} from nonmitochondrial intracellular Ca^{2+} stores in pancreatic acinar cells (Streb *et al.*, 1983), a mechanism later confirmed in other cell types such as insulin-secreting cells (Prentki *et al.*, 1984), leukocytes (Burgess *et al.*, 1984) and Swiss 3T3 cells (Berridge *et al.*, 1984), as a secondary messenger in cellular signal transduction (Berridge & Irvine, 1984) and suggesting a significant role in the maintenance of intracellular calcium concentration (reviewed in: Berridge, 2009).

Malfuctions of the inositol pathway have been implicated in the pathogenesis of a number of mood disorders, including bipolar disorder, with Barkai *et al.* (1978) and Frey *et al.* (1998) reporting that patients with depression had significantly lower levels of cerebrospinal fluid inositol. Although this same reduction in cerebrospinal fluid inositol was not noted in the study by Levine *et al.* (1995b), a placebo-controlled double-blind study comparing the effects of 12 g/day inositol versus glucose in depressed patients found significant improvement in symptoms in the inositol treatment group versus glucose placebo. Double-blind studies treating patients suffering from obsessive compulsive disorder found improvement in symptoms when treated with inositol compared to the glucose placebo control groups, with significantly lower scores measured on the Yale-Brown Obsessive Compulsive Scale (Fux *et al.*, 1996, 1999). In the studies described, inositol has been described as having the clinical profile of a serotonin selective reuptake inhibitor (reviewed in Parthasarathy *et al.*, 2006).

Inositol is also considered to be a successful alternative to traditional insulin-sensitizing drugs in management of polycystic ovary syndrome, by regulating steroid metabolism downstream through pathways independent of insulin signalling, which therefore reduces hyperandrogenism (Croze and Soulage, 2013; Monastra *et al.*, 2017).

The study of inositol is as vast as it is varied, with an example of wider applications of inositol and its derivatives, at the American Chemical Society conference in 1936, Professor Edward Bartow from the University of Iowa

suggested inositol nitrate extracted from waste corn could function as an alternative to nitro-glycerine used in the explosive cordite (Laurence, 1936), and this compound is today used to gelatinize nitrocellulose or “gun cotton” for use in explosives (Ledgard, 2007). The following sections will focus largely on the roles of inositol studied in the context of dietary inositol and inositol phosphates, and the implications for metabolism.

1.2.2 Link between *myo*-inositol and glucose metabolism

In humans and animals, research has shown that inositol shows promise in improving peripheral insulin sensitivity in studies with women with polycystic ovary syndrome (Genazzani *et al.*, 2008; Costantino *et al.*, 2009).

Randomized control studies also showed beneficial effects of inositol supplementation on the occurrence of gestational diabetes mellitus and Type 2 diabetes (Kim *et al.*, 2012; D’Anna *et al.*, 2015), while meta analyses of human studies indicating that inositol supplementation decreases blood glucose through an improvement in insulin sensitivity (Miñambres *et al.*, 2019). Previously, negative associations had been observed between dietary phytate levels and the glycaemic index of cereals and legumes from which phytate, inositol and glucose metabolism were presumed to interact (Yoon, Thompson and Jenkins, 1983), supported by later research showing that *myo*-inositol inhibits duodenal glucose absorption in rat models and reduces blood glucose rise with the suggestion of a competitive uptake model using the same transporters (Chukwuma, Ibrahim and Islam, 2016).

The model for the interaction between glucose and *myo*-inositol has been found to be more complex and multi-faceted. *Myo*-inositol and glucose compete for sodium as a co-transported analyte of the sodium ion-coupled transporters for *myo*-inositol (SMIT1 and SMIT2) and glucose (sodium-linked glucose transporter 1) (Greene and Lattimer, 1982; Schneider, 2015).

As previously mentioned, *myo*-inositol has also shown promise as an insulin mimetic, with dietary inositol shown to reduce postprandial glucose levels

and improve insulin sensitivity in humans and rhesus monkey studies (Ortmeyer, 1996; Corrado *et al.*, 2011; Kim, Han and Kim, 2014). Additionally, as well as *de novo myo*-inositol synthesis requiring glucose-6-phosphate, glucose may inversely induce *myo*-inositol depletion by activation of the glucose-sorbitol pathway, as seen in diabetic patients (Greene, Lattimer and Sima, 1987). In poultry, supplemental dietary *myo*-inositol has been shown to increase circulatory glucose, insulin and glucagon concentrations in low calcium and phosphorous diets, and improved feed conversion ratio and body weight gain (Cowieson *et al.*, 2013).

1.2.3 Inositol phosphates in plants

Inositol hexakisphosphate (InsP₆), or phytic acid, is the phosphate ester of inositol, containing six partially ionized phosphate groups. InsP₆ acts as an essential phosphorous store in a number of plant tissues and organs, including seeds and bran (Lopez *et al.*, 2002).

As the second most abundant inositol polyphosphate in cells, the roles of InsP₅ have long been questioned (Shears, 1992). Historically, InsP₅ and InsP₆ were considered to be metabolically lethargic (Menniti *et al.*, 1993), due to the known role of InsP₆ as a phosphorous store in seeds. However, InsP₃, InsP₄ and InsP₅ do not serve solely as metabolic precursors to production of InsP₆, with studies using conventional radiolabelling approaches in animal cells demonstrating that InsP₆ labelling is fairly unresponsive compared to the short-term receptor activated cell signalling of Ins(1,4,5)P₃ (Desfougères *et al.*, 2019). Findings have shown that the abundance of cellular InsP₅ contributes to processes in eukaryotic cells beyond a simple storage function, with research showing that the Jasmonic acid hormone response to plant wounding is linked to InsP₅ in *Arabidopsis thaliana* (Mosblech *et al.*, 2011). Further studies have shown that the inositol polyphosphates are not just co-factors of this process, but that InsP₅ binds specifically to the jasmonate receptor complex with a higher affinity than InsP₆ with a role in its activation (Laha *et al.*, 2016).

1.2.4 Inositol phosphates in human health and disease

Phytic acid is considered to be an “anti-nutrient” due to the affinity with which it binds to ions such as calcium, iron and zinc (Dendougui and Schwedt, 2004; Lemma *et al.*, 2007). The chelating properties of phytic acid have been linked to diets with mineral deficiencies and seen to some extent in vegetarians, in which the main dietary source of calories and minerals are plant tissues containing indigestible phytate (Committee on Food Protection and Food and Nutritional Board, 1973; Hurrell, 2003). Diets high in phytic acid have also been linked to the development of symptoms of osteomalacia, or rickets as it is known in children, due to its negative impact on phosphorous and calcium uptake (Mellanby, 1949).

One particular isomer of inositol triphosphate, Ins(1,4,5)P₃, commonly called InsP₃, is formed from hydrolysis of the cell membrane component PIP₂ (phosphatidylinositol 4,5-bisphosphate), also producing DAG (Michell, 1975). This soluble InsP₃ is free to diffuse through the cell membrane and bind to its receptor in the endoplasmic reticulum to release Ca²⁺ (Steelman *et al.*, 2015), important for secondary signal transduction particularly in the nervous system (Worley, Baraban and Snyder, 1989; Barski *et al.*, 2003). Dysfunction in the sensitivity of InsP₃ receptors involved in calcium signalling has been linked to a number of pathological conditions in humans. For example, in the development of genetically heritable Alzheimer’s disease, a mutation in the *PSEN1* gene encoding the presellin-1 protein has been linked to an increase in calcium release mediated directly by InsP₃ signalling, with treatment methods mediating InsP₃-mediated Ca²⁺ signalling showing promise as a treatment method (Stutzmann, 2005; Berridge, 2016).

Research has also linked InsP₅ to the induction of apoptosis in cancer cells as a result of its inhibition of the Akt/PKB kinase in the PI 3-K/Akt signalling pathway, associated with the development of lung cancer as well as ovarian and breast cancer cell lines (Burgering and Coffey, 1995; Piccolo *et al.*,

2004). InsP₆ has been implicated in viral capsid formation in HIV-1, increasing capsid stability and promoting the accumulation of DNA inside structures (Mallery *et al.*, 2018, 2019), and may become a focused target for treatments with evidence showing removal of IPMKs decreases viral production (Mallery *et al.*, 2021).

Due to their wide ranging roles, and thus implications in a number of myopathies, inositol phosphates and the enzymes that interconvert them are more commonly becoming a focus for disease interventions, with beneficial uses for inositol phosphates in cancer treatment (Vucenik, Druzijanic and Druzijanic, 2020), in treating diabetes mellitus (Omoruyi *et al.*, 2020) and in prevention of colitis and colitis-induced carcinogenesis (Weinberg *et al.*, 2021), and therapeutic approaches targeting enzymes involved in the synthesis pathways of inositol pyrophosphates as potential targets for metabolic diseases (Minini *et al.*, 2020; Mukherjee, Haubner and Chakraborty, 2020).

1.2.5 Roles of *myo*-inositol in poultry

With knowledge of functions of *myo*-inositol in humans and non-human animal species, interest for its potential role in poultry (specifically, *Gallus gallus*) arose from studies showing: 1) that phytase enzymes are able to release *myo*-inositol from InsP₆ in the intestinal tract of poultry (Walk, Santos and Bedford, 2014; Sommerfeld *et al.*, 2018b; Pirgozliev *et al.*, 2019a), and 2) evidence for the absorption of *myo*-inositol in poultry (Lee and Bedford, 2016; Sommerfeld *et al.*, 2018a). Our understanding of how *myo*-inositol is absorbed from the gastrointestinal tract, transported in the body and used thereafter, is limited, with knowledge of transport and uptake often being translated from other animal models including humans. Indeed, it is assumed that *de novo* synthesis of *myo*-inositol in *Gallus gallus* proceeds from glucose 6-phosphate (Sherman, Stewart and Zinbo, 1969; Loewus and Loewus, 1973, 1983), with potential for release from phosphatidylinositol phosphates and inositol phosphates, and that inositol transport (uptake) mechanisms are

conserved (Kanehisa *et al.*, 2017, 2019; summarised in Gonzalez-Uarquin, Rodehutsord and Huber, 2020). Irrespective of uptake mechanism, the majority of *myo*-inositol available from dietary uptake is a result of InsP_6 hydrolysis by phytase activity (Selle and Ravindran, 2007; Kim *et al.*, 2017), with lower inositol phosphates and inositol present in very low and variable concentrations in cereal grains (Rodehutsord *et al.*, 2016). A number of studies have focused on supplementation of *myo*-inositol into poultry diets, and have reported mixed effects on animal performance, including feed conversion ratio and bone strength, with studies reporting 1 g/kg inositol supplementation increased feed intake and body weight gain in broilers (Zyla *et al.*, 2013), though very high inositol doses (30 g/kg inositol) are associated with a significant reduction in feed conversion compared to control diets (Arthur *et al.*, 2019), and some studies have reported no interaction between inositol provision and bird performance (Farhadi *et al.*, 2017).

1.2.6 Importance of inositol and inositol phosphates for agriculture

In the case of farmed poultry, birds generally have a diet consisting of corn and soybean meal (Casartelli *et al.*, 2005). In crops, approximately one third of phosphorous is available for digestion, and the remaining two-thirds are bound as phytic acid (Lucca *et al.*, 2016). As a result of this, previous efforts to improve animal nutrition in agriculture focused on the addition of inorganic phosphate to diets. However, studies have shown that alongside the phosphorous bound in phytic acid, a large proportion of additional inorganic phosphate is also lost through excretion (Fireman and Fireman, 1998). The addition of inorganic phosphate sources can be costly, however, particularly in the case of poultry farming, and whilst particle size of defluorinated phosphate has not been found to affect phosphate uptake when measured as feed intake, weight gain and bone strength (Burnell, Cromwell and Stahly, 1990), but separate findings in Hubbard broiler chickens report that in comparison of monocalcium phosphate, dicalcium phosphate, defluorinated rock phosphate and bone ash as phosphate sources, dicalcium phosphate

outcompeted other sources in terms of digestibility measured as increased plasma concentrations of P but this did not translate to improvements in growth performance when all phosphate sources are supplied at the same level of available P (Khattak *et al.*, 2017). In poultry, deficiencies in phosphorous are similar to those described in humans, leading to poor growth performance and rickets, as well as reduced bone development (Scott, Nesheim and Young, 1982). In dairy cows, reduced dietary phosphorous availability is linked to limited milk production and infertility (Brooks *et al.*, 1984). Caged layer fatigue syndrome also occurs from reduced phosphorous availability in laying hens, in which the leg bones become brittle so that the bird can no longer stand (Simpson *et al.*, 1964). The effects of insufficient phosphorous overall constitutes an economic loss for the producer in reducing bird weight and carcass quality and increasing bird mortality (Waldroup, 1999) meaning fewer birds would reach adequate slaughter weight for sale, and the costly supplementation of inorganic P likely leading to increased consumer costs as the costs to farmers inevitably need to be passed on through the supply chain.

1.2.7 Environmental implications

Land used for agriculture accounts for approximately 38% of all global land use, or half of the habitable land on earth, with one third of this land used for crop production and the remaining two thirds for pastoral farming (Ritchie and Roser, 2019). In order to sustain the predicted global population increase to approximately 9 billion by the year 2050, models have suggested that food demand will increase by 54-96% (Valin *et al.*, 2014), and a projected doubling of meat and dairy intake in this same time period (Steinfeld *et al.*, 2006; Ros *et al.*, 2020). The limited availability of further land suitable for agricultural expansion means that, to meet this increased food demand to support the future population, agricultural and scientific efforts must focus on the sustainable improvement of outputs from current land available for agriculture.

Increasing food supply to maintain food security for a growing population, without the real possibility of increasing land use for agriculture, will rely heavily on increasing intensification of farming, which would lie in direct opposition to efforts to alleviate agricultural impacts on the climate, with current intensive poultry production and waste by-products linked to NH₃, N₂O and CH₄ emissions (Gržinić *et al.*, 2023). Efforts would also need to take into account the underlying impacts that climate change will have on food security and agricultural outputs (Gregory, Ingram and Brklacich, 2005), and how changes to livestock farming will impact downstream cost to the consumer when projections estimate increasing food costs as a result of climate change (Wollenberg *et al.*, 2016). Phosphate availability for agricultural systems is a major limiting factor for system output, and in crop production as well as arable farming, input of rock phosphate sourced inorganic phosphate is the main method for circumventing this issue. As previously discussed in section 1.2.6, inefficient use of dietary phosphate already poses an issue for non-ruminant animal rearing, with further environmental impacts including the leaching of phosphorous into the environment, linked to eutrophication and algal bloom (Djodjic, Börling and Bergström, 2004; Fortune *et al.*, 2005). Agricultural activities are responsible for 20-30% of phosphorous pollution in waterways in the United Kingdom (Environmental Agency, 2019), and combined with the necessity to mine for minerals for use as feed supplements, the overall environmental impact of such animal rearing practices are significant (Harper, Kornegay and Schell, 1997; Metzler *et al.*, 2008). As inorganic phosphate sources through mining are non-renewable, the potential future problems associated with continued overuse are unquantifiable, further encouraging the importance of improving the efficiency of available phosphorous utilization from crop sources.

1.3 Phytases

1.3.1 Background to phytases

The name phytase (*myo*-inositol hexakisphosphate phosphohydrolase) refers to a class of phosphatase enzymes that catalyse the hydrolysis of *myo*-inositol hexakisphosphate, releasing inorganic phosphate at each sequential hydrolysis step (Mullaney, Daly and Ullah, 2000).

First characterized in 1907 from rice bran (Suzuki, U., Yoshimura, K., Takaishi, 1907), phytases are now considered to be one of the most important feed additives in animal nutrition (Gen Lei *et al.*, 2013). Phytases are categorised into four broad classes based on their catalytic mechanism/structural fold: Histidine Acid Phosphatases (HAPhys); Purple Acid Phosphatases (PAPhys); β -propeller phytases, or alkaline phytases (BPPhys); and Protein Tyrosine Phosphatase-like phytases (PTPhys) (Table 1.1).

Table 1.1: Phytase classification based on catalytic mechanism.

Class	pH range	End product of hydrolysis	Prevalence
Histidine acid phosphatase (HAPhy)	4.0-4.5	Inositol-2-monophosphate (InsP ₁)	Bacteria, yeast and fungi
Purple Acid Phosphatase (PAPhy)	4.0-5.5	Inositol-2,3,4,5-tetraphosphate/inositol-1,2,5,6-tetraphosphate (InsP ₄)	Plants
Alkaline phytase β -propeller (BPPhy)	7.0-8.0	Inositol trisphosphate (InsP ₃)	<i>Bacillus</i> , legume seeds, lily
Protein Tyrosine Phosphatase-like phytases (PTPhy)	4.5-5.0	Inositol-2-monophosphate (InsP ₁)	Bacteria

^aInformation obtained from Shi, Potts and Kennelly (1998) and Gontia-Mishra and Tiwari (2013)

Enzyme Nomenclature Committee refers to phytases based on the position on the *myo*-inositol ring from which the first phosphate is cleaved by the enzyme activity: 3-phytases (D-3-phytase or L-1-phytase; EC 3.1.3.8); 6-phytases (D-4-phytase or L-6-phytase; EC 2.1.2.26) and 5-phytases (EC 3.1.3.72); additionally, a separate class of phytases known as MINPPs or multiple inositol-polyphosphate phosphatases (EC 3.1.3.62) (Table 1.2).

Table 1.2: Classification of phytases based on carbon position for first dephosphorylation.

Class	IUPAC nomenclature	Prevalence
3-phytase (EC 3.1.3.8)	<i>Myo</i> -inositol hexakisphosphate 3-phosphohydrolase	Most bacteria and Ascomycetes phylum ^{a,b}
6-phytase (EC 3.1.3.26)	<i>Myo</i> -inositol hexakisphosphate 6-phosphohydrolase	Plant grains/oilseeds, ferns, Basidiomycetes ^{c,d,e}
5-phytase (EC 3.1.3.72)	<i>Myo</i> -inositol hexakisphosphate 5-phosphohydrolase	<i>Lily, alfalfa, beans, peas,</i> <i>S. ruminantium</i> ^{f,g,h,i}
MINPP (EC 3.1.3.62)	multiple inositol-polyphosphate phosphatase	Bacteria, plants, animals ^j

^a Gao *et al.* (2007); ^b Lee *et al.* (2007); ^c Johnson, Yang and Murthy(2010); ^d Tu, Ma and Rathinasabapathi (2011); ^e Lassen *et al.*(2001); ^f Barrientos, Scott and Murthy (1994); ^g Chu *et al.* (2004); ^h Puhl, Greiner and Selinger (2008); ⁱ Yao *et al.* (2012); ^j Stentz *et al.* (2014)

Phytases occur across kingdoms, with example enzymes isolated in the animal kingdom in the liver and blood of calves (McCollum and Hart, 1908) and the plasma and erythrocytes of a number of vertebrate species (Rapoport, Leva and Guest, 1941); plant species such as the crops soybean (Hamada, 1996) and wheat (Nakano *et al.*, 1999); and a number of microbial species including filamentous fungi (Gargova, Roshkova and Vancheva, 1997), various bacteria species such as *E. coli sp.* and *Klebsiella sp.* (Greiner, Konietzny and Jany, 1993; Greiner *et al.*, 1997) and yeast species such as *S. cerevisiae* (Nakamura, Fukuhara and Sano, 2000).

The evaluation of effective pH range of phytases is imperative from a biotechnology standpoint, when selective enzymes as targets for engineering for use in agriculture, as it is necessary for phytases to be active at a pH relevant to the digestive tract (Tomschy *et al.*, 2002), with efforts often taken to modify enzymes for improved pH stability such as in the case of modification of phytase from *A. niger* to change the pKa of catalytic residues, resulting in an improved pH optimum from 2.5 to 3.2 for better performance in the monogastric gut (Usharsree *et al.*, 2015). Additionally important in this consideration is the negative effects of phytate under these conditions, with InsP₆ binding of protein reportedly occurring mainly in acidic environments

(Morales *et al.*, 2011), such as the crop, proventriculus gizzard in poultry. As well as this, the effect endogenous enzymes will have on supplemented phytases active in the complex gut matrix must be taken into account, with exogenous phytases unable to survive proteolytic digestion in the intestine (Kumar *et al.*, 2003). These considerations for pH tolerance, along with the final product of hydrolysis InsP_1 (Table 1.1), near complete hydrolysis, make Histidine Acid Phytases ideal biotechnology targets for industry applications.

1.3.2 Phytases in plants

With phytic acid the predominant phosphorous store in plant seeds and bran, several studies aiming to improve phosphate utilisation by crop plants have investigated the regulation of plant endogenous phytases (reviewed in: Brinch-Pedersen *et al.*, 2002). Total degradation of seed phytate would be an unsustainable solution, leading to the production of nonviable seeds, as phytate and its lower esters are central to a number of plant pathways and thus the complete removal of phytate would generate low yield or stress susceptible plants (Raboy, 2009), but molecular genetic methods have allowed for the development of low phytic acid crops such as the common bean (Campion *et al.*, 2009) which show promise in human nutritional studies for the reduction of anti-nutritive phytate properties (Mendoza *et al.*, 1998).

Plant phytase activity has been detected in roots and root exudates, though the majority of phytase activity in plants is detected in grains during the early stages of seed germination, with notable crop plants wheat and barley expressing PAPHy and MINPP phytases concurrently for the liberation of phosphate during germination (Dionisio *et al.*, 2011). The specific activity of plant endogenous phytases is very low (Rao *et al.*, 2009; Reddy *et al.*, 2013), and whilst significant research exists and is underway for the production of low phytic acid crop strains (Dorsch *et al.*, 2003; Shi *et al.*, 2005; Stevenson-Paulik *et al.*, 2005), for the direct downstream influence on eutrophication arising from high grain phytate used in feed products microbial and fungal phytases have been shown to be better biotechnology candidates for

agricultural applications (Spencer, Allee and Sauber, 2000; Colombo *et al.*, 2020; Dwivedi and Ortiz, 2021).

1.3.3 Use of phytases in agriculture

Phosphate is one of the most limiting minerals present in livestock feed naturally, with approximately 3 grams per kilogram of phosphorous in feedstuffs existing as phytate (Selle *et al.*, 2007) and, similar to arable farming, animal production relies on exogenous inputs of inorganic phosphate from mined rock phosphate sources. Rock phosphate, like many other ores, is a non-renewable resource, with the U.S. Geological Survey 2022 estimates of 71 million metric tons total remaining in global reserves. With a current mine production capacity of 220,000 metric tons estimated in 2021, global consumption is estimated at 47 million tons in 2020 and expected to rise to 48 million tons by 2024 (U.S. Geological Survey, 2021, 2022). Estimates for “peak phosphorous”, that is, the time point at which maximum global production rate of phosphorous is reached, varies from predictions between 2030-2136 (Cordell and White, 2011; Walan *et al.*, 2014) after which production will decline. However, despite having not reached this point of peak production yet, prices for rock phosphate have rocketed in recent years – though the COVID-19 pandemic disproportionately affected prices, with 2020 rock phosphate prices at decade-long lows – the price per metric tonne of unprocessed rock phosphate and diammonium phosphate as a fertiliser has more than doubled from 2019 to February 2022 (World Bank, 2022). In real world terms, this means that the cost for rearing livestock is increasing exponentially and unsustainably, and to avoid passing these costs on to consumers it is necessary to find alternative, cheaper, and more sustainable sources of phosphate for feed input.

Alongside associated problems with phosphate supplementation, the high phytic acid content of animal feeds is considered a potent anti-nutrient by virtue of chelation of divalent cations. Consequently, the use of the enzyme phytase to release available phosphate, to alleviate metal ion sequestration

and improve nutritional availability from food sources has moved to the forefront of agricultural animal nutrition.

Ruminant animals, those with multiple-compartment stomachs, such as sheep, cows and goats, are able to digest phytate as the rumen gut microorganisms produce the enzyme phytase (Klopfenstein *et al.*, 2002). Monogastric animals have far reduced gut phytase activity by comparison, and as such the inositol and phosphate stored in phytate is not readily bioavailable. As grains are the main component of feed for pastoral and intensive livestock farming, including the rearing of monogastric animals in commercial farming of swine and poultry, this then means the inositol and phosphate in phytates is not readily bioavailable, and so passes through the gut system (Pointillart, 1994; YI *et al.*, 1996). In terms of implications for agriculture, not only does this mean that additional input of inorganic phosphate sources is required to maintain animal nutrition, but also that large amounts of phosphorous are lost to the environment through these practices (Correll, 1998; Humer, Schwarz and Schedle, 2015).

Trials have been carried out to assess the benefits of the addition of microbial phytase to monogastric animals by measurements of weight gain and bone ash percentage since the 1970s, with pioneering work carried out by Nelson and colleagues measuring the effect of increasing doses of supplemental *Aspergillus ficuum* phytase on the utilisation of phytate phosphorous by broilers (Nelson *et al.*, 1971).

The first attempt to produce a commercial phytase enzyme for use in the animal-feed industry was undertaken by International Minerals & Chemicals (IMC) in 1962, though the first commercially sold phytase only became available in 1991, marketed by the German chemical company BASF (Lei *et al.*, 2013), as an *Aspergillus niger* phytase isolate. Phytase is now one of the most commonly used animal-feed enzyme additives, representing almost two-thirds of feed-enzyme sales (Adeola and Cowieson, 2011). Phytase is most commonly used to reduce diet costs by avoiding the requirement to supplement with increasingly expensive inorganic phosphate sources.

Studies have found that the use of phytase as a feed supplement in laying hens and broilers has led to improved utilization of phosphorous, with commercial Single Comb White Leghorn laying hens fed 300 FTU/kg phytase in low available phosphorous diets (0.1%) performing comparably to birds fed adequate available phosphorous (0.45%) with no supplemented phytase (Boling *et al.*, 2000) and the conclusion reached by Ceylan *et al.* that inclusion of 500 FTU phytase to broiler diets allows for a reduction of total phosphorous by 0.13% (Ceylan *et al.*, 2012). Laying hens fed with supplemented phytase also demonstrated improved eggshell quality, with maintenance of proper balance of calcium and phosphate ratio critical for eggshell quality (Ousterhout, 1979), and reducing supplemented inorganic phosphorous when phytase was added to the diet did not reduce hen performance or the quality of the eggshells produced (Casartelli *et al.*, 2005).

1.3.4 Phytase use in poultry production

The inclusion of phytase in poultry feed is by no means a new concept, it has for some time enabled a reduction in the production costs of poultry for human consumption as well as a reduction in the losses of phytate-P to the environment from poultry farming. Several studies and reviews have considered the variability of the amount of phytase needed to be added to the diet to replace added phosphorous adequately (Kornegay *et al.*, 1996; Bedford, 2000). A second, important consideration for the inclusion of phytase in poultry diets is the required calcium and phosphorous content of the diet, and the impact of increased calcium content on phytase activity, with greater calcium diets decreasing the efficiency of phytase hydrolysis of phytate (Fisher, 1992; Sebastian *et al.*, 1996).

Supplementation of poultry diets with phytase have been shown to go further than simply improving feed conversion ratio and weight gain for meat production by improving phosphate utilisation. One example of this is the potential for improving meat quality and therefore reducing wastage in

poultry production posited in a recent study by Greene *et al.* (2019), in which phytase supplementation was shown to reduce the occurrence of woody breast, a myopathy ascribed to broiler chickens attributed to muscle hypoxia that in addition to being a welfare issue for birds also contributes to economic losses due to the negative impact on meat texture, and whilst the mechanisms by which phytase supplementation improves this are not yet fully elucidated, the study by Green and colleagues suggests that Quantum Blue phytase provision may modulate a number of metabolites including s-adenosyl-homocystein, arginine, tricarballic acid, NAD⁺, glucosamine phosphate, AMP, histamine and pyridoxate, and may do so through improved solubility and digestibility of dietary nutrients (Tamin *et al.*, 2004). Similarly in laying hens, phytase supplementation has been shown to improve egg production (Sahara, Despedia and Aminah, 2018), egg weight (Um and Paik, 1999), and decrease broken and soft egg production rate (Lim, Namkung and Paik, 2003).

1.3.5 Superdosing

The use of super-doses of phytase has become the focus of phytase dietary inclusion research in recent years, as the inclusion of phytate is now well known to have benefits in terms of animal performance for the reduction of InsP₆ in the gut lumen and provision of plant phosphate sources.

“Superdosing” is the name given to the use of unconventionally high doses of phytase, defined as supplementation with over 1,500 FTU/kg phytase (Walk, Santos and Bedford, 2014) or greater than 2,500 FTU/kg phytase (Adeola and Cowieson, 2011). The term is more loosely defined as supplementing phytase at 2 to 5 times the standard phytase dose, at which levels the dose is associated with a rapid complete or near complete hydrolysis of InsP₆ in the digestive tract, with an associated significant increase in feed conversion ratio (Walk *et al.*, 2013; Walk, Santos and Bedford, 2014).

Though the first research using super-doses of phytase was conducted by Nelson and colleagues using doses up to approximately 7,600 FTU/kg of

feed of an *Aspergillus ficuum* phytase preparation in broiler chick experiments (Nelson *et al.*, 1971), and reporting approximately 95% phytate-P hydrolysis alongside log-linear increases in weight gain and bone ash, little was understood about the mechanisms of the advantages provided by use of high phytase doses. Several more recent studies have suggested that the use of unconventionally high phytase doses has benefits for animal performance on multiple fronts, not only the liberation of more phosphate from inositol phosphate species, but the reduction of antinutritive effects of phytate presence leading to improved mineral utilisation (Pirgozliev *et al.*, 2008; Rutherfurd *et al.*, 2012) and improvements in apparent metabolizable energy (AME), bone development (Fernandes *et al.*, 2019) and amino acid digestibility (Zeng *et al.*, 2014). These benefits, unrelated to those resulting directly from increased free inorganic phosphate from phytate degradation, are referred to as “extra-phosphoric”. That is, the growth performance of animals exceeds that obtainable with equivalent (to complete phytate dephosphorylation) provision of inorganic phosphate. An indication that *myo*-inositol provision, from phytate, might confer benefit was reported in a seminal study of broilers (Walk, Santos and Bedford, 2014).

1.4 Aims

The overarching aim of the project was to investigate the separable contributions that inositol, inositol phosphates and phosphate released from dietary phytate, by phytase activity in the gastrointestinal tract, make to poultry performance. This aim was to be achieved through the development of extraction and analysis techniques for first time measurements of inositol phosphates in poultry tissues without the use of radioisotope labelling to investigate the effects of phosphate release on animal performance and tissue response. In order to achieve this, the project aimed to:

1. Develop a method for the synthesis of stable isotope labelled *myo*-inositol. The results of which are presented in chapter 2, where a chemoenzymatic synthesis method was developed to produce $^{13}\text{C}(\text{U})$ -

labelled *myo*-inositol from a more affordable and more readily available $^{13}\text{C}(\text{U})$ -labelled glucose precursor.

2. Develop a method for the extraction and analysis of inositol phosphates from poultry tissues. Existing published methods allowed for the extraction and analysis of inositol from tissue samples, but optimisation of a solid phase extraction method published by Wilson *et al.* (2015) enabled first time measurements of inositol phosphates in poultry tissues, as is presented in Chapter 3.
3. Using the methods developed as parts 1 and 2 of the aims, measure the effect that graded phytase supplementation has on tissue inositol phosphate levels in broiler chickens to make advances in the understanding of the whole animal response to phytase supplementation, through use of a poultry feeding experiment, presented in Chapters 4 and 5, and in part in chapter 6.

2. Producing stable isotope labelled *myo*-inositol from glucose

2.1 The biosynthetic pathway for the production of *myo*-inositol

The biological significance of inositol is demonstrated by the prevalence of enzymes for the synthesis of inositol from glucose, with inositol-1-phosphate synthase genes ubiquitously expressed across kingdoms (Majumder *et al.*, 2003). The inositol-3-phosphate synthase gene, referred to from herein as IPS, is found in most archaea and it is predicted that *myo*-inositol emerged in early archaea approximately 3500 million years ago (Michell, 2007). Few bacteria encode an inositol phosphate synthase, though those that do – mostly actinomyces such as *Streptomyces* or hyperthermophilic bacteria - have been found to be genetically more similar to archaeal IPS as opposed to those found in eukaryotes; it has been suggested in these groups that accumulation of *myo*-inositol phosphodiester is related to high temperature stress and survival (Bachhawat and Mande, 2000; Nesbo *et al.*, 2001; Kulis-Horn *et al.*, 2017).

In humans, *myo*-inositol is synthesised *de novo* in the kidney from glucose (Fig. 2.1). The first step of the reaction requires the enzyme *myo*-inositol phosphate synthase to convert G6P into D-inositol 3-phosphate in an NAD⁺ dependent reaction (Loewus and Loewus, 1983), and is the rate limiting step (Hasegawa and Eisenberg, 1981). An example of this enzyme is the human ISYNA1, which converts G6P to *myo*-inositol 1-phosphate (Ju *et al.*, 2004). Genes encoding the 1-*myo*-inositol-1-phosphate synthase, referred to from herein as MIPS *in planta* and in *S. cerevisiae* as INO1, have been found to be relatively highly conserved, with orthologs of the *INO1* gene found in a range of higher eukaryotes and eukaryotic microorganisms (Majumder, Johnson and Henry, 1997). An inositol monophosphatase enzyme then dephosphorylates the inositol 3-phosphate intermediate, resulting in free

myo-inositol (McAllister *et al.*, 1992). In rats, this process has been found to take place at the highest concentration in the testes (Hasegawa, Eisenberg and Jr, 1981). This process occurs similarly in most Archaea, where it is believed that inositol was derived by early archaeal inositol synthesis from G6P with evolutionary evidence that the evolution of inositol and its functions occurred prior to the evolutionary separation of Archaea/Bacteria from the primitive Eukaryota clade (Michell, 2007).

Figure 2.1 below shows the generalised pathway for *de novo* synthesis of *myo*-inositol from a D-glucose precursor, adapted from Croze and Soulage (2013).

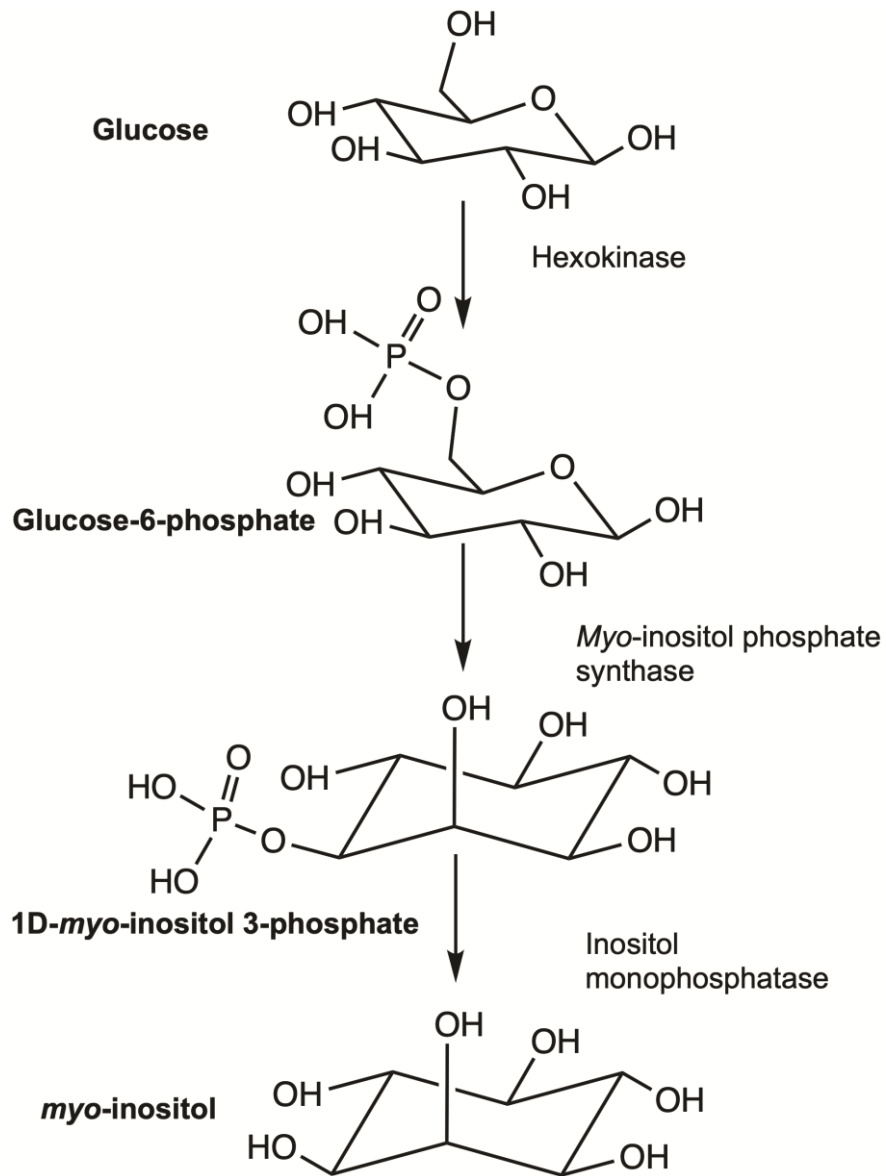


Figure 2.1: *De novo* biosynthesis pathway of *myo*-inositol from glucose. Figure adapted from Croze and Soulage (2013). Scheme produced using Chemdraw v19.0

2.2 Methods and materials

2.2.1 Materials

2.2.1.1 Media and reagents

2.2.1.1.1 Standard reagents

Lysogeny broth (LB) – Lysogeny broth was made up from components in the lab, consisting of 10 g Tryptone (Formedium), 5 g Yeast Extract (Formedium), 10 g NaCl (Fisher Chemicals) and pH adjusted to 7.5 with NaOH in 1 L of sterile water, sterilised by autoclave.

LB agar was also made fresh in the lab for each use from 5 g Tryptone (Formedium), 2.5 g yeast extract (Formedium), 5 g NaCl (Fisher), 7.5 g agar (Formedium) in 500 mL of water and sterilised by autoclave.

SOB media – In 500 mL sterile water, 10 g Tryptone (Formedium); 2.5 g yeast extract (Formedium), 0.295 g NaCl (Fisher Chemicals), 0.093 g KCl (Sigma), 1.015 g MgCl₂.6H₂O (Sigma); 1.235 g MgSO₄.7H₂O (Sigma); sterilised by autoclave.

SOC media was made from SOB medium with the addition of 2 mL of 1 M glucose (Sigma) per 100 mL SOB and filter sterilised through a 0.2 µM syringe filter.

½ MS plates for Arabidopsis in 250 mL of sterile water: 0.5375 g Murashige and Skoog media (Formedium), 2.5 g sucrose (Fisher), 175 mL sterile water – pH 5.7; 2.5 g agar (Formedium), sterilised by autoclave.

E. coli TB buffer - 10 mM PIPES (Sigma) pH 6.7 (3.0236 g); 55 mM magnesium chloride (5.2366 g (Sigma)); 15 mM CaCl₂ (1.6647 g) (VWR Chemicals); 250 mM KCl (18.63783 g) (Sigma); added up to 1 litre with sterile water and filter sterilized using a syringe and 0.22 µm filter (Sartorius).

Alternatively: 1 M MOPS (Melford) pH 6.7 2.093 g (using KOH); $\text{MnCl}_2 \cdot 4\text{H}_2\text{O}$ 5.44 g (Sigma), $\text{CaCl}_2 \cdot 2\text{H}_2\text{O}$ 1.10 g (VWR Chemicals); KCl 9.32 g (Sigma); added up to 250 mL and filter sterilized through a 0.22 μm syringe filter (Sartorius).

YPD -

For 500 mL liquid media: 10 g peptone (Formedium); 5 g Yeast extract (Formedium); 5 g sucrose (Formedium), added up to 500 mL with sterile water and autoclaved

For 200 mL solid media for plates: 4 g Peptone (Formedium); 2 g Yeast extract (Formedium); 2 g sucrose (Formedium); 4 g agar (Formedium); added up to 200 mL with sterile water and sterilized by autoclave.

1 M Tris pH 8.5 - 30.285 g Tris Ultra Pure (Formedium) dissolved in 250 mL distilled water and autoclaved, and pH adjusted using concentrated HCl.

1 M Tris pH 6.8 - 30.285 g Tris Ultra Pure (Formedium) dissolved in 250 mL distilled and autoclaved, and pH adjusted using concentrated HCl.

1 M Lithium Acetate pH 7.6 (Sigma-Aldrich) – 6.598 g dissolved in 100 mL sterile distilled water and sterilized by autoclaving.

0.2 M NaOH (Fisher Chemicals)- 1.99985 g dissolved in 250 mL sterile distilled water and sterilized by autoclaving.

50% PEG₃₃₅₀ (w/v) (Sigma)

0.5 M EDTA (Fisher Chemicals) – 14.612 g dissolved in 100 mL sterile distilled water and sterilised by autoclaving.

5 M NaCl (Fisher Chemicals) - 29.22 g in 100 mL of sterile distilled water, dissolved by heated stirring and autoclaved.

10% Sodium Dodecyl Sulphate (w/v) (Fisher Chemicals) – 10 g sodium dodecyl sulphate added up to 100 mL using sterile distilled water and dissolved by gentle stirring over heat.

2.2.1.1.2 Antibiotic stocks: (All antibiotics sourced from Duchefa Biochemie)

- 50 mg/mL Gentamicin (in sterile distilled water)
- 50 mg/mL Kanamycin (in sterile distilled water)
- 100 mg/mL Ampicillin (in sterile distilled water)
- 25 mg/mL Chloramphenicol (in 95% EtOH)

2.2.1.1.3 Protein purification buffers

For the purification of the *Archaeoglobus fulgidus* myo-inositol phosphate synthase, the following buffers were used with the Äkta Pure system:

Lysis buffer – 50 mM Tris-HCl (Formedium) pH 7.5, 150 mM NaCl (Fisher Chemicals), 10 mM Imidazole, 1% Triton-X-100 (Fisher Chemicals)

Loading buffer – 50 mM Tris-HCl pH 7.5 (Formedium), 150 mM NaCl (Fisher Chemicals), 10 mM Imidazole (Sigma-Aldrich)

Elution Buffer – 50 mM Tris-HCl pH 7.5 (Formedium), 150 mM NaCl (Fisher Chemicals), 500 mM Imidazole (Sigma-Aldrich)

Sepharose buffer – 50 mM Tris-HCl pH 7.5 (Formedium), 150 mM NaCl (Fisher Chemicals)

2.2.1.1.4 SDS PAGE

10x SDS PAGE running buffer – 1 litre: 30.3 g Tris Ultra Pure (Formedium), 144 g Glycine (Fisher Chemicals), 10 g SDS (Fisher Chemicals) and add to a final volume of 1 L using sterile distilled H₂O. Diluted to 1x running stock of final concentration 25 mM Tris, 192 mM glycine, 0.1% SDS.

SDS PAGE polyacrylamide gels were hand cast using the Bio-Rad Mini-PROTEAN® Cell, with a thickness of 1.0 mm (Bio-Rad Laboratories Inc., 2014). The recipe used for casting the gels is in Table 2.1:

Table 2.1: 12% SDS PAGE resolving gel recipe. All reagents sourced from Sigma.

Component	Stacking gel (5%)	Resolving gel (12%)
30% Bis/polyacrylamide	0.83 mL	5 mL
1.5M Tris pH 8.8	-	2.3 mL
1M Tris pH 6.8	0.63 mL	-
10% (w/v) ammonium persulfate	0.05 mL	0.1 mL
10% (w/v) SDS	0.05 mL	0.1 mL
Tetramethylethylenediamine (TEMED)	5 μ L	4 μ L
Water	3.4 mL	2.3 mL

2.2.1.2 Yeast strains

The wild type *Saccharomyces cerevisiae* haploid strain S288C, common baker's yeast, was grown on YPD nutrient-rich medium. The strain was obtained with permission from the National Collection of Yeast Cultures strain NCYC 3466.

Adolfo Saiardi at the University College London gifted the *S. cerevisiae* strains BY4741, W303 and DDY1810 and their knockout and overexpression constructs listed in Appendix 1. The BY4741 mutant lines carry a resistance cassette for G418 and are protease-deficient. The DDY1810 constructs carry a Leu2 cassette and G418 resistance. Strain W303 and its mutant lines are *ade2-1* mutants (Matheson, Parsons and Gammie, 2017), with significant similarity to the common lab reference strain S288C but divergent mutation allowing for strain survival carrying mutations which would be lethal in the S288C strain, such as survival carrying components of the *SWI/SNF* complex (Cairns *et al.*, 1998).

2.2.1.3 Gateway cloning materials

For use in Gateway cloning, the following bacterial vectors were obtained with thanks to Melissa Salmon: pDONR207, pH9GW, pDEST17.

2.2.1.3.1 Bacterial vectors

Table 2.2: Bacterial vectors for Gateway cloning

Vector name	Type	Size	Selectable marker
pDONR207	Entry vector	5585bp	Gentamicin resistance
pH9GW	Destination vector	6990bp	Kanamycin resistance
pDEST17	Destination vector	6354bp	Ampicillin resistance
pET23a:IPS	Expression vector	3666bp	Ampicillin resistance
pENTR D-TOPO	Entry vector	2580bp	Kanamycin resistance

The pET23a:IPS vector was a gift from Prof. Adolfo Saiardi at University College London. The p-ENTR D-TOPO directional Gateway entry vector was purchased from Invitrogen (K240020) (Invitrogen, 2012).

2.2.1.3.2 Yeast expression vectors

Table 2.3: Yeast vectors for Gateway cloning

Vector name	Type	Size	Selectable marker
pAG413GPD-ccdB-HA	Destination vector	7668bp	HIS3; Chloramphenicol and Ampicillin resistance
pYES2.1-cerMET8	Expression vector	6705bp	URA3; Ampicillin resistance
pE1n	Modified GATEWAY entry vector	2349bp	Kanamycin

The yeast vector was pAG413GPD-ccdB-HA was a gift from Dr. Mark Bailey, University of Birmingham department of Plant Proteomics and Signalling.

pE1n was a gift from Giovanna Benvenuto (Addgene plasmid #17441; <http://n2t.net/addgene:17441>; RRID:Addgene_17441) (Dubin, Bowler and Benvenuto, 2008)

pYES2.1-cerMET8 was a gift from Clare O'Connor (Addgene plasmid #107439; <http://n2t.net/addgene:107439>; RRID:Addgene_107439) (Reeves *et al.*, 2018)

2.2.2 Methods

2.2.2.1 Arabidopsis plating

Arabidopsis thaliana Columbia-0 (Col0) seeds were sterilized in 10% bleach and imbibed in sterile distilled water. Seeds were plated onto half strength Murashige and Skoog agar medium and separated into two conditions – 2 of the four plates of Col0 seeds were vernalized for 2 days prior to being moved to growth conditions, and the remaining two plates were transferred immediately to growth conditions after plating. All seeds were grown in long day conditions – 16 hours light, 8 hours dark – at a constant temperature of 22°C for 9 days prior to stress treatment.

2.2.2.2 Arabidopsis stress treatment

Seedlings were exposed to abiotic stress conditions based on the AtGenExpress global stress expression data set showing the upregulation of AtMIPS1 and AtMIPS2 during stress (Kilian *et al.*, 2007).

One plate of vernalized seedlings and one plate of un-vernalized seedlings remained sealed and were transferred into an icebox and stored at 4°C on day 9 for 24 hours.

2.2.2.3 RNA extraction

Seedlings were flash frozen after stress treatment in liquid nitrogen and ground using a pestle and mortar under liquid nitrogen into a fine powder. RNA extraction from 100 mg of frozen and ground seedlings was performed using the QIAGEN RNeasy Kit as per manufacturer's instructions (QIAGEN, 2012).

2.2.2.4 DNase treatment for RNA

Mix: 0.8-2 µg RNA per extraction (maximum 8 µL per tube); 1 µL DNase (Promega RQ1 RNase-Free DNase); 1µL 10x Reaction Buffer (Promega) – added up to 10µl using sterile deionized water. Incubate at 37°C for 30 minutes, then add 1 µL RQ1 Stop Solution (Promega) and incubate at 65°C

for 10 minutes, then chill on ice for 5 minutes and proceed to cDNA synthesis.

2.2.2.5 cDNA synthesis protocol

To DNase treated RNA add: 1 μ L Oligo dT and 1 μ L dNTP mix and heat at 65°C for 5 minutes. Chill briefly (30 seconds) on ice and centrifuge for 10 seconds, then add 4 μ L 5x First Strand Buffer, 2 μ L 0.1 M DTT and 1 μ L RNaseOUT, mix by inversion and heat at 42°C for 2 minutes. Add 1 μ L Superscript II Reverse Transcriptase (Invitrogen) and heat at 42°C for 50 minutes, inactivate at 70°C for 15 minutes. Add 79 μ L sterile deionized water to add up to a total of 100 μ L and proceed to cloning.

Method and materials sourced from Invitrogen RT kit (Kotewicz *et al.*, 1985).

2.2.2.6 PCR cloning of genes of interest

Using synthesised cDNA as the PCR template with specific primers, the following reaction mix (Table 2.4) was used:

Table 2.4: Reaction mix for Phusion PCR amplification

Reaction Mix	Per sample
Phusion	0.2 μ L
cDNA	1 μ L
Forward primer	1.5 μ L
Reverse primer	1.5 μ L
10 mM dNTPs	0.4 μ L
5x Buffer	4 μ L
Sterile distilled water	11.4 μ L

Two different PCR approaches were used for amplification of target genes from cDNA. For the cloning of ScINO1 from *S. cerevisiae* cDNA and genomic DNA, the PCR conditions used are described in Table 2.5.

Table 2.5: PCR conditions for the amplification of ScINO1 from *S. cerevisiae* DNA.

		38 cycles				
Temperature (°C)	98	98	58	72	72	10
Time ('min "sec)	30"	10"	30"	20"/kb	5'	∞

For AtMIPS1 and AtMIPS2 from *Arabidopsis thaliana* Columbia-0 background, using cDNA from wild type seedlings as well as cold shock and osmotic stress seedlings as described above, a Touchdown PCR was used following unsuccessful amplification using the standard "middle of the road" PCR protocol used for cloning ScINO1. Conditions are described in Table 2.6.

Table 2.6: PCR conditions for the amplification of AtMIPS1 and AtMIPS2 from *A. thaliana* cDNA.

		11 cycles (-1°C/cycle)			25 cycles				
Temperature (°C)	98	98	60	72	98	50	72	72	10
Time ('min "sec)	30"	10"	30"	20"/kb	30"	30"	20"/kb	5'	∞

PCR products were run on 0.8% TAE agarose gels with Ethidium Bromide at 100 V for 45 minutes.

Addition of C-terminal 6xHIS tag by PCR cloning

The following primers (Table 2.7) were designed in order to add a 6xHIS tag onto the 3' end of the cloned genes, using existing gel extracted gene fragments as the DNA template for PCR cloning.

Table 2.7: Primers for the PCR addition of c-terminal 6xHIS tag.

Oligonucleotide	Sequence
ScINO1 reverse primer + 6xHIS	TTACAGCAAACGTTTCCTCAACATCATCACCATCACCAT
AtMIPS2 reverse primer + 6xHIS	TCACTTGTACTIONCCATGATCATGCATCATCACCATCACCAT

PCR conditions used were as follows:

Table 2.8: PCR conditions for the addition of 3' 6xHIS to ScINO1 purified gene fragment

		38 cycles				
Temperature (°C)	98	98	69.1	72	72	10
Time ('min "sec)	30"	10"	30"	1'	5'	∞

Table 2.9: PCR conditions for the addition of 3' 6xHIS to AtMIPS2 purified gene fragment

		38 cycles				
Temperature (°C)	98	98	66	72	72	10
Time ('min "sec)	30"	10"	30"	1'	5'	∞

2.2.2.7 Gel electrophoresis

PCR reaction products were analysed by gel electrophoresis using 0.8% agarose-TAE gels. Gels were run at 100 V for 45 minutes in 1x TAE buffer and imaged using the Bio-Rad Gel Doc XR+ system using trans-UV illumination at 302 nm (Bio-Rad Laboratories, 2015).

2.2.2.8 Preparation of competent cells

Mach1 DH5 α from commercial one-shot was streaked onto LB agar with no antibiotic selection and grown at 37°C overnight for 16 hours. From this, a single colony was inoculated into a 10 mL liquid LB culture and grown overnight at 37°C with 200 rpm shaking until OD₆₀₀ of 0.6 was reached. Into two separate 250 mL subcultures of SOB medium, 0.5 mL and 2 mL of overnight culture was added and grown at 18°C with 220 rpm shaking until an OD₆₀₀ of 0.55-0.6 is reached – approximately 17 hours for Mach1 DH5 α . The conical flask was immediately submerged in ice for 10 minutes and decanted into 50 mL falcon tubes, then centrifuged at 4000 rpm at 4°C for 10 minutes. The pellet was resuspended in 80 mL of chilled TB buffer and incubated in ice for a further 10 minutes then centrifuged again, and resuspended in 20 mL TB buffer with 1.5 mL DMSO. Cells were then divided into 100 μ L aliquots into pre-chilled 1.5 mL tubes, snap frozen in liquid nitrogen and stored at -80°C.

Method adapted from Untergasser (2015).

2.2.2.9 Transformation

2.2.2.9.1 BP Reaction

Table 2.10: Reaction mixture for BP Clonase II reaction

Reaction mix:	For one sample:
PCR product	~15-150 ng per reaction, maximum 7 μ L
Donor vector	1 μ l (150 ng/ μ L)
TE Buffer (pH 8.0)	Add up to total reaction mix 8 μ L

To each reaction mixture, 2 μ L of BP Clonase II enzyme was added and reactions were incubated at 25°C for 1 hour. Following incubation, 1 μ L of Proteinase K solution was added to each sample to terminate the reaction and samples were incubated at 37°C for 10 minutes. The entire reaction mix

(Table 2.10) was used to transform 50 μ L of chemically competent *E. coli* cells.

2.2.2.9.2 Ligation reaction

The following reaction mixture (Table 2.11) for the Gateway Ligation Reaction was used for shuttling gene of interest from entry vector to destination vector.

Table 2.11: Reaction mix for the Gateway Ligation Reaction using LR Clonase II

Reaction mix:	Per sample:
Entry clone	75 ng
Destination vector	75 ng
TE buffer	Add final mix up to 4 μ L
LR clonase II	0.5 μ L

The mixture was incubated at room temperature for 90 minutes, then 0.5 μ L of Proteinase K was added and the sample was incubated at 37°C for 10 minutes. The entire reaction mix was used to transform chemically competent cells and plated onto LB agar with appropriate selection for the destination vector and grown overnight at 37°C.

2.2.2.9.3 Transformation of *E. coli*

50 μ L of chemically competent *E. coli* DH5 α was thawed on ice and entire reaction mix from BP or LR reaction was added. Cells were then incubated on ice for 10 minutes before heat shocking for exactly 30 seconds in a water bath at 42°C. 950 μ L of SOC mixture was then aseptically added to cell mixture and incubated at 37°C for one hour with shaking at 220 rpm. Serial dilution were plated on LB agar with appropriate selection for transformation vector and incubated at 37°C overnight (for approximately 16 hours).

2.2.2.9.4 Transformation of *S. cerevisiae*

Method adapted from Kawai, Hashimoto and Murata (2010).

Table 2.12: Recipe for Transformation buffer (TB) for *S. cerevisiae* transformation.

Component	Stock concentration	Final concentration
PEG ₃₃₅₀	50%	400 μ L
Lithium Acetate	1 M	200 μ L
β -mercaptoethanol	-	4 μ L

2 μ g of yeast expression vector was mixed with 100 μ L of yeast TB buffer (Table 2.12), to which one 1 μ L loop of yeast was added and mixed. The mixture was incubated at 37°C with 200 rpm shaking for 45 minutes, mounted at a 45° angle before being immediately transferred to an agar plate with appropriate Drop Out selection and incubated at 30°C for 48 hours.

2.2.2.10 Expression and purification of *A. fulgidus myo-inositol-1-phosphate synthase*

Expression vector pET23a:IPS was transformed into commercial Rosetta™ 2 (DE3)pLysS (Novagen) and plated on LB agar with Ampicillin selection at a concentration of 100 μ g/mL overnight at 37°C as per method in section 2.2.2.9.3. Single colonies were inoculated into 10 mL LB broth with antibiotic selection and grown for 16 hours at 37°C 220 rpm shaking.

From this, an expression trial was conducted in which pET23a:IPS Rosetta™ 2 cells were sub-cultured into 100 mL LB media with antibiotic selection and grown at 16°C, 18°C, 24°C, 30°C and 37°C for 18 hours with 0.1 M IPTG induction. Cells were pelleted by centrifugation at 6000 x *g* for 20 minutes and pellets resuspended in 2 volumes of lysis buffer (3.2.1.1.3). Cell slurry was subsequently lysed by three rounds of French Press at 1000psi and cellular debris centrifuged at 20,000 x *g* for 45 minutes. 6 μ L of the

supernatant was loaded onto a hand cast 12% SDS-PAGE at 100V for 60 minutes and stained using InstantBlue™ (Sigma-Aldrich) protein stain for 15 minutes and destained using sterile distilled water for a further hour. Gels were imaged using the Bio-Rad Gel Doc XR+ system with epi white illumination.

2.2.2.11 Purification of *A. fulgidus* myo-inositol-1-phosphate synthase using the ÄKTA Pure system by immobilised metal ion affinity chromatography

pET23a:IPS in commercial Rosetta™ 2 (DE3)pLysS (Novagen) was grown in four 2 litre conical flasks with Ampicillin selection at a concentration of 100 µg/mL for 16 hours at 30°C with 160 rpm shaking and induced with 1 mM IPTG at OD₆₀₀ ≈ 0.7, then grown for a following 4 hours to an OD₆₀₀ of <1.0. Cells were pelleted by centrifugation at 20,000 x G and resuspended in 50mM Tris-HCl lysis buffer (as detailed in 3.2.1.1.3). Cells were lysed by French press at 1000 psi and cleared lysate following centrifugation was syringe-filtered through a 0.45 µm filter to ensure correct viscosity.

The sample was purified using the ÄKTA Pure immobilised metal ion affinity chromatography (IMAC) system using a 1 mL HisTrap HP Affinity IMAC column (GE Healthcare) equilibrated into binding buffer, the sample was applied to the column at a flow rate of 1 mL min⁻¹. The column was washed with binding buffer until stable UV conditions were met, with an acceptable baseline signal of 0.10 mAU. Protein was eluted with a linear elution of 0-100% A:B with a gradient from 10 mM to 500 mM imidazole at a flow rate of 1 mL min⁻¹. Fractions containing protein, monitored at a wavelength of 280 nm, were pooled and concentrated using a Vivaspin™ protein concentrator spin column (GE Healthcare) with 10 kDa cut off of by centrifugation at 6000 rpm to a total volume of 1.5 mL. A 6 µL aliquot of this concentrated protein fraction was checked by SDS PAGE as described in section 2.2.1.1.4

Concentrated protein from the HisTrap purification stage was further purified using the ÄKTA Pure Sepharose gel filtration column (HiLoad 16/600

Superdex 75 PG column) for size-exclusion chromatography equilibrated into 50 mM Tris-HCl pH 7.5, 150 mM NaCl (Section 3.2.1.1.3) and manually loaded from the sample loop. Protein was eluted isocratically with 50 mM Tris-HCl pH 7.5, 150 mM NaCl for 120 minutes at a flow rate of 1 mL min⁻¹, and fractions (2 mL) collected for analysis by SDS PAGE.

2.2.2.12 Glucose and *myo*-inositol measurement

Suppressed ion conductivity HPLC analysis of G6P and inositol monophosphate separations: HPLC was performed using a Dionex™ ICS-2000 Ion Conductivity System (Dionex, 2006). Samples injected were separated by ion exchange on a 2 x 250 mm Thermo Scientific™ Dionex™ IonPac™ AS18 IC column eluted isocratically with 27 mM potassium hydroxide at a flow rate of 0.5 mL min⁻¹. Anions were detected by suppressed conductivity measurement.

HPLC-pulsed amperometry for the separation of glucose and inositol: Glucose, *myo*-inositol and other sugars from chemoenzymatic synthesis assays were analysed following 100-fold dilutions in 18.2 megaohm water by HPLC-pulsed amperometry on an Antec Carbohydrate Analyser fitted with a 3 mm gold HyRef electrode. Separation of saccharides from inositol was achieved by 2-D HPLC on a 4 mm x 50 mm CarboPac PA1 column (Dionex™) in series with a 4 mm x 250 mm CarboPac MA1 column eluted isocratically with 150 mM sodium hydroxide as described in Lee *et al.* (Lee *et al.*, 2018; Greene *et al.*, 2019).

2.2.2.13 Yeast crude total protein extraction

The method used was adapted from (Kushnirov and Kushnirov, 2000). Buffers were made to a total volume of 1 mL.

A single colony of yeast was selected and grown overnight in 10 mL of Drop Out media with appropriate selection at 30°C with 220 rpm shaking until OD₆₀₀ > 0.4 is reached. The culture was then pelleted at 3000 x g for 20

minutes, the resulting pellet resuspended in chilled water by inversion and centrifugation repeated a further two times before freezing in liquid nitrogen for storage at -80°C.

Table 2.13: Components of extraction buffer A for yeast crude total protein extraction

Component	Stock concentration	Final concentration
NaOH	0.2 M	0.1 M
EDTA	0.5 M	50 mM
SDS	10%	1%
β-mercaptoethanol	-	2%
Water	-	-

Table 2.14: Components of extraction buffer B for yeast crude total protein extraction

Component	Stock concentration	Final concentration
Tris pH 6.8	1 M	250 mM
Glycerol	-	50%
Bromophenol blue	1%	0.05%
Water	-	-

Pelleted yeast cells were resuspended in 50 µL of Buffer A and heated at 90°C for 10 minutes. To this, 0.67 µL of 3 M acetic acid was added and mixed by vortex for 30 seconds before heating again at 90°C for a further 10 minutes. Following heating, 12.5 µL of buffer B was added and mixed by vortex for 2 seconds before centrifuging at 12,000 x g for 5 minutes. Supernatant was transferred to a new tube on ice and boiled at 98°C for 1 minute before storing at -20°C or proceeding to SDS PAGE analysis.

2.2.2.14 Final optimised method for the production of *myo*-inositol from glucose

The enzymes required for the production of *myo*-inositol from glucose are as follows: Hexokinase (from *S. cerevisiae*, Invitrogen), IPS (cloned from *A. fulgidus*) and alkaline phosphatase (Calf intestinal mucosa, Rockland Inc.), with Creatine Kinase (from rabbit, lyophilised, Invitrogen; enzyme should be made up fresh in 0.5 M diglycine buffer for use) for the regeneration of ATP. ATP is the limiting factor in the reaction, and use of a coupled ATP regeneration system allows for use of lower cost substrate (phosphocreatine) to maintain ATP levels for the forward reaction.

For the initial step of the reaction, mixture comprises of: 10 mM glucose, 1.5 mM ATP, 10 mM phosphocreatine, 5 mM MgCl₂, 1 unit Hexokinase, 15 units Creatine Kinase, made up in 50 mM Tris-Acetate buffer at pH 7.5. This mixture is incubated at 30°C for 4 hours.

Following incubation, to the mixture from the previous step add: 5 mM Zinc sulphate, 1 mM NAD⁺, 20 µg IPS (purified). Concentrations given are final concentrations in the mixture. Incubate mix at 80°C for a further 4 hours. Heating at 80°C denatures the hexokinase from the previous step. Following this stage, the mixture can be stored at -20°C, or proceed to the next step.

For the final alkaline phosphatase step, dilute the reaction mixture 1:1 with 50 mM Tris-Acetate buffer pH 9.5 and add 5 units of alkaline phosphatase (Rockland Inc.). Incubate the reaction at 37°C for 2 hours.

Freeze-thawing the final mixture precipitates out protein added in previous steps, which can be removed by centrifuging at 15,000 x *g* for 5 minutes, but this is not essential. Take 1 µL aliquot of the mixture after final phosphatase reaction and dilute for HPLC analysis.

2.2.2.15 Isotope Ratio Mass Spectrometry measurement of $\delta^{13}\text{C}_6$ -*myo*-inositol in poultry tissues and digesta

Enzymatically synthesized $\delta^{13}\text{C}_6$ -*myo*-inositol was added to poultry diets in the trial described in Chapter 4.2 to a final total supplemented inositol concentration of 2 g/kg inositol. Inositol was premixed at UEA to a final concentration of d30‰ $^{13}\text{C}_6$ -*myo*-inositol into 500 g *myo*-inositol (Sigma) before being added to diets at the Nottingham Trent University trial facility.

For analysis following the animal feeding trial, 0.5 mg samples of freeze dried and milled gizzard and ileal digesta, and 0.5 mg of freeze dried tissue samples, were analysed for ratio of $\delta^{13}\text{C}$ to ^{12}C using a Thermo Finnigan Delta plus XP IRMS connected via a Conflo IV to Flash HT for bulk analysis $\delta^{13}\text{C}$ by Dr. Sarah Wexler at the Stable Isotope Analysis Platform (Stable Isotope Laboratory, School of Environmental Sciences, University of East Anglia).

2.3 Results

2.3.1 Cloning and expression of *myo*-inositol phosphate synthase proteins

The initial research aim was to produce a traceable form of inositol for use in feed trials, by reproducing the biochemical synthesis pathway of inositol from glucose *in vitro*.

The biosynthetic pathway for the production of *myo*-inositol from glucose is formed of three basic steps – the conversion of glucose to G6P, the conversion of G6P to *myo*-inositol-1-phosphate, and the dephosphorylation of *myo*-inositol-1-phosphate to *myo*-inositol. 3 enzymes catalyse these 3 steps: a hexokinase, a *myo*-inositol phosphate synthase, and a *myo*-inositol-1-monophosphatase (Loewus and Loewus, 1983). As the rate-limiting step of this biosynthesis pathway is the conversion of G6P to *myo*-inositol-1-phosphate, the initial focus for synthesizing this biosynthetic pathway was selecting a suitable *myo*-inositol phosphate synthase. A literature search provided candidate genes for *myo*-inositol phosphate synthase enzymes from *Arabidopsis thaliana* and *Saccharomyces cerevisiae* to be cloned and expressed. Table 2.15 shows the *myo*-inositol phosphate synthase genes initially selected for cloning and expression.

Table 2.15: *Myo*-inositol phosphate synthase genes selected for cloning and transformation ^a

Gene	Gene code	Length (kb)	Location	Protein length (aa)	Protein size (kDa)
AtMIPS1	AT4G39800	2794	Chromosome 4	511	56.5
AtMIPS2	AT2G22240	2696	Chromosome 2	510	56.3
ScINO1	YJL153C	1602	Chromosome X	533	59.6
AfINO1	AF_1794	1176		392	43.7

^a Gene information accessed from UniProtKB accessions P42801, Q38862, P11986 and O28480 respectively

Table 2.16: Michaelis-Menten constants of selected *myo*-inositol phosphate synthases for D-G6P^b

Gene	Origin	K _m (D-G6P)	Specific activity
AtMIPS1 ^c	<i>A. thaliana</i>	0.68mM	9.4±0.9 mM ⁻¹ min ⁻¹ (at 30°C)
AtMIPS2 ^c	<i>A. thaliana</i>	0.45mM	8.8±0.9 mM ⁻¹ min ⁻¹ (at 30°C)
ScINO1 ^{d, e}	<i>S. cerevisiae</i>	1.18mM	3.1 μmol min ⁻¹ mg ⁻¹ (at 55°C)
AfINO1 ^d	<i>A. fulgidus</i>	0.12mM	11.8 μmol min ⁻¹ mg ⁻¹ (at 90°C)

^b Gene information accessed from UniProtKB accessions P42801, Q38862, P11986 and O28480 respectively

^c Enzyme catalytic efficiency data accessed from Donahue *et al.* (2010) for *A. thaliana* MIPS enzymes

^d Enzyme catalytic efficiency data accessed from Chen *et al.* (2000) for *A. fulgidus* IPS enzyme and ScINO1

^e Enzyme catalytic efficiency data accessed from Majumder *et al.* (Majumder, Johnson and Henry, 1997)

The above named genes were selected on consideration of a relatively high specific activity, size of the enzyme and requirement for particular buffer components for catalytic activity (Table 2.16). Our intention to couple the MIPS enzyme to hexokinase demands that MIPS is more active in the couple than hexokinase. Moreover, the need to clone and express these enzymes in a system for rapid production, such as in *E. coli* or *S. cerevisiae* with a short life span, requires relatively small enzymes for ease of cloning and transformation.

Eukaryotic MIPS enzymes were the primary selection due to ease of using *S. cerevisiae* as model organism for producing the eukaryotic MIPS in laboratory conditions. The *Arabidopsis thaliana myo*-inositol phosphate synthases both have highest activity at 30°C at pH 7.5, ideal for reproducibility in the lab. These genes were cloned from a cDNA library produced from RNA extracted from *Arabidopsis thaliana* Columbia-0 background, with previous research showing that AtMIPS1 had highest expression in cauline leaf and vascular tissues, and AtMIPS2 highest

expression in seeds and seedlings (Schmid *et al.*, 2005; Winter *et al.*, 2007). Reflected additionally in the difference in V_{max} in Table 2, Donahue *et al.* (2010) found AtMIPS1 to have a larger role in the turnover of G6P to *myo*-inositol than MIPS2 and MIPS3. Whilst a great amount of research has been carried out characterizing the *A. thaliana myo*-inositol phosphate synthases, no crystal structure of these enzymes has been published to date.

Similarly, research has also historically utilized and characterized the ortholog in *Saccharomyces cerevisiae*, INO1 (Greenberg and Lopes, 1996; Carman and Henry, 1999; Henry, Kohlwein and Carman, 2012). The gene length of the *S. cerevisiae myo*-inositol phosphate synthase is considerably shorter than its higher eukaryotic equivalents, facilitating its use in the Gateway cloning system with greater success than the longer Arabidopsis MIPS. The highest activity of ScINO1 is also at 30°C, easily achievable in lab conditions both *in vivo* and *in vitro*, at pH 5.5.

Though the yeast INO1 is reported to be most highly expressed when grown in inositol-deficient media, cDNA was prepared from yeast grown in a standard complete synthetic media.

The final inositol phosphate synthase, from the hyper-thermophile *Archaeoglobus fulgidus* (Klenk *et al.*, 1997). was gifted in plasmid from Adolfo Saiardi (University College London), The enzyme is active at 90°C at a neutral pH, with specific activity recorded of 11.8 $\mu\text{mol min mg}^{-1}$ (Chen *et al.*, 2000), and has the highest reported specific activity of a MIPS enzyme to date.

Figure 2.2 shows the successful cloning PCR of ScINO1 and AtMIPS1 with 5' CACC for Gateway cloning using Phusion High Fidelity DNA polymerase and touchdown PCR conditions. ScINO1 length is 1602 bp, coding sequence length for AtMIPS1 is 2095 bp. Bands were excised from gel using a scalpel and extracted using Qiagen Gel Extraction kit (QIAGEN, 2001).

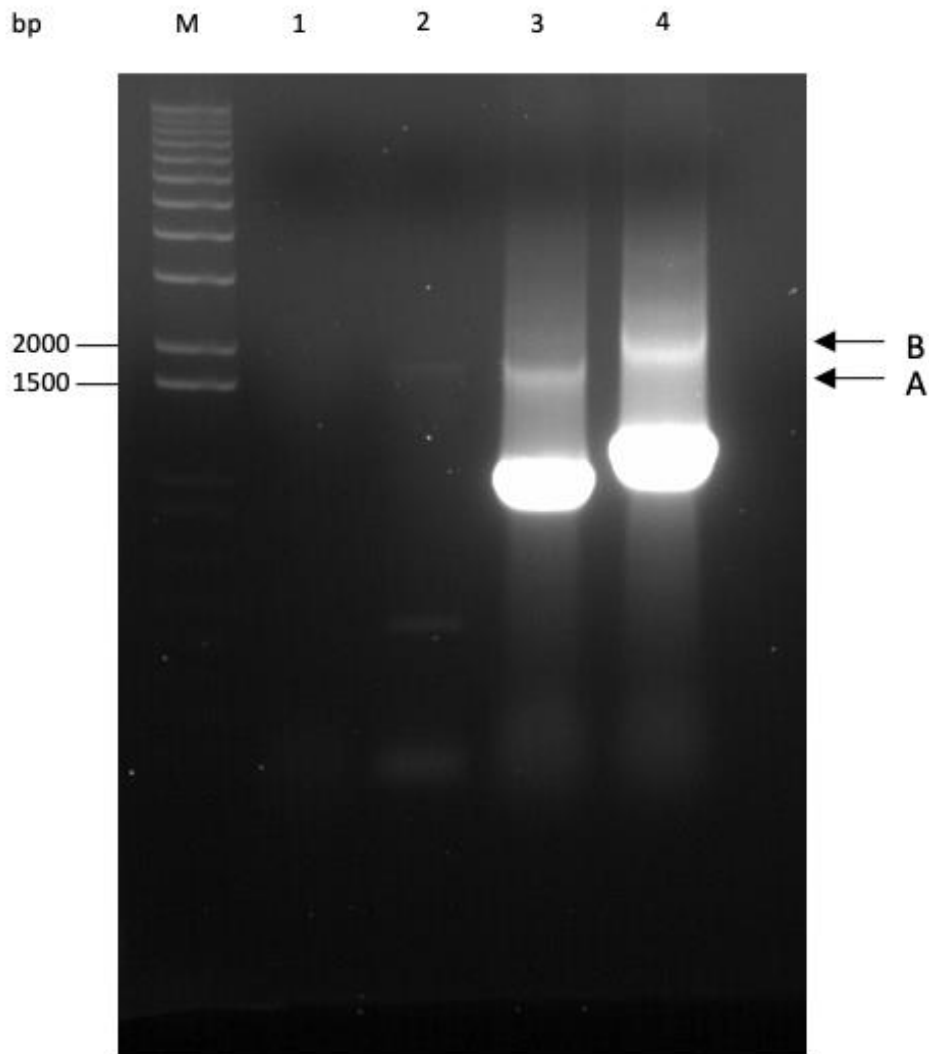


Figure 2.2: Agarose gel electrophoresis (1% agarose, TAE) from Touchdown PCR of ScINO1 (Lane 3, A) and AtMIPS1 (Lane 4, B). Lane M denotes 1kb+ ladder DNA marker. Lane 1 was a PCR of AtMIPS1 which did not amplify from template. Lane 2 a PCR of ScINO1 which did not sufficiently amplify from template.

Figure 2.3 shows the band for successful PCR of AtMIPS2 from *A. thaliana* cold shock cDNA library using touchdown PCR conditions with Phusion High Fidelity DNA polymerase, with addition of 5' CACC for Gateway cloning. The coding sequence length for AtMIPS2 is 1533bp. The band was excised from the gel and DNA extracted using Qiagen Gel Extraction Kit (QIAGEN, 2001).

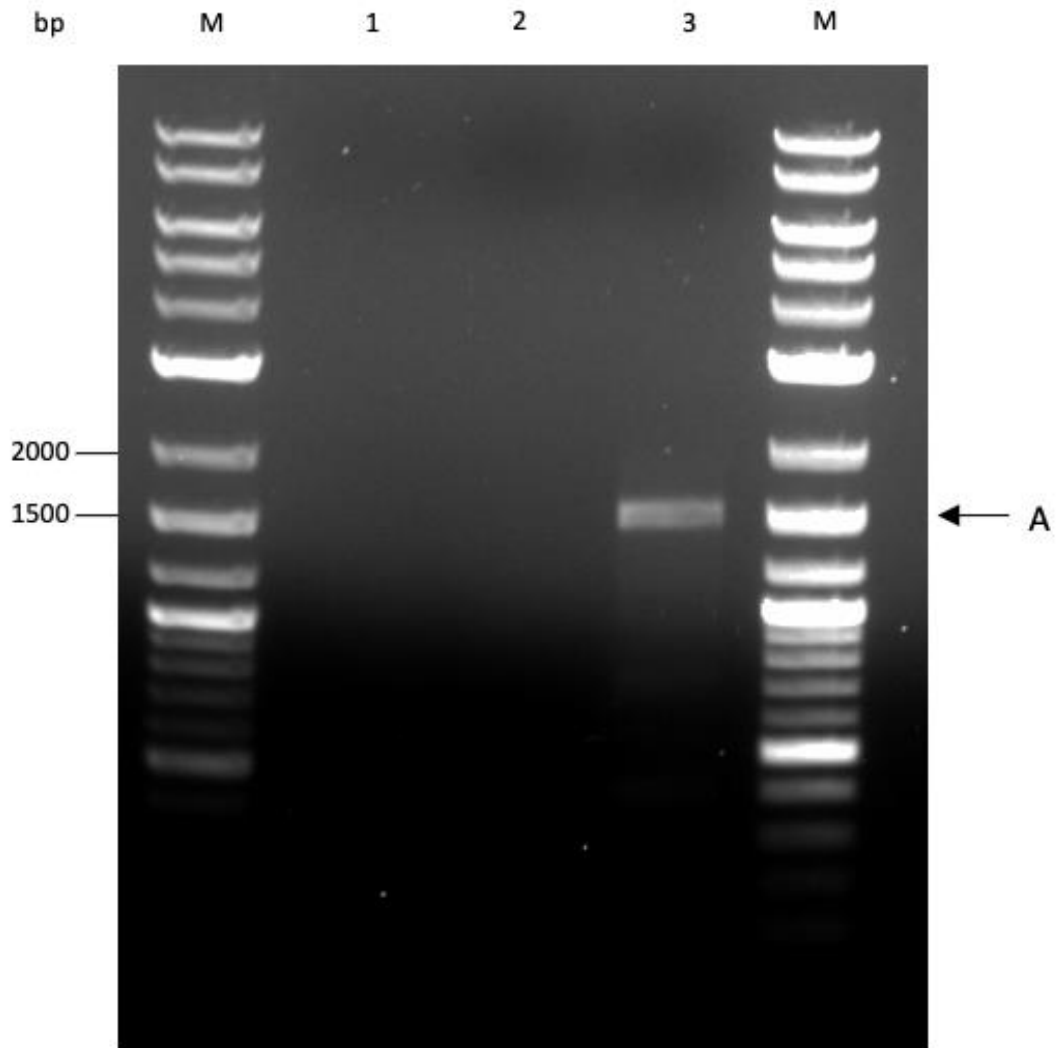


Figure 2.3: Agarose gel electrophoresis (1% agarose, TAE) of AtMIPS2 gene cloned using touchdown PCR, where A marks AtMIPS2 (lane 3). M denotes 1kb+ ladder DNA marker. Lanes 1 and 2 were additional PCR reactions for AtMIPS2 which failed to amplify.

Arabidopsis thaliana MIPS1 and MIPS2 were cloned out of *Arabidopsis* cDNA libraries produced in stress conditions to improve mRNA expression prior to RNA extraction of these genes, however these genes proved difficult in transforming into bacterial entry vectors. This may have been due to the size of the genes, with their size being over half the size of the bacterial entry vector which may have resulted in the gene being cleaved from the vector; this would allow for positive colonies to grow on selection plates that later

yielded negative colony PCR results. In addition, this may have been due to the nature of the genes being expressed: as the *myo*-inositol phosphate synthase genes are important regulatory genes, also linked to stress responses, increasing the production of these proteins and therefore increasing inositol and phosphate turnover in the cell by expressing them with a constitutive promoter in a vector may be lethal to the cells involved.

Instead, Gateway constructs were prepared for expression of yeast MIPS (Ino1) in yeast using the pDONR207 Entry Vector. Figure 2.4 shows the successful bands showing full length coding sequence insertion (lane marked F+R for priming with Gene Forward and Gene Reverse primers) as well as insertion into the vector, primed using cloning vectors T7 Forward primer and the reverse primer for the ScINO1 gene (lane marked T7+R).

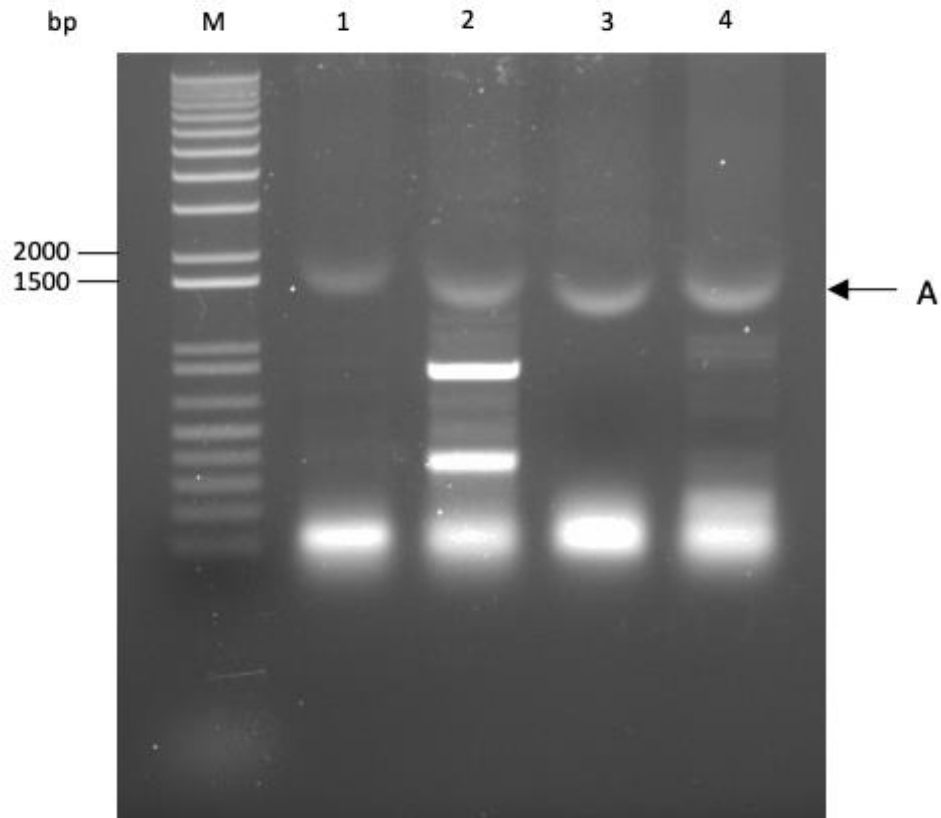


Figure 2.4: Agarose gel electrophoresis (1% agarose, TAE) of PCR products resulting from Colony PCR of ScINO1 in pDONR207 Gateway Entry Vector, where A denotes size of tagged ScINO1 (Lanes 1 to 4) and M denotes 1kb+ DNA ladder.

Colonies were picked at random from a selection plate and resuspended in 20 μ L of sterile distilled water, 1 μ L of this suspension was used as the template for PCR. Colonies that showed a successful PCR for gene insertion were inoculated into 10 mL LB liquid media with gentamicin and grown overnight for vector to be purified using Qiagen Mini Prep kit (Quaigen, 2015).

The *S. cerevisiae* INO1 gene was cloned out of the yeast cDNA library produced and transformed into a Gateway entry vector and a bacterial destination vector later found to be unsuitable for downstream purification using the ÄKTA Pure system. As such, a C terminal 6xHIS tag was added by PCR cloning to the ScINO1 fragment (method listed in section 2.2.2.6), and

this was cloned using the Gateway cloning system into the p-ENTR-D-TOPO entry vector, and ligated from this to the yeast expression vector construct pAG413-GPD-cHA gifted from Dr. Mark Bailey (University of Birmingham), as shown in figure 2.5.

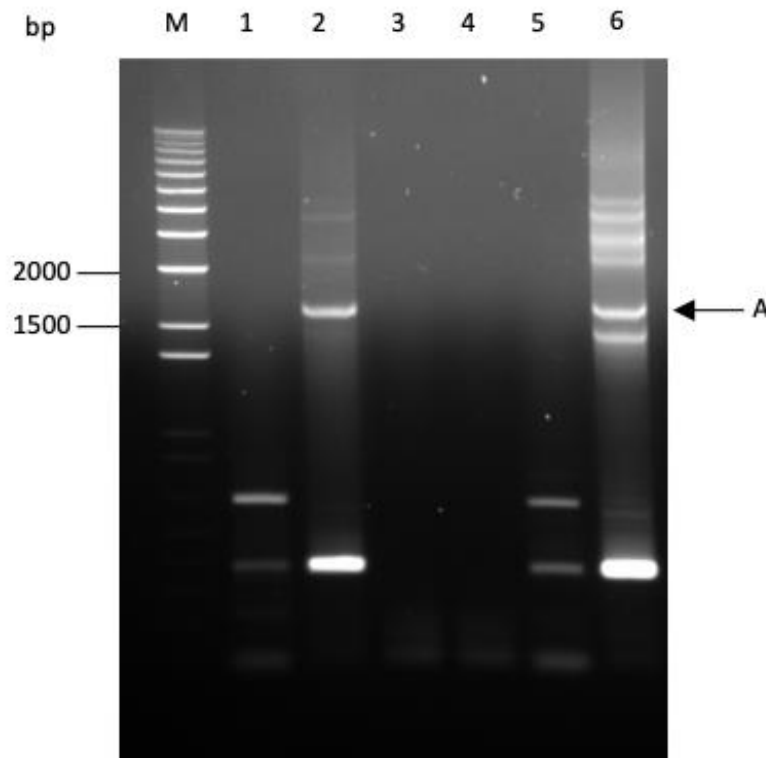


Figure 2.5: Agarose gel electrophoresis (1% TAE agarose) of PCR products of colony PCR conditions for c-terminal 6xHIS tagged ScINO1 (band size denoted **A**), where lanes 1-6 are PCR amplified reaction products. Lane M, 1kb+ ladder.

The resulting construct from the Gateway ligation reaction, ScINO1 pAG413-GPD-cHA, was transformed into NCYC3466 wild type *S. cerevisiae* using the method adapted from Kawai, Hashimoto and Murata (2010) (Method detailed in section 2.2.2.9.4. Transformed yeast were induced and grown overnight for preliminary analysis of protein expression. Crude protein was extracted from cultures using the method described in section 2.2.2.13 adapted from Kushnirov and Kushnirov (2000). The results of typical expression trials are

shown in Figure 2.6 (detection with InVision HIS tag stain) and Figure 2.7 (stained for total protein with Instant Blue).

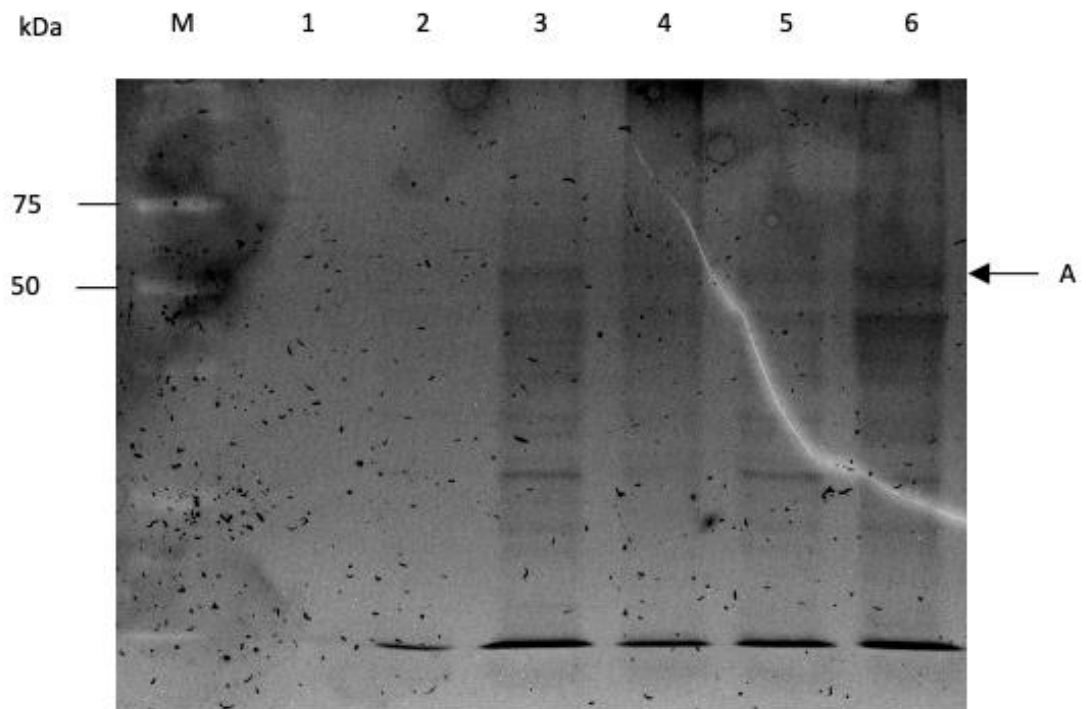


Figure 2.6: SDS PAGE analysis of crude total protein extraction of the ScINO1 overexpression line of *S. cerevisiae* NCYC3466 stained using InVision HIS-tag in-gel stain. The band corresponding to the approximate size of INO1 with 6xHIS tag is marked A. Lanes 1 to 6 are biological replicate samples of ScINO1 carrying *S. cerevisiae* NCYC3466 cultures.

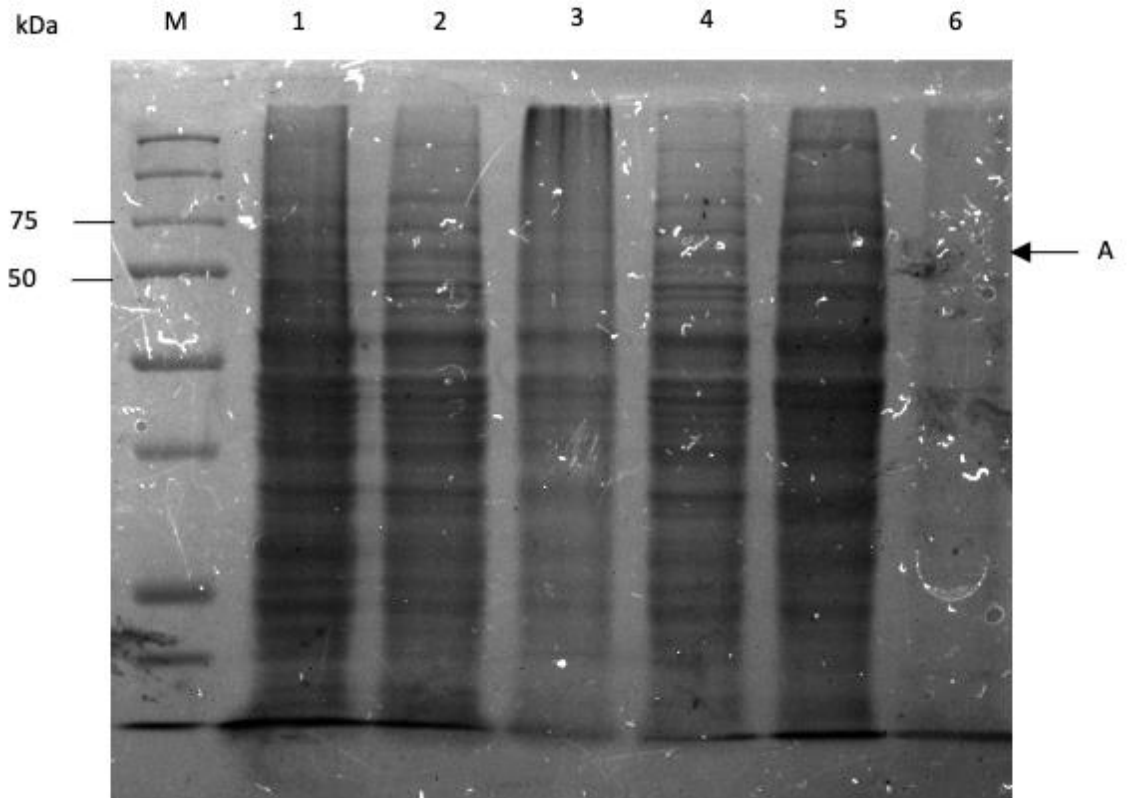


Figure 2.7: SDS PAGE analysis of crude total protein extraction of the ScINO1 overexpression line of *S. cerevisiae* NCYC3466 stained using Instant Blue total protein stain. The band corresponding to the approximate size of INO1 with 6xHIS tag is marked A. Lanes 1 to 6 are extracts from biological replicates of ScINO1 vector *S. cerevisiae* NCYC3466 cultures.

The band of approximately 61 kDa corresponds to the predicted size of ScINO1 with the addition of a 6XHIS tag at the C terminal of the protein. Further purification from cultures expressing the ScINO1 pAG413-GPD-cHA construct with purification by hand through a 1 mL HisTrap HP Affinity IMAC column (GE Healthcare) was not wholly successful, with multiple bands evident on the gel (Figure 2.8).

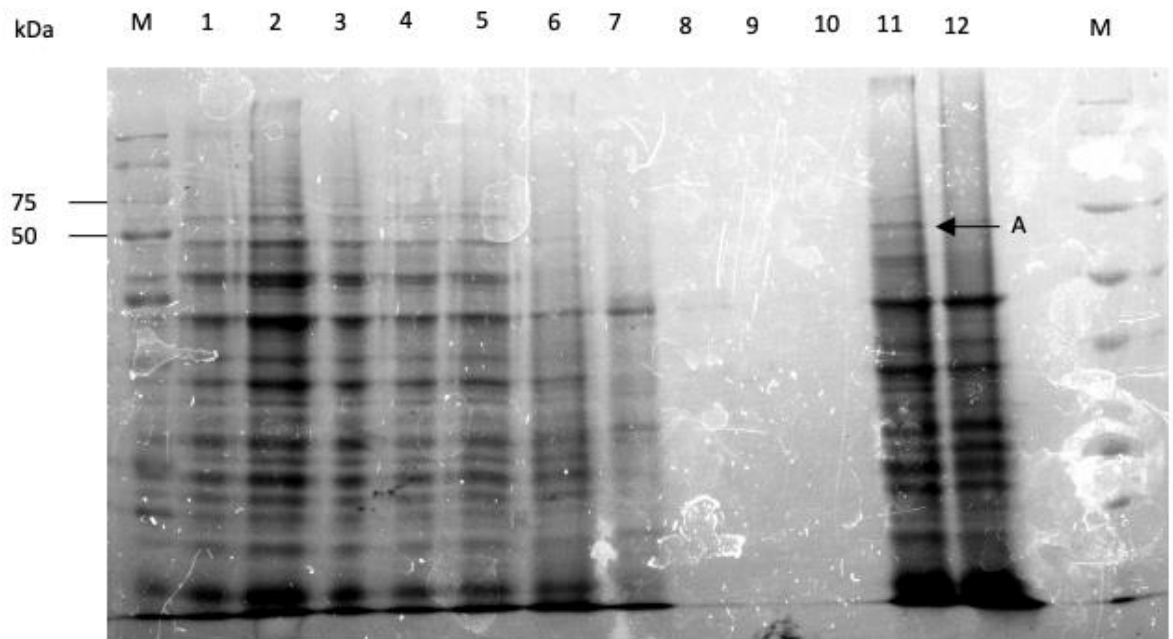


Figure 2.8: SDS PAGE analysis of cleared cell lysate and protein following manual purification using HisTrap HP Affinity IMAC column for enrichment of HIS tagged proteins. Lanes marked M correspond with Precision Plus Protein Standards, where lanes 1 to 5 are successive 1 mL load fractions, lanes 6 to 10 are successive 1 mL elution fractions, lane 11 is cleared cell lysate and lane 12 is cell pellet. Band corresponding to ScINO1 is marked A.

The lack of success in yeast prompted reappraisal of strategy, both of the expression host and the encoded transformation sequence. At this stage of the experimentation the Fiedler group reported successful expression of archaeal enzyme in a bacterial expression system (Harmel *et al.*, 2019). A construct encoding IPS from *A. fulgidus* in pET23a was subsequently obtained from Adolfo Saiardi (UCL) .

2.3.2 Purification of IPS

pET23a:IPS was transformed into commercial Rosetta™ 2 (DE3)pLysS (Novagen) *E. coli* cells. Protein expression trials were conducted at UEA (Fig. 2.9), comparing the relative protein expression of IPS in *E. coli* grown at 18°C, 24°C, 30°C and 37°C. Cultures were OD adjusted to lowest OD equivalent and total protein was analysed by SDS PAGE gel for expression (Figure 2.9).

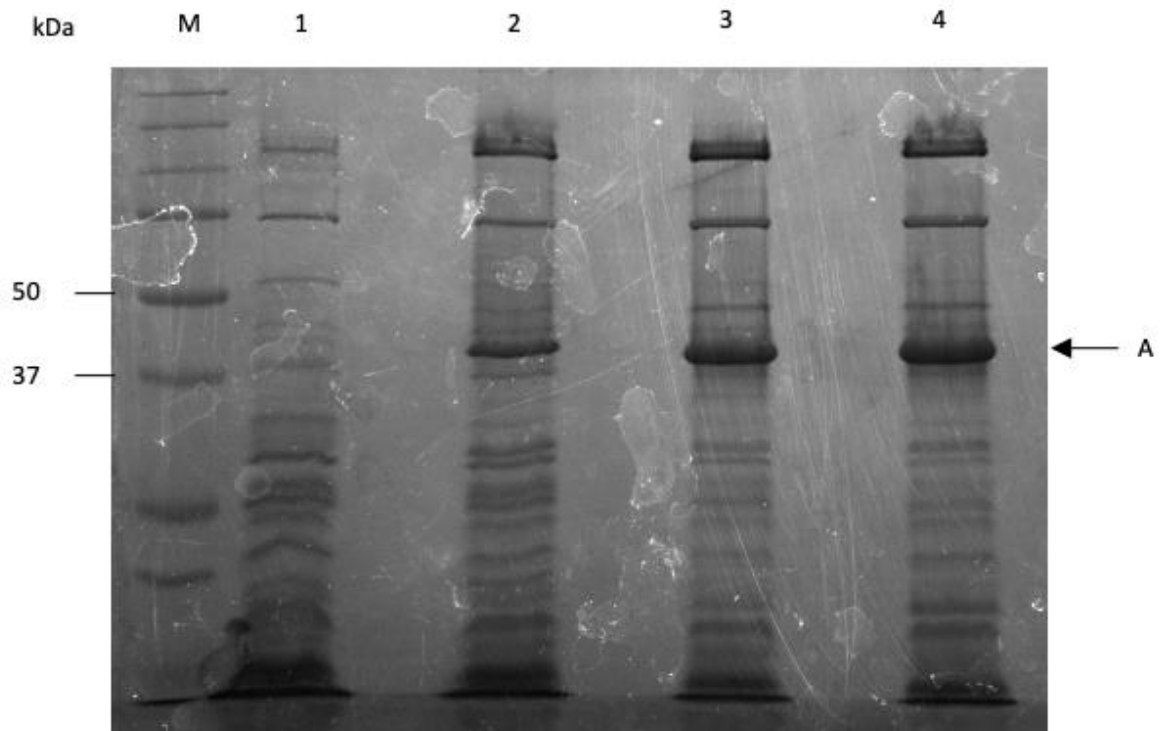


Figure 2.9: SDS PAGE gel electrophoresis of total expressed protein from expression trials of pET23a:IPS in Rosetta™ 2 (DE3)pLysS, where lane 1 to 4 are samples of *E. coli* grown at 18°C (lane 1), 24°C (lane 2), 30°C (lane 3) and 37°C (lane 4) respectively, and lane M is Precision Plus Protein Standard. Arrow marked A denotes approximate size of *A. fulgidus* IPS protein.

Following expression trials, pET23a: IPS was expressed in commercial Rosetta™ 2 (DE3)pLysS (Novagen). Cells were, grown at 30°C with 160 rpm shaking for 18 hours, induced with 0.1 M IPTG for 4 hours in four 1 litre flasks of LB medium with ampicillin and chloramphenicol selection. At OD₆₀₀

of ≈ 1.0 , cultures were centrifuged, the cells resuspended in lysis buffer and lysed by French press. The cleared cell lysate was purified using the ÄKTA Pure system (methods detailed in section 2.2.2.11). The following figures (Fig 2.10 & 2.13) show UV traces for the purification of IPS from Rosetta 2.

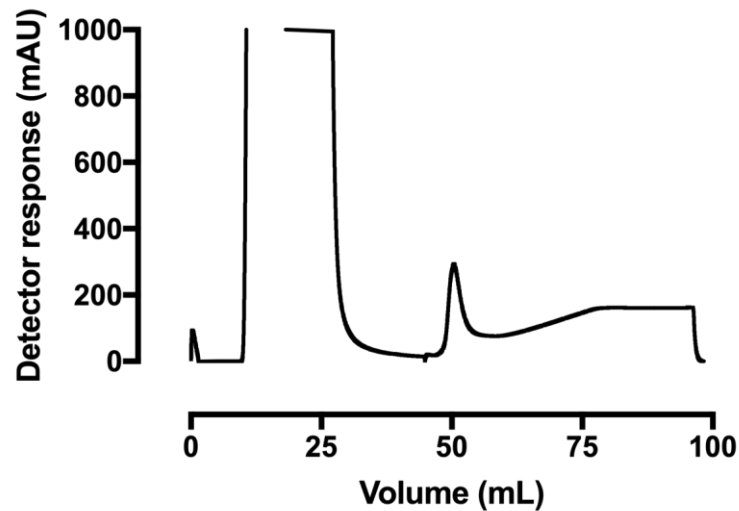


Figure 2.10: UV trace from ÄKTA Pure system of IMAC HiTrap purification of IPS. Thirty six mL of a cell lysate of pET23a:IPS expressing Rosetta™ 2 (DE3)pLysS was obtained from four litres of culture and loaded onto the column.

Protein fractions collected from IMAC purification were analysed by SDS PAGE (Fig 2.11, 2.12)

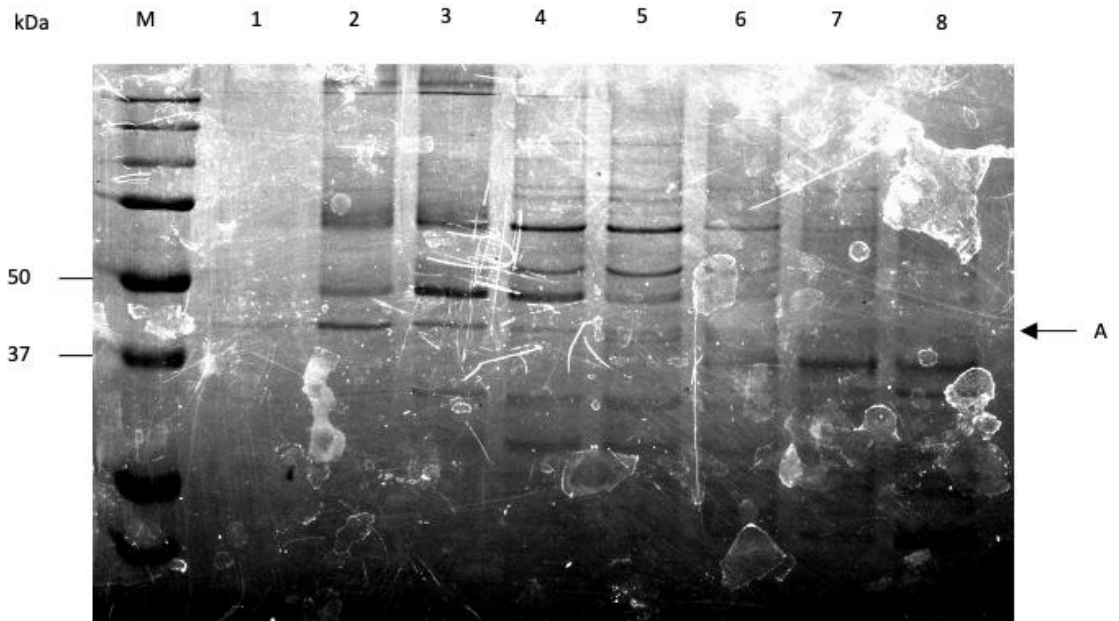


Figure 2.11: SDS PAGE of 50 μ L samples from unconcentrated sequentially eluted 2 mL fractions (lanes 1-8) from ÄKTA Pure purification of IPS protein following IMAC purification. Lane M is Precision Plus Protein Standards. Band corresponding to AfIPS is marked A.

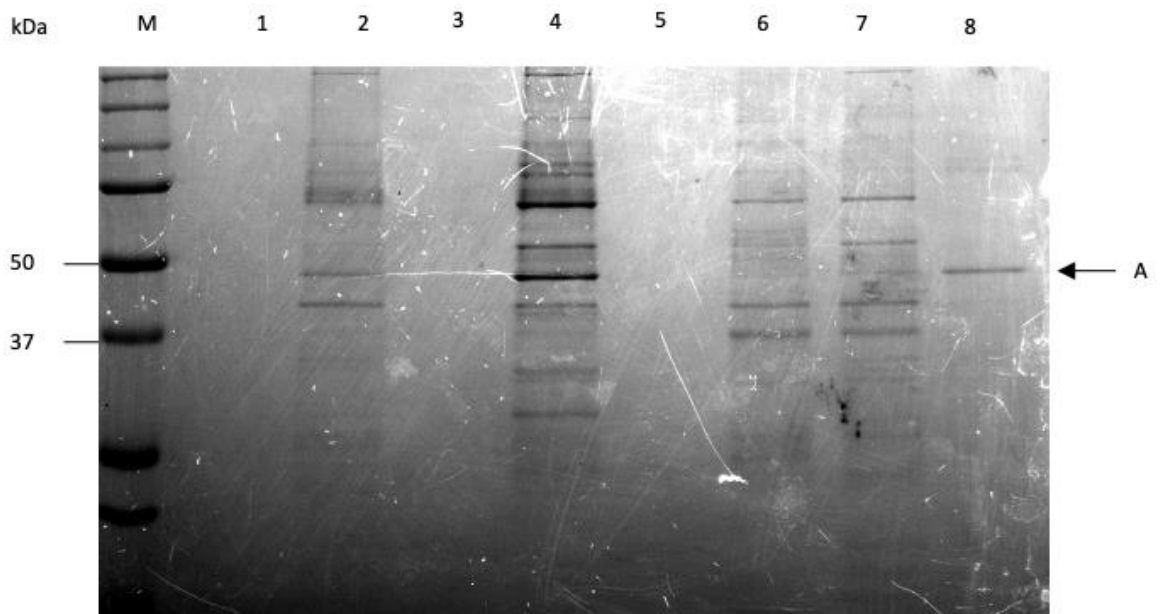


Figure 2.12: SDS PAGE of 5 μ L loads of concentrated IPS fractions prior to Sepharose gel filtration for purity (Lanes 1 to 8 represent concentrated aliquots from sequential fractions eluted and analysed as lanes 1 to 8 in fig 2.11). Lane M is Precision Plus Protein Standards. Band corresponding to AfIPS is marked A.

Samples from the gel fractions labelled in Figure 10 were pooled and concentrated using a 10 kDa cut-off Vivaspin™ protein concentrator spin column (GE Healthcare) before loading onto a HiLoad 16/600 Superdex 75 PG column for further purification of IPS by size-exclusion chromatography from contaminating proteins in the IMAC eluate. The results are shown in Figure 2.13.

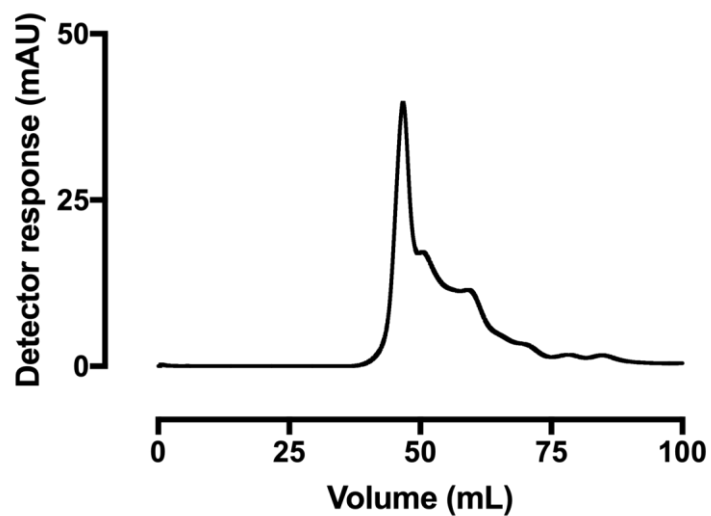


Figure 2.13: Size exclusion chromatography (Gel filtration) of IMAC purified IPS fractions.

Peaks corresponding with UV absorbing fractions shown in the gel filtration chromatogram from this purification were analysed by SDS PAGE for the presence of a band corresponding to the expected size of IPS protein (Figure 2.14).

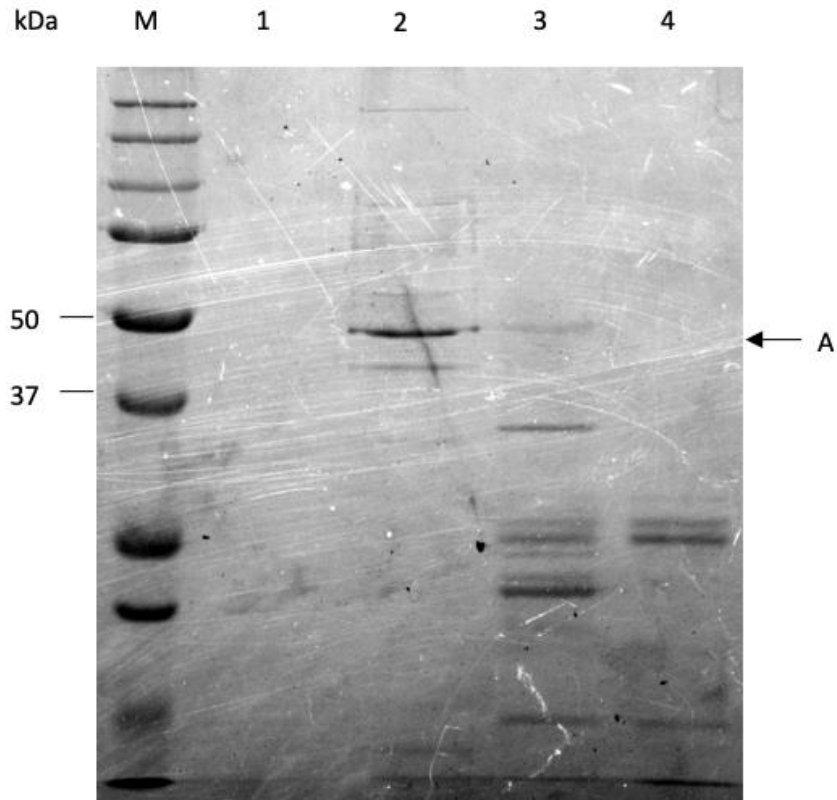


Figure 2.14: SDS PAGE of Sepharose purified IPS protein, where lanes 1 to 4 denote sequential elution fractions from Sepharose gel filtration purification of protein fractions. Lane M is Precision Plus Protein Standards. Band corresponding to AfIPS is marked A.

Finally, IPS protein purified using the ÄKTA pure system was concentrated using a Vivaspin™ protein concentrator spin column (GE Healthcare) to a final concentration of 0.46 mg/mL in a total volume of 1.2 mL as determined by nanodrop (NanoDrop 2000c, Thermo Scientific) and stored as 50 μ L aliquots at -20°C for use future use in chemoenzymatic assays.

2.3.3 Function and activity of *Archaeoglobus fulgidus* IPS

Previous studies have shown the optimal activity of the *A. fulgidus* inositol phosphate synthase, hereby known as IPS, is within the range of 65-95°C, reflecting its hyperthermophile origins (Chen *et al.*, 2000; Fujisawa, Fujinaga and Atomi, 2017). Following purification of IPS from its bacterial expression host, the next logical step was to determine suitable reaction conditions to

verify catalytic activity of the purified protein. IPS catalyses conversion of G6P (hereafter G6P) to 1L-*myo*-inositol-1-phosphate, known also as 1D-*myo*-inositol 3-phosphate (Figure 2.15). Relaxation of IUPAC rules for numbering of carbons in *myo*-inositol, only, among inositol isomers (Biochem J., 1989), allows the use of the D-nomenclature for numbering of carbons. This convention has universally been accepted for description of inositol phosphates in biological systems where, with very few exceptions, *myo*-inositol and its phosphorylated derivatives prevail (Thomas et al., 2016).

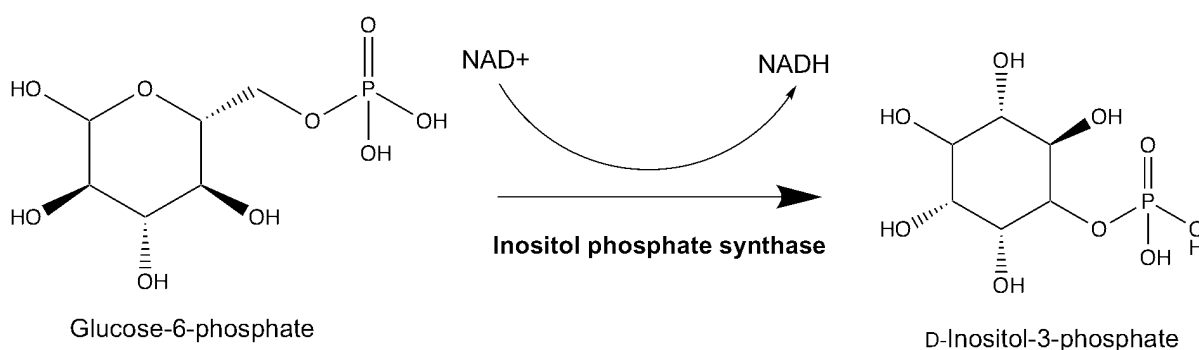


Figure 2.15: Scheme for the isomerization reaction for the conversion of G6P to inositol monophosphate by inositol phosphate synthase (IPS), requiring NAD⁺ as a co-factor. Figure produced using ChemDraw (v. 20.1), substrate and product are shown in ring form.

Previous research has shown that IPS is a Class II aldolase dependent on the presence of a divalent metal ion such as Zn²⁺ or Mn²⁺ for activity, and relatively unaffected by the presence of ammonium cations, in contrast to most inositol phosphate synthase enzymes (Chen *et al.*, 2000; Neelon *et al.*, 2005). As such, assay conditions to this effect utilised the optimum temperature range of the enzyme and its previously reported high activity in the presence of zinc cations, and the assay conditions were as follows: total concentration of 5 mM glucose-6-phosphate, 1 mM NAD⁺, 1 mM ZnSO₄, 20 µg IPS enzyme in 1 mL of 50 mM Tris-AC buffer pH 7.5

The reaction to establish functional activity of IPS was carried out at 85°C for 4 hours, with 200 µL of the reaction sampled every hour and stored at -20°C for later analysis. The assay products were analysed by HPLC using the

Dionex™ ICS-2000 Ion Conductivity System using suppressed ion conductivity detection, as described in section 2.2.2.12 (Dionex, 2006).

Initial experiments were conducted to find conditions for separation of substrate, G6P, and product (1L-Ins1P, 1D-Ins3P, hereafter Ins3P). The AS18 IC column was chosen as it is commonly used to separate anions such as chloride, sulphate, nitrate and phosphate (Thermo Fisher Application Note 154, (Borba and Rohrer, 2016)). It was postulated that G6P and Ins3P would differ in retention time by virtue of the different pKa's of sugar and cyclitol hydroxyls, and that by virtue of the esterified phosphate would elute before non-esterified inorganic phosphate. The suppressed-ion conductivity method also allows collection of separated ions in water, the eluate from the suppression module of the chromatograph when used in 'external water' mode. Here, the machine was used in standard 'eluent recycle' mode. Standards (50 μ M) of G6P (Sigma) and Ins3P (Cayman, CAY10007778, sodium salt) were initially run as control samples alongside diluted assay samples to determine the positions of elution of substrate, product and potentially interfering buffer components: the buffer components are present at 5-fold higher concentration than the G6P substrate.

The results (Figure 2.16) shows the comparison of the 50 μ M standards of G6P and Ins3P (Figure 2.16 A and B respectively) alongside a 1 in 10 diluted sample of the IPS assay following 4 hour incubation at 85°C of 20 μ g IPS with 5 mM G6P (Figure 2.16C).

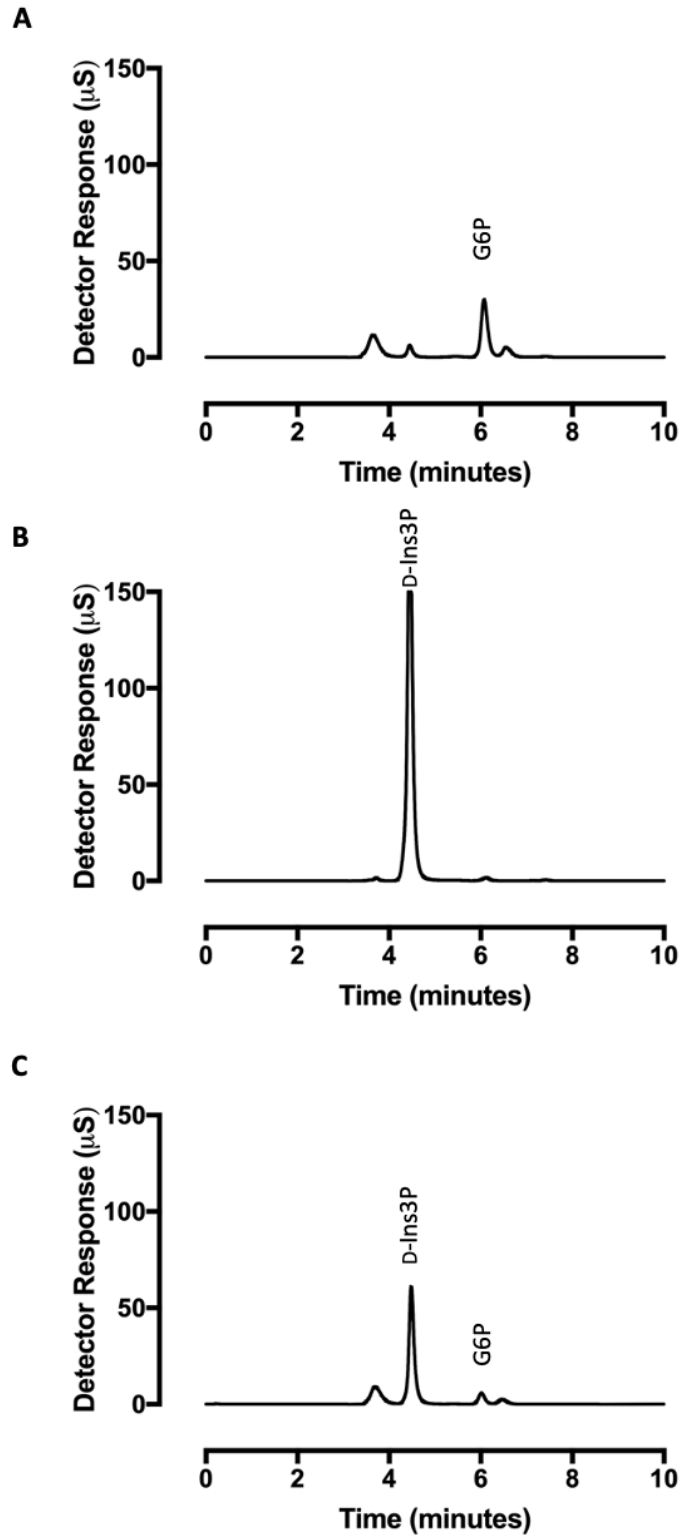


Figure 2.16: Separations of G6P and Ins3P by Ion Exchange Chromatography where **A** 50 μM G6P; **B** 50 μM D-Inositol-3-phosphate and **C** 1 in 10 dilution of 4 hour sample of IPS assay for conversion of G6P to inositol monophosphate.

Clearly, isocratic elution of the AS18 HC column with 27 mM KOH, is sufficient to resolve Ins3P and G6P, with retention times of 4.1 minutes and 6 minutes, respectively. Comparison of the traces, Figure 2.16A & B with Figure 2.16C, further reveal that the assay was successful, evidenced by the presence of a peak co-eluting with the Ins3P standard concomitant with a reduction in peak co-eluting with the G6P standard. Integrations of the peak areas of the assay dilution sample and the standards suggests that approximately 80% of the starting G6P has been converted to Ins3P by the 4 hour time point of the assay. The chromatographic method also separates the substrate and product from other buffer components. Previously published literature utilising a similar method reported a 50% yield at gram-scale, with purification and yield assessed by NMR (Harmel *et al.*, 2019), following enzymatic methods devised for synthesis of ^{13}C *myo*-inositol (Saiardi *et al.*, 2014).

2.3.4 Enzyme coupled assays

2.3.4.1 Experiments using commercial hexokinase for conversion of glucose to G6P

Due to the scale demanded of *in vivo* experiments for which this chemo-enzymatic synthesis is purposed, it was deemed necessary to synthesize G6P from glucose. While ^{14}C *myo*-inositol is commercially available, it is c. 100-fold more expensive than ^{14}C glucose, from which Ins3P can be synthesized by coupling hexokinase to IPS. Moreover, it was recognized that the methods in development here would be equally appropriate for the synthesis of stable isotope [^{13}C] *myo*-inositol, raising the possibility of use of [^{13}C] *myo*-inositol and analysis of metabolism by Isotope Ratio approaches. In order to test the feasibility of coupling the two enzymes, initial studies were undertaken with a commercially available *Saccharomyces cerevisiae* hexokinase, sourced from Sigma-Aldrich (H4502). Figure 2.17 shows the reaction scheme for the phosphorylation of glucose to G6P.

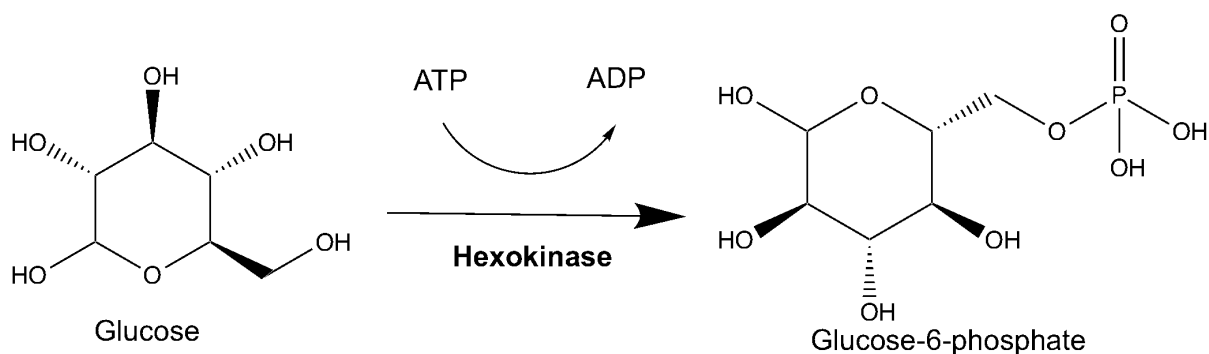


Figure 2.17: Reaction scheme for the phosphorylation of glucose to G6P by hexokinase, with ATP as a phosphate donor. Figure produced using ChemDraw (v. 20.1), substrate and product are shown in ring form.

K_M is the substrate concentration at which half of the maximum velocity of the enzyme-catalysed reaction is reached, determining the binding affinity of an enzyme towards a particular substrate (Michaelis & Menten, 1913, in: Johnson & Goody, 2011). The yeast hexokinase (Sigma) used in the reactions described here has a K_M for glucose of 0.12 mM at pH 7.5 at 30°C and this reaction for the phosphorylation of glucose to G6P by yeast hexokinase requires Mg^{2+} as an activator (Kunitz and McDonald, 1946; Pollard-Knight and Cornish-Bowden, 1982; Cardenas, Rabajille and Niemeyer, 1984). None of these components are known interferences in the MIP-catalysed reaction.

The end point hexokinase assay was made up as two separate mixtures of 400 μ L, in 50 mM pH 7.5 and 100 mM pH 9.0 Tris-Acetate buffer, containing a final concentration of: 0.75 mM ATP (Sigma), 7.5 mM $MgCl_2$ (Sigma), 10 mM D-Glucose (Sigma) and 20 units/mL Yeast Hexokinase (Invitrogen).

The assay was run in pH 7.5 Tris-acetate buffer, the most suitable for coupling this step to the IPS assay for isomerisation of the produced G6P to Ins3P, as well as at an alkaline pH (Tris-Ac pH 9.0) specified by manufacturers guidelines as the upper optimal pH for hexokinase activity (Sigma-Aldrich, 2017). The assay was run for a total of 4 hours at 30°C as 100 μ L reactions in 0.2 mL tubes, with samples removed and frozen at -20°C at hour intervals. One hundred-fold dilutions of the assay at 1 hour and 4-

hour time points were analysed by ion exchange chromatography. The HPLC resolution of G6P production is shown in Figure 2.18.

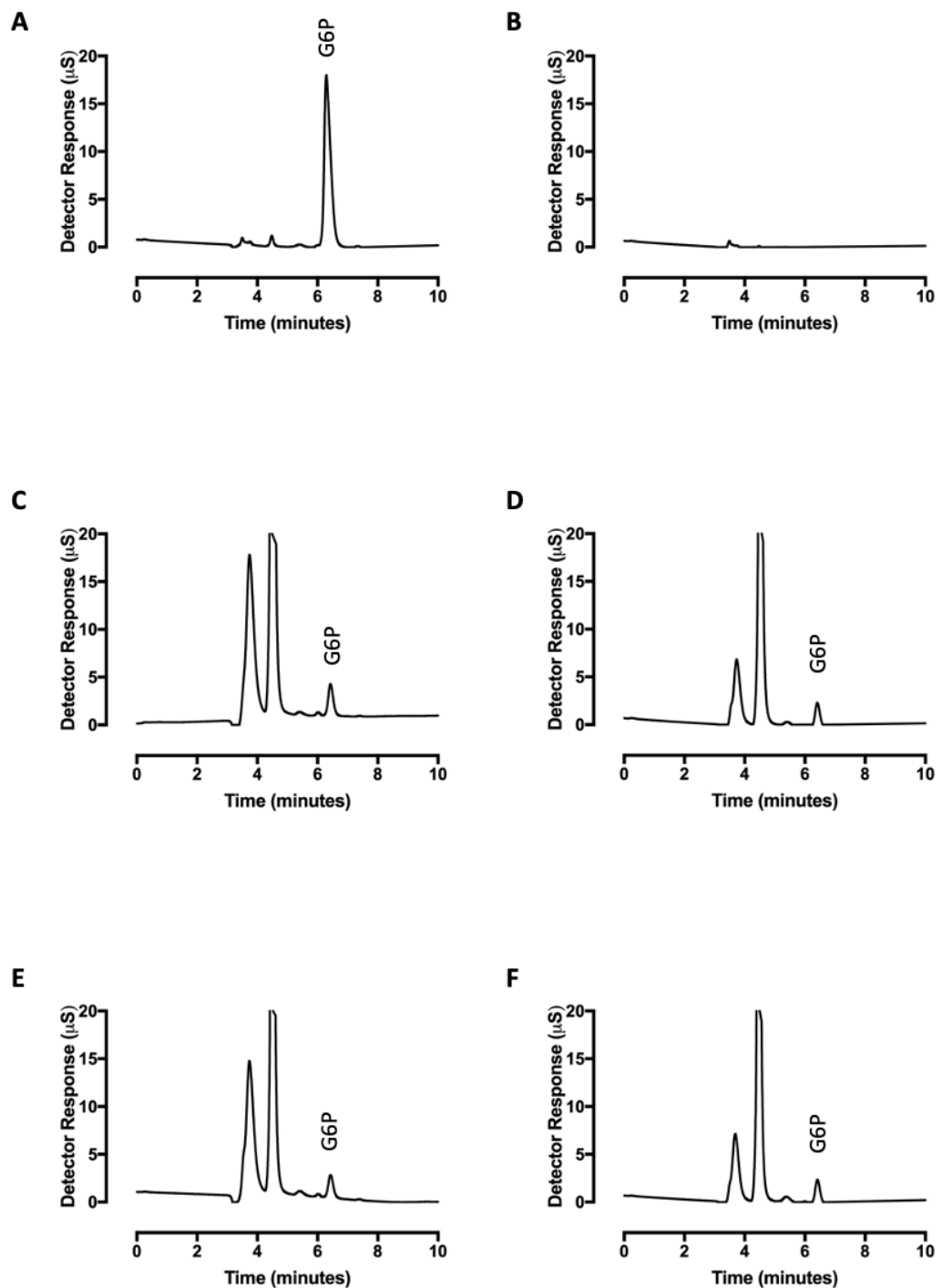


Figure 2.18: Chromatographic separation on a Dionex AS18 IC column of hexokinase reaction products and standards, measured by suppressed ion conductivity. **A** 100 μM G6P standard in 18.2 Megohm water, **B** 100 μM

glucose; **C** 1/100 dilution of the hexokinase assay after 1 hour in pH 7.5 buffer; **D** 1/100 dilution of the hexokinase assay after 1 hour in pH 9.0 buffer, **E** 1/100 dilution of the hexokinase assay after 4 hours in pH 7.5 buffer and **F** 1/100 dilution of the hexokinase assay after 4 hours in pH 9.0 G6P elutes at 6.43 minutes.

Figure 2.18 shows the separation of G6P from assay and buffer components on the AS18 IC column eluted isocratically with a 27 mM KOH. While glucose is not detectable by this method, anions components in the buffer can be detected eluting at approximately 3.5 and 4.5 minutes.

Calculations taking account of the 1:100 dilution and the initial assay concentration of 10 mM glucose and 0.75 mM ATP, set an upper limit of product of 0.75 mM G6P, which with a 20 μ L injection of this 100 μ L final dilution would suggest the maximum detector response available would be for a peak of approximately 15 μ M G6P. Comparison of the detector response obtained for the assay products with that for a 20 μ L injection of the 100 μ M G6P standard, suggests complete conversion of glucose using the available phosphate for G6P production by the 4 hour assay time point, with approximately 90% conversion at 1 hour. Moreover, there was no difference in the efficiency of phosphorylation between the pH 7.5 and pH 9.0 buffer conditions used for this assay.

2.3.4.2 ATP regeneration coupled hexokinase assays for conversion of glucose to G6P

In the hexokinase reaction shown in section 2.3.4.1, ATP as the phosphate donor is the limiting factor, in that the absence of available ATP limits the turnover of glucose to G6P by hexokinase even when glucose is 100-fold in excess of the K_M of hexokinase. As this chemoenzymatic synthesis is ultimately devised for use with a universally labelled glucose precursor – such as U- $^{13}\text{C}_6$ -glucose or U- $^{14}\text{C}_6$ -glucose, which are more expensive than conventional $^{12}\text{C}_6$ -glucose (glucose), or which pose additional problems of

purification arising from incomplete conversion or general considerations of use of radioisotope– it was necessary to improve the turnover of glucose to G6P by hexokinase by providing an alternative phosphate donor in the reactions. The rationale here was to reduce the amount (and cost) of ATP. The solution tested in the following used an ATP-regenerating system whereby ADP produced during kinase reaction is recycled to ATP by the action of creatine kinase action on sacrificial creatine phosphate substrate, shown in Figure 2.19.

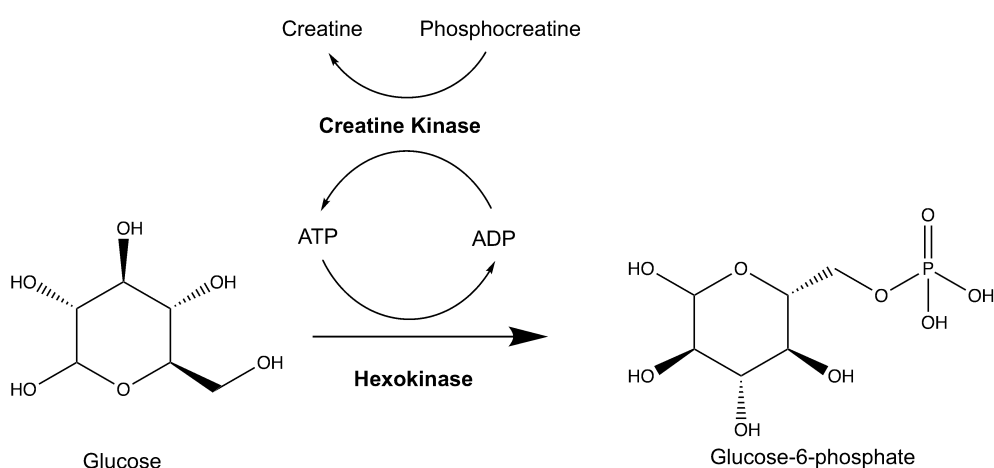


Figure 2.19: Reaction scheme of the conversion of glucose to G6P by hexokinase, using ATP as a phosphate source. Coupled to this is the regeneration of ATP from ADP by creatine kinase, using phosphocreatine to regenerate ATP and producing creatine as a by-product of this regeneration. Figure produced using ChemDraw (v. 20.1), substrate and product are shown in ring form.

For the ATP-regeneration coupled hexokinase assay, the reaction was carried out in a 500 μL mix made up in 50 mM Tris-Ac pH 7.5 buffer containing final concentration: 50 mM D-glucose, 1.5 mM ATP, 5 mM phosphocreatine, 5 mM MgCl_2 , 0.4 units yeast hexokinase and 6 units of creatine kinase.

Using this assay mix, ATP is maintained above the K_M of hexokinase by the action of creatine kinase, which under the conditions of the assay has a higher rate than hexokinase itself. The concentration of available phosphate in terms of starting ATP and phosphocreatine is in excess of the starting concentration of glucose, glucose becomes the limiting factor of the reaction. This is important, particularly in terms of formulating this assay for its use with ^{13}C and ^{14}C D-glucose, in which its total conversion through the *myo*-inositol is required to prevent losses of more expensive heavy or radiolabelled isotope through incomplete conversion.

Products generated from coupled assays were analysed by HPLC on the AS18 HC column by the standard method. Typical results are shown in Figure 2.20.

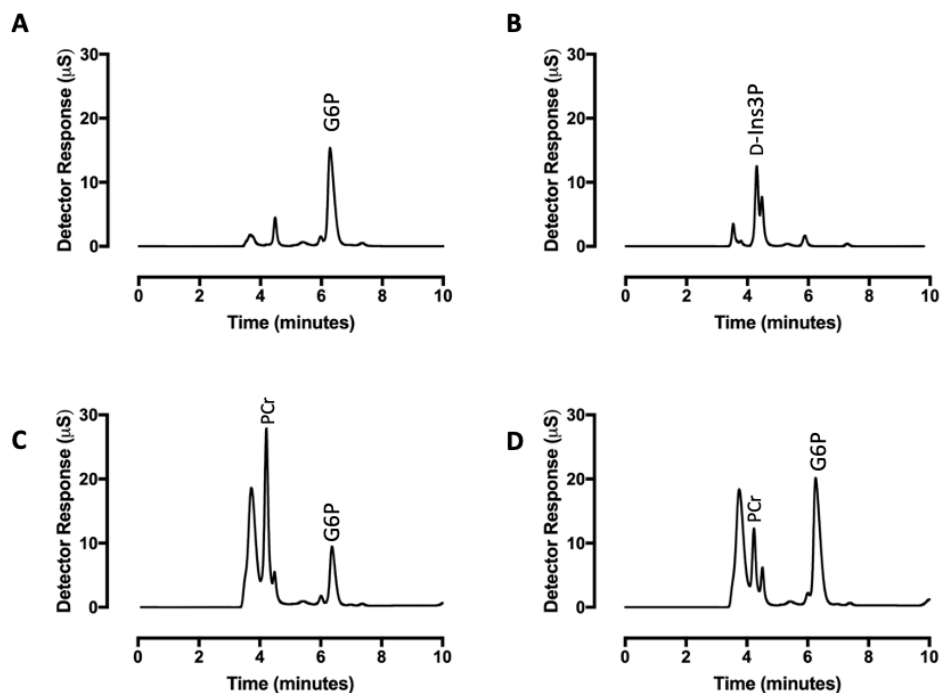


Figure 2.20: Separation of ATP-regeneration coupled hexokinase assay products by Ion Exchange Chromatography. **A** 50 μM G6P standard; **B** 50 μM D-Ins3P standard; **C** 1:100 dilution of assay at 2-hour time point and **D** 1:100 dilution of assay at 4-hour time point. Elution time for G6P is 6.4

minutes, elution time for D-Ins3P is 4.5 minutes. Unlabelled peaks running before this correspond to buffer components absent in the G6P standard. The HPLC column was eluted with a potassium hydroxide isocratic gradient.

By comparison of the data in Figure 2.20 to the results shown for the end-point assay in Figure 2.18, it is apparent that inclusion of the ATP-regenerating system has, by 4 hours, increased G6P production. Peak area calculations suggest complete phosphorylation of glucose to G6P from the available ATP and phosphocreatine.

Considering the ultimate goal of efficient, cost-effective conversion of glucose to inositol, the advantage of the coupled assay that it limits the concentration of expensive starting reagents such as ATP. The foregoing data show that a starting concentration of 50 mM ATP, to match the starting glucose, is simply not necessary. Indeed, inclusion of the coupling reagents allows linear conversion of glucose to G6P over 4 hours, evidenced by the doubling of G6P peak area between 2 and 4 hours.

2.3.4.3 Hexokinase and *myo*-inositol phosphate synthase coupled assay

The next step for the chemo-enzymatic synthesis focused on coupling the two enzymatic reactions in one reaction mixture. The significant difference in the active temperature range for the two enzymes, with the yeast hexokinase active at 25-30°C and the *A. fulgidus* IPS active at 65-90°C with very little activity below this temperature range (Chen *et al.*, 2000) means that it would be impossible for both enzymatic steps in the assay to proceed simultaneously, and therefore it is necessary to allow the first enzymatic reaction to proceed first at 30°C. Following a 2-hour reaction, the hexokinase reaction products were stored at -20°C overnight, and the following day IPS and the cofactors necessary for this reaction were added in to the reaction and the incubation temperature increased to 80°C for the IPS synthesis step, which also heat inactivated the hexokinase enzyme allowing for it to be removed from the reaction mix at a later stage. Figure 2.21 shows the

reaction scheme for this coupled assay, with Table 2.17 detailing the reaction mix and the addition of IPS components after 2 hours.

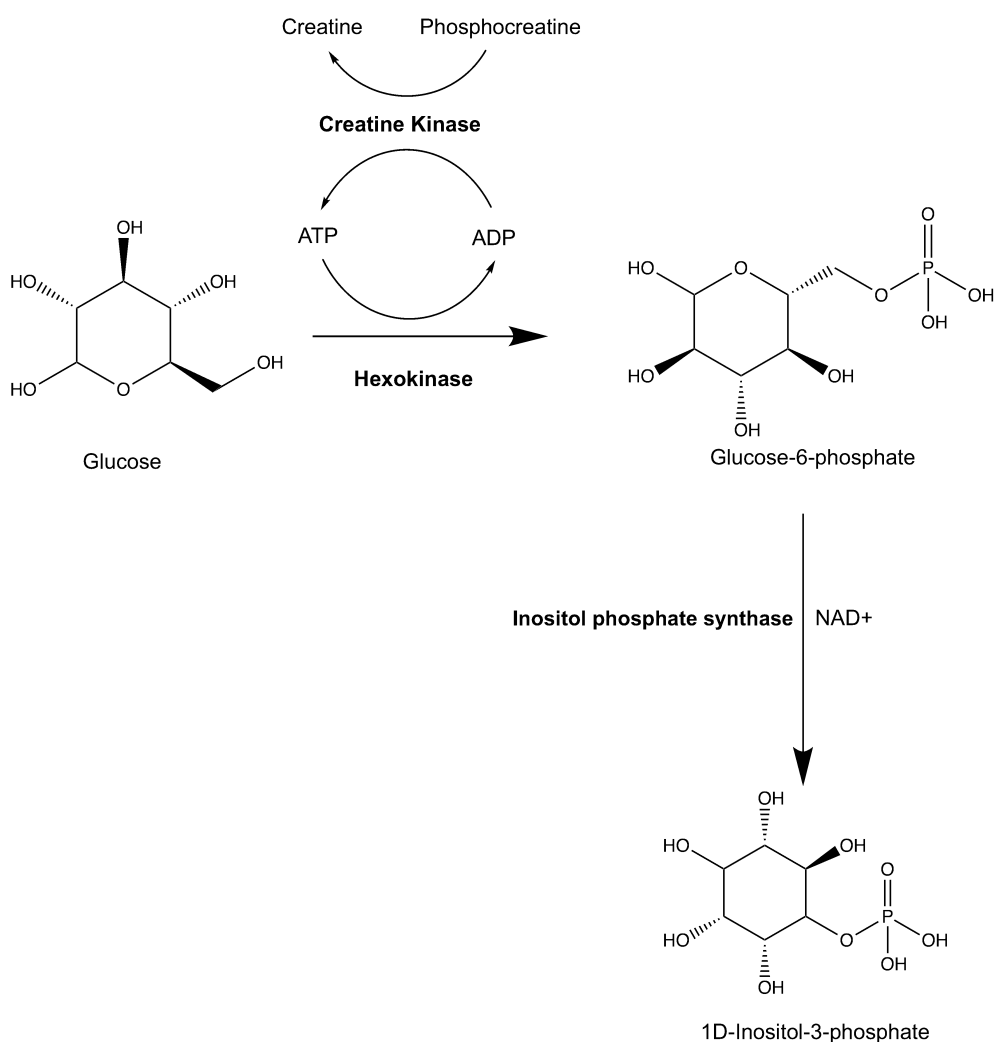


Figure 2.21: Reaction scheme for the conversion of glucose to Ins3P by hexokinase and inositol phosphate synthase, with G6P as an intermediate. The hexokinase-catalyzed reaction is coupled to creatine kinase reaction for the regeneration of ATP from ADP by dephosphorylation of phosphocreatine. Figure produced using ChemDraw (v. 20.1), substrate and products are shown in ring form.

Table 2.17: Reaction mix for the ATP-regenerating hexokinase-coupled IPS assay for the conversion of glucose-6-phosphate to inositol monophosphate

Component	Final concentration ^f
Glucose	50 mM
ATP	1.5 mM
Phosphocreatine	5 mM
MgCl ₂	5 mM
Hexokinase	0.4 units
Creatine kinase	6 units

^f This reaction was incubated at 30°C for 2 hours and then stored at -20°C overnight, after which point the following was added

Component	Final concentration ^g
Zinc sulphate	5 mM
NAD ⁺	1 mM
IPS	20 µg

^g Following which the reaction was incubated at 80°C for a further 4 hours.

The assay for coupled reaction from glucose to inositol-1-phosphate contained: 50 mM D-Glucose, 1.5 mM ATP, 5 mM phosphocreatine, 5 mM MgCl₂, 0.4 units yeast hexokinase and 6 units of creatine kinase. This reaction was incubated at 30°C for 2 hours, after which point the following was added and the reaction was incubated at 80°C for a further 4 hours: 5 mM ZnSO₄, 1 mM NAD⁺, 20 µg IPS. The reaction was carried out in multiple 100 µL aliquots from the same master mix of starting components. Results are shown in Figure 2.22.

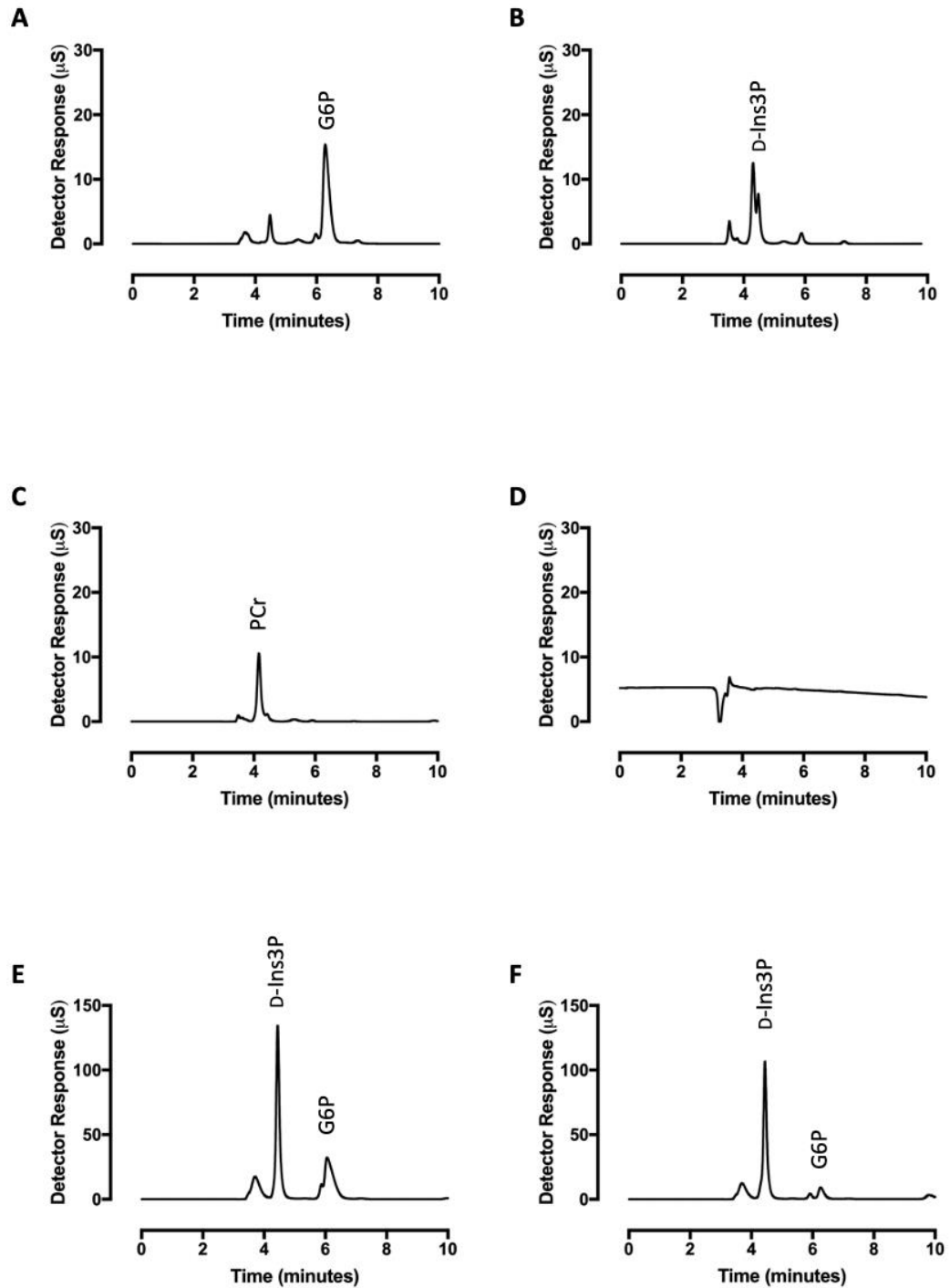


Figure 2.22: Separation of Ins3P and G6P by Ion Exchange

Chromatography. **A** 50 μM G6P, **B** 50 μM Ins3P standard, **C** 50 μM phosphocreatine (PCr), **D** 50 μM ATP standard, all prepared in 18.2 MOhm.cm water, **E** 1 in 100 dilution of IPS assay using commercial G6P as the starting material and **F** 1 in 100 dilution of Hexokinase-IPS coupled assay with glucose as the starting material.

The hexokinase-IPS coupled assay was run alongside a control assay using the IPS enzyme and commercial G6P as the starting material, as in section 3.3.3 for comparison of the efficiency of the IPS enzyme in the buffer components from the hexokinase assay. By comparison of the relative peak area for Ins3P and remaining G6P, identified by their co-elution with known standards at 4.5 minutes and 6.3 minutes respectively, as shown in Fig. 2.22 – with parallel assays run for the same length of time at the same temperature – approximately 90% of the G6P precursor, be that commercial or enzymatically synthesised, was converted to Ins3P.

The purification of inositol phosphates, whether isolated from environmental samples or labelled tissue, or whether generated *in vitro* in enzyme assays, has been a perennial problem since first description of separations of inositol phosphates (Tomlinson and Ballou, 1962; Anderson, 1964; Irving and Cosgrove, 1972). Purification from other inositol phosphates, buffer components and other interferences has exercised the modern inositol phosphate community, with relatively few developments since detailed metabolic studies of the 1980's, exemplified by Stephens and co-workers (Stephens and Downes, 1990a). Commonly, HPLC-resolved peaks of labelled material were desalted in batch-mode on Dowex ion-exchange media with eluting volatile eluents removed by multiple cycles of freeze-drying, before use as substrates for further study. One recent development that has perhaps not received the scrutiny, verification of efficacy, that earlier methods have, is the use of titanium dioxide (TiO₂) beads for purification of total inositol phosphates. The method derives from the use of TiO₂ for pre-enrichment of phosphor-peptides for proteomic studies (Matsuda, Nakamura and Nakajima, 1990). The method has been used recently for enrichment of inositol phosphates from biological samples (Wilson *et al.*, 2015). The method involves adsorption of inositol phosphates under acid conditions to TiO₂ beads (approximately 5 mg per sample), washing of the beads with acid and elution of inositol phosphates by raising of pH, the bicarbonate or ammonium hydroxide commonly used can be removed easily under reduced pressure – effectively desalting the sample.

2.3.4.4 Using titanium dioxide beads for inositol monophosphate purification

Using a method adapted from Wilson and Saiardi (2018), products from the hexokinase and IPS coupled assay were mixed with 1 volume of 1 M HClO₄, 3 mM EDTA and incubated with 5 mg of TiO₂ beads, eluted with 2.8% NH₄OH and dried completely before resuspending in 18.2 Mohm.cm water. TiO₂ beads have been previously reported to bind phosphorylated compounds and inorganic phosphate with high affinity. The method was employed here to attempt purification of the Ins3P product and remnant G6P from remaining trace metals and proteins, as the high thermostability and pH activity range of the IPS enzyme made precipitation of the protein difficult, though other phosphate containing compounds present in the buffer would be similarly enriched by this method, and the resulting clean up products would retain the phosphocreatine used in the ATP regeneration for the hexokinase assay. The results of which are shown in Figure 2.23.

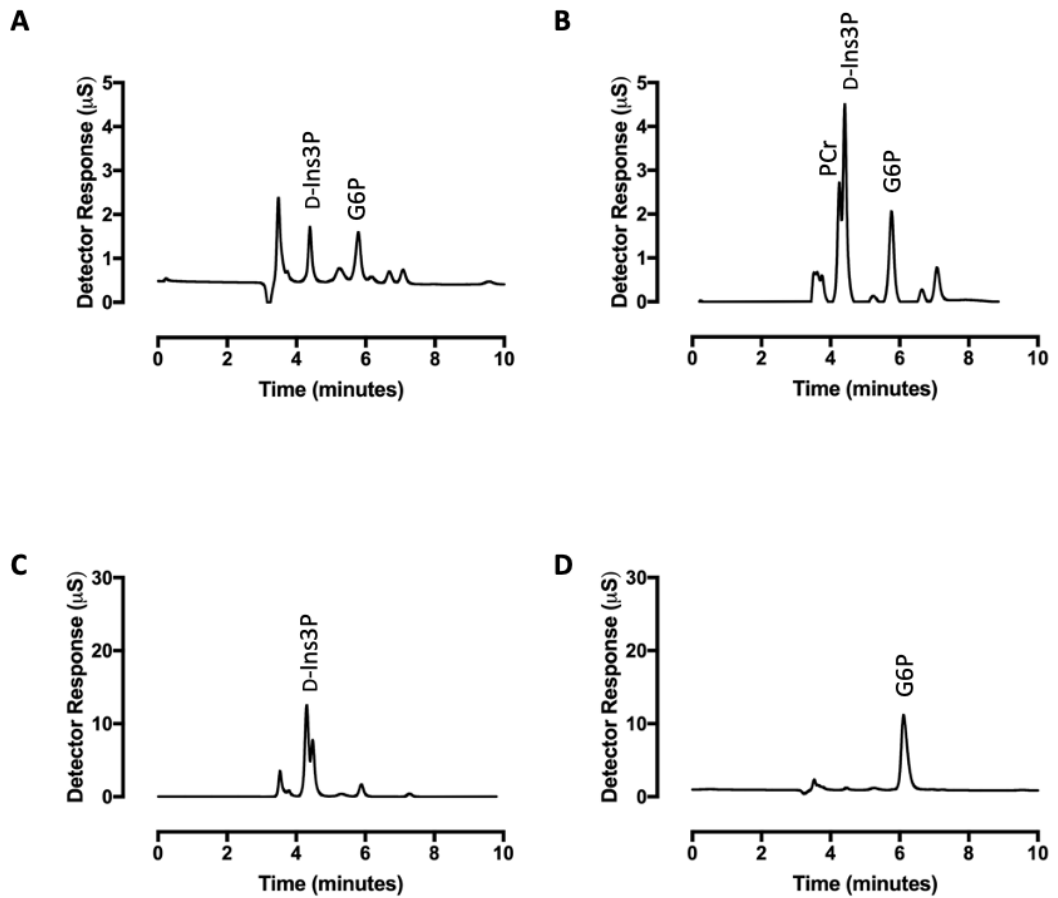


Figure 2.23: Suppressed ion chromatography separation of D-Ins3P and G6P in **A**, IPS reaction from G6P following TiO₂ clean up; **B**, hexokinase-coupled IPS reaction from glucose following TiO₂ clean up; **C**, D-Ins3P standard; **D**, Glucose-6-phosphate standard.

Consistent with speculation of the affinity of TiO₂ for multiple assay components, those bearing phosphate moieties, the employ of the TiO₂ purification method as a clean-up step for enzymatically synthesized *myo*-inositol resulted in a concentration of the co-substrates for coupled assay steps, evidenced as a shoulder peak corresponding to the near co-elution of phosphocreatine (PCr) and D-Ins3P in Fig 2.23B.

2.3.5 Three step coupled enzymatic assay from glucose to *myo*-inositol

The final step in the chemo-enzymatic synthesis of inositol from glucose involves dephosphorylation of the resultant Ins3P. This was achieved using a commercial alkaline phosphatase, with a broader effective pH range and higher efficiency than other potential phosphatases that might be cloned and expressed for this purpose. Calf intestinal mucosa (unconjugated) alkaline phosphatase was chosen on grounds of cost and specific activity and purchased from Rockland Inc. (Rockland Immunochemicals, 2020). The specific activity for hydrolysis of *p*-nitrophenol phosphate of 6 mM per minute at pH 9.8 at 37°C is well-suited for assays run in neutral to basic buffers. The complete reaction scheme for all components included in the buffer for this assay is shown in Figure 2.24, with each enzyme added into the reaction in a stepwise manner following incubation for the accumulation of precursors from previous enzymatic steps.

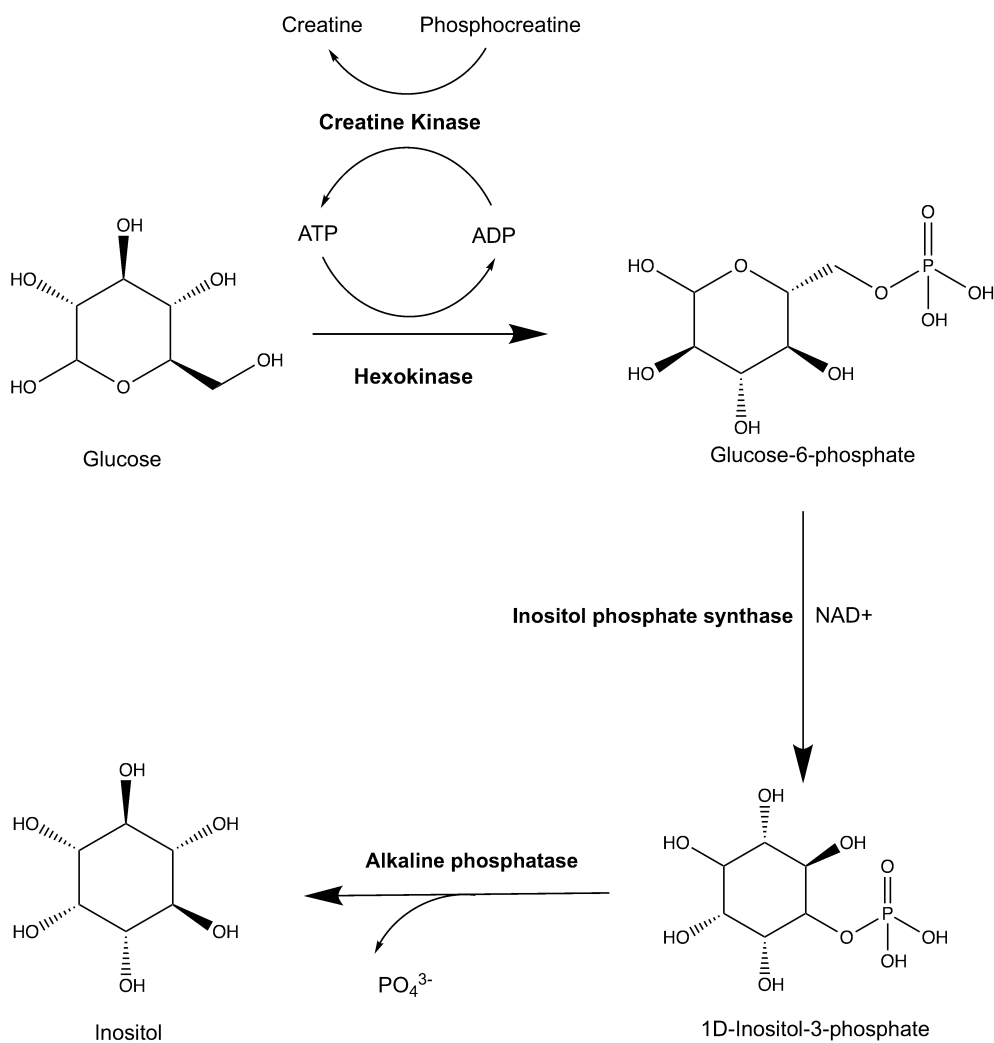


Figure 2.24: Reaction scheme for the stepwise conversion of glucose to inositol by hexokinase, inositol phosphate synthase and alkaline phosphatase enzymes, with G6P and Ins3P as reaction intermediates. Figure produced using ChemDraw (v. 20.1), substrate and products are shown in ring form.

Assay conditions were trialled for efficient dephosphorylation of inositol monophosphate in the existing buffer conditions, knowing that use of a powerful phosphatase such as the one used from Rockland Immunochemicals would also dephosphorylate remaining G6P, phosphocreatine and ATP in the buffer from previous enzymatic steps. Adding the phosphatase to the assay in situ instead of first purifying inositol-

1-phosphate from the previous enzymatic assay steps reduces endogenous losses from purification steps (Table 2.18).

Table 2.18: Assay mixture for the 3-step enzymatic coupled assay for the generation of *myo*-inositol from glucose. Final concentrations are given as a concentration in a total reaction of 500 μ L, from which four 100 μ L aliquots were used as separate reaction mixtures.

Component	Final concentration ^f
Glucose	50 mM
ATP	1.5 mM
Phosphocreatine	5 mM
MgCl ₂	5 mM
Hexokinase	0.4 units
Creatine kinase	6 units

^f This reaction was incubated at 30°C for 2 hours, after which point the following was added

Component	Final concentration ^g
Zinc sulphate	5 mM
NAD ⁺	1 mM
IPS	20 μ g

^g Following which the reaction was incubated at 80°C for a further 3 hours.

Component	Final concentration ^h
Alkaline phosphatase	2 units

^h Following which the reaction was incubated at 37°C for 1 hour.

Following enzymatic steps, the reaction products were subjected to HPLC and pulsed amperometric detection. Pulsed amperometry of analytes in hydroxide eluents on gold electrodes is a sensitive method for the detection of saccharides. A discussion of the optimization of waveforms for detection can be found in Rohrer (2013), following the work of LaCourse & Johnson (1993). The approach works for cyclitols and has been used for

measurement of inositol in feed and digesta sample samples in later chapters of this thesis.

A calibration curve generated by injection of 10 μL aliquots of 1-10 μM inositol is shown in Figure 2.25.

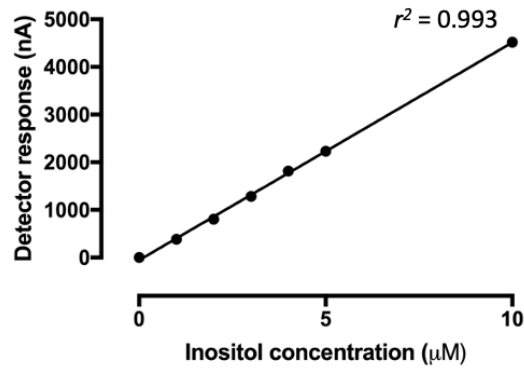


Figure 2.25: Calibration of detector response (integrated peak area) for *myo*-inositol derived from 2D HPLC-PAD of inositol standards.

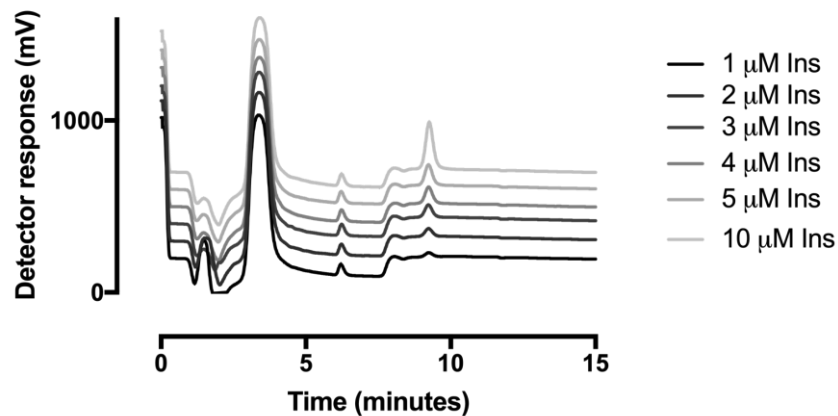


Figure 2.26: Overlay of inositol standards from 20 μL injections (1 μM , 2 μM , 3 μM , 4 μM , 5 μM , 10 μM) separated by 2D HPLC-PAD with a gradient of 150 mM NaOH used to generate calibration curve in figure 2.25.

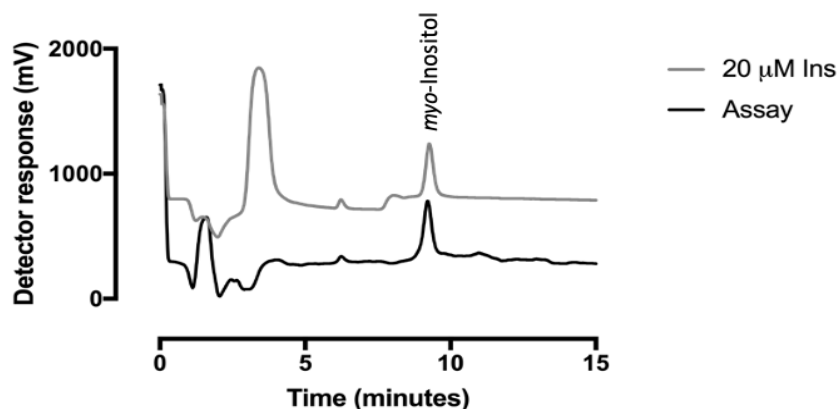


Figure 2.27: Separation of *myo*-inositol from glucose and glycerol as a buffer component by 2D HPLC-PAD with a gradient of 150 mM NaOH.

Inositol was separated from its buffer components by 2-dimensional HPLC-pulsed amperometry (method described fully in section 2.2.2.12). The commercial alkaline phosphatase was supplied in a buffer containing glycerol, which runs close to but separable from *myo*-inositol, labelled in figure 2.27. The alkaline phosphatase used in this assay is capable of dephosphorylating all phosphate containing compounds present in the buffer, including glucose 6P and Ins3P. Nevertheless, the 2-dimensional HPLC allows inositol which elutes early from the 1st column onto the main separating column, but switches the later eluting glucose to waste before it reaches the separating column. Consequently, glucose while electrochemically active on gold electrodes at this pH, is not detected or reported in this chromatogram. Inositol production was determined by comparison to a calibration curve of known standard concentrations of injected inositol, and the estimations of percentage conversion of glucose to inositol were made from the known starting concentration of glucose and the calculated recovery of inositol, as measured by PAD, suggesting an approximately 80% conversion of *myo*-inositol from starting glucose based on HPLC measurement, though this is without purification.

2.3.6 Chemoenzymatic synthesis of $^{13}\text{C}(\text{U})$ -*myo*-inositol

The use of a stable isotope e.g. ^{12}C or ^{13}C instead of radiolabelled (^{14}C) precursor, potentially affords a number of benefits, not only to help define optimal conditions for radiolabel conversion but also in final metabolic use of the synthesized labelled (^{13}C or ^{14}C inositol). Firstly, all enzyme assays demand use of substrate in/above the K_m of individual enzymes to drive reactions forward. Use of ^{14}C alone would poise substrate concentrations below K_m , because of the specific activity of the radiolabel. Consequently, even radiolabelled assays demand inclusion of un(radio)labelled 'carrier', usually ^{12}C . The methods chosen for assessment of conversion of glucose to G6P to Ins3P and hence to inositol, suppressed ion conductivity and pulsed amperometry do not rely on measurement of radioactivity and are as applicable to ^{13}C precursors as they are to ^{12}C precursors, of course, one would not by choice to use ^{14}C if one didn't have to. The constraints of the Radioactive Substances Act (1993) limiting open source radiation use to license holders in full compliance with regulations, and the high cost of purchasing radioisotopes compared to the stable isotope equivalents as well as the required safety materials for handling of radioisotopes such as shielding and the cost associated with safe storage and disposal, preclude this. A second benefit of the use of stable isotope, ^{13}C in particular, is that it opens up the use of sophisticated Isotope Ratio Spectrometry methods for study of metabolic conversions relevant to inositol (Harmel et al., 2019). Such methods can be applied against a physiological metabolic background of ^{12}C metabolism. A third benefit is that the use of ^{13}C glucose to generate ^{13}C inositol affords opportunity for the production of standard compounds that can be powerfully combined with ^{12}C inositol in further experiments. Indeed, one such possibility is the tracing of inositol between metabolic pools of inositol phosphates generated e.g. from ^{12}C glucose via (M)IPS with those that bypass this enzyme when experimental systems can be supplied with exogenous ^{13}C inositol or *vice versa* (Desfougères et al., 2019).

Table 2.19: Hexokinase and IPS coupled assay mixture for $^{13}\text{C}(\text{U})$ D-glucose conversion to *myo*-inositol monophosphate. Concentrations are in a total of 200 μL reaction mix split into two 100 μL reactions for 2-hour and 4-hour incubation periods at 30°C for the hexokinase reaction. The assay mix was made up to a total of 200 μL with 50 mM Tris-Acetate buffer at pH 7.5.

Component	Final concentration ^f
$^{13}\text{C}(\text{U})$ D-glucose	10 mM
ATP	1.5 mM
Phosphocreatine	5 mM
MgCl ₂	5 mM
Hexokinase	1 unit
Creatine kinase	15 units

Using multiple reaction mixes as described in Table 2.19, and through the method development steps described earlier in this chapter, $^{13}\text{C}(\text{U})$ -Inositol was synthesised through from D-Glucose- $^{13}\text{C}_6$ (Aldrich). Chromatograms for the conversion from glucose-6-phosphate to inositol-3-phosphate by IPS are shown in Figure 2.28.

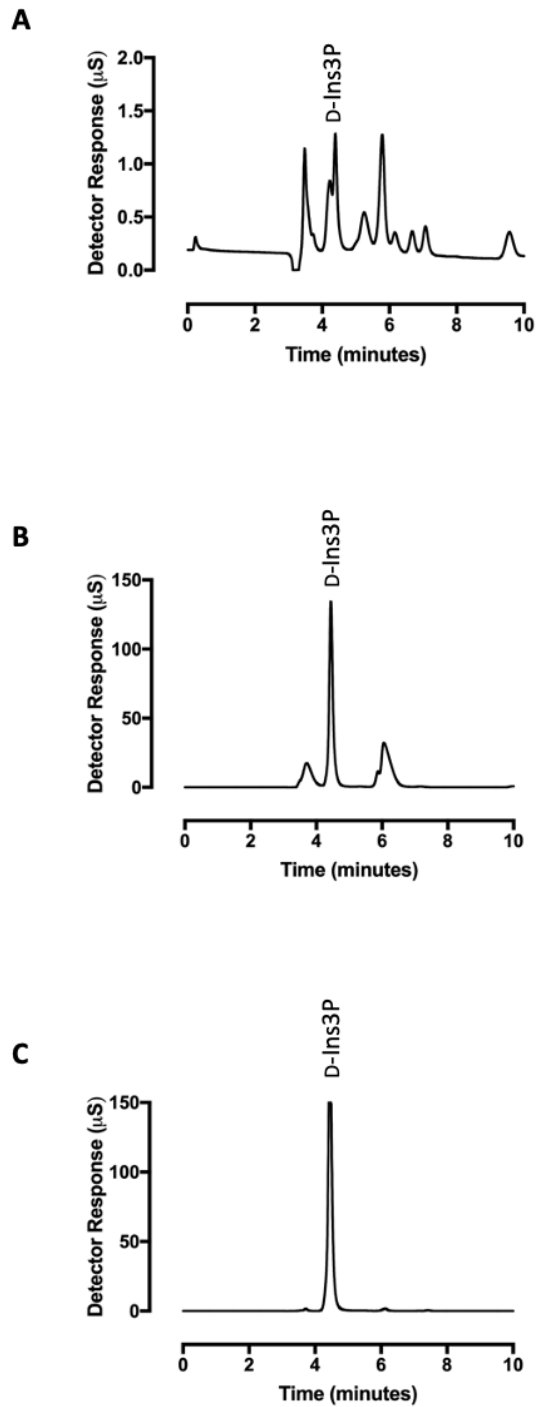


Figure 2.28: Suppressed ion chromatography separation of D-Ins3P in **A**, IPS reaction from G6P synthesised using hexokinase from D-Glucose- $^{13}\text{C}_6$; **B**, 1 in 100 dilution of IPS assay using commercial G6P as the starting material; **C**, D-Ins3P standard run alongside samples.

2.3.6.1 Use of ^{13}C Inositol in Animal Feeding Experiments

Typically, metabolic tracers used in animal feeding studies of this nature require use of radioisotope labelling, restrictive to many research groups with limited locations licensed to carry out animal experiments feeding radioisotopes outside of mouse and rat studies. Research involving stable isotope measurements in poultry is limited, and has focussed on measuring natural variations in stable isotope concentrations arising from crops with C_3/C_4 photosynthetic pathways for the purpose of determining geographic provenance of meat samples (Department for Environment Food and Rural Affairs, 2013) and to trace the sources of atmospheric aerosol particles in poultry housing as a tool for improving animal husbandry conditions (Skipitytė *et al.*, 2017). Recently, the use of diets of different plant origin, with significantly different naturally occurring levels of Carbon-13, has been employed to estimate metabolic rate of broiler tissues through measurement of Carbon-13 turnover (Pelícia *et al.*, 2018).

Without being able to vary diet composition in the experimental design, a trial was carried out (described in full in Chapter 4) which attempted to also employ the use of Carbon-13 as a metabolic tracer, but specifically for the measurement of the metabolic fate of dietary inositol rather than total consumed carbon, and so employed the method described above for the synthesis of ^{13}C *myo*-inositol as a dietary supplement. Based on the limits of detection of the Thermo Finnigan Delta plus XP isotope ratio mass spectrometer, $^{13}\text{C}_6$ -*myo*-inositol was synthesized based on the final optimised protocol described in section 2.2.2.14, and was added to poultry diets at a final concentration of $\text{d}30\%$ $^{13}\text{C}_6$ -*myo*-inositol in a mixture of 500 g natural *myo*-inositol (Sigma) before being added to poultry diets at 2 g/kg at the Nottingham Trent University poultry trial facility.

Following the animal feeding trial, 0.5 mg samples of freeze dried and milled gizzard and ileal digesta, 0.5 mg samples of ground and milled diets and 0.5

mg of freeze dried tissue samples (from 100 mg samples lysed for extractions described in chapter 5), were analysed from ratio of $\delta^{13}\text{C}$ to ^{12}C at the Stable Isotope Analysis Platform (Stable Isotope Laboratory, School of Environmental Sciences, University of East Anglia) but no significant difference was found in any sample compared to the Pee Dee Belemnite standard. Full tabulated results are provided in the appendices (Appendix 2).

2.4 Discussion

Historically, metabolic or enzymatic research using a traceable form of *myo*-inositol relied on tritiated [^3H]-*myo*-inositol for detection of picomolar concentrations of inputted label in order to follow metabolic pathways to higher inositol polyphosphates or pyrophosphates, easily discernible from the relative initial pool of unlabelled species (Mayr, 1988; Harmel *et al.*, 2019). Traditionally, these studies of isolated cells, cell lines and sometimes tissue slices, have been analysed by strong anion exchange (SAX) HPLC with coupled scintillation counting for detection. However, for longer term studies of whole complex organism metabolism, in which the pharmacokinetics of labelling of different tissues is undefined and consequently dose of labelled precursor required is unknown, a stable isotope might be more appropriate. Like many fields of research, inositol phosphate research could benefit from alternatives to radiolabelling, for legislative and democratizing purposes. Indeed, the availability and ability to handle commercial labelled *myo*-inositol and its phosphates is restrictive by virtue of cost and facility to handle radioisotopes. Both radio-labelled and stable isotope-labelled inositol are more expensive than common sugars such as glucose, particularly for universally-labelled structures.

The generation of an *in vitro* chemoenzymatic synthesis assay for the generation of a stable isotope labelled *myo*-inositol will likely be instrumental in tackling the question of the metabolic fate of inositol in poultry. Without which, the determination of the physiological explanation of the benefits of phytase, will remain obscure – evidenced by correlative studies alone –

those which relate measured inositol with growth performance without insight into use of inositol by different organs.

Work by Harmel *et al.* (2019) made great strides in successful gram scale synthesis of ^{13}C stable isotope-labelled *myo*-inositol for metabolic labelling of mammalian HCT116 cells for NMR analysis, building on previous research using the Archaeoglobus IPS by Adolfo Saiardi and colleagues (Saiardi *et al.*, 2014). The method employed by both groups used chemical derivatization, normal phase chromatography and saponification to purify the resulting ^{13}C *myo*-inositol, with a final yield of approximately 50% in respect to initial [$^{13}\text{C}_6$] glucose input. For the downstream applications, proposed of this thesis, further purification may not be necessary to remove buffer components for feed trial use in whole animal experiments.

The use of $^{13}\text{C}_6$ *myo*-inositol as a metabolic tracer in the feeding trial described in this thesis was unsuccessful, in that the isotopic label was not detectable in feed, digesta or tissues at the levels used. In the absence of description of whole animal experiments with $^{13}\text{C}_6$ *myo*-inositol, the method was adopted from geological use of IRS. Despite its ultimate failure, it is a promising advance in the move away from the use of radioisotope tracers in longitudinal metabolic studies using whole animals. It is likely that the inclusion rate of $^{13}\text{C}_6$ *myo*-inositol in this case was insufficient for detection once diluted into animal feed, taking into account the additional carbon load in the feedstuff that would further dilute the ^{13}C supplemented. The experiments, nevertheless, provide useful insight into the inclusion rates required for detection in a whole-animal feeding trial context as opposed to when included in cell line, bacterial cell and *in vitro* experiments for measurements.

3. Improving the efficiency of inositol phosphate extraction from biological tissues

3.1 Introduction

As with all life systems, phosphorous is considered an essential nutrient for poultry development (National Research Council, 1994), with the majority of dietary phosphate in animal feed provided from plant sources, namely grains. Approximately two thirds of phosphate in grains is bound in the form of phytate and is thus unavailable for digestion (Lucca *et al.*, 2016). In order to circumvent the need for the addition of inorganic rock phosphate and to reduce costs to the producer and consumer, poultry diets are now often supplemented with microbial phytase (Selle and Ravindran, 2007) with the intention of accessing phytate-bound phosphate as an economical phosphate source and reduce pollution from phosphate run off.

The benefits of the addition of phytases to animal performance include improvement of feed conversion ratio as well as the reduction in myopathies such as woody breast disorder which reduce meat quality (Greene *et al.*, 2019). The economic benefits for farmers are widely tested in animal feeding trials (Schmeisser *et al.*, 2017; Pirgozliev *et al.*, 2019b). Whilst performance parameters such as weight gain and feed conversion ratio convey the significance of the importance of the use of phytase to consumers most easily, a mechanistic understanding of these benefits is crucial. Of particular interest is phytate degradation within the digestive tract, the reduction in phytate-P excretion and understanding the causes of these poultry growth benefits rather than just correlating their use with increases in bird weight. The benefits to furthering this understanding are multiple, with the research field aiming for complete phytate hydrolysis within the gut lumen and thus complete Pi release, as well as with interest in understanding the mechanisms of these enzymes in alleviating costly conditions for meat production such as woody breast (Greene *et al.*, 2019).

Within these feeding trials, biochemical measurement, typically of bone or blood parameters, are routinely taken alongside bird performance measurements to investigate the physiological mechanism(s) underlying the benefits of addition of phytases to diets. Increasing numbers of studies formally address the degradation of phytate during passage through the gastro-intestinal tract. Here, freeze dried and milled feed and digesta are extracted using e.g. NaF-EDTA solution pH 10 (Zeller *et al.*, 2015a) and InsP₃₋₆ analysed by high performance liquid chromatography with post-column complexation with ferric ion under acid conditions and detection of complexes by UV at 290 nm for inositol phosphates. Inositol can be measured in the same samples from dilutions of these NaF-EDTA extractions, as well as from dilutions of extracted blood plasma, by HPLC pulsed amperometry (Laird *et al.*, 2016).

For biological tissue samples, however, the methods of extraction and analyses of inositol and its phosphates are markedly different from the relatively simple, high throughput methods applied to digesta (Zeller *et al.*, 2015b). Due to the high levels of phosphate-containing protein and lipid contaminants, relative to InsPs, measurement of tissue inositol and InsPs has previously proved difficult, with analysis limited to *myo*-inositol measurements with more consistent reproducibility by tissue lysis under acidic conditions (Greene *et al.*, 2019). In recent years, attention is now being focused on tissues and organs, predominantly by targeted gene expression, such as on inositol or phosphate transporters (Hu *et al.*, 2018; Walk, Bedford and Olukosi, 2018; Sommerfeld *et al.*, 2020), signalling pathways (Schmeisser *et al.*, 2017; Greene *et al.*, 2019; Greene, Mallmann, *et al.*, 2020) or metabolic pathways (F. Gonzalez-Uarquin *et al.*, 2020; Greene *et al.*, 2020a; Gonzalez-Uarquin *et al.*, 2021). Western blot analyses of proteins involved in signalling or transport from tissues samples taken from mucosa, liver or muscle have also been described (Huber, Zeller and Rodehutscord, 2015; Greene *et al.*, 2019; Whitfield *et al.*, 2022), but not beside measurements of InsPs in tissue samples and certainly not from large scale feeding trials where analysis would have most statistical value.

Methods had previously been developed for the clean-up of inositol phosphates from complex tissue samples, namely in isolated skeletal muscles from *Xenopus laevis* and rat samples in stages of isometric and isotonic tetanus. This method is complex with multiple steps following extraction in 2M perchloric acid, including the addition of EDTA and acetic acid, pH adjustment to mild acidity with KOH and subsequent charcoal treatment and freeze drying before samples could be analysed by HPLC (Mayr *et al.*, 1992).

In recent research in the animal cell biology field where InsPs are most widely studied as agents of cell signalling, controlling diverse, biochemical, physiological and developmental phenomena, researchers have begun to exploit the phosphate binding property of TiO₂ to enrich low concentration inositol phosphates from mammalian cell extracts (Wilson *et al.*, 2015). The use of TiO₂ beads allows purification of inositol phosphates by virtue of the binding of phosphate groups under acidic conditions, and elution under basic conditions, from which point the enriched sample can be concentrated to allow analysis of samples with previously too low concentrations for analysis by traditional methods such as PAGE or HPLC. The phosphate adsorbing properties of titanium were first documented in 1990 (Matsuda, Nakamura and Nakajima, 1990), but only in recent years have methods been developed utilising these properties for sample enrichment from low concentrations in relatively easily disrupted sample types.

To make complementary inositol phosphate measurements in tissues and organs to accompany measurements of inositol phosphate and inositol levels in digesta, method development was required to test the suitability of the use of TiO₂ as an extraction method for poultry tissue inositol phosphates.

3.2 Methods and materials

3.2.1 Materials

Reagents used for extractions were as follows:

1 M HClO₄ perchloric acid (Sigma 244252)

2.8% NH₄OH Ammonium Hydroxide diluted from stock (28-30% NH₃ in H₂O, Sigma)

Hichrom Titansphere® TiO₂ 5 µM bulk material (GL Sciences)

IKA T-10 Ultra-Turrax® High-Speed Homogeniser

3.2.1.1 Animal tissues

Poultry tissues used in this chapter were provided from an animal feeding trial conducted at Harper Adams University by C. Arthur (Arthur *et al.*, 2019). The study was approved by Harper Adams University Research Ethics. Animals in the feeding trial were supplied a mash basal diet split into six diets, three diets supplemented with one of three levels of inositol (1.5 g/kg, 3 g/kg or 30 g/kg), two diets supplemented with two levels (1500 or 4500 FTU/kg) of Quantum Blue™ phytase (AB Vista, UK), and one control diet. Diets were supplied to 480 male Ross 308 from 0 to 21 days of age in 60 raised floor pens at eight birds per pen. At day 21, one bird per pen was killed and blood collected, tissue and digesta samples taken and immediately frozen at -80°C.

3.2.2 Methods

3.2.2.1 Tissue disruption

Tissues from 192 male Ross 308 broiler chicks reared to 21 days in inositol and phytase “super-dosing” feed trials conducted at Harper Adams University were collected from random birds and immediately frozen at -80°C following necropsy. Varying sample weights from 100 mg up to whole organ

(frozen weight) of kidney, brain tissue, leg and breast muscle, were homogenised by Ultra-Turrax in 600 μL 1 M perchloric acid (pH 1.0) on ice and transferred to a 1.5 mL tube. Tubes were rinsed with a further 200 μL of 1 M perchloric acid which was pooled with the initial volume used for lysis. Samples were kept on ice for 20 minutes with vortex mixing every 5 minutes, then samples were centrifuged at 13,000 $\times g$ for 10 minutes at 4°C. The resulting cleared lysate was transferred to a clean 1.5 mL tube.

3.2.2.2 Titanium dioxide bead extraction

The following extraction method is adapted from Wilson *et al.* (2015). All steps were carried out at 4°C for the prevention of much-vaunted acid degradation of inositol phosphates. However, we note the stability of inositol phosphates revealed in the pioneering work of Cosgrove and colleagues and others whereby migration of phosphate between cis vicinal positions of incompletely substituted inositol rings requires boiling in 1M-HCl for ca. 10 minutes to move, but not lose, phosphate (Cosgrove and Irving, 1980; Stephens, Hawkins and Downes, 1989). Prior to extraction, the TiO_2 beads (Titansphere® TiO_2 5 μM) were weighed and washed in 1M perchloric acid, weighed out for 5 mg of beads per sample and resuspended in perchloric acid at 5 mg in 50 μL .

To each cleared lysate, 5 mg of Titansphere® TiO_2 beads (Hichrom) was added from a total resuspension of TiO_2 5 μM bulk. Samples were vortexed briefly and incubated on a fixed speed tube rotator for 30 minutes. Samples were then centrifuged at 3500 $\times g$ for 5 minutes to pellet the TiO_2 beads and HClO_4 supernatant discarded.

To elute the bound inositol phosphates, the TiO_2 was resuspended in 200 μL ~2.8-3% ammonium hydroxide solution (pH 10.0) and resuspended by vortex before fixed speed rotation for 5 minutes at 4°C. Samples were centrifuged at 3500 $\times g$ for 1 minute and supernatant containing the inositol phosphates were transferred to a clean 1.5 mL tube. A further 200 μL elution in fresh 3% ammonium hydroxide was carried out as before for full recovery and the

supernatants pooled. Samples were then vacuum evaporated until dry and resuspended in 100 μ L of 18.2 mOhm.cm water for further analysis by HPLC or stored at -20°C prior to downstream analysis.

3.2.2.3 HPLC separation of inositol phosphates

Inositol phosphates were resolved by anion exchange HPLC on a 250 x 3 mm Thermo Scientific™ Dionex™ CarboPac™ PA200 column (Dionex™) and guard column 50 x 3 mm of the same material, eluted at a flow rate of 0.4 mL min⁻¹ with a methanesulfonic acid gradient. Inositol phosphates were detected after post-column addition of 0.1% (w/v) ferric nitrate in 2% HClO₄ (Phillippy and Bland, 1988) delivered at a flow rate of 0.2 mL min⁻¹. The gradient was (A) water, (B) 0.6M methanesulfonic acid: time (minutes), %B; 0, 0; 25, 100; 38, 100. (Whitfield *et al.*, 2018).

For separation of inositol phosphates including later eluting inositol pyrophosphate species (InsP₇ and InsP₈), inositol phosphates were resolved by anion exchange HPLC on a 250 x 3 mm Thermo Scientific™ Dionex™ CarboPac™ PA200 column (Dionex™) and guard column 50 x 3 mm of the same material, eluted at a flow rate of 0.4 mL min⁻¹ as above, with a gradient of HCl (Blaabjerg, Hansen-Møller and Poulsen, 2010), resulting in earlier elution of InsP₂₋₆. Inositol phosphates were similarly detected as above following post-column addition of 0.1% (w/v) ferric nitrate in 2% HClO₄ (Phillippy and Bland, 1988). All separable inositol are identified in Appendix 3.

3.3 Results

3.3.1 Whole organ extractions

Initial extractions were performed using whole kidneys, to reduce potential variability across tissue (Fig. 3.1). One might envisage hypothetical differential inositol phosphate metabolism between distal tubules and ducts or in respiring muscle tissue e.g. with distance from vasculature. Samples were homogenized from frozen in ice-cold 1 M HClO₄.

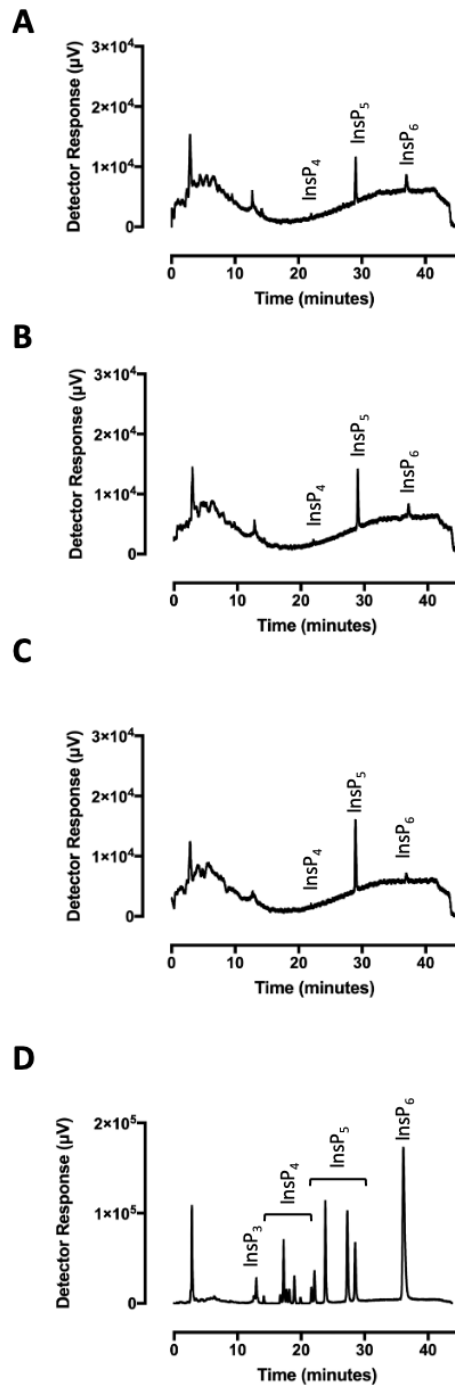


Figure 3.1: Profile of inositol phosphates in whole broiler kidneys. **A**, **B** and **C** are 20-fold diluted extracts of whole kidneys extracted using TiO₂. **D**, standards run beside the sample set from which **A-C** were obtained.

Kidneys selected for whole organ extraction were obtained from birds fed the same experimental diet during the animal feeding trial, the basal Control diet without supplementation of phytase or additional inositol, and thus variation

in the levels of each inositol phosphate species obtained during extraction can only be attributed to bird-to-bird differences as whole organs were used. Samples were diluted to reduce potential variation in detector response due to signal saturation of the UV detector, and in doing so increased the baseline noise-to-signal ratio seen in the chromatograms (Fig 3.1A, 3.1B, 3.1C). Critically, the peaks identified in these samples co-elute with known inositol phosphates identified in the acid-hydrolysed InsP₆ standard (Fig 3.1D), with peaks eluting at the same retention time for *myo*-InsP₆, as well as co-eluting with species in the regions of InsP₃, InsP₄ and InsP₅ when eluted using the 0.6 M methanesulfonic acid gradient for separation.

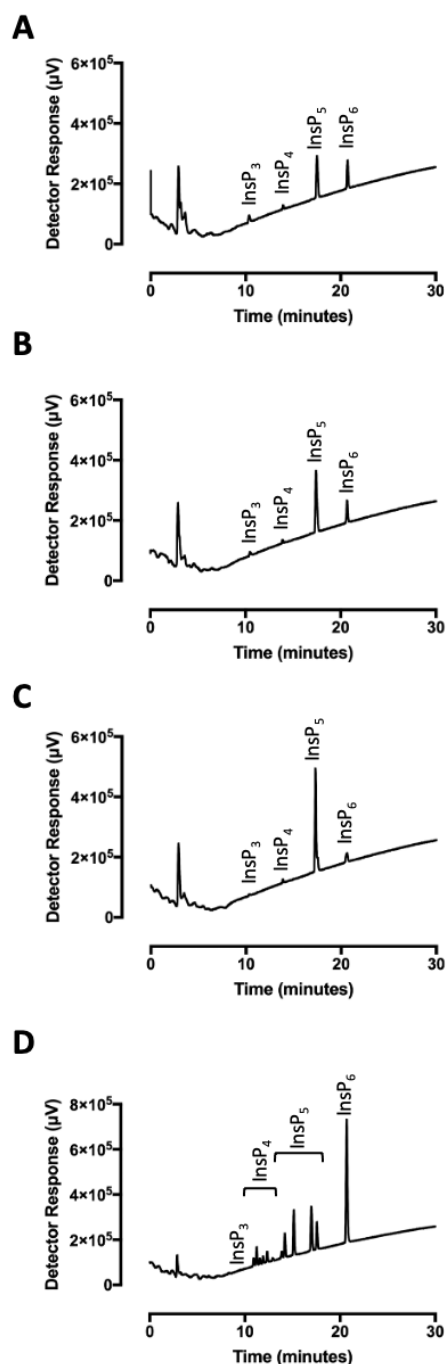


Figure 3.2: Profile of inositol phosphates in whole broiler kidneys on 0.8 M HCl gradient. **A**, **B** and **C** are concentrated extracts of whole kidneys purified using TiO₂. **D**, standards run beside the sample set from which **A-C** were obtained.

The same samples as presented in Fig 3.1 (Fig 3.1 A-C) were subsequently separated using a higher strength gradient of 0.8 M HCl (Fig 3.2 A-C), a stronger acid and more powerful eluent which allows for separation of the

more highly charged and therefore later eluting inositol pyrophosphate species of InsP₇ and InsP₈. No higher inositol pyrophosphates were detectable in the whole organs extracted and analysed by this method.

3.3.2 Technical replicability of extraction

To ascertain the reproducibility of profiles analysed in extracted poultry tissue samples, replicate extractions were performed in triplicate using three samples of 100 mg slices taken from the sample bird tissue sample, each of four tissue types – brain tissue (Fig 3.3), kidney tissue (Fig 3.4), breast muscle (Fig 3.5) and leg muscle (Fig 3.6). 100 mg slices were taken from still frozen tissue samples and extracted side by side using the adapted TiO₂ extraction method described above, with the resulting freeze-dried extractant resuspended in 100 µL of 18.2 mOhm.cm water, with 20 µL injections for HPLC analysis.

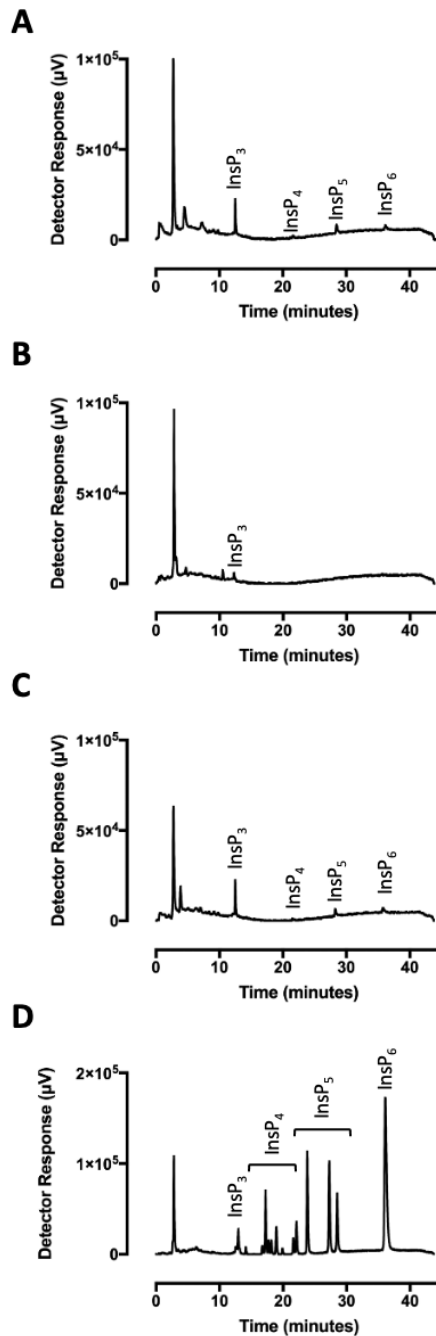


Figure 3.3: Reproducibility of broiler brain tissue extractions. **A**, **B** and **C** are replicate extractions of 100 mg samples taken from the same broiler brain. **D**, standards run beside the same set from which A-C were obtained.

The same inositol phosphate species, identified by retention time, were detected in all of the replicate samples of brain tissue extracted, though in one replicate sample (Fig 3.3B) levels were near the limited of detection to

definitively separate peaks from baseline noise for integration. Clear discernible peaks were identified in two replicates (Fig 3.3A, C) as separable from baseline noise, and co-eluting with peaks in the hydrolysed InsP₆ standard (Fig 3.3D) in the regions of known InsP₃, InsP₄ and InsP₅ species as well as a peak co-eluting with *myo*-InsP₆. Variation in samples may result from use of transverse slices of tissue from the same brain as replicate samples, resulting in differing inclusion of superficial veins in the cerebrum in the three samples extracted.

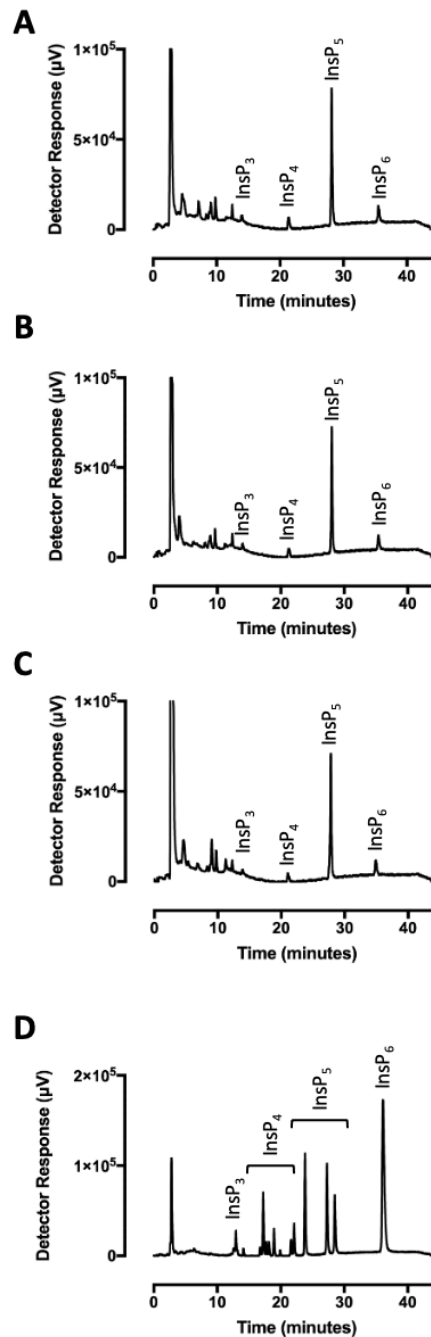


Figure 3.4: Reproducibility of broiler kidney tissue extractions. **A**, **B** and **C** are replicate extractions of 100 mg samples taken from the same broiler kidney. **D**, standards run beside the same set from which A-C were obtained.

Variability in detectable inositol phosphates was reduced in kidney tissue replicate extractions, where there were higher overall detectable levels of

individual inositol phosphate species (Fig 3.4A-C). All peaks detected after retention time of approximately 10 minutes co-eluted with known *myo*-InsP species identified in the standard run alongside the samples (Fig 3.4D) from which Figure 3.4A-C originated.

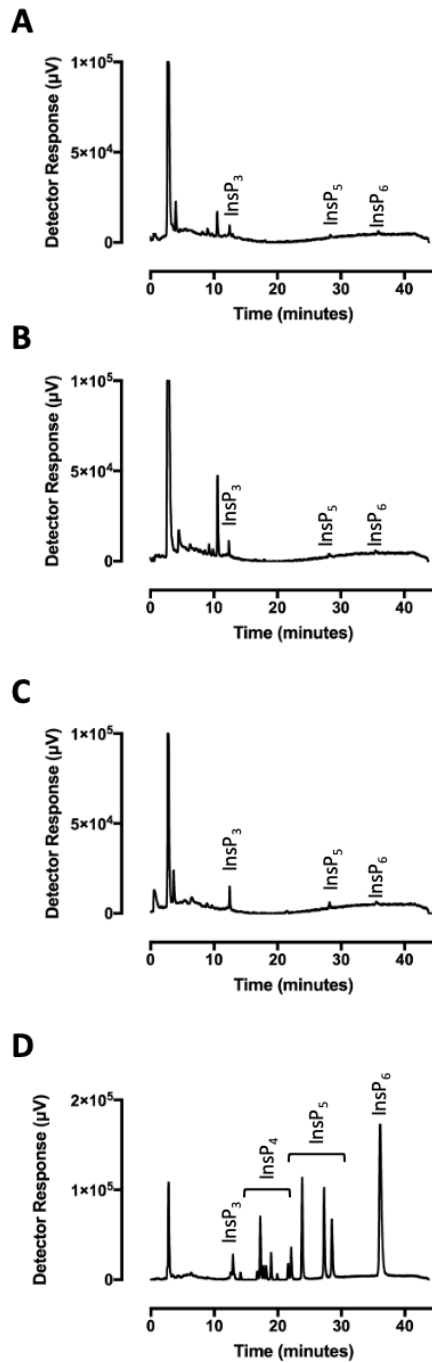


Figure 3.5: Reproducibility of broiler breast muscle extractions. **A**, **B** and **C** are replicate extractions of 100 mg samples taken from the same broiler breast muscle. **D**, standards run beside the same set from which A-C were obtained.

Similarly, minimal variation in detected inositol phosphate levels following TiO_2 extraction and concentration was measured in breast muscle replicate extractions. All peaks were separable from baseline noise (Fig 3.5A-C), though levels were far lower than measured in kidney tissue (Fig 3.4). Identifiable inositol phosphate species were consistent across replicate extractions and eluted at retention times of known inositol phosphate species, as identified by comparison to the standard run alongside the sample set (Fig 3.5D).

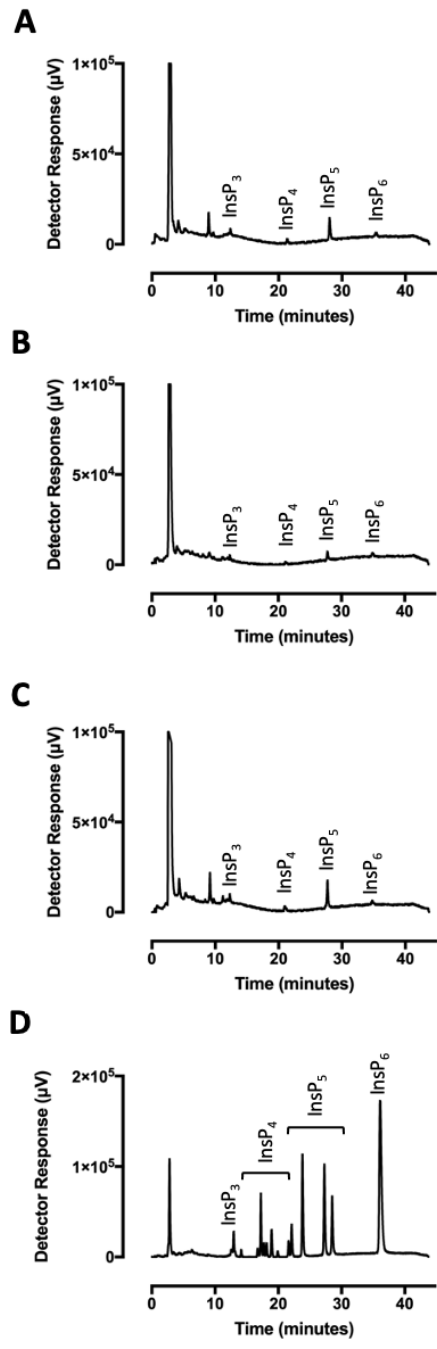


Figure 3.6: Reproducibility of broiler leg muscle extractions. **A**, **B** and **C** are replicate extractions of 100 mg samples taken from the same broiler leg muscle. **D**, standards run beside the same set from which A-C were obtained.

Larger variation in levels of extracted inositol phosphates was seen in leg muscle compared breast muscle. As noted in all tissue types trialled, the same InsP species were detected across the triplicate tissue extractions (Fig 3.6A-C), with InsP₄ and InsP₅ species identifiable compared to the *myo*-InsP₆ hydrolysed standard run alongside the samples, and detectable InsP₆ (Fig 3.6D).

3.3.3 Standardised extraction procedure as applied to multiple tissue types

Chromatograms in Fig 3.7(A-D) show identified profiles of inositol phosphates extracted from 100 mg of organ samples from kidney (Fig 3.7A), brain (Fig 3.7B), breast muscle (Fig 3.7C) and leg muscle (Fig 3.7D) from the same bird fed the Control basal diet meeting total bird requirements (described in brief in section 3.2.1.1, further elaborated in Arthur *et al.* (2019)).

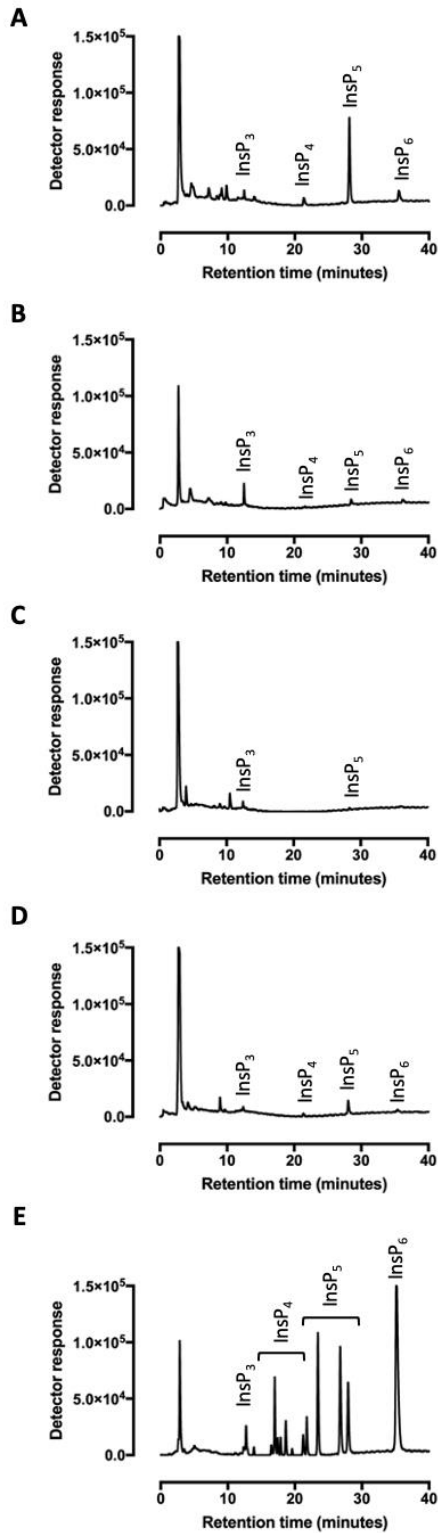


Figure 3.7: Inositol phosphates in broiler tissue. Extracts of **A**, kidney; **B**, brain; **C**, breast muscle; **D**, leg muscle; from a single bird. **E**, standards run besides the sample set from which A, B, C and D were obtained. Inositol phosphate classes are identified in the standard.

In these sample dissections, samples were taken along the coronal plane of the brain, so that only forebrain tissue was extracted, with no visible cerebrum veins present in the tissue. Species of distinct inositol phosphate classes identified in each tissue type were common to all tissue types, with no identifiable tissue-specific species of inositol phosphates separable, and all peaks were identified as *myo*-inositol phosphates based on co-elution with peaks in the hydrolysed *myo*-InsP₆ standard (Fig 3.7E) which gives rise to all separable lower inositol phosphate species.

Different organs show differing concentrations of inositol phosphates, with the highest detectable total inositol phosphate levels noted in kidney tissue samples (Fig 3.7A), followed by leg muscle (Fig 3.7D). Concentrations of InsPs detected in extracted brain and breast muscle samples from the selected bird were low, but identifiable as distinct from baseline noise in the resolved chromatography.

3.3.4 Comparative capacity of feed grade titanium dioxide to extract inositol phosphates

TiO₂, as previously mentioned, is commonly used as an inert digestibility index marker for monogastric animal feeding trials where treatments varying in nature are tested for effect on apparent ileal digestibility of gross energy and nitrogen. The use of TiO₂ by cell biologists as an enrichment method for phosphopeptide and inositol phosphate research (Wilson *et al.*, 2015), and the benefits in applying this method to extraction and analysis of inositol phosphates in poultry tissues (Sprigg *et al.*, 2022), raised concerns as to whether the TiO₂ manufactured for use as a common digestibility index marker can be considered inert, or whether it would behave similarly to the fixed size TiO₂ beads manufactured and marketed for phosphopeptide enrichment purposes.

As such, mixed particle size titanium (IV) oxide manufactured and distributed as an inert digestibility index marker for monogastric feeding trials obtained from Target Feeds was directly compared to Titansphere® spherical (mixed,

5 μm and 10 μm ; GL Sciences Inc.) bulk material for its capacity to enrich inositol phosphates in solution, and thus its potential for interference in the context of an animal feeding trial. Aliquots, 5 μg , of both TiO_2 types were applied to diluted acid hydrolysed InsP_6 as a representative sample, with the samples extracted as described in section 3.2.2.2, and analysed by HPLC. Resulting chromatograms following resuspension of enriched samples are shown in Figure 3.8.

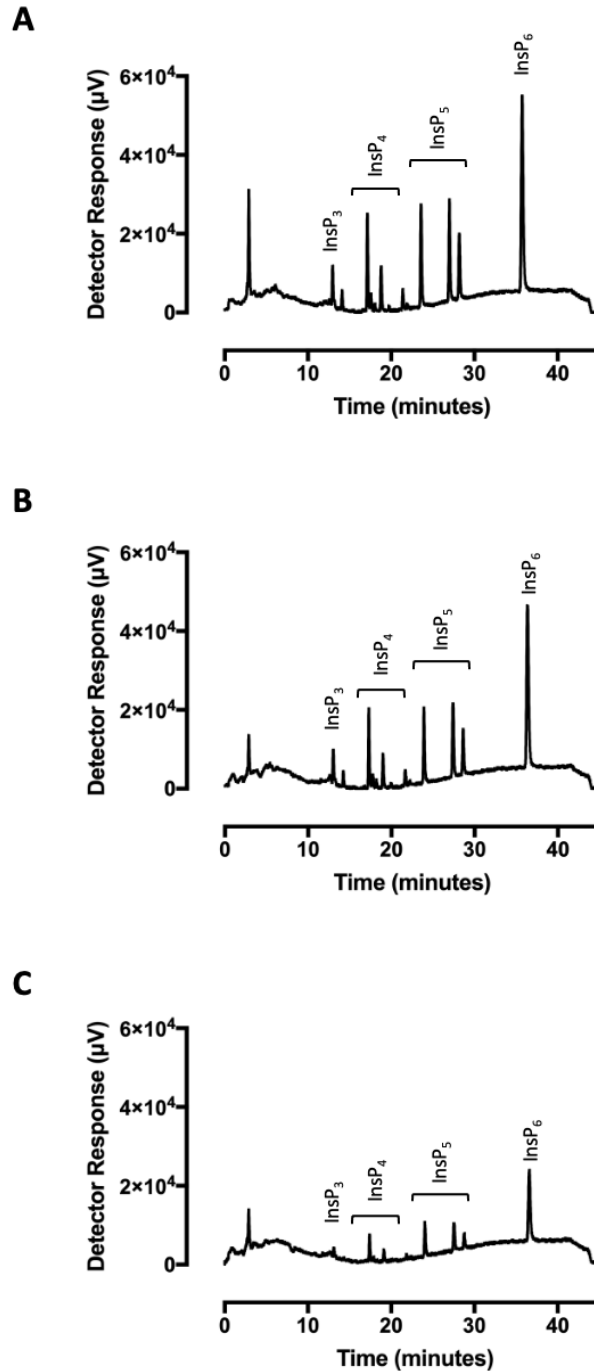


Figure 3.8: Chromatograms for comparative purification of acid-hydrolysed InsP₆, where **A** is the starting sample of acid hydrolysed InsP₆, **B** is the resulting sample following purification with Titansphere® TiO (GL Sciences Inc.) and **C** is the resulting sample following purification with feed grade TiO₂ (Target Feeds).

With comparison to the known spiked concentration of InsP₆ hydrolysate used as a model sample, the commercial Titansphere® TiO₂ had over twice the binding capacity of the feed grade TiO₂ mixture obtained from Target feeds, with calculated recovery of InsP₆ hydrolysate following processing through the extraction protocol 79% of total from the Titansphere® TiO₂ compared with 32% from the feed grade TiO₂. This difference in extraction capacity may be due to the difference in particle size, with the TiO₂ manufactured for phosphopeptide enrichment of a fixed 5 µm and 10 µm spherical shape, as opposed to mixed particle size of the bulk material in the indigestible marker. However, the ability of the feed grade TiO₂ to bind and retain the InsP₆ hydrolysate through the extraction protocol for enrichment suggests that the material used is not as inert as considered, and the TiO₂ formulated for use as a digestibility index marker retains the same chemical ability to interact with phosphates under *in vitro* conditions as the commercial phosphopeptide enrichment brand.

3.4 Discussion

3.4.1 Chromatographic resolution of tissue inositol phosphate species

The use of TiO₂ as both bulk material and pre-packed columns have proven useful tools for the enrichment of phosphopeptides (Pinkse *et al.*, 2004), and has been proven effective for the purification of low concentration inositol phosphates from large volumes of acidified mammalian cell extracts (Wilson *et al.*, 2015). Nevertheless, the published method of Wilson and colleagues couples extraction of TiO₂ enriched inositol phosphates with PAGE analysis which broadly limits separation to inositol phosphate classes. Additionally, it is restricted to higher inositol phosphate classes as lower inositol phosphates (i.e. InsP₃) stain poorly by toluidine blue and cannot be quantified by gel electrophoresis. The coupling of this TiO₂ enrichment extraction method with existing HPLC methods (Whitfield *et al.*, 2018) allows for easy separation of inositol phosphate classes and species (with the exception of paired enantiomers, phosphorylated on the 1- or 3- position and/or the 4- or 6-

position of the inositol ring). Moreover, it offers far simpler quantification of inositol phosphates in samples by direct comparison to detector response to standards of known concentrations, rather than quantification of band density on gels by colorimetric methods.

The acronym QuEChERS is given to sample extraction methods designed for chromatographic analysis of analytes in a variety of samples, first introduced for pesticide residues analysis in high moisture fruit and vegetables, and expands to describe methods that are: Quick, Easy, Cheap, Effective, Rugged and Safe, including using small amounts of material and solvent (Rejczak and Tuzimski, 2015). Whilst this refers to a specific method (Anastassiades *et al.*, 2003), the concepts are broadly applicable to the design and optimisation of disruptive extraction methods. Typically, extraction of inositol phosphates from animal organs in this context would require extensive whole animal radiolabelling with ^3H -inositol, making analysis expensive, problematic and unattainable for the majority of research groups without access to facilities licensed to carry out this work and the methods for later analysis of the findings. This restricts such work to cultured tissue or small animal work, not relevant for this type of study. The method described here removes the obstacle presented by large-scale radioisotope feeding trials in animals, utilising TiO_2 beads instead for enrichment of low concentration acid-soluble inositol phosphates for purification from tissue samples. It can be carried out in multi-sample batches as well as on low volumes of tissue samples allowing for replicate measurements without exhausting whole organs for single measurements.

3.4.2 Potential implications for the suitability of titanium dioxide as a digestibility index marker

Inert digestibility index markers are the anchor of many animal feeding trials designed to analyse nutrient utilisation and amino acid digestibility along the gastrointestinal tract. Their use is widely accepted as a method less labour intensive than simple balance sheets of quantitative analysis of feed intake vs faeces and urine. Digestibility markers, chromium dioxide, CrO_2 , or

chromic oxide, Cr₂O₃; titanium dioxide, TiO₂ and acid-insoluble ash, AIA; are commonly used at inclusion level of 0.1 to 0.5% (Zhang and Adeola, 2017), though the rational of choice of marker in individual studies is rarely qualified. A meta-analysis of poultry studies revealed substantive differences in ileal amino acid digestibility coefficients between CrO₂, TiO₂- or acid insoluble ash-normalized feeding trials (Cowieson *et al.*, 2017). An explanation of the differences was beyond the scope of the study, but one might hypothesize variability in recovery of the marker through the digestive tract, biochemical reactions of the marker with the tract and its contents as potential explanations.

Several studies have compared the use of chromic oxide (Cr₂O₃), a widely accepted digestibility index marker in ruminant animals, with the commonly used inert marker TiO₂ in monogastrics, for the effect on apparent ileal digestibility of gross energy and nitrogen. Some have reported inconsistent results pertaining to the effects of the type of digestibility index marker on the apparent ileal digestibility and apparent total tract digestibility of amino acids and gross energy, and the recovery of the marker itself, and that this affect can be diet dependent (Wang and Adeola, 2018). Nevertheless, the reproducibility of measurements of TiO₂ post recovery, and the safety of TiO₂ compared to the carcinogenic properties of Cr₂O₃, have positioned TiO₂ as the most suitable marker for use in most animal feeding trials. However, the interest in the comparison of different digestibility index markers has brought to the fore the disparities in results with different markers which implies they may have specific interactions with dietary components.

Quite separately, the employ of TiO₂ has grown in popularity in a parallel field of study, that of intracellular cell biology where it has been used as a solid phase extraction medium for concentration of inositol phosphates (Wilson *et al.*, 2015), with adapted methods for use in extraction and concentration of inositol phosphates in poultry tissues described in this chapter. The method of extraction for inositol phosphates using TiO₂ (section 3.2.2.2; published Wilson *et al.*, 2015; Sprigg *et al.*, 2022) requires incubation at an acidic pH for an extended period for phosphate containing compounds

to be adsorbed to the surface of the TiO₂ particles, before subsequent elution steps at a basic pH of approximately pH 10.0. This transition from binding in acidic to eluting in basic conditions mirrors the transit time and pH changes measured in different segments of the digestive tract of broiler chickens, from acidic pH (2.5 – 3.5) in the proventriculus/gizzard to basic in the terminal ileum and cecum/colon (pH 8.0) (Ravindran, 2013). Crucially, it eludes to theoretical possibility that the digestive tract provides opportunity for *in vivo* interactions between TiO₂ as a marker and phosphopeptides in the digestive tract, with the acidic pH of the early tract ideal for binding phosphate containing compounds to TiO₂ which would then be later extractable by basic digesta extraction methods usually carried out at pH 8.0-10.0 (Ajuwon *et al.*, 2020; Whitfield *et al.*, 2022). Additionally, the indiscriminate binding of TiO₂ to all inositol phosphate isomers could also have the potential of interrupting phytase degradation of inositol phosphates bound to TiO₂ during gut transit should these interactions occur *in vivo*, which may in part be reflected in the oft noted phenomena of complete InsP₆ hydrolysis in the gizzard in poultry that then reappears in ileal digesta samples.

For all the foregoing reasons, it became evident that the effect of the addition of TiO₂ as a digestibility index marker on the measurement of dietary inositol phosphates required further investigation in the context of poultry feeding trials in order to ascertain any potential effect the inclusion of TiO₂ may have on the subsequent recovery of inositol phosphates when *in vitro* assays show feed supplemented TiO₂ is capable of interacting with inositol phosphates. It is, however, important to note that, as of 5th May 2021, official Regulation came into place regarding the safety of use of titanium dioxide in animal feed due to potential for genotoxicity, requiring the withdrawal of additive TiO₂ or premixes for animal consumption containing TiO₂ from by 20th June 2022 in the EU (Bampidis *et al.*, 2021). The feeding trial carried out as part of this research, as described in later chapters 4, 5 and 6, were carried out prior to this change in legislation in accordance with Home Office Regulations.

4. The effect of phytase supplementation on the appearance of lower inositol phosphate esters in the broiler digestive tract

4.1 Introduction

Feeds formulated for intensely reared poultry are produced largely of wheat and wheat by-products, maize and maize by-products, cereals and grain legumes and meal (McDonald, Edwards and Greenhalgh, 1990). Therefore, depending on cereal source, a broad variety of basal phosphate concentrations and endogenous grain phytase activity exists in the feedstuffs (Eeckhout and De Paepe, 1994). The majority of dietary phosphate in animal feed mash is present as phytate, the salt form of phytic acid (*myo*-inositol 1,2,3,4,5,6-hexakisphosphate; InsP₆), the primary storage form of phosphate in plant tissues, but a form with largely reduced availability for digestion by non-ruminant animals (Lucca *et al.*, 2016).

Poultry diets are now often supplemented with microbial phytase (Selle and Ravindran, 2007) with the intention of accessing phytate-bound phosphate as an economical phosphate source in order to circumvent the need for the addition of inorganic rock phosphate.

Phytate as a phosphate source had been previously assumed to be poorly utilised by poultry species because of a lack of enzymes capable of InsP₆ hydrolysis naturally available in the avian digestive tract, though endogenous phytase enzymes in avian species have been described (Alaeldein M. Abudabos, 2012). Poultry and swine do both possess small intestinal phytases, and in very low calcium diets chickens are capable of breaking down as much as 70% of the phytate bound phosphorous, however when fed commercial diets with sufficient calcium levels the intestinal phytase in poultry is largely ineffective (Maenz and Classen, 1998). This is partly explained by the ability of phytate to readily form both soluble and insoluble chelates with multivalent cations (Cheryan, 1980), and these associations are postulated to decrease association of mineral co-factors with intestinal phosphatases and thus shift equilibriums toward less active conformations

(Maenz and Classen, 1998). The impact of poultry endogenous enzymes on dietary phytate degradation is considered to be insignificant, and the involvement of plant endogenous phytase activity still present in grain derived food is believed to also be limited. The changing gut pH is likely to reduce plant phytase stability (Leytem, Widyaratne and Thacker, 2008), which coupled with the impact of high-temperature pelleting of mash diets renders grain endogenous phytases ineffective in degrading phytate in poultry diets.

The ability of non-ruminant animals, those with single stomachs, to digest phytate P varies considerably, with reports citing loss of phytate from the digestive tract between 10 to 50% (Cowieson, Acamovic and Bedford, 2006). Endogenous phytase activity has been found to be higher in the duodenum than in any other intestinal segment in poultry (Maenz and Classen, 1998), with phytase activity attributed to the small intestinal brush border mucosa. Studies in rats have shown that the production of these endogenous intestinal phytases is stimulated by the presence of phytic acid in the duodenum and jejunum (Lopez *et al.*, 2000), though these studies also state that whilst these endogenous enzymes show high activity when animals are fed a diet containing purified phytic acid, the activity is negligible in the hydrolysis of normal dietary phytate (Jongbloed, Mroz and Kemme, 1992; Rapp, Lantzsich and Drochner, 2001), and is inhibited by increased concentration of inorganic phosphate in the gut lumen (Greiner, Konietzny and Jany, 1993; Hu, Wise and Henderson, 1996).

Previous studies have characterised InsP₆ hydrolysis and the lower InsP isomer products in different segments of the digestive tract of broilers with the addition of supplementary exogenous phytases of a variety of origins to the feed (Zeller *et al.*, 2015b), with most added microbial phytase activity occurring in the crop and gizzard due to their active pH range suited to the acid environment found here (Yu *et al.*, 2004; Onyango, Bedford and Adeola, 2005), though exogenous supplementary phytases of bacterial origin are more likely to retain activity into the jejunum and ileum than fungal phytases (Simon and Igbasan, 2002). In the present study, digesta analysis was

carried out to confirm previously established patterns for gastrointestinal phytase-mediated generation of inositol phosphates in different parts of the digestive tract, and to confirm that these effects are separable from the effects of inositol supplementation at the predicted concentration of released inositol from complete phytate hydrolysis by phytase addition.

4.2 Materials and methods

4.2.1 Animals and management

The study was performed at Nottingham Trent University (NTU) Poultry Research Unit, School of Animal, Rural and Environmental Sciences, NTU. Institutional and UK national NC3R ARRIVE guidelines for the care, use and reporting of animals in research (Kilkenny *et al.*, 2010) were followed during the study and all experimental procedures were approved by Nottingham Trent University's animal ethics review committee (internal code ARE202134). Birds underwent routine vaccination for Marek's Disease and Infectious Bronchitis (IBH120) at the commercial hatchery.

An Owner Informed Consent form was signed by the legal owner of the animals and the use of the animals authorised in this study, confirming compliance with all study protocol requirements and legal requirements including safe disposal of animals in this study. All regulatory requirements including applicable animal welfare regulations were strictly complied with by Nottingham Trent University, and conduct of the study was authorised by Nottingham County Council Trading Standards and the Food Standards Agency.

A total of 480 male Ross 308 broiler chicks were supplied from a commercial hatchery (PD Hook, Cote, Oxford, UK) in a 21 day experiment. On day 1, chicks were randomly allocated to one of 8 dietary treatments; each of which had 6 replicate floor pens (0.8 x 0.8 m, stocking density 15.2 birds/m² i.e. approximately 15 kg per m² at trial end) bedded on wood shavings, with each

pen containing 10 birds. Light was provided for 23 hours with 30-40 lux intensity, 1 hour dark, and gradually adjusted to achieve 4-6 hours of dark by day 7, with 30 minutes of dawn/dusk lighting applied either side of dark period. The temperature of the housing unit was set to 30°C at day 1 and gradually decreased to 22°C over the rearing period. Air quality measurements of carbon dioxide and ammonia levels were monitored, with ammonia not exceeding 25ppm. Diets and water were offered *ad libitum* for consumption until euthanasia at d 21.

Data for mean gizzard and ileal inositol contents in responses to phytase with N and standard error reported by Walk *et al.* (2018) was used to conduct a power calculation indicating 6 replicates per treatment were sufficient to identify treatment differences at a power setting of 80% and a type 1 error rate of 5%.

Table 4.1: Animal feeding trial study design

Number of treatments:	8
Replicates per treatment:	6
Animals per replicate:	10
Randomisation plan for treatment allocation:	Randomised within regional blocks in single pen room
Diet phases:	Starter – 0-21d

Table 4.2: Animal feeding trial study parameters

Parameter	Study Day	Comments
Body weights, g	0, 7, 14, 21,	Animals were weighed on a per pen basis. Aim to weigh birds at approximately the same time on each day of weighing. Aim to weigh the birds using the same sequence of pens on each weighing occasion. On Day 0, weighing will take place prior to the feeding of the Test Diets and on Day 21 prior to slaughter.
Feed intake, g	0, 7, 14, 21,	Recorded weight of all feed offered (including any additional feed offered in between) on Days 0, 7, 14, 21) . Recorded weight of all soiled feed removed on Days 0, 7, 14, 21, and throughout the rest of the study as necessary. Weighed the feed from any pen where an animal has been withdrawn at the time of withdrawal in order to adjust feed intake for mortality by calculating bird days.
Feed conversion	0, 7, 14, 21,	To be calculated (and added to the data set) by: Feed consumed /Total weight gain over each weekly period per treatment group.
Mortality	Daily	Dead weight (g) and record cause.
Culls	Daily	Live weight (g) and record cause.
Measure of health status	Daily	Including litter consistency.
Undesirable consequences of treatment structure	Daily	Determined from the above measurement of health status.
Therapeutic/preventative treatments	As it occurs	Plans to record each therapeutic intervention as a result of daily measurement of health status, though no interventions were necessary during the trial.
Digesta collection	21 d	Euthanise 2 birds per pen by schedule one method. Collect material from gizzard and ileum on marked, individual bird basis.
Tissue collection	21d	From the same 2 birds collect brain, kidney, liver and leg/breast muscle samples and digestive tissues

Table 4.3: Pen layout and assigned blocks

pen number	block identifier	treatment	pen number	block identifier	treatment
1	1	D	25	4	A
2	1	F	26	4	C
3	1	E	27	4	D
4	1	A	28	4	F
5	1	B	29	4	E
6	1	H	30	4	H
7	1	C	31	4	B
8	1	G	32	4	G
9	2	D	33	5	H
10	2	G	34	5	D
11	2	F	35	5	C
12	2	H	36	5	F
13	2	C	37	5	B
14	2	B	38	5	A
15	2	E	39	5	G
16	2	A	40	5	E
17	3	F	41	6	A
18	3	G	42	6	F
19	3	A	43	6	G
20	3	E	44	6	B
21	3	B	45	6	E
22	3	H	46	6	C
23	3	C	47	6	H
24	3	D	48	6	D

Birds were weighed by pen before placement (day 0) and on day 7, day 14 and day 21 to measure mean bird weight (BW) and calculate mean BW gain. Feed intake (FI) was also measured for day 0 to 7, day 7 to 14 and day 14 to 21 and used to calculate feed conversion ratio (FCR). Mortality was recorded daily, and any culled or dead birds were weighed. Treatment FI and FCR were adjusted according to the number of bird days, defined as the number

of days alive in each pen multiplied by the number of days without incidence of mortality. Two birds per pen were randomly selected for sampling on day 21 post-hatch and were euthanized via cervical dislocation without prior stunning by a trained personnel in accordance to the Welfare of Animals at the Time of Killing (England) Regulations (2015) guidelines for poultry.

Average bird weight was calculated as follows:

$$\text{Average bird weight} = \frac{\text{Total pen weight} - \text{Weighing bucket}}{\text{Number of birds alive in pen}}$$

And body weight gain at each measurement interval (Day 7, 14 and 21) as:

$$\text{Body weight gain} = \text{Total pen weight} - \text{Day 0 weight}$$

Individual feed intake was calculated by averaging method, taking into account “bird-days”, as follows:

$$\text{Individual feed intake} = \frac{\text{Total pen feed intake} \times \text{number of days in experimental period}}{\text{sum of the number of alive birds in each day}}$$

This method is limited by the assumption that birds in each pen consume the same amount of feed regardless of their body weight.

From the above data, Feed Conversion Ratio (FCR) was calculated at each measurement interval (Day 7, 14 and 21) as follows:

$$\text{FCR} = \frac{\text{Total weight of feed}}{\text{Net production (Final bird weight} - \text{starting weight)}}$$

4.2.2 Test diet and digesta sampling

Each of eight test diets (Table 4.4) was fed to birds in a total of 6 pens, on an ad libitum basis with the amount consumed recorded on a weekly basis.

Feed samples were collected at the start and end of the phase (days 0 and 21). The study was comprised of one diet phase – a starter, during which birds were offered a crumbled diet ad libitum from Study Day 0 to Day 21.

Formulations of base diet (T1) and others containing test substances (T2-T8) are shown in Table 4.5.

Basal diet preparation and manufacture was provided by Target Feeds, and test substance Quantum Blue 5 g (QB) was provided by the trial sponsor AB Vista. Inositol treatments were prepared at UEA for inclusion in the test diets, with ¹³C Inositol (produced as described in Chapter 3) hand mixed into 500 g commercial ¹²C Inositol (*myo*-Inositol, Thermo Scientific) at a final ratio of d30‰, or 30 parts per thousand ¹³C Inositol to ¹²C inositol.

Table 4.4: Dietary treatments and Test Substance inclusion rates

Dietary Treatment (T)		Test Substance inclusion rates to the basal diet			
		Quantum Blue g/tonne	¹³ C Inositol mix g/tonne	¹² C Inositol mix g/tonne	Titanium Dioxide g/tonne
T1	Control	-	-	-	-
T2	2 g/kg Ins	-	2000	-	-
T3	Phy500	100	-	-	-
T4	Phy6000	1200	-	-	-
T5	Control Ti	-	-	-	5000
T6	2 g/kg InsTi	-	2000	-	5000
T7	Phy500 Ti	100	-	-	5000
T8	Phy6000 Ti	1200	-	-	5000

All Test substances were mixed into the basal diet at the appropriate rates at Target Feeds.

Table 4.5: Ingredient composition and calculated nutrient concentrations of the basal diet.

Ingredient	Starter	Nutrient	Calculated
Wheat	63.12%	Crude protein (%)	21.55
Soybean meal ¹	30.59%	Poultry AME kcal/kg	2961.14
Soy oil	2.70%	Calcium (%)	0.95
Salt	0.35%	Total phosphate (%)	0.73
DL Methionine	0.17%	Available phosphate ³ (%)	0.45
Lysine HCl	0.12%	Phytate P (%)	0.23
Limestone	0.95%	Crude fat (%)	4.11
Dicalcium Phosphate	1.50%	Poultry ME MJ/kg	12.39
Vitamin premix ²	0.50%	Poultry NE Kcal/kg	1952.36

¹48% minimum declared crude protein; sourced from USA.

²Vitamin and Mineral Premix content (per kg diet): Manganese 100 mg, Zinc 88 mg, Iron 20 mg, Copper 10 mg, Iodine 1 mg, Magnesium 0.48 mg, Selenium 0.2 mg, Retinol 13.5 mg, Cholecalciferol 3 mg, Tocopherol 25 mg, Menadione 5.0 mg, Thiamine 3 mg, Riboflavin 10.0 mg, Pantothenic acid 15 mg, Pyroxidine 3.0 mg, Niacin 60 mg, Cobalamin 30 µg, Folic acid 1.5 mg, Biotin 125 µg.

³ Available phosphate (%) does not account for phytate P contribution

From each euthanised bird, the gizzard was excised and opened so the contents could be scraped into a 100 mL container as a pooled sample from both birds, prior to storage at -20°C prior to freeze drying. For ileal digesta collection, digesta from the same two birds was collected by gentle digital pressure into one pot and stored at -20°C prior to freeze drying. Once freeze dried, samples were finely ground with a pestle and mortar and stored at 4°C until analysis.

4.2.3 Diet and digesta extraction

For inositol phosphate analysis, 100 mg of each milled dry feed and digesta sample was extracted with 5 mL of a solution containing 0.02 M EDTA and

0.1 M sodium fluoride (pH 10) as a phytase inhibitor. Samples were incubated shaking for 30 minutes at room temperature, following which samples were sonicated in a chilled sonicator bath for 30 minutes and then incubated at 4°C for 2 hours. Samples were then centrifuged at 9000 x *g* for 15 minutes at 4°C and 1 mL of the supernatant fraction removed and filtered through a 0.45 µm PTFE filter (Kinesis, UK) into 2 ml vials. HCl extracts were additionally performed on 100 mg milled dry feed and digesta samples by incubating by shaking for 30 minutes in 5 mL 0.5 M HCl at room temperature, followed by bath sonicating for 30 minutes and then 2 hour incubation at 4°C, following which samples were centrifuged at 9000 x *g* for 15 minutes at 4°C and 1 mL of cleared supernatant transferred to vials.

4.2.4 HPLC analysis for inositol and inositol phosphates

Samples (20 µL) were analysed by high-performance liquid chromatography and UV detection at 254 nm and 290 nm after post-column complexation with ferric nitrate. Separation of inositol phosphates was achieved on a Dionex CarboPac PA200 column with a corresponding 3 x 50 mm guard column eluted at a flow rate of 0.4 mL min⁻¹ with a linear gradient of methanesulfonic acid, reaching 0.6 M (Lu *et al.*, 2019). Fe(NO₃)₃ solution in 2% HClO₄ was used as the reagent for detection (Phillippy and Bland, 1988) added at a flow rate of 0.2 mL min⁻¹. The elution order of InsPs was established using acid hydrolysed InsP₆ standards. Concentration of InsPs was established by reference to UV detector response to injection of 1 mM InsP₆ (Merck).

For inositol analysis, samples extracted as above were diluted 50-fold in 18.2 MOhm.cm water. Inositol was determined by 2d-HPLC with pulsed amperometric detection of 20 µL aliquots according to Lee *et al.* (2018) on Dionex CarboPac PA1 and MA1 columns. Concentration of inositol was determined using a linear calibration curve from inositol standards (0.01-0.2 nmole in 20 µL, *r*² > 0.995).

4.2.5 Statistical analysis

Inositol phosphates and total inositol phosphates for all 8 treatment groups in the study were compared by two-way ANOVA with Tukey's multiple comparisons test using GraphPad Prism, version 7.0e, for Mac OS X (GraphPad Software, La Jolla, CA); inositol was compared separately by one-way ANOVA with Dunnett's multiple comparisons test using the same software. Individual treatment groups were further compared to the Control by multiple T tests with statistical significance determined using the Holm-Šídák method, with $\alpha = 0.05$, and each row analysed individually without assuming a consistent standard deviation, using the same software. Analysis of difference between groups for the inclusion of TiO_2 as an indigestible marker was performed using regression analysis using the same software. The level of significance for all tests was set at $p < 0.05$. Adjusted p values are presented in the text.

4.3 Results

For analytical comparisons, the dietary groups supplemented with 2 g/kg ^{13}C inositol mixture (d30‰) will in this chapter be considered as a standard inositol dose to be compared to the response from released phytate inositol and phosphates from phytase supplementation.

4.3.1 Diets and bird performance

Diet content was analysed to measure variability between calculated inositol and inositol phosphate contents of basal diets, with predicted increased inositol content in the 2 g/kg Ins and 2 g/kg Ins Ti supplemented diets (Fig 4.1 & 4.2). Diets annotated 'Ti' contain 5 g/kg TiO_2 as a digestibility index marker, absent in those without annotation. Diets Phy500 and Phy500 Ti were supplemented with 500 FTU Quantum Blue phytase, Phy6000 and

Phy6000 Ti were supplemented with 6000 FTU Quantum Blue phytase. Phytase added to the diets should have minimal activity in the dry feed matter.

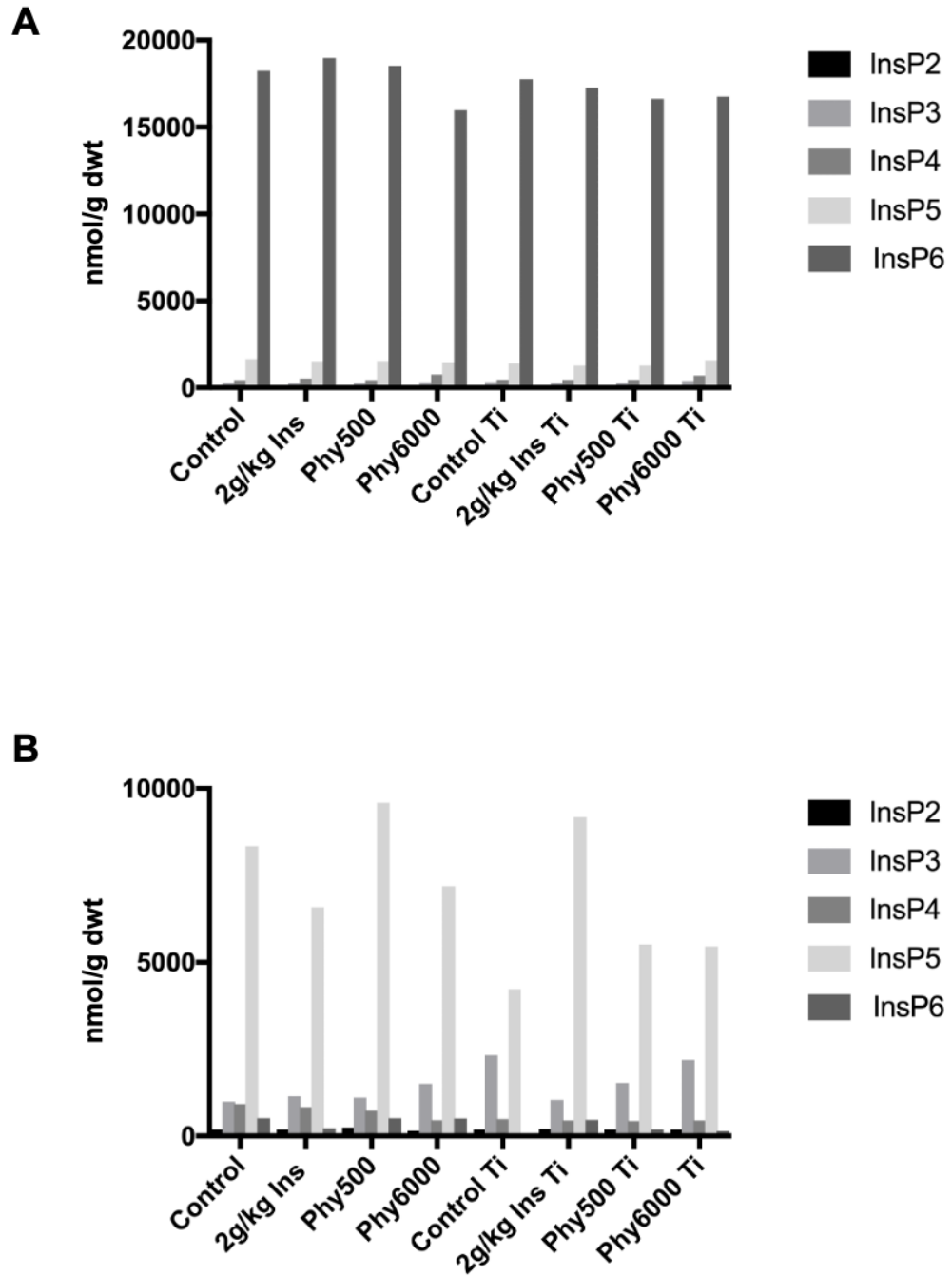


Figure 4.1: Inositol phosphate (InsP₂₋₆) levels (nmol/g dwt) in single measurements of diets fed to broilers from 0-21 days. **A**, diets extracted using adapted method in 0.5 M HCl; **B**, diets extracted using published NaF EDTA extraction method; extracts analysed and quantified by HPLC.

A published method for extraction of inositol phosphates from digesta and diets (Zeller *et al.*, 2015a), that employs sodium fluoride-EDTA buffer (pH 10.0), was used initially for extraction of the diets used in this trial (Figure 4.1 B). However, HPLC analysis found significant variation in the inositol phosphate levels in the diets, most notably a significant reduction in InsP₆ suggesting measurements were impacted by activation of plant endogenous phytases in the basal diets by rehydration at pH 10. This is a commonly observed consequence of the continued activity of these phytases when diets rich in endogenous phytase are used as 'mash' as opposed to a heat-pelleted diet in the feeding trial (Cavalcanti and Behnke, 2004; Moss *et al.*, 2017). As a result of this, diet extractions were repeated using 0.5 M HCl to extract acid soluble inositol phosphates and prevent phytate degradation during the extraction process, the results of which are shown in Figure 4.1 A. Summed totals for inositol phosphates recovered by the two extraction methods are shown in Figure 4.2 AB.

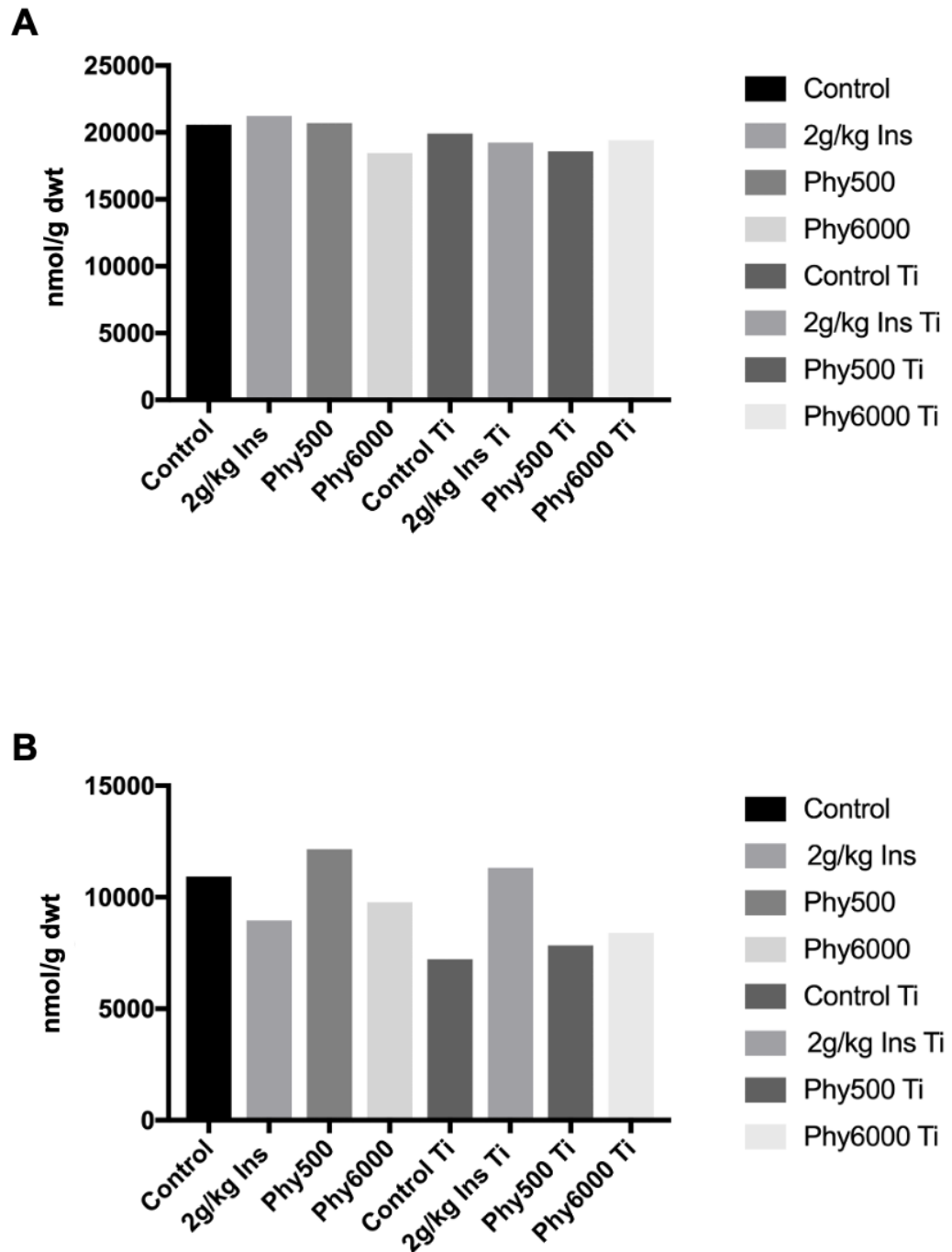


Figure 4.2: Total inositol phosphate (InsP₂₋₆) levels (nmol/g dwt) in single measurements of diets fed to broilers from 0-21 days. **A**, diets extracted using adapted method in 0.5 M HCl; **B**, diets extracted using published NaF-EDTA extraction method; extracts analysed and quantified by HPLC.

In HCl extracts the major constituent of the diet was InsP₆, as expected, with very little variability of this or inositol phosphates between diets. Comparison

with NaF-EDTA extractions indicates that the use of HCl to extract the diets in this instance reduced the impact of endogenous phytase activity on the measurements produced, allowing for confirmation that starting inositol phosphate levels were equal across all diets. Inositol and inositol phosphate concentrations quantified by HPLC are shown in Table 4.6.

Table 4.6. Measured inositol and inositol phosphate levels of basal diets from single measurements. Concentrations given as nmol per gram dry weight.

Diet	Inositol	InsP ₃	InsP ₄	InsP ₅	InsP ₆
Control	80	260	430	1660	18240
2g/kg Ins	6700	190	540	1530	18980
Phy500	100	210	430	1540	18520
Phy6000	60	290	750	1460	15980
Control Ti	160	300	480	1390	17760
2g/kg Ins Ti	7420	230	460	1280	17270
Phy500 Ti	90	220	460	1270	16630
Phy6000 Ti	180	70	690	1600	16760

In respect to inositol concentration, the basal control diets and phytase-supplemented diets contained similar concentrations of inositol, whilst the two inositol supplemented diets measured similarly to each other and subsequently far removed from the other dietary conditions.

Growth performance data is presented in table 4.7, 4.8, and full growth performance data and mortality is presented in Appendix 4. In this study, feed intake (FI) was not influenced by diet during the trial ($p > 0.05$), and whilst there are numerical differences in bird weight (BW) gain and feed conversion ratio (FCR) compared to the Control diet, these differences are also not significant overall for the study period ($p > 0.05$), apart from during the first week of the feeding period where the FCR for Phy6000 was significantly lower ($p = 0.0399$) compared to the Control. Birds in the 2 g/kg Ins-supplemented group showed a significant increase in weight gain (BW)

compared to the Control treatment group over the 21 day period ($p = 0.0089$).

Table 4.7: Influence of diet on growth of broilers¹ from day 0 to day 21

Diet	Week 1 FI, g	Week 2 FI, g	Week 3 FI, g	BW gain, g
Control	172	290	589	700 ^a
2g/kg Ins	159	268	568	769 ^a
Phy500	167	294	617	703
Phy6000	158	305	624	706
Control Ti	148	256	553	726
2g/kg Ins Ti	172	288	582	779
Phy500 Ti	167	293	597	736
Phy6000 Ti	165	300	624	716

¹ Means represent response of 6 replicate pens (60 chicks total, 10 per pen/treatment)

^a Significant difference in BW gain between Control vs. 2 g/kg Ins, $p = 0.0089$

Table 4.8: Growth performance of broilers¹ from day 0 to day 21 calculated feed conversion ratios²

Diet	Week 1 FCR	Week 2 FCR	Week 3 FCR	Total FCR
Control	1.97 ^a	1.38	1.40	1.58
2g/kg Ins	2.01	1.32	1.46	1.60
Phy500	1.76	1.26	1.46	1.49
Phy6000	1.60 ^a	1.23	1.44	1.42
Control Ti	1.73	1.27	1.52	1.51
2g/kg Ins Ti	2.03	1.34	1.43	1.60
Phy500 Ti	1.84	1.35	1.50	1.56
Phy6000 Ti	1.71	1.23	1.42	1.45

¹ Means represent response of 6 replicate pens (60 chicks total, 10 per pen)/treatment

² Feed:gain; corrected for mortality

^a Significant difference in FCR Week 1 between Control vs. Phy6000

4.3.2 Gizzard digesta

The proventriculus and gizzard function as the true stomach in poultry for the mechanical processing of food, where the muscular movements on the gizzard function to grind food mixed with pepsin and hydrochloric acid secreted by the proventriculus, and many birds consume grit and small stones to aid with mechanical digestion of food in the gizzard (Svihus, 2014; Takasaki and Kobayashi, 2020). The gizzard has been shown to be the primary location for phytate hydrolysis by exogenous supplemented phytases in the digestive tract of broilers, with phytase activity declining in later segments of the digestive tract (Truong *et al.*, 2016; Chowdhury and Koh, 2018). In *in vitro* digestion studies, Quantum Blue, the commercial *E. coli* 6-phytase supplemented in this trial, has been shown to be optimally active in an acidic pH range of 3.5-5.0, with similar activity at pH 3.0 and pH 5.5 (Menezes-Blackburn, Gabler and Greiner, 2015), making it ideally suited to the acidic environment of the foregut segments of the crop, proventriculus and gizzard. Given that dietary phytate has also been reported to decrease endogenous carbohydrase activity (Liu *et al.*, 2007), protease activity and peptidase and messengers in the gastrointestinal tract (Liu *et al.*, 2009, 2010), the additional impact of phytate on protein, carbohydrate and nutrient digestibility, and therefore the benefits of phytase activity early in the digestive tract to enable digestion of feed nutrients, cannot be understated.

As differences were noted in the total extractable phytate levels in feed by acidic or basic extraction methods, in relation to endogenous grain phytase activity through rehydration during extraction, gizzard digesta was similarly extracted by both methods for analysis of inositol and inositol phosphates (Fig 4.3 & 4.4).

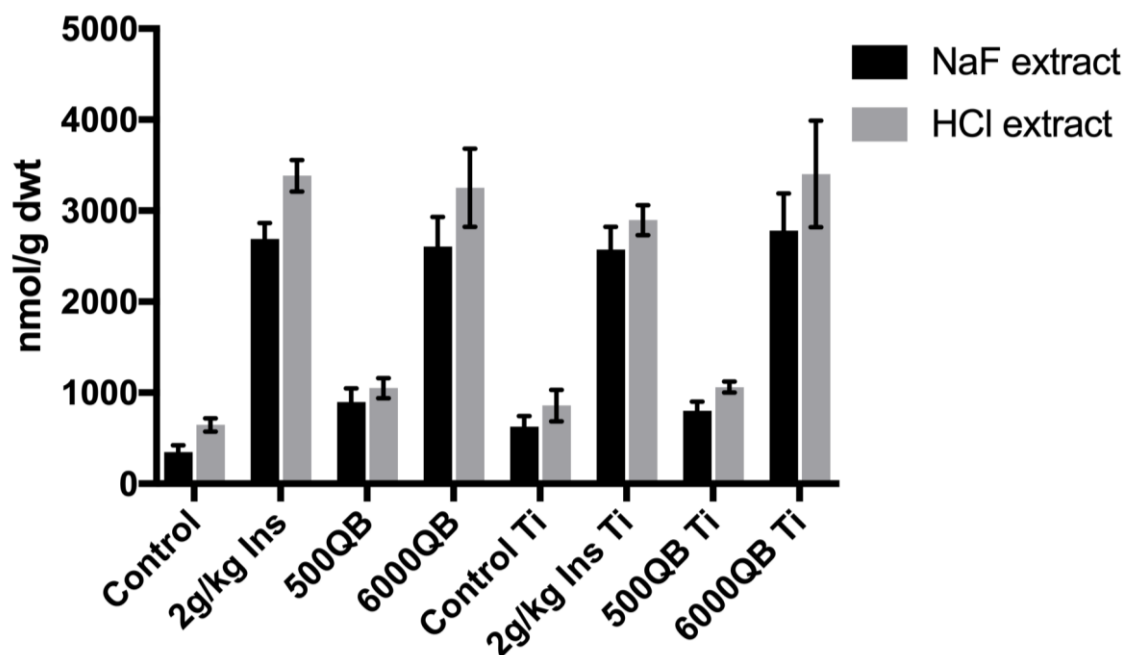


Figure 4.3: Inositol levels (nmol/g dwt) in gizzard digesta of day 21 broilers (6 pens per treatment, with samples pooled from 2 birds per pen). Bars represent standard error of the mean.

Variation in extractable inositol was also noted in the gizzard as in the diets when acid extraction using HCl was compared to sodium fluoride-EDTA (pH 10) buffer (Fig 4.3). Across all treatment groups, HCl extracted more inositol. Analysis of the speciation, InsP_3 vs InsP_4 , InsP_5 , InsP_6 , of inositol phosphates between sodium fluoride-EDTA and HCl extractions is shown in Figure 4.4.

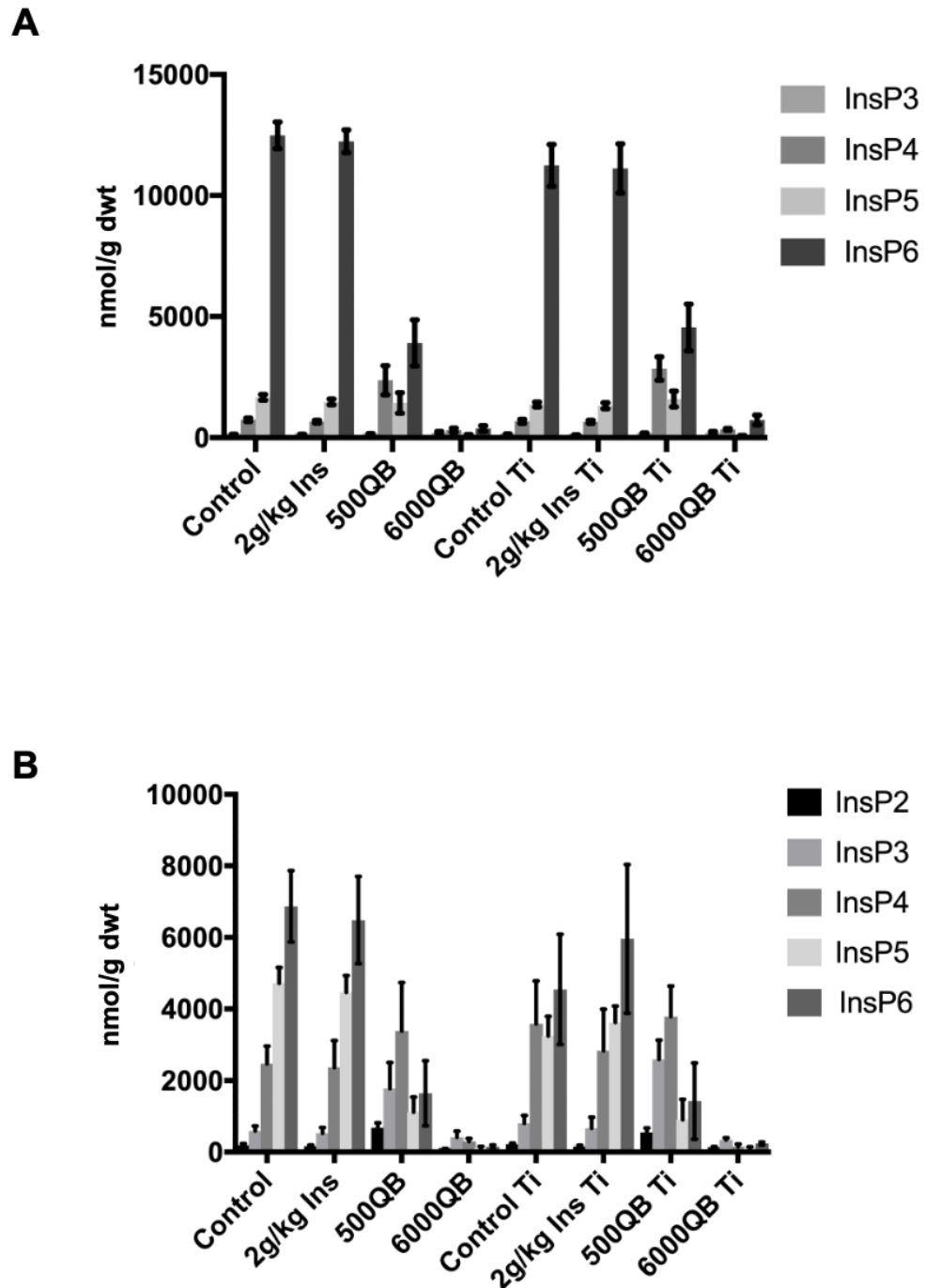


Figure 4.4: Inositol phosphate (InsP₃₋₆) levels (nmol/g dwt) in **A** acid-extracted gizzard digesta samples and **B** NaF-EDTA-extracted gizzard digesta samples of day 21 broilers (6 pens per diet with samples pooled from 2 broilers per pen per treatment). Bars represent standard error of the mean.

The most striking difference between the NaF-EDTA and HCl-extracted samples, is the much-elevated levels of lower inositol phosphates in NaF-

EDTA extracts, across all treatment groups, with a concomitant reduction of InsP₆. Comparing the Control groups, ie. without added phytase, the reduction in InsP₆ (approximately 45%, 5500 nmol/ g d wt) between HCl and NaF-EDTA is not reflected in an increase inositol in the NaF-EDTA extraction: indeed, the inositol content of the NaF-EDTA extract (approximately 350 nmol/ g d wt) is less than that of the HCl extract (approximately 550 nmol/g d wt). While the extent to which inositol is absorbed from the gizzard is unknown, it does seem that the appearance of lower inositol phosphates in the NaF-EDTA-extracted samples arises from feedstuff phytase activities that have not been destroyed during collection and freeze-drying, but which do not progress as far as releasing inositol.

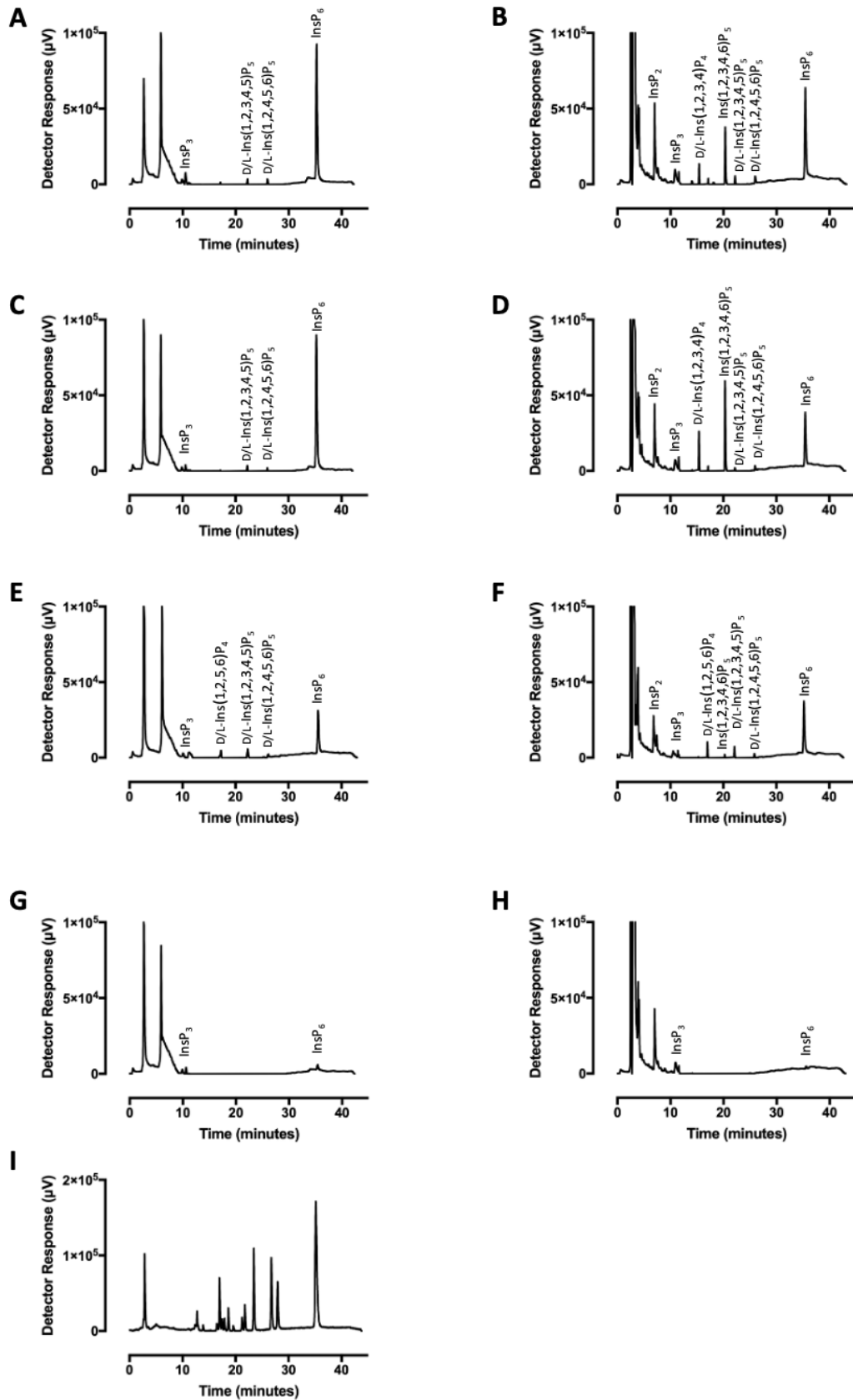


Figure 4.5: Inositol phosphates in broiler gizzard digesta. Extracts of **A**, Control diet gizzard contents from 2 pooled birds extracted in 0.5M HCl; **B**,

the same Control diet gizzard contents extracted in sodium fluoride-EDTA; **C**, 2 g/kg Ins diet gizzard contents from 2 pooled birds extracted in 0.5M HCl; **D**, the same 2 g/kg Ins diet gizzard contents extracted in NaF-EDTA; **E**, Phy500 diet gizzard contents from 2 pooled birds extracted in 0.5M HCl; **F**, the same Phy500 diet digesta extracted in sodium fluoride-EDTA; **G**, Phy6000 diet gizzard contents pooled from 2 birds extracted in 0.5M HCl; **H**, the same Phy6000 diet digesta extracted in sodium fluoride-EDTA. **I**, standards run beside the different samples from which A-H were obtained. Inositol phosphate classes and individual isomers are identified.

Figure 4.5 shows the speciation of lower inositol phosphates for matched samples of both Control and Phy500 diets extracted using the published sodium fluoride-EDTA method (Figure 4.5A, E) and using 0.5 M HCl (Figure 4.5B, F). The identities of the peaks in the set of standards (Figure 4.5I) have been described previously (Rix *et al.*, 2021; Whitfield *et al.*, 2022).

Differences in isomers identified in the same samples between extraction methods can be seen, notably the occurrence of a peak of Ins(1,2,3,4,6)P₅ in the gizzard contents of both Control and Phy500 diet-fed birds but only when extracted under alkali conditions of NaF-EDTA buffer. A peak of D/L-Ins(1,2,3,4)P₄ was similarly observed in the Control diet under alkali extraction, while absent in the acid extracted sample. At the high phytase dose of 6000 FTU, near total phytate hydrolysis is achieved and no difference in extracted inositol phosphate isomers can be identified (Fig 4.5G, H).

The occurrence of peaks of D- and/or L-Ins(1,2,3,4,5)P₅ and D- and/or L-Ins(1,2,4,5,6)P₅ was common to both extraction methods in the Phy500 diet. These isomers are known products of phytase degradation in Quantum Blue supplemented diets. Accordingly, negligible amounts of both isomers, in comparison to InsP₆, were present in the Control-fed gizzard contents.

Diets in this study were fed as a mash, and might therefore have been expected to allow endogenous feedstuff phytase activities to manifest themselves. However phytases have distinct pH optima that may or may not

be matched to the prevailing pH of the gastrointestinal tract. Dionisio and co-workers (Dionisio *et al.*, 2010) have attributed the high mature grain phytase activity of wheat, among cereals, to PAPhy with a pH optimum of 5.5. The other phytase activity of cereals is associated with Multiple Inositol Polyphosphate Phosphatase (MINPP). The former produces a predominant D- and/or L-Ins(1,2,3,4,5)P₅ product, while the latter, a recognized alkaline phytase produces a predominant Ins(1,2,3,4,6)P₅ product, among InsP₅s (Mehta *et al.*, 2006). The absence of Ins(1,2,3,4,6)P₅ in acid extracts, but presence in sodium fluoride-EDTA extracts, may therefore be indicative of persistent feedstuff MINPP activity in the food bolus of the gizzard that became apparent only on rehydration of the milled digesta contents. Ordinarily, heat treatment of pelleted feeds is assumed to degrade endogenous feedstuff phytase activities allowing activity only of adjunct enzyme that is commonly selected for its tolerance of the low pH of the gizzard (Farner, 1942; Dionisio *et al.*, 2011). Collectively, these facets of phytase behaviour could explain the absence of the product associated with MINPP degradation of phytate, Ins(1,2,3,4,6)P₅, in acidic extraction conditions but its presence in basic conditions due to rehydration and extended incubation of the enzymes during the extraction procedure prior to analysis by HPLC.

Table 4.9: Inositol and inositol phosphate (InsP₃₋₆) levels (nmol/g dwt) in acid extracted gizzard digesta of day 21 broilers (6 pens per diet with samples pooled from 2 broilers per pen per treatment). ^{1, 2}

Diet	Inositol	InsP ₃	InsP ₄	InsP ₅	InsP ₆	Σ InsP
Control	646±72 ^a	114±27	743±69 ^b	1668±117	12482±550 ^c	15008±615 ^d
2g/kg Ins	3384±174 ^a	122±26	666±55	1478±116	12238±471	14505±535
Phy500	1051±110	130±45	2374±598 ^b	1453±421	3915±948 ^c	7854±1831 ^d
Phy6000	3252±430 ^a	199±57	319±82	101±33	381±114 ^c	1000±222 ^d
Control Ti	860±173	118±35	678±80	1374±97	11248±869	13419±933
2g/kg Ins Ti	2896±164 ^a	86±28	654±61	1321±123	11122±1012	13182±1094
Phy500 Ti	1062±60	171±18	2853±481	1600±325	4550±966 ^c	9175±1102 ^d
Phy6000 Ti	3404±584 ^a	194±65	349±37	70±27	733±195 ^c	1346±190 ^d

Abbreviations: Σ InsP, total InsP₂ to InsP₆; InsP₆, inositol hexakisphosphate; InsP₅, inositol pentakisphosphate; InsP₄, inositol tetrakisphosphate; InsP₃, inositol trisphosphate; InsP₂, inositol bisphosphate.

¹The control group was fed with a diet with 0.45% calculated available phosphate. Groups Phy500 and Phy6000 were fed with the control diet supplemented with 500 or 6,000 FTU of phytase per kilogram of feed, respectively.

²Data are given as group means ± SEM, n = 6.

In the acid extracted gizzard digesta, significant reductions were measured in InsP₆ and total InsPs for all phytase supplemented diets compared to the Control (for all, $p < 0.0001$). Additionally, InsP₄ concentration in the Phy500 diet was significantly increased at 2374±598 nmol/g dwt compared to 743±69 nmol/g dwt in the Control, representing a 219% increase ($p = 0.0464$).

Inositol extracts were significantly increased in the 2 g/kg Ins and 2 g/kg Ins Ti diets at 3384±174 nmol/g dwt (424% increase) and 2896±164 nmol/g dwt (348% increase) respectively compared to 646±72 nmol/g dwt in the Control (for both, $p < 0.0001$). Supplementation with the “super-dose” of 6000 phytase units, both with and without TiO₂, also significantly increased inositol

in the gizzard measured in the acid extracted samples, at 3252 ± 430 nmol/g dwt in the Phy6000 group (403% increase) and 3404 ± 584 nmol/g dwt in the Phy6000 Ti group (426% increase) compared to the Control (for both, $p < 0.0001$).

Table 4.10: Inositol and inositol phosphate (InsP₂₋₆) levels (nmol/g dwt) in NaF extracted gizzard digesta of day 21 broilers (6 pens per diet with samples pooled from 2 broilers per pen per treatment).^{1, 2}

Diet	Inositol	InsP ₂	InsP ₃	InsP ₄	InsP ₅	InsP ₆	Σ InsPs
Control	348±77 ^a	193±42	591±137	2474±485	4722±441 ^b	6873±996 ^c	14852±817 ^d
2g/kg Ins	2691±174 ^a	167±27	527±159	2368±752	4462±469	6483±1218	14008±884
Phy500	900±147	677±139	1777±728	3387±1354	1122±419 ^b	1645±907 ^c	8606±1757 ^d
Phy6000	2606±326 ^a	75±22	417±166	299±81	97±61 ^b	142±57 ^c	1030±183 ^d
Control Ti	629±116	220±27	806±221	3586±1196	3249±545	4548±1540	12410±720
2g/kg Ins Ti	2573±248 ^a	154±36	670±306	2836±1160	3625±460	5959±2076	13245±1220
Phy500 Ti	802±99	546±126	2593±535	3788±850	906±572 ^b	1426±1065 ^c	9257±1676 ^d
Phy6000 Ti	2782±408 ^a	117±39	344±54	149±73	101±46 ^b	239±39 ^c	950±68 ^d

Abbreviations: Σ InsP, total InsP₂ to InsP₆; InsP₆, inositol

hexakisphosphate; InsP₅, inositol pentakisphosphate; InsP₄, inositol tetrakisphosphate; InsP₃, inositol trisphosphate; InsP₂, inositol bisphosphate.

¹The control group was fed with a diet with 0.45% calculated available phosphate. Groups Phy500 and Phy6000 were fed with the control diet supplemented with 500 or 6,000 FTU of phytase per kilogram of feed, respectively.

²Data are given as group means ± SEM, n = 6.

For NaF-EDTA-extracted samples, supplementation of the diet with Phy500 and Phy6000 reduced total inositol phosphates significantly (for Phy500, $p = 0.037$; for Phy6000, $p < 0.0001$) in gizzard contents (Table 4.9 and 4.10), with reductions in InsP₆ and total inositol phosphates proportional with increasing phytase dose. Total inositol phosphate levels were reduced from 14852 ± 817 nmol/g dwt (dry weight) in the Control group to 8606 ± 176 nmol/g dwt at Phy500 (42% decrease) and to 1029 ± 183 nmol/g dwt at Phy6000 (93% decrease). Phytase at 500 FTU/kg reduced InsP₅ and InsP₆ significantly (for InsP₅, $p = 0.001$; for InsP₆, $p = 0.018$), from 4721 ± 440

nmol/g dwt and 6872 ± 995 nmol/g dwt, respectively, to 1121 ± 419 and 1645 ± 905 nmol/g dwt (76.26% decrease in InsP₅ and 76.06% decrease in InsP₆). The “super dosed” group at Phy6000 also showed highly significant reductions (for InsP₅, $p = 0.0003$; for InsP₆, $p < 0.0001$) in InsP₅ (96 ± 61 nmol/g dwt, 97.97% decrease) and InsP₆ (142 ± 57 nmol/g dwt, 97.93% decrease). InsP₂ levels were also significantly increased in the Phy500 inclusion diet (677 ± 139 nmol/g dwt) compared to the Control (193 ± 42 nmol/g dwt) ($p = 0.037$, 250% increase). Numerical reductions are noted in the InsP₃ and InsP₄ concentrations in the phytase-supplemented diets, but these differences are not significantly different from the Control.

Inositol levels in the gizzard contents were impacted by both the inclusion of dietary phytase and dietary inositol (Table 4.10). Highly significant increases in inositol were measured with the inclusion of 2 g/kg Inositol ($p < 0.0001$) and at Phy6000 ($p < 0.0001$), and significant but less so at Phy500 ($p = 0.037$) compared to the Control. Inositol levels were measured at 348 ± 77 nmol/g dwt in the gizzard digesta for the Control group, 2691 ± 174 nmol/g dwt at 2 g/kg Ins (673% increase), 900 ± 147 nmol/g dwt at Phy500 (158% increase) and 2606 ± 326 nmol/g dwt at Phy6000 (649% increase).

Numerical differences between replicate treatment groups with and without the inclusion of 5 g/kg TiO₂ as a digestibility index marker were deemed not significant by ANOVA comparison for inositol phosphates and inositol, and regression analysis (Appendix 5) showed differences between measured slopes for phytase dose with and without TiO₂ are not significant ($p = 0.9231$).

4.3.3 Ileal digesta

It has previously been reported that the lower gut segments of the duodenum, jejunum and ileum are the sites of inositol and phosphate absorption in birds (Huber, Zeller and Rodehutschord, 2015; Huber, 2016; Hu *et al.*, 2018). Studies have found that, in the absence of supplemented phytase, the majority of InsP₆ hydrolysis occurs by the end of the duodenum

and jejunum, though can continue into the ileum and caeca, with endogenous mucosa phytase activity reportedly highest in the duodenum and jejunum (Maenz and Classen, 1998; Alaeldein M. Abudabos, 2012). Lactic acid bacteria isolated from chicken intestines have also been noted to carry out phytate hydrolysis (Raghavendra and Halami, 2009), and therefore intestinal InsP₆ hydrolysis in the absence of exogenous supplemented phytase is likely a result of a combination of endogenous and microbiota phytase activity.

Ileal samples were extracted in both sodium fluoride-EDTA and HCl. Again, like the analysis of gizzard contents, HCl was a more efficient extractant of inositol than NaF-EDTA (Figure 4.8) across all treatment groups. In contrast, to the gizzard analyses, however, HCl and NaF-EDTA were remarkably similar in their extraction efficiency for inositol phosphates (Figure 4.7). Thus, across treatment groups, HCl extracted between 520 and 72495 nmol InsP₆ per gram dwt, while NaF-EDTA extracted between 859 and 65168 nmol InsP₆ per gram dwt. The profiles of inositol phosphates extracted with the two extractants were very similar also, suggesting that the endogenous phytase activities that confound measurements of inositol phosphates in gizzard contents of birds fed mash diets do not persist in the ileum. This conclusion is further justified by analysis of the speciation of InsP₄ and InsP₅ within these classes, which shows the lack of Ins(1,2,3,4,6)P₅ among InsP₅s within the phytase-supplemented groups.

The presence of InsP₅ and lower inositol phosphates in the Control and Inositol-supplemented groups is common across both extraction methods, suggesting these peaks are not an artefact of the extraction technique but instead have arisen from gut endogenous phytase and/or phosphatase activities (Fig 4.6, A-D). Interestingly, these isomers share similarities with those generated by exogenous phytase supplementation, though at different ratios compared to the InsP₆ concentrations present, with D/L-Ins(1,2,3,4,5)P₅ the dominant InsP₅ isomer in phytase supplemented groups (Fig 4.6E-H), and present to a lesser extent in the Phy500 diet D/L-Ins(1,2,4,5,6)P₅ (Fig 4.6E, F). In both phytase-supplemented groups, D/L-

Ins(1,2,5,6)P₄ is the dominant InsP₄ present in the samples. In the groups without added phytase, Control and 2 g/kg Ins, D/L-Ins(1,2,3,4,5)P₅ is also the dominant InsP₅ species, though with near equal levels of D/L-Ins(1,2,4,5,6)P₅ and reduced but measurable levels of Ins(1,2,3,4,6)P₅. The predominant InsP₄ species in these samples is also D/L-Ins(1,2,5,6)P₄, with measurable peaks corresponding to D/L-Ins(1,2,3,4)P₄ (Fig 4.6A-D). The differing profiles for InsP₅ and InsP₄ in the absence of supplemented phytase suggest the involvement of phosphatases of different origin later in the digestive tract, particularly when compared to the ratios of profiles observed in the gizzard contents in these same samples.

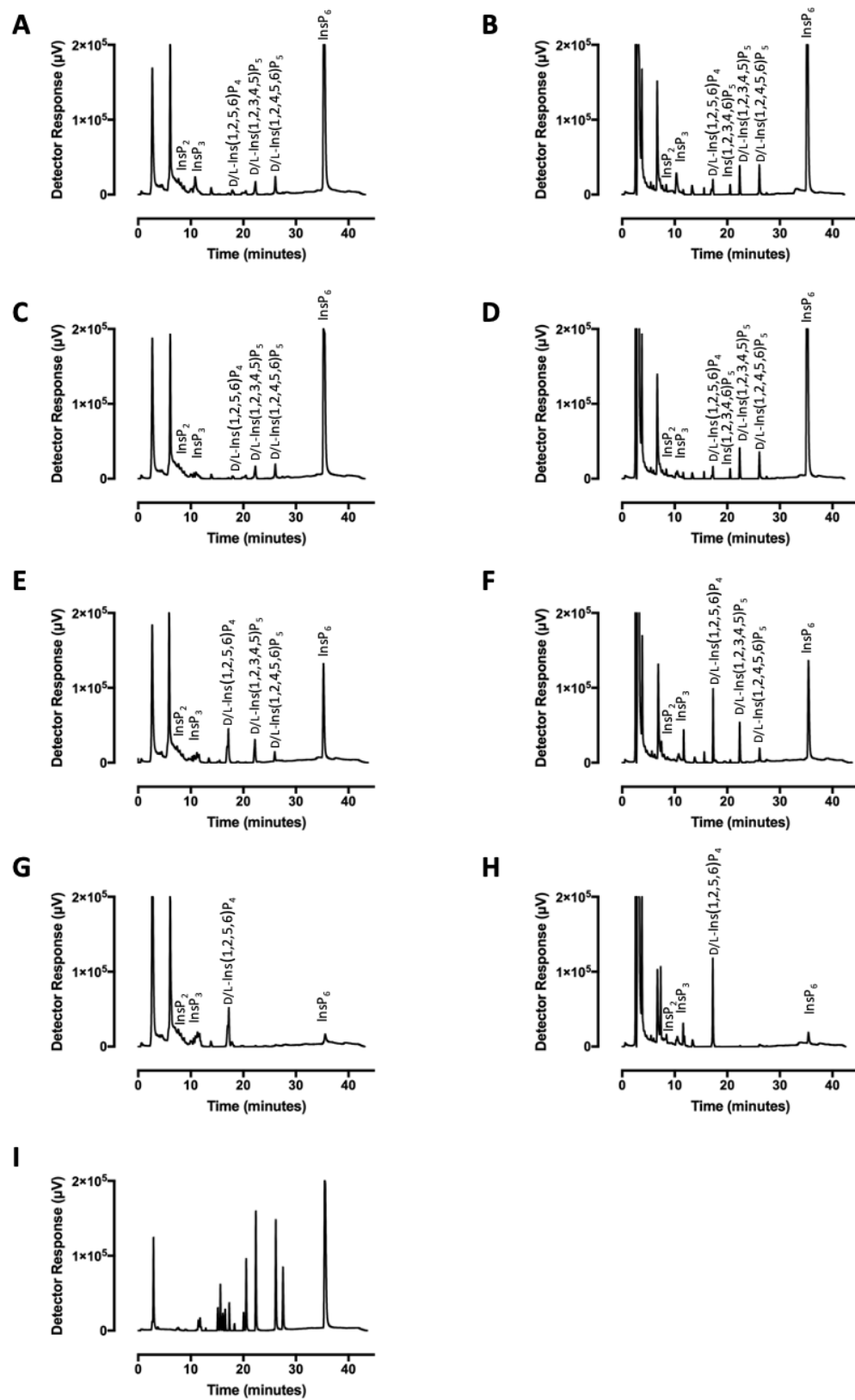


Figure 4.6: Inositol phosphates in broiler ileal digesta. Extracts of **A**, Control diet ileum contents from 2 pooled birds extracted in 0.5M HCl; **B**, the same

Control diet ileum contents extracted in NaF-EDTA; **C**, 2 g/kg Ins diet ileum contents from 2 pooled birds extracted in 0.5M HCl; **D**, the same 2 g/kg Ins diet ileum contents extracted in NaF-EDTA; **E**, Phy500 diet ileum contents from 2 pooled birds extracted in 0.5M HCl; **F**, the same Phy500 diet ileum digesta extracted in NaF-EDTA; **G**, Phy6000 diet ileum contents pooled from 2 birds extracted in 0.5M HCl; **H**, the same Phy6000 diet ileum digesta extracted in NaF-EDTA. **I**, standards run beside the different samples from which A-H were obtained. Inositol phosphate classes and individual isomers are identified.

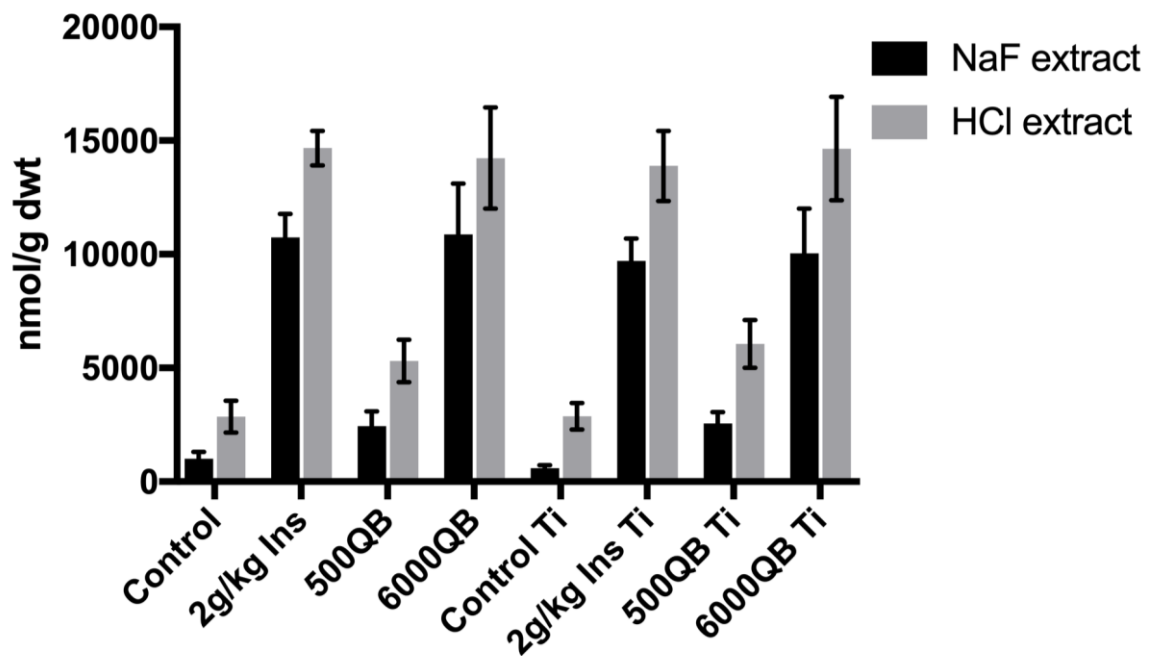


Figure 4.7: Inositol levels (nmol/g dwt) in ileal digesta of day 21 broilers (6 pens per treatment, with samples pooled from 2 birds per pen). Bars represent standard error of the mean.

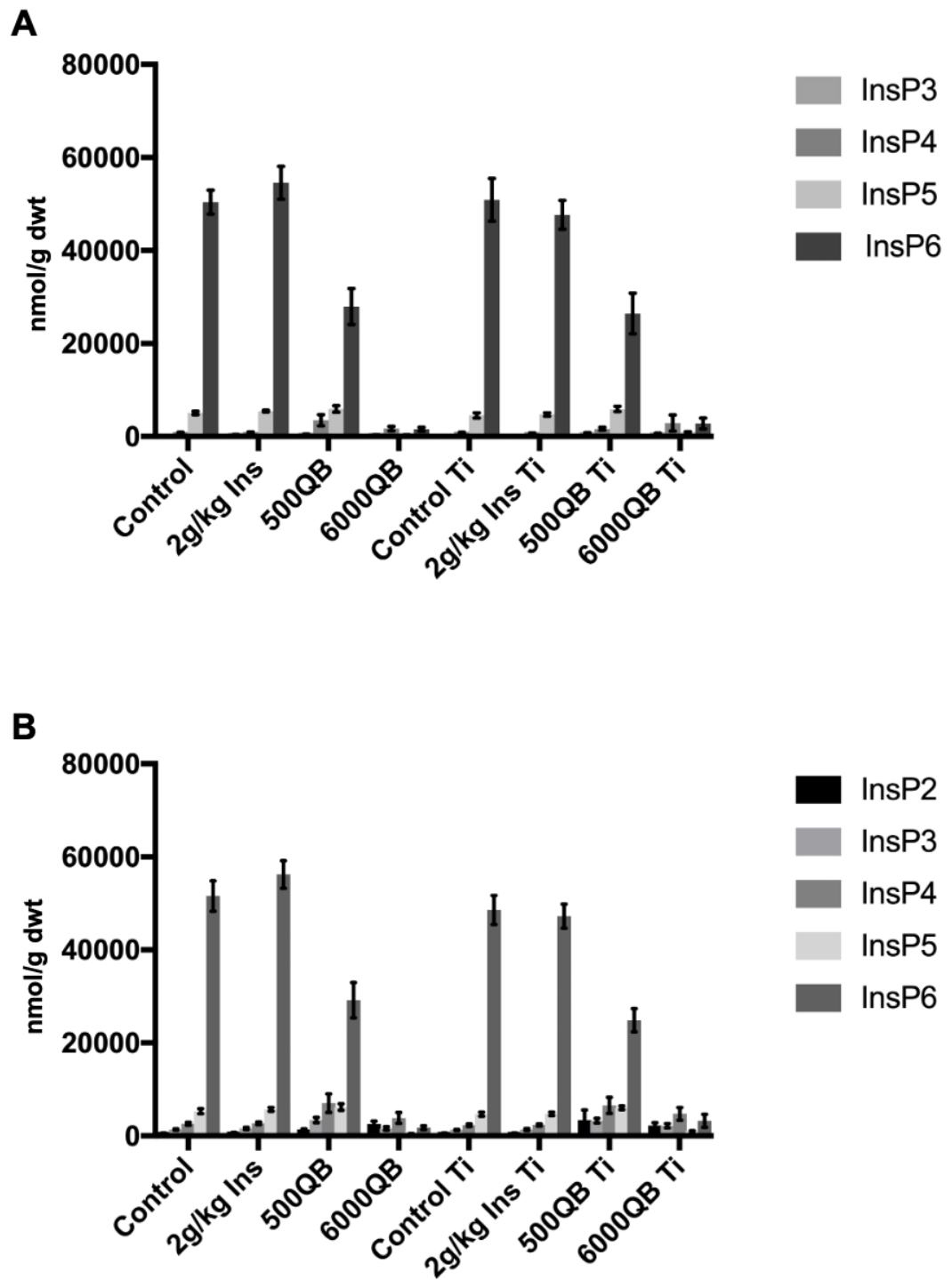


Figure 4.8: Inositol phosphate (InsP₃₋₆) levels (nmol/g dwt) in **A** acid-extracted ileal digesta samples and **B** NaF-EDTA-extracted ileal digesta samples of day 21 broilers (6 pens per diet with samples pooled from 2 broilers per pen per treatment). Bars represent standard error of the mean.

Table 4.11: Inositol and inositol phosphate (InsP₃₋₆) levels (nmol/g dwt) in ileal digesta of day 21 broilers (6 pens per diet with samples pooled from 2 broilers per pen per treatment, 0.5M HCl extracted). ^{1, 2}

Diet	Inositol	InsP ₃	InsP ₄	InsP ₅	InsP ₆	Σ InsP
Control	2854±702	31±10	762±170	5083±364	50393±2571	56269±2853
2 g/kg Ins	14671±756	216±168	780±199	5466±199	54571±3544	61033±3434
Phy500	5305±936	323±136	3510±1183	5937±707	27971±3883	37741±3433
Phy6000	14231±2226	241±92	1697±477	293±54	1579±391	3810±893
Control Ti	2869±583	41±16	806±100	4536±592	50902±4604	56285±5259
2 g/kg Ins Ti	13886±1542	33±8	612±129	4739±390	47662±3078	53047±3317
Phy500 Ti	6062±1053	571±196	1650±306	5931±538	26458±4386	34609±4572
Phy6000 Ti	14644±2275	451±176	2893±1752	755±270	2812±1150	6910±2420

Abbreviations: Σ InsP, total InsP₂ to InsP₆; InsP₆, inositol hexakisphosphate; InsP₅, inositol pentakisphosphate; InsP₄, inositol tetrakisphosphate; InsP₃, inositol trisphosphate; InsP₂, inositol bisphosphate.

¹The control group was fed with a diet with 0.45% calculated available phosphate. Groups Phy500 and Phy6000 were fed with the control diet supplemented with 500 or 6,000 FTU of phytase per kilogram of feed, respectively.

²Data are given as group means ± SEM, n = 6.

In samples extracted using HCl compared to the published sodium fluoride-EDTA method, total inositol phosphates were significantly reduced in the groups fed 500 and 6000 FTU Quantum Blue, both with and without the inclusion of TiO₂ in the diet. Compared to 56269±2853 nmol/g dwt in the Control fed group, total inositol phosphate levels were reduced to 37741±3433 nmol/g dwt and 34609±4572 nmol/g dwt in the Phy500 (32.92% reduction) and Phy500 Ti groups (38.49% reduction) respectively (for both, *p* < 0.0001); values were further reduced at the higher phytase inclusion level, to 3810±893 nmol/g dwt in the Phy6000 diet (93.23% reduction) and 6910±2420 nmol/g dwt in the Phy6000 Ti diet (87.72% reduction) (for both, *p* < 0.0001). InsP₆ levels were similarly significantly reduced by both inclusion levels of phytase in the ileal contents, by

comparison to the Control fed group at 50393 ± 2571 nmol/g dwt InsP₆, inclusion of 500 FTU phytase reduced the acid-extractable InsP₆ levels to 27971 ± 3883 nmol/ dwt in the Phy500 group (44.49% reduction) and to 26458 ± 4386 nmol/g dwt in the Phy500 Ti group (47.5% reduction) (for both, $p < 0.0001$), and similarly further reduced in the higher phytase supplemented group to 1579 ± 391 nmol/g dwt and 2812 ± 1150 nmol/g dwt for Phy6000 (96.87% reduction) and Phy6000 Ti (94.42% reduction) respectively (for both, $p < 0.0001$).

Acid-extractable inositol levels were significantly increased in the diets supplemented with 2 g/kg inositol and 6000 FTU phytase, with and without TiO₂, compared to the Control group. Inclusion of 2 g/kg inositol increased the ileal digesta inositol levels to 14671 ± 756 nmol/g dwt in the 2 g/kg Ins group (414% increase) and 13886 ± 1542 nmol/g dwt in the 2 g/kg Ins Ti group compared (386.5% increase) to 2854 ± 702 nmol/g dwt in the Control fed group (for both, $p < 0.0001$). With the inclusion of 6000 FTU phytase, inositol levels were similarly significantly increased, to levels comparable to the inclusion of 2 g/kg inositol calculated to be the predicted potential liberated quantity of inositol from complete hydrolysis of dietary phytate, at 14231 ± 2226 nmol/g dwt in the Phy6000 diet (398.6% increase) and 14644 ± 2275 nmol/g dwt in the Phy6000 Ti diet (413.1% increase) (for both, $p < 0.0001$).

Table 4.12: Inositol and inositol phosphate (InsP₃₋₆) levels (nmol/g dwt) in ileal digesta of day 21 broilers (6 pens per diet with samples pooled from 2 broilers per pen per treatment, NaF-EDTA extracted).^{1, 2}

Diet	Inositol	InsP ₂	InsP ₃	InsP ₄	InsP ₅	InsP ₆	Σ InsP
Control	1008±297	502±131	1358±156	2613±307	5285±519	51588±3269	61347±3702
2 g/kg Ins	10742±1035	656±122	1610±224	2711±265	5715±409	56214±2966	66905±3306
Phy500	2434±654	1349±173	3401±584	7038±2014	6199±682	29190±3804	40411±3922
Phy6000	10870±2233	2536±660	1614±358	3843±1173	433±97	1748±386	10174±2236
Control Ti	593±138	523±93	1270±114	2315±259	4683±447	48564±3126	57356±3599
2g/kg Ins Ti	9709±981	487±138	1371±181	2338±224	4738±379	47216±2585	56145±2940
Phy500 Ti	2552±507	3338±2200	3250±515	6596±1734	6045±403	24865±2489	44094±2938
Phy6000 Ti	10047±1954	2257±565	2169±484	4760±1361	819±308	3217±1388	13221±2886

Abbreviations: Σ InsP, total InsP₂ to InsP₆; InsP₆, inositol hexakisphosphate; InsP₅, inositol pentakisphosphate; InsP₄, inositol tetrakisphosphate; InsP₃, inositol trisphosphate; InsP₂, inositol bisphosphate.

¹The control group was fed with a diet with 0.45% calculated available phosphate. Groups Phy500 and Phy6000 were fed with the control diet supplemented with 500 or 6,000 FTU of phytase per kilogram of feed, respectively.

²Data are given as group means ± SEM, n = 6.

Total inositol phosphate levels were reduced significantly from 61347±3702 nmol/g dwt in ileal contents for the Control group to 40411±3922 nmol/g dwt at Phy500 (34.13% decrease, $p = 0.018$) and to 10174±2236 nmol/g dwt at Phy6000 (83.42% decrease, $p < 0.0001$) (Table 4.12), with a similar linear reduction in total InsPs compared to the gizzard digesta response observed with increasing phytase dose. Effects on InsP₆ levels were highly significant at both Phy500 and Phy6000 (for Phy500, $p = 0.008$; for Phy6000, $p < 0.0001$), with InsP₆ reduced from 51588±3269 nmol/g dwt in the Control group to 29190±3804 nmol/g dwt and 1748±386 for Phy500 (43.42% decrease) and Phy6000 (96.61% decrease) respectively. No significant difference was observed in the 2 g/kg Ins diet compared to the Control. Significant reductions were also measured in InsP₅ levels for Phy6000 group

(433±97 nmol/g dwt) compared to the Control (5285±519 nmol/g dwt) ($p < 0.0001$), with InsP₅ decreased by 91.81% with the inclusion of 6000 FTU/kg Quantum Blue. In both phytase doses, InsP₂ levels were significantly increased compared to the Control diet (for Phy500, $p = 0.018$; for Phy6000, $p = 0.038$).

Inositol levels in the ileal contents were altered by the addition of inositol and phytase to the diet (Table 4.12), with increases in detectable free inositol similar to those observed in the gizzard digesta. Highly significant differences were measured at 2 g/kg Ins ($p < 0.0001$) and at Phy6000 ($p = 0.004$) but not at Phy500 ($p = 0.1024$) when compared to the Control. Inositol levels were measured at 1008±297 nmol/g dwt in the Control group, 10742±1035 nmol/g dwt in 2 g/kg Ins, 2434±654 nmol/g dwt at Phy500 and 10870±2233 nmol/g dwt at Phy6000.

Regression analysis of the differences arising between groups with and without TiO₂ as a digestibility index marker concluded that differences between slopes was not significant ($p = 0.8473$), with regression outputs shown in Appendix 5. Though, ANOVA comparisons showed significant differences between the groups including 2 g/kg Ins with and without TiO₂ for measurements of InsP₆ and total inositol phosphates in the ileal digesta (for InsP₆, $p = 0.014$; for total InsPs, $p = 0.0012$).

4.4 Discussion

4.4.1 Influence of phytase dose on weight gain and feed conversion ratio

The term 'superdosing' first coined in 2013 (Walk *et al.*, 2013) has become synonymous with 'extra-phosphoric' effects of doses of phytase that surpass the dietary requirements for phosphorus (phosphate) that can be provided by supplementing feed with 1,500 units/kg of phytase. Since then, much research has been conducted into the benefit of superdosing and the associated benefits of such doses with the hypothesised near total

destruction of dietary phytate on feed conversion ratio (Walk *et al.*, 2013). Cobb male broilers fed diets supplemented with 1500 FTU have been shown to have increased gizzard digesta inositol, and by contrast reduced gizzard phytate content, compared to lower phytase doses supplemented. However, in supplementing diets with the predicted comparative released phosphate, the same feed conversion ratio as with 1500 FTU could not be achieved, instead suggesting that the benefits of the addition of phytase to the diet are 'extra-phosphoric', in that they also lie in the reduction of anti-nutrient effects of grain phytate (Walk, Santos and Bedford, 2014). Similar results were seen in the comparison of female Ross broiler chicks fed 2 g/kg available P with exogenous phytase compared to chicks fed solely 5 g/kg available P: the addition of high dose phytase, over 1000FTU, increased the availability of dietary nutrients (Cowieson, Acamovic and Bedford, 2006).

Since 2013, superdosing has come to convey the benefits arising from provision of inositol through adding phytase to animal feed. As such, it has been accepted as a standard term in academia and industry, with more than 600 citations in Google Scholar since 2013. A more nuanced understanding of the mechanisms by which inositol contributes to the growth performance benefits of superdosing, has arisen from studies that have 'progressively' followed the influence of increases in gastro-intestinal tract inositol from the gizzard contents to ileal contents, to gut tissue, to plasma (blood) and to other organs including, liver, kidney and muscle. Suffice to say, not a single study has made measurements in all these tissues/organs. The experiments described in this thesis were explicitly designed to redress this, so that correlations could be drawn between inositol phosphate degradation in the gut, release of inositol and, by measurement of inositol phosphates and inositol in tissue, proxy assessment of effect of released inositol on animal physiology. Irrespective of mechanism of phytase or inositol action, for commercial poultry production growth performance is a primary concern. The growth performance of birds in this study is described in Table 4.8. It is important to note that on average bird weights at day 21 were typically low for the bird age in this study (Appendix 4), and this may be attributed to the use of a mash diet, as previous studies have found that although mash diet

feeding is generally associated with lower mortality, this is due to reduced growth rate, and mash-fed birds show reduced body weight gain compared to crumbled-pellet fed birds (Proudfoot and Sefton, 1978; Jafarnejad *et al.*, 2011).

The initial body weight of birds used in this trial was similar at an average day 0 weight of 43.5 grams across all pens and all treatment groups (ANOVA $p = 0.969$). Results from this study did not show a significant difference in the feed conversion ratio calculated for the different diets fed during the trial phase, though phytase dose improved FCR numerically. Previous trials have shown that birds fed high levels of supplementary phytase have improved FCR in comparison to birds fed diets with sufficient available phosphate (Pirgozliev *et al.*, 2011). The basal diet used in this trial, as the diet fed to the Control groups, was formulated to mimic commercial diet formulation in terms of calcium and phosphate content and is therefore not deficient in either Ca or P, with basal diet formulated available P calculated at 0.45%. Studies have shown that the requirement for optimal bird performance from day 0 to 21 is 0.39% P (Waldroup *et al.*, 2000), which may account for the lack of significant difference in BW and FCR between Control and phytase-containing diets as birds were able to obtain sufficient phosphorus from the basal diet. Several studies have shown little response to phytase supplementation when diets already contained sufficient dietary non-phytate P (Wu, Ravindran and Hendriks, 2003; Driver *et al.*, 2005). A 2013 study using Arbor Acres broilers to measure the effect of high phytase inclusion rates on animal performance in diets without limiting calcium and phosphorus similarly noted impacts on BW gain by day 21 related to phytase inclusion rate but with overall no significant difference in FCR ratio in this time period (Dos Santos *et al.*, 2013). However, the authors noted significant differences in feed conversion ratios emerging at 35 days of feeding, but only in comparison to a reduced available P diet compared to commercial formulations. This supports previous observations that high dose phytase inclusion influences improvement in growth performance separately from the impact of improved phosphate nutrition, relating to the reduction in endogenous phytate-related losses of protein and amino acid digestibility. In

the study presented in this chapter, significant differences were only measured in body weight gain between Control and 2 g/kg Inositol supplemented groups in the absence of TiO₂ as an indigestible marker (700.1 ± 19.59 vs. 768.8 ± 16.76, $p = 0.0089$), with all other differences not significant ($p > 0.05$), which supports the interpretation that the basal diet formulation met the birds' total requirements for phosphate without the addition of phytase (Table 4.7). A potential simplistic explanation for the improved performance in the inositol-fed group compared to the Control may be the increased calorie content of the feed with 2 g/kg added inositol, though this was not a measured parameter in the trial. Other studies that have reported improvements in FCR and BWG with *myo*-inositol supplementation (Cowieson *et al.*, 2013) have attempted to explain this improvement to the effect of inositol on gastrointestinal microbial flora (Jiang *et al.*, 2009a) or to a reduction in antioxidative stress (Jiang *et al.*, 2009b), but the mechanism in poultry is not yet fully elucidated.

A complicating factor, or, alternatively, a potential explanation of the lack of effect of treatment on FCR, is that phytase activity is inhibited by inorganic phosphate, the product of its action (Greiner, Konietzny and Jany, 1993; Sommerfeld, Schollenberger, *et al.*, 2018). It has been suggested that the addition of supplementary phytases to diets with high levels of non-phytate available phosphate reduces the effectiveness of the added phytase in improving bird performance, with phytase most effective when dietary available phosphate is as low as possible (Manangi and Coon, 2008). Diet supplementation with monoammonium phosphate has been shown also to decrease phytase efficacy in Atlantic salmon (Greiling *et al.*, 2019). Moreover, there is evidence for poultry that interactions between phosphatases and phosphate in the gut may be responsible for reduced gastrointestinal InsP₆ hydrolysis when diets are supplemented with additional sufficient non-phytate phosphorus (Shastak *et al.*, 2014; Sommerfeld, Schollenberger, *et al.*, 2018). Despite the foregoing, results from the study presented in this chapter still showed significant phytate hydrolysis in the presence of sufficient non-phytate available phosphate in the diet (Figure 4.4, 4.8).

4.4.2 The impact of endogenous plant phytases on phytate digestibility

The differences in lower inositol phosphate isomers in the gizzard and ileal digesta in the Control and inositol-supplemented dietary groups, when compared to the diet suggests the presence of phytase activity distinct from the supplemented Quantum Blue present in other groups. Grain phytases originating from the feedstuffs, not inactivated in the feed in this trial in the absence of heat pelleting, may account for some of this activity – as shown by the impact of differential extraction methods on the resulting analysed inositol phosphate levels and profiles (figure 4.4, 4.5). However, it is likely that the low pH of the early avian digestive tract, particularly in the gizzard with a fluctuating acidic pH of 0.6 – 3.8 (Farner, 1942; Lee *et al.*, 2017), where this impact was more noticeable, will limit grain endogenous phytase activity. Indeed, wheat grain phytases are particularly susceptible to inactivation within the digestive system (Phillippy, 1999). An alternate explanation for this may lie in a significant contribution from digestive microbiota phytase activity in diets without supplemented exogenous phytase. Interestingly, the InsP₅ isomers observed, predominantly Ins(1,2,3,4,6)P₅ with notable but far reduced, by comparison, peaks of D/L-Ins(1,2,3,4,5)P₅ and D/L-Ins(1,2,4,5,6)P₅, (Figure 4.5) could arise from the action of microbial Multiple Inositol Polyphosphate Phosphatase (MINPP, a phytase) or from cereal MINPP activity. Among plants, wheat, which formed the largest proportion of the feed constituents, has a particularly high mature grain phytase activity attributed to enzyme of the purple acid class (Brinch-Pedersen *et al.*, 2003). Recent characterization of the wheat enzyme (Faba-Rodriguez *et al.*, 2022) reveals a predominant 4/6-phytase activity, fitting with early characterization of 6-phytase activity of wheat bran (Lim and Tate, 1973). Nevertheless, plant MINPPs also present in wheat, have been characterized as 5-phytases (Barrientos, Scott and Murthy, 1994). These two activities which would produce predominant D/L-Ins(1,2,3,4,5)P₅ and/or Ins(1,2,3,4,6)P₅ products (Sprigg *et al.*, 2022) need to be considered beside microbial originating adjunct phytases, here a 6-phytase (Sommerfeld,

Künzel, *et al.*, 2018), but also frequently 3- or 6-phytases (Shin *et al.*, 2001; Andlid, Veide and Sandberg, 2004; Kumar and Sinha, 2018).

In the gizzard digesta of birds supplemented with high phytase doses, the only detectable InsP₅ isomer was negligible amounts of Ins(1,2,3,4,6)P₅, as well as D- and/or L-Ins(1,2,3,4)P₄ and D- and/or L-Ins(1,2,5,6)P₄, known products of phytase degradation in Quantum Blue-supplemented diets (Sommerfeld, Künzel, *et al.*, 2018). It is possible that InsP₅ residues produced by hydrolysis of InsP₆ in the gizzard are further broken down to lower inositol phosphates rapidly by concerted action of phytase.

4.4.3 Phytase supplementation improves phytate digestibility in the gizzard and ileum

Supplementation with phytase at both 500 FTU and 6000 FTU showed highly significant improvement in phytate reduction in the gizzard digesta, with significant reductions in InsP₅, InsP₆ and total inositol phosphate levels (Figure 4.4). The phytase used in this trial, Quantum Blue, is a modified *E. coli* 6-phytase, shown in *in vitro* digestion studies to be most active in an acidic pH range, with highest reported activity at pH 3.5 (Tao, 2018), and highest enzyme tolerance to degradation at an acidic pH range closest to that of the crop, proventriculus and gizzard (Igbasan *et al.*, 2000; Garrett *et al.*, 2004; Elkhailil *et al.*, 2007), which may explain the apparent improved activity in the gizzard. The effect observed here of greater effect on total inositol phosphates in the gizzard as opposed to the ileal digesta (Figure 4.8) has been noted previously (Onyango, Bedford and Adeola, 2005; reviewed in Selle and Ravindran, 2007). In these reports, non-digestible markers of titanium dioxide and chromic oxide have been used. The apparent greater effect in gizzard may arise from the faster transit of soluble InsPs through the gizzard in comparison to the digestibility index marker, leading to subsequent apparent concentration in the terminal ileum. Additionally, inositol phosphate isomers are highly soluble in acidic conditions in the gizzard, as are the mineral complexes that lower inositol phosphates form. Consequently, the absence of changes in concentrations of 'lower' inositol phosphates in the

gizzard may be due to increased transit rate or increased breakdown of InsP₂₋₄ in the gizzard (Zeller, Schollenberger, Kühn, *et al.*, 2015).

Highly significant reduction in InsP₆ and total inositol phosphates was also measured in the ileal digesta of birds with phytase supplemented diets, at both 500 FTU and 6000 FTU (Table 4.12). Though not significant, numerical increases in total InsP₅ isomers present in 500 FTU phytase treatment group ileal digesta compared to the control and inositol treatment groups suggests that some phytase activity continues into this gut segment. Previous research has demonstrated that when phytase is provided at 500 FTU/kg, birds appear less able to degrade lower inositol phosphate esters of InsP₃ and InsP₄ (Zeller, Schollenberger, Kühn, *et al.*, 2015; Zeller, Schollenberger, Witzig, *et al.*, 2015; Bedford and Walk, 2016) which have been shown to retain the same antinutritive properties as InsP₆ in the gut of broilers (Persson *et al.*, 1998; Yu *et al.*, 2012) and therefore, in the context of improvements to animal performance, the reduction of all lower inositol phosphate esters and their hydrolysis to *myo*-inositol must be considered. In the 'super-dosed' phytase group, at 6000 FTU, highly significant reductions in InsP₅ were also measured, as well as significant increases in InsP₂ and free detectable inositol (Figure 4.12), with values suggesting almost complete destruction of dietary phytate by the terminal ileum at this phytase dose. The dose of 2 grams of inositol per kilogram of feed was selected as, approximately, a typical commercial poultry diet would contain 2-2.5 grams of inositol per kilogram of feed in the form of InsP₆ (Eeckhout and De Paepe, 1994), and thus if this was completely dephosphorylated through superdosing of phytase it would yield approximately 2-2.5 grams of inositol per kilogram of feed provided. The measured significant difference in inositol in the 2 g/kg Ins dosed diet compared the Control, and lack of significant difference between Phy6000 and 2 g/kg Ins treatment groups in terms of measured inositol contents, supports that near complete hydrolysis of dietary InsP₆ is achieved in the 'super-dosed' 6000 FTU group.

Previous studies have shown that broiler intestinal endogenous phytases and the phytase activity provided by their gut microbiota have a high capacity

to hydrolyse InsP₆ in the intestine (Zeller *et al.*, 2015a). Supplementary phytase activity is considered to contribute largely to hydrolysis in the anterior digestive system segments of the crop and gizzard, supported by the modification of dietary supplement phytases for activity in the acidic pH of the early digestive tract prior to inactivation by pepsin in later stage digestion (Simon and Igbasan, 2002).

Phytate degradation by phytase is often investigated in the context of calcium and available phosphate, with focus on calcium to phosphate ratios and amino acid digestibility (Cowieson *et al.*, 2017; Sommerfeld *et al.*, 2018b). Calcium and phosphate act antagonistically in the gut, and the requirements for calcium and phosphate differ greatly between broilers and layers – with broilers requiring of higher levels of non-phytate P for improved growth performance, whilst layers are able to retain more calcium and are better able to tolerate reduced available phosphorus with improved phytate P utilisation (Edwards Jr, 1983; Edwards Jr and Veltmann Jr, 1983), and improved with reduced dietary calcium (Fisher, 1992). It is important to optimise calcium to phosphate ratios, particularly in calculating available phosphate and phytate-P liberated inorganic phosphate, to promote bone deposition as opposed to bone resorption (Manangi and Coon, 2008).

In the context of protein and amino acid digestibility, the presence of high levels of phytic acid in the ileum has been shown to reduce digestibility of nitrogen and all essential amino acids (Ravindran *et al.*, 2000). The proposed mechanisms for this interference by phytic acid in protein and amino acid digestibility include the formation of electrostatic bonds between phytate and protein under acidic conditions in the proventriculus and gizzard (Kies *et al.*, 2006); the complex formation between phytic acid, minerals and proteins due to charge differences in the small intestine rendering them resistant to enzymatic hydrolysis (Maenz, 2001). Additionally, endogenous proteolytic enzymes themselves can be bound by phytate in the small intestine, preventing their ability to digest protein (Selle *et al.*, 2006). The near complete hydrolysis of InsP₆ to free inositol by superdosing with supplementary phytase at 6000 FTU, a higher level than usually

supplemented in poultry diets by commercial users, shows the potential extra phosphoric benefits of superdosing by removing phytate before it reaches the terminal ileum.

Supplementation of the basal diet with both levels of phytase, 500 FTU and the super-dosed 6000 FTU, significantly improved phytate reduction and free detectable inositol concentrations in the gizzard and ileal digesta of broilers. However, this improvement in available phosphate and inositol did not, in this study, translate to significantly improved feed conversion or body weight gain, and it is possible that the basal diet formulation to contain sufficient available non-phytate phosphorus for optimal broiler growth in this trial may have reduced any potential significant impact phytase inclusion would have had on feed conversion ratio.

Both levels of inclusion of Quantum Blue in the diets had a more visible impact on gizzard phytate degradation than in the terminal ileum. Quantum Blue is formulated for activity at an acidic pH range of 3.5 – 5.5, most suited to activity in the fluctuating acidic pH of the anterior digestive tract segments of the crop, proventriculus and gizzard, though altered lower inositol phosphate profiles show that some phytase activity remains into the ileum.

The inclusion of inositol at 2 g/kg as a treatment diet allows for comparison to the predicted liberated inositol from complete phytate hydrolysis, and comparable inositol concentrations in the ileum between the inositol supplemented diet and the super-dosed phytase treatment at 6000 FTU suggests this phytase level achieves near complete phytate hydrolysis during feed transit. Additionally, the absence of altered InsP status in the 2 g/kg inositol supplemented diet compared to the Control diet confirms that no inositol phosphate synthesis occurs within the digestive tract, and that all changing levels of inositol phosphates throughout the digestive tract can be attributed to phytate degradation by both supplemented and endogenous phytases.

5. Inositol phosphate species in tissues of broiler chickens

Data presented in this chapter is partially published in Sprigg *et al.* (2022).

5.1 Introduction

As noted in previous chapters, research into the impact of phytase dosing in poultry has focused largely on animal performance matrices such as feed conversion ratio and bone ash mineralisation. Commonly, this is coupled with biochemical measurements of blood plasma parameters and phytate hydrolysis in gizzard and ileal digesta in attempt to provide a mechanistic explanation of the role of phytate degradation in improving animal performance.

In more recent research, studies have focused on tissues and organs, largely by targeted gene expression, such as on inositol or phosphate transporters (Hu *et al.*, 2018; Walk, Bedford and Olukosi, 2018; Sommerfeld *et al.*, 2020; Zanu *et al.*, 2020), signalling pathways (Schmeisser *et al.*, 2017; Greene *et al.*, 2019; Greene *et al.*, 2020b) or by metabolomics (Gonzalez-Uarquin, Rodehutscord and Huber, 2020; Greene *et al.*, 2020a; Gonzalez-Uarquin *et al.*, 2021). Both approaches have been complemented by Western blot of transporters or signalling components in tissues such as intestinal mucosa, liver and muscle (Huber, Zeller and Rodehutscord, 2015; Greene *et al.*, 2019; Greene *et al.*, 2020a; Whitfield *et al.*, 2022). Given the importance of inositol phosphates and phosphatidylinositol phosphates to intracellular signalling, it is noteworthy that the study of effect of phytase has not extended to measurement of these molecules in tissues, except for blood (Whitfield *et al.*, 2022), though until recently methods for the measurement of these molecules remained limited, complex and involved extractions methods, and often requiring of inaccessible expensive analytical equipment.

For feed and digesta, freeze dried and milled samples are typically extracted using sodium fluoride and EDTA solution, pH 10 (Zeller *et al.*, 2015a; Walk, Bedford and Olukosi, 2018; Zanu *et al.*, 2020) and InsP₃₋₆ analysed by high

performance liquid chromatography (HPLC) with post-column complexation with ferric ion and detection by UV at 290nm. Commonly, inositol is measured by HPLC-pulsed amperometry (Walk, Santos and Bedford, 2014; Laird *et al.*, 2016; Walk, Bedford and Olukosi, 2018; Pirgozliev *et al.*, 2019b; Kriseldi *et al.*, 2021) by GC (Sommerfeld *et al.*, 2018b; Ajuwon *et al.*, 2020) or by enzymatic assay (Gonzalez-Uarquin *et al.*, 2020; Gonzalez-Uarquin, Rodehutschord and Huber, 2020; Gonzalez-Uarquin *et al.*, 2021). For tissue samples, however, the methods of extraction and analyses are markedly different. Analysis of avian erythrocyte inositol phosphates by acid gradient HPLC has been reported (Mayr, 1988; Casals, Villar and Riera-Codina, 2002; Whitfield *et al.*, 2020), but for other avian organs analysis has been limited to *myo*-inositol (Greene *et al.*, 2019; Gonzalez-Uarquin, Rodehutschord and Huber, 2020). Others have concluded that inositol phosphates are absent from human plasma (Letcher, Schell and Irvine, 2008; Wilson *et al.*, 2015) and for poultry (Whitfield *et al.*, 2022).

Despite the relatively early elaboration of techniques capable of measuring inositol phosphates in animal tissues by Georg Mayr (Mayr, 1988), the identification of inositol phosphates in animal cells has predominantly employed radiolabelling of cell lines, tissue slices or, only when easily isolated, primary cells, for example of blood (Watson, McConnell and Lapetina, 1984). The consequence of this is that our understanding of whole animal responses to dietary conditions that might be expected to influence tissue or organ inositol phosphate metabolism is lacking, as is a description of the inositol phosphate profile of different tissues. Only very recently has description of inositol phosphates in different mouse tissues been reported (Qiu *et al.*, 2020).

Radiolabelling with metabolic precursors such as ^{32}P [inorganic phosphate], ^3H [*myo*-inositol] and ^{32}P [ATP], in permeabilized cells, has been the mainstay of research into the cell signalling role of inositol phosphates since the early work on ^{32}P -labelling of pancreatic slices (Hokin and Hokin, 1953). The approach was used incisively to determine the pathways of synthesis of phosphoinositides including $\text{PtdIns}(3,4,5)\text{P}_3$ in Swiss 3T3 cells (Hawkins,

Jackson and Stephens, 1992), PtdIns(3,5)P₂ in mouse fibroblasts (Whiteford, Brearley and Ulug, 1997), of InsP₆ in the duckweed *Spirodela polyrhiza* (Brearley and Hanke, 1996a, 1996b) and more widely in the pathways of metabolism of Ins(1,4,5)P₃ emanating from receptor-activation of phospholipase C (Irvine and Schell, 2001). The field of inositol phosphate research is vast, and as of July 2022 the phrase “inositol phosphate” garners more than 23,000 discrete publications in PubMed alone. The addition of the term “poultry” returns approximately 480 citations. While the former almost exclusively addresses intracellular metabolism and signalling process of discrete cells lines, the latter almost exclusively addresses the digestive fate of phytate, and the two sets barely intersect. Replacing the term “poultry” with “avian” reveals the detailed studies in avian erythrocytes of inositol phosphate metabolism performed by radiolabelling in the late 1980s by the groups of Michell, Downes and Irvine in the UK (King *et al.*, 1989; Stephens, Hawkins and Downes, 1989; Stephens and Downes, 1990b) and, quite separately, non-radioactive analysis by the metal-dye-detection technique (Mayr and Dietrich, 1987). Nevertheless, the analysis of inositol phosphate function does not extend far beyond this dominant cell type of this major tissue, the blood.

In the present study, development of a HPLC method that obviates the need to radiolabel tissues has allowed for previously unobtainable identification and quantification of inositol phosphates in poultry tissues. Moreover, it has allowed assessment of tissue/organ response to dietary phytase dosage, beside digesta measurements.

5.2 Materials and methods

5.2.1 Animal tissue sampling

For tissue analysis, from each of the two birds from which digesta was pooled for analysis, brain, kidney, liver and leg/breast muscle samples were collected and stored in polythene bags and immediately frozen at -20°C before shipping on dry ice to UEA for inositol phosphate and inositol

analysis. Samples were stored thereafter at -80°C . After defrosting, 100 mg samples of tissue were taken for InsP extraction and analysis. Storage at these temperatures is not anticipated to effect phytate stability or result in phytate degradation prior to analysis, based on phytate stability in long term wheat storage (Schollenberger *et al.*, 2021).

5.2.2 Tissue extraction

Methods are as described in chapter 3. Briefly:

For inositol phosphate analysis, 100 mg (frozen weight) of poultry tissue was homogenised by Ultra-Turrax (IKA T-10 Ultra-Turrax® High-Speed Homogeniser) in 600 μL : 1 M HClO_4 on ice and transferred to a 1.5 mL tube. Samples were kept on ice for 20 minutes with vortex mixing every 10 minutes and centrifuged at $13,000 \times g$ for 10 minutes at 4°C . The resulting cleared lysate was transferred to a clean 1.5 mL tube, and 20 μL of which was taken and diluted to 1000 μL with 18.2 Megohm.cm water for inositol analysis.

The following extraction method is adapted from Wilson *et al.* (2015). All steps were carried out at 4°C for the prevention of acid degradation of inositol phosphates. Prior to extraction, TiO_2 beads (Titansphere® TiO_2 5 μM , Hichrom) were washed in 1 M HClO_4 . Then, to each cleared lysate, 5 mg of Titansphere® TiO_2 beads in 50 μL HClO_4 was added. Samples were vortexed briefly and extracted for 30 minutes with mixing on a rotator. Samples were centrifuged at $3500 \times g$ for 5 minutes to pellet the TiO_2 beads and the HClO_4 supernatant discarded.

In order to elute the bound inositol phosphates, the TiO_2 beads were resuspended in 200 μL 3% ammonium hydroxide solution (pH 10) vortexed and incubated with rotation for 5 minutes at 4°C . Samples were centrifuged at $3500 \times g$ for 1 minute and supernatant containing the inositol phosphates were transferred to a clean 1.5 mL tube. A further 200 μL elution in fresh 3% ammonium hydroxide was carried out and the supernatants pooled. Samples were vacuum evaporated until dry and resuspended in 100 μL of 18.2

MOhm.cm water for further analysis by HPLC or stored at -20°C prior to downstream analysis.

5.2.3 HPLC analysis of inositol and inositol phosphates

50 µL samples were analysed by high-performance liquid chromatography and UV detection at 290 nm after post-column reaction with ferric ion, on a 250 x 3 mm Thermo Scientific™ Dionex™ CarboPac™ PA200 column (Dionex™) with a corresponding 3 x 50 mm guard column of the same material. The column was eluted at a flow rate of 0.4 mL min⁻¹ with a gradient derived from buffer reservoirs containing (A) water and (B) 0.6 M methanesulfonic acid, by mixing according to the following schedule: time (minutes), %B; 0, 0; 25, 100; 38, 100 (Whitfield *et al.*, 2018). Fe(NO₃)₃ in 2% HClO₄ was used as the post-column reagent (Phillippy and Bland, 1988) added at a flow rate of 0.2 mL min⁻¹. The elution order of InsPs was established using acid-hydrolysed InsP₆ standards. Concentration of InsPs was established by reference to UV detector response to injection of InsP₆ (Merck).

For inositol analysis, samples extracted as above were diluted 50-fold in 18.2 MOhm.cm water. Inositol was determined by HPLC pulsed amperometry of 20 µL aliquots after separation by 2-dimensional HPLC on Dionex CarboPac PA1 and MA1 columns (Lee *et al.*, 2018).

5.2.4 Statistical analysis

For each tissue set, results were first analysed by two-way ANOVA with Dunnett's multiple comparisons test to determine source of variation as diet and whether the presence or absence of TiO₂ significantly impacted results. For all tissue types, presence of TiO₂ was not a significant source of variation ($p > 0.5$ for all groups).

Tissue inositol, inositol phosphates and total inositol phosphates were compared by multiple T tests with correction for multiple comparisons using the Holm-Šídák method. All statistical tests were performed using GraphPad Prism, version 7.0e, for Mac OS X (GraphPad Software, La Jolla, CA). The

level of significance for all tests was set at $\alpha = 0.05$ and each set was analysed individually, without assuming a consistent standard deviation.

5.3 Results and Discussion

The principal objectives of this study were to identify inositol phosphate species in different tissues and investigate the effect of the addition of dietary phytase on the inositol phosphate levels observed in different poultry tissues. The experiments were designed from the premise that release of inositol and phosphate in the digestive tract and uptake into the systemic circulation might be expected to influence the synthesis of inositol- and phosphate-containing metabolites, specifically inositol phosphates, in distal organs. From our understanding of the cell-biology of inositol phosphates, we might expect differential effects in different organs to manifest in the physiology of the animal. Previous studies have identified changes in plasma inositol levels in relation to changes in gizzard and ileal phytate hydrolysis (Pirgozliev *et al.*, 2019a; Gonzalez-Uarquin, Rodehutscord and Huber, 2020; Whitfield *et al.*, 2022), but have been unable to access tissue inositol phosphates by commonly used analytical methods. The use of TiO_2 as a pre-concentration method for inositol phosphates enabled first time measurement of inositol phosphate levels in poultry tissues in combination with existing analytical (HPLC) methods.

5.3.1 Digestive tissue inositol phosphates

The avian small intestine, comprising the digestive tissues of the duodenum, jejunum and ileum, aids in digestion and nutrient absorption from the diet. Randomised feeding trials with phytase supplemented broilers suggest that not only does endogenous intestinal mucosa-derived phosphatase activity aid in phytate degradation in low phosphorus and low calcium diets (Sommerfeld *et al.*, 2019), but that the availability of dietary phosphorus, both supplemented and through phytase supplementation, alters the expression of jejunal sodium-dependent phosphate transporters (Huber, Zeller and Rodehutscord, 2015). With the digestive tissues serving as the entry point of

the known absorbable co-products of phytase action, inositol and phosphate, into the circulatory system and thereafter to distal organs, initial experiments tested effect of phytase supplementation on gastro-intestinal tract tissues.

Food ingested by the bird passes from the oesophagus to the crop, then to the proventriculus (a muscular stomach) to the gizzard (ventriculus). Gizzard contents are commonly analysed for phytate degradation products (Walk *et al.*, 2014; Beeson *et al.*, 2017; Kriseldi *et al.*, 2021), the low pH favours the activity of adjunct phytases of the histidine acid class but nevertheless in mash diets with high wheat contents (where feed phytases are not degraded by the pelleting process) the activity of the high mature grain phytase activity is evidenced as the isomer Ins(1,2,3,4,6)P₅ (Rodehutscord *et al.*, 2016) beside the known Ins(1,2,3,4,5)P₅ product of the commonly used feed additive *E. coli* 6-phytases (Greiner, Konietzny and Jany, 1993). From the gizzard, the food bolus passes through the duodenum, jejunum and ileum. These sections of the gut, particularly the ileum, are commonly assessed for phytate degradation and occasionally the caecal contents also. Much of the phytase feeding trial literature addresses ileal digestibility coefficients, of protein, phosphorus and calcium, and consequently ileal inositol phosphate contents are widely reported (Selle, Ravindran and Partridge, 2009; Cowieson *et al.*, 2017; Walk and Rama Rao, 2020).

In Chapter 4, the inositol phosphate profile of gizzard and ileal contents was reported. The results are typical of many phytase studies, with near complete removal of phytate (and lower inositol phosphates) from gut contents evident in ileal samples. In this chapter, analysis of the inositol phosphate profile of duodenal, jejunal and ileal tissues is reported. The small intestine is the site of Pi absorption across the brush border membrane by a secondary active, Na⁺-dependent process, mediated by proteins of the solute carrier (SLC) 34 family (Murer, Forster and Biber, 2004; Huber, Hempel and Rodehutscord, 2006). NaPi IIb, SLC34A2 is expressed in the small intestine, and NaPi IIa, SLC34A1 is expressed in the kidney (Werner and Kinne, 2001). The small intestine also expresses alkaline phosphatase activities (Huber, Hempel and Rodehutscord, 2006; Gonzalez-Uarquin *et al.*, 2020), that are reported to

contribute to phytate degradation critically in the 'final' removal of the axial-positioned 2-phosphate, to liberate inositol (Maenz and Classen, 1998; Adeola and Cowieson, 2011; Hirvonen *et al.*, 2019). In hens, much of the control of phosphate uptake, at least in response to altered dietary phosphate, is mediated by reabsorption by the kidney, rather than jejunal absorption (Huber, Hempel and Rodehutschord, 2006). A similar conclusion was reached by Rodehutschord *et al.* (2002), whereas others have noted the responsiveness of duodenal phosphate transport to dietary P restriction in young cockerels (Quamme, 1985).

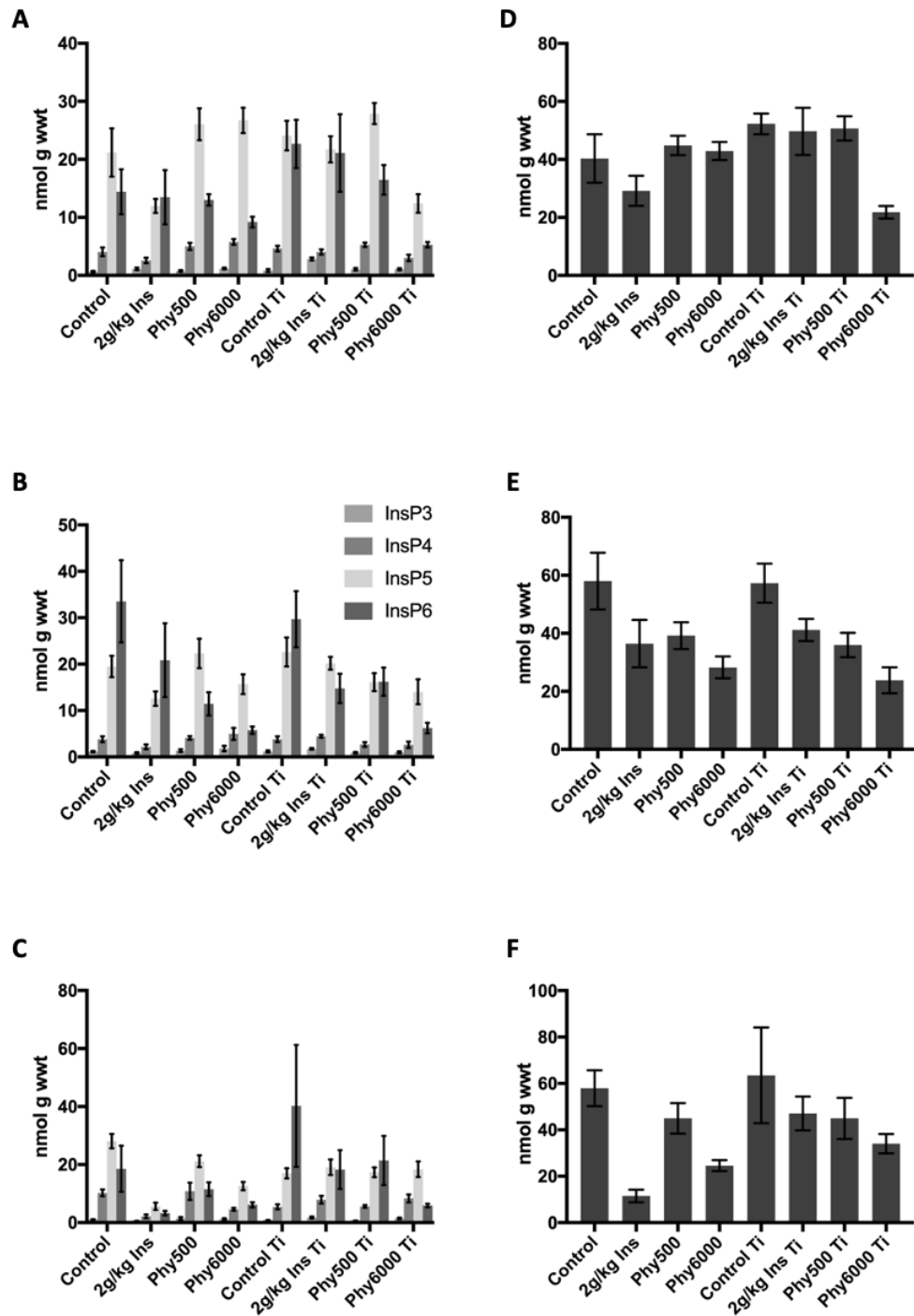


Figure 5.1: Inositol phosphate (InsP₃₋₆) levels (nmol/g wwt) in duodenum, jejunum and ileum tissue of day 21 broilers in different trial diets (see Table 5.1 legend notes for diet descriptions). **A**, duodenum tissue; **B**, jejunum tissue; **C**, ileum tissue; **D**, total inositol phosphate levels (sum of InsP₃₋₆) for duodenum tissues; **E**, total inositol phosphates for jejunum tissues; and **F**, total inositol phosphates for ileum tissues. Bars on the graph indicate calculated standard error of the mean for each group, n=12 for all except

duodenal tissue apart from 2 g/kg Ins where inositol data is n=11 to remove an outlier value.

Table 5.1: Inositol and inositol phosphate (InsP₃₋₆) levels (nmol/g wwt) in duodenal segments of day 21 broilers (6 pens per diet with samples from 2 broilers per pen per treatment).^{1, 2}

Diet	Inositol	InsP ₃	InsP ₄	InsP ₅	InsP ₆	ΣInsP
Control	3409±217	0.6±0.1	4.1±0.7	21.2±4.2	14.4±3.9	40.3±8.4
2g/kg Ins	4842±313	1.1±0.2	2.6±0.5	12.0±1.2	13.5±4.7	29.2±5.2
Phy500	3412±300	0.8±0.1	5.0±0.6	26.1±2.7	13.0±1.0	44.9±3.3
Phy6000	3561±190	1.2±0.1	5.8±0.5	26.7±2.2	9.2±0.9	42.9±3.1
Control Ti	3280±197	0.9±0.2	4.6±0.5	24.1±2.6	22.7±4.2	52.3±3.6
2g/kg Ins Ti	4552±263	2.8±0.2	4.0±0.5	21.7±2.3	21.1±6.7	49.7±8.1
Phy500 Ti	3251±199	1.1±0.2	5.3±0.4	27.9±1.8	16.5±2.6	50.7±4.2
Phy6000 Ti	3740±126	1.1±0.2	3.0±0.6	12.4±1.6	13.5±0.5	21.8±2.1

Abbreviations: Σ InsP, total InsP₂ to InsP₆; InsP₆, inositol

hexakisphosphate; InsP₅, inositol pentakisphosphate; InsP₄, inositol tetrakisphosphate; InsP₃, inositol trisphosphate; InsP₂, inositol bisphosphate.

¹The control group was fed with a diet with 0.45% calculated available phosphate. Groups Phy500 and Phy6000 and Phy500 Ti and Phy6000 Ti were fed with the control diet supplemented with 500 or 6,000 FTU of phytase per kilogram of feed, respectively. Groups 2 g/kg Ins and 2 g/kg Ins Ti were fed with the control diet supplemented with 2 grams per kilogram of ¹³C inositol (d30‰)

²Data are given as group means ± SEM, n = 12, apart from 2 g/kg Ins where inositol data is n=11 to remove an outlier value. Statistical analysis was performed by multiple T-tests with correction for multiple comparisons using the Holm-Šídák method.

Phytase supplementation had no significant effects on the measured concentrations of individual species of inositol phosphates extracted.

Significant differences were measured in the InsP₃ levels between the 2 g/kg Ins Ti group compared to the Control, with values increased to 1.1±0.2 nmol/g wwt in the inositol supplemented group compared with 0.6±0.1 nmol/g wwt in the Control group representing an 83% increase in InsP₃, though no other significant effects were measured ($p > 0.05$) (Table 5.1).

Duodenal tissue inositol levels were significantly increased by the inclusion of 2g/kg inositol in the diets, in both inositol treatment groups. In the 2 g/kg Ins treatment group, inositol levels were measured at 4842±313 nmol/g wwt , 42% increased compared to 3409±217 nmol/g wwt in the Control group ($p = 0.0027$); in the 2 g/kg Ins Ti group, with the inclusion of 5g/kg TiO₂, duodenal tissue inositol levels were 4552±263 nmol/g wwt (33.5% increased) in comparison to Control levels ($p = 0.0246$). Differences between matched pair Control groups with and without TiO₂ as an indigestible marker were not significant ($p = 0.9979$).

Table 5.2: Inositol and inositol phosphate (InsP₃₋₆) levels (nmol/g wwt) in jejunum segments of day 21 broilers (6 pens per diet with samples from 2 broilers per pen per treatment).^{1, 2}

Diet	Inositol	InsP ₃	InsP ₄	InsP ₅	InsP ₆	ΣInsP
Control	3820±148	1.2±0.1	3.8±0.6	19.5±2.3	33.5±8.9	58.0±9.8
2g/kg Ins	5798±255	0.8±0.2	2.2±0.5	12.6±1.6	20.9±8.0	36.4±8.2
Phy500	4305±192	1.4±0.3	4.1±0.4	22.3±3.2	11.4±2.5	39.2±4.6
Phy6000	5168±339	1.8±0.6	5.0±1.3	15.7±2.1	5.8±0.8	28.3±2.8
Control Ti	4332±350	1.2±0.2	3.8±0.6	22.6±3.1	29.7±6.0	57.3±6.7
2g/kg Ins Ti	5670±252	1.7±0.2	4.5±0.3	20.2±1.4	14.8±3.2	41.2±3.8
Phy500 Ti	4622±396	0.9±0.2	2.7±0.5	16.1±1.9	16.2±3.0	25.9±4.2
Phy6000 Ti	5323±260	1.0±0.2	2.6±0.7	14.0±2.7	6.2±1.1	23.9±4.5

Abbreviations: Σ InsP, total InsP₂ to InsP₆; InsP₆, inositol

hexakisphosphate; InsP₅, inositol pentakisphosphate; InsP₄, inositol tetrakisphosphate; InsP₃, inositol trisphosphate; InsP₂, inositol bisphosphate.

¹The control group was fed with a diet with 0.45% calculated available phosphate. Groups Phy500 and Phy6000 and Phy500 Ti and Phy6000 Ti were fed with the control diet supplemented with 500 or 6,000 FTU of phytase per kilogram of feed, respectively. Groups 2g/kg Ins and 2g/kg Ins Ti were fed with the control diet supplemented with 2 grams per kilogram of ¹³C inositol (d30‰)

²Data are given as group means ± SEM, n = 12. Statistical analysis was performed by multiple T-tests with correction for multiple comparisons using the Holm-Šídák method.

There was no significant impact of dietary inositol supplementation on measured acid extractable inositol phosphates or total inositol phosphates (for both 2 g/kg Ins and 2 g/kg Ins Ti, *p* > 0.05) (Table 5.2). Phytase supplementation at 6000 FTU had a highly significant impact on InsP₆ and total inositol phosphate (InsP₃₋₆) levels in both groups with and without TiO₂,

with InsP₆ reduced from 33.5±8.9 nmol/g wwt in the Control group to 5.8±0.8 nmol/g wwt in Phy6000 (82.7% reduction) and 6.2±1.1 nmol/g wwt in Phy6000 Ti (81.5% reduction) (for Phy6000, $p = 0.0014$, for Phy6000 Ti, $p = 0.0017$). Total inositol phosphates were also significantly reduced in both 6000 FTU groups, from 58.0±9.8 nmol/g wwt in the Control group to 28.3±2.8 nmol/g wwt in Phy6000 (51.2% reduction) and 23.9±4.5 nmol/g wwt in Phy6000 Ti (58.8% reduction) ($p = 0.0051$ and $p = 0.0010$ respectively). InsP₆ was also significantly reduced in the Phy500 group compared to the Control, to 11.4±2.5 nmol/g wwt in the Phy500 group (66% reduction, $p = 0.0163$), but total inositol phosphate levels were not significantly different in this diet.

In the jejunal tissue samples, inositol levels were significantly increased in diets with the inclusion of 2g/kg inositol compared to the Control. In the 2g/kg Ins treatment group, without the addition of TiO₂, inositol levels were 5798±255 nmol/g wwt compared to 3820±148 nmol/g wwt in the Control group (51.78% increase, $p < 0.0001$). In the 2g/kg Ins Ti diet, including TiO₂ as an indigestible marker, inositol levels were measured to be 5670±252 nmol/g wwt (48.43% increased, $p = 0.004$). The inclusion of 6000 FTU phytase also significantly increased inositol measured in jejunum tissue samples, at 5168±339 nmol/g wwt for the Phy6000 group (35.3% increased compared to the Control) and 5323±260 nmol/g wwt for the Phy6000 Ti group (39.35% increased) compared to the Control (for Phy6000, $p = 0.0223$; for Phy6000 Ti, $p = 0.0082$). Both Control diets, with and without TiO₂, were not significantly different ($p = 0.78$).

Table 5.3: Inositol and inositol phosphate (InsP₃₋₆) levels (nmol/g wwt) in ileum segments of day 21 broilers (6 pens per diet with samples from 2 broilers per pen per treatment).^{1, 2}

Diet	Inositol	InsP ₃	InsP ₄	InsP ₅	InsP ₆	ΣInsP
Control	7405±427	1.0±0.1	10.2±1.2	28.1±2.5	18.6±7.9	58.0±7.8
2g/kg Ins	10089±862	0.4±0.2	2.2±5.6	5.6±2.7	3.3±0.8	11.5±2.7
Phy500	8469±381	1.4±0.5	10.8±3.0	21.2±2.1	11.5±2.4	45.0±6.6
Phy6000	10207±468	1.2±0.3	4.6±0.5	12.6±1.4	6.1±0.9	24.6±2.4
Control Ti	6886±516	0.8±0.1	5.4±0.9	17.0±1.8	40.3±21.0	63.5±20.6
2g/kg Ins Ti	10676±405	1.8±0.2	7.9±1.3	19.1±2.7	18.3±6.7	47.1±7.3
Phy500 Ti	7719±488	0.6±0.1	5.6±0.4	17.3±1.7	21.4±8.5	44.9±8.9
Phy6000 Ti	8299±489	1.4±0.3	8.3±1.4	18.4±2.7	5.9±0.6	34.0±4.2

Abbreviations: Σ InsP, total InsP₂ to InsP₆; InsP₆, inositol

hexakisphosphate; InsP₅, inositol pentakisphosphate; InsP₄, inositol tetrakisphosphate; InsP₃, inositol trisphosphate; InsP₂, inositol bisphosphate.

¹The control group was fed with a diet with 0.45% calculated available phosphate. Groups Phy500 and Phy6000 and Phy500 Ti and Phy6000 Ti were fed with the control diet supplemented with 500 or 6,000 FTU of phytase per kilogram of feed, respectively. Groups 2g/kg Ins and 2g/kg Ins Ti were fed with the control diet supplemented with 2 grams per kilogram of ¹³C inositol (d30‰)

²Data are given as group means ± SEM, n = 12. Statistical analysis was performed by multiple T-tests with correction for multiple comparisons using the Holm-Šídák method.

There was no significant difference in the measured InsP₃ concentrations in the ileum tissue in all groups compared to the Control fed group (Table 5.3). For InsP₄ measurements, both the 2 g/kg Ins and the Phy6000 diets were significantly reduced compared to the Control, with 2g/kg Ins reduced to 2.2±5.6 nmol/g wwt InsP₄ compared to 10.2±1.2 nmol/g wwt InsP₄ in the Control diet (78.4% decreased, *p* = 0.0007) and to 4.6±0.5 nmol/g wwt InP₄

measured in the Phy6000 group (54.9% decreased, $p = 0.0307$). The significant differences seen in these two diet groups compared to the Control fed group were also seen in total inositol phosphate levels measured, reduced from 58.0 ± 7.8 nmol/g wwt in the Control fed group to 11.5 ± 2.7 nmol/g wwt in the 2 g/kg Ins treatment group (80.8% decreased, $p = <0.0001$) and 24.6 ± 2.4 nmol/g wwt in the Phy6000 group (57.6% decreased, $p = 0.0027$). For total inositol phosphate levels, the Phy6000 Ti group was also reduced compared to the control (41.4% decreased to 34.0 ± 4.2 nmol/g wwt) approaching traditional significance levels ($p = 0.0560$) but all other groups were not significantly different ($p > 0.5$). No significant differences in InsP₆ levels were measured in any dietary treatment group.

InsP₅ levels in the ileum tissue were significantly different in almost all groups compared to the Control fed group, with the exception of Phy500 where reduction in InsP₅ to 21.2 ± 2.1 nmol/g wwt was not significantly different to concentrations measured in the Control group at 28.1 ± 2.5 nmol/g wwt (24.6% reduced, $p = 0.1079$). All other groups were significantly reduced (for all, $p < 0.05$).

Ileal tissue inositol levels were significantly increased by the inclusion of 2 g/kg Ins in the diet, in both groups 2 g/kg Ins (36.25% increased) and 2 g/kg Ins Ti (44.17% increased), in the absence and presence of TiO₂ in the diet at 10089 ± 862 nmol/g wwt and 10676 ± 405 nmol/g wwt respectively compared to 7405 ± 427 nmol/g wwt in the Control (for 2 g/kg Ins, $p = 0.0157$; for 2 g/kg Ins Ti, $p = 0.0014$). Inositol levels in the ileal tissue were also significantly increased in the Phy6000 group ($p = 0.0015$) to 10207 ± 468 nmol/g wwt (37.83% increased) in comparison to the Control. Increases in other treatment groups compared to the Control were not significantly different.

5.3.2 Liver tissue inositol phosphates

The liver in poultry, as in humans, has multiple functions. For its role in the digestive system, the liver is an accessory organ to digestion, producing and secreting bile and processing nutrients transported in blood received from

the digestive system (Akers and Denbow, 2013). In addition to these auxiliary digestive roles, the liver is the major detoxification organ and is responsible for the conversion of toxins to water-soluble waste products to be removed via the kidneys and gall bladder (Akers and Denbow, 2013). The liver in birds plays a greater role in lipogenesis than adipose tissue in mammals and the conversion of glucose to triglycerides important for the fattening of poultry (Hermier, 1997). It is the major site of phospholipid and cholesterol synthesis (Zaefarian *et al.*, 2019). The liver, along with the pancreas, maintains constant blood glucose concentrations through mobilisation of glycogen stores to glucose as well as conversion of amino acids, fats and lactic acid in immediate glucose demand, and reduction of blood glucose levels through glycogenesis (Freeman, 1969; Duke, 1986; Akers and Denbow, 2013).

The liver additionally has important functions in protein metabolism, representing 11% of all protein synthesis in the bird, and is the site of dietary protein hydrolysis from the intestine before transport via systemic circulation to other organs and tissues (Denbow, 2000). Finally, the liver is involved in the storage of fat-soluble vitamins A, D, E and K, and along with the kidneys synthesises 1,23 dihydroxycholecalciferol from vitamin D₃, by metabolising vitamin D into 25-hydroxycholecalciferol (25(OH)D₃) before it is subsequently converted to the active metabolite 1,25-dihydroxycholecalciferol (1,25(OH)₂D₃) in the kidneys (Garcia *et al.*, 2013).

There are no known publications regarding the effect phytase supplementation has on liver inositol phosphate concentrations, though research feeding graded *myo*-inositol to male Ross 308 broilers resulted in a linear increase in liver weight and hepatic nitrogen content, but linearly reduced fat concentration, and increased circulatory alkaline phosphatase levels at high inositol doses (30 g/kg feed Ins) (Pirgozliev *et al.*, 2019a). The same group reported correlation between inositol content of jejunum digesta and jejunum tissue, plasma inositol and kidney tissue (C Arthur *et al.*, 2021).

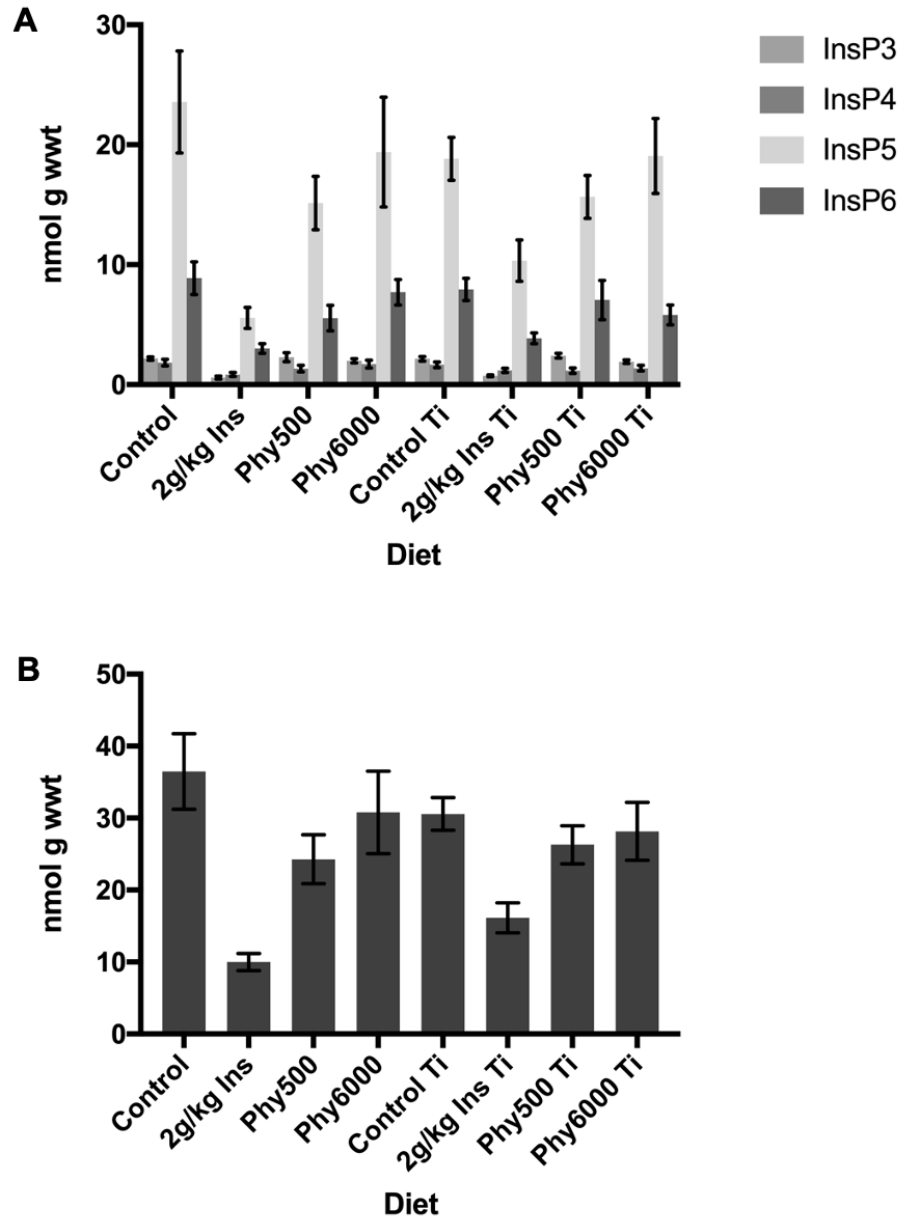


Figure 5.2: Inositol phosphate (InsP₃₋₆) levels (nmol/g wwt) in livers of day 21 broilers, where **A** shows inositol phosphate levels for InsP₃₋₆, and **B** total inositol phosphate levels (sum of InsP₃₋₆) for the same extracts. Bars on the graph indicate calculated standard error of the mean for each group, n=12 for all groups.

Table 5.4: Inositol and inositol phosphate (InsP₃₋₆) levels (nmol/g wwt) in liver of day 21 broilers (6 pens per diet with samples from 2 broilers per pen per treatment).^{1, 2}

Diet	Inositol	InsP ₃	InsP ₄	InsP ₅	InsP ₆	ΣInsP
Control	15924±870	2.2±0.1	1.8±0.3	23.6±4.3	8.9±1.4	36.5±5.3
2g/kg Ins	22071±614	0.6±0.1	0.8±0.2	5.6±0.9	3.0±0.4	10.0±1.2
Phy500	16063±547	2.3±0.4	1.3±0.3	15.1±2.2	5.5±1.1	24.3±3.4
Phy6000	18109±987	2.0±0.2	1.7±0.3	19.4±4.6	7.7±1.1	30.8±5.7
Control Ti	17107±1254	2.2±0.2	1.7±0.2	18.8±1.8	7.9±0.9	30.6±2.3
2g/kg Ins Ti	24454±1346	0.7±0.1	1.2±0.2	10.3±1.7	3.9±0.4	16.1±2.1
Phy500 Ti	16860±905	2.4±0.2	1.2±0.2	15.7±1.8	7.1±1.6	26.3±2.6
Phy6000 Ti	16657±1096	1.9±0.2	1.4±0.2	19.1±3.1	5.8±0.8	28.2±4.0

Abbreviations: Σ InsP, total InsP₂ to InsP₆; InsP₆, inositol

hexakisphosphate; InsP₅, inositol pentakisphosphate; InsP₄, inositol tetrakisphosphate; InsP₃, inositol trisphosphate; InsP₂, inositol bisphosphate.

¹The control group was fed with a diet with 0.45% calculated available phosphate. Groups Phy500 and Phy6000 and Phy500 Ti and Phy6000 Ti were fed with the control diet supplemented with 500 or 6,000 FTU of phytase per kilogram of feed, respectively. Groups 2g/kg Ins and 2g/kg Ins Ti were fed with the control diet supplemented with 2 grams per kilogram of ¹³C inositol (d30‰)

²Data are given as group means ± SEM, n = 12. Statistical analysis was performed by multiple T-tests with correction for multiple comparisons using the Holm-Šídák method.

Ins(1,3,4,5,6)P₅ was the dominant inositol phosphate in liver (Table 5.4, Figure 5.2A), and although in this case InsP₆ was the next most abundant species, at approximately 2-fold lower, the identities of inositol phosphates were similar to kidney. Liver inositol phosphate levels showed a reduction in inositol phosphates from 36.5 ± 5.3 nmol/g wwt for the Control group to 24.3 ± 3.4 nmol/g wwt on addition of Phy500 (33.4% decreased), though further reduction with increasing, Phy6000, was not observed, 30.8 ± 5.7 nmol/g

wwt (15.6% decreased), and neither treatment was not significantly different from Control group (for Phy500, $p = 0.281$; for Phy6000, $p = 0.927$).

Inclusion of 2 g/kg inositol in the diet resulted in significant reductions in individual inositol phosphate species and total inositol phosphates in the liver tissue: for InsP₃, reduced from 2.2 ± 0.1 nmol/g wwt in the Control to 0.6 ± 0.1 nmol/g wwt (reduction of 72.7%, $p < 0.0001$); for InsP₄, reduced from 1.8 ± 0.3 nmol/g wwt in the Control to 0.8 ± 0.2 nmol/g wwt (55.6% reduced, $p = 0.004$); for InsP₅, reduced from 23.6 ± 4.3 nmol/g wwt in the Control to 5.6 ± 0.9 nmol/g wwt (76.3% reduced, $p = 0.0004$); for InsP₆, reduced from 8.9 ± 1.4 nmol/g wwt in the Control to 3.0 ± 0.4 nmol/g wwt (66.3% reduction, $p = 0.0004$); and for total InsPs, reduced from 36.5 ± 5.3 nmol/g wwt in the Control to 10.0 ± 1.2 nmol/g wwt (72.6% reduction, $p < 0.0001$). Similarly, for the 2g/kg Ins Ti group, significant reductions in inositol phosphates and total inositol phosphates were observed: for InsP₃, reduced to 0.7 ± 0.1 nmol/g wwt (68.2% decrease, $p < 0.0001$); for InsP₅, reduced to 10.3 ± 1.7 nmol/g wwt (56.4% decrease, $p = 0.0088$); for InsP₆, reduced to 3.9 ± 0.4 nmol/g wwt (56.2% decrease, $p = 0.002$); and for total InsPs, reduced to 16.1 ± 2.1 nmol/g wwt (55.9% decrease, $p = 0.0016$).

Similar to the kidney, sample inositol levels were increased in the liver tissue from 15920 ± 870 nmol/g wwt in the Control group to 16060 ± 550 nmol/g wwt at Phy500 (0.9% increase), and 18110 ± 990 nmol/g wwt at Phy6000 (13.8% increase), but again these differences were not significant (Control vs. Phy500, $p = 0.964$; Control vs. Phy6000, $p = 0.507$), and similarly in the TiO₂ containing groups slight increases were observed in Phy500 Ti (5.9% increase) to 16860 ± 905 nmol/g wwt and 16657 ± 1096 nmol/g wwt in Phy6000 Ti (4.6% increase) but these differences were also not significantly different (Control vs. Phy500 Ti, $p = 0.0975$; Control vs. Phy6000 Ti, $p = 0.993$) (Table 5.4). In the study of Gonzalez-Uarquin et al., (2020), a statistically significant increase in tissue inositol was observed in kidney of d 22 broilers at 1500 FTU/kg, but not at 3000 FTU/kg; while liver levels of inositol did not differ between treatments. In contrast, Whitfield et al., (2022), reported increase in liver inositol of d 18 broilers at 2000FTU/kg, but not at d 38 or d 56, and no

effect on kidney inositol of phytase at d 18, 36 or 52. Here, significant increases in liver inositol concentration were observed in the inositol supplemented groups, with increases to 22071 ± 614 nmol/g wwt in the 2 g/kg Ins group (38.6% increase) and 24454 ± 1346 nmol/g wwt in the 2 g/kg Ins Ti group (53.6% increase) compared to 15924 ± 870 nmol/g wwt in the Control group (Control vs. 2 g/kg Ins, $p = 0.0206$; Control vs. 2 g/kg Ins Ti, $p = 0.0001$).

5.3.3 Kidney tissue inositol phosphates

The primary defined roles of the kidneys in poultry, as in other vertebrate species, is waste removal and osmoregulation, similar to all vertebrates, but with the same reduced capacity for urine concentration as reptile kidneys (Skadhauge and Schmidt-Nielsen, 1967). Additionally, as in other vertebrates, the kidney occupies a vital role in a number of homeostasis pathways, most importantly for the maintenance of the calcium to phosphate ratio in coordination with the parathyroid. Decades of research, in humans and animals, have focused on the importance of parathyroid hormone (PTH) and $1,25(\text{OH})_2\text{D}_3$ (Calcitriol) in regulating phosphate and calcium homeostasis in the complex axis involving crosstalk between many tissues and organs including but not limited to bone, kidneys, parathyroid gland and the small intestine (Portale *et al.*, 1984; Michigami *et al.*, 2018). Studies have demonstrated that in response to depleted calcium levels, birds display altered renal $25(\text{OH})\text{D}_3$ -1-hydroxylase activity and thus reduced biosynthesis of $1,25(\text{OH})_2\text{D}_3$, linked to increased rate of cracked or soft-shelled eggs associated with older laying hens due to the importance of $1,25(\text{OH})_2\text{D}_3$ in regulating Ca homeostasis (Elaroussi *et al.*, 1994). Similarly in phosphorus (phosphate)-restricted diets, layers show decreased circulatory phosphate and FGF23 levels increasing kidney expression of NPT2a, responsible for phosphate resorption (Gattineni *et al.*, 2009), and conversely FGF23 secretion is triggered by increased circulatory phosphate leading to phosphate excretion to avoid phosphate toxicity in laying hens (Ren *et al.*, 2017a; 2017b).

PTH stimulates release of Ca from bones, stimulates absorption of Ca from the gut, stimulates conservation of Ca by the kidneys and induces biochemical transformation of vit D in the kidney that convert weaker gut-acting (Ca-uptake stimulating) $25(\text{OH})\text{D}_3$ form to stronger $1,25(\text{OH})_2\text{D}_3$ form. Thus, at high dietary Ca we would expect PTH to be low. Again, under the conditions of adequate phosphate and calcium of this feeding trial, it is consistent that neither phytase- nor inositol-supplementation was of effect on PTH levels (Chapter 6), though the impact phytase supplementation would have on kidney InsP levels (Fig 5.3, Table 5.5) under adequate phosphate and calcium was unknown.

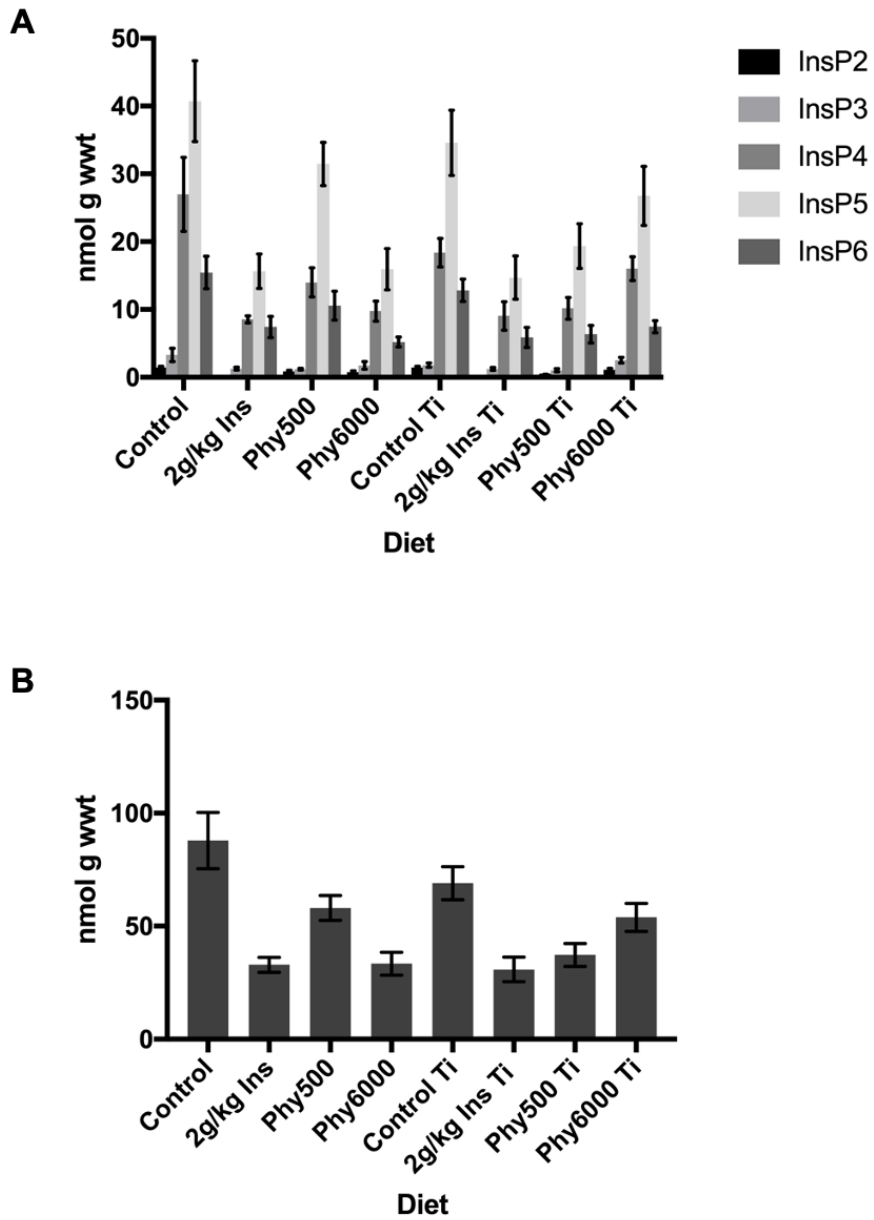


Figure 5.3: Inositol phosphate (InsP₂₋₆) levels (nmol/g wwt) in kidneys of day 21 broilers, where **A** shows inositol phosphate levels for InsP₂₋₆, and **B** total inositol phosphate levels (sum of InsP₂₋₆) for the same extracts. Bars on the graph indicate calculated standard error of the mean for each group, n=12 for all groups except Phy500 Ti where n = 11.

Table 5.5: Inositol and inositol phosphate (InsP₂₋₆) levels (nmol/g wwt) in kidney of day 21 broilers (6 pens per diet with samples from 2 broilers per pen per treatment).^{1, 2}

Diet	Inositol	InsP ₂	InsP ₃	InsP ₄	InsP ₅	InsP ₆	ΣInsP
Control	6432±483	1.4±0.2	3.3±1.0	27.0±5.4	40.7±6.0	15.4±2.4	87.9±12.5
2g/kg Ins	8200±554	n.d.	1.3±0.2	8.5±0.5	15.6±1.6	7.4±1.6	32.9±3.4
Phy500	6600±264	0.9±0.2	1.2±0.1	14.0±2.1	31.5±3.0	10.6±2.1	58.1±5.5
Phy6000	7529±309	0.7±0.2	1.7±0.6	9.8±1.5	15.9±3.1	5.2±0.7	33.4±5.1
Control Ti	6962±622	1.5±0.2	1.8±0.3	18.4±2.1	34.6±4.8	12.8±1.6	69.0±7.3
2g/kg Ins Ti	8188±334	n.d.	1.2±0.2	9.1±2.1	14.7±3.2	5.9±1.5	30.9±5.5
Phy500 Ti	6059±322	0.3±0.1	1.0±0.2	10.2±1.6	19.4±2.5	6.4±1.3	37.3±5.1
Phy6000 Ti	7306±184	1.1±0.2	2.5±0.4	16.0±1.7	26.8±4.2	7.5±0.9	53.9±5.9

Abbreviations: Σ InsP, total InsP₂ to InsP₆; InsP₆, inositol

hexakisphosphate; InsP₅, inositol pentakisphosphate; InsP₄, inositol tetrakisphosphate; InsP₃, inositol trisphosphate; InsP₂, inositol bisphosphate.

¹The control group was fed with a diet with 0.45% calculated available phosphate. Groups Phy500 and Phy6000 and Phy500 Ti and Phy6000 Ti were fed with the control diet supplemented with 500 or 6,000 FTU of phytase per kilogram of feed, respectively. Groups 2g/kg Ins and 2g/kg Ins Ti were fed with the control diet supplemented with 2 grams per kilogram of ¹³C inositol (d30‰)

²Data are given as group means ± SEM, n = 12, except Phy500 Ti where n = 11. Statistical analysis was performed by multiple T-tests with correction for multiple comparisons using the Holm-Šídák method.

Kidney tissue inositol phosphates (Table 5.5) show a similar reduction with increasing phytase to digesta response to phytase dose. Ins(1,3,4,5,6)P₅ is the dominant inositol phosphate measured in these tissues followed by D- and/or L-Ins(3,4,5,6)P₄, with InsP₅ over 3-fold higher than InsP₆ in these samples (Figure 5.3B). Significant differences were measured between the Control and Phy6000 diets for: InsP₄ (63.7% decrease, *p* = 0.017), 27.0 ± 5.4 nmol/g wwt and 9.8 ± 1.5 nmol/g wwt, respectively; InsP₅ (85.3% decrease, *p*

= 0.005), 40.7 ± 6.0 nmol/g wwt and 15.9 ± 3.1 nmol/g wwt, respectively; InsP₆ (66.2% decrease, $p = 0.003$), 15.4 ± 2.4 nmol/g wwt and 5.2 ± 0.73 nmol/g wwt, respectively. At Phy500, individual and total inositol phosphate levels were not statistically significantly different. With the addition of 2 g/kg inositol, the kidney showed significant differences in InsP₄ ($p = 0.008$), InsP₅ ($p = 0.003$), InsP₆ ($p = 0.02$) and total InsPs ($p = 0.002$).

Total inositol phosphate levels were reduced significantly ($p = 0.003$) in the kidney from a Control value of 87.9 ± 12.5 nmol/g wwt, at Phy6000, 33.4 ± 5.1 nmol/g wwt (Table 5.5), a reduction of 62%.

For the treatment groups additionally containing TiO₂ as an indigestible marker, significant differences were measured in the Phy500 and the 2 g/kg inositol supplemented diets compared to the Control fed group. For 2 g/kg Ins Ti: InsP₃ ($p = 0.0494$); InsP₄ ($p = 0.0056$); for InsP₅ ($p = 0.0009$); for InsP₆ ($p = 0.003$) and total InsPs ($p = 0.0004$). For Phy500 Ti compared to the Control: InsP₂ ($p < 0.0001$); InsP₃ ($p = 0.0413$); InsP₄ ($p = 0.0097$); InsP₅ ($p = 0.006$); InsP₆ ($p = 0.0038$) and total InsPs ($p = 0.0016$). For the Phy6000 Ti, significant differences were only measured in InsP₆ levels, with levels reduced by 51.3% to 7.5 ± 0.9 nmol/g wwt compared to 15.4 ± 2.4 nmol/g wwt in the Control ($p = 0.0492$).

Kidney inositol levels were not significantly affected by the addition of phytase to the control diet despite changes to inositol phosphate levels observed in the same sample (Table 5.5). Slight numerical increases in the inositol levels were measured in the kidney tissue between different dietary phytase doses, with 6430 ± 480 nmol/g wwt in the Control group; 6600 ± 260 nmol/g wwt with Phy500 (2.6% increase) and 7530 ± 310 nmol/g wwt with Phy6000 (17.1% increase). The differences were not significant (Control vs. Phy500, $p = 0.182$; Control vs. Phy6000, $p = 0.133$). Equally, no significant differences in inositol measured in the kidney tissue of the phytase treated groups additionally supplemented with TiO₂ were measured, with concentrations at 6059 ± 322 nmol/g wwt with Phy500 Ti (5.7% decrease) and

7306±184 nmol/g wwt with Phy6000 Ti (13.6% increase) (Control vs. Phy500 Ti, $p = 0.954$; Control vs. Phy6000 Ti, $p = 0.293$).

Significant differences in inositol concentration were, however, measured in the inositol treatment groups. With 2 g/kg of feed supplementation of inositol, extractable inositol in the kidney tissue increased to 8200±554 nmol/g wwt in the 2 g/kg Ins group (27.5% increase) and 8188±334 nmol/g wwt in the 2 g/kg Ins Ti group (27.3% increase) compared to 6432±483 nmol/g wwt in the Control (for both, $p < 0.0001$). Two-way ANOVA showed no significant variance resulted from the inclusion of TiO₂ in the diets.

To the knowledge of this author, there are no reported measurements of inositol phosphates in poultry tissues other than blood and only a limited number of reports of inositol levels in other tissues. (Charlotte Arthur, Rose, *et al.*, 2021) reported a positive correlation between plasma and kidney inositol levels of day 21 broilers with inositol supplementation in the range 0-13.5 g/kg. More physiologically, perhaps, phytase supplementation at 1500 FTU/kg increased kidney inositol (Charlotte Arthur, Mansbridge, *et al.*, 2021), suggesting increasing dietary inositol is associated with increased inositol uptake. Similarly, plasma and kidney inositol of day 22 broilers was increased at 1500 FTU/kg but not at 3000 FTU/kg (F. Gonzalez-Uarquin *et al.*, 2020). The same study reported that phytase was of no effect on liver inositol or on liver inositol monophosphatase or kidney *myo*-inositol oxygenase activities. These limited data, and the generalized observation of no deleterious effect of inositol on growth performance of birds (summarised, Pirgozliev, C. A. Brearley, *et al.*, 2019), even at supra-dietary levels (30kg, Pirgozliev *et al.*, 2019) suggests that whole animal broiler metabolism can exploit the inositol liberated by 'recommended' and 'supra-dosed' phytase.

The remarkably similar effect of supplementation with 2 g/kg inositol or 6000FTU/kg phytase on total and individual inositol phosphates (Table 5.5) implies that the sensitivity of kidney to inositol, rather than phosphate, underlies this organ's inositol phosphate response. While recent work in rats (Moritoh *et al.*, 2021) highlights the sensitivity of kidney inositol

pyrophosphate (InsP₇) level to pharmacological inhibition of IP6K, interpreted in context of a much vaunted regulatory role for inositol pyrophosphate and IP6K in phosphate homeostasis (Azevedo and Saiardi, 2017; Wilson, Jessen and Saiardi, 2019; Zhu *et al.*, 2019), similar effect on liver and muscle InsP₇ does not discriminate the relative contribution of the inositol phosphate metabolism of individual organs to phosphate homeostasis. Indeed, inhibition of IP6K was without effect on gut absorption or kidney reabsorption of phosphate (Moritoh *et al.*, 2021), but suppressed phosphate exporter function of XPR1, in kidney epithelial 293 cells. XPR1 is the single SPX domain protein 'receptor' of vertebrate InsP₇ and/or InsP₈ (Li *et al.*, 2020; Moritoh *et al.*, 2021).

Much of the foregoing deserves placing in context of the phosphate-uptake stimulatory (Pi-US) function (Yagci *et al.*, 1992; Norbis *et al.*, 1997) of the InsP₇-synthesizing inositol hexakisphosphate kinase subsequently characterized by Schell *et al.* (Schell *et al.*, 1999). Injection of a mRNA encoding the kinase conferred phosphate uptake on *Xenopus* oocytes, similar to that afforded by a mRNA population isolated from the duodenum of rabbit showing elevated 1,25(OH)₂D₃ levels. 1,25(OH)₂D₃ is the cognate physiological ligand of the vitamin D receptor, activation of which stimulates Ca²⁺ uptake from the gut (and associated phosphate uptake) increasing blood Ca²⁺. The kinetic parameters of the phosphate uptake that was stimulated by Pi-US mRNA, *K_M* 0.26 mM, is similar to that of human kidney phosphate transporter NPT-1, 0.29 mM (Miyamoto *et al.*, 1995). The lack of effect of pharmacological inhibition of IP6K on phosphate uptake, albeit of 293 cells (Moritoh *et al.*, 2021), is therefore at variance with our understanding of whole animal physiology and the recognized function of renal phosphate reabsorption (at least in normophosphataemic situations).

In summary, the data presented in Table 5.5 offer a whole animal, physiological, perspective to kidney inositol phosphate metabolism. Thus, reductions in kidney inositol phosphates in response to dietary phytase are mimicked by supplementation of diet with inositol. It seems likely that InsP₇ and InsP₈ levels are similarly reduced by phytase and inositol. In this study,

the inositol phosphate response is that of a phosphate- and Ca-replete animal, provided at 0.45% and 0.95%, respectively, evidenced also in phytase-mediated reduction of 25(OH)D₃ : 24,25(OH)₂D₃ ratio of plasma (Chapter 6). Indeed, the 24-hydroxylase activity of kidney is commonly interpreted to buffer 1,25(OH)₂D₃ levels, by metabolism of the 25(OH)D₃ precursor when Ca and phosphate are replete (Warren *et al.*, 2020).

In a separate study of ‘inositol phosphate-mediated’ responses in 5 week-old broilers, IP6K isoform expression showed complex post-prandial behaviour in broilers fed phytase (Greene, Mallmann, *et al.*, 2020). Circulatory (cell) IP6K1 was reduced by phytase at all periods (up to 30 h) after feeding, whereas IP6K2, IP6K3 and MINPP1 were transiently upregulated at 8 h post-prandial, but otherwise were reduced by phytase. Interestingly, circulatory *myo*-inositol 3-phosphate synthase, ISYNA, was downregulated at all periods after feeding with phytase – consistent with the reductions in kidney inositol phosphate levels observed with phytase here.

These exciting data show how the cell biology of kidney is integrated with animal physiology and, for the first time, how diet influences inositol phosphate metabolism-related cell biology of phosphate homeostasis.

5.3.4 Breast and leg muscle inositol phosphates

Broilers have been selectively bred primarily for efficient growth and feed conversion to lean muscle (Griffin and Goddard, 1994), with increased feed conversion to breast and leg muscle gain of the most economic value to farmers, with reducing the cost of feed inputs increasingly important. As with any advantageous selected trait, the selection for birds with rapid breast muscle growth has given rise to related myopathies, with the most efficient breast muscle development associated with white striping (fibrotic and lipid-laden regions leading to white striations parallel to muscle fibres) and woody breast (hardened breast tissue), both of which reduce the physical quality characteristics of breast meat and consequently reduce the appeal to consumers, leading to economic losses for producers (Mazzoni *et al.*, 2015;

Kuttappan, Hargis and Owens, 2016). These myopathies are thought to result from muscle growth outpacing vascular development, leading to areas of hypoxic tissue (Boerboom *et al.*, 2018; Livingston *et al.*, 2019; Özbek, Petek and Ardiçll, 2020). Recently, research has shown that supplementation with dietary phytase reduces the severity of woody breast by reversing the down-regulation of oxygen homeostasis-related genes in Cobb broilers (Greene *et al.*, 2020a). The relationship between circulatory inositol and muscle inositol phosphates or between muscle inositol and muscle inositol phosphates is not evident in the literature. Experiments were undertaken, therefore, to determine whether inositol phosphates of leg or breast muscle are influenced by supplementation of diet with phytase or inositol (Table 5.6, 5.7).

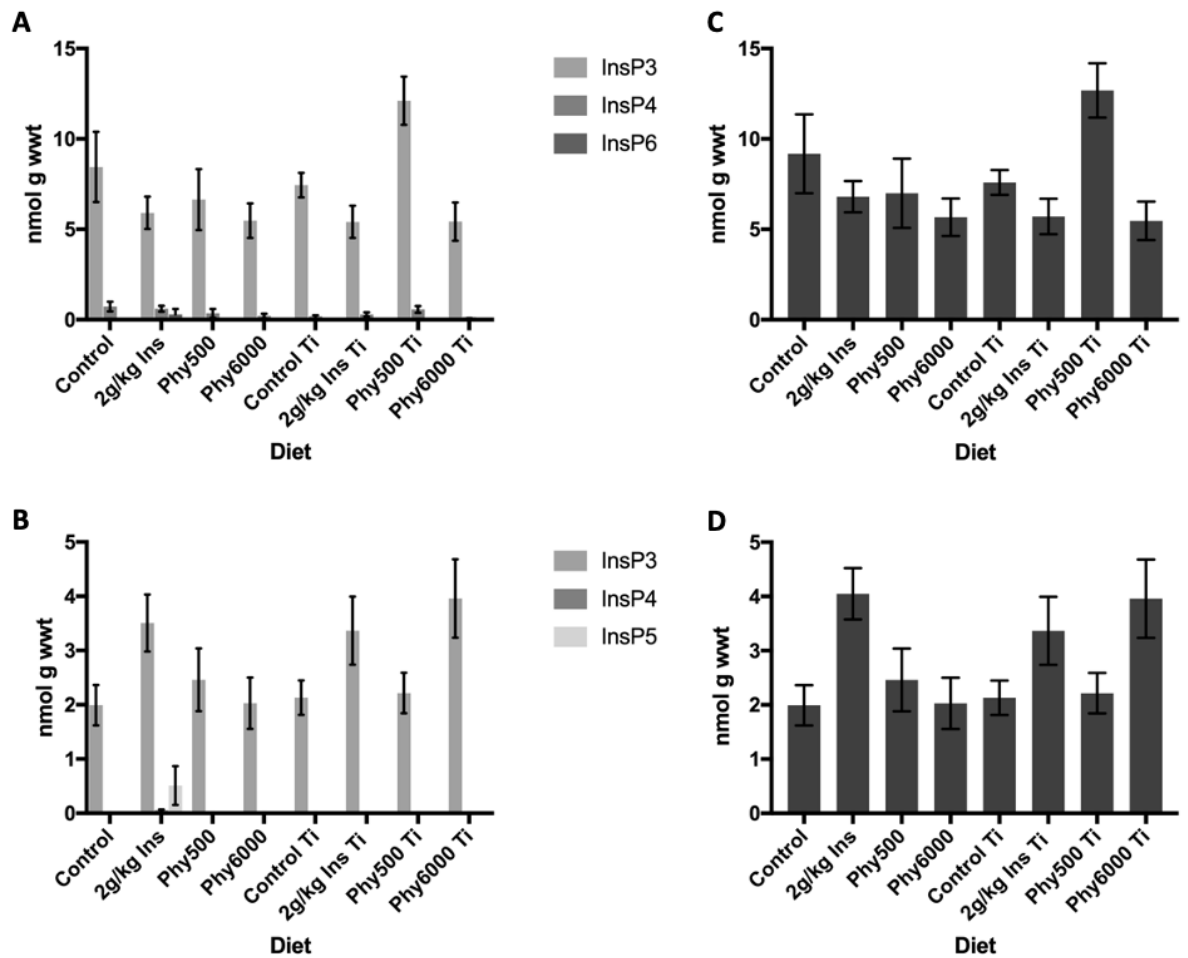


Figure 5.4: Inositol phosphate (InsP₃₋₆) levels (nmol/g wwt) in breast and leg muscles of day 21 broilers. **A**, InsP₃₋₆ in breast muscle; **B**, total inositol phosphate levels (sum of InsP₃₋₆) for the same extracts; **C**, InsP₃₋₆ in leg muscle; **D**, total inositol phosphate levels (sum of InsP₃₋₆) for the same extracts. Bars on the graph indicate calculated standard error of the mean for each group, n=12 for all.

Table 5.6: Inositol and inositol phosphate (InsP₃₋₆) levels (nmol/g wwt) in breast muscle of day 21 broilers (6 pens per diet with samples from 2 broilers per pen per treatment).^{1, 2}

Diet	Inositol	InsP ₃	InsP ₄	InsP ₅	InsP ₆	ΣInsP
Control	558±46	8.4±1.9	0.7±0.3	n.d.	n.d.	9.2±2.2
2g/kg Ins	772±50	5.9±0.9	0.6±0.2	n.d.	0.3±0.3	6.8±0.9
Phy500	656±56	6.6±1.7	0.4±0.2	n.d.	n.d.	7.0±1.9
Phy6000	694±41	5.5±1.0	0.2±0.1	n.d.	n.d.	5.7±1.0
Control Ti	566±50	7.4±0.7	0.1±0.1	n.d.	n.d.	7.6±0.7
2g/kg Ins Ti	727±42	5.4±0.9	0.3±0.1	n.d.	n.d.	5.7±1.0
Phy500 Ti	569±44	12.1±1.3	0.6±0.2	n.d.	n.d.	12.7±1.5
Phy6000 Ti	730±57	5.4±1.1	n.d.	n.d.	n.d.	5.4±1.1

Abbreviations: Σ InsP, total InsP₂ to InsP₆; InsP₆, inositol hexakisphosphate; InsP₅, inositol pentakisphosphate; InsP₄, inositol tetrakisphosphate; InsP₃, inositol trisphosphate; InsP₂, inositol bisphosphate.

¹The control group was fed with a diet with 0.45% calculated available phosphate. Groups Phy500 and Phy6000 and Phy500 Ti and Phy6000 Ti were fed with the control diet supplemented with 500 or 6,000 FTU of phytase per kilogram of feed, respectively. Groups 2g/kg Ins and 2g/kg Ins Ti were fed with the control diet supplemented with 2 grams per kilogram of ¹³C inositol (d30‰)

²Data are given as group means ± SEM, n = 12. Statistical analysis was performed by multiple T-tests with correction for multiple comparisons using the Holm-Šídák method.

Table 5.7: Inositol and inositol phosphate (InsP₃₋₆) levels (nmol/g wwt) in leg muscle of day 21 broilers (6 pens per diet with samples from 2 broilers per pen per treatment).^{1, 2}

Diet	Inositol	InsP ₃	InsP ₄	InsP ₅	InsP ₆	ΣInsP
Control	612±75	2.0±0.4	n.d.	n.d.	n.d.	2.0±0.4
2g/kg Ins	1486±120	3.5±0.5	n.d.	0.5±0.4	n.d.	4.0±0.5
Phy500	744±66	2.5±0.6	n.d.	n.d.	n.d.	2.5±0.6
Phy6000	880±81	2.0±0.5	n.d.	n.d.	n.d.	2.0±0.5
Control Ti	685±76	2.1±0.3	n.d.	n.d.	n.d.	2.1±0.3
2g/kg Ins Ti	1185±102	3.4±0.6	n.d.	n.d.	n.d.	3.4±0.6
Phy500 Ti	677±75	2.2±0.4	n.d.	n.d.	n.d.	2.2±0.4
Phy6000 Ti	804±76	4.0±0.7	n.d.	n.d.	n.d.	4.0±0.7

Abbreviations: Σ InsP, total InsP₂ to InsP₆; InsP₆, inositol

hexakisphosphate; InsP₅, inositol pentakisphosphate; InsP₄, inositol tetrakisphosphate; InsP₃, inositol trisphosphate; InsP₂, inositol bisphosphate.

¹The control group was fed with a diet with 0.45% calculated available phosphate. Groups Phy500 and Phy6000 and Phy500 Ti and Phy6000 Ti were fed with the control diet supplemented with 500 or 6,000 FTU of phytase per kilogram of feed, respectively. Groups 2g/kg Ins and 2g/kg Ins Ti were fed with the control diet supplemented with 2 grams per kilogram of ¹³C inositol (d30‰)

²Data are given as group means ± SEM, n = 12, apart from Phy500 Ti where 2 values have been removed as outliers for Ins values (inositol average n=10). Statistical analysis was performed by multiple T-tests with correction for multiple comparisons using the Holm-Šídák method.

InsP₃ was the dominant inositol phosphate detected in breast muscle and leg muscle samples across dietary treatments. Supplementation with either 2 g/kg Ins or phytase had no significant effect on inositol phosphate or total inositol phosphate levels compared to the Control diet ($p > 0.1$).

Overall there were no diets in which the extractable inositol measured in breast muscle different significantly from the Control diet, though the inclusion of 2 g/kg Ins approached traditional significance thresholds at $p = 0.0506$ compared to the Control fed group.

Inclusion of 2g/kg Ins in the diet significantly increased measurable tissue inositol concentration in the leg muscle compared to the Control, in both groups with and without the inclusion of TiO_2 (for 2 g/kg Ins, 142% increase observed; for 2 g/kg Ins Ti, 93% increase observed; for both, $p < 0.0001$). There was no significant difference between inositol levels with and without the inclusion of dietary phytase in the leg muscle (for all groups, $p > 0.1$).

InsP_3 was the only significant detectable inositol phosphate species in leg muscle extracts, and the dominant inositol phosphate in breast muscle extracts. Mayr and Thieleczek (1991) using tetanically stimulated skeletal muscles from *Xenopus laevis* (sartorius, tibialis anterior, iliofibularis muscles) and rat (gastrocnemius and soleus muscles) measured InsP_3 concentrations comparable to that seen in the leg muscle extracts here of poultry. The authors reported ca. 1.2 - 2.5 μM $\text{Ins}(1,4,5)\text{P}_3$ in resting state muscle and lower concentrations (0.2-0.9 μM) of D and/or L- $\text{Ins}(3,4,5,6)\text{P}_4$ (when corrected for myoplasmic space of muscle by assuming 0.58 mL/g muscle wet weight (Baylor, Chandler and Marshall, 1983). The same study, using *in vitro* radiolabelling experiments of contracting muscle, also detected higher inositol phosphates, InsP_5 and InsP_6 , but these higher inositol phosphates were not detectable in the muscle extracts from poultry in the trial presented here. The evidence of a role for InsP_3 in contraction of skeletal muscle, as opposed to smooth muscle is weak. Thus, while InsP_3 receptors are identifiable in smooth muscle (Marks *et al.*, 1990; Salanova *et al.*, 2002), evidence that InsP_3 is directly involved in stimulating skeletal muscle contraction has been attributed to artificial Ca^{2+} release in disrupted cell preparations (Hannon *et al.*, 1992). In cardiac and skeletal muscle, which shows excitation-contraction coupling, the release of calcium from sarcoplasmic reticulum is mediated via ryanodine receptors.

In birds, like other vertebrates, muscle fibre density is specified before birth. Vertebrate muscle fibres can be distinguished as 'slow twitch', Type I, or 'fast-twitch', Type II, with further sub-division of Type II according to expression of myosin heavy chain isoforms. Distinction can also be made according to predominant biochemistry of ATP production viz. oxidative (eg. Type I and IIA) or glycolytic (Type IIB) (Talbot and Maves, 2016). Chicken breast muscle, *pectoralis major*, is exclusively composed of Type IIB fibres, whereas leg muscle, gastrocnemius, has ca. 18% Type I fibres, the remainder Type IIB (Huo *et al.*, 2022). Although, the levels of inositol were generally similar between the different treatment groups in breast and leg muscle, and also in their response to phytase, inositol content of leg muscle was more responsive to (increased by) inositol-supplementation than was breast muscle, with numerical increase in inositol phosphate content for leg muscle also. These observations are broadly consistent with the study of (Charlotte Arthur, Mansbridge, *et al.*, 2021) that showed correlation between increases in plasma inositol and both breast and leg muscle inositol content with inositol-supplementation of diet. In a larger study, (Greene *et al.*, 2019) observed inositol supplementation- and phytase supplementation - (at > 1000 FTU/kg) dependent increases in muscle inositol.

5.3.5 Brain tissue inositol phosphates

Functionally, like in all other organisms, the brain in poultry is a complex organ forming part of the central nervous system, and responsible for the voluntary control of a number of tissues and organs, separated from circulating blood solutes by the highly selective semipermeable border of the blood-brain barrier (Vadlamudi and Hanson, 1966). Morphologically, the domestication of poultry over millennia has led not only to intentional physiological differences, with conscious selection for large body size, high feeding efficiency and larger pectoral muscles in broilers. This has led to unconscious selection for smaller brains in comparison to their wild relatives the Red Junglefowl (Jackson and Diamond, 1996), with similar reductions seen in high performing layer lines compared with lower performing lines or

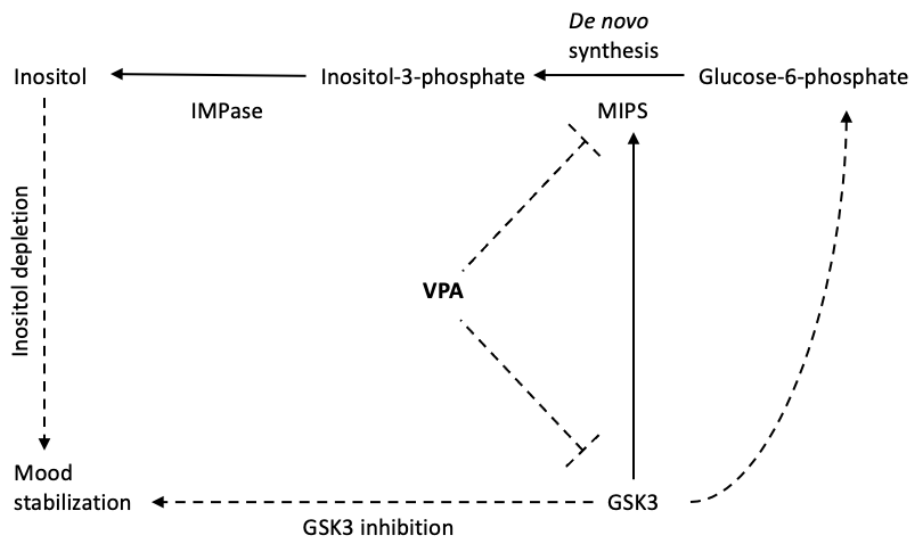
less intensively bred so-called “fancy breeds” still kept domestically but for pleasure rather than performance, though any functional consequences of this reduction in brain size have yet to be elucidated (Mehlhorn and Petow, 2020; Mehlhorn and Caspers, 2021).

Research into the role of inositol and inositol phosphates in the brains of poultry is limited, outside of animal behavioural studies investigating the use of inositol to ameliorate fearfulness, aggression and stress levels in laying hens (Herwig *et al.*, 2019). In animal models of psychiatric disorders and in human psychiatric studies, inositol deficiency has been correlated with increased memory loss (Priya, Bhyvaneswari and Patwari, 2013) and greater incidences of depression and anxiety and obsessive-compulsive disorder (Einat and Belmaker, 2001; Fisher, Novak and Agranoff, 2002; Shirayama *et al.*, 2017). The role of inositol phospholipids in signal transduction in the central nervous system is well established (Fisher and Agranoff, 1987; Fisher, Heacock and Agranoff, 1992), with functional roles assigned for inositol triphosphate in intercellular calcium signalling (Leybaert *et al.*, 1998) and InsP_6 in the modulation of circadian rhythms with suspected roles for inositol pyrophosphates (Wei *et al.*, 2018).

The inositol depletion hypothesis of lithium action, as explanation of treatment for bipolar disorder, is a long-standing, though not universally accepted, example of inositol involvement in brain function that has its origins in Berridge and colleagues' (Berridge, Downes and Hanley, 1982) observation that lithium amplifies agonist-dependent phosphatidylinositol responses in brain. The hypothesis (Yu and Greenberg, 2016) posits that inhibition of inositol recycling within the PI (phosphoinositide) cycle, after receptor-activation of $\text{PtdIns}(4,5)\text{P}_2$ hydrolysis by phospholipase C is manifest most strongly at the level of the inositol monophosphate (inositol monophosphatase). This prevents recycling of the inositol moiety of released $\text{Ins}(1,4,5)\text{P}_3$, otherwise used for resynthesis of PtdIns and successively $\text{PtdIns}4\text{P}$ and $\text{PtdIns}(4,5)\text{P}_2$. The well-characterized blockade of $\text{PtdIns}(4,5)\text{P}_2$ resynthesis results in depletion of $\text{PtdIns}(4,5)\text{P}_2$, elevation of $\text{Ins}(1,4,5)\text{P}_3$ and depletion of inositol (Yu and Greenberg, 2016). Inositol

depletion within the brain is a reported action of psychoactive drugs such as valproate and lithium, measured by NMR. Figure 5.5 shows the dual inhibition model proposed by Yu and Greenberg (2016).

Valproate (VPA) effects



Lithium effects

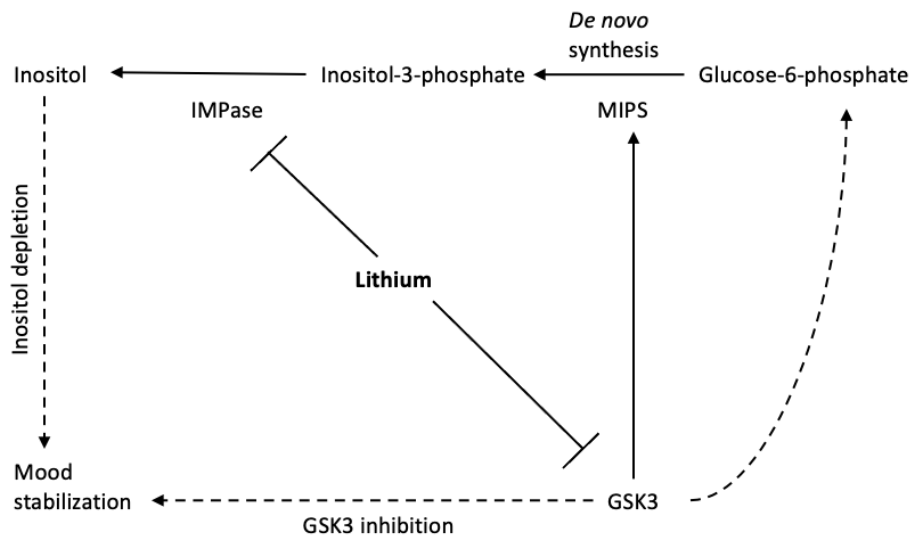


Figure 5.5: Model of the dual effects of Valproic Acid (VPA) and lithium on inositol depletion and GSK3 inhibition to contribute to mood stabilization. VPA directly inhibits MIPS, with proposed mode of action of inhibiting GSK3 to do so, reducing intracellular inositol. Lithium depletes inositol by inhibiting

IMPase, as well as inhibiting GSK3. GSK3 may also affect glucose-6-phosphate metabolism, but this is currently unknown. Inositol depletion affects numerous cellular functions, some of which are associated with mood stabilization. Figure reproduced from Yu and Greenberg (2016).

Valproate inhibits *myo*-inositol 3 phosphate synthase which converts D-glucose 6-phosphate to D-Ins3P. The latter is dephosphorylated by inositol monophosphatase which is inhibited uncompetitively by lithium. The brain exhibits very high levels of inositol, and its inositol metabolism is isolated to large extent by the blood-brain barrier. Measured inositol and inositol phosphates are presented in Figure 5.6, Table 5.8.

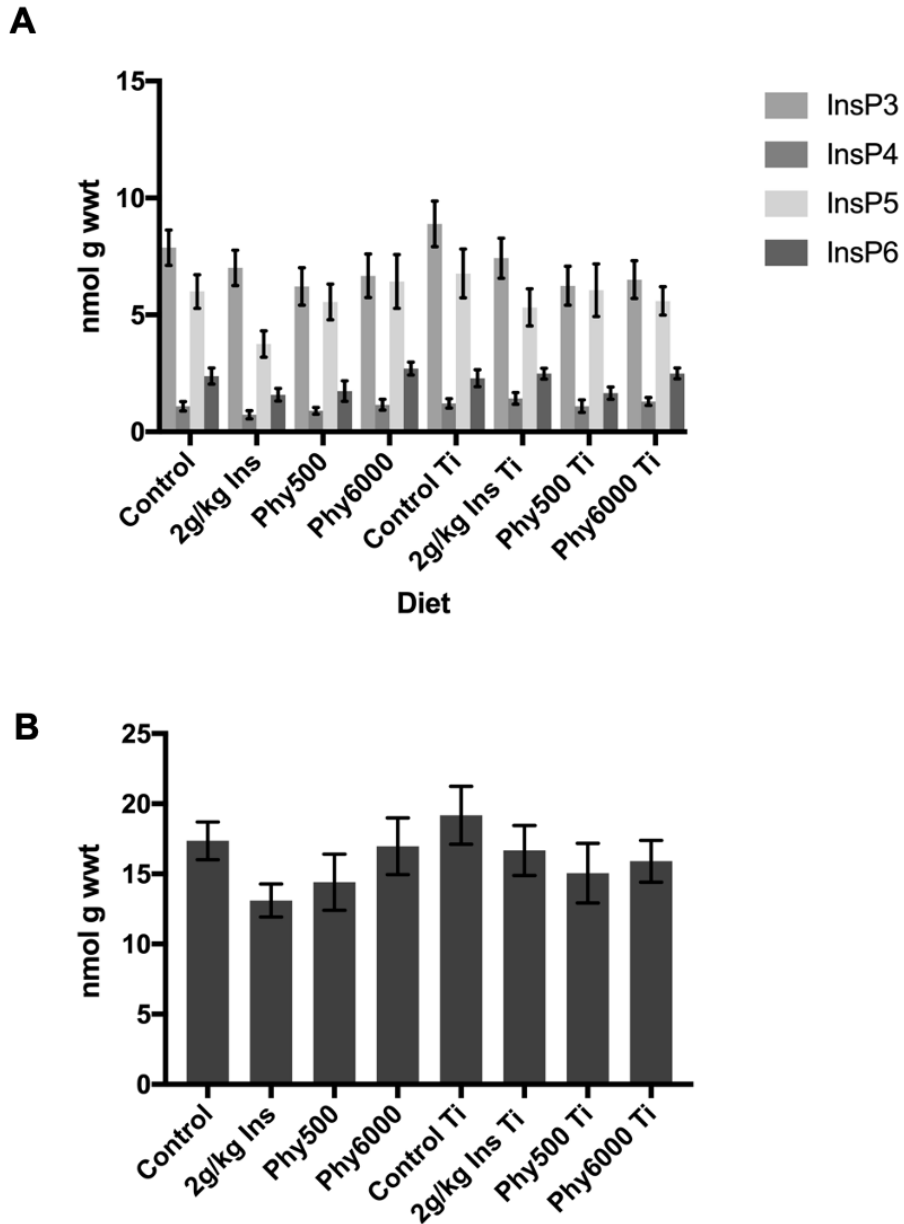


Figure 5.6 Inositol phosphate (InsP₃₋₆) levels (nmol/g wwt) in brain tissue of day 21 broilers, where **A** shows inositol phosphate levels for InsP₃₋₆ in brain tissue, and **B** total inositol phosphate levels (sum of InsP₃₋₆) for the same extracts. Bars on the graph indicate calculated standard error of the mean for each group, n = 12 for all groups except 2g/kg Ins where n = 11.

Table 5.8: Inositol and inositol phosphate (InsP₃₋₆) levels (nmol/g wwt) in brains of day 21 broilers (6 pens per diet with samples from 2 broilers per pen per treatment).^{1, 2}

Diet	Inositol	InsP ₃	InsP ₄	InsP ₅	InsP ₆	ΣInsP
Control	20092±624	7.8±0.8	1.1±0.2	6.0±0.7	2.4±0.3	17.4±1.3
2g/kg Ins	23519±1210	7.0±0.8	0.7±0.2	3.8±0.6	1.6±0.3	13.1±1.2
Phy500	21162±596	6.2±0.8	0.9±0.1	5.6±0.8	1.7±0.4	14.4±2.0
Phy6000	21030±854	6.7±0.9	1.2±0.2	6.4±1.2	2.7±0.4	17.0±2.0
Control Ti	20014±843	8.9±1.0	1.2±0.2	6.8±1.0	2.3±0.4	19.2±2.1
2g/kg Ins Ti	24926±1207	7.4±0.9	1.4±0.3	5.3±0.8	2.5±0.2	16.7±1.8
Phy500 Ti	20022±848	6.2±0.8	1.1±0.2	6.1±1.1	1.7±0.3	15.1±2.1
Phy6000 Ti	21275±1447	6.5±0.8	1.3±0.2	5.6±0.6	2.5±0.2	15.9±1.5

Abbreviations: Σ InsP, total InsP₂ to InsP₆; InsP₆, inositol

hexakisphosphate; InsP₅, inositol pentakisphosphate; InsP₄, inositol tetrakisphosphate; InsP₃, inositol trisphosphate; InsP₂, inositol bisphosphate.

¹The control group was fed with a diet with 0.45% calculated available phosphate. Groups Phy500 and Phy6000 and Phy500 Ti and Phy6000 Ti were fed with the control diet supplemented with 500 or 6,000 FTU of phytase per kilogram of feed, respectively. Groups 2 g/kg Ins and 2 g/kg Ins Ti were fed with the control diet supplemented with 2 grams per kilogram of ¹³C inositol (d30‰)

²Data are given as group means ± SEM, n = 12, except 2 g/kg Ins where n = 11. Statistical analysis was performed by multiple T-tests with correction for multiple comparisons using the Holm-Šídák method.

Brain inositol levels were increased by 17.06% with the inclusion of 2 g/kg Ins in the diet, from 20092±624 nmol/g wwt in the Control diet to 23519±1210 nmol/g wwt in 2 g/kg Ins ($p = 0.0942$) and significantly increased by 24.06% in the 2 g/kg Ins Ti diet with the additional inclusion of TiO₂ to 24926±1207 nmol/g wwt ($p = 0.0049$) (Table 5.8). At present, it is unknown the role that dietary *myo*-inositol plays in brain function, though transporters SMIT1 and SMIT2 have been identified predominantly in the brain of a number of

animals (Aouameur *et al.*, 2007). *Myo*-inositol is known to play a role as an osmolyte in the brains of rats and in human cell lines (Macrì *et al.*, 2006; Dai *et al.*, 2016). Amplification of Band q22 of human chromosome 21, containing SMIT, is observed in Down's syndrome (Berry *et al.*, 1995) and is associated with substantial elevations of inositol (Shetty *et al.*, 1995; Berry *et al.*, 1999; Fisher, Novak and Agranoff, 2002). In poultry, *myo*-inositol has been associated with increased plasma concentrations of the neurotransmitters serotonin and dopamine (Herwig *et al.*, 2019; F. Gonzalez-Uarquin *et al.*, 2020). It will be interesting to determine whether SMIT expression is influenced by dietary interventions of the nature employed here.

InsP₃ and Ins(1,3,4,5,6)P₅ were the dominant inositol phosphates in the brain tissue, at almost equal levels, and at 3-4 fold higher concentrations than InsP₄ and InsP₆, these increased levels of notable Ins(1,3,4,5,6)P₅ compared to InsP₄ levels have been observed in radiolabelled differentiating neurons (Ucuncu *et al.*, 2020), with species Ins(1,3,4)P₃ and Ins(1,4,5)P₃ as well as Ins(1,3,4,5)P₄ identified in Li⁺ treated cholinergically stimulated brain slices of guinea pig, mouse and rat brains by radiolabelling (Lee *et al.*, 1992). Despite numerous studies of the response of neuronal cell inositol phosphate metabolism to agonists such as carbachol, that targets muscarinic M3 receptors (Nahorski, Tobin and Willars, 1997), it is remarkable that the higher inositol phosphate profile of brain tissues or neuronal cells is relatively undescribed. A recent study of MINPP deletion (Ucuncu *et al.*, 2020) offers some assistance, but among different classes of [³H]inositol-labelled inositol phosphates identified only Ins(1,3,4,5,6)P₅ and InsP₆ as discrete isomers in day 10 differentiating neurones or their induced pluripotent stem cell precursors. Vallejo and colleagues' study (Vallejo *et al.*, 1987) identified the same two isomers in [³H]inositol-labelled, by microinjection, of anaesthetized, rat brain, but noted a failure to detect InsP₄. This may reflect the limitations of the *in vivo* approach, as the data of Table 5.8 makes clear that lower and higher inositol phosphates are readily detectable by the methods of this study in poultry. Brain total inositol phosphates showed no significant differences in response to different diets compared to the Control

diet (Control vs. 2 g/kg Ins, $p = 0.118$; Control vs. Phy500, $p = 0.657$; Control vs. Phy6000, $p = 0.985$). The inclusion of dietary phytase had no significant difference on the measured inositol levels in brain tissue compared to the Control diet (for all phytase doses, with and without Ti, $p > 0.9$).

5.3.6 Inositol phosphate identities in poultry tissues

Other than in erythrocytes (Mayr and Dietrich, 1987; Stephens, Hawkins and Downes, 1989; Casals, Villar and Riera-Codina, 2002; Whitfield *et al.*, 2022), inositol phosphates isomers have not been identified in poultry organs. In this chapter experiments are described that were designed to identify isomers of inositol phosphates in different tissues. Amongst the thousands of radiolabelling studies of inositol phosphate metabolism of isolated cells and tissue slices, there are barely any comparisons of the inositol phosphate speciation of different cell types, let alone organs of a single species. This, no doubt, reflects the constraints of radiolabelling, but nevertheless leaves the physiology of digestive influence on tissue and organ inositol phosphate metabolism and associated pathologies wholly unstudied. The experiments in this chapter seek to redress this (Figure 5.7).

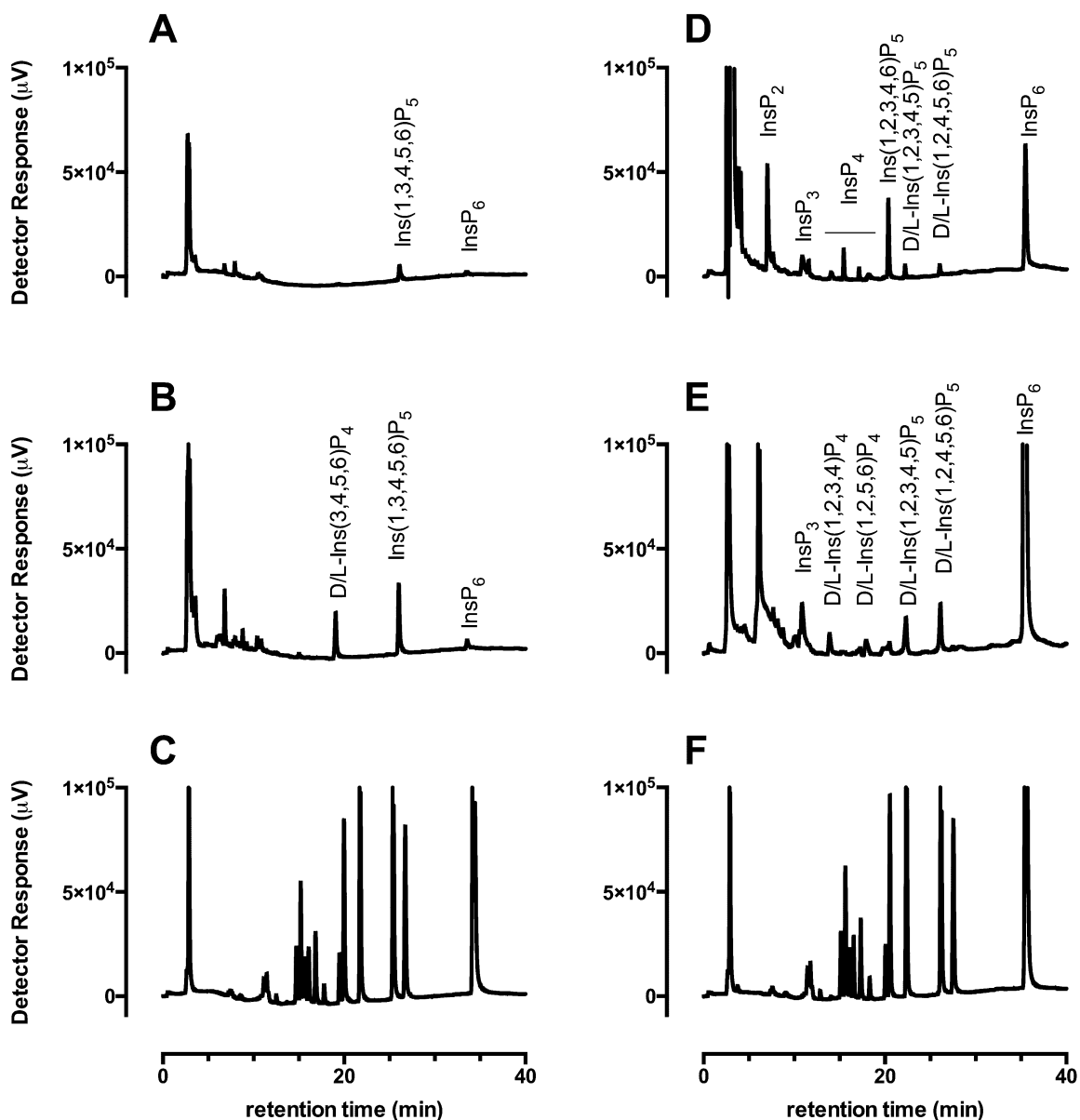


Figure 5.7 Figure previously published in Sprigg *et al.* 2022. Inositol phosphates in broiler digesta and tissue. Extracts of **A**, liver; **B**, kidney; **D**, gizzard contents; **E**, ileal contents; from a single bird (A, B) or pooled from 2 birds (D, E) fed the Control diet were analysed by HPLC. **C** and **F**, standards run beside the different sample sets from which A, B and D, E, respectively, were obtained. Inositol phosphate classes and individual isomers are identified.

The peaks identified in figure 5.7A in liver tissue and figure 5.7B in kidney tissue extracts, are identified as D-and/or L-Ins(3,4,5,6)P₄ and Ins(1,3,4,5,6)P₅. Similarly, peaks of the same identities were identified in

duodenum, jejunum and ileum tissue extracts (Appendix 6). Peaks in the standards (Fig 5.7C and 5.7F) are used as reference for identification of these isomers. The isomers identified in the tissue extracts differ from those identified in the gizzard and ileal contents (Fig 5.6D, E), identified as D- and/or L-Ins(1,2,3,4)P₄, D- and/or L-Ins(1,2,5,6)P₄, Ins(1,2,3,4,6)P₅, D- and/or L-Ins(1,2,3,4,5)P₅, D- and/or L-Ins(1,2,4,5,6)P₅ and InsP₆.

5.4 Conclusions

5.4.1 Inositol phosphates in poultry tissues

The peaks identified in Figure 5.7B for kidney tissue samples are also the isomers present in liver tissue samples (Figure 5.7A), and the same isomers are identified in all other tissue types described in this chapter (see Appendix 6). The identities of peaks in the set of standards (Figure 5.7C) have been described (Whitfield *et al.*, 2018, 2022; Rix *et al.*, 2021). The isomers detected in tissues, D-and/or L-Ins(3,4,5,6)P₄ and Ins(1,3,4,5,6)P₅, differ from the known products of phytase degradation in Quantum Blue-supplemented diets, D- and/or L-Ins(1,2,3,4)P₄, D-and/or L-Ins(1,2,5,6)P₄, Ins(1,2,3,4,6)P₅, D- and/or L-Ins(1,2,3,4,5)P₅ and D- and/or L-Ins(1,2,4,5,6)P₅ (Sommerfeld, Künzel, *et al.*, 2018) (Figure 5.6D,E). As diets were fed as a mash in this study, as opposed to the usual application of heat pelleted diets which renders endogenous plant phytases present in the feed substance from wheat and soybean inactive, the presence of Ins(1,2,3,4,6)P₅ in the gizzard and ileal digesta inositol phosphate profile is noted as a known product of endogenous MINPP phytase. HPLC methods utilised in this analysis are unable to distinguish hydrolysis products arising from phytase activity by wheat 4-phytases (PAPhy) and the supplemented *E. coli* 6-phytase, either at the InsP₅ level of generation of Ins(1,2,3,5,6)P₅ or Ins(1,2,3,4,5)P₅, or at the InsP₄ level of Ins(1,2,5,6)P₄ or Ins(2,3,4,5)P₄ and Ins(1,2,3,4)P₄ versus Ins(1,2,3,6)P₄., hence the 5-OH product of cereal MINPP proving especially diagnostic. The tissue inositol phosphates, (Figure 5.7 A,B) are similar to

those identified in avian erythrocytes (Stephens and Downes, 1990a; Mayr and Thieleczek, 1991; Whitfield *et al.*, 2022).

The significance of the inositol phosphate isomers identified in these tissues is that, despite the clear impact of dietary phytase on inositol phosphates in gizzard and ileal contents, and on total tissue inositol phosphates, the tissue isomers of inositol phosphates are phosphorylated in positions not expected from phytate degradation by Quantum Blue (*E. coli*) phytase used here or from endogenous feed phytase. Instead, they reflect the isomers expected from *de novo* inositol phosphate synthesis (Stephens and Downes, 1990a) and they match the isomers reported in both *Xenopus* and rat skeletal muscle tissues analysed by different methods (Mayr and Thieleczek, 1991). It is widely accepted that the products of phytase degradation retain phosphate in the 2-position, and equally that the final step in inositol hexakisphosphate biosynthesis involves the addition of a phosphate to the 2-position (Letcher, Schell and Irvine, 2008). It is from this that it can be concluded that the effect seen in different dietary conditions (0, 500FTU and 6000FTU Quantum Blue) in kidney inositol phosphate levels have not arisen as a result of uptake of inositol phosphates following gut phytate hydrolysis, with the isomers identified lacking a phosphate on the 2-position.

5.4.2 Kidney inositol phosphate levels are responsive to dietary phytase dose

Kidney tissue inositol phosphate levels, as individual InsP₄, InsP₅ and InsP₆ isomers, as well as total inositol phosphate levels, decrease with increasing phytase dose. This pattern suggests that the response is due to the influence of increasing free inorganic Pi and/or inositol in the gut, and/or their tissue-specific influence on inositol phosphate biosynthetic gene expression.

Despite numerous studies describing the impact of dietary phytase on free inositol, specifically on the increase in circulatory inositol (Walk, Santos and Bedford, 2014; Sommerfeld *et al.*, 2018b; Pirgozliev *et al.*, 2019a; Ajuwon *et al.*, 2020; Gonzalez-Uarquin *et al.*, 2020; Gonzalez-Uarquin, Rodehutscord

and Huber, 2020; Gonzalez-Uarquin *et al.*, 2021; Kriseldi *et al.*, 2021), few studies measure any tissue specific responses other than in chicken erythrocytes (Whitfield *et al.*, 2022). Recent research of pharmacological inhibition of IP6K, an enzyme responsible for the conversion of InsP₆ to InsP₇ has been shown to cause a transient reduction in plasma phosphate in rats and monkeys (Moritoh *et al.*, 2021). Circulating phosphate levels are known to be tightly controlled within a narrow range in mammals, and IP6K inhibition resulted in reductions in InsP₇ in liver, muscle and, most significantly, in the kidney, but without effect of renal reabsorption of phosphate (Moritoh *et al.*, 2021).

In animal models and in humans, research has shown that the kidney is the most important organ for maintenance of blood plasma inositol concentration (Holub, 1986b) and the main location for inositol catabolism as shown in rats (Howard and Anderson, 1967), with *myo*-inositol reportedly an important organic osmolyte in mammalian kidneys (Sizeland *et al.*, 1993) and brains (Córdoba, Gottstein and Blei, 1996; Soupart *et al.*, 2002; Haris *et al.*, 2011), though there is no research to date in poultry to suggest the same holds true in avian systems (Gonzalez-Uarquin, Rodehutschord and Huber, 2020). As such, there is equally minimal research considering how changes in circulatory inositol, or inositol and phosphate as the absorbable co-products of phytase action in the gut, modifies tissue inositol phosphate synthesis (Sprigg *et al.*, 2022).

Whilst it cannot be excluded that potential selective inositol phosphate absorption and metabolism contributes to the tissue profile observed, at present no inositol phosphate transporters have been described in animals, though a plethora of studies describing the expression of inositol and phosphate transporters in the gastrointestinal tract of poultry have been published. As such, the data presented here suggests that the changing profile with phytase dose seen in the kidney is a result of tissue response to changing phosphate and/or inositol availability in terms of influence on tissue specific inositol phosphate synthesis.

5.4.3 Liver inositol phosphate levels are impacted by inositol supplementation

Similarly to in mammalian systems, the liver in poultry is a vital organ which carries out many metabolic functions, including but not limited to bile secretion and lipid, carbohydrate and protein metabolism as an accessory organ to the digestive system (Zaefarian *et al.*, 2019). Despite the importance of the liver in a number of roles in birds, very little is known about the influence of diet on liver size, development, and function, with limited studies focussing solely on specific pathologies.

The liver contains high concentrations of inositol (Eisenberg and Bolden, 1963; Croze and Soulage, 2013). *Myo*-inositol has been reported to be a hepatic lipid exporter, based on study showing the accumulation of triglycerides in inositol-deficient diets and the absence of this accumulation in inositol replete diets (Hayashi, Maeda and Tomita, 1974), though the mechanisms for this are not yet known. Similarly, studies investigating phytase addition to broiler diets have shown modified liver lipid profiles (Liu *et al.*, 2010), and the presence of dietary phytate in the form of supplemented sodium phytate increases liver weight, lipids, triglyceride and cholesterol content of the liver and decreases hepatic lipogenic enzyme activity in rats (Katayama, 1995). Research by Croze *et al.* (Croze, G elo en and Soulage, 2015) investigating the role of chronic inositol supplementation on insulin sensitivity suggests that the possible mechanism for the role of inositol in fatty acid transport could be reducing fatty acid synthase activity in epididymal white adipose tissue.

Though limited access to appropriate methodology has dictated that previous studies have been unable to measure the impact of phytase supplementation on inositol phosphate profile in liver tissues, it has been noted that phytase supplementation at 500, 1000 and 1500 FTU has no effect on liver weight (Sharma *et al.*, 2016). The significant impact of inositol supplementation on

overall extractable inositol concentration in the liver was anticipated, as previous research has noted that massively supra-physiological inositol dose significantly increases tissue inositol concentration in leg muscle, breast muscle and kidney tissue (C Arthur *et al.*, 2021), as also seen in this study in digestive tissues in addition to muscle and metabolic tissues. However, research to date has not proposed a potential mechanism for the phenomenon seen here, by which inositol supplementation decreases inositol phosphate concentration in the liver. It has been hypothesised in other animal models that inositol phosphates might alter secondary messengers in the energy metabolism pathways of insulin sensitive tissues, including the liver (Chatree *et al.*, 2020), therefore there is potential that significant increases in *myo*-inositol concentrations in this tissue, a product of glucose metabolism, may alter synthesis of inositol phosphates forming part of a signalling cascade for energy metabolism.

5.4.4 Inclusion of titanium dioxide as a digestibility index marker does not impact extractable inositol phosphates in tissues

The use of TiO₂ as a pre-concentration method for the extraction of inositol phosphates has been recently applied for analysis of poultry tissues, as in this chapter (Wilson *et al.*, 2015), though has been used routinely by the cell biology field for phosphopeptide research for many years. In addition, the use of TiO₂ as a digestibility index marker in the animal feed industry has been relatively commonplace in monogastrics, though its use in animal feed is no longer considered safe in the EU due to potential concerns of genotoxicity (Bampidis *et al.*, 2021).

In light of the widespread use of TiO₂, both as a digestibility index marker in animal feeding trials still in use in the UK and USA, and as an enrichment method for phosphopeptide and inositol phosphate research, this study additionally aimed to investigate the effect of the inclusion of TiO₂ impacted the effect of dietary supplemented phytase or the extraction of inositol phosphates from diet, digesta and tissues. Results in Chapter 4 present that the inclusion of TiO₂ has no significant effect on the extraction and analysis

of inositol phosphates from poultry diets or gizzard and ileal digesta. By two-way ANOVA for each tissue type, inclusion of TiO_2 is not found to be a source of variance in analysed inositol phosphate levels in tissues, and matched T-tests also showed no significant differences between matched diet conditions with and without TiO_2 .

Presented in this chapter are the first measurements of the profiles of inositol phosphates in poultry tissues. They were achieved without the use of radiolabelling, which is not only labour intensive and restrictive in both research use and animal husbandry in feeding radioisotope. The inositol phosphate species described here match those described in other animal models by traditionally accepted radioisotope methods.

The inositol phosphate isomers described in this chapter not only describe the native state profiles in poultry tissues, but also the identification of these isomers as those resulting from *de novo* synthesis show how addition of phytase to poultry diets - and the inositol and phosphate released thereof - alters ratios of inositol phosphates in kidney and liver tissues. Not only that, but evidence here suggests that the kidney is especially responsive, directly or indirectly, to phosphate from the diet, and liver similarly responsive to dietary inositol. The methods elaborated here have enabled a first look at the integrated whole-bird response to phytase supplementation in terms of inositol phosphate status in an organ specific manner.

6. The effect of phytase supplementation on circulating metabolites implicated in phosphate homeostasis

6.1 Introduction

Chapter 5 described the decrease in inositol phosphates in kidney tissue observed with increasing phytase dose, and that the isomers observed reflect those expected from *de novo* synthesis of inositol phosphates. It is likely that the effect seen in the kidney arises from tissue response to changing phosphate and/or inositol supply in the blood, as these are metabolic precursors of tissue inositol phosphates in poultry as in other species.

Response of poultry to phytase is commonly interpreted in the context of interaction of calcium and phytate, their matrix values and interaction with the gut; though in comparison to calcium homeostasis which has been extensively studied, the mechanisms underpinning phosphate homeostasis is less understood. The interaction of the gut with distal organs is mediated by a major tissue, the blood, and human and mammalian studies show that phosphate homeostasis is controlled by inter-organ signalling between the gut, kidney, parathyroid gland and bone, mediated by vitamin D along with parathyroid hormone (PTH), which serves as the primary regulator of serum calcium with an additional role in decreasing phosphate reabsorption at the proximal convoluted tubule in the kidney (Weinman & Lederer, 2012) and the bone-derived hormone fibroblast growth factor 23 (FGF23) (Bergwitz and Jüppner, 2010), with FGF23 shown to inhibit renal tubular reabsorption of phosphate through mechanisms independent of PTH (Quarles, 2012).

Vitamin D₃ (cholecalciferol) is provided in poultry diets for avoidance of tibial dyschondroplasia and is especially important in provision of adequate calcium supply for egg (shell) production in layers (Whitehead *et al.*, 2004; Mattila, Valkonen and Valaja, 2011). The effects of combination of phytase

and cholecalciferol on growth performance have previously been established (Qian, Kornegay and Denbow, 1997), but to date studies are not published of the effect of phytase supplementation on levels of vitamin D or its metabolites.

The results presented in Chapter 5 speak to a phytase-dependent modulation of tissue inositol phosphate levels in the kidney of poultry fed diets supplemented with vitamin D₃ as standard (Sprigg *et al.*, 2022), and postulated potential explanations for this observation in the alteration of phosphate homeostasis mechanisms resulting from the increase in free available phosphate with phytase supplementation. This is not a naïve premise given a known central role for the kidney in phosphate homeostasis (Warren and Livingston, 2021), and the effects of systemic inhibition of inositol hexakisphosphate kinase on serum phosphate levels of rats and monkeys (Moritoh *et al.*, 2021).

The kidney also retains a central role in vitamin D processing for the maintenance of phosphate homeostasis. There are two major classes of vitamin D: ergocalciferol (D₂), which is primarily synthesized by algae and fungi (Holick *et al.*, 1973; Holick, 1989); and cholecalciferol (D₃), which is synthesized *de novo* by animals, the metabolic pathway of which is depicted in Figure 6.1. In poultry, vitamin D₃ is taken up by the liver, where it is hydroxylated at the side chain C-25 to 25-OH-D₃, the predominant circulatory form of vitamin D₃ (Tucker, Gagnon and Haussler, 1973; Clark and Potts, 1976) by 25-hydroxylase. Circulating 25-OH-D₃ in adult chickens is thought to be approximately 25 ng/mL (Horst *et al.*, 1981). 25-OH-D₃ is further hydroxylated at the 1-C position by 1 α -hydroxylase in the kidney to yield 1,25-(OH)₂-D₃ (Shanmugasundaram and Selvaraj, 2012). 1,25-(OH)₂-D₃ is the active form of vitamin D, as a ligand for the transcription regulator VDR (Kongsbak *et al.*, 2013), and so 1 α -hydroxylase activity is tightly regulated to avoid homeostatic imbalance by parathyroid hormone (PTH), fibroblast growth factor 23 (FGF23), circulatory calcium and phosphate, and 1,25-

(OH)₂-D₃ (Boyle, Gray and DeLuca, 1971; Hughes *et al.*, 1975; Shimada *et al.*, 2004a).

Hydroxylation at C-24 can occur with either 1,25-(OH)₂-D₃ or 25-OH-D₃, resulting in 1,24,25-(OH)₂-D₃ or 24,25-(OH)₂-D₃ (Holick *et al.*, 1973). 24,25-(OH)₂-D₃ is considered an inactive form of vitamin D, and inhibits signalling cascades involved in calcium and phosphorus absorption, which in turn inhibits bone mineralisation (St-Arnaud *et al.*, 2000). The 24-hydroxylase is responsible for this and is tightly regulated by 1,25-(OH)₂-D₃, though maintains an important role in calcium homeostasis by preventing hypercalcaemia (Veldurthy *et al.*, 2016).

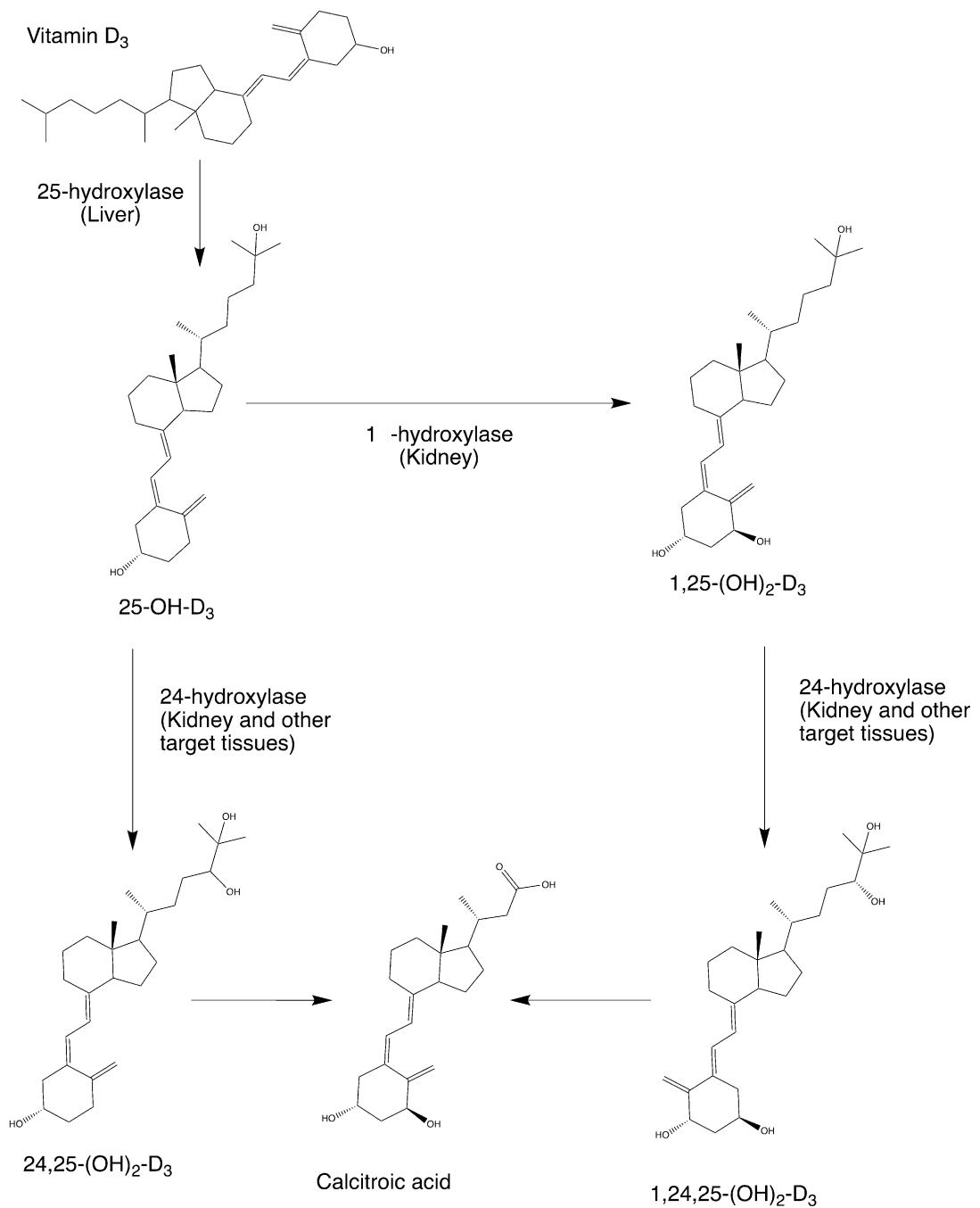


Figure 6.1: Metabolic pathway of Vitamin D₃ to its metabolites. Figure adapted from Holick (1994) and Warren and Livingston (2021).

In the context of phosphate homeostasis, vitamin D - specifically, 1,25-(OH)₂-D₃ - is considered to be a hormone, with circulatory serum 1,25-(OH)₂-D₃, PTH and tibia FGF23 partly responsible for the regulation of bone phosphorus retention and bone development (Cao *et al.*, 2021). Similarly important in this homeostasis network, FGF23 has been shown in mice to be a physiological regulator of circulatory phosphate and 1,25-(OH)₂-D₃ levels

(Shimada *et al.*, 2004b), and its overexpression is linked to renal phosphate wasting disorders or oncogenic hypophosphatemic osteomalacia (Shimada *et al.*, 2001; White *et al.*, 2001a) and the hereditary disorder autosomal-dominant hypophosphatemic rickets (White *et al.*, 2001b). These hormones are also major regulators of serum calcium, in combination with parathyroid hormone (PTH), with PTH regulating calcium homeostasis by modulating bone metabolism, synthesis of 1,25-(OH)₂-D₃ and calcium reabsorption (Kumar and Thompson, 2011; Khundmiri, Murray and Lederer, 2016). The skeleton is the major reserve for calcium and phosphate stores, with bone mineralisation the most sensitive measure of phosphate utilisation (Shastak *et al.*, 2012; Li *et al.*, 2015); and maintenance of each mineral to prevent deviation from its basal condition is achieved through these hormones signalling for either increased uptake from the gastrointestinal tract, altered excretion via the kidneys, or by either increasing sequestration of or utilisation of reserves in the bone (Bruder, Guise and Mundy, 2001; Blaine, Chonchol and Levi, 2015).

Because the kidney is part of the inter-organ axis responsible for phosphate homeostasis, with a notable response to phytase supplementation observed in the profiles, measurements were made of circulatory nutrients and hormones of the gut, parathyroid gland, kidney, and bone axis, to further understand the role of the products of phytase action in maintenance of broiler phosphate homeostasis.

6.2 Materials and methods

6.2.1 Animals, Diet and Experimental Design

Animals, husbandry and basal diet composition in this trial were previously described in Chapters 4 and 5. Briefly, 480 male Ross 308 hatchlings were

randomly allocated to 48 pens, with a 2 x 4 factorial arrangement of treatments [2 TiO₂ levels, one inositol level and 3 phytase levels (0, 500 and 6000 FTU)]. The study was made of one diet phase – a starter – offered as a mash, and the basal diets were mixed in two separate lots, each divided into 4 equal parts, and formulated to contain adequate levels of all nutrients according to the Ross Management Manual 2018. Study diets were supplemented with 3 µg/kg diet cholecalciferol (Vitamin D₃) as part of the originally supplemented vitamin and mineral premix, components of which are described in Chapter 4.2 (Table 4.5).

Two birds per pen were randomly selected for sampling on day 21 post-hatch and were euthanised via cervical dislocation without prior stunning in accordance with the Welfare of Animals at the Time of Killing (England) Regulations (2015) guidelines for poultry. Blood was collected from each bird of the two birds following post-mortem examination, pooled and separated into heparinised tubes and immediately frozen at -20°C before shipping to UEA for analysis. Samples were stored thereafter at -80°C.

6.2.2 Plasma Hormones

Analysis of vitamin D metabolites, 25(OH)D₂, 25(OH)D₃, 24,25(OH)₂D₂ and 24,25(OH)₂D₃, in plasma was performed by a clinically validated LC-MS/MS method performed using Micromass Quattro Ultima Pt electrospray ionisation (ESI) tandem mass spectrometer (Waters Corp., Milford, MA, USA), and chromatographic separation was achieved using a core-shell C18 50x2.1 mm 2.6 µm reversed-phase column with an in-line 2 µm, 6.35 mm x 24 mm guard filter (Restek, Bellefonte, PA, USA). Analysis for vitamin D metabolites was performed by Rachel Dunn at the Norwich Medical School, the method of which is published in full in Tang *et al.* (2017).

Fibroblast Growth Factor 23 (FGF23) was determined using an enzyme-linked immunosorbent assay kit as per manufacturer's instructions (ELISA; Abnova Ltd., Cambridge, UK.) with detectable range 0-1000 pg ml⁻¹,

sensitivity 9.38 pg ml⁻¹. Parathyroid Hormone (PTH) was determined using chicken-specific enzyme-linked immunosorbent assay kit as per manufacturer's instructions (ELISA; Cusabio Technology LLC, USA) with a detection range 0-1000 pg ml⁻¹, sensitivity of 6.25 pg ml⁻¹.

6.2.3 Plasma minerals

Total plasma calcium and phosphate was measured by inductively coupled plasma atomic emission spectroscopy using an Agilent Vista Pro from dilutions of plasma into 18.2 MOhm.cm water.

6.2.4 Plasma inositol

For inositol analysis, 200 µL aliquots of blood plasma were deproteinated using 10% trichloroacetic acid and diluted 50-fold in 18.2 MOhm.cm water. Inositol was determined by HPLC pulsed amperometry of 20 µL aliquots after separation by 2-dimensional HPLC on Dionex CarboPac PA1 and MA1 columns (method described fully in section 3.2.2.12).

6.2.5 Statistical analysis

All results are expressed as mean ± SEM (standard error). The differences between means were tested by two-way ANOVA with Dunnett's correction for multiple comparisons to determine source of variation. Inclusion of TiO₂ was found to be not significant as a source of variation (P = 0.6847) and data was pooled from matched groups and compared by one-way ANOVA with Dunnett's multiple comparisons test. All statistical tests were performed using GraphPad Prism, version 7.0e, for Mac OS X (GraphPad Software, La Jolla, CA). Alpha for all statistical tests was set at 0.05. Adjusted ANOVA P values are presented in the tables, and group specific P values presented in the text.

6.3 Results

6.3.1 Plasma inositol and metabolites

Plasma inositol content was numerically different but not statistically significantly altered between groups compared to Control: for 2 g/kg Ins, $p = 0.073$; for Phy500, $p = 0.297$; for Phy6000, $p = 0.206$ (Table 6.1). The range of values of inositol measured in plasma are similar to values reported for phytase treatments in other studies in which phytase was shown to increase plasma inositol (Gonzalez-Uarquin *et al.*, 2020). Because the kidney is a key organ for inositol metabolism and because kidney inositol phosphates are responsive to phytase (Sprigg *et al.*, 2022), a range of blood parameters reflecting metabolic and endocrine function of the kidney were tested. In chickens, calcium and phosphate are tightly controlled in a narrow physiological range (Warren and Livingston, 2021). Phytase treatment was without effect on plasma ionized calcium or phosphate (Table 6.1), but Ca:P ratio was numerically reduced in Phy500 and Phy6000 Groups compared to Control Group. Plasma PTH was unaffected by treatment, falling in the range 19-40 pg/mL comparable to the value ca. 50 pg/mL reported for Lohman Selected Leghorn (LSL) and Lohman Brown (LB) layers (Reyer *et al.*, 2021). Plasma FGF23 was unaffected by treatment, falling in the range 10.9-13.5 pg/mL. Others, Ren *et al.* (2017), have reported reduction in both FGF23 and PTH by vaccination of laying hens with FGF23 peptide, with FGF23 values in the range 273-466 pg/mL and PTH values in the range 11.6-21.9 pg/mL.

Table 6.1: Plasma parameters in day 21 broilers. ^{1,2,3}

Diet	Inositol	Calcium	Phosphate	Ca:P	PTH	FGF23
Control	255±33	0.80±0.12	1.09±0.13	0.72±0.04	30.98±4.72	12.33±0.92
2g/kg Ins	326±33	0.96±0.07	1.30±0.10	0.74±0.03	36.58±5.51	11.33±0.53
Phy500	235±19	0.66±0.06	0.95±0.07	0.69±0.04	24.64±4.46	12.08±0.45
Phy6000	293±31	0.72±0.05	1.13±0.08	0.63±0.02	31.75±4.92	12.19±0.91
<i>P</i> -value	0.1519	0.2413	0.1948	0.1148	0.7206	0.8386

¹The control group was fed with a diet with 0.45% calculated available phosphate. Groups 2 g/kg Ins were fed with 2 g supplemented d30% ¹³C inositol mix per kilogram of feed; groups Phy500 and Phy6000 were fed with the control diet supplemented with 500 or 6,000 FTU of phytase per kilogram of feed, respectively.

²Data are given as group means ± SEM, n = 12, of 12 replicate pens with samples pooled from 2 broilers per pen per treatment.

³ Calcium and phosphate measurements are given as mmol/L concentrations; inositol measurements as nmol/mL; and PTH and FGF23 as pg/mL.

6.3.2 Effect of phytase treatments on vitamin D metabolites

Following on from results in Chapter 5 showing the notable impact of dietary phytase supplementation on kidney inositol phosphate levels, and the known role of the kidney in vitamin D processing, measurements were undertaken of the impact supplementation with Quantum Blue had on the detectable levels of circulating vitamin D metabolites. Measurements of these were carried out by Dr. Jonathan Tang and colleagues (Norwich Medical School), and are presented in Table 6.2.

Table 6.2: Plasma concentration of vitamin D metabolites (nmol/L) in day 21 broilers. ^{1,2}

Diet	Total 25(OH)D	Total 24,25(OH)D	Total 25(OH)D: total 24,25(OH)D
Control	41.83±3.08	5.28±0.45	8.17±0.34
2g/kg Ins	42.13±5.03	5.21±0.61	8.25±0.37
Phy500	33.24±2.65	4.73±0.37	7.08±0.19
Phy6000	39.20±3.46	5.84±0.56	6.92±0.23
<i>P</i> -value	0.7188	0.8851	0.0045

¹The control group was fed with a diet with 0.45% calculated available phosphate. Groups 2 g/kg Ins were fed with 2 g supplemented d30‰ ¹³C inositol mix per kilogram of feed; groups Phy500 and Phy6000 were fed with the control diet supplemented with 500 or 6,000 FTU of phytase per kilogram of feed, respectively.

²Data are given as group means ± SEM, n = 12, of 12 replicate pens with samples pooled from 2 broilers per pen per treatment.

No significant differences were measured in the individual metabolites of vitamin D, in total measured 25(OH)D or total 24,25(OH)D, between dietary conditions either with the addition of phytase or 2 g/kg *myo*-inositol. Nevertheless, the level of total 25(OH)D (D₂ and D₃), ranging 14.9-57 nmol/L with bird to bird differences, giving a total average of 39 nmol/L, measured by LC-MS-MS (Table 6.2) is similar to the values (20-22 nmol/L reported by radioimmunoassay for male birds fed 40 µg/kg vitamin D (Sedrani, 1984) and (ca. 52 nmol/L) for 35 d old Ross 708 broilers at Ca inclusion rates of 0.54-1.2% (Warren *et al.*, 2020). Similarly, Reyer *et al.* (2021) reported 25(OH)D levels of ca. 15 ng/mL (37.4 nmol/L) in LSL and ca. 35 ng/mL (87.4 nmol/L) in LB hens in control (adequate Ca and P) diets without added phytase, with measurements made by ELISA. Similarly, the levels of 1,25(OH)₂D were ca. 450 pg/mL (1.1 nmol/L) for LSL and ca. 420 pg/mL (1.0 nmol/L) for LB hens.

Significant differences were measured in the ratio of total 25(OH)D: total 24,25(OH)D with phytase supplementation, with decreasing 25(OH)D:

24,25(OH)D with increasing phytase dose, decreasing from 8.17 ± 0.34 in the Control to 7.08 ± 0.19 in the Phy500 fed group and 6.92 ± 0.23 in the Phy6000 group. The 2 g/kg Inositol fed group did not significantly differ from the Control fed group, at a ratio of 8.25 ± 0.37 for total 25(OH)D: total 24,25(OH)D.

6.4 Discussion

In the present study, measured concentrations of FGF23 were far lower than expected, having been reported in other studies as ranging from 60-240 pg/mL in birds of the same age (Horvat-Gordon *et al.*, 2019), and it is unknown if this is an artefact of the technique used to measure FGF23 in these plasma samples, the age and storage conditions of the plasma by the time these measurements were taken – with the samples having been stored frozen – or a true result. Whilst studies have reported that immunosuppression of FGF23 improves P utilisation in young birds (Ren, Bütz, Sand, *et al.*, 2017), high P availability has been shown to increase concentrations of circulating FGF23 (when P availability is as 0.8% available non-phytate P as opposed to 0.4% non-phytate P in Control diets) (Ren, Bütz, Wahhab, *et al.*, 2017), with FGF23 providing a protective effect against P toxicity (Razzaque, 2011).

Similarly, no significant differences were measured in plasma PTH. PTH has been shown to be a major determinant of the quantity of inorganic phosphate excreted by avian kidneys, with increases in PTH triggering net P secretion in the urine (Wideman Jr. and Braun, 1981; Wideman Jr., 1984). The consensus for human phosphate homeostasis modelling is that PTH exhibits direct control of sodium/phosphate transporters in the kidney, but indirectly controls sodium/phosphate transporter expression in the gut through stimulating $1,25(\text{OH})_2\text{D}_3$ which then enhances NaPi IIb expression in the small intestine (Marks, Debnam and Unwin, 2010).

The liver is the major organ contributing to the conversion of dietary or endogenous vitamin D to 25(OH)D₃ which is the major circulating metabolite (Warren *et al.*, 2020). Here, 25(OH)D₃ was the major vitamin D metabolite detected in plasma (Table 6.2). No significant differences were detected between treatments. There are very few reports of measurements of vitamin D metabolites in broiler plasma, not least because of the technical difficulty of identifying and quantifying isomers but also, perhaps, because poultry diets are universally supplemented with vitamin D. In conditions of adequate Ca²⁺, 25(OH)D₃ is converted by the kidney to 24,25(OH)₂D₃ (Warren *et al.*, 2020). Here, in Ross 308 birds, available P was provided at 0.45% and Ca²⁺ at 0.95%, and total 24,25(OH)₂D (D₂ and D₃) was unaffected by phytase treatment with levels of 4.7-5.9 nmol/L (Table 6.2). Warren *et al.* (2020) reported that 24,25(OH)₂D₃ levels are increased in 35 d old broilers from ca. 2.7 ng/ml (ca. 6.5 nmol/L) at Ca²⁺ inclusion rate of 0.54% to ca. 3.4 ng/mL (ca. 8.2 nmol/L) at 1.2%. Here, significant differences were detected in the ratio 25(OH)D:24,25(OH)₂D, for Phy500 (P = 0.0118) and Phy6000 (P = 0.007) groups compared to Control group (Table 6.2). These data suggest that phytase has a specific effect on vitamin D metabolism mediated by the kidney and may be linked to the response of kidney inositol phosphates to phytase (Sprigg *et al.*, 2022). The lack of this observation in the group supplemented with the predicted released inositol from 6000 units of phytase suggests that if the differences are at all related to inositol they are modified by the effect of phytase on phosphorous and calcium released.

Previously published work analysing the kidney inositol phosphates of the same birds presented here shows altered kidney tissue InsP levels in phytase supplemented diets in comparison to the Control and inositol supplemented birds (Sprigg *et al.* 2022). In the data presented here, this story is further complicated by the observations that phytase mediated reduction in 25(OH)D:24,25(OH)₂D ratio is not mimicked by supplementation with inositol, whilst the inositol levels, calcium and phosphate levels in the plasma are largely unaltered, though numerical reductions in Ca:P ratio are observed also in the presence of phytase in the diet. It can be inferred from

the data presented here that the changes seen with phytase treatment do not result from the increase in free inositol, as these changes are absent with inositol supplementation, and that the effects are likely a consequence of effects other than inositol release by phytase activity in the gut.

It is anticipated that the results of the present study may focus attention on the relationship(s) between cellular inositol phosphate metabolism and kidney function as they pertain to phosphate homeostasis in poultry. The most obvious next steps would be to analyse gene expression of calcium, phosphate and inositol transporters in kidney tissue. Expression of sodium/phosphate NaPi IIb transporters in jejunum tissue has been shown to be altered with phytase supplementation, with decreased transporter expression in the jejunum tissue of broilers fed high phytase doses (Huber, Zeller and Rodehutschord, 2015). Activity of renal proximal tubular apical Na/Pi-cotransporters have been characterized in the capacity of kidney cortex brush border membranes in rabbits exposed to adapted low dietary phosphate, with overall activity and thus reabsorption of Pi increased (Murer, Forster and Biber, 2004). Also notably, phytase supplementation has been shown to influence *myo*-inositol transporter gene expression in both the kidney and liver (Walk, Bedford and Olukosi, 2018), particularly as these organs have known important roles in both *de novo* synthesis and excretion of *myo*-inositol (Holub, 1986a; Lahjouji *et al.*, 2007; Marine L. Croze and Soulage, 2013).

For the role of inositol phosphates in whole animal phosphate homeostasis, the inositol pyrophosphates have come to the fore in recent years for their potential role in control of both cellular and circulating phosphate as metabolic messengers (Shears, 2009), and the kinases responsible for their generation investigated as potential novel treatments for hyperphosphatemia. With inositol pyrophosphate levels in mammalian cells reported to be approximately 3-6% of the concentration of measurable InsP₆ (Laussmann *et al.*, 2000; Pisani *et al.*, 2014), the pyrophosphates InsP₇ and InsP₈ were undetectable by conventional HPLC methods employed in chapters 4 and 5 in the tissue samples arising from this trial. However,

despite their low concentrations, inositol pyrophosphates have been suggested as conserved regulators of phosphate homeostasis.

In studies in rats and monkey, pharmacological inhibition of IP6K, an enzyme for the conversion of InsP₆ to InsP₇, decreases InsP₇ and phosphate export, causing a transient reduction in plasma phosphate that correlates with the pharmacokinetics of the IP6K inhibitor (SC-919) treatment. The use of the SC-919 IP6K inhibitor in this study was as a single dose treatment to rescue adenine-treated rats modelling chronic kidney disease hyperphosphatemia. In the same study, reductions in InsP₇ were measured in liver, muscle and, most prominently, in kidney. The inhibitor was without effect on renal reabsorption of phosphate (Moritoh *et al.*, 2021), but was able to alleviate kidney disease modelled hyperphosphatemia. It is possible that the phytase-mediated reductions in kidney inositol phosphates in broilers (Sprigg *et al.*, 2022) are accompanied by reductions in the InsP₇ product of IP6K. Irrespective of mechanism, the reduced numerically Ca:P ratio (Table 6.1) and significantly reduced 25(OH)D:24,25(OH)₂D ratio (Table 6.2) are indicative of phytase influence on kidney function.

7. Final Discussion and Future Work

7.1 Producing stable isotope labelled *myo*-inositol from glucose

The development of a method for a simple and efficient enzymatic synthesis of ^{13}C stable isotope-labelled *myo*-inositol would be of value to animal nutritionists. It would allow study of the metabolic fate of ingested *myo*-inositol and also of the fate of *myo*-inositol released from digestion of dietary phytate. Not only are inositol phosphates a major component of animal feedstuff, the principle source of phosphorus therein, but they are also endogenous metabolites that are either synthesized from glucose-6-phosphate or from *myo*-inositol absorbed by cells, tissues and organs. Consequently, in an experimental setting, supplementation of animal diet with labelled *myo*-inositol would allow address to questions such as: is inositol absorbed from the digestive tract, by what manner of cellular process, to which organs and for what ultimate metabolic purpose. Harmel *et al.* (2019), in work up of gram scale synthesis of ^{13}C stable isotope labelled *myo*-inositol, tested for the labelling of HCT116 cells, exploited Saiardi's elaboration of the use of a highly efficient inositol phosphate synthase isolated from *Archaeoglobus fulgidus* (Saiardi *et al.*, 2014). Together, these studies provided a basis for the method further developed in this study for use in whole animal metabolic studies. The same enzyme strain, gifted from Adolfo Saiardi, was employed for the cycloaldolisation reaction as part of the coupled enzyme reaction described in this study. Its use resulted in a high yield of ^{13}C *myo*-inositol from the starting, relatively low-cost, ^{13}C D-glucose, employing commercially available enzymes for phosphorylation and dephosphorylation steps.

Previous work involving either stable isotope labelling or measurement in whole birds utilised the naturally occurring variability in $^{12}\text{C}/^{13}\text{C}$ ratio in animal feed arising from C_3/C_4 photosynthetic pathways in feedstuff, either directly manipulating the feed formulation to use ^{13}C as a metabolic tracer of total carbon (Pelícia *et al.*, 2018), or by measuring differences in $^{12}\text{C}/^{13}\text{C}$ ratio as a

way of assigning geographic provenance to samples based on known variability arising in different regions naturally (Department for Environment Food and Rural Affairs, 2013). These methods had great success in the synthesis of a stable isotope label safe for use in an animal feeding trial, with no impact on mortality with label inclusion, but did not go so far as to label a specific low-level molecule to use as a tracer.

The study presented in this thesis attempted to address this, with the production of a specific stable-isotope labelled molecule of interest to follow through the animal model. Whilst the dosage of stable isotope labelled tracer supplemented in the animal feeding trial described in this thesis proved undetectable in the conditions of the trial, and can be assumed that the supplemented level of tracer was in fact ultimately too low in concentration when further diluted by other carbon sources present in the feed, the approach is a promising advance in the move away from the use of radioisotope tracers in long-term metabolic studies using whole animals, with its safe use in animal feeding trials demonstrated here. A more thorough investigation using a wider range of concentrations of stable isotope label needs to be undertaken, with comparison to the use of radioisotope labelling in the same context, to ascertain not only the ideal dose for the stable isotope label to be detected readily, but also to determine its cost effectiveness compared to the current preferred radioisotope labelled method.

7.2 Improving the efficiency of inositol phosphate extraction from biological tissues

For the purposes of understanding the benefits of phytase to animal performance, biochemical measurements are often taken alongside bird performance parameters, to attribute improvements in weight gain, feed conversion ratio and amino acid digestibility with phytase-mediated release of inositol and phosphate along the digestive tract. Even so the understanding of the effects of these increases in available products of

phytate degradation in tissues has been constrained by the absence of description of inositol phosphates – arising from the lack of methods suitable for high throughput sample extraction and analysis of inositol phosphates in tissues.

The popularity of TiO₂ as a solid phase extraction medium for concentration of inositol phosphates in cell biology, first published by Wilson *et al.* (2015), gave rise to the method adapted here for purification of inositol phosphates from biological tissues. This, coupled with HPLC analysis, enabled for the identification of inositol phosphate species in a number of poultry tissues without the use of radioisotope labelling or labour intensive methods, achieving one of the main aims of this study to develop an accessible method to allow for study of inositol phosphates in tissues. Henceforth, this relatively simple solid phase extraction method will allow for greater understanding of the impact of phytase supplementation in enabling measurements of the whole animal response in a tissue-specific manner when measurements are taken alongside routinely measured digesta hydrolysis analyses, and was utilised for this purpose in the results presented in Chapter 5.

7.3 The effect of phytase supplementation on the appearance of lower inositol phosphate esters in the broiler digestive tract

Supplementation of poultry diets with microbial phytase as a way of accessing phytate-bound phosphate, a more economical phosphate source than inorganic rock phosphate, is now fairly commonplace. Previous studies have characterised InsP₆ hydrolysis and the resultant occurrence of lower InsP isomers in different segments of the digestive tract of broilers fed supplementary phytases, and found most added microbial phytase activity to occur in the crop and gizzard (Yu *et al.*, 2004; Onyango, Bedford and Adeola, 2005). Similar observations were made in this study, with apparent reappearance of InsPs in the terminal ileum. This observation may be

attributed to faster transit of lower InsPs, relative to higher InsPs, through the digestive tract.

Analysis of inositol phosphate speciation in the gizzard and ileum by differential extraction methods designed for disruption of any remaining phytase activity during extraction in this study was indicative of persistent feedstuff MINPP activity in the food bolus of the gizzard that only became apparent on rehydration of the milled digesta contents. It is likely that this occurrence was due to the use of starter-phase mash diets in this trial, whereas the usual heat treatment of pelleted feeds ordinarily degrades endogenous feedstuff phytase activities.

In the use of a superdose of microbial phytase, at 6000 FTU, phytate hydrolysis was significantly improved in comparison to the addition of 500 FTU phytase, and both significantly increased free *myo*-inositol and reduced InsP₆ compared to the control diet in the absence of added phytase, in both the gizzard and the ileum. The application of the superdose of phytase removed the often-reported bottleneck of hydrolysis seen with lower supplemented phytase doses, where a build up of lower esters InsP₃ and InsP₄ is seen (Zeller *et al.*, 2015a; Zeller *et al.*, 2015b; Bedford and Walk, 2016), as was noted in the 500 FTU group in this trial. This is of great importance, as these lower esters have been shown to retain the same antinutritive properties as InsP₆ in the gut of broilers (Persson *et al.*, 1998; Yu *et al.*, 2012), and therefore in improving animal performance the aim must be for the reduction of all lower inositol phosphate esters in the gut lumen.

The use of only two phytase levels in this study, at 500 FTU/kg as the commercially recommended dose compared with a superdose of 6000 FTU/kg, does not allow for test of a theoretical optimum dose for the reduction of lower inositol phosphate esters from the data collected as part of this study. The determination of this will be of vital importance to the field, particularly for the farmers purchasing commercial phytases for use, to avoid overuse of supplemental enzymes at high cost whilst still achieving near complete gut hydrolysis of inositol phosphates and aim to overall reduce the

impact of inositol phosphate excretion on phosphorus pollution, and this is an important area of study for future research.

7.4 Inositol phosphate species in tissues of broiler chickens

This thesis presents the first measurements of the profiles of inositol phosphates in poultry tissues, achieved without the restrictive and limiting practice of whole animal radioisotope labelling. HPLC analysis coupled with the method described in Chapter 3 for enrichment of low concentration inositol phosphates allowed for identification of inositol phosphate species within these tissues. These matched those described in other animal models (Mayr and Thieleczek, 1991) and in avian erythrocytes (Whitfield *et al.*, 2022). They were identified as arising from *de novo* synthesis of inositol phosphates within tissues rather than from gut uptake of phytate hydrolysis products of lower InsP esters.

In addition to these measurements of the differing levels of inositol phosphates in different tissues, this chapter described for the first time the differing responses of different tissues to the changing availability of inositol and/or phosphate with dietary inositol and phytase supplementation. The responsiveness of the kidney to phytase supplementation, with decreasing concentrations of *de novo* synthesized InsPs with increasing phytase dose, and the response of liver InsP concentrations to increased dietary inositol, are unprecedented observations with the kidney's known role in phosphate homeostasis. It is tempting to speculate that phytase supplementation, whilst increasing available P, may alter the manner in which birds utilise phosphate. The methods elaborated here will allow for further research in understanding whole-bird responses to phytase supplementation in an organ specific manner.

Separately, the use of TiO₂ as a solid phase extractant in this context raised concerns over the potential interference of TiO₂ in inositol phosphate measurements when employed as a digestibility index marker. Data

presented here for tissues, and in Chapter 4 for digesta, suggest that the inclusion of TiO_2 has no significant effect on the extraction and analysis of inositol phosphates from tissues, from digesta or from the parent diet, and shows that its inclusion in previous studies of inositol phosphates with phytase supplementation are unlikely to have been impacted by the use of TiO_2 as a digestibility index marker.

7.5 The effect of phytase supplementation on circulating metabolites implicated in phosphate homeostasis

Following on from the significant responsiveness of the kidney to phytase supplementation described in Chapter 5, the next logical step for investigation was to measure other markers of phosphate homeostasis. This was not an initial aim of this thesis, but the need for these measurements arose from the results presented in chapter 5 suggesting a whole-animal response to phytase in terms of the effect on inositol phosphates in specific tissues, and as a reduction rather than increase in inositol phosphates suggesting that the response may be a change in phosphate use within the animal rather than simply increased phosphate uptake and delivery to target tissues. Phytase mediated release of phosphate is often investigated in the context of calcium, and calcium/phosphate ratios. While the metabolites measured here – PTH, FGF23, and vitamin D – as well as circulatory inositol and phosphate are known for their roles in the maintenance of calcium and phosphate, these metabolites are rarely measured in poultry with the exception of plasma inositol, not least because diets are almost universally supplemented with vitamin D_3 .

No significant differences were measured in PTH or FGF23, though it is noted that measured concentrations of FGF23 in this study were far lower than reported in other studies and may speak to the limitations of the use of ELISA for long term stored plasma. However, ratios of vitamin D metabolites, total $25(\text{OH})\text{D}$: total $24,25(\text{OH})_2\text{D}$, were reduced in birds fed diets with supplemented phytase. This is notable, with 25-OH-D_3 considered

metabolically active in the release of bone calcium and phosphorus and 24,25-(OH)₂-D₃ considered the inactive form, and the 24-hydroxylation of 25-OH-D₃ a function of the kidney.

These data, coupled with the kidney inositol phosphate data presented in chapter 5, suggest that phytase has a specific effect on vitamin D metabolism mediated by the kidney, which may be linked to the response of kidney inositol phosphates to phytase supplementation. Further work is needed to investigate the link between cellular inositol phosphate metabolism and kidney function as they pertain to phosphate homeostasis in poultry. This thesis provides pointers to further study. The demonstrated effect of phytase on vitamin D deserves to be put in context of study of sodium/phosphate cotransporters and the known influence of phytase supplementation on kidney *myo*-inositol transporters, particularly in light of the interaction of phytase and cholecalciferol on growth performance (Qian, Kornegay and Denbow, 1997).

7.6 Limitations

The primary success in this study lies in the use of novel methodology for the extraction and analysis of inositol phosphates in poultry tissues, and the use of this method to elucidate a phytase dose-dependent response of kidney inositol phosphate levels in poultry tissues, which has subsequently been published in Sprigg *et al.* (2022). This data suggests that tissue inositol phosphate concentrations can be influenced by dietary phytase inclusion rate, and that such effects are tissue specific, though the consequences for physiology of such changes have yet to be elucidated.

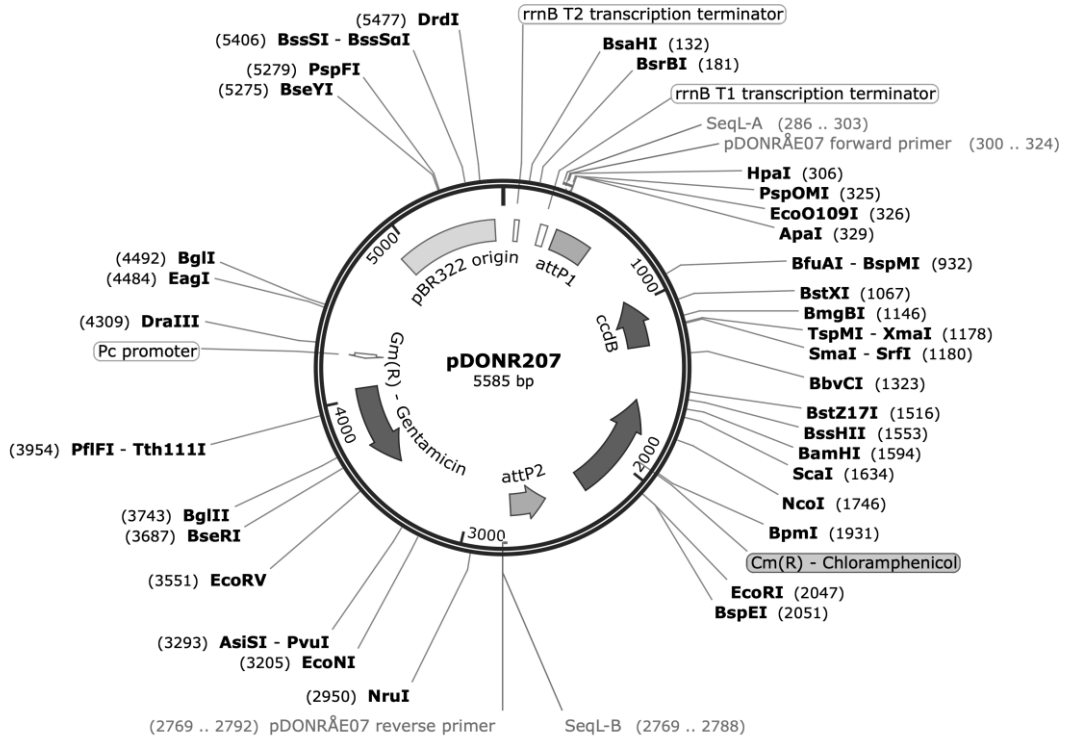
Whilst previous studies have shown the impact of phytase supplementation on the release of phosphorus in the digestive tract of broilers, and have shown that this allows for a reduction in supplementary phosphorus without negatively impacting growth performance, improvements in growth performance were not measured in this study with phytase inclusion. This

may be attributed to the length of the study, lasting only 21 days, and future studies would be encouraged to continue beyond this period. Additionally, the responses seen in kidney inositol phosphate levels noted in this study, a progressive reduction in inositol phosphates with increasing phytase supplementation, has only been measured in 2 phytase concentrations – 500 FTU/kg and 6000 FTU/kg compared to a 0 FTU/kg Control. Further understanding of the effect of phytase in these tissues is necessary in order to be able to draw conclusions relevant to the agricultural community, that would come from repetition of the study with interval phytase doses between those tested here to measure the nature of the relationship between phytase dose and tissue inositol phosphate levels. Any future work ought to additionally seek to understand the mechanisms underpinning this relationship, particularly in the effects on circulating metabolites and inositol and phosphate transporters within these tissues in response to phytase.

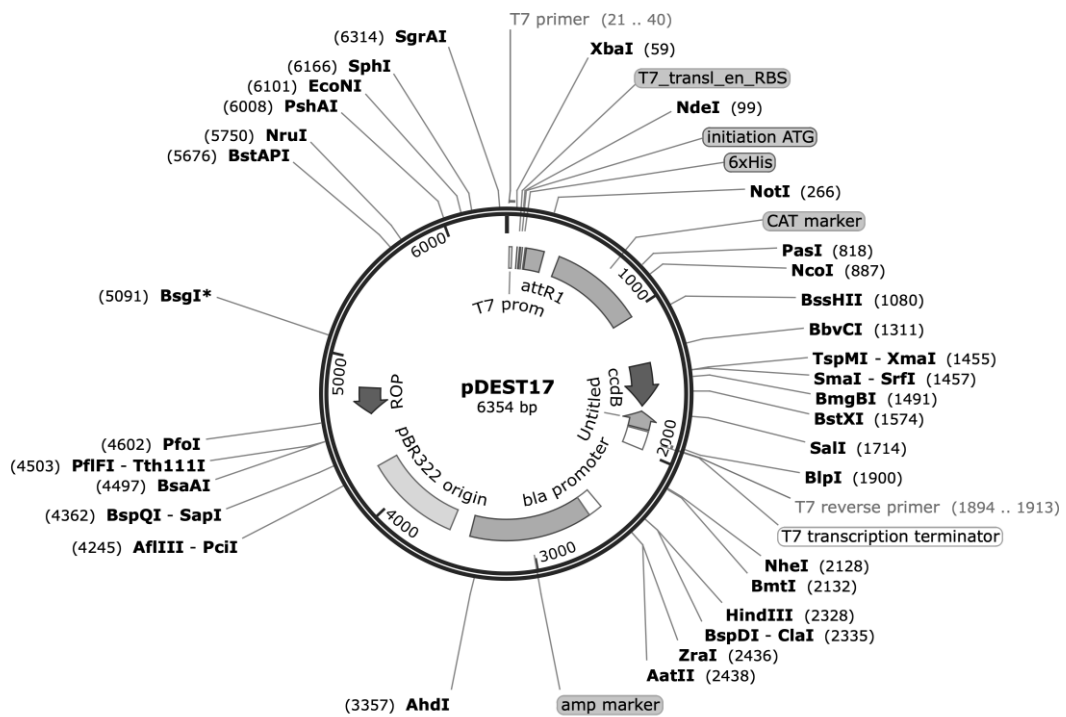
Appendices

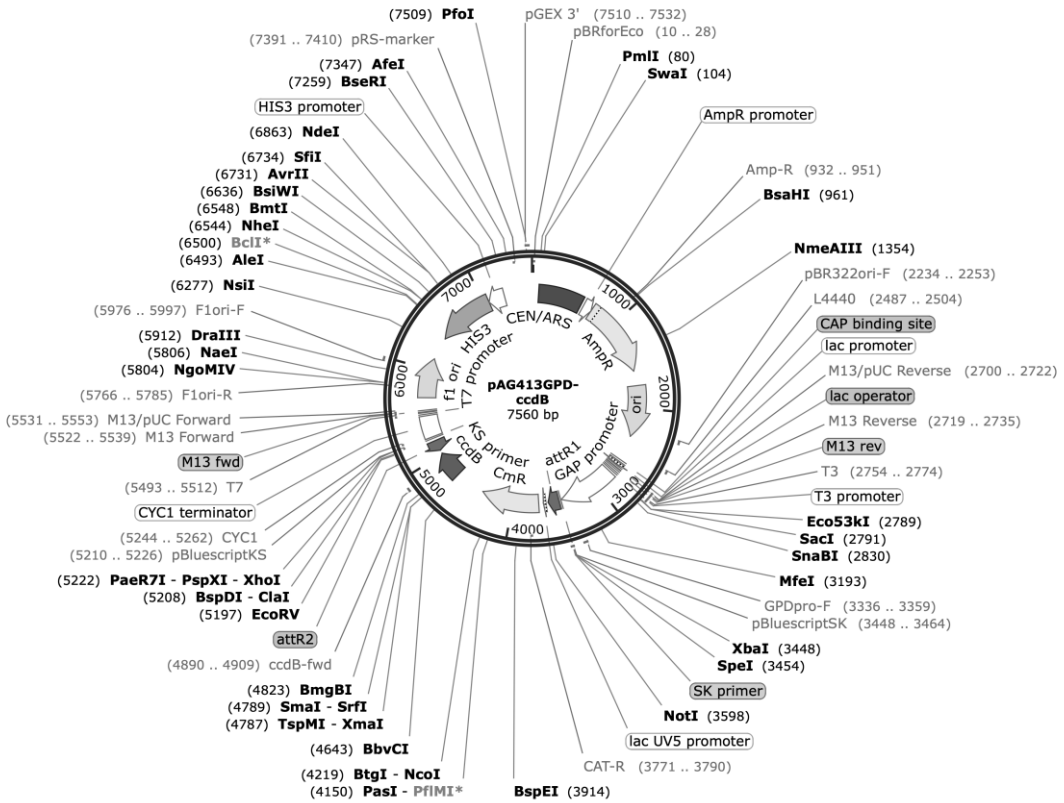
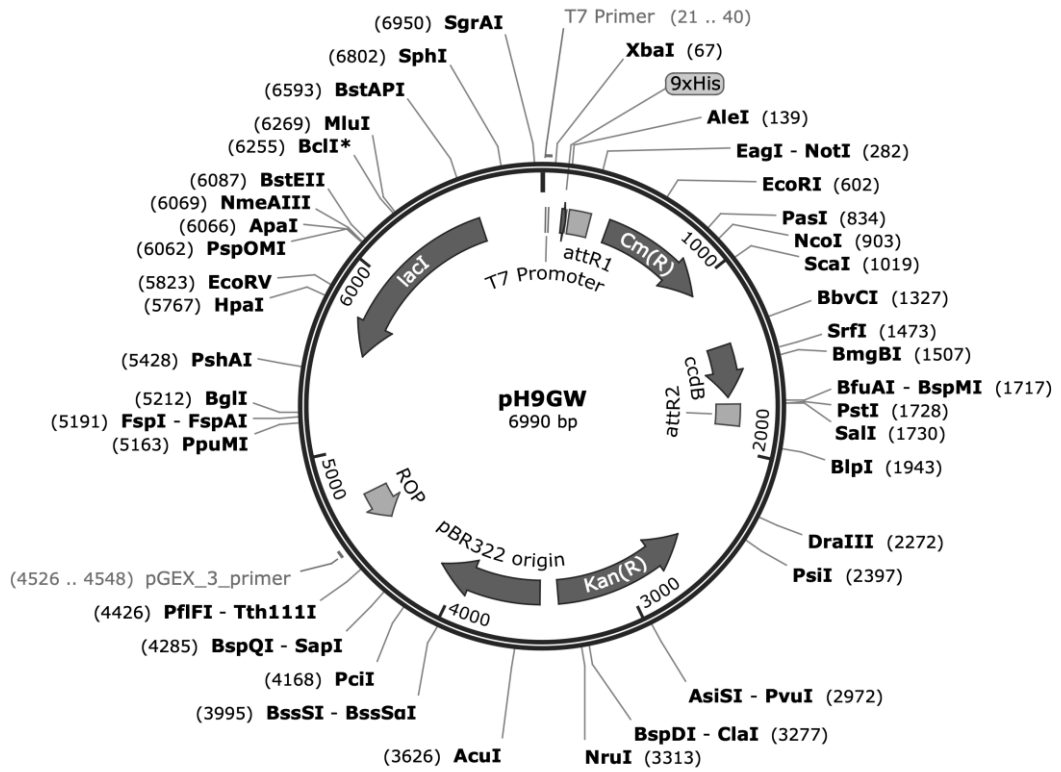
Appendix 1: Vectors and yeast strains

Created by SnapGene



Created by SnapGene





Inositol phosphate synthase coding sequence from *Archaeoglobus fulgidus*:

```
>sp|O29976|DIPPS_ARCFU Bifunctional IPC transferase and DIPP
synthase OS=Archaeoglobus fulgidus (strain ATCC 49558 / DSM 4304 /
JCM 9628 / NBRC 100126 / VC-16) OX=224325 GN=AF_0263 PE=1 SV=1
MILPCESFNGVPSGCLIIEMNWYSVLKASTAIFFFPEKYSSSTSSLSKRSPISAPMINVDG
EYLKIFAGRIKLMKAVILAAGLGTRLGGVPKPLVVRVGGCEIILRTMKLLSPHVSEFIIVA
SRYADDIDAFLLKDKGFNYKIVRHDRPEKNGYSLLVAKNHVEDRFDILTMGDHVYSQQFIE
KAVRGEVVIADREPRFVDIGEATKIRVEDGRVAKIGKDLREFDCVDTGFFVLDDSI FEHA
EKLRDREEIPLSEIVKLARLPVTVYVDGELWMDVDTKEDVRRANRALVSAAVKSGSDGFIS
RKINRKISTRISAAIVNKVNPQMTLISFLVGAFSALASFFSIPLAGLLYQFSSILDGCD
GEIARASLKMSKGGYVDSILDRFVDFLFLAI IALLYPKTATVAMFAIFGSVMVSYTSEK
YKAEFGESIFGKFRVLNYIPGKRDERIFLIMIFCLLSAISLQWIFWMFLVAAISLTRVV
VTL LAVLVSK
```

The IPS-gene from *A. fulgidus* cloned into a pET23a vector (Prof. Helena Santos, Universidade Nova de Lisboa) was received from Prof. Adolfo Saiardi (University College London) (Rodrigues *et al.*, 2007)

***Arabidopsis thaliana* MIPS1 coding sequence:**

```
>sp|P42801|INO1_ARATH Inositol-3-phosphate synthase isozyme 1
OS=Arabidopsis thaliana OX=3702 GN=IPS1 PE=1 SV=3
MFIESFKVESPNVKYteneIHSVYDYETTEVVHEKTVNGTYQWIVKPKTVKYDFKTDIRV
PKLGVMLVGLGGNNGSTLTAGVIANKEGISWATKDKVQQANYFGSLTQASSIRVGSFNGE
EIIYAPFKSLLPMVNPDDVVFVGGWDISDMNLADAMARARVLDIDLQKQLRPYMENIVPLPG
IFDPDFIAANQGSRRANHVIKGTTKEQVDHI IKDMREFKEKNKVDKVVVLWTANTERYSNV
VVGMDTMENTLMEVDRDEAEISPSTLYAIACVLEGI PFINGSPQNTFVPLIDMAIRNN
VLIGGDDFKSGQTKMKSVLVDFLVGAGIKPTSIVSYNHLGNNDGMNLSAPQTFRSKEISK
SNVDDMVASNGILFEPGEHPDHVVVIKYVPYVADSKRAMDEYTSEIFMGGKNTIVMHNT
CEDSLLAAPI IIDLVL LLAELSTRIQFKSEGEKGFHSFHPVATILSYLTKAPLVPPGTPVI
NALSKQRAMLENIMRACVGLAPENNMIMEFK
```

***Arabidopsis thaliana* MIPS2 coding sequence:**

```
>sp|Q38862|INO2_ARATH Inositol-3-phosphate synthase isozyme 2
OS=Arabidopsis thaliana OX=3702 GN=IPS2 PE=1 SV=2
MFIESFKVESPNVKYteneINSVYDYETTEVVHENRNGTYQWVVKPKTVKYDFKTDTRVP
KLGVMVLVGGNNGSTLTAGVIANKEGISWATKDKVQQANYFGSLTQASSIRVGSYNGEE
IYAPFKSLLPMVNPEDVVFVGGWDISDMNLADAMARARVLDIDLQKQLRPYMENMIPLPGI
YDPDFIAANQGSRRANSVIKGTKEQVDHI IKDMREFKEKNKVDKLVVLWTANTERYSNVI
VGLNDTTENLLASVEKDESEISPSTLYAIACVLEGI PFINGSPQNTFVPLIELAISKNK
LIGGDDFKSGQTKMKSVLVDFLVGAGIKPTSIVSYNHLGNNDGMNLSAPQTFRSKEISKS
NVVDDMVASNGILFEPGEHPDHVVVIKYVPYVADSKRAMDEYTSEIFMGGKNTIVLHNTC
EDSLLAAPI IIDLVL LLAELSTRIQFKAEGEGKGFHSFHPVATILSYLTKAPLVPPGTPVVN
ALSKQRAMLENILRACVGLAPENNMIMEYK
```

***Saccharomyces cerevisiae* INO1 coding sequence:**

```
>INO1 YJL153C SGDID:S000003689
ATGACAGAAGATAATATTGCTCCAATCACCTCCGTTAAAGTAGTTACCGACAAGTGCACG
TACAAGGACAACGAGCTGCTCACCAAGTACAGCTACGAAAATGCTGTAGTTACGAAGACA
GCTAGTGGCCGCTTCGATGTAACGCCACTGTTCAAGACTACGTGTTCAAACCTTGACTTG
AAAAAGCCGGA AAAA ACTAGGAATTATGCTCATTGGGTTAGGTGGCAACAATGGCTCCACT
TTAGTGGCCTCGGTATTGGCGAATAAGCACAAATGTGGAGTTTCAAAC TAAGGAAGGCGTT
AAGCAACCAA ACTACTTCGGCTCCATGACTCAATGTTCTACCTTGAAACTGGGTATCGAT
GCGGAGGGGAATGACGTTTATGCTCCTTTTAACTCTCTGTTGCCCATGGTTAGCCCAAAC
GACTTTGTCTGCTCTGTTGGGACATCAATAACGCAGATCTATACGAAGCTATGCAGAGA
AGTCAAGTTCTCGAATATGATCTGCAACAACGCTTGAAGGCGAAGATGTCTTGGTGAAG
CCTCTTCTTCCATTTACTACCCTGATTTTCAATTGCAGCTAATCAAGATGAGAGAGCCAAT
AACTGCATCAATTTGGATGAAAAAGGCAACGTAACCACGAGGGGTAAGTGGACCCATCTG
CAACGCATCAGACGCGATATCCAGAATTTCAAAGAAGAAAACGCCCTTGATAAAGTAATC
GTTCTTTGGACTGCAAACTACTGAGAGGTACGTAGAAAGTATCTCCTGGTGTAAATGACACC
ATGGAAAACCTCTTGCACTTATTAAGAATGACCATGAAGAGATTGCTCCTTCCACGATC
```

TTTGCAGCAGCATCTATCTTGGAAGGTGTCCCCTATATTAATGGTTCACCGCAGAATACT
TTTGTTCCCGGCTTGGTTCAGCTGGCTGAGCATGAGGGTACATTCATTGCGGGAGACGAT
CTCAAGTCGGGACAAACCAAGTTGAAGTCTGTTCTGGCCAGTTCCTTAGTGGATGCAGGT
ATTAAACCGGTCTCCATTGCATCCTATAACCATTTAGGCAATAATGACGGTTATAACTTA
TCTGCTCCAAAACAATTTAGGTCTAAGGAGATTTCCAAAAGTTCTGTCATAGATGACATC
ATCGCGTCTAATGATATCTTGTACAATGATAAACTGGGTAAAAAAGTTGACCACTGCATT
GTCATCAAATATATGAAGCCCGTCGGGGACTCAAAAGTGGCAATGGACGAGTATTACAGT
GAGTTGATGTTAGGTGGCCATAACCGGATTTCCATTCACAATGTTTGCGAAGATTCTTTA
CTGGCTACGCCCTTGATCATCGATCTTTTAGTCATGACTGAGTTTTGTACAAGAGTGTC
TATAAGAAGGTGGACCCAGTTAAAGAAGATGCTGGCAAATTCGAGAACTTTTATCCAGTT
TTAACCTTCTTGAGTTACTGGTTAAAAGCTCCATTAACAAGACCAGGATTCACCCGGTG
AATGGCTTAAACAAGCAAAGAACCGCCTTAGAAAATTTTTTAAGATTGTTGATTGGATTG
CCTTCTCAAAACGAACTAAGATTCTGAAGAGAGATTGTTGTAA

Yeast strains:

Strain:	Background:	Received from:
BY4741	<i>MATa his3Δ 1 leu2Δ0 met15Δ0 ura3Δ0</i>	Adolfo Saiardi
<i>kcs1Δ</i>	<i>MATa his3Δ 1 leu2Δ0 met15Δ0 ura3Δ0 kcs1Δ::KanMX6</i>	Adolfo Saiardi
<i>vip1Δ</i>	<i>MATa his3Δ 1 leu2Δ0 met15Δ0 ura3Δ0 vip1Δ::KanMX6</i>	Adolfo Saiardi
<i>ipk1Δ</i>	<i>MATa his3Δ 1 leu2Δ0 met15Δ0 ura3Δ0 ipk1Δ::KanMX6</i>	Adolfo Saiardi
<i>ino1Δ</i>	<i>MATa his3Δ 1 leu2Δ0 met15Δ0 ura3Δ0 ino1Δ::KanMX6</i>	Adolfo Saiardi
<i>arg82Δ</i>	<i>MATa his3Δ 1 leu2Δ0 met15Δ0 ura3Δ0 arg82Δ::KanMX6</i>	Adolfo Saiardi
W303	<i>MATa/MATα {leu2-3,112 trp1-1 can1-100 ura3-1 ade2-1 his3-11,15} [phi+]</i>	Adolfo Saiardi
<i>ino1Δ</i>	<i>MATa/MATα {leu2-3,112 trp1-1 can1-100 ura3-1 ade2-1 his3-11,15} [phi+] ino1Δ::KanMX4</i>	Adolfo Saiardi
<i>kcs1Δ</i>	<i>MATa/MATα {leu2-3,112 trp1-1 can1-100 ura3-1 ade2-1 his3-11,15} [phi+] kcs1Δ::KanMX4</i>	Adolfo Saiardi
DDY1810	<i>MATa leu2-3,112 trp1-Δ901 ura3-52 prb1-1122 pep4-3 prc1-407</i>	Adolfo Saiardi
<i>kcs1Δ</i>	<i>MATa leu2-3,112 trp1-Δ901 ura3-52 prb1-1122 pep4-3 prc1-407 kcs1::Leu2</i>	Adolfo Saiardi
<i>ipk1Δ</i>	<i>MATa leu2-3,112 trp1-Δ901 ura3-52 prb1-1122 pep4-3 prc1-407 ipk1::kanMX4</i>	Adolfo Saiardi
<i>arg82Δ</i>	<i>MATa leu2-3,112 trp1-Δ901 ura3-52 prb1-1122 pep4-3 prc1-407 arg82::kanMX4</i>	Adolfo Saiardi
NCYC 3466	OS96, S288C haploid strain	National Collection of Yeast Cultures

Appendix 2: Isotope Ratios for tissue samples and digesta and diets

Sample ID	d13C‰ final VPDB	R sample	Atom %
Brain 5A	-24.02	0.010911	1.079363
Brain 5B	-24.50	0.010906	1.078848
Brain 14A	-23.92	0.010913	1.079479
Brain 14B	-24.48	0.010906	1.078867
Brain 21A	-24.06	0.010911	1.079319
Brain 21B	-25.45	0.010895	1.077803
Brain 31A	-25.63	0.010893	1.07761
Brain 31B	-25.56	0.010894	1.077688
Brain 37A	-24.84	0.010902	1.078476
Brain 37B	-24.27	0.010909	1.079096
Brain 44A	sample missing from 96 well plate		
Brain 44B	-23.80	0.010914	1.079611
Brain 2A	-25.29	0.010897	1.077974
Brain 2B	-25.31	0.010897	1.077962
Brain 11A	-25.24	0.010898	1.078029
Brain 11B	-25.47	0.010895	1.077782
Brain 17A	-25.19	0.010898	1.078083
Brain 17B	-25.14	0.010899	1.078144
Brain 28A	-25.32	0.010897	1.077946
Brain 28B	-25.25	0.010898	1.078026
Brain 36A	-25.24	0.010898	1.078036
Brain 36B	-25.64	0.010893	1.077591
Brain 42A	-24.77	0.010903	1.078544
Brain 42B	-26.59	0.010883	1.076557
Leg 5A	-17.46	0.010985	1.086542
Leg 5B	-22.20	0.010932	1.081358
Leg 14A	-22.55	0.010928	1.080972
Leg 14B	-21.21	0.010943	1.082447
Leg 21A	-19.57	0.010961	1.084232
Leg 21B	-21.47	0.01094	1.082158
Leg 31A	-22.47	0.010929	1.081069
Leg 31B	-19.79	0.010959	1.083993
Leg 37A	-21.39	0.010941	1.082245
Leg 37B	-20.11	0.010955	1.083645
Leg 44A	-22.59	0.010927	1.080934
Leg 44B	-23.33	0.010919	1.080126
Leg 2A	-10.39	0.011064	1.094272
Leg 2B	-23.07	0.010922	1.080408
Leg 11A	-27.35	0.010874	1.07572
Leg 11B	-24.07	0.010911	1.079314
Leg 17A	-20.93	0.010946	1.082744
Leg 17B	-23.51	0.010917	1.079925
Leg 28A	-25.59	0.010894	1.077647
Leg 28B	-25.85	0.010891	1.077371
Leg 36A	-21.95	0.010935	1.08163
Leg 36B	-25.96	0.01089	1.077249
Leg 42A	-25.63	0.010893	1.077609
Leg 42B	-24.02	0.010911	1.079363

Sample ID	d13C‰ final VPDB	R sample	Atom %
Liver 5A	-25.30	0.010897	1.077965
Liver 5B	-24.78	0.010903	1.078535
Liver 14A	-24.78	0.010903	1.078539
Liver 14B	-25.52	0.010895	1.077732
Liver 21A	-25.25	0.010898	1.07802
Liver 21B	-25.49	0.010895	1.077764
Liver 31A	-25.02	0.0109	1.07827
Liver 31B	-25.74	0.010892	1.077486
Liver 37A	-24.68	0.010904	1.078648
Liver 37B	-25.51	0.010895	1.07774
Liver 44A	-25.48	0.010895	1.077769
Liver 44B	-25.53	0.010895	1.077711
Liver 2A	-25.70	0.010893	1.077536
Liver 2B	-25.44	0.010896	1.07782
Liver 11A	-25.79	0.010892	1.077435
Liver 11B	-25.57	0.010894	1.077676
Liver 17A	-25.28	0.010897	1.077985
Liver 17B	-25.71	0.010893	1.077524
Liver 28A	-26.00	0.010889	1.077207
Liver 28B	-25.69	0.010893	1.077539
Liver 36A	-25.85	0.010891	1.077369
Liver 36B	-25.80	0.010892	1.077418
Liver 42A	-25.57	0.010894	1.077676
Liver 42B	-25.64	0.010893	1.077591
Kidney 5A	-24.02	0.010911	1.079368
Kidney 5B	-24.35	0.010908	1.079003
Kidney 14A	-24.07	0.010911	1.079318
Kidney 14B	-24.05	0.010911	1.079336
Kidney 21A	-24.24	0.010909	1.079129
Kidney 21B	-24.36	0.010908	1.078999
Kidney 31A	-24.22	0.010909	1.079146
Kidney 31B	-24.54	0.010906	1.078801
Kidney 37A	-22.99	0.010923	1.0805
Kidney 37B	-24.66	0.010904	1.078667
Kidney 44A	-23.61	0.010916	1.079815
Kidney 44B	-24.36	0.010908	1.078992
Kidney 2A	-23.66	0.010915	1.079758
Kidney 2B	-24.10	0.010911	1.079284
Kidney 11A	-24.61	0.010905	1.078721
Kidney 11B	-23.19	0.010921	1.080274
Kidney 17A	-22.95	0.010923	1.080541
Kidney 17B	-23.37	0.010919	1.080075
Kidney 28A	-23.71	0.010915	1.079707
Kidney 28B	-22.02	0.010934	1.081562
Kidney 36A	-21.47	0.01094	1.082163
Kidney 36B	-23.67	0.010915	1.079751
Kidney 42A	-22.51	0.010928	1.081022
Kidney 42B	-22.78	0.010925	1.080726

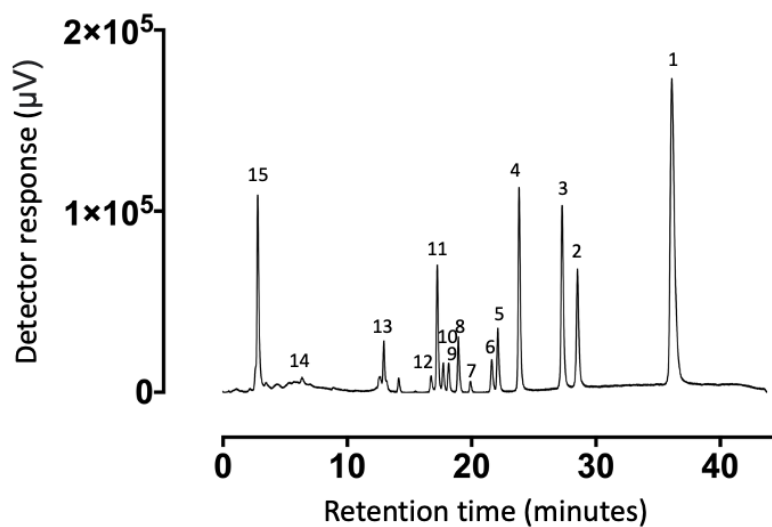
Sample ID	d13C‰ final VPDB	R sample	Atom %
Ileum 5A	-25.28	0.010897	1.077992
Ileum 5B	-26.04	0.010889	1.077155
Ileum 14A	-25.72	0.010892	1.077512
Ileum 14B	-25.35	0.010897	1.077916
Ileum 21A	-26.04	0.010889	1.077157
Ileum 21B	-25.16	0.010899	1.078126
Ileum 31A	-25.33	0.010897	1.077936
Ileum 31B	-25.55	0.010894	1.077695
Ileum 37A	-25.82	0.010891	1.077398
Ileum 37B	-24.73	0.010903	1.078587
Ileum 44A	-25.63	0.010893	1.077606
Ileum 44B	-24.98	0.010901	1.078322
Ileum 2A	-25.94	0.01089	1.077268
Ileum 2B	-26.88	0.01088	1.076242
Ileum 11A	-25.90	0.01089	1.077313
Ileum 11B	-26.35	0.010885	1.076822
Ileum 17A	-27.62	0.010871	1.075429
Ileum 17B	-26.65	0.010882	1.076491
Ileum 28A	-26.36	0.010885	1.076805
Ileum 28B	-26.44	0.010884	1.076721
Ileum 36A	-25.96	0.01089	1.077249
Ileum 36B	-25.98	0.01089	1.077226
Ileum 42A	-27.61	0.010871	1.075444
Ileum 42B	-26.73	0.010881	1.076408
Jejunum 5A	-26.64	0.010882	1.076506
Jejunum 5B	-26.34	0.010885	1.076825
Jejunum 14A	-26.59	0.010883	1.076557
Jejunum 14B	-26.60	0.010883	1.076546
Jejunum 21A	-26.67	0.010882	1.076464
Jejunum 21B	-26.83	0.01088	1.076292
Jejunum 31A	-26.77	0.010881	1.076354
Jejunum 31B	-26.81	0.01088	1.076313
Jejunum 37A	-27.01	0.010878	1.076095
Jejunum 37B	-27.42	0.010873	1.075645
Jejunum 44A	-26.67	0.010882	1.076466
Jejunum 44B	-26.72	0.010881	1.076419
Jejunum 2A	-27.64	0.010871	1.075406
Jejunum 2B	-26.74	0.010881	1.076389
Jejunum 11A	-28.25	0.010864	1.074742
Jejunum 11B	-26.63	0.010882	1.07651
Jejunum 17A	-26.64	0.010882	1.076497
Jejunum 17B	-27.22	0.010876	1.075868
Jejunum 28A	-27.29	0.010875	1.075787
Jejunum 28B	-27.52	0.010872	1.075534
Jejunum 36A	-27.10	0.010877	1.075999
Jejunum 36B	-27.29	0.010875	1.075787
Jejunum 42A	-26.70	0.010882	1.076441
Jejunum 42B	-26.68	0.010882	1.076461

Sample ID	d13C‰ final VPDB	R sample	Atom %
Duodenum 5A	-25.88	0.010891	1.077332
Duodenum 5B	-25.14	0.010899	1.078141
Duodenum 14A	-26.84	0.01088	1.076278
Duodenum 14B	-25.87	0.010891	1.077348
Duodenum 21A	-26.04	0.010889	1.077153
Duodenum 21B	-26.03	0.010889	1.077166
Duodenum 31A	-25.81	0.010891	1.077412
Duodenum 31B	-27.19	0.010876	1.075895
Duodenum 37A	-26.34	0.010886	1.076832
Duodenum 37B	-25.63	0.010893	1.077604
Duodenum 44A	-26.64	0.010882	1.076498
Duodenum 44B	-27.81	0.010869	1.075224
Duodenum 2A	-26.32	0.010886	1.076851
Duodenum 2B	-26.80	0.01088	1.076323
Duodenum 11A	-26.18	0.010887	1.07701
Duodenum 11B	-25.77	0.010892	1.077451
Duodenum 17A	-26.16	0.010888	1.077027
Duodenum 17B	-25.85	0.010891	1.077361
Duodenum 28A	-25.77	0.010892	1.07745
Duodenum 28B	-26.45	0.010884	1.076713
Duodenum 36A	-25.78	0.010892	1.077446
Duodenum 36B	-26.17	0.010887	1.077016
Duodenum 42A	-26.93	0.010879	1.07618
Duodenum 42B	-26.39	0.010885	1.076778
Breast 5A	-26.48	0.010884	1.076682
Breast 5B	-27.28	0.010875	1.075802
Breast 14A	-26.90	0.010879	1.076216
Breast 14B	-27.84	0.010869	1.075184
Breast 21A	-27.28	0.010875	1.075807
Breast 21B	-26.62	0.010882	1.076526
Breast 31A	-26.50	0.010884	1.076657
Breast 31B	-26.97	0.010878	1.076138
Breast 37A	-26.89	0.010879	1.076227
Breast 37B	-26.70	0.010882	1.07644
Breast 44A	-25.98	0.01089	1.077226
Breast 44B	-26.35	0.010885	1.076814
Breast 2A	-26.19	0.010887	1.076999
Breast 2B	-26.20	0.010887	1.076978
Breast 11A	-27.04	0.010878	1.076069
Breast 11B	-25.97	0.01089	1.077233
Breast 17A	-26.61	0.010882	1.076531
Breast 17B	-25.93	0.01089	1.077279
Breast 28A	-25.49	0.010895	1.077759
Breast 28B	-26.21	0.010887	1.076972
Breast 36A	-27.31	0.010875	1.075765
Breast 36B	-25.10	0.010899	1.078185
Breast 42A	-24.12	0.01091	1.079257
Breast 42B	-22.96	0.010923	1.08053

Sample ID	d13C‰ final VPDB	R sample	Atom %
Plasma 5	-2.91	0.011147	1.102456
Plasma 14	-26.14	0.010888	1.077051
Plasma 21	-26.25	0.010887	1.07693
Plasma 31	-25.99	0.010889	1.077208
Plasma 37	-25.95	0.01089	1.07726
Plasma 44	-25.77	0.010892	1.077455
Plasma 2	-25.47	0.010895	1.077779
Plasma 11	-26.09	0.010888	1.077103
Plasma 17	-26.01	0.010889	1.077191
Plasma 28	-26.16	0.010888	1.077032
Plasma 36	-26.22	0.010887	1.07696
Plasma 42	-26.33	0.010886	1.076846
Gizzard digesta 5	-27.19	0.010876	1.075901
Gizzard digesta 14	-27.75	0.01087	1.075287
Gizzard digesta 21	-26.88	0.010879	1.076237
Gizzard digesta 31	-27.31	0.010875	1.075771
Gizzard digesta 37	-27.59	0.010872	1.075461
Gizzard digesta 44	-29.15	0.010854	1.073754
Gizzard digesta 2	-27.47	0.010873	1.075589
Gizzard digesta 11	-28.30	0.010864	1.07469
Gizzard digesta 17	-26.85	0.01088	1.076271
Gizzard digesta 28	-28.76	0.010858	1.074179
Gizzard digesta 36	-27.96	0.010867	1.075055
Gizzard digesta 42	-28.50	0.010861	1.07447
Ileum digesta 5	-27.02	0.010878	1.076089
Ileum digesta 14	-26.64	0.010882	1.076504
Ileum digesta 21	-26.93	0.010879	1.076186
Ileum digesta 31	-27.21	0.010876	1.075882
Ileum digesta 37	-26.64	0.010882	1.0765
Ileum digesta 44	-27.71	0.01087	1.075332
Ileum digesta 2	-27.62	0.010871	1.075433
Ileum digesta 11	-27.46	0.010873	1.075608
Ileum digesta 17	-27.19	0.010876	1.075898
Ileum digesta 28	-26.76	0.010881	1.076373
Ileum digesta 36	-26.85	0.01088	1.076268
Ileum digesta 42	-26.94	0.010879	1.076178
diet A	-26.78	0.0107579	1.06434
diet B	-27.01	0.0107554	1.064095
diet C	-26.99	0.0107556	1.064115
diet D	-26.91	0.0107565	1.064203
diet E	-27.06	0.0107548	1.064037
diet F	-27.35	0.0107516	1.063723
diet G	-27.18	0.0107535	1.063909
diet H	-26.77	0.010758	1.06435
control 1	-26.68	0.0107591	1.064457
control 2	-26.94	0.0107561	1.064164
blank	-27.50	0.0107499	1.063557

Reference for offset correction	$\delta^{13}\text{C}\text{‰}$ measured	Reference check (offset corrected)	$\delta^{13}\text{C}\text{‰}$ corrected VPDB
Casein d13C measured		Collagen d13C after offset correction	
	-34.32		-18.33
	-34.37		-17.73
	-34.40		-18.21
	-34.27		-17.91
	-34.49		-18.19
	-34.53		-18.11
	-34.52		-18.25
	-34.50		-18.10
	-34.53		-17.98
	-34.60		-17.89
	-34.54		-18.15
	-34.39		-17.98
mean	-34.45	mean	-18.07
SD	0.10	SD	0.17
accepted	-23.37	accepted	-17.98
Offset correction	11.08	Accuracy +/-	0.09 per mil

Appendix 3: Identities of separable inositol phosphate species as separated by HPLC on a CarboPac PA200 column with a guard column of the same material by a 0.6M Methanesulfonic acid gradient giving rise to known elution order.



Separation of hydrolysed InsP standards prepared by acid reflux of phytate: the peaks identified are 1: InsP₆, 2: InsP₅ (13456), 3: InsP₅ (23456/12456), 4: InsP₅ (12356/12345), 5: InsP₅ (12346), 6: InsP₄(1456/3456), 7: InsP₄ (2456), 8: InsP₄ (1256/2345), 9: InsP₄ (1345/1356), 10: InsP₄(1245,2356), 11: InsP₄ (1234/1236), 12: InsP₄ (1246), 13: InsP₃, 14: InsP₂ and 15: InsP₁/P_i.

Appendix 4: Recorded bird weights and feed intake measured at day 0, 7, 14 and 21 (at euthanasia)

pen	diet	pen wt	minus bucket	n of birds	d0 brd wt	D07 pen wt	bucket weight	no of birds	D07 Bird Wt	D7 BWG	D07 feed wt	wk1 FI/Brd	wk1 FCR
1	4	965	428	10	42.8	2042.1	537	10	150.5	107.7	4621.6	142.4	1.32
2	6	973	436	10	43.6	1787	537	10	125.0	81.4	4776.7	126.9	1.56
3	5	978	441	10	44.1	1832	537	10	129.5	85.4	4539.9	150.6	1.76
4	1	973	436	10	43.6	1810.7	537	10	127.4	83.8	4662.1	138.4	1.65
5	2	969	432	10	43.2	1839.3	537	10	130.2	87.0	4620.2	142.6	1.64
6	8	973	436	10	43.6	1831.9	537	10	129.5	85.9	4516.1	153.0	1.78
7	3	977	440	10	44	1958.6	537	10	142.2	98.2	4505.4	154.1	1.57
8	7	965	428	10	42.8	1805.5	537	10	126.9	84.1	4688.2	135.8	1.62
9	4	978	441	10	44.1	1744	537	10	120.7	76.6	4520.8	152.5	1.99
10	7	969	432	10	43.2	1667.9	537	9	125.7	82.5	4761.1	142.8	1.73
11	6	982	445	10	44.5	1615.3	537	9	119.8	75.3	4444.2	178.0	2.36
12	8	984	447	10	44.7	1896.5	537	10	136.0	91.3	4419.7	162.6	1.78
13	3	983	446	10	44.6	1746.5	537	10	121.0	76.4	4543.3	150.3	1.97
14	2	984	447	10	44.7	1736.7	537	10	120.0	75.3	4440.7	160.5	2.13
15	5	961	424	10	42.4	1870.5	537	10	133.4	91.0	4390.4	165.6	1.82
16	1	974	437	10	43.7	2045.1	537	10	150.8	107.1	4563	148.3	1.38
17	6	966	429	10	42.9	1706.4	537	10	116.9	74.0	3903.8	214.2	2.89
18	7	986	449	10	44.9	1961.3	537	10	142.4	97.5	4245.6	180.0	1.85
19	1	970	433	10	43.3	1901.1	537	10	136.4	93.1	4032.7	205.9	2.21
20	5	971	434	10	43.4	1807.5	537	10	127.1	83.7	4620.4	142.6	1.70
21	2	969	432	10	43.2	1747.1	537	10	121.0	77.8	4377.7	166.8	2.14
22	8	964	427	10	42.7	1895.1	537	10	135.8	93.1	4139.5	195.3	2.10
23	3	966	429	10	42.9	1906.9	537	10	137.0	94.1	4224.2	182.2	1.94

pen	diet	pen wt	minus bucket	n of birds	d0 brd wt	D07 pen wt	bucket weight	no of birds	D07 Bird Wt	D7 BWG	D07 feed wt	wk1 FI/Brd	wk1 FCR
24	4	971	434	10	43.4	1848	537	10	131.1	87.7	4755.1	129.1	1.47
25	1	963	426	10	42.6	1690.9	537	10	115.4	72.8	3837	220.9	3.03
26	3	964	427	10	42.7	2033.7	537	10	149.7	107.0	4361.1	168.5	1.58
27	4	952	415	10	41.5	2034.7	537	10	149.8	108.3	4487.9	155.8	1.44
28	6	953	416	10	41.6	1816.7	537	10	128.0	86.4	4701.4	134.5	1.56
29	5	980	443	10	44.3	1899.3	537	10	136.2	91.9	4281.3	181.1	1.97
30	8	956	419	10	41.9	2085.9	537	10	154.9	113.0	4541.8	150.4	1.33
31	2	968	431	10	43.1	1909.5	537	10	137.3	94.2	4711.8	133.4	1.42
32	7	971	434	10	43.4	1970.2	537	10	143.3	99.9	4553.1	149.3	1.49
33	8	982	445	10	44.5	2139.8	537	10	160.3	115.8	4214	183.2	1.58
34	4	975	438	10	43.8	1950.6	537	9	157.1	113.3	4334.7	190.1	1.68
35	3	970	433	10	43.3	1921.9	537	10	138.5	95.2	4571.8	147.4	1.55
36	6	984	447	10	44.7	1935.9	537	9	155.4	110.7	3985.1	229.0	2.07
37	2	951	414	10	41.4	1797.7	537	10	126.1	84.7	4314.5	173.2	2.04
38	1	966	429	10	42.9	1886.6	537	10	135.0	92.1	4315.3	173.1	1.88
39	7	981	444	10	44.4	1911.6	537	10	137.5	93.1	4740.8	130.5	1.40
40	5	984	447	10	44.7	1879.7	537	10	134.3	89.6	4791.8	125.4	1.40
41	1	989	452	10	45.2	1878.2	537	10	134.1	88.9	4597.1	144.9	1.63
42	6	967	430	10	43	1707.7	537	9	130.1	87.1	4674.3	152.4	1.75
43	7	970	433	10	43.3	1749	537	10	121.2	77.9	3746.9	229.9	2.95
44	2	970	433	10	43.3	1626.9	537	10	109.0	65.7	4268.6	177.7	2.71
45	5	975	438	10	43.8	1696.2	537	10	115.9	72.1	4814.2	123.2	1.71
46	3	965	428	10	42.8	1827.5	537	9	143.4	100.6	4274.3	196.9	1.96
47	8	968	431	10	43.1	1828.4	537	10	129.1	86.0	4597	144.9	1.68
48	4	983	446	10	44.6	2064.9	537	10	152.8	108.2	4240.3	180.6	1.67

pen	diet	pen wt	minus bucket	n of birds	d0 brd wt	D07 pen wt	bucket weight	no of birds	D07 Bird Wt	D7 BWG	D07 feed wt	wk1 FI/Brd	wk1 FCR
Mean		971.625	434.625	10	43.4625	1859.302083	537	9.875	133.9623611	90.49986	4443.09375	162.8471759	1.83038255
st.Dev		9.120062	9.12006	0	0.912006	122.6785204	0	0.334218682	12.26276762	12.26064	257.9577018	27.44982257	0.408264761
2		989.8651	452.865	10	45.28651	2104.659124	537	10.54343736	158.4878963	115.0211	4959.009154	217.7468211	2.646912073
-2		953.3849	416.385	10	41.63849	1613.945043	537	9.206562635	109.4368259	65.97858	3927.178346	107.9475308	1.013853028

pen	diet	D14 pen wt	minus bucket	no of birds	D14 Bird Wt	D14 BWG	D14 feed wt	wk2 FI/Brd	wk2 FCR	Runt cull	D14 pen wt	minus bucket	no of birds	D14 Bird Wt
1	4	4726.8	887	10	384.0	233.5	1471.8	315.0	1.35		4726.8	887	10	384.0
2	6	4287.5	887	10	340.1	215.1	1776.6	300.0	1.40		4287.5	887	10	340.1
3	5	4035	887	10	314.8	185.3	2205.5	233.4	1.26	Cull	3706	887	8	352.4
4	1	4242.3	887	10	335.5	208.2	1754.9	290.7	1.40		4242.3	887	10	335.5
5	2	4306.7	887	10	342.0	211.7	1805.2	281.5	1.33		4306.7	887	10	342.0
6	8	4725.9	887	10	383.9	254.4	1508.3	300.8	1.18		4725.9	887	10	383.9
7	3	4786.6	887	10	390.0	247.8	1572.6	293.3	1.18		4786.6	887	10	390.0
8	7	4201.1	887	9	368.2	241.4	1820	318.7	1.32		4201.1	887	9	368.2
9	4	4358	887	10	347.1	226.4	1999.5	252.1	1.11		4358	887	10	347.1
10	7	3901.1	887	9	334.9	209.2	2448.9	256.9	1.23		3901.1	887	9	334.9
11	6	3938.7	887	9	339.1	219.3	2046.4	266.4	1.22		3938.7	887	9	339.1
12	8	4761	887	10	387.4	251.5	1477.3	294.2	1.17		4761	887	10	387.4
13	3	4313.3	887	10	342.6	221.7	1649.4	289.4	1.31	Cull	4210.3	887	9	369.3
14	2	4123.1	887	10	323.6	203.6	1731.4	270.9	1.33		4123.1	887	10	323.6
15	5	4414.1	887	10	352.7	219.4	1638.5	275.2	1.25		4414.1	887	10	352.7
16	1	4691.8	887	10	380.5	229.7	1652.2	291.1	1.27		4691.8	887	10	380.5
17	6	3912.1	887	10	302.5	185.6	696.8	320.7	1.73		3912.1	887	10	302.5
18	7	4599	887	10	371.2	228.8	828	341.8	1.49	Cull	4445	887	9	395.3
19	1	4455.7	887	10	356.9	220.5	834.2	319.9	1.45		4455.7	887	10	356.9
20	5	4213.3	887	10	332.6	205.6	1996.1	262.4	1.28		4213.3	887	10	332.6
21	2	4139.1	887	10	325.2	204.2	1884.5	249.3	1.22		4139.1	887	10	325.2
22	8	4720.1	887	10	383.3	247.5	1193.6	294.6	1.19	Cull	4561.1	887	9	408.2
23	3	4344.5	887	10	345.8	208.8	1347.6	287.7	1.38		4344.5	887	10	345.8
24	4	4546.6	887	10	366.0	234.9	1752.2	300.3	1.28		4546.6	887	10	366.0

pen	diet	D14 pen wt	minus bucket	no of birds	D14 Bird Wt	D14 BWG	D14 feed wt	wk2 Fl/Brd	wk2 FCR	Runt cull	D14 pen wt	minus bucket	no of birds	D14 Bird Wt
25	1	3988.6	887	10	310.2	194.8	1248.4	258.9	1.33	Cull	3870.6	887	9	331.5
26	3	4885.3	887	10	399.8	250.2	1278.4	308.3	1.23		4885.3	887	10	399.8
27	4	4879.1	887	10	399.2	249.4	1423.2	306.5	1.23		4879.1	887	10	399.2
28	6	4242.8	887	10	335.6	207.6	2061.7	264.0	1.27		4242.8	887	10	335.6
29	5	4387	887	10	350.0	213.8	1506.2	277.5	1.30		4387	887	10	350.0
30	8	4767.1	887	10	388.0	233.1	1566.5	297.5	1.28		4767.1	887	10	388.0
31	2	4443.2	887	10	355.6	218.4	1736.7	297.5	1.36		4443.2	887	10	355.6
32	7	4742.7	887	10	385.6	242.3	1330	322.3	1.33		4742.7	887	10	385.6
33	8	4903.3	887	10	401.6	241.4	976.1	323.8	1.34		4903.3	887	10	401.6
34	4	4734.8	887	9	427.5	270.5	1247.7	343.0	1.27		4734.8	887	9	427.5
35	3	4442	887	10	355.5	217.0	1903.3	266.9	1.23		4442	887	10	355.5
36	6	4632.6	887	9	416.2	260.7	1289.9	299.5	1.15		4632.6	887	9	416.2
37	2	4168.4	887	10	328.1	202.1	1439.4	287.5	1.42		4168.4	887	10	328.1
38	1	4228.8	887	10	334.2	199.2	1211	310.4	1.56		4228.8	887	10	334.2
39	7	4445.1	887	10	355.8	218.4	1779.2	296.2	1.36		4445.1	887	10	355.8
40	5	4369.6	887	10	348.3	214.0	2213	257.9	1.21		4369.6	887	10	348.3
41	1	4374	887	10	348.7	214.6	1910.2	268.7	1.25		4374	887	10	348.7
42	6	4019.2	887	9	348.0	217.9	2176.7	277.5	1.27	Cull	3883.2	887	8	374.5
43	7	3947.9	887	10	306.1	184.9	1220	252.7	1.37	Cull	3862.9	887	9	330.7
44	2	3738.6	887	10	285.2	176.2	2045	222.4	1.26		3738.6	887	10	285.2
45	5	3804.9	887	10	291.8	175.9	2493	232.1	1.32		3804.9	887	10	291.8
46	3	4472.8	887	9	398.4	255.0	1411	318.1	1.25		4472.8	887	9	398.4
47	8	4514.1	887	10	362.7	233.6	1717.5	288.0	1.23	Cull	4339.1	887	9	383.6
48	4	5150.6	887	10	426.4	273.6	1130.7	311.0	1.14		5150.6	887	10	426.4

pen	diet	D14 pen wt	minus bucket	no of birds	D14 Bird Wt	D14 BWG	D14 feed wt	wk2 Fl/Brd	wk2 FCR	Post cull	D14 pen wt	minus bucket	no of birds	D14 Bird Wt
Mean		4396.3729	887	9.85416667	356.421389	222.459	1612.63125	287.37988	1.297256		4370.1438	887	9.66666667	360.724167
st.Dev		326.1219	0	0.35667396	33.7430131	23.62422	408.28511	27.73808	0.110361		342.92875	0	0.55862039	33.1683056
2		5048.6167	887	10.5675146	423.907415	269.7075	2429.20147	342.85604	1.517977		5056.0013	887	10.7839074	427.060778
-2		3744.1291	887	9.14081875	288.935363	175.2106	796.061031	231.90372	1.076535		3684.2862	887	8.54942589	294.387555

pen	diet	Bird 1	Bird 2	Bird 3	Bird 4	Bird 5	Bird 6	Bird 7	Bird 8	No of birds	S Bird 1	S Bird 2	Ave bird wt D21	BWG D14-21	SD week 3	D21 feed left	FI/bird D14-21	FCR w3
1	4	936.7	862.2	985.6	508.8	899	752	674.5	788.9	10	877	934	821.87	437.9	144.8681	1430.6	608.22	1.388979
2	6	897.9	690.1	987.2	469.8	915.1	682.9	620.5	474.5	10	603	696	703.7	363.7	178.8101	2661.8	515.58	1.417792
3	5	654.7			633.2	526.3		720.1	408	7	819	919	668.6142857	316.2	172.0371	4102.5	592	1.872
4	1	922	543.3	617.3	816.1	786.4	704.8	783.2	886.1	10	803	756	761.82	426.3	114.8568	2329.8	546.61	1.282249
5	2	831	650.5	531.2	479.8	743.1	855.4	727	535.5	10	624	850	682.75	340.8	139.7176	2397.9	544.83	1.598773
6	8	777.3	804.7	738.9	813.7	826.4	991	628	910.9	10	724	791	800.59	416.7	99.65082	2301.3	524.8	1.259419
7	3	848.6	803	942.6	845.8	998.2	839.3	1072.3	920	10	833	884	898.68	508.7	84.94832	897.5	671.61	1.320196
8	7	915.3	704.2	823	905.5	788.2	588.4	854.5		9	940	706	802.7888889	434.6	117.4633	2326	615	1.415239
9	4	832.8	466.3	813.5	848.1	771.9	692	792.3	865	10	784	810	767.59	420.5	116.1977	2660.8	537.97	1.279388
10	7	780	773.1	488.4	583.7	828.7	845.8	589.6		9	583	906	708.7	373.8	148.1119	3384.5	567.2666667	1.517567
11	6	633.8	826.2	716.4	833	796.6	827.4	732		9	690	759	757.1555556	418.1	69.85104	3092.3	555.0111111	1.327531
12	8	719.2	898.1	848	945.2	934.4	980.1	981	1036.5	10	907	774	902.35	515.0	97.8103	1161.6	635.67	1.234431
13	3	459.9	834.9	743	612	907.3	755.3	820		9	771	656	728.8222222	359.6	134.8012	2506	576.0444444	1.602052
14	2	773.9	527.1	912.8	528.1	922.6	536.1	811	855.7	10	628	672	716.73	393.1	158.5825	2196.2	557.62	1.418447
15	5	921.5	760.1	642.6	881.6	796.8	655	553.1	831.9	10	651	569	726.26	373.6	129.9513	2354.3	532.52	1.425566
16	1	620.1	385.7	806.4	938.1	896.2	975.9	929.8	954.3	10	897	885	828.85	448.4	186.2745	1511.1	618.21	1.378794
17	6	491.5	702.4	859.5	758.4	626.9	684.9	867	474	10	554	744	676.26	373.8	139.2366	1786.4	495.14	1.324789
18	7	616.5	926.4	1011.5	468.3	949.4	877.2	984.9		9	671	761	807.3555556	412.0	188.5967	1749.4	568.8444444	1.380616
19	1	852.4	789.4	862.2	781.9	819.4	693.1	796.6	408.5	10	821	582	740.65	383.8	143.3268	1569.1	530.61	1.382589
20	5	927	769.2	843.6	926.9	447.4	451.3	626	910.6	10	549	771	722.2	389.6	190.5613	2735.9	530.12	1.360782

pen	diet	Bird 1	Bird 2	Bird 3	Bird 4	Bird 5	Bird 6	Bird 7	Bird 8	No of birds	S Bird 1	S Bird 2	Ave bird wt D21	BWG D14-21	SD week 3	D21 feed left	FI/bird D14-21	FCR w3
21	2	805	733.9	462.6	730.9	616.6	805.6	709.6	866.8	10	646	802	717.9	392.7	118.1454	2709.1	521.64	1.328376
22	8	760	917.1	710.7	938.2	964.6	792.8	701.3		9	709	740	803.7444444	395.5	106.6698	2080.1	572.7222222	1.448056
23	3	999.6	753.5	397.7	589.9	854.1	696	611		9	806	779	720.7555555	375.0	173.7143	1738.5	627.7888889	1.674079
24	4	767.1	722	1035.3	867.1	692.5	673.7	853	813	10	762	751	793.67	427.7	105.9167	1801.8	599.14	1.400809
25	1	712	660.5	481.9	917.2	761.2	892.7	997		9	761	556	748.8333333	417.3	169.0156	1855.1	603.8111111	1.446871
26	3	892.1	932	863.6	732.4	863	890	712.7	887.3	10	767	736	827.61	427.8	81.23668	1364.8	595.46	1.391977
27	4	907.4	949	819.2	846	665.1	793.6	1008.1	620.2	10	726	759	809.36	410.2	123.0961	1443.2	602.1	1.468
28	6	742.2	947.7	711.7	523.3	879	853.5	834.9	712.9	10	512	553	727.02	391.4	155.6762	2473.2	562.95	1.438151
29	5	826.7	611.6	471.6	684.4	836.3	609.2	466.6	631.4	10	942	744	682.38	332.4	156.2322	2109.7	543.75	1.635929
30	8	964.6	946.9	925.4	797.6	946.1	822.2	662	811.7	10	736	624	823.65	435.6	122.4298	1285.5	632.2	1.451198
31	2	814.4	564.2	808.7	901.7	451.7	943.2	937.4	615.2	10	745	733	751.45	395.8	164.9981	1077.6	670.01	1.692671
32	7	874.3	813.9	755.1	874.9	911.7	873	458.4	723.7	10	880	806	797.1	411.5	133.3374	548.3	682.27	1.657886
33	8	1052.9	1017.1	795	927.5	1011.1	964.1	674.8	375.7	10	850	782	845.02	443.4	204.7018	333.5	668.36	1.507386
34	4	1039.7	945.8	1048.9	519.9	1050.7	974.3	824.5		9	698	882	887.0888889	459.6	180.9074	648.5	737.8	1.605464
35	3	813.5	937.9	682.6	613.8	815.8	523.5	820.5	1028.7	10	781	896	791.33	435.8	151.2551	1710.9	623.34	1.430237
36	6	1056.7	916.9	1014.2	492.3	858.3	888.3	1043.9		9	775	806	872.4	456.2	174.7461	1154.5	686.2666667	1.504238
37	2	516.1	910.7	602.9	411.9	740.5	1023.5	956.2	902.1	10	827	702.3	759.32	431.2	201.2088	1411.9	606.85	1.407417
38	1	881	997.6	621.5	595.1	731.7	724.8	762.1	864.5	10	675	797	765.03	430.9	124.1749	832.5	641.95	1.489962
39	7	855.9	984.7	476.7	698.9	917.6	955.1	841.3	681.7	10	675	841	792.79	437.0	157.182	1474.3	634.59	1.452217
40	5	723.7	712	804.6	885.7	929.5	678	1046.2	652.5	10	863	653	794.82	446.6	133.4441	2224.1	602.99	1.3503

pen	diet	Bird 1	Bird 2	Bird 3	Bird 4	Bird 5	Bird 6	Bird 7	Bird 8	No of birds	S Bird 1	S Bird 2	Ave bird wt D21	BWG D14-21	SD week 3	D21 feed left	FI/bird D14-21	FCR w3
41	1	645	607.1	798.1	999.8	1013.8	438.2	839.2	660.9	10	782	824	760.81	412.1	177.7	2031.2	592	1.43651
42	6	510.4	895.9	678.6	800	916.3	1049.4			8	767	866	810.45	435.9	163.9252	2810.9	675.85	1.550381
43	7	735.6	533	754.7	542.1	392.3	953.5	831.5		9	967	705	712.7444444	382.1	194.6686	1765	610.6666666	1.598232
44	2	666.9	970.9	839.5	632.4	553.5	395	513.8	740.6	10	654	708	667.46	382.3	163.6086	3011.2	507.48	1.327439
45	5	647.9	688.1	642.3	531.5	672.7	763.6	549.7	443.4	10	716	790	644.52	352.7	108.2062	3355.7	517.83	1.468063
46	3	1063.3	902.8	634.2	942	591.3	921.4	847.9		9	817	917	848.5444444	450.1	150.3768	2008.3	604.8555555	1.343758
47	8	898.9	785.8	723.6	941.7	694.8	892.2	876.2		9	889	703	822.8	439.2	96.12782	1350.6	711.9888888	1.620981
48	4	881.5	995.3	1001.1	903.9	873.6	1104.4	874.1	499	10	760	840	873.29	446.9	163.1886	600.3	657.14	1.470342

S bird = bird sampled for digesta and tissues, where S Bird 1 = Bird A, S Bird 2 = Bird B

Mortality record:

Pen	Diet	Day	Weight	Reason recorded	Technician reporting initials
10	7	3	50.5g	Died	J.O.
11	6	6	74g	Culled	D.S.
34	4	5	87.9g	Died	J.O.
36	6	6	83g	Culled	J.O.
42	6	6	97.1g	Died	J.O.
46	3	6	86g	Culled (wry neck)	J.O.
8	7	9	76.3g	Died	B.G.
3	5	14	142g	Runt culled	B.G.
3	5	14	187g	Runt culled	B.G.
13	3	14	103g	Runt culled	B.G.
18	7	14	154g	Runt culled	B.G.
22	8	14	159g	Runt culled	B.G.
25	1	14	118g	Runt culled	B.G.
42	6	14	136g	Runt culled	B.G.
43	7	14	85g	Runt culled	B.G.
47	8	14	175g	Runt culled	B.G.
3	5	17	599.1g	Died	B.G.
23	3	20	701.9g	Died	B.G.

Diet	Sum deaths reported	Percentage mortality (%)
1	1	1.25
2	0	0
3	3	3.75
4	1	1.25
5	3	3.75
6	4	5
7	4	5
8	2	2.5

Appendix 5: Regression outputs

Gizzard digesta (HCl extracted) -

<i>Linear regression: Gizzard digesta (HCl extracted)</i>	<i>Without Titanium</i>	<i>With titanium</i>
<i>Best-fit values ± SE</i>		
<i>Slope</i>	-1.885±0.9357	-1.769 ± 0.506
<i>Y-intercept</i>	12037±3252	11812 ± 1759
<i>X-intercept</i>	6387	6679
<i>1/slope</i>	-0.5306	-0.5654
<i>95% Confidence Intervals</i>		
<i>Slope</i>	-13.77 to 10	-8.198 to 4.661
<i>Y-intercept</i>	-29289 to 53363	-10538 to 34163
<i>X-intercept</i>	-infinity to +infinity	-infinity to +infinity
<i>Goodness of Fit</i>		
<i>R square</i>	0.8023	0.9243
<i>Sy.x</i>	4405	2382
<i>Is slope significantly non-zero?</i>		
<i>F</i>	4.057	12.22
<i>DFn, DFd</i>	1, 1	1, 1
<i>P value</i>	0.2934	0.1774
<i>Deviation from zero?</i>	Not Significant	Not Significant
<i>Equation</i>	Y = -1.885*X + 12037	Y = -1.769*X + 11812

Are the slopes equal? F = 0.01189. DF_n = 1, DF_d = 2. P = 0.9231.

Are the elevations or intercepts equal? F = 0.0001226. DF_n = 1. DF_d = 3. P=0.9919.

Gizzard digesta (NaF-EDTA extracted) -
 Linear regression: Gizzard
 digesta (NaF-EDTA
 extracted)

Without Titanium

With titanium

Best-fit values \pm SE	Without Titanium	With titanium
Slope	-1.921 \pm 0.7957	-1.745 \pm 0.3434
Y-intercept	12325 \pm 2766	11319 \pm 1194
X-intercept	6417	6487
1/slope	-0.5206	-0.5731
95% Confidence Intervals		
Slope	-12.03 to 8.19	-6.108 to 2.618
Y-intercept	-22821 to 47472	-3847 to 26485
X-intercept	-infinity to +infinity	-infinity to +infinity
Goodness of Fit		
R square	0.8535	0.9627
Sy.x	3746	1617
Is slope significantly non-zero?		
F	5.827	25.82
DFn, DFd	1, 1	1, 1
P value	0.2500	0.1237
Deviation from zero?	Not Significant	Not Significant
Equation	Y = -1.921*X + 12325	Y = -1.745*X + 11319

Are the slopes equal? F = 0.04128. DF_n = 1, DF_d = 2. P = 0.8578.

Are the elevations or intercepts equal? F = 0.1033. DF_n = 1. DF_d = 3. P=0.7690.

Ileal digesta (HCI extracted) –

<i>Linear regression: Ileal digesta (HCI extracted)</i>	<i>Without Titanium</i>	<i>With titanium</i>
<i>Best-fit values ± SE</i>		
<i>Slope</i>	-7.679 ± 2.212	-6.909 ± 2.744
<i>Y-intercept</i>	49244 ± 7690	47570 ± 9540
<i>X-intercept</i>	6413	6886
<i>1/slope</i>	-0.1302	-0.1447
<i>95% Confidence Intervals</i>		
<i>Slope</i>	-35.79 to 20.43	-41.78 to 27.96
<i>Y-intercept</i>	-48467 to 146956	-73644 to 168785
<i>X-intercept</i>	-infinity to +infinity	-infinity to +infinity
<i>Goodness of Fit</i>		
<i>R square</i>	0.9234	0.8637
<i>Sy.x</i>	10416	12921
<i>Is slope significantly non-zero?</i>		
<i>F</i>	12.05	6.337
<i>DFn, DFd</i>	1, 1	1, 1
<i>P value</i>	0.1786	0.2407
<i>Deviation from zero?</i>	Not Significant	Not Significant
<i>Equation</i>	Y = -7.679*X + 49244	Y = -6.909*X + 47570

Are the slopes equal? F = 0.04773. DF_n = 1, DF_d = 2. P = 0.8473.

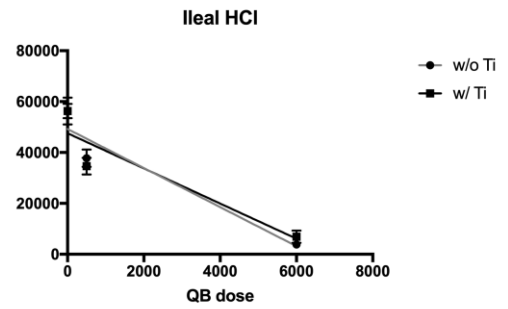
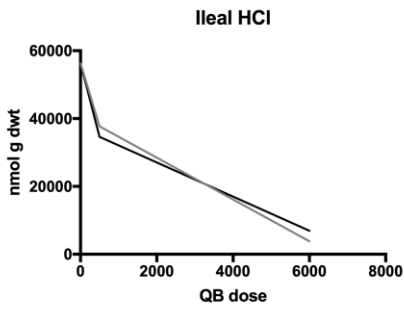
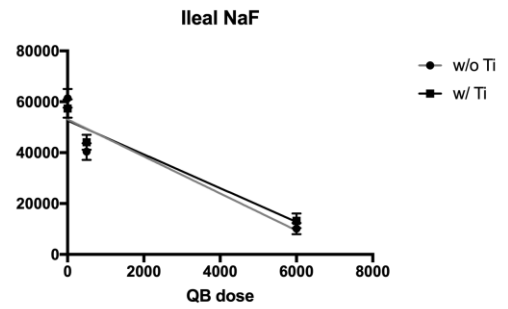
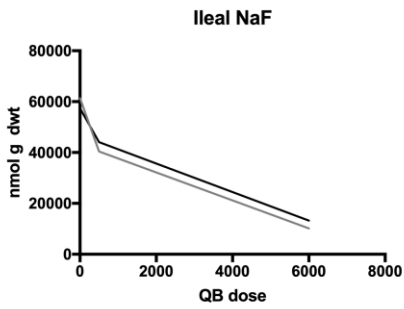
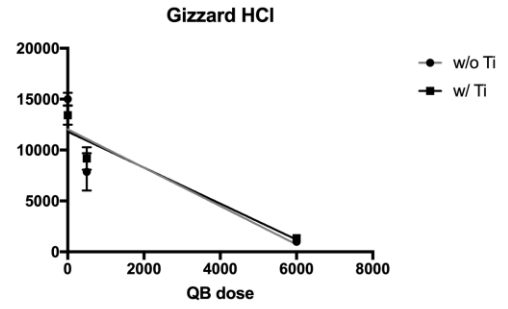
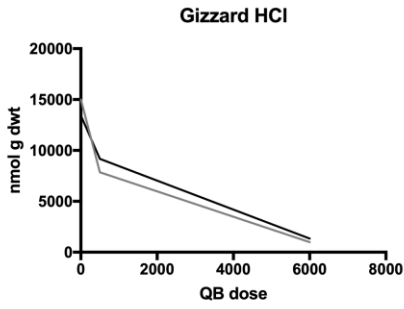
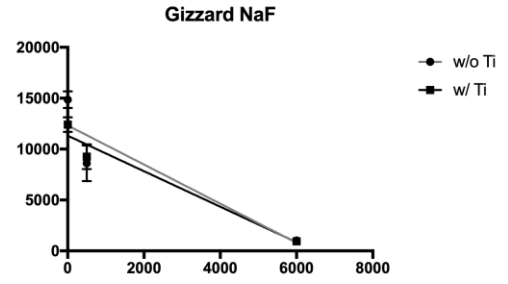
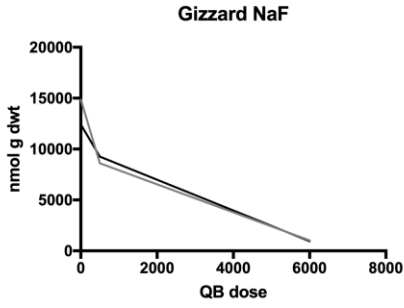
Are the elevations or intercepts equal? F = 4.574e-007. DF_n = 1. DF_d = 3. P=0.9995.

Ileal digesta (NaF-EDTA extracted) –

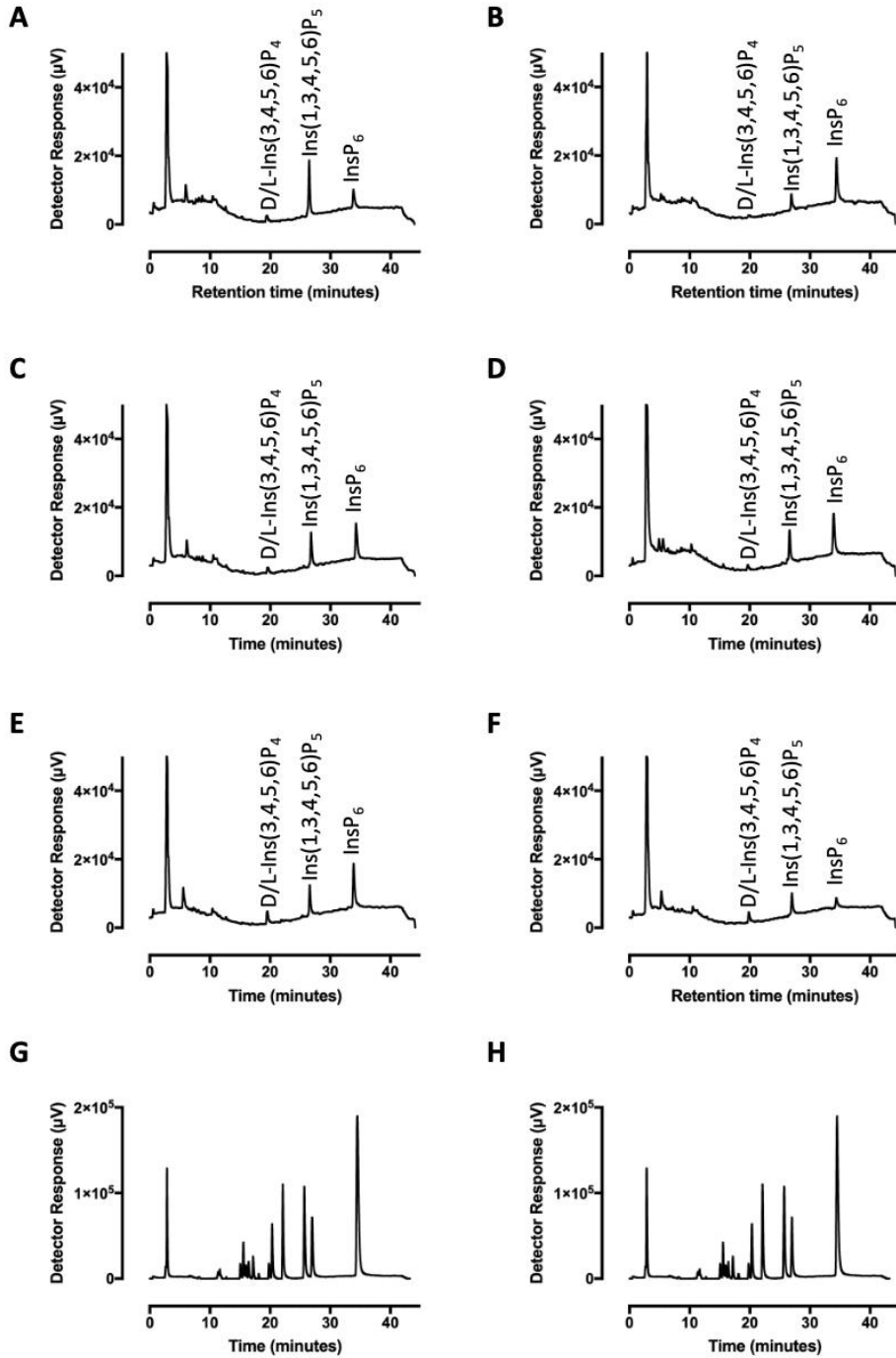
<i>Linear regression: Ileal digesta (NaF-EDTA extracted)</i>	<i>Without Titanium</i>	<i>With titanium</i>
<i>Best-fit values ± SE</i>		
<i>Slope</i>	-7.275 ± 2.605	-6.635 ± 1.498
<i>Y-intercept</i>	53074 ± 9057	52600 ± 5206
<i>X-intercept</i>	7295	7927
<i>1/slope</i>	-0.1375	-0.1507
<i>95% Confidence Intervals</i>		
<i>Slope</i>	-40.38 to 25.83	-25.67 to 12.4
<i>Y-intercept</i>	-62001 to 168148	-13551 to 118752
<i>X-intercept</i>	-infinity to +infinity	-infinity to +infinity
<i>Goodness of Fit</i>		
<i>R square</i>	0.8863	0.9515
<i>Sy.x</i>	12266	7051
<i>Is slope significantly non-zero?</i>		
<i>F</i>	7.798	19.63
<i>DFn, DFd</i>	1, 1	1, 1
<i>P value</i>	0.2189	0.1413
<i>Deviation from zero?</i>	Not Significant	Not Significant
<i>Equation</i>	Y = -7.275*X + 53074	Y = -6.635*X + 52600

Are the slopes equal? F = 0.04537. DFn = 1, DFd = 2. P = 0.8511.

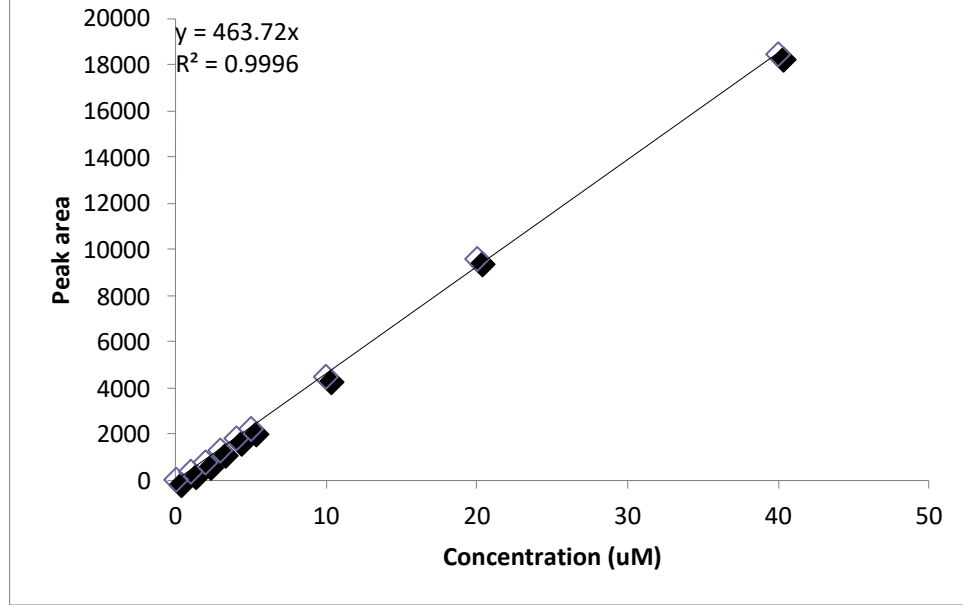
Are the elevations or intercepts equal? F = 0.01833. DFn = 1. DFd = 3. P=0.9009.



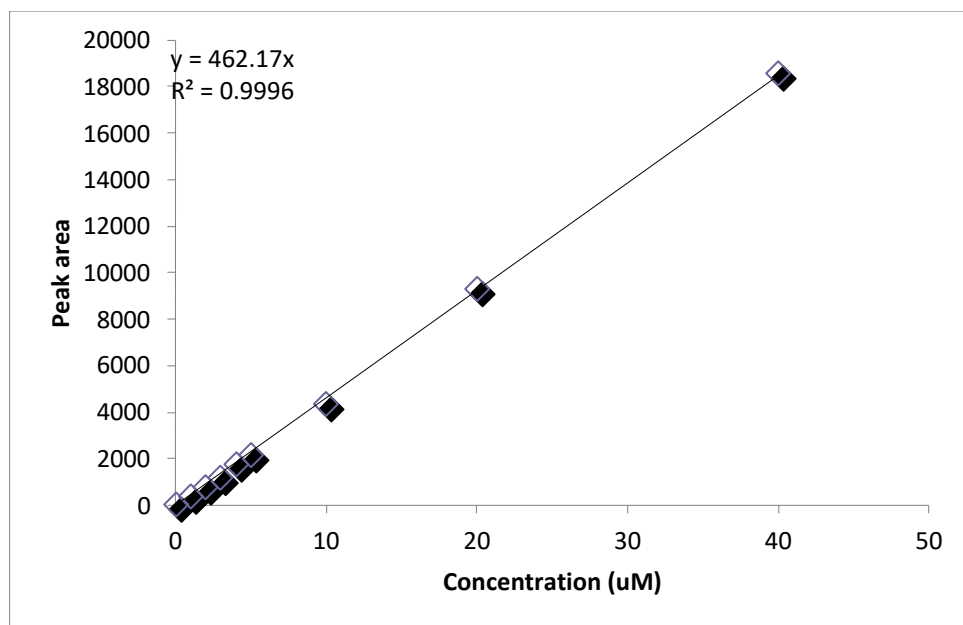
Appendix 6: Inositol phosphate profiles in duodenum tissue (A and B), jejunum tissue (C and D) and ileum tissue (E and F). G and H, InsP₆ hydrolysate standards run alongside sample sets. Major peaks identified.



Appendix 7: Digesta and diet inositol and inositol phosphate raw measurements



Standard curve for inositol used to calculate ileal digesta concentrations



Standard curve for inositol used to calculate gizzard digesta concentrations

Run	Peak	Retention Time (min)	Area (nA)	Sample ID	nmol / g d wt inositol	g/kg
CS_diet_A	1	9.826	15.438	Diet 1 Control	83	0.0150
CS_diet_B	1	9.826	1239.745	Diet 2 13C Ins	6695	1.2051
CS_diet_C	1	9.826	18.72	Diet 3 500QB	101	0.0182
CS_diet_D	1	9.826	10.627	Diet 4 6000QB	57	0.0103
CS_diet_E	1	9.826	30.095	Diet 5 Control Ti	163	0.0293
CS_diet_F	1	9.826	1374.425	Diet 6 13C Ins Ti	7422	1.3360
CS_diet_G	1	9.826	16.575	Diet 7 500QB Ti	90	0.0161
CS_diet_H	1	9.826	33.475	Diet 8 6000QB Ti	181	0.0325

Ileal digesta (HCl extracted) inositol:

Run	Peak	Retention Time (min)	Area (nA)	nmol / g d wt	g / kg										
CS_ileal acid_001	1	9.501	1361.945	6910	1.2										
CS_ileal acid_002	1	9.501	1883.7	9557	1.7			Run	Peak	Retention Time (min)	Area (nA)	uM	nmol	area	
CS_ileal acid_003	1	9.403	201.565	1023	0.2							0	0	0	
CS_ileal acid_004	1	9.403	150.41	763	0.1			1uM Ins.csi	1	9.328	467.09	1	0.01	467.09	
CS_ileal acid_005	1	9.49	2777.71	14092	2.5			2uM Ins.csi	1	9.328	948.285	2	0.02	948.285	
CS_ileal acid_006	1	9.457	1770.6	8983	1.6			3uM Ins.csi	1	9.328	1419.047	3	0.03	1419.047	
CS_ileal acid_007	1	9.436	281.71	1429	0.3			4uM Ins.csi	1	9.328	1870.602	4	0.04	1870.602	
CS_ileal acid_008	1	9.436	837.103	4247	0.8			5uM Ins.csi	1	9.273	2241.655	5	0.05	2241.655	
CS_ileal acid_009	1	9.436	1926.21	9772	1.8			10uM Ins.csi	1	9.284	4527.868	10	0.1	4527.868	
CS_ileal acid_010	1	9.425	715	3627	0.7			20uM Ins.csi	1	9.273	10017.15	20	0.2	10017.15	
CS_ileal acid_011	1	9.414	2571.66	13047	2.3			40uM Ins.csi	1	9.328	19774.658	40	0.4	19774.658	
CS_ileal acid_012	1	9.403	1923.545	9759	1.8										
CS_ileal acid_013	1	9.393	881.758	4473	0.8										
CS_ileal acid_014	1	9.393	2776.02	14084	2.5										
CS_ileal acid_015	1	9.393	610.74	3099	0.6										
CS_ileal acid_016	1	9.349	235.267	1194	0.2										
CS_ileal acid_017	1	9.393	2129.4	10803	1.9										
CS_ileal acid_018	1	9.382	756.34	3837	0.7										

Run	Peak	Retention Time (min)	Area (nA)		nnol / g d wt	g/kg												
CS_ileal acid_019	1	9.382	685.035		3475	0.6												
CS_ileal acid_020	1	9.36	345.117		1751	0.3												
CS_ileal acid_021	1	9.403	3284.223		16662	3												
CS_ileal acid_022	1	9.403	2152.8		10922	2												
CS_ileal acid_023	1	9.393	1562.145		7925	1.4												
CS_ileal acid_024	1	9.403	2550.925		12942	2.3												
CS_ileal acid_025	1	9.349	785.33		3984	0.7												
CS_ileal acid_026	1	9.36	1233.505		6258	1.1												
CS_ileal acid_027	1	9.371	4287.92		21754	3.9												
CS_ileal acid_028	1	9.382	2831.465		14365	2.6												
CS_ileal acid_029	1	9.36	520.78		2642	0.5												
CS_ileal acid_030	1	9.382	3567.33		18098	3.3												
CS_ileal acid_031	1	9.382	2389.953		12125	2.2												
CS_ileal acid_032	1	9.36	1449.175		7352	1.3												
CS_ileal acid_033	1	9.36	3409.25		17296	3.1												
CS_ileal acid_034	1	9.36	3524.722		17882	3.2												
CS_ileal acid_035	1	9.36	1362.335		6912	1.2												
CS_ileal acid_036	1	9.371	3020.485		15324	2.8												
CS_ileal acid_037	1	9.338	2763.8		14022	2.5												
CS_ileal acid_038	1	9.338	1038.408		5268	0.9												

Run	Peak	Retention Time (min)	Area (nA)		nnol / g d wt	g/kg										
CS_ileal acid_039	1	9.349	1426.23		7236	1.3										
CS_ileal acid_040	1	9.328	713.18		3618	0.7										
CS_ileal acid_041	1	9.328	481.13		2441	0.4										
CS_ileal acid_042	1	9.338	3985.475		20220	3.6										
CS_ileal acid_043	1	9.338	1984.84		10070	1.8										
CS_ileal acid_044	1	9.338	3358.355		17038	3.1										
CS_ileal acid_045	1	9.328	1001.293		5080	0.9										
CS_ileal acid_046	1	9.328	952.64		4833	0.9										
CS_ileal acid_047	1	9.338	4494.88		22804	4.1										
CS_ileal acid_048	1	9.338	3178.143		16124	2.9										

Ileal digesta inositol (NaF-EDTA extracted):

Run	Peak	Retention Time (min)	Area (nA)				mean	sd	SEM	nmol / g d wt	nmol / g d wt	
CS_ileal_004			nd	Diet 1 Control		Control	187	135	55.0119951	1008 (mean)	728 (sd)	297 (sem)
CS_ileal_016			nd	Diet 1 Control		13C Ins	1989	469	191.588149	10743	2534	1035
CS_ileal_019	1	8.656	136.37	Diet 1 Control		500QB	451	297	121.045993	2434	1601	654
CS_ileal_025	1	8.569	195.195	Diet 1 Control		6000QB	2013	1013	413.423416	10870	5469	2233
CS_ileal_038	1	8.515	367.217	Diet 1 Control		Control TI	110	62	25.4645781	593	337	138
CS_ileal_041		8.656	47.84	Diet 1 Control		13C Ins Ti	1798	445	181.629434	9709	2403	981
CS_ileal_005.1	1	8.688	2156.862	Diet 2 13C Ins		500QB Ti	473	230	93.8169921	2552	1241	507
CS_ileal_014	1	8.667	1322.815	Diet 2 13C Ins		6000QB Ti	1860	887	361.918916	10047	4787	1954
CS_ileal_021	1	8.678	2503.28	Diet 2 13C Ins		Formula to calculate nmol/g dwt using standard curve =PRODUCT(Cell/46294,5000/10,1000/20,1000/100)						
CS_ileal_031	1	8.656	1525.843	Diet 2 13C Ins								
CS_ileal_037	1	8.623	2370.55	Diet 2 13C Ins								
CS_ileal_044	1	8.613	2056.99	Diet 2 13C Ins								
CS_ileal_007		8.656	35.63	Diet 3 500QB								
CS_ileal_013	1	8.569	406.672	Diet 3 500QB								
CS_ileal_023	1	8.656	846.852	Diet 3 500QB								
CS_ileal_026	1	8.537	443.3	Diet 3 500QB								
CS_ileal_035	1	8.613	716.137	Diet 3 500QB								
CS_ileal_046	1	8.58	256.035	Diet 3 500QB								
CS_ileal_001	1	8.482	564.785	Diet 4 6000QB								
CS_ileal_009	1	8.678	1113.515	Diet 4 6000QB								
CS_ileal_024	1	8.667	2108.925	Diet 4 6000QB								

Run	Peak	Retention Time (min)	Area (nA)	Diet
CS_ileal_027	1	8.645	3283.67	Diet 4 6000QB
CS_ileal_034	1	8.623	2744.95	Diet 4 6000QB
CS_ileal_048	1	8.602	2261.22	Diet 4 6000QB
CS_ileal_003			nd	Diet 5 Control Ti
CS_ileal_015	1	8.623	151.093	Diet 5 Control Ti
CS_ileal_020		8.656	35.63	Diet 5 Control Ti
CS_ileal_029		8.656	63.407	Diet 5 Control Ti
CS_ileal_040	1	8.558	110.175	Diet 5 Control Ti
CS_ileal_045	1	8.547	188.565	Diet 5 Control Ti
CS_ileal_002	1	8.634	1057.615	Diet 6 13C Ins Ti
CS_ileal_011	1	8.678	1865.63	Diet 6 13C Ins Ti
CS_ileal_017	1	8.667	1906.06	Diet 6 13C Ins Ti
CS_ileal_028	1	8.656	2081.43	Diet 6 13C Ins Ti
CS_ileal_036	1	8.623	1547.52	Diet 6 13C Ins Ti
CS_ileal_042	1	8.613	2329.21	Diet 6 13C Ins Ti
CS_ileal_008	1	8.547	316.225	Diet 7 500QB Ti
CS_ileal_010	1	8.613	219.05	Diet 7 500QB Ti
CS_ileal_018	1	8.58	262.535	Diet 7 500QB Ti
CS_ileal_032	1	8.526	705.217	Diet 7 500QB Ti
CS_ileal_039	1	8.623	697.84	Diet 7 500QB Ti
CS_ileal_043	1	8.58	634.887	Diet 7 500QB Ti
CS_ileal_006	1	8.699	1278.745	Diet 8 6000QB Ti
CS_ileal_012	1	8.656	739.278	Diet 8 6000QB Ti

Run	Peak	Retention Time (min)	Area (nA)	Diet
CS_ileal_022	1	8.656	1381.12	Diet 8 6000QB Ti
CS_ileal_030	1	8.667	2941.673	Diet 8 6000QB Ti
CS_ileal_033	1	8.634	2005.51	Diet 8 6000QB Ti
CS_ileal_047	1	8.602	2816.645	Diet 8 6000QB Ti

Gizzard digesta inositol (NaF-EDTA extracted):

Run	Peak	Retention Time (min)	Area (nA)	Diet			mean	sd	sem	nmol / g d wt	nmol / g d wt	
CS_gizzard_004	1	9.078	38.025	Diet 1 Control		Control	65	35	14.2681152	348	189	77
CS_gizzard_016	1	9.631	49.335	Diet 1 Control		13C Ins	498	79	32.2104015	2691	426	174
CS_gizzard_019	1	9.631	79.235	Diet 1 Control		500QB	167	67	27.1519528	900	359	147
CS_gizzard_025	1	9.696	127.693	Diet 1 Control		6000QB	482	148	60.4260791	2606	799	326
CS_gizzard_038	1	9.761	58.89	Diet 1 Control		Control TI	117	53	21.4627533	629	284	116
CS_gizzard_041	1	9.793	33.93	Diet 1 Control		13C Ins Ti	149	45	18.3095952	802	242	99
CS_gizzard_005	1	9.295	410.345	Diet 2 13C Ins		500QB Ti	498	79	32.2104015	2691	426	174
CS_gizzard_014	1	9.631	573.885	Diet 2 13C Ins		6000QB Ti	515	185	75.5454463	2782	999	408
CS_gizzard_021	1	9.707	546.325	Diet 2 13C Ins		Formula to calculate nmol/g dwt using standard curve =PRODUCT(Cell/46294,5000/10,1000/20,1000/100)						
CS_gizzard_031	1	9.783	516.978	Diet 2 13C Ins								
CS_gizzard_037	1	9.815	388.797	Diet 2 13C Ins								
CS_gizzard_044	1	9.837	553.345	Diet 2 13C Ins								
CS_gizzard_007	1	9.306	192.952	Diet 3 500QB								
CS_gizzard_013	1	9.631	168.383	Diet 3 500QB								
CS_gizzard_023	1	9.707	233.903	Diet 3 500QB								
CS_gizzard_026	1	9.728	230.88	Diet 3 500QB								
CS_gizzard_035	1	9.75	79.918	Diet 3 500QB								
CS_gizzard_046	1	9.783	94.185	Diet 3 500QB								
CS_gizzard_001	1	8.938	241.02	Diet 4 6000QB								
CS_gizzard_009	1	9.382	554.548	Diet 4 6000QB								
CS_gizzard_024	1	9.728	540.54	Diet 4 6000QB								

Run	Peak	Retention Time (min)	Area (nA)	Diet	
CS_gizzard_027	1	9.761	672.36	Diet 4 6000QB	
CS_gizzard_034	1	9.793	401.18	Diet 4 6000QB	
CS_gizzard_048	1	9.815	485.225	Diet 4 6000QB	
CS_gizzard_003				Diet 5 Control Ti	
CS_gizzard_015	1	9.631	120.185	Diet 5 Control Ti	
CS_gizzard_020	1	9.642	174.2	Diet 5 Control Ti	
CS_gizzard_029	1	9.739	159.575	Diet 5 Control Ti	
CS_gizzard_040	1	9.75	79.105	Diet 5 Control Ti	
CS_gizzard_045	1	9.772	49.725	Diet 5 Control Ti	
CS_gizzard_002	1	9.013	668.46	Diet 6 13C Ins Ti	
CS_gizzard_011	1	9.631	490.425	Diet 6 13C Ins Ti	
CS_gizzard_017	1	9.631	448.825	Diet 6 13C Ins Ti	
CS_gizzard_028	1	9.772	320.645	Diet 6 13C Ins Ti	
CS_gizzard_036	1	9.804	484.25	Diet 6 13C Ins Ti	
CS_gizzard_042	1	9.837	446.55	Diet 6 13C Ins Ti	
CS_gizzard_008	1	9.295	154.31	Diet 7 500QB Ti	
CS_gizzard_010	1	9.382	222.885	Diet 7 500QB Ti	
CS_gizzard_018	1	9.631	86.71	Diet 7 500QB Ti	
CS_gizzard_032	1	9.804	161.687	Diet 7 500QB Ti	
CS_gizzard_039	1	9.685	132.827	Diet 7 500QB Ti	
CS_gizzard_043	1	9.728	132.6	Diet 7 500QB Ti	

Run	Peak	Retention Time (min)	Area (nA)	Diet	
CS_gizzard_006	1	9.295	537.16	Diet 8 6000QB Ti	
CS_gizzard_012	1	9.631	288.665	Diet 8 6000QB Ti	
CS_gizzard_022	1	9.696	289.835	Diet 8 6000QB Ti	
CS_gizzard_030	1	9.783	590.233	Diet 8 6000QB Ti	
CS_gizzard_033	1	9.783	686.66	Diet 8 6000QB Ti	
CS_gizzard_047	1	9.826	698.49	Diet 8 6000QB Ti	

Gizzard digesta inositol (HCl extracted):

Run	Peak	Retention Time (min)	Area (nA)	Diet		mean	sd	sem	nmol / g d wt	nmol / g d wt	
CS_gizzard acid_004	1	9.577	104.162	Diet 1 Control	Control	121	33	13.5568923	646	177	72
CS_gizzard acid_016	1	9.555	128.733	Diet 1 Control	13C Ins	634	80	32.6279986	3384	426	174
CS_gizzard acid_019	1	9.555	105.658	Diet 1 Control	500QB	197	50	20.5342451	1051	268	110
CS_gizzard acid_025	1	9.479	175.078	Diet 1 Control	6000QB	610	197	80.5611382	3253	1053	430
CS_gizzard acid_038	1	9.479	135.07	Diet 1 Control	Control Ti	161	80	32.4769781	860	424	173
CS_gizzard acid_041	1	9.533	78.423	Diet 1 Control	13C Ins Ti	543	75	30.7202649	2896	401	164
CS_gizzard acid_005	1	9.642	613.99	Diet 2 13C Ins	500QB Ti	199	28	11.2379998	1062	147	60
CS_gizzard acid_014	1	9.577	655.005	Diet 2 13C Ins	6000QB Ti	638	268	109.399261	3404	1430	584
CS_gizzard acid_021	1	9.588	613.275	Diet 2 13C Ins	Formulae to caculate nmol/g dwt from peak area =PRODUCT(H2/46863,5000/10,1000/20,1000/100)						
CS_gizzard acid_031	1	9.609	645.028	Diet 2 13C Ins							
CS_gizzard acid_037	1	9.544	515.873	Diet 2 13C Ins							
CS_gizzard acid_044	1	9.588	762.808	Diet 2 13C Ins							
CS_gizzard acid_007	1	9.577	239.655	Diet 3 500QB							
CS_gizzard acid_013	1	9.479	161.72	Diet 3 500QB							
CS_gizzard acid_023	1	9.566	265.817	Diet 3 500QB							
CS_gizzard acid_026	1	9.479	213.07	Diet 3 500QB							
CS_gizzard acid_035	1	9.544	137.93	Diet 3 500QB							
CS_gizzard acid_046	1	9.436	163.8	Diet 3 500QB							
CS_gizzard acid_001	1	9.642	295.425	Diet 4 6000QB							
CS_gizzard acid_009	1	9.598	812.077	Diet 4 6000QB							
CS_gizzard acid_024	1	9.588	699.563	Diet 4 6000QB							

Run	Peak	Retention Time (min)	Area (nA)	Diet
CS_gizzard acid_027	1	9.577	786.662	Diet 4 6000QB
CS_gizzard acid_034	1	9.577	489.775	Diet 4 6000QB
CS_gizzard acid_048	1	9.566	574.99	Diet 4 6000QB
CS_gizzard acid_003	1	9.598	81.835	Diet 5 Control Ti
CS_gizzard acid_015	1	9.555	150.215	Diet 5 Control Ti
CS_gizzard acid_020	1	9.588	154.993	Diet 5 Control Ti
CS_gizzard acid_029	1	9.588	305.792	Diet 5 Control Ti
CS_gizzard acid_040	1	9.479	176.313	Diet 5 Control Ti
CS_gizzard acid_045	1	9.501	97.565	Diet 5 Control Ti
CS_gizzard acid_002	1	9.652	504.172	Diet 6 13C Ins Ti
CS_gizzard acid_011	1	9.566	504.498	Diet 6 13C Ins Ti
CS_gizzard acid_017	1	9.577	545.448	Diet 6 13C Ins Ti
CS_gizzard acid_028	1	9.588	443.852	Diet 6 13C Ins Ti
CS_gizzard acid_036	1	9.577	612.495	Diet 6 13C Ins Ti
CS_gizzard acid_042	1	9.588	646.23	Diet 6 13C Ins Ti
CS_gizzard acid_008	1	9.544	199.225	Diet 7 500QB Ti
CS_gizzard acid_010	1	9.479	200.395	Diet 7 500QB Ti
CS_gizzard acid_018	1	9.577	159.38	Diet 7 500QB Ti
CS_gizzard acid_032	1	9.577	181.675	Diet 7 500QB Ti
CS_gizzard acid_039	1	9.479	240.337	Diet 7 500QB Ti
CS_gizzard acid_043	1	9.566	213.428	Diet 7 500QB Ti
CS_gizzard acid_006	1	9.62	622.765	Diet 8 6000QB Ti
CS_gizzard acid_012	1	9.566	396.923	Diet 8 6000QB Ti

Run	Peak	Retention Time (min)	Area (nA)	Diet	
CS_gizzard acid_022	1	9.588	321.295	Diet 8 6000QB Ti	
CS_gizzard acid_030	1	9.598	775.45	Diet 8 6000QB Ti	
CS_gizzard acid_033	1	9.598	1063.92	Diet 8 6000QB Ti	
CS_gizzard acid_047	1	9.577	647.66	Diet 8 6000QB Ti	

Gizzard digesta (NaF-EDTA extracted) inositol phosphates:

	Peak area							nmol g dwt				
	IP2	IP3	IP4	IP5	IP6			IP2	IP3	IP4	IP5	IP6
Gizzard digesta 01	19297	161488	9316	37203	22616		Gizzard digesta 01	145.7749	1219.925	70.37563	281.0417	170.8475
Gizzard digesta 02	25963	19132	105554	316605	1956543		Gizzard digesta 02	196.1317	144.5284	797.384	2391.722	14780.27
Gizzard digesta 03	28715	30450	116504	362670	1059792		Gizzard digesta 03	216.921	230.0277	880.1034	2739.709	8005.961
Gizzard digesta 04	33289	49801	173733	500099	1003201		Gizzard digesta 04	251.4743	376.2105	1312.427	3777.886	7578.457
Gizzard digesta 05	30261	63238	282036	669988	579035		Gizzard digesta 05	228.5999	477.7173	2130.578	5061.274	4374.19
Gizzard digesta 06	13040	18878	0	42239	16325		Gizzard digesta 06	98.50776	142.6096	0	319.0851	123.3236
Gizzard digesta 07	167917	45160	137716	50917	13862		Gizzard digesta 07	1268.491	341.1511	1040.345	384.6411	104.7174
Gizzard digesta 08	145675	352237	144919	0	0		Gizzard digesta 08	1100.469	2660.896	1094.758	0	0
Gizzard digesta 09	15210	22849	15512	39561	0		Gizzard digesta 09	114.9005	172.6077	117.1819	298.8547	0
Gizzard digesta 10	84314	244388	797625	185409	206227		Gizzard digesta 10	636.9312	1846.174	6025.479	1400.631	1557.896
Gizzard digesta 11	38498	53283	173814	472331	1082784		Gizzard digesta 11	290.8245	402.5145	1313.039	3568.119	8179.649
Gizzard digesta 12	16008	60649	10396	11365	28306		Gizzard digesta 12	120.9288	458.1593	78.53425	85.85435	213.8313
Gizzard digesta 13	49334	107767	434083	369722	612377		Gizzard digesta 13	372.6827	814.1017	3279.183	2792.982	4626.065
Gizzard digesta 14	31204	48559	179882	479027	1282834		Gizzard digesta 14	235.7236	366.8281	1358.878	3618.702	9690.882
Gizzard digesta 15	32683	202152	1090142	479601	62281		Gizzard digesta 15	246.8964	1527.112	8235.234	3623.038	470.4879
Gizzard digesta 16	33303	85769	376501	775820	539319		Gizzard digesta 16	251.5801	647.9227	2844.192	5860.758	4074.165
Gizzard digesta 17	25574	49671	229083	678705	786030		Gizzard digesta 17	193.1931	375.2284	1730.556	5127.125	5937.888
Gizzard digesta 18	68267	452478	795739	39012	0		Gizzard digesta 18	515.7078	3418.144	6011.232	294.7074	0
Gizzard digesta 19	45358	161812	604003	807674	665347		Gizzard digesta 19	342.6468	1222.373	4562.805	6101.392	5026.215
Gizzard digesta 20	43044	41308	106162	307951	1237752		Gizzard digesta 20	325.1663	312.052	801.977	2326.347	9350.32
Gizzard digesta 21	25570	20890	88541	353561	904164		Gizzard digesta 21	193.1628	157.8088	668.8631	2670.897	6830.304

	Peak area							nmol g dwt				
	IP2	IP3	IP4	IP5	IP6			IP2	IP3	IP4	IP5	IP6
Gizzard digesta 22	35344	60475	0	3975	49866		Gizzard digesta 22	266.9983	456.8448	0	30.02825	376.7015
Gizzard digesta 23	55400	38185	133280	179208	580185		Gizzard digesta 23	418.5069	288.46	1006.834	1353.787	4382.878
Gizzard digesta 24	0	15207	53009	0	50480		Gizzard digesta 24	0	114.8779	400.4446	0	381.3399
Gizzard digesta 25	12938	39275	196224	453508	1364764		Gizzard digesta 25	97.73722	296.6942	1482.33	3425.925	10309.8
Gizzard digesta 26	61626	568249	1242059	71277	35396		Gizzard digesta 26	465.5398	4292.71	9382.856	538.4461	267.3912
Gizzard digesta 27	8698	42713	78150	0	21108		Gizzard digesta 27	65.70709	322.6658	590.3667	0	159.4557
Gizzard digesta 28	6476	35708	211758	494940	495609		Gizzard digesta 28	48.92149	269.7481	1599.678	3738.913	3743.967
Gizzard digesta 29	26701	87215	410885	646450	437852		Gizzard digesta 29	201.7067	658.8462	3103.939	4883.462	3307.655
Gizzard digesta 30	5942	49396	51204	10263	32492		Gizzard digesta 30	44.88751	373.151	386.8091	77.52953	245.4535
Gizzard digesta 31	8273	42419	261231	737894	1091097		Gizzard digesta 31	62.49653	320.4448	1973.411	5574.255	8242.448
Gizzard digesta 32	28307	91208	623448	470940	875213		Gizzard digesta 32	213.8389	689.0104	4709.698	3557.611	6611.601
Gizzard digesta 33	0	28651	48673	0	42207		Gizzard digesta 33	0	216.4376	367.6893	0	318.8433
Gizzard digesta 34	3474	36066	52720	0	18747		Gizzard digesta 34	26.24355	272.4525	398.2614	0	141.62
Gizzard digesta 35	92462	499465	120961	0	0		Gizzard digesta 35	698.4835	3773.096	913.7728	0	0
Gizzard digesta 36	13191	285928	1112912	310564	47239		Gizzard digesta 36	99.64845	2159.979	8407.244	2346.086	356.8564
Gizzard digesta 37	20536	167976	786998	728445	212859		Gizzard digesta 37	155.1346	1268.937	5945.2	5502.875	1607.996
Gizzard digesta 38	18023	77069	344902	616732	1173519		Gizzard digesta 38	136.1507	582.2005	2605.485	4658.964	8865.086
Gizzard digesta 39	46055	320991	326059	8490	29676		Gizzard digesta 39	347.9122	2424.855	2463.14	64.1358	224.1807
Gizzard digesta 40	26832	95654	351233	597477	753150		Gizzard digesta 40	202.6963	722.5967	2653.311	4513.506	5689.503
Gizzard digesta 41	10687	55400	269436	596252	712632		Gizzard digesta 41	80.73255	418.5069	2035.394	4504.252	5383.419
Gizzard digesta 42	12803	88078	419747	606287	364991		Gizzard digesta 42	96.7174	665.3655	3170.885	4580.059	2757.243
Gizzard digesta 43	60950	597844	320487	15564	21168		Gizzard digesta 43	460.4331	4516.279	2421.047	117.5748	159.9089
Gizzard digesta 44	17148	75542	281846	575338	1079299		Gizzard digesta 44	129.5407	570.6651	2129.142	4346.262	8153.322
Gizzard digesta 45	16437	183434	773608	186570	61636		Gizzard digesta 45	124.1696	1385.711	5844.048	1409.401	465.6154

	Peak area							nmol/g dwt				
	IP2	IP3	IP4	IP5	IP6			IP2	IP3	IP4	IP5	IP6
Gizzard digesta 46	111105	152728	622388	219651	64742		Gizzard digesta 46	839.3178	1153.749	4701.691	1659.304	489.0789
Gizzard digesta 47	22524	54954	8034	12404	20674		Gizzard digesta 47	170.1525	415.1377	60.69105	93.70324	156.1771
Gizzard digesta 48	12716	53234	28604	0	0		Gizzard digesta 48	96.06017	402.1443	216.0825	0	0
							Equation to calculate from peak area sum to nmol/g dwt =PRODUCT(Cell/3309384,5000/20,1000/100,10/1)					

Gizzard digesta (HCl extracted) Inositol phosphates:

Row Labels	peak area					Row Labels	nmol g dwt			
	IP2	IP3	IP4	IP5	IP6		IP3	IP4	IP5	IP6
1mM Merck InsP6.a	0	0	0	0	3320171	1mM Merck InsP6.a	0	0	0	10000
Gizzard digesta 01 0.5M HCl	0	24498	37031	18445	57795	Gizzard digesta 01 0.5M HCl	184.4634	278.8335	138.8859	435.1809
Gizzard digesta 02 0.5M HCl	0	2200	76443	147943	1729515	Gizzard digesta 02 0.5M HCl	16.56541	575.5954	1113.971	13022.79
Gizzard digesta 03 0.5M HCl	0	4214	87646	152579	1215928	Gizzard digesta 03 0.5M HCl	31.73029	659.9509	1148.879	9155.613
Gizzard digesta 04 0.5M HCl	0	4490	120122	200261	1553840	Gizzard digesta 04 0.5M HCl	33.8085	904.4865	1507.912	11700
Gizzard digesta 05 0.5M HCl	0	6825	102673	186519	1564949	Gizzard digesta 05 0.5M HCl	51.39043	773.1002	1404.438	11783.65
Gizzard digesta 06 0.5M HCl	0	54424	42380	0	56963	Gizzard digesta 06 0.5M HCl	409.7982	319.1101	0	428.9162
Gizzard digesta 07 0.5M HCl	0	3334	99654	9715	46812	Gizzard digesta 07 0.5M HCl	25.10413	750.368	73.15135	352.4818
Gizzard digesta 08 0.5M HCl	0	14131	398414	66047	220698	Gizzard digesta 08 0.5M HCl	106.4027	2999.951	497.3163	1661.797
Gizzard digesta 09 0.5M HCl	0	21726	60414	25051	15915	Gizzard digesta 09 0.5M HCl	163.591	454.9013	188.6273	119.8357
Gizzard digesta 10 0.5M HCl	0	20303	603127	136386	268124	Gizzard digesta 10 0.5M HCl	152.8762	4541.385	1026.95	2018.902
Gizzard digesta 11 0.5M HCl	0	7570	124843	201992	1663078	Gizzard digesta 11 0.5M HCl	57.00008	940.0344	1520.946	12522.53
Gizzard digesta 12 0.5M HCl	0	1354	53985	22202	220848	Gizzard digesta 12 0.5M HCl	10.19526	406.4926	167.1751	1662.926
Gizzard digesta 13 0.5M HCl	0	13623	493206	342751	988749	Gizzard digesta 13 0.5M HCl	102.5775	3713.709	2580.823	7445.016
Gizzard digesta 14 0.5M HCl	0	6780	76415	251113	1857111	Gizzard digesta 14 0.5M HCl	51.05159	575.3845	1890.814	13983.55
Gizzard digesta 15 0.5M HCl	0	6679	77176	206882	2027844	Gizzard digesta 15 0.5M HCl	50.29108	581.1146	1557.766	15269.12
Gizzard digesta 16 0.5M HCl	0	7074	68468	196819	1742470	Gizzard digesta 16 0.5M HCl	53.26533	515.5457	1481.994	13120.33
Gizzard digesta 17 0.5M HCl	0	6955	74171	231105	1743799	Gizzard digesta 17 0.5M HCl	52.36929	558.4878	1740.159	13130.34

Row Labels	Peak area					Row Labels	nmol/g dwt			
	IP2	IP3	IP4	IP5	IP6		IP3	IP4	IP5	IP6
Gizzard digesta 18 0.5M HCl	0	18791	469855	290160	711090	Gizzard digesta 18 0.5M HCl	141.4912	3537.883	2184.827	5354.318
Gizzard digesta 19 0.5M HCl	0	11090	83985	289798	1945070	Gizzard digesta 19 0.5M HCl	83.50474	632.3846	2182.101	14645.86
Gizzard digesta 20 0.5M HCl	0	5507	64624	144793	1370091	Gizzard digesta 20 0.5M HCl	41.46624	486.6014	1090.253	10316.42
Gizzard digesta 21 0.5M HCl	0	18664	85000	166265	1516642	Gizzard digesta 21 0.5M HCl	140.5349	640.0273	1251.931	11419.91
Gizzard digesta 22 0.5M HCl	0	5635	44924	16890	101703	Gizzard digesta 22 0.5M HCl	42.43004	338.2657	127.1772	765.7964
Gizzard digesta 23 0.5M HCl	0	5305	58344	148128	489667	Gizzard digesta 23 0.5M HCl	39.94523	439.3147	1115.364	3687.062
Gizzard digesta 24 0.5M HCl	0	0	0	0	10141	Gizzard digesta 24 0.5M HCl	0	0	0	76.35902
Gizzard digesta 25 0.5M HCl	0	25931	103365	241403	1720982	Gizzard digesta 25 0.5M HCl	195.2535	778.3108	1817.7	12958.53
Gizzard digesta 26 0.5M HCl	0	43917	496877	365019	625247	Gizzard digesta 26 0.5M HCl	330.6833	3741.351	2748.495	4707.943
Gizzard digesta 27 0.5M HCl	0	47134	79163	21584	81116	Gizzard digesta 27 0.5M HCl	354.9064	596.0762	162.5217	610.7818
Gizzard digesta 28 0.5M HCl	0	21974	71780	117326	933211	Gizzard digesta 28 0.5M HCl	165.4583	540.4842	883.4334	7026.829
Gizzard digesta 29 0.5M HCl	0	28228	111042	168899	1349993	Gizzard digesta 29 0.5M HCl	212.5493	836.1166	1271.764	10165.09
Gizzard digesta 30 0.5M HCl	0	41109	52963	8185	80497	Gizzard digesta 30 0.5M HCl	309.5398	398.7972	61.63086	606.1209
Gizzard digesta 31 0.5M HCl	0	23306	65186	146164	1549137	Gizzard digesta 31 0.5M HCl	175.4879	490.8332	1100.576	11664.59
Gizzard digesta 32 0.5M HCl	0	27610	398579	338008	753766	Gizzard digesta 32 0.5M HCl	207.8959	3001.193	2545.11	5675.656
Gizzard digesta 33 0.5M HCl	0	35162	58759	0	48718	Gizzard digesta 33 0.5M HCl	264.7605	442.4396	0	366.8335
Gizzard digesta 34 0.5M HCl	0	48145	39935	0	34983	Gizzard digesta 34 0.5M HCl	362.519	300.6999	0	263.4126
Gizzard digesta 35 0.5M HCl	0	16709	426185	131599	391040	Gizzard digesta 35 0.5M HCl	125.8143	3209.059	990.9053	2944.427
Gizzard digesta 36 0.5M HCl	0	6136	81429	181920	1574848	Gizzard digesta 36 0.5M HCl	46.20244	613.1386	1369.809	11858.18
Gizzard digesta 37 0.5M HCl	0	27439	114586	208975	1486630	Gizzard digesta 37 0.5M HCl	206.6083	862.8019	1573.526	11193.93

	Peak area							nmol/g dwt			
Row Labels	IP2	IP3	IP4	IP5	IP6		Row Labels	IP3	IP4	IP5	IP6
Gizzard digesta 38 0.5M HCl	0	22444	127393	209998	1512649		Gizzard digesta 38 0.5M HCl	168.9973	959.2352	1581.229	11389.84
Gizzard digesta 39 0.5M HCl	0	25939	190829	163993	621368		Gizzard digesta 39 0.5M HCl	195.3137	1436.891	1234.823	4678.735
Gizzard digesta 40 0.5M HCl	0	27720	131034	222606	1523487		Gizzard digesta 40 0.5M HCl	208.7242	986.651	1676.164	11471.45
Gizzard digesta 41 0.5M HCl	0	20201	88903	190975	1471488		Gizzard digesta 41 0.5M HCl	152.1081	669.4158	1437.991	11079.91
Gizzard digesta 42 0.5M HCl	0	23475	92288	172170	1217733		Gizzard digesta 42 0.5M HCl	176.7605	694.904	1296.394	9169.204
Gizzard digesta 43 0.5M HCl	0	29879	212569	280736	1050501		Gizzard digesta 43 0.5M HCl	224.9809	1600.588	2113.867	7909.992
Gizzard digesta 44 0.5M HCl	0	14080	87130	218674	1777190		Gizzard digesta 44 0.5M HCl	106.0186	656.0656	1646.557	13381.77
Gizzard digesta 45 0.5M HCl	0	21816	68911	199224	1475889		Gizzard digesta 45 0.5M HCl	164.2686	518.8814	1500.103	11113.05
Gizzard digesta 46 0.5M HCl	0	20691	317579	146002	577977		Gizzard digesta 46 0.5M HCl	155.7977	2391.285	1099.356	4352.012
Gizzard digesta 47 0.5M HCl	0	17148	25305	8251	75437		Gizzard digesta 47 0.5M HCl	129.1199	190.5399	62.12782	568.0204
Gizzard digesta 48 0.5M HCl	0	16886	37508	15374	103680		Gizzard digesta 48 0.5M HCl	127.1471	282.4252	115.7621	780.6827
							Equation to calculate from peak area sum to nmol/g dwt =PRODUCT(Cell/3320171,5000/20,1000/100,10/1)				

Ileal digesta (HCl extracted) inositol phosphates:

Sum of Area	Column Labels		Peak area					Sum of Area	nmol g dwt				
Row Labels	IP2	IP3	IP4	IP5	IP6	Grand Total		Row Labels	IP3	IP4	IP5	IP6	Total
1mM InsP6.b	0	0	0	0	3452701	3452701		1mM InsP6.b	0	0	0	25000	25000
Ileal digesta 01 0.5M HCl	0	47825	333665	31172	275622	688284		Ileal digesta 01 0.5M HCl	346.2869	2415.971	225.7074	1995.698	4983.664
Ileal digesta 02 0.5M HCl	0	0	85932	519380	7098558	7703870		Ileal digesta 02 0.5M HCl	0	622.2085	3760.679	51398.59	55781.47
Ileal digesta 03 0.5M HCl	0	15678	173443	974335	10012176	11175632		Ileal digesta 03 0.5M HCl	113.5198	1255.85	7054.875	72495.24	80919.49
Ileal digesta 04 0.5M HCl	0	5347	171562	681086	7528123	8386118		Ileal digesta 04 0.5M HCl	38.71607	1242.23	4931.545	54508.94	60721.43
Ileal digesta 05 0.5M HCl	0	145419	97084	647837	7512617	8402957		Ileal digesta 05 0.5M HCl	1052.937	702.9569	4690.799	54396.67	60843.36
Ileal digesta 06 0.5M HCl	0	76885	326957	43435	299733	747010		Ileal digesta 06 0.5M HCl	556.7018	2367.4	314.5002	2170.279	5408.881
Ileal digesta 07 0.5M HCl	0	131844	619362	1193982	3834419	5779607		Ileal digesta 07 0.5M HCl	954.6439	4484.619	8645.275	27763.91	41848.45
Ileal digesta 08 0.5M HCl	0	191653	240969	1074792	3485206	4992620		Ileal digesta 08 0.5M HCl	1387.703	1744.786	7782.255	25235.36	36150.1
Ileal digesta 09 0.5M HCl	0	88275	353551	58395	432630	932851		Ileal digesta 09 0.5M HCl	639.1735	2559.96	422.8211	3132.548	6754.502
Ileal digesta 10 0.5M HCl	0	45363	423790	529415	1830129	2828697		Ileal digesta 10 0.5M HCl	328.4602	3068.54	3833.339	13251.43	20481.77
Ileal digesta 11 0.5M HCl	0	8385	145878	713841	5860799	6728903		Ileal digesta 11 0.5M HCl	60.71334	1056.26	5168.714	42436.33	48722.02
Ileal digesta 12 0.5M HCl	0	171430	1589829	176568	270106	2207933		Ileal digesta 12 0.5M HCl	1241.275	11511.49	1278.477	1955.759	15987
Ileal digesta 13 0.5M HCl	0	35075	810179	845182	3731874	5422310		Ileal digesta 13 0.5M HCl	253.9678	5866.27	6119.716	27021.41	39261.36
Ileal digesta 14 0.5M HCl	0	9710	163132	812177	7398199	8383218		Ileal digesta 14 0.5M HCl	70.30728	1181.191	5880.737	53568.2	60700.43
Ileal digesta 15 0.5M HCl	0	4034	120239	384056	5704530	6212859		Ileal digesta 15 0.5M HCl	29.20902	870.6155	2780.837	41304.84	44985.5
Ileal digesta 16 0.5M HCl	0	8761	133245	867857	7081783	8091646		Ileal digesta 16 0.5M HCl	63.43584	964.7881	6283.899	51277.12	58589.25
Ileal digesta 17 0.5M HCl	0	4563	111803	549007	6183145	6848518		Ileal digesta 17 0.5M HCl	33.03935	809.5329	3975.199	44770.35	49588.12
Ileal digesta 18 0.5M HCl	0	83847	217995	809366	4755479	5866687		Ileal digesta 18 0.5M HCl	607.1116	1578.438	5860.383	34433.04	42478.97

	Peak area								nmol/g dwt				
	IP2	IP3	IP4	IP5	IP6	Grand total			IP3	IP4	IP5	IP6	Grand total
Ileal digesta 19 0.5M HCl	0	5539	140749	506306	6288239	6940833		Ileal digesta 19 0.5M HCl	40.10628	1019.122	3666.014	45531.3	50256.55
Ileal digesta 20 0.5M HCl	0	5717	112210	500198	5894313	6512438		Ileal digesta 20 0.5M HCl	41.39513	812.4799	3621.788	42679	47154.66
Ileal digesta 21 0.5M HCl	0	12967	199029	775628	6319940	7307564		Ileal digesta 21 0.5M HCl	93.89026	1441.111	5616.096	45760.84	52911.94
Ileal digesta 22 0.5M HCl	0	63306	244085	256542	1176362	1740295		Ileal digesta 22 0.5M HCl	458.3803	1767.348	1857.546	8517.694	12600.97
Ileal digesta 23 0.5M HCl	0	37606	271903	624152	2080760	3014421		Ileal digesta 23 0.5M HCl	272.2941	1968.77	4519.302	15066.18	21826.54
Ileal digesta 24 0.5M HCl	0	20250	444599	16179	258374	739402		Ileal digesta 24 0.5M HCl	146.6243	3219.212	117.1474	1870.811	5353.794
Ileal digesta 25 0.5M HCl	0	0	94409	737148	8055547	8887104		Ileal digesta 25 0.5M HCl	0	683.588	5337.473	58327.86	64348.93
Ileal digesta 26 0.5M HCl	0	6058	92745	632742	5155806	5887351		Ileal digesta 26 0.5M HCl	43.86421	671.5395	4581.5	37331.69	42628.59
Ileal digesta 27 0.5M HCl	0	1537	73971	35444	108992	219944		Ileal digesta 27 0.5M HCl	11.12897	535.6024	256.6397	789.1793	1592.55
Ileal digesta 28 0.5M HCl	0	6501	15853	616510	5450928	6089792		Ileal digesta 28 0.5M HCl	47.07184	114.7869	4463.969	39468.58	44094.41
Ileal digesta 29 0.5M HCl	0	0	83765	613763	7033906	7731434		Ileal digesta 29 0.5M HCl	0	606.5179	4444.079	50930.46	55981.06
Ileal digesta 30 0.5M HCl	0	17267	55138	54297	221257	347959		Ileal digesta 30 0.5M HCl	125.0253	399.2382	393.1487	1602.057	2519.47
Ileal digesta 31 0.5M HCl	0	0	8335	801484	9755032	10564851		Ileal digesta 31 0.5M HCl	0	60.3513	5803.312	70633.34	76497
Ileal digesta 32 0.5M HCl	0	24216	131925	731152	2289438	3176731		Ileal digesta 32 0.5M HCl	175.341	955.2304	5294.058	16577.15	23001.78
Ileal digesta 33 0.5M HCl	0	37075	69458	63386	178203	348122		Ileal digesta 33 0.5M HCl	268.4493	502.9251	458.9595	1290.316	2520.65
Ileal digesta 34 0.5M HCl	0	13413	88517	35755	71793	209478		Ileal digesta 34 0.5M HCl	97.11962	640.9258	258.8915	519.8322	1516.769
Ileal digesta 35 0.5M HCl	0	49593	1040630	1001717	2855431	4947371		Ileal digesta 35 0.5M HCl	359.0884	7534.898	7253.14	20675.34	35822.47
Ileal digesta 36 0.5M HCl	0	3256	71161	644272	6532630	7251319		Ileal digesta 36 0.5M HCl	23.57575	515.256	4664.985	47300.87	52504.68
Ileal digesta 37 0.5M HCl	0	4975	105234	695542	6661484	7467235		Ileal digesta 37 0.5M HCl	36.02252	761.9687	5036.217	48233.86	54068.07
Ileal digesta 38 0.5M HCl	0	6149	7550	645079	5637149	6295927		Ileal digesta 38 0.5M HCl	44.52311	54.66735	4670.829	40816.95	45586.97

	Peak area								nmol/g dwt				
	IP2	IP3	IP4	IP5	IP6	Grand total			IP3	IP4	IP5	IP6	Grand total
Ileal digesta 39 0.5M HCl	0	112540	186550	880638	3773818	4953546		Ileal digesta 39 0.5M HCl	814.8693	1350.754	6376.443	27325.11	35867.18
Ileal digesta 40 0.5M HCl	0	2992	86262	688495	6925951	7703700		Ileal digesta 40 0.5M HCl	21.6642	624.598	4985.191	50148.79	55780.24
Ileal digesta 41 0.5M HCl	0	0	83956	774807	7166911	8025674		Ileal digesta 41 0.5M HCl	0	607.9009	5610.151	51893.51	58111.56
Ileal digesta 42 0.5M HCl	0	4988	76636	884127	8369117	9334868		Ileal digesta 42 0.5M HCl	36.11665	554.8989	6401.706	60598.33	67591.05
Ileal digesta 43 0.5M HCl	0	15426	165814	889348	5789967	6860555		Ileal digesta 43 0.5M HCl	111.6952	1200.611	6439.509	41923.46	49675.28
Ileal digesta 44 0.5M HCl	0	5936	73231	796808	7572703	8448678		Ileal digesta 44 0.5M HCl	42.98084	530.2443	5769.454	54831.73	61174.41
Ileal digesta 45 0.5M HCl	0	5322	91845	598308	6608894	7304369		Ileal digesta 45 0.5M HCl	38.53505	665.0228	4332.174	47853.07	52888.8
Ileal digesta 46 0.5M HCl	0	7858	73570	622110	5519669	6223207		Ileal digesta 46 0.5M HCl	56.89748	532.6989	4504.517	39966.31	45060.43
Ileal digesta 47 0.5M HCl	0	7648	111457	31367	184165	334637		Ileal digesta 47 0.5M HCl	55.37694	807.0276	227.1193	1333.485	2423.009
Ileal digesta 48 0.5M HCl	0	28041	111785	65761	161420	367007		Ileal digesta 48 0.5M HCl	203.0367	809.4026	476.1562	1168.795	2657.391
							Formula to calculate nmol/ g dwt from peak area =PRODUCT(Cell/3452701,5000/20,1000/100,10/1)						

Ileal digesta inositol phosphates (NaF-EDTA extracted):

Row Labels	Peak area					Row Labels	nmol g dwt				
	IP2	IP3	IP4	IP5	IP6		IP2	IP3	IP4	IP5	IP6
1mM InsP6.a	0	0	0	0	3576364	1mM InsP6.a	0	0	0	0	10000
Ileal digesta 01	702190	239211	1137015	51648	233339	Ileal digesta 01	4908.547	1672.166	7948.121	361.0371	1631.119
Ileal digesta 02	25784	119957	327400	613381	7650407	Ileal digesta 02	180.2389	838.5402	2288.637	4287.742	53478.95
Ileal digesta 03	65420	239488	368910	960184	9070432	Ileal digesta 03	457.308	1674.103	2578.806	6712.013	63405.4
Ileal digesta 04	0	135264	528368	840086	7618969	Ileal digesta 04	0	945.5413	3693.472	5872.487	53259.18
Ileal digesta 05	30304	155221	432280	884924	8279133	Ileal digesta 05	211.8353	1085.048	3021.784	6185.92	57873.95
Ileal digesta 06	527543	391550	1144605	71674	299291	Ileal digesta 06	3687.705	2737.068	8001.178	501.0256	2092.146
Ileal digesta 07	147757	749477	2272116	1289317	4070771	Ileal digesta 07	1032.872	5239.099	15882.86	9012.764	28456.07
Ileal digesta 08	243186	634037	1183207	1059071	3404446	Ileal digesta 08	1699.953	4432.134	8271.019	7403.266	23798.23
Ileal digesta 09	580329	410421	913572	95881	231332	Ileal digesta 09	4056.697	2868.982	6386.179	670.2408	1617.089
Ileal digesta 10	2045872	715919	2063563	767726	2378429	Ileal digesta 10	14301.34	5004.517	14425.01	5366.666	16626.03
Ileal digesta 11	111562	224585	322009	777801	7063438	Ileal digesta 11	779.8563	1569.925	2250.952	5437.093	49375.83
Ileal digesta 12	600957	577289	1368936	128308	267819	Ileal digesta 12	4200.894	4035.446	9569.328	896.9165	1872.146
Ileal digesta 13	239180	574989	1165291	989448	4721835	Ileal digesta 13	1671.949	4019.369	8145.78	6916.578	33007.23
Ileal digesta 14	78387	167979	278513	650858	6519911	Ileal digesta 14	547.9518	1174.23	1946.901	4549.719	45576.39
Ileal digesta 15	39784	130592	200900	507789	6919713	Ileal digesta 15	278.1037	912.8825	1404.359	3549.618	48371.15
Ileal digesta 16	46089	232015	442537	995051	8335670	Ileal digesta 16	322.1778	1621.864	3093.484	6955.745	58269.17
Ileal digesta 17	0	190871	357069	753017	7148267	Ileal digesta 17	0	1334.253	2496.034	5263.845	49968.82
Ileal digesta 18	78408	285760	550453	756592	4312423	Ileal digesta 18	548.0986	1997.56	3847.854	5288.835	30145.3

	Peak area							nmol/g dwt				
	IP2	IP3	IP4	IP5	IP6			IP2	IP3	IP4	IP5	IP6
Ileal digesta 19	76487	182073	318406	622206	6961039		Ileal digesta 19	534.6701	1272.752	2225.766	4349.431	48660.03
Ileal digesta 20	36267	162036	317274	661753	6133522		Ileal digesta 20	253.5187	1132.687	2217.853	4625.878	42875.4
Ileal digesta 21	86671	294795	482718	928489	7444507		Ileal digesta 21	605.8598	2060.717	3374.363	6490.454	52039.63
Ileal digesta 22	265572	335063	562979	321820	1448291		Ileal digesta 22	1856.439	2342.204	3935.415	2249.631	10124.05
Ileal digesta 23	183368	447409	861687	724281	2331394		Ileal digesta 23	1281.805	3127.541	6023.485	5062.97	16297.24
Ileal digesta 24	281410	237700	345434	67559	503446		Ileal digesta 24	1967.152	1661.604	2414.701	472.2604	3519.259
Ileal digesta 25	118905	159106	215583	581804	7157415		Ileal digesta 25	831.1864	1112.205	1506.998	4067.008	50032.76
Ileal digesta 26	206848	285468	399593	669240	5373720		Ileal digesta 26	1445.938	1995.518	2793.291	4678.215	37564.13
Ileal digesta 27	100270	33630	41007	0	149204		Ileal digesta 27	700.9214	235.0851	286.6529	0	1042.987
Ileal digesta 28	124421	290266	290292	532546	5534989		Ileal digesta 28	869.7451	2029.058	2029.24	3722.678	38691.45
Ileal digesta 29	95180	161707	471823	564857	6916705		Ileal digesta 29	665.3406	1130.387	3298.203	3948.542	48350.12
Ileal digesta 30	191654	213532	457552	44268	308989		Ileal digesta 30	1339.727	1492.661	3198.444	309.4484	2159.938
Ileal digesta 31	82966	155588	301232	740575	9322613		Ileal digesta 31	579.9605	1087.613	2105.714	5176.871	65168.23
Ileal digesta 32	110455	375501	623122	955597	2722175		Ileal digesta 32	772.118	2624.88	4355.835	6679.948	19028.93
Ileal digesta 33	256735	266342	444688	113706	178134		Ileal digesta 33	1794.665	1861.821	3108.52	794.8436	1245.217
Ileal digesta 34	199626	171326	292183	70918	122826		Ileal digesta 34	1395.454	1197.627	2042.458	495.7409	858.5955
Ileal digesta 35	273987	636581	1023900	949773	2915356		Ileal digesta 35	1915.262	4449.918	7157.409	6639.236	20379.33
Ileal digesta 36	76237	131734	238087	540157	5702136		Ileal digesta 36	532.9225	920.8654	1664.309	3775.881	39859.87
Ileal digesta 37	141327	287246	491155	1008029	8994364		Ileal digesta 37	987.9238	2007.947	3433.34	7046.465	62873.66
Ileal digesta 38	122026	284617	347680	585941	5488593		Ileal digesta 38	853.0032	1989.57	2430.401	4095.927	38367.13

	Peak area							nmol/g dwt				
	IP2	IP3	IP4	IP5	IP6			IP2	IP3	IP4	IP5	IP6
Ileal digesta 39	226969	488862	803582	946611	4007563		Ileal digesta 39	1586.59	3417.312	5617.311	6617.133	28014.23
Ileal digesta 40	111936	180055	281916	641684	6470466		Ileal digesta 40	782.4707	1258.646	1970.689	4485.589	45230.76
Ileal digesta 41	67526	172642	390550	911552	8717529		Ileal digesta 41	472.0297	1206.826	2730.077	6372.058	60938.49
Ileal digesta 42	79637	218941	471831	846400	7427916		Ileal digesta 42	556.6897	1530.472	3298.259	5916.624	51923.66
Ileal digesta 43	160339	289783	437224	703226	4517191		Ileal digesta 43	1120.824	2025.682	3056.344	4915.789	31576.7
Ileal digesta 44	143084	321252	341253	692209	7689161		Ileal digesta 44	1000.206	2245.661	2385.474	4838.776	53749.85
Ileal digesta 45	100513	216164	346315	683628	6173207		Ileal digesta 45	702.62	1511.06	2420.86	4778.792	43152.82
Ileal digesta 46	106874	225661	318055	698295	5641559		Ileal digesta 46	747.0856	1577.447	2223.313	4881.319	39436.42
Ileal digesta 47	94512	77569	107221	22844	258649		Ileal digesta 47	660.671	542.2337	749.5112	159.6873	1808.044
Ileal digesta 48	312866	293042	569550	85604	260028		Ileal digesta 48	2187.04	2048.463	3981.348	598.4011	1817.684
							Formula to calculate nmol/g dwt from peak area =PRODUCT(Cell/3576364,5000/20,1000/100,10/1)					

Diet Inositol phosphates, HCl extractions:

Row Labels	peak areas							nmol g dwt					
	IP2	IP3	IP4	IP5	IP6			IP2	IP3	IP4	IP5	IP6	
Control 0.5M HCl	0	34315	57663	220823	2422042		Control 0.5M HCl	0	258.3828	434.187	1662.738	18237.33	20592.64
13C Ins 0.5M HCl	0	25223	71979	202782	2520104		13C Ins 0.5M HCl	0	189.9224	541.9826	1526.894	18975.71	
Phy500 0.5M HCl	0	27579	57593	204762	2459807		Phy500 0.5M HCl	0	207.6625	433.6599	1541.803	18521.69	
Phy6000 0.5M HCl	0	37868	99863	194098	2121762		Phy6000 0.5M HCl	0	285.1359	751.9417	1461.506	15976.3	
Control Ti 0.5M HCl	0	40184	63817	184698	2358895		Control Ti 0.5M HCl	0	302.5748	480.5249	1390.727	17761.85	
13C Ins Ti 0.5M HCl	0	30466	61351	169767	2293344		13C Ins Ti 0.5M HCl	0	229.4008	461.9566	1278.3	17268.27	
Phy500 Ti 0.5M HCl	0	29604	61277	168999	2208786		Phy500 Ti 0.5M HCl	0	222.9102	461.3994	1272.517	16631.57	
Phy6000 Ti 0.5M HCl	0	50035	91887	212055	2225573		Phy6000 Ti 0.5M HCl	0	376.7502	691.8845	1596.717	16757.97	
							Equation to calculate from peak area sum to nmol/g dwt =PRODUCT(Cell/3320171,5000/20,1000/100,10/1)						

Diet Inositol phosphates, NaF-EDTA extractions:

Sum of Area	Column Labels	Peak areas					nmol g dwt				
Row Labels	IP2	IP3	IP4	IP5	IP6		IP2	IP3	IP4	IP5	IP6
Control NaF	24845	130372	121697	1103149	66534		187.685986	984.866066	919.332722	8333.49197	502.616197
13C Ins NaF	25007	151893	109941	870880	28657		188.909779	1147.44164	830.524654	6578.86785	216.482886
Phy500 NaF	31690	145774	95999	1268921	66226		239.395005	1101.21702	725.202938	9585.77941	500.28948
Phy6000 NaF	18964	198833	59937	951606	66108		143.259289	1502.03935	452.780638	7188.69433	499.398075
Control Ti NaF	24869	307952	64140	558745	0		187.867289	2326.35439	484.53126	4220.91392	0
13C Ins Ti NaF	27460	137334	59554	1213840	60084		207.440418	1037.45893	449.887351	9169.68233	453.891117
Phy500 Ti NaF	25257	202264	56368	730247	23699		190.798348	1527.95807	425.819427	5516.48736	179.028786
Phy6000 Ti NaF	24444	289439	58926	722402	15405		184.656722	2186.50208	445.143265	5457.22406	116.373621
							Equation to calculate from peak area sum to nmol/g dwt =PRODUCT(B3/3309384,5000/20,1000/100,10/1)				

Appendix 8: Tissue raw measurements for inositol

Run	Inositol nmol/g fwt	Run	Inositol nmol/g fwt	Run	Inositol nmol/g fwt	Run	Inositol nmol/g fwt
CS_Brain A_001	18204.0759	CS_Brain A_033	14727.2473	CS_Brain B_018	18509.7013	CS_13C Brain A_005	17239.4617
CS_Brain A_003	23290.1312	CS_Brain A_034	18763.9587	CS_Brain B_019	21876.8501	CS_13C Brain A_014	26434.496
CS_Brain A_004	21764.5868	CS_Brain A_035	22863.6935	CS_Brain B_020	21294.3886	CS_13C Brain A_021	28373.83
CS_Brain A_006	21747.7312	CS_Brain A_038	19563.0932	CS_Brain B_022	16108.0402	CS_13C Brain A_031	missing
CS_Brain A_007	24530.8487	CS_Brain A_039	18144.7859	CS_Brain B_023	21591.0804	CS_13C Brain A_037	22232.5495
CS_Brain A_008	27118.4394	CS_Brain A_040	16379.048	CS_Brain B_024	24180.3462	CS_13C Brain A_044	24096.9222
CS_Brain A_009	24801.0888	CS_Brain A_041	22479.0276	CS_Brain B_025	19494.0676	CS_13C Brain B_005	24182.291
CS_Brain A_010	21006.77	CS_Brain A_043	16070.3163	CS_Brain B_026	20397.2641	CS_13C Brain B_014	29057.4271
CS_Brain A_012	20420.8543	CS_Brain A_045	22036.3624	CS_Brain B_027	21514.0983	CS_13C Brain B_021	20926.8492
CS_Brain A_013	20980.0391	CS_Brain A_046	18968.7326	CS_Brain B_029	20205.6812	CS_13C Brain B_031	27115.2361
CS_Brain A_015	22887.9816	CS_Brain A_047	29758.2356	CS_Brain B_030	17399.3579	CS_13C Brain B_037	21090.2403
CS_Brain A_016	20449.8185	CS_Brain A_048	17849.2462	CS_Brain B_032	19352.3171	CS_13C Brain B_044	17962.5455
CS_Brain A_018	22660.1061	CS_Brain B_001	25062.8141	CS_Brain B_033	23220.2326	CS_13C Brain A_002	33858.5207
CS_Brain A_019	16658.8842	CS_Brain B_003	21748.325	CS_Brain B_034	20915.5145	CS_13C Brain A_011	23609.3338
CS_Brain A_020	19626.7448	CS_Brain B_004	22401.9059	CS_Brain B_035	17166.5969	CS_13C Brain A_017	27664.7254
CS_Brain A_022	29787.1655	CS_Brain B_006	20149.7069	CS_Brain B_038	16580.576	CS_13C Brain A_028	20706.3188
CS_Brain A_023	20999.5114	CS_Brain B_007	23753.6991	CS_Brain B_039	19803.8805	CS_13C Brain A_036	22891.8278
CS_Brain A_024	19186.837	CS_Brain B_008	19709.0313	CS_Brain B_040	23396.9151	CS_13C Brain A_042	31353.6774
CS_Brain A_025	19221.7337	CS_Brain B_009	23647.5433	CS_Brain B_041	22394.6817	CS_13C Brain B_002	26867.4285
CS_Brain A_026	22376.7448	CS_Brain B_010	19052.7638	CS_Brain B_043	16870.1145	CS_13C Brain B_011	21511.0982
CS_Brain A_027	16392.3088	CS_Brain B_012	25345.5815	CS_Brain B_045	15489.8445	CS_13C Brain B_017	21242.5782
CS_Brain A_029	17738.4487	CS_Brain B_013	19484.7152	CS_Brain B_046	20835.2532	CS_13C Brain B_028	23606.4768
CS_Brain A_030	16405.0112	CS_Brain B_015	16069.6893	CS_Brain B_047	20225.0838	CS_13C Brain B_036	22005.2168
CS_Brain A_032	21962.3814	CS_Brain B_016	18223.9671	CS_Brain B_048	21838.9522	CS_13C Brain B_042	24030.3278

Run	Inositol nmol/g fwt	Run	Inositol nmol/g fwt	Run	Inositol nmol/g fwt	Run	Inositol nmol/g fwt
CS_Liver A_001	18790.3172	CS_Liver A_033	13099.5191	CS_Liver B_018	20235.2795	CS_13C Liver A_005	18926.7027
CS_Liver A_003	14504.6164	CS_Liver A_034	23100.6111	CS_Liver B_019	20232.5913	CS_13C Liver A_014	23073.9252
CS_Liver A_004	16814.8848	CS_Liver A_035	15979.1189	CS_Liver B_020	16581.8258	CS_13C Liver A_021	23050.5253
CS_Liver A_006	23820.8337	CS_Liver A_038	17853.992	CS_Liver B_022	14993.9662	CS_13C Liver A_031	20121.8657
CS_Liver A_007	16829.8701	CS_Liver A_039	17766.3034	CS_Liver B_023	18042.3469	CS_13C Liver A_037	23085.9988
CS_Liver A_008	19746.468	CS_Liver A_040	16802.0517	CS_Liver B_024	19217.0733	CS_13C Liver A_044	25353.646
CS_Liver A_009	26232.6663	CS_Liver A_041	20644.2541	CS_Liver B_025	25352.9474	CS_13C Liver B_005	21870.8715
CS_Liver A_010	11554.2126	CS_Liver A_043	19049.2598	CS_Liver B_026	19067.3645	CS_13C Liver B_014	19914.8384
CS_Liver A_012	13664.2969	CS_Liver A_045	28981.7718	CS_Liver B_027	13135.3689	CS_13C Liver B_021	25941.9764
CS_Liver A_013	18047.2942	CS_Liver A_046	15824.893	CS_Liver B_029	14664.0763	CS_13C Liver B_031	21611.0919
CS_Liver A_015	15426.3513	CS_Liver A_047	19223.4546	CS_Liver B_030	11652.7643	CS_13C Liver B_037	20978.037
CS_Liver A_016	13921.4117	CS_Liver A_048	17569.7031	CS_Liver B_032	14635.7902	CS_13C Liver B_044	20928.1751
CS_Liver A_018	24190.9107	CS_Liver B_001	18434.6872	CS_Liver B_033	23045.8326	CS_13C Liver A_002	20781.076
CS_Liver A_019	15280.0477	CS_Liver B_003	22852.7455	CS_Liver B_034	21269.5464	CS_13C Liver A_011	18196.782
CS_Liver A_020	21126.434	CS_Liver B_004	17105.9864	CS_Liver B_035	19734.8162	CS_13C Liver A_017	23567.8398
CS_Liver A_022	19807.053	CS_Liver B_006	20408.0039	CS_Liver B_038	17116.3464	CS_13C Liver A_028	20754.479
CS_Liver A_023	16258.1021	CS_Liver B_007	19222.7376	CS_Liver B_039	22731.0713	CS_13C Liver A_036	28808.3271
CS_Liver A_024	21284.6033	CS_Liver B_008	17844.7428	CS_Liver B_040	18829.6803	CS_13C Liver A_042	26273.7923
CS_Liver A_025	17315.7066	CS_Liver B_009	21533.7959	CS_Liver B_041	16447.8556	CS_13C Liver B_002	22881.8965
CS_Liver A_026	14404.6671	CS_Liver B_010	18390.3768	CS_Liver B_043	16009.7346	CS_13C Liver B_011	20468.069
CS_Liver A_027	14841.4611	CS_Liver B_012	18654.1244	CS_Liver B_045	25441.1015	CS_13C Liver B_017	31232.8007
CS_Liver A_029	17510.049	CS_Liver B_013	17135.7053	CS_Liver B_046	22078.7482	CS_13C Liver B_028	28790.369
CS_Liver A_030	18463.4387	CS_Liver B_015	13727.0341	CS_Liver B_047	23658.5411	CS_13C Liver B_036	20245.5314
CS_Liver A_032	21015.3713	CS_Liver B_016	12701.3711	CS_Liver B_048	24296.0587	CS_13C Liver B_042	31442.5824

Run	Inositol nmol/g fwt	Run	Inositol nmol/g fwt	Run	Inositol nmol/g fwt	Run	Inositol nmol/g fwt
CS_Kidney A_001	5411.72009	CS_Kidney A_034	7861.11523	CS_Kidney B_019	4908.77312	CS_13C Kidney A_005	7821.20955
CS_Kidney A_003	6122.12665	CS_Kidney A_035	5922.58639	CS_Kidney B_022	7168.71465	CS_13C Kidney A_014	7690.40144
CS_Kidney A_004	5409.82712	CS_Kidney A_038	5734.85413	CS_Kidney B_023	6493.87195	CS_13C Kidney A_021	9840.91214
CS_Kidney A_006	8089.9536	CS_Kidney A_039	4829.79704	CS_Kidney B_024	7932.2419	CS_13C Kidney A_031	6474.08326
CS_Kidney A_007	7380.44215	CS_Kidney A_040	5619.69556	CS_Kidney B_025	6460.89066	CS_13C Kidney A_037	9853.36138
CS_Kidney A_008	4580.40614	CS_Kidney A_041	8125.92954	CS_Kidney B_026	6470.97837	CS_13C Kidney A_044	8565.31249
CS_Kidney A_009	6787.53628	CS_Kidney A_043	6569.88729	CS_Kidney B_027	6034.3372	CS_13C Kidney B_005	8916.65097
CS_Kidney A_010	5078.63711	CS_Kidney A_045	11567.4827	CS_Kidney B_029	5174.20711	CS_13C Kidney B_014	9506.13776
CS_Kidney A_012	6000.73621	CS_Kidney A_046	4663.58234	CS_Kidney B_030	7795.70348	CS_13C Kidney B_021	8605.24195
CS_Kidney A_013	7445.8539	CS_Kidney A_047	8142.69507	CS_Kidney B_032	6729.00998	CS_13C Kidney B_031	10555.5276
CS_Kidney A_015	6972.27283	CS_Kidney A_048	8690.2947	CS_Kidney B_033	6627.86276	CS_13C Kidney B_037	3468.21759
CS_Kidney A_016	10930.0968	CS_Kidney B_001	7302.91201	CS_Kidney B_034	8253.79229	CS_13C Kidney B_044	7104.31579
CS_Kidney A_018	7961.57391	CS_Kidney B_003	7762.48173	CS_Kidney B_038	5393.23319	CS_13C Kidney A_002	7750.94186
CS_Kidney A_019	6222.24105	CS_Kidney B_004	5768.9371	CS_Kidney B_039	6874.91261	CS_13C Kidney A_011	6101.4536
CS_Kidney A_020	8183.69844	CS_Kidney B_006	7988.22059	CS_Kidney B_040	5706.07402	CS_13C Kidney A_017	8055.6166
CS_Kidney A_022	7122.23788	CS_Kidney B_007	7243.21519	CS_Kidney B_041	4984.51304	CS_13C Kidney A_028	7912.19076
CS_Kidney A_023	6288.13479	CS_Kidney B_008	6909.33984	CS_Kidney B_043	6217.55895	CS_13C Kidney A_036	8672.65269
CS_Kidney A_024	7635.61683	CS_Kidney B_009	9069.7178	CS_Kidney B_045	5620.3841	CS_13C Kidney A_042	6860.24949
CS_Kidney A_025	6317.67335	CS_Kidney B_010	5840.99383	CS_Kidney B_046	6011.47751	CS_13C Kidney B_002	9585.11239
CS_Kidney A_026	7630.21228	CS_Kidney B_012	7454.46071	CS_Kidney B_047	6969.65636	CS_13C Kidney B_011	6858.14078
CS_Kidney A_027	8280.8182	CS_Kidney B_013	7050.2161	CS_Kidney B_048	7090.77138	CS_13C Kidney B_017	8483.65147
CS_Kidney A_029	9191.9006	CS_Kidney B_015	4664.71791	CS_Kidney B_035	5115.839	CS_13C Kidney B_028	9133.47357
CS_Kidney A_030	6953.13129	CS_Kidney B_016	6937.01934			CS_13C Kidney B_036	9839.45017
CS_Kidney A_033	7362.12686	CS_Kidney B_018	5057.08565			CS_13C Kidney B_042	8998.61861

Run	Inositol nmol/g fwt	Run	Inositol nmol/g fwt	Run	Inositol nmol/g fwt	Run	Inositol nmol/g fwt
CS_ Jejunat tissue B_041	3608.77058	CS_ Jejunat tissue B_046	4089.46362	CS_ Jejunat tissue B_045	3916.36855	CS_ Jejunat tissue B_043	3506.79637
CS_ Jejunat tissue B_038	3036.52406	CS_ Jejunat tissue B_035	5276.45833	CS_ Jejunat tissue B_040	7479.92007	CS_ Jejunat tissue B_039	3000.75808
CS_ Jejunat tissue B_025	3716.62506	CS_ Jejunat tissue B_026	4713.70153	CS_ Jejunat tissue B_029	3858.90571	CS_ Jejunat tissue B_032	4272.04956
CS_ Jejunat tissue B_019	3231.0194	CS_ Jejunat tissue B_023	5191.52944	CS_ Jejunat tissue B_020	4087.9383	CS_ Jejunat tissue B_018	3944.69001
CS_ Jejunat tissue B_016	4603.94957	CS_ Jejunat tissue B_013	3445.5752	CS_ Jejunat tissue B_015	4264.23402	CS_ Jejunat tissue B_010	5313.63855
CS_ Jejunat tissue B_004	3723.24966	CS_ Jejunat tissue B_007	4402.60633	CS_ Jejunat tissue B_003	4069.55317	CS_ Jejunat tissue B_008	3611.71129
CS_ Jejunat tissue A_041	4278.59973	CS_ Jejunat tissue A_046	4143.35364	CS_ Jejunat tissue A_045	3626.93241	CS_ Jejunat tissue A_043	3488.3746
CS_ Jejunat tissue A_038	3564.85468	CS_ Jejunat tissue A_035	4327.61491	CS_ Jejunat tissue A_040	2337.36802	CS_ Jejunat tissue A_039	4865.80743
CS_ Jejunat tissue A_025	3301.17376	CS_ Jejunat tissue A_026	4755.57108	CS_ Jejunat tissue A_029	4834.76857	CS_ Jejunat tissue A_032	6012.68236
CS_ Jejunat tissue A_019	3964.48938	CS_ Jejunat tissue A_023	3094.69459	CS_ Jejunat tissue A_020	4832.27447	CS_ Jejunat tissue A_018	5317.84348
CS_ Jejunat tissue A_016	4379.383	CS_ Jejunat tissue A_013	4556.05089	CS_ Jejunat tissue A_015	4956.02112	CS_ Jejunat tissue A_010	4209.30193
CS_ Jejunat tissue A_004	4426.49955	CS_ Jejunat tissue A_007	3667.2755	CS_ Jejunat tissue A_003	3721.64876	CS_ Jejunat tissue A_008	7918.18588
CS_ 13C Jejunat tissue A_005	11280.5379	CS_ Jejunat tissue B_048	4288.64828	CS_ 13C Jejunat tissue A_002	6758.91384	CS_ Jejunat tissue B_047	5138.12267
CS_ 13C Jejunat tissue A_014	6525.93211	CS_ Jejunat tissue B_034	5518.29352	CS_ 13C Jejunat tissue A_011	6087.80157	CS_ Jejunat tissue B_033	5040.57783
CS_ 13C Jejunat tissue A_021	5021.80157	CS_ Jejunat tissue B_027	4283.21462	CS_ 13C Jejunat tissue A_017	4389.51958	CS_ Jejunat tissue B_030	5555.95699
CS_ 13C Jejunat tissue A_031	6573.99478	CS_ Jejunat tissue B_024	5815.65628	CS_ 13C Jejunat tissue A_028	6897.16136	CS_ Jejunat tissue B_022	5086.72675
CS_ 13C Jejunat tissue A_037	5183.06319	CS_ Jejunat tissue B_009	6140.29842	CS_ 13C Jejunat tissue A_036	6866.47833	CS_ Jejunat tissue B_012	4383.62572
CS_ 13C Jejunat tissue A_044	5749.46214	CS_ Jejunat tissue B_001	4877.04693	CS_ 13C Jejunat tissue A_042	5881.49869	CS_ Jejunat tissue B_006	5874.23562

Run	Inositol nmol/g fwt						
CS_Duodenal tissue A_041	4049.39401	CS_Duodenal tissue A_045	4611.59101	CS_Duodenal tissue B_041	4647.36448	CS_Duodenal tissue B_045	3773.88167
CS_Duodenal tissue A_038	2943.76377	CS_Duodenal tissue A_040	3147.8019	CS_Duodenal tissue B_038	3042.16615	CS_Duodenal tissue B_040	2953.79022
CS_Duodenal tissue A_025	3276.49846	CS_Duodenal tissue A_029	4232.01851	CS_Duodenal tissue B_025	3316.67585	CS_Duodenal tissue B_029	2992.60688
CS_Duodenal tissue A_019	3175.76906	CS_Duodenal tissue A_020	3259.16703	CS_Duodenal tissue B_019	2394.09982	CS_Duodenal tissue B_020	3572.56501
CS_Duodenal tissue A_016	3973.76598	CS_Duodenal tissue A_015	2836.80366	CS_Duodenal tissue B_016	3972.33363	CS_Duodenal tissue B_015	3217.01961
CS_Duodenal tissue A_004	4045.74152	CS_Duodenal tissue A_003	2622.48788	CS_Duodenal tissue B_004	2071.53482	CS_Duodenal tissue B_003	2143.22389
CS_13C Duodenal tissue A_005	3200.37598	CS_13C Duodenal tissue A_002	4472.23708	CS_13C Duodenal tissue B_005	6166.17546	CS_13C Duodenal tissue B_002	3487.53003
CS_13C Duodenal tissue A_014	5337.06005	CS_13C Duodenal tissue A_011	4993.90078	CS_13C Duodenal tissue B_014	5555.58225	CS_13C Duodenal tissue B_011	4458.6611
CS_13C Duodenal tissue A_021	12000.0522	CS_13C Duodenal tissue A_017	4487.40992	CS_13C Duodenal tissue B_021	4204.73629	CS_13C Duodenal tissue B_017	3727.36815
CS_13C Duodenal tissue A_031	6213.38903	CS_13C Duodenal tissue A_028	6538.96606	CS_13C Duodenal tissue B_031	4140.58486	CS_13C Duodenal tissue B_028	4122.45953
CS_13C Duodenal tissue A_037	5568.68407	CS_13C Duodenal tissue A_036	5781.36815	CS_13C Duodenal tissue B_037	4271.80679	CS_13C Duodenal tissue B_036	3524.66319
CS_13C Duodenal tissue A_044	3446.90026	CS_13C Duodenal tissue A_042	4052.8094	CS_13C Duodenal tissue B_044	4961.85901	CS_13C Duodenal tissue B_042	4974.6893
CS_Duodenal tissue A_046	4762.41736	CS_Duodenal tissue A_043	2425.75474	CS_Duodenal tissue B_046	2466.2186	CS_Duodenal tissue B_043	3435.95527
CS_Duodenal tissue A_035	4203.08506	CS_Duodenal tissue A_039	2693.17431	CS_Duodenal tissue B_035	4175.83517	CS_Duodenal tissue B_039	3893.48281
CS_Duodenal tissue A_026	2882.316	CS_Duodenal tissue A_032	3269.33671	CS_Duodenal tissue B_026	2494.43587	CS_Duodenal tissue B_032	4224.60555
CS_Duodenal tissue A_023	4548.20956	CS_Duodenal tissue A_018	2305.93874	CS_Duodenal tissue B_023	2894.2045	CS_Duodenal tissue B_018	4180.81203
CS_Duodenal tissue A_013	2300.92552	CS_Duodenal tissue A_010	3703.69656	CS_Duodenal tissue B_013	5184.45901	CS_Duodenal tissue B_010	2739.79727
CS_Duodenal tissue A_007	2856.4621	CS_Duodenal tissue A_008	2555.45394	CS_Duodenal tissue B_007	2177.20692	CS_Duodenal tissue B_008	3588.03438
CS_Duodenal tissue A_048	3496.79374	CS_Duodenal tissue A_047	3559.67387	CS_Duodenal tissue B_048	3920.9123	CS_Duodenal tissue B_047	3544.56258
CS_Duodenal tissue A_034	4293.39467	CS_Duodenal tissue A_033	4333.35721	CS_Duodenal tissue B_034	3815.09806	CS_Duodenal tissue B_033	3472.15734

Run	Inositol nmol/g fwt	Run	Inositol nmol/g fwt	Run	Inositol nmol/g fwt	Run	Inositol nmol/g fwt
CS_Duodenal tissue A_027	4507.60247	CS_Duodenal tissue A_030	3542.987	CS_Duodenal tissue B_027	3155.32173	CS_Duodenal tissue B_030	3737.28515
CS_Duodenal tissue A_024	3818.06963	CS_Duodenal tissue A_022	3330.64125	CS_Duodenal tissue B_024	3889.50749	CS_Duodenal tissue B_022	4330.20604
CS_Duodenal tissue A_009	2428.29661	CS_Duodenal tissue A_012	3057.1342	CS_Duodenal tissue B_009	2821.33319	CS_Duodenal tissue B_012	3468.79132
CS_Duodenal tissue A_001	3939.8193	CS_Duodenal tissue A_006	4345.06611	CS_Duodenal tissue B_001	2645.47708	CS_Duodenal tissue B_006	4153.38255

Run	Inositol nmol/g fwt	Run	Inositol nmol/g fwt	Run	Inositol nmol/g fwt	Run	Inositol nmol/g fwt
CS_Ileal tissue A_041	8491.90405	CS_Ileal tissue A_045	6303.08346	CS_Ileal tissue B_041	6411.25437	CS_Ileal tissue B_045	6347.0015
CS_Ileal tissue A_038	6803.13843	CS_Ileal tissue A_040	7880.23488	CS_Ileal tissue B_038	6577.57121	CS_Ileal tissue B_040	3150.63268
CS_Ileal tissue A_025	9106.13993	CS_Ileal tissue A_029	5673.28836	CS_Ileal tissue B_025	6721.01949	CS_Ileal tissue B_029	7417.21139
CS_Ileal tissue A_019	6609.21039	CS_Ileal tissue A_020	9931.87706	CS_Ileal tissue B_019	5726.49675	CS_Ileal tissue B_020	6588.42079
CS_Ileal tissue A_016	9040.29485	CS_Ileal tissue A_015	5961.22439	CS_Ileal tissue B_016	10255.3173	CS_Ileal tissue B_003	9515.14243
CS_Ileal tissue A_004	5594.06097	CS_Ileal tissue A_003	7526.81159	CS_Ileal tissue B_004	7529.28036	CS_Ileal tissue B_003	6340.82959
CS_13C Ileal tissue A_005	6585.80679	CS_13C Ileal tissue A_002	10478.7123	CS_13C Ileal tissue B_005	16162.564	CS_13C Ileal tissue B_002	7459.42037
CS_13C Ileal tissue A_014	10040.4125	CS_13C Ileal tissue A_011	9485.7577	CS_13C Ileal tissue B_014	12155.2376	CS_13C Ileal tissue B_011	11447.8413
CS_13C Ileal tissue A_021	4443.8611	CS_13C Ileal tissue A_017	9913.12794	CS_13C Ileal tissue B_021	10487.9112	CS_13C Ileal tissue B_017	11233.765
CS_13C Ileal tissue A_031	13065.9509	CS_13C Ileal tissue A_028	12230.8616	CS_13C Ileal tissue B_031	8822.2141	CS_13C Ileal tissue B_028	10627.5175
CS_13C Ileal tissue A_037	10801.201	CS_13C Ileal tissue A_036	12981.1624	CS_13C Ileal tissue B_037	9882.85117	CS_13C Ileal tissue B_036	10304.0449
CS_13C Ileal tissue A_044	9762.96606	CS_13C Ileal tissue A_042	11385.4204	CS_13C Ileal tissue B_044	8854.45953	CS_13C Ileal tissue B_042	10566.5901
CS_Ileal tissue A_046	7690.2049	CS_Ileal tissue A_043	8823.62819	CS_Ileal tissue B_046	10651.2944	CS_Ileal tissue B_043	7757.12144
CS_Ileal tissue A_035	9105.06747	CS_Ileal tissue A_039	6424.37781	CS_Ileal tissue B_035	8521.88606	CS_Ileal tissue B_039	5117.16642
CS_Ileal tissue A_026	6181.82109	CS_Ileal tissue A_032	6425.77411	CS_Ileal tissue B_026	8067.991	CS_Ileal tissue B_032	8428.88556
CS_Ileal tissue A_023	7630.88956	CS_Ileal tissue A_018	10062.3638	CS_Ileal tissue B_023	10255.5122	CS_Ileal tissue B_018	8023.48826
CS_Ileal tissue A_013	10081.7241	CS_Ileal tissue A_010	6995.92904	CS_Ileal tissue B_013	7429.55522	CS_Ileal tissue B_010	9661.38431
CS_Ileal tissue A_007	7890.56472	CS_Ileal tissue A_008	9649.62519	CS_Ileal tissue B_007	8122.17391	CS_Ileal tissue B_008	5262.72664
CS_Ileal tissue A_048	9708.77761	CS_Ileal tissue A_047	9471.22439	CS_Ileal tissue B_048	12598.046	CS_Ileal tissue B_047	9235.81409
CS_Ileal tissue A_034	12947.7661	CS_Ileal tissue A_033	7537.95302	CS_Ileal tissue B_034	10845.6772	CS_Ileal tissue B_033	8387.63118
CS_Ileal tissue A_027	9558.54073	CS_Ileal tissue A_030	8847.01649	CS_Ileal tissue B_027	7179.26837	CS_Ileal tissue B_030	5941.63718
CS_Ileal tissue A_024	9513.68116	CS_Ileal tissue A_022	10896.2869	CS_Ileal tissue B_024	10478.3508	CS_Ileal tissue B_022	9575.75712
CS_Ileal tissue A_009	9388.42279	CS_Ileal tissue A_012	7794.73763	CS_Ileal tissue B_009	8479.23538	CS_Ileal tissue B_012	6709.06547
CS_Ileal tissue A_001	11305.4523	CS_Ileal tissue A_006	5286.76462	CS_Ileal tissue B_001	10479.3253	CS_Ileal tissue B_006	9905.53223

Run	Inositol nmol/g fwt	Run	Inositol nmol/g fwt	Run	Inositol nmol/g fwt	Run	Inositol nmol/g fwt
CS_Breast Muscle A_004	353.160821	CS_Breast Muscle A_003	631.589828	CS_Breast Muscle B_004	641.220453	CS_Breast Muscle B_003	704.528748
CS_Breast Muscle A_016	628.304964	CS_Breast Muscle A_015	615.986723	CS_Breast Muscle B_016	609.156272	CS_Breast Muscle B_015	511.990903
CS_Breast Muscle A_019	344.612133	CS_Breast Muscle A_020	977.620426	CS_Breast Muscle B_019	369.621896	CS_Breast Muscle B_020	655.927687
CS_Breast Muscle A_025	521.13569	CS_Breast Muscle A_029	302.132865	CS_Breast Muscle B_025	586.161073	CS_Breast Muscle B_029	461.859968
CS_Breast Muscle A_038	666.827464	CS_Breast Muscle A_040	387.725404	CS_Breast Muscle B_038	905.016884	CS_Breast Muscle B_040	479.067604
CS_Breast Muscle A_041	553.910826	CS_Breast Muscle A_045	580.002527	CS_Breast Muscle B_041	518.262008	CS_Breast Muscle B_045	487.205109
CS_13C Breast muscle A_005	601.834987	CS_13C Breast muscle A_002	717.409922	CS_13C Breast muscle B_005	892.689295	CS_13C Breast muscle B_002	836.955614
CS_13C Breast muscle A_014	605.806789	CS_13C Breast muscle A_011	711.436031	CS_13C Breast muscle B_014	836.073107	CS_13C Breast muscle B_011	607.436031
CS_13C Breast muscle A_021	784.073107	CS_13C Breast muscle A_017	582.217232	CS_13C Breast muscle B_021	718.496084	CS_13C Breast muscle B_017	727.389034
CS_13C Breast muscle A_031	784.684073	CS_13C Breast muscle A_028	577.023499	CS_13C Breast muscle B_031	718.156658	CS_13C Breast muscle B_028	863.159269
CS_13C Breast muscle A_037	747.448564	CS_13C Breast muscle A_036	795.953003	CS_13C Breast muscle B_037	955.483029	CS_13C Breast muscle B_036	481.033943
CS_13C Breast muscle A_044	1135.98956	CS_13C Breast muscle A_042	868.013577	CS_13C Breast muscle B_044	482.018799	CS_13C Breast muscle B_042	960.099217
CS_Breast Muscle A_007	718.937358	CS_Breast Muscle A_008	692.359819	CS_Breast Muscle B_007	620.80261	CS_Breast Muscle B_008	612.403234
CS_Breast Muscle A_013	917.895619	CS_Breast Muscle A_010	253.382491	CS_Breast Muscle B_013	623.825604	CS_Breast Muscle B_010	525.616199
CS_Breast Muscle A_023	483.696276	CS_Breast Muscle A_018	758.803666	CS_Breast Muscle B_023	700.124044	CS_Breast Muscle B_018	615.240163
CS_Breast Muscle A_026	502.771461	CS_Breast Muscle A_032	660.92964	CS_Breast Muscle B_026	1042.42184	CS_Breast Muscle B_032	688.328395
CS_Breast Muscle A_035	700.795948	CS_Breast Muscle A_039	369.733306	CS_Breast Muscle B_035	719.45995	CS_Breast Muscle B_039	610.760802
CS_Breast Muscle A_046	332.368548	CS_Breast Muscle A_043	399.334987	CS_Breast Muscle B_046	514.155928	CS_Breast Muscle B_043	644.65463
CS_Breast Muscle A_001	463.315186	CS_Breast Muscle A_006	576.382285	CS_Breast Muscle B_001	909.832771	CS_Breast Muscle B_006	676.084809
CS_Breast Muscle A_009	730.359727	CS_Breast Muscle A_012	901.769922	CS_Breast Muscle B_009	753.540992	CS_Breast Muscle B_012	839.058875

Run	Inositol nmol/g fwt	Run	Inositol nmol/g fwt	Run	Inositol nmol/g fwt	Run	Inositol nmol/g fwt
CS_Breast Muscle A_024	665.185032	CS_Breast Muscle A_022	694.151563	CS_Breast Muscle B_024	811.92199	CS_Breast Muscle B_022	941.412262
CS_Breast Muscle A_027	574.514736	CS_Breast Muscle A_030	563.689615	CS_Breast Muscle B_027	932.566099	CS_Breast Muscle B_030	515.015046
CS_Breast Muscle A_034	554.918108	CS_Breast Muscle A_033	475.148738	CS_Breast Muscle B_034	579.703903	CS_Breast Muscle B_033	887.249902
CS_Breast Muscle A_048	639.279397	CS_Breast Muscle A_047	1098.04057	CS_Breast Muscle B_048	707.962925	CS_Breast Muscle B_047	597.173409

Run	Inositol nmol/g fwt	Run	Inositol nmol/g fwt	Run	Inositol nmol/g fwt	Run	Inositol nmol/g fwt
CS_Leg Muscle A_004	478.157809	CS_Leg Muscle A_003	624.638626	CS_Leg Muscle B_004	559.363113	CS_Leg Muscle B_003	630.36083
CS_Leg Muscle A_016	594.68536	CS_Leg Muscle A_015	551.662863	CS_Leg Muscle B_016	462.50951	CS_Leg Muscle B_015	951.228127
CS_Leg Muscle A_019	368.622976	CS_Leg Muscle A_020	1347.26117	CS_Leg Muscle B_019	366.927508	CS_Leg Muscle B_020	875.214651
CS_Leg Muscle A_025	1257.11879	CS_Leg Muscle A_029	607.118791	CS_Leg Muscle B_025	439.832627	CS_Leg Muscle B_029	578.507771
CS_Leg Muscle A_038	756.461254	CS_Leg Muscle A_040	337.186175	CS_Leg Muscle B_038	593.696337	CS_Leg Muscle B_040	482.643191
CS_Leg Muscle A_041	534.072383	CS_Leg Muscle A_045	596.910118	CS_Leg Muscle B_041	929.929356	CS_Leg Muscle B_045	638.379524
CS_13C Leg muscle A_005	1049.25384	CS_13C Leg muscle A_002	1175.09628	CS_13C Leg muscle B_005	2360.396	CS_13C Leg muscle B_002	1161.01553
CS_13C Leg muscle A_014	1073.33396	CS_13C Leg muscle A_011	1063.13052	CS_13C Leg muscle B_014	1679.48637	CS_13C Leg muscle B_011	830.696136
CS_13C Leg muscle A_021	1767.9162	CS_13C Leg muscle A_017	1298.2178	CS_13C Leg muscle B_021	1487.72971	CS_13C Leg muscle B_017	1645.16932
CS_13C Leg muscle A_031	1151.22023	CS_13C Leg muscle A_028	890.284231	CS_13C Leg muscle B_031	1738.8704	CS_13C Leg muscle B_028	1387.73599
CS_13C Leg muscle A_037	1236.2489	CS_13C Leg muscle A_036	1888.62343	CS_13C Leg muscle B_037	1131.49357	CS_13C Leg muscle B_036	1159.92716
CS_13C Leg muscle A_044	1196.38746	CS_13C Leg muscle A_042	1151.93499	CS_13C Leg muscle B_044	1959.87693	CS_13C Leg muscle B_042	572.685127
CS_Leg Muscle A_007	677.268775	CS_Leg Muscle A_008	776.841648	CS_Leg Muscle B_007	933.143137	CS_Leg Muscle B_008	451.206391
CS_Leg Muscle A_013	680.554288	CS_Leg Muscle A_010	369.789153	CS_Leg Muscle B_013	958.468645	CS_Leg Muscle B_010	571.548745
CS_Leg Muscle A_023	571.690034	CS_Leg Muscle A_018	765.892838	CS_Leg Muscle B_023	1095.80154	CS_Leg Muscle B_018	5982.14107
CS_Leg Muscle A_026	502.918161	CS_Leg Muscle A_032	1020.14238	CS_Leg Muscle B_026	878.464297	CS_Leg Muscle B_032	833.039887
CS_Leg Muscle A_035	365.161396	CS_Leg Muscle A_039	4559.14792	CS_Leg Muscle B_035	1014.80817	CS_Leg Muscle B_039	595.956961
CS_Leg Muscle A_046	721.986741	CS_Leg Muscle A_043	995.875448	CS_Leg Muscle B_046	532.800783	CS_Leg Muscle B_043	394.690794
CS_Leg Muscle A_001	567.840452	CS_Leg Muscle A_006	838.408869	CS_Leg Muscle B_001	606.906858	CS_Leg Muscle B_006	867.161178
CS_Leg Muscle A_009	1216.85143	CS_Leg Muscle A_012	876.556896	CS_Leg Muscle B_009	1227.16553	CS_Leg Muscle B_012	1160.54777

Run	Inositol nmol/g fwt	Run	Inositol nmol/g fwt	Run	Inositol nmol/g fwt	Run	Inositol nmol/g fwt
CS_Leg Muscle A_024	550.320617	CS_Leg Muscle A_022	1209.39789	CS_Leg Muscle B_024	1067.57961	CS_Leg Muscle B_022	607.118791
CS_Leg Muscle A_027	820.323878	CS_Leg Muscle A_030	535.132051	CS_Leg Muscle B_027	1109.96631	CS_Leg Muscle B_030	445.484187
CS_Leg Muscle A_034	586.208021	CS_Leg Muscle A_033	800.366265	CS_Leg Muscle B_034	968.677318	CS_Leg Muscle B_033	590.164113
CS_Leg Muscle A_048	1207.73829	CS_Leg Muscle A_047	1152.98881	CS_Leg Muscle B_048	627.393762	CS_Leg Muscle B_047	559.752201

Appendix 9: Tissue raw inositol phosphate measurements

nmol g wwt					
Row Labels	IP3	IP4	IP5	IP6	Grand Total
Duodenal tissue 13B	0.6388327	3.92761144	28.9581598	19.137331	52.6619349
Ileum tissue 10A	0.42656052	3.97743924	9.4779386	1.22884569	15.110784
Ileum tissue 10B	0	5.32898228	8.31231373	5.25265646	18.8939525
Ileum tissue 12A	3.18897913	13.5656902	28.77757	8.39627213	53.9285115
Ileum tissue 12B	1.21127635	4.72903254	17.2392663	7.12825546	30.3078307
Ileum tissue 13A	1.64762962	7.9538704	11.2155751	5.17892284	25.9959979
Ileum tissue 13B	0	3.6044508	21.4658446	4.02424281	29.0945382
Ileum tissue 15A	1.11018064	4.96305038	23.1680543	11.3958768	40.6371622
Ileum tissue 15B	0	3.67055184	13.7668736	4.21678549	21.6542109
Ileum tissue 16A	1.30445145	9.85035099	35.9095697	10.309602	57.3739742
Ileum tissue 16B	1.38092128	11.4727787	36.5609314	14.7069773	64.1216086
Ileum tissue 18A	0.98805933	3.70468244	23.6286014	17.7142145	46.0355578
Ileum tissue 18B	0	5.51043612	14.4218355	9.29749284	29.2297645
Ileum tissue 19A	0.69182875	12.9801416	38.523225	11.2458174	63.4410127
Ileum tissue 19B	0.81812637	3.87864771	20.0270309	10.9773809	35.7011859
Ileum tissue 1A	4.05736533	6.96307486	13.7109973	7.22171858	31.9531561
Ileum tissue 1B	0.96127329	2.5537467	10.4446843	5.11987834	19.0795826
Ileum tissue 20A	0.61377479	5.96104647	20.5338055	17.9442001	45.0528268
Ileum tissue 20B	0.35657118	5.38658667	18.376233	15.0216412	39.1410321
Ileum tissue 22A	2.65973878	15.9830585	37.1086052	8.56922932	64.3206318
Ileum tissue 22B	2.37906138	12.447589	19.5103195	7.88834541	42.2253153
Ileum tissue 23A	1.30257931	4.53188151	17.8331676	6.22919491	29.8968233
Ileum tissue 23B	0.86464192	9.92235648	23.3971758	9.42667069	43.6108449
Ileum tissue 24B	2.0239303	3.20798858	10.4563492	3.23160638	18.9198745
Ileum tissue 25A	0.78428379	8.87294847	18.1463915	6.90561448	34.7092382
Ileum tissue 25B	2.15987667	15.3841169	35.3729848	10.4842873	63.4012657
Ileum tissue 26A	2.7085585	11.7566243	36.6047107	9.13159219	60.2014858
Ileum tissue 26B	1.42642875	6.14120421	24.9452938	7.80582712	40.3187539
Ileum tissue 27A	0.78370775	5.6584794	18.3825695	5.92792394	30.7526806
Ileum tissue 29A	1.08800295	4.48795816	14.4229876	253.236683	273.235631
Ileum tissue 29B	1.17282542	11.6569687	29.3852963	9.94899851	52.164089
Ileum tissue 30A	0.56581914	15.3223362	6.46335677	2.45236297	24.803875
Ileum tissue 30B	0.60743831	1.72769972	11.2857084	4.29109515	17.9119416
Ileum tissue 32A	0.47998859	5.7345172	22.1123098	10.191225	38.5180406
Ileum tissue 32B	1.00289246	5.61786831	10.5537006	6.78104499	23.9555064
Ileum tissue 33A	1.12414971	5.24358377	27.125476	7.78379344	41.277003
Ileum tissue 33B	1.70897829	7.52601378	25.7791174	5.07105862	40.0851681
Ileum tissue 34A	0.38018899	6.17015041	8.51320905	8.2948884	23.3584368

nmol g wwt					
Row Labels	IP3	IP4	IP5	IP6	Grand Total
Ileum tissue 34B	1.92657888	4.19907214	9.32874322	7.95747068	23.4118649
Ileum tissue 35A	0.07877401	8.15851	20.9821117	9.38649163	38.6058873
Ileum tissue 35B	0.69024462	4.21376126	9.86432006	4.82926418	19.5975901
Ileum tissue 38A	0.51483925	15.9343828	31.6147303	9.41068547	57.4746379
Ileum tissue 38B	1.4061232	5.72587654	20.881016	105.647607	133.660622
Ileum tissue 39A	0.21817663	4.68194095	15.9382711	7.08865244	27.9270412
Ileum tissue 39B	1.61105083	7.09023656	18.887472	31.3058268	58.8945861
Ileum tissue 3A	1.16231261	1.34247035	9.93243725	106.180879	118.618099
Ileum tissue 3B	0.73532006	10.7639566	23.6588438	35.0267824	70.1849029
Ileum tissue 40A	0.30155899	5.51058013	16.3024749	6.57856555	28.6931796
Ileum tissue 40B	0.34721047	2.22885793	12.6107534	9.84084627	25.0276681
Ileum tissue 41A	0.40683102	14.3469498	36.4105839	10.2675508	61.4319156
Ileum tissue 41B	0.74784902	5.00769379	14.3178596	8.96165924	29.0350616
Ileum tissue 43A	0.23776213	4.48176569	15.1251851	105.086828	124.931541
Ileum tissue 43B	0.35959542	5.44764733	22.3530962	7.48237846	35.6427174
Ileum tissue 45A	0.54032919	3.81470683	12.4640063	9.41572585	26.2347681
Ileum tissue 45B	1.85500543	5.48278601	9.56621733	4.37116526	21.275174
Ileum tissue 46A	0.29104619	8.63086602	23.89819	22.5297977	55.3498999
Ileum tissue 46B	0.80041302	9.33219949	17.5526342	10.5820708	38.2673175
Ileum tissue 47A	1.00649274	5.68252924	13.9722332	4.00883363	24.6700888
Ileum tissue 47B	0.38263717	5.22443031	9.73067787	4.9764434	20.3141888
Ileum tissue 48A	0.31466399	2.40887165	5.84670175	1.14891959	9.71915699
Ileum tissue 48B	0.77333896	2.67327581	7.08490815	2.55101049	13.0825334
Ileum tissue 4A	0.81092582	7.94566178	25.406849	8.99305363	43.1564903
Ileum tissue 4B	1.44644628	11.5989323	24.1379683	14.8293866	52.0127335
Ileum tissue 6A	0.77895539	7.3412477	10.6252741	5.69981055	24.4452877
Ileum tissue 6B	1.3339737	5.20830108	13.156411	4.43179388	24.1304797
Ileum tissue 7A	6.06084608	42.3729265	27.4077376	30.7904115	106.631922
Ileum tissue 7B	1.4323332	13.0233449	19.1705976	18.3190606	51.9453363
Ileum tissue 8A	0.77319495	9.39109998	21.4826938	46.7278185	78.3748073
Ileum tissue 8B	0.91706192	6.2290509	25.8581794	8.78639787	41.7906901
Ileum tissue 9A	0	6.4126649	13.5269513	9.72664556	29.6662618
Ileum tissue 9B	0.983739	5.6754727	14.37604	11.9040916	32.9393433

nmol g wwt					
Row Labels	IP3	IP4	IP5	IP6	Grand Total
Duodenal tissue 40A	0.61332063	3.76726295	29.7903282	10.1491061	44.3200179
Duodenal tissue 10A	1.31556179	6.96499651	36.9183254	23.0021996	68.2010833
Duodenal tissue 10B	0.73642266	5.104842	26.1582098	11.5245159	43.5239905
Duodenal tissue 12A	0.63375654	2.22873076	10.2090758	3.79913324	16.8706963
Duodenal tissue 12B	1.05001659	3.2216971	12.3853787	6.44728675	23.1043792
Duodenal tissue 13A	0.43316834	5.36673794	25.2724104	10.4315596	41.5038763
Duodenal tissue 15A	0.80709686	4.68079684	12.6671023	58.5538734	76.7088695
Duodenal tissue 15B	0.51734483	2.32774762	15.0287882	39.6151358	57.4890165
Duodenal tissue 16A	1.8911733	6.06447834	34.382691	21.1245286	63.4628713
Duodenal tissue 16B	0.46589012	3.61849438	11.6692703	9.53736685	25.2910217
Duodenal tissue 18A	2.21157919	5.49470567	23.1796758	16.5827689	47.4687296
Duodenal tissue 18B	0.76829295	7.51664447	38.2191685	39.3722161	85.876322
Duodenal tissue 19A	0.58838395	5.58107172	25.0459124	17.8193849	49.0347529
Duodenal tissue 19B	0.47002596	8.40414691	48.9746616	31.943519	89.7923535
Duodenal tissue 1A	1.67489324	5.32817732	15.0191784	12.3244359	34.3466849
Duodenal tissue 1B	1.70080305	7.32542273	33.1800133	11.7416475	53.9478866
Duodenal tissue 20A	1.3075334	4.74684863	29.3336829	20.0644157	55.4524806
Duodenal tissue 20B	0.35227619	5.57170526	29.6522641	31.423863	67.0001086
Duodenal tissue 22A	1.14988494	3.21634484	16.1700365	5.53168494	26.0679512
Duodenal tissue 22B	0.69372621	2.60679512	16.3921554	8.35415191	28.0468286
Duodenal tissue 23A	0.86791802	1.42236376	15.1550529	15.194465	32.6397997
Duodenal tissue 23B	0.19560087	5.42950538	27.4803403	13.9100437	47.0154902
Duodenal tissue 24A	1.40387413	5.53083344	24.3091248	9.49442711	40.7382595
Duodenal tissue 24B	0.53486132	4.69770513	29.981185	10.8133949	46.0271463
Duodenal tissue 25A	0.84565748	2.06451362	15.026112	4.40028963	22.3365728
Duodenal tissue 25B	0.38074049	7.27640087	38.6891944	47.3146087	93.6609445
Duodenal tissue 26A	0.54678227	2.96466686	17.1373363	15.7864982	36.4352837
Duodenal tissue 26B	0.5868026	5.67534453	39.4084655	13.8736726	59.5442853
Duodenal tissue 27A	0.6445827	8.64183602	41.2611998	10.7663193	61.3139379
Duodenal tissue 27B	0.40555553	2.88511277	16.0915772	3.10212269	22.4843682
Duodenal tissue 29A	0.41273242	5.24570382	34.8895746	16.6379946	57.1860054
Duodenal tissue 29B	0.66246413	6.16690118	19.2008768	11.0632482	37.0934903
Duodenal tissue 30A	0.47574315	2.64365275	17.1575289	3.78538765	24.0623125
Duodenal tissue 30B	1.05220615	3.57251358	14.8093454	6.65456528	26.0886304
Duodenal tissue 32A	0.8365343	4.73955009	25.1795973	10.2655178	41.0211995
Duodenal tissue 32B	0.38463305	5.52171027	33.5248693	10.0375601	49.4687727
Duodenal tissue 33A	0.90027488	3.65960949	20.5359014	6.11252706	31.2083128
Duodenal tissue 33B	2.535756	8.27946352	12.1371067	5.06190226	28.0142285
Duodenal tissue 34A	0.75418244	6.52282664	28.0908632	7.37493116	42.7428034
Duodenal tissue 34B	1.85516717	7.99737496	29.0419845	13.8904593	52.7849859

nmol g wwt					
Row Labels	IP3	IP4	IP5	IP6	Grand Total
Duodenal tissue 35A	0.70516058	3.61642646	24.3669049	7.54048637	36.2289783
Duodenal tissue 35B	1.64946999	7.61748596	35.5140863	16.1886478	60.9696901
Duodenal tissue 38A	0.26627506	3.86007604	15.2315659	9.36487803	28.7227951
Duodenal tissue 38B	1.17469998	5.20252079	22.4608912	7.73633052	36.5744425
Duodenal tissue 39A	0.72182558	3.52969548	17.5898458	9.00384359	30.8452104
Duodenal tissue 39B	0.18501798	3.64051164	23.6972639	13.3391762	40.8619697
Duodenal tissue 3A	0.40020326	2.81723635	6.90672983	25.5637438	35.6879132
Duodenal tissue 3B	3.22449487	8.57773051	27.8223985	19.0052759	58.6298999
Duodenal tissue 40B	0.43876388	4.35211927	21.9666584	13.462035	40.2195766
Duodenal tissue 41A	0.37453673	1.05731513	11.1774704	5.11408682	17.7234091
Duodenal tissue 41B	0.35118141	4.24118146	27.3353427	9.18326603	41.1109716
Duodenal tissue 43A	1.57782266	4.05494706	31.0434874	12.610417	49.2866742
Duodenal tissue 43B	1.26799964	4.40746653	25.2823851	13.1002707	44.0581219
Duodenal tissue 45A	1.09502425	4.23485606	29.019724	10.9894113	45.3390157
Duodenal tissue 45B	0.48486633	3.16707969	32.8609455	15.5607301	52.0736216
Duodenal tissue 46A	0.42428845	7.81114055	21.1363279	10.464403	39.8361599
Duodenal tissue 46B	1.22433005	8.58004172	42.4271416	10.583126	62.8146393
Duodenal tissue 47A	1.15852155	2.53721571	14.2207182	5.78080843	23.6972639
Duodenal tissue 47B	0.51333063	1.2259114	9.96445307	5.38778206	17.0914772
Duodenal tissue 48A	1.69411272	5.87033718	34.3435222	8.40633647	50.3143086
Duodenal tissue 48B	1.26033618	3.6260362	24.6105545	4.35114613	33.848073
Duodenal tissue 4A	0.38633604	0.93980864	3.03716569	8.84047794	13.2037883
Duodenal tissue 4B	0.60334595	0.47404016	1.26885114	0.65516559	3.00140284
Duodenal tissue 6A	0.71026956	0	1.92888242	4.33825204	6.97740402
Duodenal tissue 6B	1.9862976	3.15418561	3.04762693	2.25427565	10.4423858
Duodenal tissue 7A	1.58852718	3.72590456	24.5747916	9.02646907	38.9156924
Duodenal tissue 7B	0.32514995	3.95702498	11.3461883	14.0669623	29.6953255
Duodenal tissue 8A	2.48551772	6.8144033	22.423547	26.0265928	57.7500609
Duodenal tissue 8B	0.27892586	5.66524822	31.500376	12.7404527	50.1850028
Duodenal tissue 9A	1.34706716	4.8614357	22.8507549	7.42796721	36.487225
Duodenal tissue 9B	1.10244443	6.14476228	22.0726089	10.7623051	40.0821207

nmol g wwt					
Row Labels	IP3	IP4	IP5	IP6	Grand Total
Jejunal tissue 10B	2.21030476	6.59147105	27.0858777	30.3434683	66.2311219
Jejunal tissue 12B	0.68425971	2.16529744	13.8288714	7.48518792	24.1636165
Jejunal tissue 13B	0.65606831	6.65403618	39.2806371	10.1688115	56.759553
Jejunal tissue 15A	2.11769354	5.35092576	29.3578821	14.8682438	51.6947452
Jejunal tissue 15B	1.85012252	8.27442351	36.6360858	9.54946617	56.310098
Jejunal tissue 16A	1.00623518	0	5.96483061	51.4661229	58.4371887
Jejunal tissue 16B	1.81747984	6.95907208	34.0568199	9.58421084	52.4175827
Jejunal tissue 18A	1.3727234	2.47429003	20.6044521	11.8074985	36.258964
Jejunal tissue 18B	0	2.09457164	10.4175882	36.9129303	49.4250902
Jejunal tissue 19A	1.22867523	4.49393189	20.0814274	31.2782358	57.0822704
Jejunal tissue 19B	0.70985453	5.22122058	16.9704816	9.80801099	32.7095677
Jejunal tissue 1B	8.03628035	17.928371	13.8521169	9.15985606	48.9766243
Jejunal tissue 20A	0.37736911	2.52102841	9.98025056	10.9874749	23.866123
Jejunal tissue 20B	0.88184681	3.75366032	26.3556215	29.2030767	60.1942054
Jejunal tissue 22A	1.34156448	4.3950147	17.5127951	7.9906548	31.2400291
Jejunal tissue 22B	0.32692134	1.81488327	9.91632533	4.83841103	16.896541
Jejunal tissue 23A	1.43541217	4.41368532	25.0438559	33.9886907	64.881644
Jejunal tissue 23B	2.95478031	3.70716924	19.8422951	10.6820681	37.1863127
Jejunal tissue 24A	0.90632881	0.76833933	8.65587295	1.14941783	11.4799589
Jejunal tissue 24B	1.3461394	8.06286435	30.2070862	11.5911171	51.2072071
Jejunal tissue 25A	0.80506233	1.0286152	7.68277502	4.88416023	14.4006128
Jejunal tissue 25B	1.73364752	2.03979624	16.5270852	6.20606492	26.5065939
Jejunal tissue 26A	0.79986918	3.78803405	19.7172885	4.58666677	28.8918585
Jejunal tissue 26B	1.42638598	4.54178309	36.134081	6.89428132	48.9965314
Jejunal tissue 27A	1.3142386	4.25022465	7.45872757	5.63457082	18.6577616
Jejunal tissue 27B	1.05247897	4.61226159	21.0191624	5.39692225	32.0808252
Jejunal tissue 29A	1.3144859	2.17914584	16.9342531	35.0874134	55.5152983
Jejunal tissue 29B	1.06645103	1.72449768	11.0601791	4.35136748	18.2024952
Jejunal tissue 30A	0.53650215	0	3.86790968	3.37134536	7.77575719
Jejunal tissue 30B	0.91152197	0.36364434	5.13330792	0.99807451	7.40654875
Jejunal tissue 32A	0.38243861	1.36011145	17.4189474	7.53143171	26.6929292
Jejunal tissue 32B	0.59127754	0.67350246	11.6095404	3.84293309	16.7172535
Jejunal tissue 33A	1.65587387	2.02607148	11.888116	5.96272862	21.53279
Jejunal tissue 33B	0.64234355	4.1639194	22.9454512	8.92492772	36.6766418
Jejunal tissue 34A	2.21166487	1.74935062	12.5459154	3.98512656	20.4920574
Jejunal tissue 34B	1.19689808	5.79902066	18.4928172	5.97595879	31.4646948
Jejunal tissue 35A	2.81839823	2.5688796	1.20592427	9.79601728	16.3892194
Jejunal tissue 35B	0.5188207	5.73571365	24.4874466	7.22392288	37.9659039
Jejunal tissue 38A	1.57253613	4.9561225	23.3993575	86.236754	116.16477
Jejunal tissue 38B	1.00289673	2.87329727	14.4862998	9.02384492	27.3863387

nmol g wwt					
Row Labels	IP3	IP4	IP5	IP6	Grand Total
Jejunal tissue 39A	1.11677515	3.15360388	17.4298283	8.5727825	30.2729898
Jejunal tissue 39B	0.74422826	1.05136615	10.9653422	2.47206439	15.233001
Jejunal tissue 3B	0.53897508	0	6.95276611	32.6456424	40.1373836
Jejunal tissue 40A	2.69635914	4.55995912	23.7862474	38.7263298	69.7688954
Jejunal tissue 40B	0.5044777	4.87538133	19.6166402	52.437737	77.4342363
Jejunal tissue 41A	0.98064036	2.16245357	18.896523	36.0592749	58.0988918
Jejunal tissue 41B	0.76833933	5.04168587	29.0062315	34.078458	68.8947147
Jejunal tissue 43A	1.10552332	0.7552328	4.15563508	22.8085745	28.8249657
Jejunal tissue 43B	0.55257619	2.59002315	9.88937039	16.7709161	29.8028858
Jejunal tissue 45A	0.69748988	3.11552076	27.0609012	29.2673729	60.1412847
Jejunal tissue 45B	1.23535214	5.59933157	42.8038203	19.8647987	69.5033028
Jejunal tissue 46A	1.42119282	3.29653923	11.2848447	5.85490887	21.8574857
Jejunal tissue 46B	2.82309679	4.15959177	26.4928692	23.6679177	57.1434754
Jejunal tissue 47A	1.70928916	2.97023612	6.92086532	3.62234774	15.2227383
Jejunal tissue 47B	0	0.45971767	1.1185062	0	1.57822387
Jejunal tissue 48A	1.39015755	2.79910937	6.07030107	4.23316143	14.4927294
Jejunal tissue 48B	1.35281631	2.55255826	12.4235053	3.0980866	19.4269665
Jejunal tissue 4B	1.56721934	5.42350625	23.7287517	27.6754242	58.3949016
Jejunal tissue 6B	0.93081082	2.08171241	19.3742931	9.7197274	32.1065437
Jejunal tissue 7B	0.53192723	1.5756273	12.0746986	5.89929797	20.081551
Jejunal tissue 8B	0.59684164	2.79614186	19.6903335	16.1262233	39.2095403
Jejunal tissue 9B	2.05178995	5.11500824	26.1626094	7.83745679	41.1668643
Jejunum Tissue 10A	1.35949322	4.20855578	20.1049202	23.079484	48.7524532
Jejunum Tissue 12A	2.49048772	8.82291936	31.0123959	13.9704466	56.2962496
Jejunum Tissue 13A	0.38849729	4.58159726	33.5689108	10.3024733	48.8414787
Jejunum Tissue 1A	0.46911481	3.53307497	17.7312785	5.02697194	26.7604402
Jejunum Tissue 3A	0.8539027	3.65597959	20.866459	79.3500151	104.726356
Jejunum Tissue 4A	0.7164078	5.66807902	23.1655419	96.0976857	125.647714
Jejunum Tissue 6A	0.48914554	2.12449409	24.8732237	7.85711658	35.3439799
Jejunum Tissue 7A	0.58348781	4.21585092	18.573682	8.26762295	31.6406437
Jejunum Tissue 8A	0.87084227	4.3612592	24.1978665	14.5327909	43.9627589
Jejunum Tissue 9A	0.4020984	2.65506121	13.6741896	6.2352455	22.9665947
Jejunum Tissue 11A	1.36705463	4.17329358	25.8939084	23.0294411	54.4636976
Jejunum Tissue 11B	1.61780371	4.73302009	25.3320835	10.5019539	42.1848612
Jejunum Tissue 14A	1.81583254	4.87767294	21.9902487	13.4824844	42.1662386
Jejunum Tissue 14B	1.66645847	5.60474036	22.9302955	8.78133257	38.9828269
Jejunum Tissue 17A	0.81611483	3.96713377	21.7474995	8.54540286	35.0761509
Jejunum Tissue 17B	1.99969771	5.52461082	24.9947788	12.5289297	45.0480171
Jejunum Tissue 21A	0.81086903	2.33595328	15.6095239	15.2223841	33.9787303
Jejunum Tissue 21B	0.536645	0.78057455	8.56284514	12.4846028	22.3646675

nmol g wwt					
Row Labels	IP3	IP4	IP5	IP6	Grand Total
Jejunum Tissue 28A	2.80269804	5.78113028	15.8900429	36.7146755	61.1885467
Jejunum Tissue 28B	2.07012253	3.17514961	15.5627051	6.48446047	27.2924378
Jejunum Tissue 2A	2.25621717	5.9187013	17.0279873	13.3933059	38.5962117
Jejunum Tissue 2B	0.85860578	3.80910415	22.3966668	9.43141793	36.4957947
Jejunum Tissue 31A	1.11840386	2.36087082	11.5393102	6.04643645	21.0650213
Jejunum Tissue 31B	0.98752123	1.48010155	12.3655232	3.7213682	18.5545142
Jejunum Tissue 36A	2.37962454	4.27270143	11.101155	10.7982103	28.5516913
Jejunum Tissue 36B	1.63262309	2.34946121	18.1783905	3.15521558	25.3156904
Jejunum Tissue 37A	0.45730233	2.53253951	10.3771039	67.3635052	80.730451
Jejunum Tissue 37B	0.18911097	1.28469562	13.9877858	3.89959414	19.3611865
Jejunum Tissue 42A	2.17359587	4.35073266	19.8089153	7.72666514	34.059909
Jejunum Tissue 42B	1.01256991	5.43700601	24.3589882	34.897007	65.7055711
Jejunum Tissue 44A	0.74385398	0	5.60788784	3.52229021	9.87403203
Jejunum Tissue 44B	0.22202835	0.47185942	7.2658219	13.1867527	21.1464623
Jejunum Tissue 5A	1.26961395	3.56386315	10.7993906	89.3027385	104.935606
Jejunum Tissue 5B	0.38084484	0.75539473	9.6579052	13.4289773	24.2231221

nmol g wwt					
Row Labels	IP3	IP4	IP5	IP6	Grand Total
Leg Muscle 10A	1.60569611	0	0	0	1.60569611
Leg Muscle 10B	3.55822637	0	0	0	3.55822637
Leg Muscle 12A	2.69072539	0	0	0	2.69072539
Leg Muscle 12B	1.57779264	0	0	0	1.57779264
Leg Muscle 13A	1.81788119	0	0	0	1.81788119
Leg Muscle 13B	0.74448825	0	0	0	0.74448825
Leg Muscle 15A	2.6901317	0	0	0	2.6901317
Leg Muscle 15B	2.67148981	0	0	0	2.67148981
Leg Muscle 16A	1.12278802	0	0	0	1.12278802
Leg Muscle 16B	1.36964465	0	0	0	1.36964465
Leg Muscle 18A	4.30520812	0	0	0	4.30520812
Leg Muscle 18B	1.88413709	0	0	0	1.88413709
Leg Muscle 19A	3.37584456	0	0	0	3.37584456
Leg Muscle 19B	1.83391085	0	0	0	1.83391085
Leg Muscle 1A	2.57091859	0	0	0	2.57091859
Leg Muscle 1B	2.47687797	0	0	0	2.47687797
Leg Muscle 20A	1.83699804	0	0	0	1.83699804
Leg Muscle 20B	1.7541188	0	0	0	1.7541188
Leg Muscle 22A	1.56722494	0	0	0	1.56722494
Leg Muscle 22B	3.65523545	0	0	0	3.65523545
Leg Muscle 23A	7.59330519	0	0	0	7.59330519
Leg Muscle 23B	2.65759745	0	0	0	2.65759745
Leg Muscle 24A	1.45644224	0	0	0	1.45644224
Leg Muscle 24B	2.73596463	0	0	0	2.73596463
Leg Muscle 25A	1.43946269	0	0	0	1.43946269
Leg Muscle 25B	2.07839271	0	0	0	2.07839271
Leg Muscle 26A	4.92953336	0	0	0	4.92953336
Leg Muscle 26B	1.1329995	0	0	0	1.1329995
Leg Muscle 27A	2.6655529	0	0	0	2.6655529
Leg Muscle 28B	0.97127813	0	0	0	0.97127813
Leg Muscle 29A	1.32488036	0	0	0	1.32488036
Leg Muscle 29B	1.43530685	0	0	0	1.43530685
Leg Muscle 30A	10.5973806	0	0	0	10.5973806
Leg Muscle 30B	5.40828561	0	0	0	5.40828561
Leg Muscle 32A	2.58979796	0	0	0	2.58979796
Leg Muscle 32B	0.9475305	0	0	0	0.9475305
Leg Muscle 33A	1.74450101	0	0	0	1.74450101
Leg Muscle 33B	4.4703729	0	0	0	4.4703729
Leg Muscle 34A	0.51924196	0	0	0	0.51924196
Leg Muscle 34B	0.81584988	0	0	0	0.81584988

nmol g wwt					
Row Labels	IP3	IP4	IP5	IP6	Grand Total
Leg Muscle 35A	2.72337839	0	0	0	2.72337839
Leg Muscle 35B	2.53042888	0	0	0	2.53042888
Leg Muscle 38A	1.16019054	0	0	0	1.16019054
Leg Muscle 38B	0.82000572	0	0	0	0.82000572
Leg Muscle 39A	3.27907296	0	0	0	3.27907296
Leg Muscle 39B	3.02521078	0	0	0	3.02521078
Leg Muscle 3A	0.63762391	0	0	0	0.63762391
Leg Muscle 3B	3.16294705	0	0	0	3.16294705
Leg Muscle 40A	1.84257873	0	0	0	1.84257873
Leg Muscle 40B	3.7689866	0	0	0	3.7689866
Leg Muscle 41A	5.16166645	0	0	0	5.16166645
Leg Muscle 41B	0.52672247	0	0	0	0.52672247
Leg Muscle 43A	0.36868198	0	0	0	0.36868198
Leg Muscle 43B	0.79982023	0	0	0	0.79982023
Leg Muscle 45A	3.81648187	0	0	0	3.81648187
Leg Muscle 45B	0.62610631	0	0	0	0.62610631
Leg Muscle 46A	0.52375401	0	0	0	0.52375401
Leg Muscle 46B	2.34947193	0	0	0	2.34947193
Leg Muscle 47A	2.76458053	0	0	0	2.76458053
Leg Muscle 47B	3.08980434	0	0	0	3.08980434
Leg Muscle 48A	0.51378001	0	0	0	0.51378001
Leg Muscle 48B	0.24412565	0	0	0	0.24412565
Leg Muscle 4A	2.24806954	0	0	0	2.24806954
Leg Muscle 4B	2.7794228	0	0	0	2.7794228
Leg Muscle 6A	4.63173806	0	0	0	4.63173806
Leg Muscle 6B	5.3055771	0	0	0	5.3055771
Leg Muscle 7A	1.24105122	0	0	0	1.24105122
Leg Muscle 7B	1.29341475	0	0	0	1.29341475
Leg Muscle 8A	0.96082917	0	0	0	0.96082917
Leg Muscle 8B	3.27289858	0	0	0	3.27289858
Leg Muscle 9A	3.0856485	0	0	0	3.0856485
Leg Muscle 9B	6.11335279	0	0	0	6.11335279

nmol g wwt					
Diet 1	IP3	IP4	IP5	IP6	Total
Breast Muscle 4A	8.52684112	0.60272675	0	0	9.12956787
Breast Muscle 4B	7.03009664	0	0	0	7.03009664
Breast Muscle 16A	3.0574524	0	0	0	3.0574524
Breast Muscle 16B	13.5311348	2.30533058	0	0	15.8364653
Breast Muscle 19A	7.9252907	0.64992736	0	0	8.57521806
Breast Muscle 19B	0.56478982	0	0	0	0.56478982
Breast Muscle 25A	8.87430228	1.27765132	0	0	10.1519536
Breast Muscle 25B	1.04194237	0	0	0	1.04194237
Breast Muscle 38A	15.6729542	1.39484411	0	0	17.0677983
Breast Muscle 38B	4.91474482	0	0	0	4.91474482
Breast Muscle 41A	5.95095254	0	0	0	5.95095254
Breast Muscle 41B	24.3086067	2.50324964	0	0	26.8118563
Breast Muscle 7A	2.49178033	0	0	0	2.49178033
Breast Muscle 7B	11.7232486	0	0	0	11.7232486
Breast Muscle 13A	2.30283086	0	0	0	2.30283086
Breast Muscle 13B	3.8042807	0	0	0	3.8042807
Breast Muscle 23A	4.36377699	0	0	0	4.36377699
Breast Muscle 23B	1.62334798	0	0	0	1.62334798
Breast Muscle 26A	21.4908334	2.75792706	0	0	24.2487604
Breast Muscle 26B	3.43888036	0	0	0	3.43888036
Breast Muscle 35A	12.5621254	1.44483852	0	0	14.0069639
Breast Muscle 35B	6.30826555	0	0	0	6.30826555
Breast Muscle 46A	6.25136014	0	0	0	6.25136014
Breast Muscle 46B	3.39315018	0	0	0	3.39315018
Breast Muscle 1A	7.78942354	0	0	0	7.78942354
Breast Muscle 1B	2.86982631	0	0	0	2.86982631
Breast Muscle 9A	11.1289032	0	0	0	11.1289032
Breast Muscle 9B	2.28959705	0	0	0	2.28959705
Breast Muscle 24A	4.11454014	0	0	0	4.11454014
Breast Muscle 24B	11.034355	1.26015328	0	0	12.2945083
Breast Muscle 27A	4.04342094	0	0	0	4.04342094
Breast Muscle 27B	5.08531399	0	0	0	5.08531399
Breast Muscle 34A	7.85323993	1.11090525	0	0	8.96414518
Breast Muscle 34B	4.20305966	0	0	0	4.20305966
Breast Muscle 48A	4.58728142	0	0	0	4.58728142
Breast Muscle 48B	0.70727389	0	0	0	0.70727389
Breast Muscle 3A	9.4786465	0.94092425	0	0	10.4195708
Breast Muscle 3B	9.76023268	0	0	0	9.76023268
Breast Muscle 15A	8.75652133	0	0	0	8.75652133
Breast Muscle 15B	11.0017116	0	0	0	11.0017116

nmol g wwt					
Diet 1	IP3	IP4	IP5	IP6	Total
Breast Muscle 29A	5.11369318	0	0	0	5.11369318
Breast Muscle 29B	3.54872103	0	0	0	3.54872103
Breast Muscle 20A	6.0715273	0.82461372	0	0	6.89614102
Breast Muscle 20B	8.39641452	0	0	0	8.39641452
Breast Muscle 40A	8.60153865	0	0	0	8.60153865
Breast Muscle 40B	4.25099548	0	0	0	4.25099548
Breast Muscle 45A	6.48442233	0	0	0	6.48442233
Breast Muscle 45B	7.89529406	0	0	0	7.89529406
Breast Muscle 8A	7.16361113	0	0	0	7.16361113
Breast Muscle 8B	13.7347885	0.95474623	0	0	14.6895347
Breast Muscle 10A	8.4508202	0	0	0	8.4508202
Breast Muscle 10B	15.8294073	0.87049095	0	0	16.6998982
Breast Muscle 18A	15.4006317	0.62213635	0	0	16.022768
Breast Muscle 18B	10.9792141	0	0	0	10.9792141
Breast Muscle 32A	9.28381534	0	0	0	9.28381534
Breast Muscle 32B	16.1467248	0.96033385	0	0	17.1070586
Breast Muscle 39A	12.5578612	0.67183668	0	0	13.2296979
Breast Muscle 39B	19.7802893	2.20754739	0	0	21.9878367
Breast Muscle 43A	13.1000065	0.52053006	0	0	13.6205365
Breast Muscle 43B	2.90982184	0	0	0	2.90982184
Breast Muscle 6A	3.10935837	0	0	0	3.10935837
Breast Muscle 6B	3.93279575	0	0	0	3.93279575
Breast Muscle 12A	10.4657421	0	0	0	10.4657421
Breast Muscle 12B	2.0209506	0	0	0	2.0209506
Breast Muscle 22A	7.02259747	0.4946506	0	0	7.51724807
Breast Muscle 22B	5.13751404	0	0	0	5.13751404
Breast Muscle 30A	7.24786641	0	0	0	7.24786641
Breast Muscle 30B	0.75800352	0	0	0	0.75800352
Breast Muscle 33A	1.38175733	0	0	0	1.38175733
Breast Muscle 33B	5.48659267	0	0	0	5.48659267
Breast Muscle 47A	13.1010358	0	0	0	13.1010358
Breast Muscle 47B	5.45674307	0	0	0	5.45674307
Breast Muscle 5A	0	0	0	3.56805979	3.56805979
Breast Muscle 5B	5.56500345	0	0	0	5.56500345
Breast Muscle 14A	12.6124691	1.0618804	0	0	13.6743495
Breast Muscle 14B	5.02481754	0	0	0	5.02481754
Breast Muscle 21A	8.42107748	1.72822773	0	0	10.1493052
Breast Muscle 21B	4.17394931	0.77860738	0	0	4.95255669
Breast Muscle 31A	6.44708417	1.15591131	0	0	7.60299548
Breast Muscle 31B	6.33600443	0.80286919	0	0	7.13887362

nmol g wwt					
Diet 1	IP3	IP4	IP5	IP6	Total
Breast Muscle 37A	3.0837416	0.38150057	0	0	3.46524217
Breast Muscle 37B	5.98886383	0.61113532	0	0	6.59999915
Breast Muscle 44A	4.86941081	0	0	0	4.86941081
Breast Muscle 44B	8.3831766	0.74805061	0	0	9.13122721
Breast Muscle 2A	7.97466018	0.72234621	0	0	8.69700639
Breast Muscle 2B	6.91461581	0.39002499	0	0	7.30464079
Breast Muscle 11A	6.77402845	0	0	0	6.77402845
Breast Muscle 11B	2.79496049	0	0	0	2.79496049
Breast Muscle 17A	10.2683848	0.84299953	0	0	11.1113843
Breast Muscle 17B	4.07585291	0	0	0	4.07585291
Breast Muscle 28A	2.04140179	0	0	0	2.04140179
Breast Muscle 28B	1.53636272	0	0	0	1.53636272
Breast Muscle 36A	0.78621378	0	0	0	0.78621378
Breast Muscle 36B	6.02610899	0.91329321	0	0	6.9394022
Breast Muscle 42A	6.74097993	0	0	0	6.74097993
Breast Muscle 42B	8.99903313	0.72772315	0	0	9.72675628

nmol/g wwt	IP3	IP4	IP5	IP6	Total
Brain 10A	7.94769057	2.29643895	7.94471858	1.3798066	19.5686547
Brain 10B	11.2728976	3.16391905	15.9467052	1.84058039	32.2241023
Brain 12A	5.3622821	1.44061822	3.30520319	2.62484458	12.7329481
Brain 12B	6.11133957	1.42392932	4.94986042	2.73035046	15.2154798
Brain 13A	8.74887228	1.34928648	8.72852554	3.42865536	22.2553397
Brain 13B	6.19478409	1.5536684	4.74467834	0	12.4931308
Brain 15A	7.89705232	1.3737483	2.5662048	2.26043207	14.0974375
Brain 15B	16.129826	2.10577393	9.78221266	3.51164265	31.5294552
Brain 16A	8.91598994	1.99786759	13.3392354	2.95050683	27.2035998
Brain 16B	6.31332103	0.69590445	3.43951458	2.73320815	13.1819482
Brain 18A	6.20438592	0.96018353	3.89457299	1.90813616	12.9672786
Brain 18B	3.12116802	1.76536601	5.79847977	0.8433612	11.528375
Brain 19A	8.31964738	0.66104064	5.7521852	2.69331481	17.426188
Brain 19B	8.53888929	1.06534649	6.70768213	0.48283515	16.7947531
Brain 1A	1.88927541	0	2.01752849	1.0277393	4.9345432
Brain 1B	5.55146112	0.80895463	3.19032409	3.83593321	13.3866731
Brain 20A	13.335006	0.47403347	4.47879895	2.29369557	20.581534
Brain 20B	6.89194592	2.58575139	5.90524303	2.33027399	17.7132143
Brain 22A	13.4767474	1.84412392	10.3934152	3.48980991	29.2040964
Brain 22B	4.35660416	0.73945563	6.16266366	1.75233495	13.0110584
Brain 23A	8.6886322	0.69338968	6.32898117	3.16243305	18.8734361
Brain 23B	6.16494981	1.45925035	5.9092438	1.47731095	15.0107549
Brain 24A	14.5843877	2.38514162	8.31564662	2.42217727	27.7073532
Brain 24B	6.87674301	1.92082429	4.911796	1.74776264	15.4571259
Brain 25A	12.4142586	1.07186202	5.75538582	3.23113189	22.4726383
Brain 25B	5.3622821	0.67029955	5.47636105	2.31621416	13.8251569
Brain 26A	2.89095258	0.59668548	1.67723488	0.80838309	5.97325603
Brain 26B	6.37276096	1.21943309	8.40194883	1.86595666	17.8600995
Brain 27A	5.10909085	0.78152081	4.03357099	3.03052212	12.9547048
Brain 27B	7.57527653	0.73408317	7.54887148	2.99794446	18.8561757
Brain 29A	11.2312896	1.71209868	11.6521701	4.4086141	29.0041725
Brain 29B	9.6649331	1.31510852	8.52151454	2.61672874	22.1182849
Brain 30A	5.46824522	1.01470824	4.57241684	1.59539066	12.650761
Brain 30B	4.19211558	0.90085791	7.33168711	2.22476811	14.6494287
Brain 32A	6.80415771	0	3.36612913	2.48664673	12.6569336
Brain 32B	1.07060464	0	0.68687415	0	1.75747879
Brain 33A	7.87979188	2.10120163	4.74970787	3.59897363	18.329675
Brain 33B	6.31229226	0.68527384	4.63037078	2.20556444	13.8335013
Brain 34A	6.61520731	1.81543272	11.3231929	4.29704992	24.0508829
Brain 34B	9.20941746	2.14429558	4.91076723	3.57062536	19.8351056
Brain 35A	11.82386	1.50428753	9.56034168	4.67335042	27.5618397

nmol/g ww	IP3	IP4	IP5	IP6	Total
Brain 35B	3.84770689	0.76140268	4.6670635	1.83372193	11.109895
Brain 38A	5.25597607	1.15850715	6.15443352	3.96109999	16.5300167
Brain 38B	5.42618003	0.57473843	4.75942402	1.53446473	12.2948072
Brain 39A	5.39760314	0.73499763	7.27624795	2.93141746	16.3402662
Brain 39B	8.50231087	1.16387961	6.9823632	2.45109708	19.0996508
Brain 3A	4.2029748	0	2.51213732	0	6.71511212
Brain 3B	6.59908994	1.01299363	6.47940992	0.97470059	15.0661941
Brain 40A	5.70063249	0.91491774	5.34319274	1.86401344	13.8227564
Brain 40B	8.37622963	1.1289015	3.71956811	1.6882084	14.9129076
Brain 41A	10.169601	0.88874131	6.15088998	3.54342016	20.7526524
Brain 41B	3.7692919	0.34418007	4.42290255	2.16612833	10.7025028
Brain 43A	9.96064676	1.20868817	6.0226369	2.02998802	19.2219599
Brain 43B	4.07346433	0.85662088	7.978325	0.75008623	13.6584964
Brain 45A	6.84142197	1.40243949	14.1312725	4.10855675	26.4836907
Brain 45B	9.84039521	0.61840392	6.19249794	1.48519817	18.1364952
Brain 46A	8.43909879	0.74242762	7.52052321	2.7204057	19.4224553
Brain 46B	3.26462401	0.63852205	4.26778719	0.94200863	9.11294187
Brain 47A	3.87022548	2.50184964	4.36094785	1.14067517	11.8736981
Brain 47B	7.75542525	0.68538815	8.20282505	3.20975638	19.8533948
Brain 48A	6.18232456	1.25566858	14.7076113	1.87544419	24.0210486
Brain 48B	8.34662397	1.45822159	9.81890539	2.67342529	22.2971762
Brain 4A	9.17066719	1.18776989	4.12501704	2.98902847	17.4724826
Brain 4B	10.8500739	2.83848541	5.92261778	0	19.6111771
Brain 6A	3.97344521	0.85010535	3.39241987	2.00026805	10.2162385
Brain 6B	9.32726856	1.41021241	5.11206285	3.40110724	19.2506511
Brain 7A	3.57302582	0	2.54437205	0	6.11739787
Brain 7B	4.60190819	0.28576891	2.28169327	0	7.16937037
Brain 8A	4.94643119	0.45151488	4.6654632	2.49201919	12.5554285
Brain 8B	5.66679745	0.56285044	2.11983376	0.70950705	9.0589887
Brain 9A	4.80789042	0.60880208	4.839325	1.93316951	12.189187
Brain 9B	3.28039845	0	1.55732624	3.12562601	7.96335071
Brain 11A	11.1997788	1.55144652	7.70708078	2.39763308	22.8559392
Brain 11B	5.4914988	0.8484434	3.10715594	1.10133394	10.5484321
Brain 14A	2.94441329	0	1.29554686	0	4.23996015
Brain 14B	6.82365649	0.15296305	4.03847522	0.81258485	11.8276796
Brain 17A	3.74270487	0	2.22197634	2.43838144	8.40306265
Brain 17B	8.03193919	0	3.27516454	2.27513727	13.582241
Brain 21A	12.1964209	1.09255738	2.44339662	1.38882925	17.1212041
Brain 21B	6.82491028	1.33341149	7.3808432	2.60062257	18.1397875
Brain 28A	10.1707889	2.21282363	6.83331071	3.35452979	22.571453
Brain 28B	11.359387	2.07440461	5.00427388	2.30397456	20.74204

nmol/g wwt	IP3	IP4	IP5	IP6	Total
Brain 2A	8.47039146	1.98488361	5.51770312	3.23404005	19.2070182
Brain 2B	3.79436124	0.68457233	2.56789851	1.45665958	8.50349166
Brain 31B	7.4396462	0.83427551	4.49498215	1.37491212	14.143816
Brain 36A	10.5900581	1.71606987	6.7205945	3.722268	22.7489905
Brain 36B	4.51767585	1.57276104	5.79353813	1.98688969	13.8708647
Brain 37A	10.4646785	0	5.99590072	1.43145829	17.8920376
Brain 37B	5.52284368	0.54715634	3.28983394	1.69262389	11.0524579
Brain 42A	7.25496213	2.65854792	11.8506241	3.41132673	25.1754608
Brain 42B	4.50087499	1.878311	3.28105738	2.19125835	11.8515017
Brain 44A	5.48109229	0.32172392	3.73568361	2.92585712	12.4643569
Brain 44B	7.08795657	1.06246628	2.23664575	2.01447319	12.4015418
Brain 5A	6.86490636	1.75092538	1.5950786	2.62256399	12.8334743
Brain 5B	5.51256256	0.9973943	4.82360195	0.59505133	11.9286101

nmol g wwt						
Chromatogram	IP2	IP3	IP4	IP5	IP6	Total
Kidney 1A	0	1.1110767	2.47985182	4.45719171	1.9030038	9.95112402
Kidney 3A	0.98966109	1.19012073	6.55941621	9.51947915	5.67580794	23.9344851
Kidney 4A	3.02485923	4.08340509	40.1900526	57.4646439	7.41762632	112.180587
Kidney 6A	0	0.46707841	8.53229593	10.9686611	1.40123522	21.3692707
Kidney 7A	0.82203322	1.26643912	7.22422861	16.142081	9.40016973	34.8549517
Kidney 8A	0	3.05546091	9.70556715	12.8045147	3.01234598	28.5778887
Kidney 9A	0	2.28310898	12.7217538	11.035068	4.85464198	30.8945728
Kidney 10A	0.90008611	0.72824585	17.8318642	40.1904243	3.00516016	62.6557806
Kidney 13A	0	0.75513074	7.55799763	28.1860137	8.20769502	44.7068371
Kidney 15A	1.05235119	4.65938586	11.1395102	23.229779	6.72543347	46.8064598
Kidney 16A	1.20127115	12.6047984	71.4750138	97.3020957	19.8559119	202.439091
Kidney 18A	0	0.85796232	4.58876658	16.3448947	3.82645002	25.6180736
Kidney 19A	1.55796047	2.76109001	12.1719146	27.7687404	13.24731	57.5070155
Kidney 20A	1.80463238	1.39516444	18.3468893	29.4411785	24.0384318	75.0262964
Kidney 22A	1.43865105	2.80655892	18.119297	27.8801207	9.00755131	59.252179
Kidney 23A	0.61835234	0.90615689	10.6949805	31.5795799	7.26523735	51.0643069
Kidney 24A	0.58849401	0.4729014	14.1481394	27.5546525	9.15634737	51.9205347
Kidney 25A	0.73580336	1.75643781	17.6928557	28.2210755	8.78714481	57.1933172
Kidney 26A	1.02038667	0.61686562	14.1216262	23.8880251	7.00233539	46.649239
Kidney 27A	0.72725471	0.29610541	4.89267728	15.1572518	4.86219948	25.9354887
Kidney 29A	0.89017463	2.91050555	29.7236556	45.2001809	15.6667018	94.3912184
Kidney 33A	1.25194358	3.85160039	11.7384113	58.3923583	11.5473676	86.7816811
Kidney 34A	2.14893235	0.81236952	19.5491516	22.1607022	6.78899083	51.4601466
Kidney 35A	2.16243674	1.05817418	25.2045172	27.0448309	8.23705778	63.7070167
Kidney 38A	0.98606818	0.8849711	9.63519566	26.4301953	12.7148158	50.6512461
Kidney 39A	0.75599799	1.08666968	22.412206	38.7247644	8.44470324	71.4243414
Kidney 40A	1.64357086	1.07849271	25.601348	25.6050648	9.75921303	63.6876893
Kidney 41A	1.44633244	2.63397531	31.2055455	33.236779	23.6502735	92.1729057
Kidney 43A	0.19265436	0.94233378	6.02097517	13.9907947	12.7709395	33.9176976
Kidney 45A	1.90064982	0.95608596	20.9663691	65.0543583	18.8252421	107.702705
Kidney 46A	1.29456293	1.18243934	15.6963123	33.2186906	31.5705357	82.9625408
Kidney 48A	1.48858012	1.11504129	7.42989178	8.4625439	6.38039014	24.8764472
Kidney 1B	1.5117482	1.07056353	8.98054253	11.679438	5.29756116	28.5398534
Kidney 3B	2.39213524	2.307516	7.39644054	21.1773597	11.7390308	45.0124823
Kidney 4B	1.03550168	2.32548055	40.7017327	22.5012854	8.80994121	75.3739415
Kidney 6B	0	0.21433571	4.91225245	2.9987177	4.36315656	12.4884624
Kidney 7B	1.29010277	0.86390921	9.82834559	34.4047228	5.9387099	52.3257903
Kidney 8B	0.35346809	0.61736119	10.4823793	9.20863042	3.54508793	24.2069269
Kidney 10B	0	0.41553872	6.25364711	7.63282929	3.57965421	17.8816693
Kidney 12B	1.6218895	2.18102076	16.2740276	39.075383	11.2048021	70.3571229

nmol g wwt						
Chromatogram	IP2	IP3	IP4	IP5	IP6	Total
Kidney 13B	1.03351938	1.21886402	16.7368936	32.2213481	12.8084793	64.0191044
Kidney 15B	1.79571205	0.85771454	26.3263726	30.8550508	9.52208091	69.3569309
Kidney 16B	2.00001239	6.86184019	43.6656363	50.8912277	27.2428126	130.661529
Kidney 18B	0.57214007	1.49675709	9.50572698	19.3723556	6.80980493	37.7567847
Kidney 19B	1.41511129	2.18535703	15.2455878	43.8654765	9.36572735	72.07726
Kidney 20B	2.14236599	1.19581983	15.840896	27.4671837	10.2497073	56.8959728
Kidney 22B	2.38953348	1.0825812	15.1810393	33.8268836	10.911794	63.3918317
Kidney 23B	0.08883162	1.02026278	17.9639346	51.6754734	8.39663258	79.145135
Kidney 25B	1.08481128	1.21787287	15.3736937	35.9686302	10.5560959	64.2011039
Kidney 26B	1.04194414	1.84725173	11.3673504	21.299147	15.2386498	50.794343
Kidney 27B	0.61760898	0.59778602	13.5930967	27.3311487	6.11748818	48.2571285
Kidney 29B	0.97330715	0.90182061	18.0491733	28.9765779	7.66950176	56.5703808
Kidney 32B	0.28768065	0.49978628	7.22967992	21.3851291	4.12639612	33.528672
Kidney 33B	1.09038649	1.52921718	21.8113226	17.0803263	5.69922381	47.2104764
Kidney 34B	0.2809904	0.57461794	4.91906659	4.58405863	1.5383853	11.8971189
Kidney 38B	1.81714562	1.4566156	10.4134945	32.1344988	32.3592415	78.180996
Kidney 39B	0.27467184	0.77544927	8.17003141	11.3205186	5.22570294	25.7663741
Kidney 40B	0.58291881	1.87203043	21.2794479	61.6947389	18.1749252	103.604061
Kidney 41B	1.00923626	0.78548464	15.8744711	33.0172398	11.2912798	61.9777116
Kidney 43B	0.42520241	0.91197988	9.63680627	21.9241896	15.660631	48.5588091
Kidney 45B	1.29171338	2.07187061	19.3749574	46.7837873	15.8918162	85.4141449
Kidney 46B	0.61240545	1.20882865	28.4570926	52.900656	9.95682312	93.1358058
Kidney 47B	1.89482683	4.04041405	27.1008307	31.3168018	8.51941101	72.8722844
Kidney 48B	0	1.40472565	4.12604581	5.02267433	0.99127519	11.544721
Kidney 11A	0	1.79593664	25.0241277	42.5569529	6.13218828	75.5092055
Kidney 11B	0	0.71654411	2.61955488	12.9015554	5.83115199	22.0688064
Kidney 14A	0	2.46822177	11.2251055	31.5500078	5.95026256	51.1935976
Kidney 14B	0	1.73675749	8.55665259	3.59776611	4.0379737	17.9291499
Kidney 17A	0	1.29642452	18.0048791	10.6069843	4.59942332	34.5077113
Kidney 17B	0	0.65485738	6.12805076	8.13412352	4.21413197	19.1311636
Kidney 21A	0	2.26786525	9.4951185	5.87164958	5.38555308	23.0201864
Kidney 21B	0	1.47772335	7.12093139	9.58175577	7.3532597	25.5336702
Kidney 28A	0	0.7595493	3.51037657	8.3610605	2.96234257	15.5933289
Kidney 28B	0	2.17044535	4.41799911	4.5431279	1.76960693	12.9011793
Kidney 2A	0	1.04679384	7.91796918	4.74699504	2.63585422	16.3476123
Kidney 2B	0	2.45543306	7.76513151	7.05498175	4.16661312	21.4421594
Kidney 31A	0	1.28940327	9.40797972	25.7474423	4.14442094	40.5892463
Kidney 31B	0	0.72732675	6.97223125	18.4687835	3.93240412	30.1007456
Kidney 36A	0	0.48020367	4.30440524	13.5712076	6.72134678	25.0771633
Kidney 36B	0	0.75942392	8.3052666	18.4979969	21.457205	49.0198924

nmol g wwt						
Chromatogram	IP2	IP3	IP4	IP5	IP6	Total
Kidney 37A	0	0.66852375	10.6632797	15.0597136	4.6326489	31.024166
Kidney 37B	0	1.08841985	9.59404297	10.512072	1.4240609	22.6185957
Kidney 42A	0	1.83154443	17.9375503	28.1576134	4.86811169	52.7948198
Kidney 42B	0	0.83540392	2.67259043	17.3224383	5.26192885	26.0923615
Kidney 44A	0	0.53863054	8.59627253	14.894338	20.715585	44.744826
Kidney 44B	0	0.15221077	6.58944749	9.29839799	5.54980029	21.5898565
Kidney 5A	0	1.79994878	4.75740155	15.2934211	13.5990418	35.4498132
Kidney 5B	0	1.10509533	9.54853019	27.8948178	12.3594143	50.9078576

nmol g ww					
Diet 1	IP3	IP4	IP5	IP6	Total
Liver 4A	1.61595828	1.20854167	13.5526846	3.14830909	19.5254936
Liver 4B	2.38818504	3.19857237	35.4282027	13.5218103	54.5367705
Liver 16A	1.6772128	1.12048831	7.7384457	2.71804554	13.2541923
Liver 16B	2.36299165	2.23443127	16.4101582	9.54347789	30.5510591
Liver 19A	2.19343027	1.99361212	25.607721	12.1054232	41.9001866
Liver 19B	2.12649489	1.09788836	25.2635349	9.3369909	37.824909
Liver 25A	1.4502253	0	2.82363547	0.9228931	5.19675388
Liver 25B	2.03597159	2.14576043	60.5593488	8.28998331	73.0310641
Liver 38A	3.13521841	3.01592031	25.771972	10.4085744	42.3316852
Liver 38B	2.46117177	2.79498417	19.5259876	17.5642377	42.3463813
Liver 41A	2.5918316	1.31351412	21.7594309	9.00021458	34.6649912
Liver 41B	2.15477571	1.99311813	28.3289775	9.98016329	42.4570346
Liver 7A	3.07149396	1.89283856	23.1816224	8.08349632	36.2294513
Liver 7B	1.56754746	2.35409987	12.566067	1.19162258	17.6793369
Liver 13A	1.66560408	0	2.84067806	0.54968516	5.0559673
Liver 13B	1.66362813	1.55470377	26.9677935	8.2451539	38.4312793
Liver 23A	6.03184061	1.35365065	20.9889331	6.47840578	34.8528302
Liver 23B	2.33693379	3.30255685	22.5877253	5.46227244	33.6894884
Liver 26A	1.75402793	1.12246426	16.4110227	4.02340886	23.3109238
Liver 26B	2.67494508	1.39168773	18.317199	13.4373384	35.8211702
Liver 35B	1.39613362	0.6018009	9.15853773	7.39500053	18.5514728
Liver 35A	1.62853986	0	8.38720315	3.64904035	13.6647834
Liver 46A	1.19285755	0.5893277	4.83120275	1.19594498	7.80933298
Liver 46B	2.37521786	1.77292297	15.3374633	6.82148045	26.3070846
Liver 1A	0.84422551	0	1.80676115	3.1643637	5.81535037
Liver 1B	1.66424561	3.15250799	43.9281309	13.0163371	61.7612216
Liver 9A	2.4475871	1.10307523	11.9646366	10.4074629	25.9227619
Liver 9B	3.21018109	2.00287439	17.0071428	9.85888924	32.0790875
Liver 24A	1.22867168	0	2.45215649	0	3.68082817
Liver 24B	1.92877619	2.68210791	34.8496192	8.56525813	48.0257615
Liver 27A	1.55680322	3.20351225	29.5900054	10.0102966	44.3606174
Liver 7B	2.20590347	2.76398642	48.4232983	10.323485	63.7166732
Liver 34A	2.48019031	1.37785606	12.4613416	10.0084441	26.3278321
Liver 34B	2.01127219	1.39736859	10.0924221	6.25561718	19.75668
Liver 48A	2.17218878	2.04548086	9.3125385	5.38446933	18.9146775
Liver 48B	2.17614069	0.78321799	10.8112981	5.40669879	19.1773556
Liver 3A	0.59199887	0	11.9339382	1.75416387	14.280101
Liver 3B	1.35859053	3.20820514	15.8908533	5.06535307	25.5230021
Liver 15A	1.67461936	1.17692644	26.7725448	9.13420882	38.7582994
Liver 15B	2.50402523	1.8293611	17.1867074	11.0344572	32.5545509

nmol g ww					
Diet 1	IP3	IP4	IP5	IP6	Total
Liver 20A	2.74682034	0.97476184	17.3500939	6.02097288	27.092649
Liver 20B	1.90555875	2.47796736	19.923401	8.89561261	33.2025397
Liver 29A	2.12933532	1.37069323	31.6096754	6.98165606	42.09136
Liver 29B	2.40794456	1.34710531	23.4438065	7.21099	34.4098464
Liver 40A	2.58380429	1.88777519	11.4076652	9.61819358	25.4974382
Liver 40B	2.21578323	1.7225362	11.5801905	6.64821416	22.166724
Liver 45A	2.67692103	2.1509473	21.056239	8.2656544	34.1497617
Liver 45B	3.03148093	1.72340068	17.8091323	14.5470825	37.1110964
Liver 8A	2.43400243	1.05256496	23.6125035	0.99081645	28.0898873
Liver 8B	2.9626931	1.00736505	11.2140218	2.7320007	17.9160807
Liver 10A	1.55433328	0.62575931	12.834426	3.06754205	18.0820607
Liver 10B	1.5535923	0	9.97312396	4.94506699	16.4717833
Liver 18A	2.32680703	1.08492117	15.0570016	22.6991196	41.1678494
Liver 18B	2.03337815	2.80387595	28.2016521	8.3975492	41.4364554
Liver 32A	2.02757379	0.85855116	23.4052755	8.73383154	35.025232
Liver 32B	2.32964746	1.74377768	13.8773582	9.40787818	27.3586615
Liver 39A	3.98994117	0.69195371	8.82336687	2.61307308	16.1183348
Liver 39B	2.16267951	0.80804089	13.927498	7.40648575	24.3047042
Liver 43A	3.38974574	0.97809626	10.4429066	5.33679948	20.147548
Liver 43B	2.23937115	2.37311841	16.5256279	8.30998983	29.4481073
Liver 6A	1.76563665	1.41243522	7.55604062	4.96606148	15.700174
Liver 6B	1.16507073	0.42371822	9.86950998	3.93251506	15.390814
Liver 12B	2.8216822	1.63185477	29.4267676	8.25266315	42.1329677
Liver 12A	1.21866842	0	8.83559307	0.72035802	10.7746195
Liver 22A	2.11859108	0.85151183	8.5253686	3.76344767	15.2589192
Liver 22B	1.76477217	1.58150262	29.7421537	5.09684481	38.1852733
Liver 30A	1.95347559	1.72105423	31.0007117	8.20230044	42.8775419
Liver 30B	1.64856149	2.94478603	35.8994673	9.75786869	50.2506835
Liver 33A	2.58602724	1.53086885	28.5710316	7.16937151	39.8572992
Liver 33B	2.04350491	1.1866827	12.8021933	5.30259081	21.3349717
Liver 47A	1.4505958	0.94858048	11.1490624	2.71656357	16.2648023
Liver 47B	2.51674542	2.26518203	15.265835	9.92298418	29.9707466
Liver 5A	0	0.81597009	3.7228949	1.9892719	6.52813689
Liver 5B	0.71779791	0.52032512	2.22009565	1.61601699	5.07423566
Liver 14A	1.53238883	1.25993907	3.66409189	2.86065975	9.31707955
Liver 14B	0	0.47243013	2.30196849	1.19436557	3.96876419
Liver 21A	0.44635119	0.68382005	3.52629977	2.45618533	7.11265634
Liver 21B	0.68933675	0.54502489	7.09786156	2.02738728	10.3596105
Liver 31A	0.53750212	0.75804474	11.1659264	2.61178135	15.0732546
Liver 31B	0.48007829	1.66290894	5.17265861	3.1356171	10.4512629

nmol g ww					
Diet 1	IP3	IP4	IP5	IP6	Total
Liver 37A	0.82474666	0	6.96094709	4.95048605	12.7361798
Liver 37B	0.32648834	1.99090183	3.46712062	4.09100925	9.87552005
Liver 44A	0.99275526	1.03576044	10.729104	5.90888731	18.666507
Liver 44B	0.59969038	0.35632867	6.59070129	3.29321919	10.8399395
Liver 2A	0.53023011	1.18935039	25.8106336	5.20525729	32.7354714
Liver 2B	1.12452916	1.37077459	12.649041	4.25488032	19.3992251
Liver 11A	0.68281702	0	4.97556196	1.55019272	7.2085717
Liver 11B	0.5253403	1.55270031	11.0456874	3.8270853	16.9508133
Liver 17A	0.71792329	0.63279058	13.6832969	2.24755377	17.2815645
Liver 17B	1.02961684	0.78951501	6.16616614	4.37223558	12.3575336
Liver 28A	0.48935637	1.3309039	7.91282862	4.19657883	13.9296677
Liver 28B	1.32751865	1.42305786	13.4645096	6.70692813	22.9220142
Liver 36A	0.58715242	0.50189433	2.77289407	1.25417161	5.11611243
Liver 36B	0.6320383	1.85461427	10.6310572	4.71301719	17.830727
Liver 42A	0.42829653	2.20304403	8.15468576	4.14417018	14.9301965
Liver 42B	0.713535	1.50505609	6.91204907	3.93002191	13.0606621

Appendix 10: Full ANOVA tables

Gizzard digesta ANOVA:

Inositol:

ANOVA table	SS	DF	MS	F (DFn, DFd)	P value
Treatment (between columns)	1722581	7	246083	F (7, 40) = 22.6	P<0.0001
Residual (within columns)	435593	40	10890		
Total	2158174	47			

InsP2 -

ANOVA table	SS	DF	MS	F (DFn, DFd)	P value
Interaction	55269	3	18423	F (3, 40) = 0.5892	P=0.6257
Titanium	4350	1	4350	F (1, 40) = 0.1391	P=0.7111
Diet	1954940	3	651647	F (3, 40) = 20.84	P<0.0001
Residual	1250770	40	31269		

InsP3 -

ANOVA table	SS	DF	MS	F (DFn, DFd)	P value
Interaction	1304077	3	434692	F (3, 40) = 0.5606	P=0.6441
Titanium	906718	1	906718	F (1, 40) = 1.169	P=0.2860
Diet	24422636	3	8140879	F (3, 40) = 10.5	P<0.0001
Residual	31015211	40	775380		

InsP4 -

ANOVA table	SS	DF	MS	F (DFn, DFd)	P value
Interaction	2404530	3	801510	F (3, 40) = 0.174	P=0.9134
Titanium	2516424	1	2516424	F (1, 40) = 0.5462	P=0.4642
Diet	78929410	3	26309803	F (3, 40) = 5.71	P=0.0024
Residual	184293144	40	4607329		

InsP5 -

ANOVA table	SS	DF	MS	F (DFn, DFd)	P value
Interaction	3979070	3	1326357	F (3, 40) = 1.236	P=0.3094
Titanium	4765416	1	4765416	F (1, 40) = 4.44	P=0.0414
Diet	148566117	3	49522039	F (3, 40) = 46.14	P<0.0001
Residual	42934923	40	1073373		

InsP6 -

ANOVA table	SS	DF	MS	F (DFn, DFd)	P value
Interaction	10586834	3	3528945	F (3, 40) = 0.4232	P=0.7374
Titanium	6620394	1	6620394	F (1, 40) = 0.7939	P=0.3782
Diet	324892877	3	108297626	F (3, 40) = 12.99	P<0.0001
Residual	333553808	40	8338845		

Total InsPs -

ANOVA table	SS	DF	MS	F (DFn, DFd)	P value
Interaction	15713780	3	5237927	F (3, 40) = 0.744	P=0.5322
Titanium	5213943	1	5213943	F (1, 40) = 0.7406	P=0.3946
Diet	1280019813	3	426673271	F (3, 40) = 60.61	P<0.0001
Residual	281603423	40	7040086		

Ileal digesta ANOVA:

Inositol:

ANOVA table	SS	DF	MS	F (DFn, DFd)	P value
Treatment (between columns)	32842005	7	4691715	F (7, 40) = 15.67	P<0.0001
Residual (within columns)	11978130	40	299453		
Total	44820134	47			

InsP2 -

ANOVA table	SS	DF	MS	F (DFn, DFd)	P value
Interaction	10360226	3	3453409	F (3, 40) = 0.8099	P=0.4959
Titanium	1829224	1	1829224	F (1, 40) = 0.429	P=0.5162
Diet	40140005	3	13380002	F (3, 40) = 3.138	P=0.0358
Residual	170565488	40	4264137		

InsP3 -

ANOVA table	SS	DF	MS	F (DFn, DFd)	P value
Interaction	1182594	3	394198	F (3, 40) = 0.4824	P=0.6963
Titanium	4287	1	4287	F (1, 40) = 0.005246	P=0.9426
Diet	30000255	3	10000085	F (3, 40) = 12.24	P<0.0001
Residual	32683500	40	817088		

InsP4 -

ANOVA table	SS	DF	MS	F (DFn, DFd)	P value
Interaction	3766004	3	1255335	F (3, 40) = 0.1583	P=0.9237
Titanium	28979	1	28979	F (1, 40) = 0.003655	P=0.9521
Diet	150683865	3	50227955	F (3, 40) = 6.335	P=0.0013
Residual	317135056	40	7928376		

InsP5 -

ANOVA table	SS	DF	MS	F (DFn, DFd)	P value
Interaction	3121822	3	1040607	F (3, 40) = 0.9171	P=0.4413
Titanium	1367597	1	1367597	F (1, 40) = 1.205	P=0.2788
Diet	217527265	3	72509088	F (3, 40) = 63.9	P<0.0001
Residual	45386543	40	1134664		

InsP6 -

ANOVA table	SS	DF	MS	F (DFn, DFd)	P value
Interaction	166881523	3	55627174	F (3, 40) = 1.264	P=0.2997
Titanium	165988123	1	165988123	F (1, 40) = 3.772	P=0.0592
Diet	19304621229	3	6434873743	F (3, 40) = 146.2	P<0.0001
Residual	1760331782	40	44008295		

Total InsPs -

ANOVA table	SS	DF	MS	F (DFn, DFd)	P value
Interaction	415432776	3	138477592	F (3, 40) = 2.209	P=0.1019
Titanium	48242970	1	48242970	F (1, 40) = 0.7697	P=0.3856
Diet	19067577340	3	6355859113	F (3, 40) = 101.4	P<0.0001
Residual	2507221417	40	62680535		

Kidney ANOVAs:

InsP2:

ANOVA table	SS (Type III)	DF	MS	F (DFn, DFd)	P value
Interaction	2.396	3	0.7986	F (3, 87) = 2.859	P=0.0416
Titanium	0.02545	1	0.02545	F (1, 87) = 0.09111	P=0.7635
Diet	26.39	3	8.797	F (3, 87) = 31.49	P<0.0001
Residual	24.3	87	0.2793		

InsP3:

ANOVA table	SS (Type III)	DF	MS	F (DFn, DFd)	P value
Interaction	16.14	3	5.379	F (3, 87) = 2.109	P=0.1049
Titanium	1.304	1	1.304	F (1, 87) = 0.5111	P=0.4766
Diet	33.7	3	11.23	F (3, 87) = 4.405	P=0.0062
Residual	221.9	87	2.55		

InsP4:

ANOVA table	SS (Type III)	DF	MS	F (DFn, DFd)	P value
Interaction	717	3	239	F (3, 87) = 3.106	P=0.0306
Titanium	47.2	1	47.2	F (1, 87) = 0.6135	P=0.4356
Diet	2569	3	856.4	F (3, 87) = 11.13	P<0.0001
Residual	6694	87	76.94		

InsP5:

ANOVA table	SS (Type III)	DF	MS	F (DFn, DFd)	P value
Interaction	1685	3	561.5	F (3, 87) = 3.013	P=0.0344
Titanium	104.2	1	104.2	F (1, 87) = 0.5591	P=0.4566
Diet	6485	3	2162	F (3, 87) = 11.6	P<0.0001
Residual	16215	87	186.4		

InsP6:

ANOVA table	SS (Type III)	DF	MS	F (DFn, DFd)	P value
Interaction	134.5	3	44.84	F (3, 87) = 1.461	P=0.2309
Titanium	54.99	1	54.99	F (1, 87) = 1.791	P=0.1843
Diet	941.6	3	313.9	F (3, 87) = 10.22	P<0.0001
Residual	2671	87	30.7		

Total InsPs:

ANOVA table	SS (Type III)	DF	MS	F (DFn, DFd)	P value
Interaction	6540	3	2180	F (3, 87) = 3.924	P=0.0112
Titanium	665.4	1	665.4	F (1, 87) = 1.198	P=0.2768
Diet	28397	3	9466	F (3, 87) = 17.04	P<0.0001
Residual	48338	87	555.6		

Inositol:

ANOVA table	SS	DF	MS	F (DFn, DFd)	P value
Treatment (between columns)	555257502	7	79322500	F (7, 85) = 59.63	P<0.0001
Residual (within columns)	113076763	85	1330315		
Total	668334265	92			

Liver ANOVA:

InsP3 –

ANOVA table	SS	DF	MS	F (DFn, DFd)	P value
Interaction	0.2187	3	0.0729	F (3, 88) = 0.1526	P=0.9278
Titanium	0.04364	1	0.04364	F (1, 88) = 0.09136	P=0.7632
Diet	42.01	3	14	F (3, 88) = 29.31	P<0.0001
Residual	42.03	88	0.4777		

InsP4 -

ANOVA table	SS	DF	MS	F (DFn, DFd)	P value
Interaction	1.627	3	0.5423	F (3, 88) = 0.7729	P=0.5122
Titanium	0.1598	1	0.1598	F (1, 88) = 0.2277	P=0.6344
Diet	7.44	3	2.48	F (3, 88) = 3.535	P=0.0180
Residual	61.75	88	0.7017		

InsP5 –

ANOVA table	SS	DF	MS	F (DFn, DFd)	P value
Interaction	274.8	3	91.58	F (3, 88) = 0.9564	P=0.4171
Titanium	0.09479	1	0.09479	F (1, 88) = 0.0009899	P=0.9750
Diet	2461	3	820.4	F (3, 88) = 8.568	P<0.0001
Residual	8427	88	95.76		

InsP6 -

ANOVA table	SS	DF	MS	F (DFn, DFd)	P value
Interaction	44.39	3	14.8	F (3, 88) = 1.13	P=0.3416
Titanium	0.3251	1	0.3251	F (1, 88) = 0.02482	P=0.8752
Diet	307.3	3	102.4	F (3, 88) = 7.82	P=0.0001
Residual	1153	88	13.1		

Total InsPs-

ANOVA table	SS	DF	MS	F (DFn, DFd)	P value
Interaction	500.8	3	166.9	F (3, 88) = 1.053	P=0.3735
Titanium	0.2054	1	0.2054	F (1, 88) = 0.001295	P=0.9714
Diet	5629	3	1876	F (3, 88) = 11.83	P<0.0001
Residual	13955	88	158.6		

Inositols:

ANOVA table	SS	DF	MS	F (DFn, DFd)	P value
Treatment (between columns)	485258942	7	69322706	F (7, 88) = 5.113	P<0.0001
Residual (within columns)	1193128339	88	13558277		
Total	1678387282	95			

Brain ANOVA:

InsP3-

ANOVA table	SS (Type III)	DF	MS	F (DFn, DFd)	P value
Interaction	4.862	3	1.621	F (3, 87) = 0.1913	P=0.9020
Titanium	2.496	1	2.496	F (1, 87) = 0.2946	P=0.5887
Diet	64.26	3	21.42	F (3, 87) = 2.528	P=0.0625
Residual	737	87	8.471		

InsP4-

ANOVA table	SS (Type III)	DF	MS	F (DFn, DFd)	P value
Interaction	1.298	3	0.4326	F (3, 87) = 0.8261	P=0.4830
Titanium	1.987	1	1.987	F (1, 87) = 3.794	P=0.0547
Diet	0.7064	3	0.2355	F (3, 87) = 0.4497	P=0.7181
Residual	45.56	87	0.5236		

InsP5 –

ANOVA table	SS (Type III)	DF	MS	F (DFn, DFd)	P value
Interaction	17.65	3	5.883	F (3, 87) = 0.6424	P=0.5898
Titanium	5.987	1	5.987	F (1, 87) = 0.6538	P=0.4210
Diet	44.83	3	14.94	F (3, 87) = 1.632	P=0.1878
Residual	796.8	87	9.158		

InsP6 –

ANOVA table	SS (Type III)	DF	MS	F (DFn, DFd)	P value
Interaction	4.707	3	1.569	F (3, 87) = 1.366	P=0.2585
Titanium	0.3851	1	0.3851	F (1, 87) = 0.3353	P=0.5640
Diet	10.98	3	3.661	F (3, 87) = 3.188	P=0.0277
Residual	99.92	87	1.149		

Total InsPs –

ANOVA table	SS (Type III)	DF	MS	F (DFn, DFd)	P value
Interaction	67.55	3	22.52	F (3, 87) = 0.5896	P=0.6234
Titanium	36.68	1	36.68	F (1, 87) = 0.9606	P=0.3298
Diet	194.4	3	64.8	F (3, 87) = 1.697	P=0.1736
Residual	3322	87	38.19		

Inositols –

ANOVA table	SS	DF	MS	F (DFn, DFd)	P value
Treatment (between columns)	268444010	7	38349144	F (7, 87) = 3.293	P=0.0037
Residual (within columns)	1013225994	87	11646276		
Total	1281670004	94			

Breast muscle ANOVA:

InsP3-

ANOVA table	SS	DF	MS	F (DFn, DFd)	P value
Interaction	163.8	3	54.59	F (3, 88) = 2.915	P=0.0387
Titanium	23	1	23	F (1, 88) = 1.228	P=0.2708
Diet	256.9	3	85.64	F (3, 88) = 4.573	P=0.0050
Residual	1648	88	18.73		

InsP4 –

ANOVA table	SS	DF	MS	F (DFn, DFd)	P value
Interaction	1.991	3	0.6637	F (3, 88) = 1.857	P=0.1428
Titanium	1.023	1	1.023	F (1, 88) = 2.863	P=0.0942
Diet	1.969	3	0.6563	F (3, 88) = 1.836	P=0.1464
Residual	31.45	88	0.3574		

InsP5 –

ANOVA table	SS	DF	MS	F (DFn, DFd)	P value
Interaction	0	3	0	F (3, 88) =	P=nan
Titanium	0	1	0	F (1, 88) =	P=nan
Diet	0	3	0	F (3, 88) =	P=nan
Residual	0	88	0		

InsP6 –

ANOVA table	SS	DF	MS	F (DFn, DFd)	P value
Interaction	0.3978	3	0.1326	F (3, 88) = 1	P=0.3968
Titanium	0.1326	1	0.1326	F (1, 88) = 1	P=0.3201
Diet	0.3978	3	0.1326	F (3, 88) = 1	P=0.3968
Residual	11.67	88	0.1326		

Total InsPs –

ANOVA table	SS	DF	MS	F (DFn, DFd)	P value
Interaction	204.6	3	68.21	F (3, 88) = 3.017	P=0.0341
Titanium	11.69	1	11.69	F (1, 88) = 0.5172	P=0.4739
Diet	276.1	3	92.04	F (3, 88) = 4.071	P=0.0093
Residual	1990	88	22.61		

Inositol –

ANOVA table	SS	DF	MS	F (DFn, DFd)	P value
Treatment (between columns)	485439	7	69348	F (7, 88) = 2.499	P=0.0217
Residual (within columns)	2442131	88	27751		
Total	2927569	95			

Ileal tissue ANOVAs:

InsP3 -

ANOVA table	SS	DF	MS	F (DFn, DFd)	P value
Interaction	15.36	3	5.119	F (3, 88) = 5.671	P=0.0013
Titanium	0.2448	1	0.2448	F (1, 88) = 0.2711	P=0.6039
Diet	2.114	3	0.7048	F (3, 88) = 0.7807	P=0.5078
Residual	79.44	88	0.9027		

InsP4 -

ANOVA table	SS	DF	MS	F (DFn, DFd)	P value
Interaction	580.2	3	193.4	F (3, 88) = 8.288	P<0.0001
Titanium	0.4816	1	0.4816	F (1, 88) = 0.02064	P=0.8861
Diet	149.7	3	49.9	F (3, 88) = 2.138	P=0.1011
Residual	2053	88	23.33		

InsP5 -

ANOVA table	SS	DF	MS	F (DFn, DFd)	P value
Interaction	2092	3	697.2	F (3, 88) = 13.51	P<0.0001
Titanium	28.09	1	28.09	F (1, 88) = 0.5443	P=0.4626
Diet	1416	3	472	F (3, 88) = 9.146	P<0.0001
Residual	4542	88	51.61		

InsP6 -

ANOVA table	SS	DF	MS	F (DFn, DFd)	P value
Interaction	1543	3	514.4	F (3, 88) = 0.5463	P=0.6520
Titanium	3226	1	3226	F (1, 88) = 3.426	P=0.0676
Diet	7357	3	2452	F (3, 88) = 2.604	P=0.0569
Residual	82872	88	941.7		

Total InsPs -

ANOVA table	SS	DF	MS	F (DFn, DFd)	P value
Interaction	4474	3	1491	F (3, 88) = 1.435	P=0.2380
Titanium	3831	1	3831	F (1, 88) = 3.687	P=0.0581
Diet	16289	3	5430	F (3, 88) = 5.225	P=0.0023
Residual	91443	88	1039		

Inositol -

ANOVA table	SS	DF	MS	F (DFn, DFd)	P value
Treatment (between columns)	139010766	7	19858681	F (7, 88) = 6.235	P<0.0001
Residual (within columns)	280260999	88	3184784		
Total	419271764	95			

Duodenum ANOVAs:

InsP3 –

ANOVA table	SS	DF	MS	F (DFn, DFd)	P value
Interaction	11.81	3	3.937	F (3, 88) = 9.1	P<0.0001
Titanium	6.537	1	6.537	F (1, 88) = 15.11	P=0.0002
Diet	21.5	3	7.168	F (3, 88) = 16.57	P<0.0001
Residual	38.08	88	0.4327		

InsP4 –

ANOVA table	SS	DF	MS	F (DFn, DFd)	P value
Interaction	60.35	3	20.12	F (3, 88) = 5.854	P=0.0011
Titanium	0.3099	1	0.3099	F (1, 88) = 0.09017	P=0.7647
Diet	40.96	3	13.65	F (3, 88) = 3.972	P=0.0105
Residual	302.4	88	3.437		

InsP5 –

ANOVA table	SS	DF	MS	F (DFn, DFd)	P value
Interaction	1872	3	623.8	F (3, 88) = 8.567	P<0.0001
Titanium	0.0346	1	0.0346	F (1, 88) = 0.0004751	P=0.9827
Diet	1357	3	452.4	F (3, 88) = 6.213	P=0.0007
Residual	6408	88	72.82		

InsP6 –

ANOVA table	SS	DF	MS	F (DFn, DFd)	P value
Interaction	564.4	3	188.1	F (3, 88) = 1.171	P=0.3253
Titanium	356.6	1	356.6	F (1, 88) = 2.22	P=0.1398
Diet	1844	3	614.6	F (3, 88) = 3.826	P=0.0126
Residual	14135	88	160.6		

Total InsPs –

ANOVA table	SS	DF	MS	F (DFn, DFd)	P value
Interaction	5822	3	1941	F (3, 88) = 5.935	P=0.0010
Titanium	443.9	1	443.9	F (1, 88) = 1.358	P=0.2471
Diet	3603	3	1201	F (3, 88) = 3.673	P=0.0152
Residual	28774	88	327		

Inositol one-way ANOVA –

ANOVA table	SS	DF	MS	F (DFn, DFd)	P value
Treatment (between columns)	21284337	7	3040620	F (7, 87) = 4.845	P=0.0001
Residual (within columns)	54598162	87	627565		
Total	75882499	94			

Jejunum ANOVAs:

InsP3 -

ANOVA table	SS	DF	MS	F (DFn, DFd)	P value
Interaction	10.06	3	3.354	F (3, 88) = 3.681	P=0.0150
Titanium	0.2065	1	0.2065	F (1, 88) = 0.2267	P=0.6352
Diet	1.026	3	0.3421	F (3, 88) = 0.3754	P=0.7709
Residual	80.18	88	0.9111		

InsP4 -

ANOVA table	SS	DF	MS	F (DFn, DFd)	P value
Interaction	73.78	3	24.59	F (3, 88) = 4.435	P=0.0060
Titanium	3.519	1	3.519	F (1, 88) = 0.6345	P=0.4278
Diet	5.021	3	1.674	F (3, 88) = 0.3018	P=0.8240
Residual	488	88	5.546		

InsP5 -

ANOVA table	SS	DF	MS	F (DFn, DFd)	P value
Interaction	640.8	3	213.6	F (3, 88) = 3.175	P=0.0281
Titanium	12.76	1	12.76	F (1, 88) = 0.1897	P=0.6642
Diet	558.4	3	186.1	F (3, 88) = 2.767	P=0.0465
Residual	5920	88	67.28		

InsP6 -

ANOVA table	SS	DF	MS	F (DFn, DFd)	P value
Interaction	417.6	3	139.2	F (3, 88) = 0.451	P=0.7172
Titanium	33.15	1	33.15	F (1, 88) = 0.1074	P=0.7439
Diet	8274	3	2758	F (3, 88) = 8.938	P<0.0001
Residual	27155	88	308.6		

Total InsPs -

ANOVA table	SS	DF	MS	F (DFn, DFd)	P value
Interaction	297.1	3	99.05	F (3, 88) = 0.2237	P=0.8797
Titanium	20.38	1	20.38	F (1, 88) = 0.04604	P=0.8306
Diet	12317	3	4106	F (3, 88) = 9.273	P<0.0001
Residual	38962	88	442.8		

Inositol one-way ANOVA -

ANOVA table	SS	DF	MS	F (DFn, DFd)	P value
Treatment (between columns)	43577509	7	6225358	F (7, 88) = 5.03	P<0.0001
Residual (within columns)	108920528	88	1237733		
Total	152498038	95			

Leg muscle ANOVA:

InsP3 –

ANOVA table	SS	DF	MS	F (DFn, DFd)	P value
Interaction	18.68	3	6.226	F (3, 88) = 1.95	P=0.1273
Titanium	4.253	1	4.253	F (1, 88) = 1.332	P=0.2515
Diet	27.95	3	9.317	F (3, 88) = 2.919	P=0.0385
Residual	280.9	88	3.192		

InsP4 –

ANOVA table	SS	DF	MS	F (DFn, DFd)	P value
Interaction	0.005306	3	0.001769	F (3, 88) = 1	P=0.3968
Titanium	0.001769	1	0.001769	F (1, 88) = 1	P=0.3201
Diet	0.005306	3	0.001769	F (3, 88) = 1	P=0.3968
Residual	0.1557	88	0.001769		

InsP5 –

ANOVA table	SS	DF	MS	F (DFn, DFd)	P value
Interaction	1.175	3	0.3916	F (3, 88) = 2.018	P=0.1172
Titanium	0.3916	1	0.3916	F (1, 88) = 2.018	P=0.1589
Diet	1.175	3	0.3916	F (3, 88) = 2.018	P=0.1172
Residual	17.08	88	0.194		

InsP6 –

ANOVA table	SS	DF	MS	F (DFn, DFd)	P value
Interaction	0	3	0	F (3, 88) =	P=nan
Titanium	0	1	0	F (1, 88) =	P=nan
Diet	0	3	0	F (3, 88) =	P=nan
Residual	0	88	0		

Total InsPs –

ANOVA table	SS	DF	MS	F (DFn, DFd)	P value
Interaction	23.68	3	7.892	F (3, 88) = 2.537	P=0.0618
Titanium	1.945	1	1.945	F (1, 88) = 0.625	P=0.4313
Diet	38.82	3	12.94	F (3, 88) = 4.159	P=0.0084
Residual	273.8	88	3.111		

Inositol one-way ANOVA –

ANOVA table	SS	DF	MS	F (DFn, DFd)	P value
Treatment (between columns)	7539082	7	1077012	F (7, 86) = 12.34	P<0.0001
Residual (within columns)	7503136	86	87246		
Total	15042218	93			

References

- Adeola, O. and Cowieson, A. J. (2011) 'BOARD-INVITED REVIEW: Opportunities and challenges in using exogenous enzymes to improve nonruminant animal production', *Journal of Animal Science*, 89(10), pp. 3189–3218.
- Agranoff, B. W. and Fisher, S. K. (2001) 'Inositol, lithium, and the brain.', *Psychopharmacology bulletin*, 35(3), pp. 5–18.
- Ajuwon, K. M., Sommerfeld, V., Paul, V., Däuber, M., Schollenberger, M., Kühn, I., Adeola, O., Rodehutschord, M. (2020) 'Phytase dosing affects phytate degradation and *Muc2* transporter gene expression in broiler starters', *Poultry Science*, 99(2), pp. 981–991.
- Akers, R. M. and Denbow, D. M. (2013) 'Digestive System', in *Anatomy and Physiology of Domestic Animals*. 2nd ed. Hoboken, NJ, USA: John Wiley & Sons, Ltd, pp. 483–527.
- Alaeldein M. Abudabos (2012) 'Intestinal phytase activity in chickens (*Gallus Domesticus*)', *African Journal of Microbiology Research*, 6(23), pp. 4932–4938.
- Anastassiades, M., Lehotay, S.J., Stajnbaher, D., Schenck, F.J. (2003) 'Fast and easy multiresidue method employing acetonitrile extraction/partitioning and "Dispersive Solid-Phase Extraction" for the determination of pesticide residues in produce', *Journal of AOAC International*, 86(2), pp. 412–431.
- Anderson, G. (1964) 'Investigations on the analysis of inositol hexaphosphate in soil', *Transactions of the International Congress of Soil Science*, 4, pp. 563–571.

Andlid, T. A., Veide, J. and Sandberg, A. S. (2004) 'Metabolism of extracellular inositol hexaphosphate (phytate) by *Saccharomyces cerevisiae*', *International Journal of Food Microbiology*, 97(2), pp. 157–169.

Aouameur, R., Da Cal, S., Bissonnette, P., Coady, M.J., Lapointe, J.-Y. (2007) 'SMIT2 mediates all *myo*-inositol uptake in apical membranes of rat small intestine', *American Journal of Physiology - Gastrointestinal and Liver Physiology*, 293(6), pp. 1300–1307.

Arthur, C., Pirgozliev, V., Rose, S., Mansbridge, S., Brearley, C., Kühn, I., Bedford, M. (2019) 'Effect of graded levels of dietary *myo*-inositol and phytase supplementation on growth performance and plasma *myo*-inositol concentrations in broilers', in *British Poultry Abstracts*, pp. 1–45.

Arthur, C., Mansbridge, S. C., Rose, S. P., Brearley, C.A., Whitfield, H., Kühn, I., Pirgozliev, V. (2021) '*myo*-Inositol concentration in chicken tissues is influenced by dietary *myo*-inositol and phytase', in *British Poultry Abstracts*, pp. 1–29.

Arthur, C., Rose, S., Mansbridge, S.C., Brearley, C., Kühn, I., Pirgozliev, V. (2021) 'The correlation between *myo*-inositol (Ins) concentration in the jejunum digesta of broiler chickens and the Ins concentrations of key tissues associated with the uptake and regulation of Ins', *British Poultry Abstracts*, 7(1), pp. 1–29.

Azevedo, C. and Saiardi, A. (2017) 'Eukaryotic Phosphate Homeostasis: The Inositol Pyrophosphate Perspective.', *Trends in biochemical sciences*. Elsevier, 42(3), pp. 219–231.

Bachhawat, N. and Mande, S. C. (2000) 'Complex evolution of the inositol-1-phosphate synthase gene among archaea and eubacteria', *Trends in Genetics*, 16(3), pp. 111–113.

Bampidis, V., Azimonti, G., de Lourdes Bastos, M., Christensen, H., Dusemund, B., Durjava, M.F., Kouba, M., López-Alonso, M., López Puente, S., Marcon, F., Mayo, B., Pechová, A., Petkova, M., Ramos, F., Sanz, Y., Villa, R.E., Woutersen, R. (2021) 'Safety and efficacy of a feed additive consisting of titanium dioxide for all animal species (Titanium Dioxide Manufacturers Association)', *EFSA Journal*, 19(6).

Barrientos, L., Scott, J. J. and Murthy, P. P. N. (1994) 'Specificity of hydrolysis of phytic acid by alkaline phytase from lily pollen', *Plant Physiology*, 106(4), pp. 1489–1495.

Barkai, A., Dunner, D.L., Gross, H.A., Mayo, P., and Fieve, R. R. (1978). 'Reduced *myo*-inositol levels in cerebrospinal fluid from patients with affective disorder.' *Biol. Psychiatry*, 13: 65-72.

Barski, J. J., Hartmann, J., Rose, C.R., Hoebeek, F., Mörl, K., Noll-Hussong, M., De Zeeuw, C.I., Konnerth, A., Meyer, M. (2003) 'Calbindin in cerebellar Purkinje cells is a critical determinant of the precision of motor coordination.', *The Journal of neuroscience : the official journal of the Society for Neuroscience*. Society for Neuroscience, 23(8), pp. 3469–77.

Baylor, S. M., Chandler, W. K. and Marshall, M. W. (1983) 'Sarcoplasmic reticulum calcium release in frog skeletal muscle fibres estimated from Arsenazo III calcium transients', *Journal of Physiology*, 344, pp. 625–666.

Bedford, M. R. (2000) 'Exogenous enzymes in monogastric nutrition - Their current value and future benefits', *Animal Feed Science and Technology*, 86(1–2), pp. 1–13.

Bedford, M. R. and Walk, C. L. (2016) 'Reduction of phytate to tetrakisphosphate (IP₄) to trisphosphate (IP₃) or perhaps even lower, does not remove its antinutritive properties', in Walk, C. L. et al. (eds) *Phytate destruction - consequences for precision animal nutrition*. Wageningen, The

Netherlands: Wageningen Academic Publishers, pp. 45–51.

Beeson, L.A., Walk, C.L., Bedford, M.R., Olukosi, O.A. (2017). 'Hydrolysis of phytate to its lower esters can influence the growth performance and nutrient utilization of broilers with regular or superdoses of phytase.' *Poultry Science* 96(7).

Bergwitz, C. and Jüppner, H. (2010) 'Regulation of phosphate homeostasis by PTH, vitamin D, and FGF23', *Annual Review of Medicine*, 61, pp. 91–104.

Berridge, M. J. (2009) 'Inositol trisphosphate and calcium signalling mechanisms', *Biochimica et Biophysica Acta (BBA) - Molecular Cell Research*, 1793(6), pp. 933–940.

Berridge, M. J. (2016) 'The Inositol Trisphosphate/Calcium Signaling Pathway in Health and Disease', *Physiological Reviews*. American Physiological Society Bethesda, MD, 96(4), pp. 1261–1296.

Berridge, M. J., Downes, C. P. and Hanley, M. R. (1982) 'Lithium amplifies agonist-dependent phosphatidylinositol responses in brain and salivary glands', *Biochemical Journal*, 206(3), pp. 587–595.

Berridge, M. J. and Irvine, R. F. (1989) 'Inositol phosphates and cell signalling', *Nature*, 341, pp. 197–205.

Berridge, M.J., Heslop, J.P., Irvine, R.F., Brown, K.D. (1984) 'Inositol trisphosphate formation and calcium mobilization in Swiss 3T3 cells in response to platelet-derived growth factor.' *Biochem. J.*, 222, pp. 196-201.

Berry, G. T., Mallee, J.J., Kwon, H.M., Rim, J.S., Mulla, W.R., Muekne, M., Spinner, N.B. (1995) 'The human osmoregulatory Na⁺/myo-inositol cotransporter gene (SLC5A3): Molecular cloning and localization to chromosome 21', *Genomics*, 25(2), pp. 507–513.

Berry, G. T., Wang, Z.J., Dreha, S.F., Finucane, B.M., Zimmerman, R.A. (1999) 'In vivo brain myo-inositol levels in children with Down syndrome', *The Journal of Pediatrics*, 135(1), pp. 94–97.

Bio-Rad Laboratories (2015) 'Gel Doc™ XR+ System', *Bio-Rad Laboratories*.

Bio-Rad Laboratories Inc. (2014) 'Handcasting Polyacrylamide Gels'.

Blaabjerg, K., Hansen-Møller, J. and Poulsen, H. D. (2010) 'High-performance ion chromatography method for separation and quantification of inositol phosphates in diets and digesta', *Journal of Chromatography B: Analytical Technologies in the Biomedical and Life Sciences*, 878(3–4), pp. 347–354.

Blaine, J., Chonchol, M. and Levi, M. (2015) 'Renal control of calcium, phosphate, and magnesium homeostasis', *Clinical Journal of the American Society of Nephrology*, 10(7), pp. 1257–1272.

Boerboom, G., van Kempen, T., Navarro-Villa, A., Pérez-Bonilla, A. (2018) 'Unraveling the cause of white striping in broilers using metabolomics', *Poultry Science*, 97(11), pp. 3977–3986.

Boling, S. D., Douglas, M.W., Johnson, M.L., Wang, X., Parsons, C.M., Koelkebeck, K.W., Zimmerman, R.A. (2000) 'The effects of dietary available phosphorus levels and phytase on performance of young and older laying hens', *Poultry Science*, 79(2), pp. 224–230.

Borba, B. De and Rohrer, J. (2016) *Thermo Fisher Scientific Application Note 154: Determination of inorganic anions in environmental waters with a hydroxide-selective column*, Thermo Fisher Scientific. Sunnyvale, CA.

Boyle, I. T., Gray, R. W. and DeLuca, H. F. (1971) 'Regulation by calcium of in vivo synthesis of 1,25-dihydroxycholecalciferol and 21,25-

dihydroxycholecalciferol.', *Proceedings of the National Academy of Sciences of the United States of America*, 68(9), pp. 2131–2134.

Brearley, C. A. and Hanke, D. E. (1996a) 'Inositol phosphates in the duckweed *Spirodela polyrhiza* L', *Biochemical Journal*, 314(1), pp. 215–225.

Brearley, C. A. and Hanke, D. E. (1996b) 'Metabolic evidence for the order of addition of individual phosphate esters to the *myo*-inositol moiety of inositol hexakisphosphate in the duckweed *Spirodela polyrhiza* L', *Biochemical Journal*, 314(1), pp. 227–233.

Brinch-Pedersen, H., Sørensen, L.D., Holm, P.B.. (2002) *Review Review Engineering crop plants: getting a handle on phosphate, TRENDS in Plant Science*.

Brinch-Pedersen, H., Hatzack, F., Sørensen, L.D., Holm, P.B. (2003) 'Concerted action of endogenous and heterologous phytase on phytic acid degradation in seed of transgenic wheat (*Triticum aestivum* L.)', *Transgenic Research*, 12(6), pp. 649–659.

Brooks, H. V., Cook, T.G., Mansell, G.P., Walker, G.A. (1984) 'Phosphorus deficiency in a dairy herd', *New Zealand Veterinary Journal*, 32(10), pp. 174–176.

Bruder, J. M., Guise, T. A. and Mundy, G. R. (2001) 'Mineral metabolism', in Felig, P. and Frohman, L. A. (eds) *Endocrinology & Metabolism*. Fourth Edi. New York: McGraw-Hill Publishing Company, pp. 1079–1159.

Burgering, B. M. T. and Coffey, P. J. (1995) 'Protein kinase B (c-Akt) in phosphatidylinositol-3-OH kinase signal transduction', *Nature*, 376(6541), pp. 599–602.

Burgess, G.M., McKinney, J.S., Irvine, R.F., Berridge, M.J., Hoyle, P.C., Putney, J.W. (1984) 'Inositol 1,4,5-trisphosphate may be a signal for f-Met-leu-Phe-induced intracellular calcium mobilization in human leukocytes (HL-

60 cells).' FEBS Let., 176, pp. 193-196.

Burnell, T. W., Cromwell, G. L. and Stahly, T. S. (1990) 'Effects of Particle Size on the Biological Availability of Calcium and Phosphorus in Defluorinated Phosphate for Chicks', *Poultry Science*, 69(7), pp. 1110–1117.

Cairns, B. R., Erdjument-Bromage, H., Tempst, P., Winston, F., Kornberg, R.D. (1998) 'Two actin-related proteins are shared functional components of the chromatin-remodeling complexes RSC and SWI/SNF.', *Molecular cell*, 2(5), pp. 639–51.

Campion, B., Sparvoli, F., Doria, E., Tagliabue, G., Galasso, I., Fileppi, M., Bollini, R., Nielsen, E. (2009) 'Isolation and characterisation of an *lpa* (low phytic acid) mutant in common bean (*Phaseolus vulgaris* L.) *Theor. appl. Genetic.* on-line. doi:10.1007/s00122-009-0975-8.

Cao, S., Li, T., Shao, Y., Zhang, L., Lu, L., Zhang, R., Hou, S., Luo, X., Liao, X. (2021) 'Regulation of bone phosphorus retention and bone development possibly by related hormones and local bone-derived regulators in broiler chicks', *Journal of Animal Science and Biotechnology*. *Journal of Animal Science and Biotechnology*, 12(1), pp. 1–16.

Cardenas, M. L., Rabajille, E. and Niemeyer, H. (1984) 'Fructose is a good substrate for rat liver "glucokinase" (hexokinase D)', *Biochemical Journal*, 222(2), pp. 363–370.

Carman, G. M. and Henry, S. A. (1999) 'Phospholipid biosynthesis in the yeast *Saccharomyces cerevisiae* and interrelationship with other metabolic processes.', *Progress in lipid research*, 38(5–6), pp. 361–99.

Casals, I., Villar, J. L. and Riera-Codina, M. (2002) 'A straightforward method for analysis of highly phosphorylated inositols in blood cells by high-performance liquid chromatography', *Analytical Biochemistry*, 300(1), pp. 69–76.

Cavalcanti, W. B. and Behnke, K. C. (2004) 'Effect of wheat bran phytase subjected to different conditioning temperatures on phosphorus utilization by broiler chicks based on body weight and toe ash measurements', *International Journal of Poultry Science*, 3(3), pp. 215–219.

Ceylan, N., Cangir, S., Corduk, M., Grigorov, A., Golzar Adabi, S.H. (2012) 'The effects of phytase supplementation and dietary phosphorus level on performance and on tibia ash and phosphorus contents in broilers fed maize-soyabased diets', *Journal of Animal and Feed Sciences*. The Kielanowski Institute of Animal Physiology and Nutrition, Polish Academy of Sciences, Jabłonna, Poland, 21(4), pp. 696–704.

Chatree, S., Thongmaen, N., Tantivejkul, K., Sitticharoon, C., Vucenik, I. (2020) 'Role of inositols and inositol phosphates in energy metabolism', *Molecules*, 25(21), pp. 1–18.

Chen, L., Zhou, C., Yang, H., Roberts, M.F. (2000) 'Inositol-1-phosphate synthase from *Archaeoglobus fulgidus* is a class II aldolase.', *Biochemistry*, 39(40), pp. 12415–23.

Chowdhury, R. and Koh, K. (2018) 'Phytase activity in the digesta from different parts of the digestive tract and ileal digestibility of nutrients in broilers fed with buckwheat diets', *Journal of Poultry Science*, 55(4), pp. 274–279.

Chu, H. M., Guo, R.-T., Lin, T.-W., Chou, C.-C., Shr, H.-L., Lai, H.-L., Tang, T.-Y., Cheng, L.-J., Selinger, B.L., Wang, A. H.-J. (2004) 'Structures of *Selenomonas ruminantium* phytase in complex with persulfated phytate: DSP phytase fold and mechanism for sequential substrate hydrolysis', *Structure*, 12(11), pp. 2015–2024.

Chukwuma, C. I., Ibrahim, M. A. and Islam, M. S. (2016) 'Myo-inositol inhibits intestinal glucose absorption and promotes muscle glucose uptake: a dual

approach study', *Journal of Physiology and Biochemistry*. *Journal of Physiology and Biochemistry*, 72(4), pp. 791–801.

Clark, M. B. and Potts, J. T. (1976) '25-Hydroxyvitamin D3 regulation', *Calcified Tissue Research*, 22(1 Supplement), pp. 29–34.

Colombo, F., Paolo, D., Cominelli, E., Sparvoli, F., Nielsen R., Pilu, R. (2020) 'MRP Transporters and Low Phytic Acid Mutants in Major Crops: Main Pleiotropic Effects and Future Perspectives', *Frontiers in Plant Science*, 11(August), pp. 1–12.

Committee on Food Protection and Food and Nutritional Board (1973) 'Toxicants Occurring Naturally in Foods', in *Committee on Food Protection*. Washington, D.C.: National Academy of Science, pp. 363–371.

Cordell, D. and White, S. (2011) 'Peak phosphorus: Clarifying the key issues of a vigorous debate about long-term phosphorus security', *Sustainability*, 3(10), pp. 2027–2049.

Córdoba, J., Gottstein, J. and Blei, A. T. (1996) 'Glutamine, *myo*-inositol, and organic brain osmolytes after portacaval anastomosis in the rat: Implications for ammonia-induced brain edema', *Hepatology*, 24(4 I), pp. 919–923.

Corrado, F., D'Anna, R., Di Vieste, G., Giordano, D., Pintaudi, B., Santamaria, A., Di Benedetto, A. (2011) 'The effect of *myo*-inositol supplementation on insulin resistance in patients with gestational diabetes', *Diabetic Medicine*, 28(8), pp. 972–975.

Correll, D. L. (1998) 'The Role of Phosphorus in the Eutrophication of Receiving Waters: A Review', *Journal of Environmental Quality*, 27(2), pp. 261–266.

Cosgrove, D. J. and Irving, G. C. J. (1980) *Inositol Phosphates: Their Chemistry, Biochemistry, and Physiology*. Amsterdam: Elsevier.

Costantino, D. *et al.* (2009) 'Metabolic and hormonal effects of *myo*-inositol in women with polycystic ovary syndrome: A double-blind trial', *European Review for Medical and Pharmacological Sciences*, 13(2), pp. 105–110.

Cowieson, A. J., Ptak, A., Maćkowiak, P., Sassek, M., Pruszyńska-Osmalek, E., Zyla, K., Świątkiewicz, S., Kaczmarek, S., Józefiak, D. (2013) 'The effect of microbial phytase and *myo*-inositol on performance and blood biochemistry of broiler chickens fed wheat/corn-based diets', *Poultry Science*, 92(8), pp. 2124–2134.

Cowieson, A. J., Ruckebusch, J.P., Sorbara, J.O.B., Wilson, J.W., Guggenbuhl, P., Roos, F.F. (2017) 'A systematic view on the effect of phytase on ileal amino acid digestibility in broilers', *Animal Feed Science and Technology*. Elsevier B.V., 225(February), pp. 182–194.

Cowieson, A. J., Acamovic, T. and Bedford, M. R. (2006) 'Supplementation of corn-soy-based diets with an *Escherichia coli*-derived phytase: Effects on broiler chick performance and the digestibility of amino acids and metabolizability of minerals and energy', *Poultry Science*. Poultry Science Association Inc., 85(8), pp. 1389–1397.

Croze, M. L., Géloën, A. and Soulage, C. O. (2015) 'Abnormalities in *myo*-inositol metabolism associated with type 2 diabetes in mice fed a high-fat diet: Benefits of a dietary *myo*-inositol supplementation', *British Journal of Nutrition*, 113(12), pp. 1862–1875.

Croze, M. L. and Soulage, C. O. (2013) 'Potential role and therapeutic interests of *myo*-inositol in metabolic diseases', *Biochimie*, 95(10), pp. 1811–1827.

D'Anna, R., Di Benedetto, A., Scilipoti, A., Santamaria, A., Interdonato, M.L., Petrella, E., Neri, I., Pintaudi, B., Corrado, F., Facchinetti, F. (2015) '*Myo*-inositol Supplementation for Prevention of Gestational Diabetes in Obese

Pregnant Women', *Obstetrics & Gynecology*, 126(2), pp. 310–315.

Dai, G., Yu, H., Kruse, M., Traynor-Kaplan, A., Hille, B. (2016) 'Osmoregulatory inositol transporter SMIT1 modulates electrical activity by adjusting PI(4,5)P2 levels', *Proceedings of the National Academy of Sciences of the United States of America*, 113(23), pp. E3290–E3299.

Denbow, D. M. (2000) 'Gastrointestinal anatomy and physiology', in Whittow, G. C. (ed.) *Sturkie's Avian Physiology*. 5th ed. New York, NY, USA: Academic Press, pp. 299–325.

Dendougui, F. and Schwedt, G. (2004) 'In vitro analysis of binding capacities of calcium to phytic acid in different food samples', *European Food Research and Technology*. Springer-Verlag, 219(4), pp. 409–415.

Department for Environment Food and Rural Affairs (2013) *TRACE WP1 Report on the bio-element (HCNS) stable isotope analysis of authentic European and Chinese chicken*.

Desfougères, Y., Wilson, M.S.C., Laha, D., Saiardi, A. (2019) 'ITPK1 mediates the lipid-independent synthesis of inositol phosphates controlled by metabolism', *Proceedings of the National Academy of Sciences of the United States of America*, 116(49), pp. 24551–24561.

Dionex (2006) 'Ics-2000 Ion Chromatography System Operator ' S Manual', (031857).

Dionisio, G., Madsen, C.K., Holm, P.B., Welinder, K.G., Jørgensen, M., Stoger, E., Arcalis, E., Brinch-Pedersen, H. (2011) 'Cloning and characterization of purple acid phosphatase phytases from wheat, barley, maize, and rice', *Plant Physiology*, 156(3), pp. 1087–1100.

Djordjic, F., Börling, K. and Bergström, L. (2004) 'Phosphorus leaching in

relation to soil type and soil phosphorus content.’, *Journal of environmental quality*, 33(2), pp. 678–84.

Donahue, J. L., Alford, S.R., Torabinejad, J., Kerwin, R.E., Nourbakhsh, A., Ray, W.K., Hernick, M., Huang, X., Lyons, B.M., Hein, P.P., Gillaspay, G.E. (2010) ‘The Arabidopsis thaliana *Myo*-inositol 1-phosphate synthase1 gene is required for *Myo*-inositol synthesis and suppression of cell death.’, *The Plant cell*. American Society of Plant Biologists, 22(3), pp. 888–903.

Donahue, T. F. and Henry, S. A. (1981) ‘*myo*-Inositol-1-phosphate synthase. Characteristics of the enzyme and identification of its structural gene in yeast.’, *The Journal of biological chemistry*, 256(13), pp. 7077–85.

Dorsch, J. A., Cook, A., Young, K.A., Anderson, J.M., Bauman, A.T., Volkmann, C.J., Murthy, P.P.N., Raboy, V. (2003) ‘Seed phosphorus and inositol phosphate phenotype of barley low phytic acid genotypes’, *Phytochemistry*, 62(5), pp. 691–706.

Driver, J. P., Pesti, G.M., Bakalli, R.I., Edwards, H.M.Jr. (2005) ‘Effects of calcium and nonphytate phosphorus concentrations on phytase efficacy in broiler chicks’, *Poultry Science*. Poultry Science Association Inc., 84(9), pp. 1406–1417.

Dubin, M. J., Bowler, C. and Benvenuto, G. (2008) ‘A modified Gateway cloning strategy for overexpressing tagged proteins in plants’, *Plant Methods*, 4(1), p. 3.

Duke, G. E. (1986) ‘Alimentary canal: Secretion and digestion, special digestive functions, and absorption’, in Sturkie, P. D. (ed.) *Avian Physiology*. New York, NY, USA: Springer, pp. 289–302.

Dwivedi, S. L. and Ortiz, R. (2021) ‘Food Crops Low in Seed-Phytate Improve Human and Other Non-Ruminant Animals’ Health’, *Crop Breeding, Genetics and Genomics*.

Edwards Jr, H. M. (1983) 'Phosphorus. 1. Effect of breed and strain on utilization of suboptimal levels of phosphorus in the ration', *Poultry Science*, 62(1), pp. 77–84.

Edwards Jr, H. M. and Veltmann Jr, J. R. (1983) 'The role of calcium and phosphorus in the etiology of tibial dyschondroplasia in young chicks', *The Journal of Nutrition*, 113(8), pp. 1568–1575.

Eeckhout, W. and De Paepe, M. (1994) 'Total phosphorus, phytate-phosphorus and phytase activity in plant feedstuffs', *Animal Feed Science and Technology*, 47(1–2), pp. 19–29.

Einat, H. and Belmaker, R. H. (2001) 'The effects of inositol treatment in animal models of psychiatric disorders', *Journal of Affective Disorders*, 62(1–2), pp. 113–121.

Eisenberg, F. and Bolden, A. (1963) 'Biosynthesis of inositol in rat testis homogenate', *Biochemical and biophysical research communications*, 12(1), pp. 72–77.

Elaroussi, M. A., Forte, L.R., Eber, S.L., Biellier, H.V. (1994) 'Calcium homeostasis in the laying hen. 1. Age and dietary calcium effects.', *Poultry science*. Poultry Science Association Inc., 73(10), pp. 1581–1589.

Elkhalil, E. A. I., Männer, K., Borriss, R., Simon, O. (2007) 'In vitro and in vivo characteristics of bacterial phytases and their efficacy in broiler chickens', *British Poultry Science*, 48(1), pp. 64–70.

Environmental Agency (2019) 'Agricultural and rural land management challenge RBMP 2021', (October 2019), pp. 1–18.

Faba-Rodriguez, R., Gu, Y., Salmon, M., Dionisio, G., Brinch-Pedersen, H., Brearley, C.A., Hemmings, A.M. (2022) 'Structure of a cereal purple acid

phytase provides new insights to phytate degradation in plants', *Plant Communications*. 3(2), p. 100305.

Farhadi, D., Karimi, A., Sadeghi, G.H., Rostamzadeh, J., Bedford, M.R. (2017) 'Effects of a high dose of microbial phytase and *myo*-inositol supplementation on growth performance, tibia mineralization, nutrient digestibility, litter moisture content, and foot problems in broiler chickens fed phosphorus-deficient diets', *Poultry Science*. Poultry Science Association Inc., 96(10), pp. 3664–3675.

Farner, D. S. (1942) 'The Hydrogen Ion Concentration in Avian Digestive Tracts', *Poultry Science*. Poultry Science Association Inc., 21(5), pp. 445–450.

Fernandes, J. I. M., Horn, D., Ronconi, E.J., Buzim, R., Lima, F.K., Pazdiora, D.A. (2019) 'Effects of Phytase Superdosing on Digestibility and Bone Integrity of Broilers', *Journal of Applied Poultry Research*. 2019 Poultry Science Association Inc., 28(2), pp. 390–398.

Fireman, A. K. B. A. T. and Fireman, F. A. T. (1998) 'Phytase in feeds for laying hens', *Ciência Rural*, 28(3), pp. 529–534.

Fisher, H. (1992) 'Low-calcium diets enhance phytate-phosphorus availability', *Nutrition Reviews*, 50(6), pp. 170–171.

Fisher, S. K. and Agranoff, B. W. (1987) 'Receptor activation and inositol lipid hydrolysis in neural tissues', *Journal of Neurochemistry*, 48, pp. 999–1017.

Fisher, S. K., Heacock, A. M. and Agranoff, B. W. (1992) 'Inositol Lipids and Signal Transduction in the Nervous System: An Update', *Journal of Neurochemistry*, 58, pp. 18–38.

Fisher, S. K., Novak, J. E. and Agranoff, B. W. (2002) 'Inositol and higher inositol phosphates in neural tissues: Homeostasis, metabolism and

functional significance', *Journal of Neurochemistry*, 82(4), pp. 736–754.

Fortune, S., Lu, J., Addiscott, T.M., Brookes, P.C. (2005) 'Assessment of phosphorus leaching losses from arable land', *Plant and Soil*. Kluwer Academic Publishers, 269(1–2), pp. 99–108.

Freeman, B. M. (1969) 'The mobilization of hepatic glycogen in *Gallus domesticus* at the end of incubation', *Comparative biochemistry and physiology*, 28(3), pp. 1169–1176.

Frey, R., Metzler, D., Fischer, P., Heiden, A., Scharfetter, J., Moser, E., and Kasper, S. (1998) 'Myo-inositol in depressive and healthy subjects determined by frontal ¹H-magnetic resonance spectroscopy at 1.5 tesla. *Journal of Psychiatric Research*, 32: 411-420.

Fujisawa, T., Fujinaga, S. and Atomi, H. (2017) 'An *in vitro* enzyme system for the production of *myo*-inositol from starch', *Applied and Environmental Microbiology*, 83(16), pp. 1–14.

Fux, M., Levine, J., Aviv, A., and Belmaker, R.H. (1996) 'Inositol treatment of obsessive compulsive disorder.' *Am. J. Psychiatry*. 153: 1219-1221.

Fux, M., Benjamin, J., and Belmaker, R.H. (1999) 'Inositol versus placebo augmentation of serotonin reuptake inhibitors in the treatment of obsessive-compulsive disorder: A double blind cross-over study.' *Int. J. Neuropsychopharmacol.*, 2:193-195.

Gao, X. R., Wang, G.K., Su, Q., Wang, Y., An, L.J.. (2007) 'Phytase expression in transgenic soybeans: Stable transformation with a vector-less construct', *Biotechnology Letters*, 29(11), pp. 1781–1787.

Garcia, A. F. Q. M., Murakami, A.E., Duarte, C.R.D.A., Rojas, I.C.O., Picoli, K.P., Puzotti, M.M. (2013) 'Use of vitamin D3 and its metabolites in broiler chicken feed on performance, bone parameters and meat quality', *Asian-*

Australasian Journal of Animal Sciences, 26(3), pp. 408–415.

Gargova, S., Roshkova, Z. and Vancheva, G. (1997) 'Screening of fungi for phytase production', *Biotechnology Techniques*, 11(4), pp. 221–224.

Garrett, J. B., Kretz, K.A., O'Donoghue, E., Kerovuo, J., Kim, W., Barton, N.R., Hazelwood, G.P., Short, J.M., Robertson, D.E., Gray, K.A. (2004) 'Enhancing the thermal tolerance and gastric performance of a microbial phytase for use as a phosphate-mobilizing monogastric-feed supplement', *Applied and Environmental Microbiology*, 70(5), pp. 3041–3046.

Gattineni, J., Gates, C., Twombly, K., Dwarakanath, V., Robinson, M.L., Goetz, R., Mohammadi, M., Baum, M. (2009) 'FGF23 decreases renal NaPi-2a and NaPi-2c expression and induces hypophosphatemia *in vivo* predominantly via FGF receptor 1', *American Journal of Physiology - Renal Physiology*, 297(2), pp. 282–291.

Gen Lei, X., Weaver, J.D., Mullaney, E., Ullah, A.H., Azain, M.J. (2013) 'Phytase, a New Life for an "Old" Enzyme', *The Annual Review of Animal Biosciences*, (1), pp. 283–309.

Genazzani, A. D., Lanzoni, C., Ricchieri, F., Jasonni, V.M. (2008) 'Myo-inositol administration positively affects hyperinsulinemia and hormonal parameters in overweight patients with polycystic ovary syndrome', *Gynecological Endocrinology*, 24(3).

Gontia-Mishra, I. and Tiwari, S. (2013) 'Molecular characterization and comparative phylogenetic analysis of phytases from fungi with their prospective applications', *Food Technology and Biotechnology*, 51(3), pp. 313–326.

Gonzalez-Uarquin, F., Kenéz, Á, Rodehutschord, M., Huber, K. (2020) 'Dietary phytase and *myo*-inositol supplementation are associated with distinct plasma metabolome profile in broiler chickens', *Animal*. Elsevier,

14(3), pp. 549–559.

Gonzalez-Uarquin, F., Molano, E., Heinrich, F., Sommerfeld, V., Rodehutscord, M., Huber, K. (2020) 'Research Note: Jejunum phosphatases and systemic *myo*-inositol in broiler chickens fed without or with supplemented phytase', *Poultry Science*. Elsevier Inc., 99(11), pp. 5972–5976.

Gonzalez-Uarquin, F., Sommerfeld, V., Rodehutscord, M., Huber, K. (2021) 'Interrelationship of *myo*-inositol pathways with systemic metabolic conditions in two strains of high-performance laying hens during their productive life span', *Scientific Reports*. Nature Publishing Group UK, 11(1), pp. 1–14.

Gonzalez-Uarquin, F., Rodehutscord, M. and Huber, K. (2020) 'Myo-inositol: its metabolism and potential implications for poultry nutrition—a review', *Poultry Science*. Elsevier Inc., 99(2), pp. 893–905.

Greenberg, M. L. and Lopes, J. M. (1996) 'Genetic regulation of phospholipid biosynthesis in *Saccharomyces cerevisiae*.', *Microbiological reviews*, 60(1), pp. 1–20.

Greene, D. A. and Lattimer, S. A. (1982) 'Sodium- and energy-dependent uptake of *myo*-inositol by rabbit peripheral nerve. Competitive inhibition by glucose and lack of an insulin effect', *Journal of Clinical Investigation*, 70(5), pp. 1009–1018.

Greene, D. A., Lattimer, S. A. and Sima, A. A. F. (1987) 'Sorbitol, phosphoinositides, and sodium-potassium-ATPase in the pathogenesis of diabetic complications', *The New England Journal of Medicine*, 315(10), pp. 599–606.

Greene, E., Flees, J., Dadgar, S., Mallmann, B., Orłowski, S., Dhamad, A., Rochell, S., Kidd, M., Laurendon, C., Whitfield, H., Brearley, C., Rajaram, N., Walk, C., Dridi, S. (2019) 'Quantum Blue Reduces the Severity of Woody

Breast Myopathy via Modulation of Oxygen Homeostasis-Related Genes in Broiler Chickens', *Frontiers in Physiology*, 10(October), pp. 1–21.

Greene, E., Cauble, R., Dhamad, A.E., Kidd, M.T., Kong, B., Howard, S.M., Castro, H.F., Campagna, S.R., Bedford, M., Dridi, S. (2020a) 'Muscle Metabolome Profiles in Woody Breast-(un)Affected Broilers: Effects of Quantum Blue Phytase-Enriched Diet', *Frontiers in Veterinary Science*, 7(August), pp. 1–15.

Greene, E., Mallmann, B., Wilson, J.W., Cowieson, A.J., Dridi, S. (2020b) 'Monitoring Phytate Hydrolysis Using Serial Blood Sampling and Feather Myo-Inositol Levels in Broilers', *Frontiers in Physiology*, 11(June), pp. 1–11.

Gregory, P. J., Ingram, J. S. I. and Brklacich, M. (2005) 'Climate change and food security', *Philosophical Transactions of the Royal Society B: Biological Sciences*, 360(1463), pp. 2139–2148.

Greiling, A. M., Tschesche, C., Baardsen, G., Kröckel, S., Koppe, W., Rodehutschord, M. (2019) 'Effects of phosphate and phytase supplementation on phytate degradation in rainbow trout (*Oncorhynchus mykiss* W.) and Atlantic salmon (*Salmo salar* L.)', *Aquaculture*. Elsevier, 503(January), pp. 467–474.

Greiner, R., Haller, E., Konietzny, U., Jany, K.D. (1997) 'Purification and characterization of a phytase from *Klebsiella terrigena*', *Archives of Biochemistry and Biophysics*, 341(2), pp. 201–206.

Greiner, R., Konietzny, U. and Jany, K. D. (1993) 'Purification and characterization of two phytases from *Escherichia coli*', *Archives of Biochemistry and Biophysics*, pp. 107–113.

Griffin, H. D. and Goddard, C. (1994) 'Rapidly growing broiler (meat-type) chickens. Their origin and use for comparative studies of the regulation of growth', *International Journal of Biochemistry*, 26(1), pp. 19–28.

Gržinić, G., Piotrowicz-Cieślak, A., Klimkowicz-Pawlas, A., Górny, R. L., Ławniczek-Wałczyk, A., Piechowicz, L., Olkowska, E., Potrykus, M., Tankiewicz, M., Krupka, M., Siebielec, M. and Wolska, L. (2023) 'Intensive poultry farming: A review of the impact on the environment and human health.' *Science of The Total Environment*, 858 (3).

Hamada, J. S. (1996) 'Isolation and identification of the multiple forms of soybean phytases', *Journal of the American Oil Chemists' Society*, 73(9), pp. 1143–1151.

Hannon, J. D., Lee, N.K., Yandong, C., Blinks, J.R. (1992) 'Inositol trisphosphate (InsP₃) causes contraction in skeletal muscle only under artificial conditions: evidence that Ca²⁺ release can result from depolarization of T-tubules', *Journal of Muscle Research and Cell Motility*, 13(4), pp. 447–456.

Haris, M., Cai, K., Singh, A., Hariharan, H., Reddy, R. (2011) 'In vivo mapping of brain *myo*-inositol', *NeuroImage*. Elsevier Inc., 54(3), pp. 2079–2085.

Harmel, R. K., Puschmann, R., Trung, M.N., Saiardi, A., Schmieder, P., Fiedler, D. (2019) 'Harnessing ¹³C-labeled *myo*-inositol to interrogate inositol phosphate messengers by NMR', *Chemical Science*. Royal Society of Chemistry, 10(20), pp. 5267–5274.

Harper, A. F., Kornegay, E. T. and Schell, T. C. (1997) 'Phytase supplementation of low-phosphorus growing-finishing pig diets improves performance, phosphorus digestibility, and bone mineralization and reduces phosphorus excretion.', *Journal of animal science*, 75(12), pp. 3174–86.

Hasegawa, R., Eisenberg, F. and Jr (1981) 'Selective hormonal control of *myo*-inositol biosynthesis in reproductive organs and liver of the male rat.', *Proceedings of the National Academy of Sciences of the United States of*

America. National Academy of Sciences, 78(8), pp. 4863–6.

Hawkins, P. T., Jackson, T. R. and Stephens, L. R. (1992) 'Platelet-derived growth factor stimulates synthesis of PtdIns(3,4,S)P₃ by activating a PtdIns(4,S)P₂ 3-OH kinase', *Nature*, 358, pp. 157–159.

Hayashi, E., Maeda, T. and Tomita, T. (1974) 'The effect of *myo*-inositol deficiency on lipid metabolism in rats: II. The mechanism of triacylglycerol accumulation in the liver of *myo*-inositol-deficient rats', *Biochimica et Biophysica Acta - Lipids and Lipid Metabolism*, 360(2), pp. 146–152.

Henry, S. A., Kohlwein, S. D. and Carman, G. M. (2012) 'Metabolism and Regulation of Glycerolipids in the Yeast *Saccharomyces cerevisiae*', *Genetics*, 190(2), pp. 317–349.

Hermier, D. (1997) 'Lipoprotein metabolism and fattening in poultry', *The Journal of Nutrition*, 127(5), pp. 805S-808S.

Herwig, E., Classen, H.L., Walk, C.L., Bedford, M., Schwean-Lardner, K. (2019) 'Dietary inositol reduces fearfulness and avoidance in laying hens', *Animals*, 9(11).

Hirvonen, J., Liljavirta, J., Saarinen, M.T., Lehtinen, M.J., Ahonen, I., Nurminen, P. (2019) 'Effect of Phytase on *in Vitro* Hydrolysis of Phytate and the Formation of *myo*-Inositol Phosphate Esters in Various Feed Materials', *Journal of Agricultural and Food Chemistry*.

Hokin, M. R. and Hokin, L. E. (1953) 'Enzyme secretion and the incorporation of P³² into phospholipides of pancreas slices', *The Journal of biological chemistry*. © 1953 ASBMB. Currently published by Elsevier Inc; originally published by American Society for Biochemistry and Molecular Biology., 203(2), pp. 967–977.

Holick, M. F., Kleiner-Bossaller, A., Schnoes, H.K., Kasten, P.M., Boyle, I.T.,

DeLuca, H.F. (1973) '1,24,25-Trihydroxyvitamin D₃: a metabolite of vitamin D₃ effective on intestine', *Journal of Biological Chemistry*, 248(19), pp. 6691–6696.

Holick, M. F. (1989) 'Phylogenetic and evolutionary aspects of vitamin D from phytoplankton to humans', in Pang, P. K. T. and Schreibman, M. P. (eds) *Vertebrate Endocrinology: Fundamentals and Biomedical Implications*. Orlando, FL., USA: Academic Press.

Holick, M. F. (1994) 'McCollum Award Lecture, 1994: Vitamin D - new horizons for the 21st century', *The American Journal of Clinical Nutrition*, 60(4), pp. 619–630.

Holub, B. J. (1986a) 'Metabolism and function of *myo*-inositol and inositol phospholipids', *Annual Review of Nutrition*, 6, pp. 563–597.

Holub, B. J. (1986b) 'Metabolism and function of phospholipids.', *Annual Review of Nutrition*, (6), pp. 563–597.

Horst, R. L., Littledike, E.T., Riley, J.L., Napoli, J.L. (1981) 'Quantitation of Vitamin Concentrations D and Its Metabolites in Five and Their of Animals ' Species', *Analytical Biochemistry*, 116, pp. 189–203.

Horvat-Gordon, M., Hadley, J.A., Ghanem, K., Leach, R.M.Jr. (2019) 'Lack of a relationship between plasma fibroblast growth factor-23 and phosphate utilization in young chicks', *Poultry Science*. Poultry Science Association Inc., 98(4), pp. 1762–1765.

Howard, C. F. and Anderson, L. (1967) 'Metabolism of *myo*-Inositol in animals', *Archives of Biochemistry and Biophysics*, 118(2), pp. 332–339.

Hu, H. L., Wise, A. and Henderson, C. (1996) 'Hydrolysis of phytate and inositol tri-, tetra-, and penta-phosphates by the intestinal mucosa of the pig', *Nutrition Research*, 16(5), pp. 781–787.

Hu, Y., Liao, X., Wen, Q., Lu, L., Zhang, L., Luo, X. (2018) 'Phosphorus absorption and gene expression levels of related transporters in the small intestine of broilers', *British Journal of Nutrition*, 119(12), pp. 1346–1354.

Huber, K. (2016) 'Cellular *myo*-inositol metabolism', in Walk, C. L. et al. (eds) *Phytate Destruction - Consequences for Precision Animal Nutrition*. Wageningen Academic Publishers, pp. 53–60.

Huber, K., Hempel, R. and Rodehutschord, M. (2006) 'Adaptation of epithelial sodium-dependent phosphate transport in jejunum and kidney of hens to variations in dietary phosphorus intake', *Poultry Science*. Poultry Science Association Inc., 85(11), pp. 1980–1986.

Huber, K., Zeller, E. and Rodehutschord, M. (2015) 'Modulation of small intestinal phosphate transporter by dietary supplements of mineral phosphorus and phytase in broilers', *Poultry Science*, 94(5), pp. 1009–1017.

Hughes, M. R., Brumbaugh, P.F., Hussler, M.R., Wergedal, J.E., Baylink, D.J. (1975) 'Regulation of serum $1\alpha,25$ -dihydroxyvitamin D3 by calcium and phosphate in the rat', *Science*, 190(4214), pp. 578–580.

Humer, E., Schwarz, C. and Schedle, K. (2015) 'Phytate in pig and poultry nutrition', *Journal of Animal Physiology and Animal Nutrition*, 99(4), pp. 605–625.

Huo, W., Weng, K., Li, Y., Zhang, Y., Zhang, Y., Xu, Q., Chen, G. (2022) 'Comparison of muscle fiber characteristics and glycolytic potential between slow- and fast-growing broilers', *Poultry Science*, 101(3), pp. 1–9.

Hurrell, R. F. (2003) 'Influence of Vegetable Protein Sources on Trace Element and Mineral Bioavailability', *The Journal of Nutrition*. Oxford University Press, 133(9), pp. 2973S-2977S.

Iemma, F., Cirillo, G., Puoci, F., Trombino, S., Castiglione, M., Picci, N. (2007) 'Iron (III) chelation and antioxidant properties of myo-inositol phosphorylated polymeric microspheres', *Journal of Pharmacy and Pharmacology*, 59(4), pp. 597–601.

Igbasan, F. A., Männer, K., Miksch, G., Borriss, R., Farouk, A., Simon, O. (2000) 'Comparative studies on the in vitro properties of phytases from various microbial origins', *Archives of Animal Nutrition*, 53(4), pp. 353–373.

Invitrogen (2012) 'pENTR Directional TOPO Cloning Kits User Guide', *Life Technologies*, (25), pp. 5–18.

Irvine, R. F. and Schell, M. J. (2001) 'Back in the water: The return of the inositol phosphates', *Nature Reviews Molecular Cell Biology*, 2(5), pp. 327–338.

Irving, G. C. and Cosgrove, D. J. (1972) 'Inositol phosphate phosphatases of microbiological origin: the inositol pentaphosphate products of *Aspergillus ficuum* phytases.', *Journal of Bacteriology*, 112(1), pp. 434–438.

Jackson, S. and Diamond, J. (1996) 'Metabolic and digestive responses to artificial selection in chickens', *Evolution*, 50(4), pp. 1638–1650.

Jafarnejad, S., Farkhoy, M., Sadegh, M. and Bahonar, A.R., 'Effect of crumble-pellet and mash diets with different levels of dietary protein and energy on the performance of broilers at the end of the third week.' (2011) *Vet. Med. Int.* Jan 23;2010:328123.

Jiang, W.-D., Feng, L., Liu, Y., Jiang, J., and Zhou, X.-Q. (2009a) 'Myo-inositol prevents oxidative damage, inhibits oxygen radical generation and increases antioxidant enzyme activities of juveniles Jian carp (*Cyprinus carpio* var. Jian).' *Aquaculture Research*, 40 (15): 1770-1776.

Jiang, W.-D., Feng, L., Liu, Y., Jiang, J., and Zhou, X.-Q. (2009b). 'Growth,

digestive capacity and intestinal microflora of juvenile Jian carp (*Cyprinus carpio* var. Jian) fed graded levels of dietary inositol.' *Aquaculture Research*, 40 (8): 955-962.

Johnson, S. C., Yang, M. and Murthy, P. P. N. (2010) 'Heterologous expression and functional characterization of a plant alkaline phytase in *Pichia pastoris*', *Protein Expression and Purification*. Elsevier Inc., 74(2), pp. 196–203.

Johnson, K.A. & Goody, R. S. (2011) 'The Original Michaelis Constant: Translation of the 1913 Michaelis-Menten Paper.' *Biochemistry*, 50(39): 8264-8269.

Jongbloed, A. W., Mroz, Z. and Kemme, P. A. (1992) 'The effect of supplementary *Aspergillus niger* phytase in diets for pigs on concentration and apparent digestibility of dry matter, total phosphorus, and phytic acid in different sections of the alimentary tract', *Journal of Animal Science*, 70(4), pp. 1159–1168.

Ju, S., Shaltiel, G., Shamir, A., Agam, G., Greenberg, M.L. (2004) 'Human 1-D- myo -Inositol-3-phosphate Synthase Is Functional in Yeast', *Journal of Biological Chemistry*, 279(21), pp. 21759–21765.

Kanehisa, M., Furumichi, M., Tanabe, M., Sato, Y., Morishima, K. (2017) 'KEGG: New perspectives on genomes, pathways, diseases and drugs', *Nucleic Acids Research*, 45(D1), pp. D353–D361.

Kanehisa, M., Sato, Y., Furumichi, M., Morishima, K., Tanabe, M. (2019) 'New approach for understanding genome variations in KEGG', *Nucleic Acids Research*. Oxford University Press, 47(D1), pp. D590–D595.

Katayama, T. (1995) 'Effect of Dietary Sodium Phytate on the Hepatic and Serum Levels of Lipids and on the Hepatic Activities of NADPH-Generating Enzymes in Rats Fed on Sucrose', *Bioscience, Biotechnology, and*

Biochemistry, 59(6), pp. 1159–1160.

Kawai, S., Hashimoto, W. and Murata, K. (2010) 'Transformation of *Saccharomyces cerevisiae* and other fungi: methods and possible underlying mechanism.', *Bioengineered bugs*. Taylor & Francis, 1(6), pp. 395–403.

Khattak, F.M., Shahzad, M.A., Pasha, T.N. and Saleem, G. (2017) 'Comparative evaluation of commercially available supplementary sources of inorganic phosphorus in broiler feed.' *The Journal of Animal and Plant Sciences*. 26 (6) p. 1576-1581 6p.

Khundmiri, S. J., Murray, R. D. and Lederer, E. (2016) 'PTH and vitamin D', *Comprehensive Physiology*, 6(2), pp. 561–601.

Kies, A. K., De Jonge, L.H., Kemme, P.A., Jongbloed, A.W. (2006) 'Interaction between protein, phytate, and microbial phytase. *In vitro* studies', *Journal of Agricultural and Food Chemistry*, 54(5), pp. 1753–1758.

Kilian, J., Whitehead, D., Horak, J., Wanke, D., Weinl, S., Batistic, O., D'Angelo, C., Bornberg-Bauer, E., Kudla, J., Harter, K. (2007) 'The AtGenExpress global stress expression data set: protocols, evaluation and model data analysis of UV-B light, drought and cold stress responses', *The Plant Journal*, 50(2), pp. 347–363.

Kilkenny, C., Browne, W., Cuthill, I.C., Emerson, M., Altman, D.G. (2010) 'Animal research: Reporting *in vivo* experiments: The ARRIVE guidelines', *British Journal of Pharmacology*, 160(7), pp. 1577–1579.

Kim, H. J. *et al.* (2012) 'Effects of Pinitol on Glycemic Control, Insulin Resistance and Adipocytokine Levels in Patients with Type 2 Diabetes Mellitus', *Annals of Nutrition and Metabolism*, 60, pp. 1–5.

Kim, J. H., Park, K.S., Lee, S.K., Min, K.W., Han, K.A., Kim, Y.K., Ku, B.J. (2017) 'Effect of superdosing phytase on productive performance and egg

quality in laying hens', *Asian-Australasian Journal of Animal Sciences*, 30(7), pp. 994–998.

Kim, J. N., Han, S. N. and Kim, H. K. (2014) 'Phytic acid and *myo*-inositol support adipocyte differentiation and improve insulin sensitivity in 3T3-L1 cells', *Nutrition Research*. Elsevier Inc., 34(8), pp. 723–731.

King, C. E., Hawkins, P.T., Stephens, L.R., Michell, R.H. (1989) 'Determination of the steady-state turnover rates of the metabolically active pools of phosphatidylinositol 4-phosphate and phosphatidylinositol 4,5-bisphosphate in human erythrocytes', *Biochemical Journal*, 259(3), pp. 893–896.

Klenk, H. P., Clayton, R. A., Tomb, J. F., White, O., Nelson, K. E., Ketchum, K. A., Dodson, R. J., Gwinn, M., Hickey, E. K., Peterson, J. D., Richardson, D. L., Kerlavage, A. R., Graham, D. E., Kyrpides, N. C., Fleischmann, R. D., Quackenbush, J., Lee, N. H., Sutton, G. G., Gill, S., Kirkness, E. F., ... Venter, J. C (1997) 'The complete genome sequence of the hyperthermophilic, sulphate-reducing archaeon *Archaeoglobus fulgidus*', *Nature*, 390(6658), pp. 364–370.

Klopfenstein, T. J., Angel, R., Cromwell, G., Erickson, G.E., Fox, D.G., Parsons, C., Satter, L.D., Sutton, A.L., Baker, D.H., Lewis, A., Meyer, D. (2002) *Animal Diet Modification to Decrease the Potential for Nitrogen and Phosphorus Pollution*.

Kongsbak, M., Levring, T.D., Geisler, C., von Esse, M.R. (2013) 'The vitamin D receptor and T cell function', *Frontiers in Immunology*, 4(JUN), pp. 1–10.

Kornegay, E. T., Denbow, D.M., Yi, Z., Ravindran, V. (1996) 'Response of broilers to graded levels of microbial phytase added to maize-soyabean-meal-based diets containing three levels of non-phytate phosphorus', *British Journal of Nutrition*, 75(6), pp. 839–852.

Kotewicz, M. L., D'Alessio, J.M., Driftmier, K.M., Blodgett, K.P., Gerard, G.F. (1985) 'SuperScript II Reverse Transcriptase Protocol', *Gene J. Virol. Acids Res*, 35(16).

Kriseldi, R. Walk, C. L., Bedford, M.R., and Dozier, W.A. (2021) 'Inositol and gradient phytase supplementation in broiler diets during a 6-week production period: 2. Effects on phytate degradation and inositol liberation in gizzard and ileal digesta contents', *Poultry Science*. Elsevier Inc., 100(3), p. 100899.

Kulis-Horn, R. K., Rückert, C., Kalinowski, J., Persicke, M. (2017) 'Sequence-based identification of inositol monophosphatase-like histidinol-phosphate phosphatases (HisN) in *Corynebacterium glutamicum*, Actinobacteria, and beyond', *BMC Microbiology*. BMC Microbiology, 17(1), pp. 1–22.

Kumar, R. and Thompson, J. R. (2011) 'The regulation of parathyroid hormone secretion and synthesis', *Journal of the American Society of Nephrology*, 22(2), pp. 216–224.

Kumar, V. and Sinha, A. K. (2018) *General aspects of phytases, Enzymes in Human and Animal Nutrition: Principles and Perspectives*. Elsevier Inc.

Kumar, V., Miasnikov, A., Sands, J.S., Simmins, P.H. (2003) 'In vitro activities of three phytases under different pH and protease challenges.' *Proceedings of the Australian Pig Science Association*. p. 164.

Kunitz, M. and McDonald, M. R. (1946) 'Crystalline hexokinase (heterophosphatase)', *The Journal of General Physiology*, 29(6), pp. 393–412.

Kushnirov, Vitaly V and Kushnirov, V V (2000) 'Yeast Functional Analysis Report Rapid and reliable protein extraction from yeast', *Yeast*, 16, pp. 857–860.

Kuttappan, V. A., Hargis, B. M. and Owens, C. M. (2016) 'White striping and woody breast myopathies in the modern poultry industry: A review', *Poultry Science*. Poultry Science Association Inc., 95(11), pp. 2724–2733.

LaCourse, W. R. and Johnson, D. C. (1993) 'Optimization of waveforms for pulsed amperometric detection of carbohydrates based on pulsed voltammetry', *Analytical Chemistry*, 65(1), pp. 50–55.

Laha, D., Parvin N., Dynowski, M., Johnen, P., Mao, H., Bitters, S.T., Zheng, N., Schaaf, G. (2016) 'Scientific Correspondence Inositol Polyphosphate Binding Specificity of the Jasmonate Receptor Complex 1[OPEN]', *Plant Physiology* *Ò*, 171, pp. 2364–2370.

Lahjouji, K., Aouameur, R., Bissonnette, P., Coady, M.J., Bichet, D.G., Lapoint, J.-Y. (2007) 'Expression and functionality of the Na⁺/myo-inositol cotransporter SMIT2 in rabbit kidney', *Biochimica et Biophysica Acta - Biomembranes*, 1768(5), pp. 1154–1159.

Laird, S., Kühn, I., Wilcock, P., Miller, H.M. (2016) 'The effects of phytase on grower pig growth performance and ileal inositol phosphate degradation', *Journal of Animal Science*, 94(7), pp. 142–145.

Larner, J. (2002) 'D-chiro-inositol--its functional role in insulin action and its deficit in insulin resistance.', *International journal of experimental diabetes research*. Hindawi Limited, 3(1), pp. 47–60.

Larner, J. and Craig J.W. (1996) 'Urinary myo-inositol to chiro-inositol ratios and insulin resistance.' *Diabetes Care* 19, (1): 76-78.

Lassen, S. F., Breinholt, J., Østergaard, P., Brugger, R., Bischoff, A., Wyss, M., Fuglsang, C. (2001) 'Expression, Gene Cloning, and Characterization of Five Novel Phytases from Four Basidiomycete Fungi: *Peniophora lycii*, *Agrocybe pediades*, a *Ceriporia* sp., and *Trametes pubescens*', *Applied and Environmental Microbiology*, 67(10), pp. 4701–4707.

Laurence, W. L. (1936) 'Corn by-product yields explosive', *The New York Times*, 17 April, p. 7.

Laussmann, T., Pikzack, C., Thiel, U., Mayr, G.W., Vogel, G. (2000) 'Diphospho-*myo*-inositol phosphates during the life cycle of *Dictyostelium* and *Polysphondylium*', *European Journal of Biochemistry*, 267(8), pp. 2447–2451.

Ledgard, J. B. (2007) *The preparatory manual of explosives : a book*.

Lee, C. H., Dixon, J.F., Reichman, M., Moumami, C., Los, G., Hokin, L.E. (1992) 'Li⁺ increases accumulation of inositol 1,4,5-trisphosphate and inositol 1,3,4,5-tetrakisphosphate in cholinergically stimulated brain cortex slices in guinea pig, mouse and rat. The increases require inositol supplementation in mouse and rat but not in gu', *Biochemical Journal*, 282(2), pp. 377–385.

Lee, J., Choi, Y., Lee, P.-C., Kang, S., Bok, J., Cho, J. (2007) 'Recombinant production of *Penicillium oxalicum* PJ3 phytase in *Pichia Pastoris*', *World Journal of Microbiology and Biotechnology*, 23(3), pp. 443–446.

Lee, S. A., Dunne, J., Mottram, T., Bedford, M.R. (2017) 'Effect of diet phase change, dietary Ca and P level and phytase on bird performance and real-time gizzard pH measurements', *British Poultry Science*, 58(3), pp. 290–297.

Lee, S. A., Dunne, J., Febery, E., Brearley, C.A., Mottram, T., Bedford, M.R. (2018) 'Exogenous phytase and xylanase exhibit opposing effects on real-time gizzard pH in broiler chickens.', *British Poultry Science*, 59(5), pp. 568–578.

Lee, S. A. and Bedford, M. R. (2016) 'Inositol - An effective growth promotor?', *World's Poultry Science Journal*, 72(4), pp. 743–760.

Letcher, A. J., Schell, M. J. and Irvine, R. F. (2008) 'Do mammals make all their own inositol hexakisphosphate?', *Biochemical Journal*, 416(2), pp. 263–270.

Levine, J., Barak, Y., Gonzales, M., Szor, H., Elizur, A., Kofman, O., and Belmarker, R.H. (1995b) Double-blind, controlled trial of inositol treatment of depression. *Am. J. Psychiatry* 152:792-794.

Leybaert, L., Paemeleire, K., Strahonja, A., Sanderson, M.J. (1998) 'Inositol-triphosphate-dependent intercellular calcium signalling in and between astrocytes and endothelial cells', *Glia*, 24, pp. 398–407.

Leytem, A. B., Widyaratne, G. P. and Thacker, P. A. (2008) 'Phosphorus utilization and characterization of ileal digesta and excreta from broiler chickens fed diets varying in cereal grain, phosphorus level, and phytase addition', *Poultry Science*. Poultry Science Association Inc., 87(12), pp. 2466–2476.

Li, W., Angel, R., Kim, S.-W., Jiménez-Moreno, E., Proszkowiec-Weglarz, M., Plumstead, P.W. (2015) 'Impact of response criteria (tibia ash weight vs. percent) on phytase relative non phytate phosphorus equivalance', *Poultry Science*, 94(9), pp. 2228–2234.

Li, X., Gu, C., Hostachy, S., Sahu, S., Wittwer, C., Jessen, H.J., Fiedler, D., Wang, H., Shears, S.B. (2020) 'Control of XPR1-dependent cellular phosphate efflux by InsP8 is an exemplar for functionally-exclusive inositol pyrophosphate signaling', *Proceedings of the National Academy of Sciences of the United States of America*, 117(7), pp. 3568–3574.

Lim, H. S., Namkung, H. and Paik, I. K. (2003) 'Effects of phytase supplementation on the performance, egg quality, and phosphorous excretion of laying hens fed different levels of dietary calcium and nonphytate phosphorous', *Poultry Science*. Poultry Science Association Inc., 82(1), pp. 92–99.

Lim, P. E. and Tate, M. E. (1973) 'The phytases. II. Properties of phytase fractions F1 and F2 from wheat bran and the *myo*-inositol phosphates produced by fraction F2', *Biochimica et Biophysica Acta*, 302(2), pp. 316–328.

Liu, N., Ru, Y.J., Li, F.D., Wang, J.-P., Lei, X.-Q. (2009) 'Effect of dietary phytate and phytase on proteolytic digestion and growth regulation of broilers', *Archives of Animal Nutrition*, 63(4), pp. 292–303.

Liu, N., Ru, Y., Wang, J., Xu, T. (2010) 'Effect of dietary sodium phytate and microbial phytase on the lipase activity and lipid metabolism of broiler chickens', *British Journal of Nutrition*, 103(6), pp. 862–868.

Liu, X., Yue, Y., Li, B., Nie, Y., Li, W., Wu, W.-H., Ma, L. (2007) 'A G Protein-Coupled Receptor Is a Plasma Membrane Receptor for the Plant Hormone Abscisic Acid', *Science*, 315(5819), pp. 1712–1716.

Livingston, M. L., Ferket, P.R., Brake, J., Livingston, K.A. (2019) 'Dietary amino acids under hypoxic conditions exacerbates muscle myopathies including wooden breast and white stripping', *Poultry Science*. 2018 Poultry Science Association Inc., 98(3), pp. 1517–1527.

Loewus, F. A. and Loewus, M. W. (1983) '*myo*-Inositol: Its Biosynthesis and Metabolism', *Annual Review of Plant Physiology*. Annual Reviews 4139 El Camino Way, P.O. Box 10139, Palo Alto, CA 94303-0139, USA , 34(1), pp. 137–161.

Loewus, M. W. and Loewus, F. A. (1973) 'D-Glucose 6-phosphate cycloaldolase: inhibition studies and aldolase function', *Plant Physiology*, 51(1), pp. 263–266.

Lopez, H. W., Vallery, F., Levrat-Verny, M.-A., Coudray, C., Demigné, C., Rémésy, C. (2000) 'Dietary phytic acid and wheat bran enhance mucosal

phytase activity in rat small intestine', *Journal of Nutrition*, 130(8), pp. 2020–2025.

Lopez, H. W., Leenhardt, F., Coudray, C., Remesy, C. (2002) 'Minerals and phytic acid interactions: is it a real problem for human nutrition?', *International Journal of Food Science and Technology*. Wiley/Blackwell (10.1111), 37(7), pp. 727–739.

Lu, H., Kühn, I., Bedford, M.R., Whitfield, H., Brearley, C., Adeola, O., Ajuwon, K.M. (2019) 'Effect of phytase on intestinal phytate breakdown, plasma inositol concentrations, and glucose transporter type 4 abundance in muscle membranes of weanling pigs', *Journal of Animal Science*, 97(9), pp. 3907–3919.

Lucca, W., Alves, D.A., Tombesi da Rocha, L., Shirmann, G.D., do Santos Camargo, C.A., Figueiredo, A.M., Zanella, I., de Oliveira, V. (2016) 'Endogenous losses and true digestibility of phosphorus in rice bran with or without phytase determined with piglets', *Ciência Rural*, 46(6), pp. 1082–1087.

Macri, M. A., D'Alessandro, N., Di Giulio, C., Di Iorio, P., Di Luzio, S., Giuliani, P., Bianchi, G., Esposito, E. (2006) 'Regional changes in the metabolite profile after long-term hypoxia-ischemia in brains of young and aged rats: A quantitative proton MRS study', *Neurobiology of Aging*, 27(1), pp. 98–104.

Maenz, D. D. (2001) *Enzymatic characteristics of phytases as they relate to their use in animal feeds*. Edited by M. R. Bedford and G. G. Partridge. Wallingford, UK: CABI Publishing.

Maenz, D. D. and Classen, H. L. (1998) 'Phytase Activity in the Small Intestinal Brush Border Membrane of the Chicken', *Poultry Science*. Poultry Science Association Inc., 77(4), pp. 557–563.

- Majumder, A. L., Chatterjee, A., Dastidar, K.G., Majee, M. (2003) 'Diversification and evolution of L - myo -inositol 1-phosphate synthase 1', *FEBS Letters*. John Wiley & Sons, Ltd, 553(1–2), pp. 3–10.
- Majumder, A. L., Johnson, M. D. and Henry, S. A. (1997) '1l-myoinositol-1-phosphate synthase', *Biochimica et Biophysica Acta (BBA) - Lipids and Lipid Metabolism*. Elsevier, 1348(1–2), pp. 245–256.
- Mallery, D. L., Márquez, C.L., McEwan, W.A., Dickson, C.F., Jacques, D.A., Anandapadamanaban, M., Bichel, K., Towers, G.T., Saiardi, A., Böcking, T., James, L.C. (2018) 'IP6 is an HIV pocket factor that prevents capsid collapse and promotes DNA synthesis', *eLife*, 7.
- Mallery, D. L., Rifat Faysal, K.M., Kleinpeter, A., Wilson, M.S.C., Vaysburd, M., Fletcher, A.J., Novikova, M., Böcking, T., Freed, E.O., Saiardi, A., James, L.C. (2019) 'Cellular IP6 levels limit HIV production while viruses that cannot efficiently package IP6 are attenuated for infection and replication', *Cell Reports*, 12, pp. 3983–3996.
- Mallery, D. L., Kleinpeter, A.B., Renner, N., Rifat Faysal, K.M., Novikova, M., Kiss, L., Wilson, M.S.C., Ahsan, B., Ke, Z., Briggs, J.A.G., Saiardi, A., Böcking, T., Freed, E.O., James, L.C. (2021) 'A stable immature lattice packages IP6 for HIV capsid maturation', *Science Advances*, 7(11).
- Manangi, M. K. and Coon, C. N. (2008) 'Phytate phosphorus hydrolysis in broilers in response to dietary phytase, calcium, and phosphorus concentrations', *Poultry Science*. Poultry Science Association Inc., 87(8), pp. 1577–1586.
- Maquenne, L. (1887a) 'Préparation, propriétés et constitution se l'inosite', *Comptes rendus hebdomadaires des séances de l'Académie des Sciences, Paris*, (104), pp. 225–227.
- Maquenne, L. (1887b) 'Sur les propriétés de l'inosite', *Comptes rendus*

hebdomadaires des séances de l'Académie des Sciences, Paris, (104), pp. 297–299.

Casartelli, E.M., Junquera, O.M., Laurentiz, A.C., Filardi, R.S., Lucas Junior, J., Araujo, L.F. (2005) 'Effect of phytase in laying hen diets with different phosphorus sources', *Brazilian Journal of Poultry Science*, 7(2), pp. 93–98.

Marks, A. R., Tempst, P., Chadwick, C. C. Riviere, L., Fleischer, S., Nadal-Ginard, B. (1990) 'Smooth muscle and brain inositol 1,4,5-trisphosphate receptors are structurally and functionally similar', *Journal of Biological Chemistry*, 265(34), pp. 20719–20722.

Marks, J., Debnam, E. S. and Unwin, R. J. (2010) 'Phosphate homeostasis and the renal-gastrointestinal axis', *American Journal of Physiology - Renal Physiology*, 299(2), pp. 285–296.

Matheson, K., Parsons, L. and Gammie, A. (2017) 'Whole-Genome Sequence and Variant Analysis of W303, a Widely-Used Strain of *Saccharomyces cerevisiae*.', *G3 (Bethesda, Md.)*. Genetics Society of America, 7(7), pp. 2219–2226.

Matsuda, H., Nakamura, H. and Nakajima, T. (1990) 'New Ceramic Titania: Selective Adsorbent for Organic Phosphates', *Analytical Sciences*, 6(December), pp. 1–2.

Mattila, P., Valkonen, E. and Valaja, J. (2011) 'Effect of Different Vitamin D Supplementations in Poultry Feed on Vitamin D Content of Eggs and Chicken Meat', *Journal of Agricultural and Food Chemistry*, 59(15), pp. 8298–8303.

Mayr, G. W. (1988) 'A novel metal-dye detection system permits picomolar-range h.p.l.c. analysis of inositol polyphosphates from non-radioactively labelled cell or tissue specimens.', *The Biochemical journal*, 254(2), pp. 585–591.

Mayr, G. W., Radenberg, T., Thiel, U., Vogel, G., Stephens, L.R. (1992) 'Phosphoinositol diphosphates: non-enzymic formation *in vitro* and occurrence *in vivo* in the cellular slime mold *Dictyostelium*', *Carbohydrate Research*, 234(C), pp. 247–262.

Mayr, G. W. and Dietrich, W. (1987) 'The only inositol tetrakisphosphate detectable in avian erythrocytes is the isomer lacking phosphate at position 3: a NMR study', *FEBS Letters*, 213(2), pp. 278–282.

Mayr, G. W. and Thieleczek, R. (1991) 'Masses of inositol phosphates in resting and tetanically stimulated vertebrate skeletal muscles', *Biochemical Journal*, 280(3), pp. 631–640.

Mazzoni, M., Petracci, M., Meluzzi, A., Cavani, C., Clavenzani, P., Sirri, F. (2015) 'Relationship between pectoralis major muscle histology and quality traits of chicken meat', *Poultry Science*. Poultry Science Association Inc., 94(1), pp. 123–130.

McAllister, G., Whiting, P., Hammond, E.A., Knowles, M.R., Atack, J.R., Bailey, F.J., Maigetter, R., Ragan, C.I. (1992) 'cDNA cloning of human and rat brain *myo*-inositol monophosphatase. Expression and characterization of the human recombinant enzyme.', *The Biochemical journal*. Portland Press Ltd, 284 (Pt 3)(Pt 3), pp. 749–54.

McCollum, E. V. and Hart, E. B. (1908) 'On the occurrence of a phytin-splitting enzyme in animal tissue', *J. Bio. Chem.*, 4, pp. 497–500.

McDonald, P., Edwards, R. A. and Greenhalgh, J. F. D. (1990) *Animal Nutrition*. 4th Editio. Harlow: Longman Sci. Tech.

McDonald, P., Edwards, R. A. and Greenhalgh, J. F.D. (1990) *Animal Nutrition*. 4th Edition. Harlow: Longman Sci. Tech.

Mehlhorn, J. and Caspers, S. (2021) 'The effects of domestication on the

brain and behavior of the chicken in the light of evolution', *Brain, Behavior and Evolution*, 95(6), pp. 287–301.

Mehlhorn, J. and Petow, S. (2020) 'Smaller brains in laying hens: New insights into the influence of pure breeding and housing conditions on brain size and brain composition', *Poultry Science*. Elsevier Inc., 99(7), pp. 3319–3327.

Mehta, B. D., Jog, S.P., Johnson, S.C., Murthy, P.P.N. (2006) 'Lily pollen alkaline phytase is a histidine phosphatase similar to mammalian multiple inositol polyphosphate phosphatase (MINPP)', *Phytochemistry*, 67(17), pp. 1874–1886.

Mellanby, E. (1949) 'The rickets-producing and anti-calcifying action of phytate.', *The Journal of physiology*. Wiley-Blackwell, 109(3–4), pp. 488–533, 2 pl.

Mendoza, C., Viteri, V.E., Lönnnerdal, B., Young, K.A., Raboy, V. and Brown, K.H. (1998) 'Effect of genetically modified, low-phytic acid maize on absorption of iron from tortillas.' *Am. J. Clin. Nutr.*, 68, pp. 1123-1128.

Menezes-Blackburn, D., Gabler, S. and Greiner, R. (2015) 'Performance of Seven Commercial Phytases in an *in Vitro* Simulation of Poultry Digestive Tract', *Journal of Agricultural and Food Chemistry*, 63(27), pp. 6142–6149.

Menniti, F. S., Oliver, K.G., Putney Jr., J.W., Shears, S.B. (1993) 'Inositol phosphates and cell signaling: new views of InsP5 and InsP6', *Trends in Biochemical Sciences*. Elsevier Current Trends, 18(2), pp. 53–56.

Metzler, B. U., Mosenthin, R., Baumgärtel, T., Rodehutschord, M. (2008) 'The effect of dietary phosphorus and calcium level, phytase supplementation, and ileal infusion of pectin on the chemical composition and carbohydrase activity of fecal bacteria and the level of microbial metabolites in the gastrointestinal tract of pigs^{1,2}', *Journal of Animal Science*, 86(7), pp. 1544–

1555.

Michell, R. H. (1975) 'Inositol phospholipids and cell surface receptor function', *Biochimica et Biophysica Acta (BBA) - Reviews on Biomembranes*. Elsevier, 415(1), pp. 81–147.

Michell, R. H. (2007) 'Evolution of the diverse biological roles of inositols', *Biochemical Society Symposium*, 74(February 2007), pp. 223–246.

Michell, R. H. (2008) 'Inositol derivatives: evolution and functions', *Nature Reviews Molecular Cell Biology*. Nature Publishing Group, 9(2), pp. 151–161.

Michigami, T., Kawai, M., Yamazaki, M., Ozono, K. (2018) 'Phosphate as a signaling molecule and its sensing mechanism', *Physiological Reviews*, 98(4), pp. 2317–2348.

Miñambres, I., Cuizart, G., Gonçalves, A., Corcoy, R. (2019) 'Effects of inositol on glucose homeostasis: Systematic review and meta-analysis of randomized controlled trials', *Clinical Nutrition*, 38(3), pp. 1146–1152.

Minini, M., Senni, A., Unfer, V., Bizzarri, M. (2020) 'The key role of IP6K: A novel target for anticancer treatments?', *Molecules*, 25(19), pp. 1–20.

Miyamoto, K., Tatsumi, S., Sonoda, T., Yamamoto, H., Minami, H., Taketani, Y., Takeda, E. (1995) 'Cloning and functional expression of a Na⁺-dependent phosphate co-transporter from human kidney: CDNA cloning and functional expression', *Biochemical Journal*, 305(1), pp. 81–85.

Monastra, G., Unfer, V., Harrath, A.H., Bizzarri, M. (2017) 'Combining treatment with *myo*-inositol and D -*chiro*-inositol (40:1) is effective in restoring ovary function and metabolic balance in PCOS patients', *Gynecological Endocrinology*, 33(1), pp. 1–9.

Morales, G.A., Moyano, F.J., Marquez, L. (2011) 'In vitro assessment of the effects of phytate and phytase on nitrogen and phosphorus bioaccessibility within fish digestive tract.' *Anim. Feed Sci. Technol.* 2011;170:209-221.

Moritoh, Y., Abe, S.-i., Akiyama, H., Kobayashi, A., Koyama, R., Hara, R., Kasai, S., Watanabe, M. (2021) 'The enzymatic activity of inositol hexakisphosphate kinase controls circulating phosphate in mammals', *Nature Communications*. Springer US, 12(1).

Mosblech, A., Thurow, C., Gatz, C., Feussner, I., Heilmann, I. (2011) 'Jasmonic acid perception by COI1 involves inositol polyphosphates in *Arabidopsis thaliana*', *The Plant Journal*. John Wiley & Sons, Ltd (10.1111), 65(6), pp. 949–957.

Moss, A. F., Chrystal, P.V., Truong, H.H., Liu, S.Y., Selle, P.H. (2017) 'Effects of phytase inclusions in diets containing ground wheat or 12.5% whole wheat (pre- and post-pellet) and phytase and protease additions, individually and in combination, to diets containing 12.5% pre-pellet whole wheat on the performance of broiler ', *Animal Feed Science and Technology*. Elsevier, 234(September), pp. 139–150.

Mukherjee, S., Haubner, J. and Chakraborty, A. (2020) 'Targeting the inositol pyrophosphate biosynthetic enzymes in metabolic diseases', *Molecules*, 25(6), pp. 1–28.

Mullaney, E. J., Daly, C. B. and Ullah, A. H. (2000) 'Advances in phytase research.', *Advances in applied microbiology*, 47, pp. 157–99.

Murer, H., Forster, I. and Biber, J. (2004) 'The sodium phosphate cotransporter family SLC34', *Pflugers Archiv European Journal of Physiology*, 447(5), pp. 763–767.

Nahorski, S. R., Tobin, A. B. and Willars, G. B. (1997) 'Muscarinic M3 receptor coupling and regulation', *Life Sciences*, 60(13–14), pp. 1039–1045.

Nakamura, Y., Fukuhara, H. and Sano, K. (2000) 'Secreted phytase activities of yeasts', *Bioscience, Biotechnology and Biochemistry*, 64(4), pp. 841–844.

Nakano, T., Joh, T., Tokumoto, E., Hayakawa, T. (1999) 'Purification and Characterization of Phytase from Bran of *Triticum aestivum* L. cv. Nourin #61', *Food Science Technology Research*, 5(1), pp. 18–23.

Neelon, K., Wang, Y., Stec, B., Roberts, M.F. (2005) 'Probing the mechanism of the *Archaeoglobus fulgidus* inositol-1-phosphate synthase', *Journal of Biological Chemistry*, 280(12), pp. 11475–11482.

Nelson, T. S., Shieh, T.R., Wodzinski, R.J., Ware, J.H. (1971) 'Effect of supplemental phytase on the utilization of phytate phosphorus by chicks.', *The Journal of nutrition*, 101(10), pp. 1289–1293.

Nesbo, C. L., L'Haridon, S., Stetter, K.O., Ford Doolittle, W. (2001) 'Phylogenetic analyses of two "archaeal" genes in *thermotoga maritima* reveal multiple transfers between archaea and bacteria', *Molecular Biology and Evolution*, 18(3), pp. 362–375.

Norbis, F., Boll, M., Stange, G., Markovich, D., Verrey, F., Biber, J., Murer, H. (1997) 'Identification of a cDNA/protein leading to an increased P(i)-uptake in *Xenopus laevis* oocytes', *Journal of Membrane Biology*, 156(1), pp. 19–24.

Oberleas, D., Li, Y.-C., Stoecker, B.J., Henley, S.A., Keim, K.S., Smith, J.C. (1990) 'The rate of chromium transit through the gastrointestinal tract.' *Nutr. Res.* 10 (1990), pp. 1189-1194.

Omoruyi, F. O., Stennett, D., Foster, S., Dilworth, L. (2020) 'New frontiers for the use of ip6 and inositol combination in treating diabetes mellitus: A review', *Molecules*, 25(7), pp. 1–15.

Onyango, E. M., Bedford, M. R. and Adeola, O. (2005) 'Phytase activity

along the digestive tract of the broiler chick: A comparative study of an *Escherichia coli*-derived and *Peniophora lycii* phytase', *Canadian Journal of Animal Science*, 85(1).

Ortmeyer, H.K., Bodkin, N.L., Lilley, K., Larner, J. and Hansen, B.C. (1993) 'Chiro-inositol deficiency and insulin resistance. I. Urinary excretion rate of chiro-inositol is directly associated with insulin resistance in spontaneously diabetic rhesus monkeys.' *Endocrinology*. 132: 640-645.

Ortmeyer, H. K. (1996) 'Dietary *myo*-inositol results in lower urine glucose and in lower postprandial plasma glucose in obese insulin resistant rhesus monkeys', *Obesity Research*, 4(6), pp. 569–575.

Ousterhout, L.E. (1980) 'Effects of Calcium and Phosphorus levels on egg weight and egg shell quality in laying hens.' *Poultry Science* 59 (7):1480-1484.

Özbek, M., Petek, M. and Ardlıll, S. (2020) 'Physical quality characteristics of breast and leg meat of slow-and fast-growing broilers raised in different housing systems', *Archives Animal Breeding*, 63(2), pp. 337–344.

Parthasarathy, L. K., Seelan, R.S., Tobias, C., Casanova, M.F.,m Parthasarathy, R.N. (2006) 'Mammalian inositol 3-phosphate synthase: its role in the biosynthesis of brain inositol and its clinical use as a psychoactive agent.', *Sub-cellular biochemistry*, 39, pp. 293–314.

Parthasarathy, R. and Eisenberg, F. (1991) 'Biochemistry, Stereochemistry, and Nomenclature of the Inositol Phosphates', *Biochemical Journal*, (235), pp. 313–322.

Pelícia, V. C., Araujo, P.C., Luiggi, F.G., Stradiotti, A.C., Denadai, J.C., Sartori, J.R., Pacheco, P.D.G., Dornelas, L.C., Silva, E.T., Souza-Kruliski, C.R., Pimenta, G.E.M., Ducatti, C. (2018) 'Estimation of the metabolic rate by assessing carbon-13 turnover in broiler tissues using the stable isotope

technique', *Livestock Science*. Elsevier B.V., 210(January), pp. 8–14.

Persson, H., Turk, M., Nyman, M., Sandberg, A.S. (1998) 'Binding of Cu^{2+} , Zn^{2+} , and Cd^{2+} to inositol tri-, tetra-, penta-, and hexaphosphates', *Journal of Agricultural and Food Chemistry*, 46, pp. 3194–3200.

Phillippy, B. Q. (1999) 'Susceptibility of wheat and *Aspergillus niger* phytases to inactivation by gastrointestinal enzymes', *Journal of Agricultural and Food Chemistry*, 47(4), pp. 1385–1388.

Phillippy, B. Q. and Bland, J. M. (1988) 'Gradient ion chromatography of inositol phosphates', *Analytical Biochemistry*, 175(1), pp. 162–166.

Piccolo, E., Vignati, S., Maffucci, T., Innominato, P.F., Riley, A.M., Potter, B.V.L., Pandolfi, P.P., Broggin, M., Iacobelli, S., Innocenti, P., Falasca, M. (2004) 'Inositol pentakisphosphate promotes apoptosis through the PI 3-K/Akt pathway', *Oncogene*. Nature Publishing Group, 23(9), pp. 1754–1765.

Pinkse, M. W. H., Uitto, P.M., Hilhorst, M.J., Ooms, B., Heck, A.J.R. (2004) 'Selective isolation at the femtomole level of phosphopeptides from proteolytic digests using 2D-NanoLC-ESI-MS/MS and titanium oxide precolumns', *Analytical Chemistry*, 76(14), pp. 3935–3943.

Pirgozliev, V., Acamovic, T., Bedford, M., Oduguwa, O. (2008) 'Effects of dietary phytase on performance and nutrient metabolism in chickens', *British Poultry Science*, 49(2), pp. 144–154.

Pirgozliev, V., Bedford, M.R., Acamovic, T., Mares, P., Allymehr, M. (2011) 'The effects of supplementary bacterial phytase on dietary energy and total tract amino acid digestibility when fed to young chickens', *British Poultry Science*, 52(2), pp. 245–254.

Pirgozliev, V., Brearley, C.A., Rose, S.P., Mansbridge, S.C. (2019a) 'Manipulation of plasma myo-inositol in broiler chickens: Effect on growth

performance, dietary energy, nutrient availability, and hepatic function', *Poultry Science*. Poultry Science Association Inc., 98(1), pp. 260–268.

Pisani, F., Livermore, t., Rose, G., Chubb, J.R., Gaspari, M., Saiardi, A. (2014) 'Analysis of Dictyostelium discoideum inositol pyrophosphate metabolism by gel electrophoresis', *PLoS ONE*, 9(1), pp. 1–9.

Pointillart, A. (Institut N. de R. A. (INRA), J.-E.-J. (France). L. de N. et S. A. (1994) 'Phytate and phytase. Their role in monogastric nutrition [swine, poultry]', *Summa (Italy)*.

Pollard-Knight, D. and Cornish-Bowden, A. (1982) 'Mechanism of liver glucokinase', *Molecular and Cellular Biochemistry*, 44(2), pp. 71–80.

Portale, A. A., Booth, B.E., Halloran, B.P., Morris Jr., R.C. (1984) 'Effect of dietary phosphorus on circulating concentrations of 1,25-dihydroxyvitamin D and immunoreactive parathyroid hormone in children with moderate renal insufficiency', *Journal of Clinical Investigation*, 73(6), pp. 1580–1589.

Prentki, M., Biden, T.J., Janjic, D., Irvine, R.F., Berridge, M.J. and Wollheim, C.B. (1984) 'Rapid mobilization of Ca²⁺ from rat insulinoma microsomes by inositol 1,4,5-trisphosphate.' *Nature*, 309, pp. 562-564.

Priya, S. S., Bhyvaneswari, K. and Patwari, P. (2013) 'A study on the effects of scyllo-inositol on learning and memory in senile swiss albino mice', *International Journal of Pharmaceutical and Biological Archives*, 4(5), pp. 868–872.

Proudfoot, F.G., Sefton, A.E. (1978) 'Feed texture and light treatment effects on the performance of chicken broilers.' *Poultry Science* 57(2):408-416.

Puhl, A. A., Greiner, R. and Selinger, B. (2008) 'A protein tyrosine phosphatase-like inositol polyphosphatase from *Selenomonas ruminantium* subsp. *lactilytica* has specificity for the 5-phosphate of *myo*-inositol

hexakisphosphate', *The International Journal of Biochemistry & Cell Biology*, 40(10), pp. 2053–2064.

QIAGEN (2001) 'QIAquick Gel Extraction Kit Protocol', *QIAquick Spin Handbook*, 03/2001(July), pp. 23–24.

QIAGEN (2012) 'RNeasy Mini Handbook', *Sample & Assay Technologies*, (June), pp. 50–54.

QIAGEN. (2015) 'QIAprep ® Miniprep Handbook For purification of molecular biology grade DNA Sample & Assay Technologies', *QIAGEN Sample and Assay Technologies*, (June), pp. 20–22.

Qian, H., Kornegay, E. T. and Denbow, D. M. (1997) 'Utilization of Phytate Phosphorus and Calcium as Influenced by Microbial Phytase, Cholecalciferol, and the Calcium:Total Phosphorus Ratio in Broiler Diets', *Poultry Science*. Poultry Science Association Inc., 76(1), pp. 37–46.

Qiu, D., Wilson, M.S., Eisenbeis, V.B., Jarmel, R.K., Riemer, E., Haas, T.M., Wittwer, C., Jork, N., Gy, C., Shears, S.B., Schaaf, G., Kammerer, B., Fiedler, D., Saiardi, A., Jessen, H.J. (2020) 'Analysis of inositol phosphate metabolism by capillary electrophoresis electrospray ionization mass spectrometry', *Nature Communications*. Springer US, 11(1), pp. 1–12.

Quamme, G. A. (1985) 'Phosphate transport in intestinal brush-border membrane vesicles: effect of pH and dietary phosphate', *American Journal of Physiology - Gastrointestinal and Liver Physiology*, 249, pp. 168–176.

Quarles, L.D. (2012) 'Role of FGF23 in vitamin D and phosphate metabolism: implications in chronic kidney disease.' *Exp. Cell Res.* May 15; 318(9):1040-8.

Raboy, V. (2009) 'Approaches and challenges to engineering seed phytate and total phosphorus', *Plant Science*, 177(4), pp. 281–296.

Radioactive Substances Act (1993). Available at <https://legislation.gov.uk/ukpga/1993/12/contents>

Raghavendra, P. and Halami, P. M. (2009) 'Screening, selection and characterization of phytic acid degrading lactic acid bacteria from chicken intestine', *International Journal of Food Microbiology*. Elsevier B.V., 133(1–2), pp. 129–134.

Rao, D. E. C. S., Rao, K. V., Reddy, T. P., Reddy, V.D. (2009) 'Molecular characterization, physicochemical properties, known and potential applications of phytases: An overview', *Critical Reviews in Biotechnology*, 29(2), pp. 182–198.

Rapoport, S., Leva, E. and Guest, G. M. (1941) 'Phytase in Plasma and Erythrocytes of Various Species of Vertebrates', *Journal of Biological Chemistry*, 139(2), pp. 621–632.

Rapp, C., Lantzsch, H. J. and Drochner, W. (2001) 'Hydrolysis of phytic acid by intrinsic plant and supplemented microbial phytase (*Aspergillus niger*) in the stomach and small intestine of minipigs fitted with re-entrant cannulas 3. Hydrolysis of phytic acid (IP6) and occurrence of hydrolysis products (IP', *Journal of Animal Physiology and Animal Nutrition*, 85(11–12), pp. 420–430.

Ravindran, V., Cabahug, S., Ravindra, G., Selle, P.H., Bryden, W.L. (2000) 'Response of broiler chickens to microbial phytase supplementation as influenced by dietary phytic acid and non-phytate phosphorous levels. II. Effects on apparent metabolisable energy, nutrient digestibility and nutrient retention', *British Poultry Science*, 41(2), pp. 193–200.

Ravindran, V. (2013) 'Feed enzymes: The science, practice, and metabolic realities', *Journal of Applied Poultry Research*, 22(3), pp. 628–636.

Razzaque, M. S. (2011) 'Phosphate toxicity: new insights into an old

problem', *Clinical Science*, 120(3), pp. 91–97.

Reddy, C. S., Vani, K., Pandey, S., Vijaylakshmi, M., Reddy, C.O., Kaul, T. (2013) 'Manipulating Microbial Phytases For Heterologous Expression In Crops For Sustainable Nutrition', *Annals of Plant Sciences*, 2, pp. 436–454.

Reeves, T. D., Warner, D.M., Ludlow, L.H., O'Connor, C.M. (2018) 'Pathways over Time: Functional Genomics Research in an Introductory Laboratory Course', *CBE—Life Sciences Education*. Edited by J. Hewlett, 17(1), p. ar1.

Rejczak, T. and Tuzimski, T. (2015) 'A review of recent developments and trends in the QuEChERS sample preparation approach', *Open Chemistry*, 13(1), pp. 980–1010.

Ren, Z., Bütz, D.E., Sand, J.M., Cook, M.E. (2017a) 'Maternally derived anti-fibroblast growth factor 23 antibody as new tool to reduce phosphorus requirement of chicks', *Poultry Science*, 96(4), pp. 878–885.

Ren, Z., Bütz, D.E., Wahhab, A.N., Piepenburg, A.J., Cook, M.E. (2017b) 'Additive effects of fibroblast growth factor 23 neutralization and dietary phytase on chick calcium and phosphorus metabolism', *Poultry Science*, 96(5), pp. 1167–1173.

Reyer, H., Oster, M., Pnsuksili, S., Trakooljul, N., Omotoso, A.O., Iqbal, M.A., Murani, E., Sommerfeld, V., Rodehutsord, M., Wimmers, K. (2021) 'Transcriptional responses in jejunum of two layer chicken strains following variations in dietary calcium and phosphorus levels', *BMC Genomics*. *BMC Genomics*, 22(1), pp. 1–12.

Ritchie, H. and Roser, M. (2019) *Land Use, Our World In Data*.

Rix, G. D., Todd, J.D., Neal, A.L., Brearley, C.A. (2021) 'Improved sensitivity, accuracy and prediction provided by a high-performance liquid

chromatography screen for the isolation of phytase-harboring organisms from environmental samples', *Microbial Biotechnology*, 14(4), pp. 1409–1421.

Roberts, M. F. (2006) 'Inositol in Bacteria and Archaea', in Majumder, A. L. and Biswas, B. B. (eds) *Biology of Inositols and Phosphoinositides. Subcellular Biochemistry*, vol. 39. Boston, MA: Springer, pp. 103–133.

Rockland Immunochemicals (2020) *Alkaline Phosphatase, Calf Intestinal (CIP), Rockland Antibodies and Assays*.

Rodehutschord, M., Rückert, C., Maurer, H.P., Schenkel, H., Schipprack, W., Knudsen, K.E.B., Schollenberger, M., Laux, M., Eklund, M., Siegert, W., Mosenthin, R. (2016) 'Variation in chemical composition and physical characteristics of cereal grains from different genotypes', *Archives of Animal Nutrition*, 70(2), pp. 87–107.

Rodehutschord, M., Sanver, F. and Timmler, R. (2002) 'Comparative Study on the Effect of Variable Phosphorus Intake at two Different Calcium Levels on P Excretion and P Flow at the Terminal Ileum of Laying Hens', *Archives of Animal Nutrition*, 56(3), pp. 189–198.

Rodrigues, M.V., Borges, N., Henriques, M., Lamosa, P., Ventura, R., Fernandes, C., Empadinhas, N., Maycock, C., da Costa, M.S., Santos, H. (2007) 'Bifunctional CTP:inositol-1-phosphate cytidyltransferase/CDP-inositol:inositol-1-phosphate transferase, the key enzyme for di-myo-inositol-phosphate synthesis in several (hyper)thermophiles. *J. Bacteriol.* 2007 Aug; 189(15): 5405-12.

Rohrer, J. (2013) 'Optimal Settings for Pulsed Amperometric Detection of Carbohydrates Using the Dionex ED40 Electrochemical Detector', *Thermo Scientific Inc*, pp. 1–4.

Ros, M. B. H., Koopmans, G.F., van Groenigen, K.J., Abalos, D., Oenema,

O., Vos, H.M.J., van Groenigen, J.W. (2020) 'Towards optimal use of phosphorus fertiliser', *Scientific Reports*. Nature Publishing Group UK, 10(1), pp. 1–8.

Rutherford, S. M., Chung, T.K., Thomas, D.V., Zou, M.L., Moughan, P.J. (2012) 'Effect of a novel phytase on growth performance, apparent metabolizable energy, and the availability of minerals and amino acids in a low-phosphorus corn-soybean meal diet for broilers', *Poultry Science*. Poultry Science Association Inc., 91(5), pp. 1118–1127.

Sahara, E., Despedia, F. and Aminah, R. A. (2018) 'The Influence of Phytase Enzyme to Laying Performance and Quality of Egg Shell of Golden Arabian Chicken', *E3S Web of Conferences*, 68, pp. 1–6.

Saiardi, A., Guillermier, C., Loss, O., Poczatek, J.C., Lechene, C. (2014) 'Quantitative imaging of inositol distribution in yeast using multi-isotope imaging mass spectrometry (MIMS)', *Surf Interface Anal.*, (46), pp. 169–172.

Salanova, M., Priori, G., Barone, V., Intravaia, E., Flucher, B., Ciruela, F., McIlhinney, R.A.J., Parys, J.B., Mikoshiba, K., Sorrentino, V. (2002) 'Homer proteins and InsP3 receptors co-localise in the longitudinal sarcoplasmic reticulum of skeletal muscle fibres', *Cell Calcium*, 32(4), pp. 193–200.

Dos Santos, T. T., Srinongkote, S., Bedford, M.R., Walk, C.L. (2013) 'Effect of high phytase inclusion rates on performance of broilers fed diets not severely limited in available phosphorus', *Asian-Australasian Journal of Animal Sciences*, 26(2), pp. 227–232.

Schell, M. J., Letcher, A.J., Brearley, C.A., Biber, J., Murer, H., Irvine, R.F. (1999) 'PiUS (Pi uptake stimulator) is an inositol hexakisphosphate kinase', *FEBS Letters*, 461(3), pp. 169–172.

Scherer, J. (1850) 'Über eine neue aus dem Muskelfleisch gewonnene Zuckerart', *Liebigs Annalen der Chemie*, (73), p. 322.

Schmeisser, J., Séon, A.-A., Aureli, R., Friedel, A., Guggenbuhl, P., Duval, S., Cowieson, A.J., Fru-Nji, F. (2017) 'Exploratory transcriptomic analysis in muscle tissue of broilers fed a phytase-supplemented diet', *Journal of Animal Physiology and Animal Nutrition*, 101(3), pp. 563–575.

Schmid, M., Davison, T.S., Henz, S.R., Pape, U.J., Demar, M., Vingron, M., Schölkopf, B., Weigel, D., Lohmann, J.U. (2005) 'A gene expression map of *Arabidopsis thaliana* development', *Nature Genetics*, 37(5), pp. 501–506.
doi: 10.1038/ng1543.

Schneider, S. (2015) 'Inositol transport proteins', *FEBS Letters*, 589(10), pp. 1049–1058.

Schollenberger, M., Sommerfeld, V., Hartung, J., Rodehutschord, M. (2022) 'Storage duration conditions change the phytate content and phytase activity of wheat grains.' *JSFA Reports*. 2022;2: 100-106.

Scott, M. L., Nesheim, M. C. and Young, R. J. (1982) *Nutrition of the chicken*. Ithaca, New York: M. L. Scott and Associates .

Sebastian, S., Touchburn, S.P., Chavez, E.R., Laguë, P.C. (1996) 'Efficacy of Supplemental Microbial Phytase at Different Dietary Calcium Levels on Growth Performance and Mineral Utilization of Broiler Chickens', *Poultry Science*, 75(12), pp. 1516–1523.

Sedrani, S. H. (1984) 'Changes in serum levels of 1,25-dihydroxyvitamin D₃, calcium and phosphorus with age and vitamin D status in chickens', *British Journal of Nutrition*, 25(2), pp. 329–334.

Selle, P. H., Ravindran, V., Bryden, W.L., Scott, T. (2006) 'Influence of dietary phytate and exogenous phytase on amino acid digestibility in poultry: a review', *The Journal of Poultry Science*, 43, pp. 89–103.

Selle, P. H., Ravindran, V., Ravindran, G., Bryden, W.L. (2007) 'Effects of dietary lysine and microbial phytase on growth performance and nutrient utilisation of broiler chickens', *Asian-Australasian Journal of Animal Sciences*, 20(7), pp. 1100–1107.

Selle, P. H. and Ravindran, V. (2007) 'Microbial phytase in poultry nutrition', *Animal Feed Science and Technology*, 135(1–2), pp. 1–41.

Selle, P. H., Ravindran, V. and Partridge, G. G. (2009) 'Beneficial effects of xylanase and/or phytase inclusions on ileal amino acid digestibility, energy utilisation, mineral retention and growth performance in wheat-based broiler diets', *Animal Feed Science and Technology*, 153(3–4), pp. 303–313.

Shanmugasundaram, R. and Selvaraj, R. K. (2012) 'Vitamin D-1 α -hydroxylase and vitamin D-24-hydroxylase mRNA studies in chickens', *Poultry Science*. Poultry Science Association Inc., 91(8), pp. 1819–1824.

Sharma, N. K., Choct, M., Wu, S.-B., Smillie, R., Morgan, N., Omar, A.S., Sharma, N., Swick, R.A. (2016) 'Performance, litter quality and gaseous odour emissions of broilers fed phytase supplemented diets', *Animal Nutrition*. Elsevier Ltd, 2(4), pp. 288–295.

Shastak, Y., Witzig, M., Hartung, K., Bessei, W., Rodehutschord, M. (2012) 'Comparison and evaluation of bone measurements for the assessment of mineral phosphorus sources in broilers', *Poultry Science*. Poultry Science Association Inc., 91(9), pp. 2210–2220.

Shastak, Y., Zeller, E., Witzig, M., Schollenberger, M., Rodehutschord, M. (2014) 'Effects of the composition of the basal diet on the evaluation of mineral phosphorus sources and interactions with phytate hydrolysis in broilers', *Poultry Science*. Poultry Science Association Inc., 93(10), pp. 2548–2559.

Shears, S. B. (1992) *Advances in Second Messenger and Phosphoprotein*

research, Vol. 26. Edited by J. W. Putney Jr. New York: Raven Press.

Shears, S. B. (2009) 'Diphosphoinositol polyphosphates: Metabolic messengers?', *Molecular Pharmacology*, 76(2), pp. 236–252.

Sherman, W. R., Stewart, M. A. and Zinbo, M. (1969) 'Mass spectrometric study on the mechanism of D-glucose 6-phosphate-L-myo-inositol 1-phosphate cyclase', *Journal of Biological Chemistry*, 244(20), pp. 5703–5708.

Shetty, H. U., Schapiro, M.B., Holloway, H.W., Rapoport, S.I. (1995) 'Polyol profiles in Down syndrome. myo-Inositol, specifically, is elevated in the cerebrospinal fluid', *Journal of Clinical Investigation*, 95(2), pp. 542–546.

Shi, J., Wang, H., Hazebroek, J., Ertl, D.S., Harp, T. (2005) 'The maize low-phytic acid 3 encodes a *myo*-inositol kinase that plays a role in phytic acid biosynthesis in developing seeds', *Plant Journal*, 42(5), pp. 708–719.

Shi, L., Potts, M. and Kennelly, P. J. (1998) 'The serine, threonine, and/or tyrosine-specific protein kinases and protein phosphatases of prokaryotic organisms: A family portrait', *FEMS Microbiology Reviews*, 22(4), pp. 229–253.

Shimada, T., Mizutani, S., Muto, T., Yoneya, T., Hino, R., Takeda, S., Takeuchi, Y., Fujita, T., Fukumoto, S., Yamashita, T. (2001) 'Cloning and characterization of FGF23 as a causative factor of tumor-induced osteomalacia', *Proceedings of the National Academy of Sciences of the United States of America*, 98(11), pp. 6500–6505.

Shimada, T., Hasegawa, H., Yamazaki, Y., Muto, T., Hino, R., Takeuchi, Y., Fujita, T., Nakahara, K., Fukumoto, S., Yamashita, T. (2004) 'FGF-23 is a potent regulator of vitamin D metabolism and phosphate homeostasis', *Journal of Bone and Mineral Research*, 19(3), pp. 429–435.

Shimada, T., Kakitani, M., Yamazaki, Y., Hasegawa, H., Takeuchi, Y., Fujita, T., Fukumoto, S., Tomizuka, K., Yamashita, T. (2004) 'Targeted ablation of Fgf23 demonstrates an essential physiological role of FGF23 in phosphate and vitamin D metabolism', *Journal of Clinical Investigation*, 113(4), pp. 561–568.

Shin, S., Ha, N.-C., Oh, B.-C., Oh, T.-K., Oh, B.-H.. (2001) 'Enzyme mechanism and catalytic property of β propeller phytase', *Structure*, 9(9), pp. 851–858.

Shirayama, Y., Takahashi, M., Osone, F., Hara, A., Okubo, T. (2017) 'Myo-inositol, Glutamate, and Glutamine in the Prefrontal Cortex, Hippocampus, and Amygdala in Major Depression', *Biological Psychiatry: Cognitive Neuroscience and Neuroimaging*. Elsevier, 2(2), pp. 196–204.

Sigma-Aldrich (2017) 'Hexokinase from *Saccharomyces cerevisiae*', *Yeast*.

Simon, O. and Igbasan, F. (2002) 'In vitro properties of phytases from various microbial origins', *International Journal of Food Science and Technology*, 37(7), pp. 813–822.

Simpson, C. F., Waldroup, P.W., Ammerman, C.B., Harms, R.H. (1964) 'Relationship of Dietary Calcium and Phosphorus Levels to the Cage Layer Fatigue Syndrome', *Avian Diseases*. American Association of Avian Pathologists, 8(1), p. 92.

Sizeland, P. C. B., Chambers, S.T., Lever, M., Bason, L.M., Robson, R.A. (1993) 'Organic osmolytes in human and other mammalian kidneys', *Kidney International*. Elsevier Masson SAS, 43(2), pp. 448–453.

Skadhauge, E. and Schmidt-Nielsen, B. (1967) 'Renal function in domestic fowl.', *The American journal of physiology*, 212(4), pp. 793–798.

Skipitytė, R., Mašalaite, A., Garbaras, A., Mickiene, R., Ragažinskiene, O.,

Baliukoniene, V., Bakutis, B., Šiugždaite, J., Petkevičius, S., Maruška, a.S., Remeikis, V. (2017) 'Stable isotope ratio method for the characterisation of the poultry house environment', *Isotopes in Environmental and Health Studies*. Taylor & Francis, 53(3), pp. 243–260.

Sommerfeld, V. Künzel, S., Schollenberger, M., Kühn, I., Rodehutsord, M. (2018a) 'Influence of phytase or *myo*-inositol supplements on performance and phytate degradation products in the crop, ileum, and blood of broiler chickens', *Poultry Science*, 97(3), pp. 920–929.

Sommerfeld, V., Schollenberger, M., Kühn, I., Rodehutsord, M. (2018b) 'Interactive effects of phosphorus, calcium, and phytase supplements on products of phytate degradation in the digestive tract of broiler chickens', *Poultry Science*, 97(4), pp. 1177–1188.

Sommerfeld, V. *et al.* (2019) 'Phytate degradation in gnotobiotic broiler chickens and effects of dietary supplements of phosphorus, calcium, and phytase', *Poultry Science*, 98(11), pp. 5562–5570.

Sommerfeld, V., Van Kessel, A.G., Classen, H.L., Schollenberger, M., Kühn, I., Rodehutsord, M. (2020) 'Phytate degradation, *myo*-inositol release, and utilization of phosphorus and calcium by two strains of laying hens in five production periods', *Poultry Science*, 99(12), pp. 6797–6808.

Sooncharernying, S., Edwards, H.M. (1993) 'Phytate content of excreta and phytate retention in the gastrointestinal tract of young chickens.' *Poultry Science* 72, pp.1906-1916.

Soupart, A., Silver, S., Schroöder, B., Sterns, R., Decaux, G. (2002) 'Rapid (24-hour) reaccumulation of brain organic osmolytes (particularly *myo*-inositol) in azotemic rats after correction of chronic hyponatremia', *Journal of the American Society of Nephrology*, 13(6), pp. 1433–1441.

Spencer, J. D., Allee, G. L. and Sauber, T. E. (2000) 'Growing-finishing

performance and carcass characteristics of pigs fed normal and genetically modified low-phytate corn', *Journal of Animal Science*, 78(6), pp. 1529–1536.

Sprigg, C., Whitfield, H., Burton, E., Scholey, D., Bedford, M.R., Brearley, C.A. (2022) 'Phytase dose-dependent response of kidney inositol phosphate levels in poultry', *PLoS ONE*, 17(10), P. e0275742.

St-Arnaud, R., Arabian, A., Travers, R., Barletta, F., Raval-Pandya, M., Chapin, K., Depovere, J., Mathieu, C., Christakos, S., Demay, M.B., Glorieux, F.H. (2000) 'Deficient mineralization of intramembranous bone in vitamin D-24-hydroxylase-ablated mice is due to elevated 1,25-dihydroxyvitamin D and not to the absence of 24,25-dihydroxyvitamin D', *Endocrinology*, 141(7), pp. 2658–2666.

Steelman, Z. A., Tolstykh, G.P., Estlack, L., Roth, C.C., Ibey, B.L. (2015) 'The role of PIP₂ and the IP₃ /DAG pathway in intracellular calcium release and cell survival during nanosecond electric pulse exposures', in Ryan, T. P. (ed.) *Proceedings of the SPIE, Volume 9326, id. 932611 6 pp. (2015).*, p. 932611.

Steinfeld, H., Gerber, P., Wassenaar, T., Castel, V., Rosales, M., de Haan, C. (2006) *Livestock's Long Shadow: Environmental Issues and Options*. Rome: FAO 2006.

Stentz, R., Osborne, S., Horn, N., Li, A.W.H., Hauteforte, I., Bongaerts, R., Rouyer, M., Bailey, P., Shears, S.B., Hemmings, A.M., Brearley, C.A., Carding, S.R. (2014) 'A Bacterial Homolog of a Eukaryotic Inositol Phosphate Signaling Enzyme Mediates Cross-kingdom Dialog in the Mammalian Gut', *Cell Reports*. The Authors, 6(4), pp. 646–656.

Stephens, L. R. and Downes, C. P. (1990) 'Product-precursor relationships amongst inositol polyphosphates', *Biochemical Journal*, 265, pp. 435–452.

Stephens, L. R., Hawkins, P. T. and Downes, C. P. (1989) 'An analysis of

myo-[3H]inositol trisphosphates found in *myo*-[3H]inositol prelabelled avian erythrocytes', *Biochemical Journal*, 262(3), pp. 727–737.

Stephens, L. R. and Irvine, R. F. (1990) 'Stepwise phosphorylation of myo-inositol leading to myo-inositol hexakisphosphate in *Dictyostelium*', *Nature*. Nature Publishing Group, 346(6284), pp. 580–583.

Stevenson-Paulik, J., Bastidas, R.J., Chiou, S.-T., Frye, R.A., York, J.D. (2005) 'Generation of phytate-free seeds in *Arabidopsis* through disruption of inositol polyphosphate kinases', *Proceedings of the National Academy of Sciences of the United States of America*, 102(35), pp. 12612–12617.

Streb, H., Irvine, R.F., Berridge, M.J. and Schulz, I. (1983) 'Release of Ca²⁺ from a nonmitochondrial intracellular store in pancreatic acinar cells by inositol 1,4,5-triphosphate.' *Nature*, 306. pp 67-69.

Stutzmann, G. E. (2005) 'Calcium Dysregulation, IP3 Signaling, and Alzheimer's Disease', *The Neuroscientist*. Sage PublicationsSage CA: Thousand Oaks, CA, 11(2), pp. 110–115.

Subcommittee on Poultry Nutrition, Board on Agriculture and National Research Council (1994) *Nutrient Requirements of Poultry: Ninth Revised Edition*. 9th edn. Washington, D.C., USA: National Academy of Sciences.

Suzuki, S., Kawasaki, H., Satoh, Y., Ohtomo, M., Hirai, M., Hirai, A., Onoda, M., Matsumoto, M., Hinokio, Y., Akai, H., Craig, J., Larner, J., and Toyota, T. (1994) 'Urinary chiro-inositol excretion is an index marker of insulin sensitivity in Japanese type II diabetes.' *Diabetes Care*, 17:1465-1468.

Suzuki, U., Yoshimura, K., Takaishi, M. (1907) *About the enzyme "phytase", which splits anhydro-oxy-methylene diphosphoric acid*, *Bulletin of the College of Agriculture*. Tokyo.

Svihus, B. (2014) 'Function of the digestive system', *Journal of Applied*

Poultry Research. Poultry Science Association Inc., 23(2), pp. 306–314.

Takasaki, R. and Kobayashi, Y. (2020) 'Takasaki R, Kobayashi Y. Effects of diet and gizzard muscularity on grit use in domestic chickens.', *Peer J*, 8, p. e10277.

Talbot, J. and Maves, L. (2016) 'Skeletal muscle fiber type: using insights from muscle developmental biology to dissect targets for susceptibility and resistance to muscle disease', *WIREs Developmental Biology*, 5(4), pp. 518–534.

Tamim, N.M., Angel, R., Christman, M. (2004) 'Influence of dietary calcium and phytase on phytate phosphorus hydrolysis in broiler chickens.' *Poultry Science*. 83:1358-67.

Tang, J. C. Y., Nicholls H., Piec, I., Washbourne, C.J., Dutton, J.J., Jackson, S., Greeves, J., Fraser, W.D. (2017) 'Reference intervals for serum 24,25-dihydroxyvitamin D and the ratio with 25-hydroxyvitamin D established using a newly developed LC–MS/MS method', *Journal of Nutritional Biochemistry*. Elsevier Inc., 46, pp. 21–29.

Tao, N. (2018) *The Performance of Quantum Blue Phytase at Different pH Levels Using Wheat Based Diet in an In Vitro Simulation of Poultry Crop*.

Tomlinson, R. V. and Ballou, C. E. (1962) 'Myo-inositol Polyphosphate Intermediates in the Dephosphorylation of Phytic Acid by Phytase', *Biochemistry*, 1(1), pp. 166–171.

Tomschy, A., Brugger, R., Lehmann, M., Svendsen, A., Vogel, K., Kostrewa, D., Lassen, S.F., Burger, D., Kronenberger, A., van Loon, A.P., Pasamontes, L., Wyss, M. (2002) 'Engineering of phytase for improved activity at low pH.' *Appl. Environ. Microbiol.* 68(4):1907-13.

Truong, H. H., Yu, S., Moss, A.F., Liu, S.Y., Selle, P.H. (2016) 'Phytate

Degradation in the Gizzard Is Pivotal To Phytase Responses in Broiler', in *Australian Poultry Science Symposium*, pp. 1–5.

Tu, S., Ma, L. and Rathinasabapathi, B. (2011) 'Characterization of phytase from three ferns with differing arsenic tolerance', *Plant Physiology and Biochemistry*, 49(2), pp. 146–150.

Tucker, G., Gagnon, R. E. and Haussler, M. R. (1973) 'Vitamin D3-25-hydroxylase: Tissue occurrence and apparent lack of regulation', *Archives of Biochemistry and Biophysics*, 155(1), pp. 47–57.

Turner, B. L., Papházy, M.J., Haygarth, P.M., McKelvie, I.D. (2002) 'Inositol phosphates in the environment', *Philosophical Transactions of the Royal Society B: Biological Sciences*, 357(1420), pp. 449–469.

U.S. Geological Survey (2021) 'Mineral Commodity Summaries, January 2021', *U.S. Geological Survey*.

U.S. Geological Survey (2022) 'Mineral commodity summaries January 2022', *U.S. Geological Survey*, (703), p. 202.

Ucuncu, E. Rajamani, K., Wilson, M.S.C., Medina-Cano, D., Altin, N., David, P., Barcia, G., Lefort, N., Banal, C., Vasilache-Dangles, M.-T., Pitelet, G., Lorino, E., Rabasse, N., Bieth, E., Zaki, M.S., Topcu, M., Sonmez, F.M., Musaev, D., Stanley, V., Bole-Feysot, C., Nitschke, P., Munnich, A., Bahi-Buisson, N., Fossoud, C., Giuliano, F., Colleaux, L., Burglen, L., Gleeson, J.G., Boddaert, N., Saiardi, A., Cantagrel, V. (2020) 'MINPP1 prevents intracellular accumulation of the chelator inositol hexakisphosphate and is mutated in Pontocerebellar Hypoplasia', *Nature Communications*, 11(1).

Um, J. S. and Paik, I. K. (1999) 'Effects of microbial phytase supplementation on egg production, eggshell quality, and mineral retention of laying hens fed different levels of phosphorus', *Poultry Science*, 78(1), pp. 75–79.

- Untergasser, A. (2015) 'Preparation of Chemical Competent Cells Commented Protocol':, *Work*, pp. 8–11.
- Ushasree, M.V., Vidya, J., Pandey, A. (2015). 'Replacement P212H altered the pH-temperature profile of phytase from *Aspergillus niger* NII 08121.' *Appl. Biochem. Biotechnol.* 175(6):3084-3092.
- Vadlamudi, S. and Hanson, R. P. (1966) 'Invasion of the Brain of Chicken by Newcastle Disease Virus', *Avian Diseases*, 10(1), pp. 122–127.
- Vadnal, R. and Parthasarathy, R. (1995) 'Myo-Inositol Monophosphatase: Diverse Effects of Lithium, Carbamazepine and Valproate'.
- Valin, H., Sands, R.D., van der Mensbrugge, D., Nelson, G.C., Ahammad, H., Blanc, E., Bodirsky, B., Fujimori, S., Hasegawa, T., Havlik, P., Heyhoe, E., Kyle, P., Mason-D'Croz, D., Paltsev, S., Rolinski, S., Tabeau, A., van Meijl, H., von Lampe, M., Willenbockel, D. (2014) 'The future of food demand: Understanding differences in global economic models', *Agricultural Economics (United Kingdom)*, 45(1), pp. 51–67.
- Vallejo, M., Jackson, T., Lightman, S., Hanley, M.R. (1987) 'Occurrence and extracellular actions of inositol pentakis- and hexakisphosphate in mammalian brain', *Nature*, 330, pp. 656–658.
- Veldurthy, V., Wei, R., Campbell, M., Lupicki, K., Dhawan, P., Christakos, S. (2016) '25-Hydroxyvitamin D3 24-Hydroxylase. A Key Regulator of 1,25(OH)₂D₃ Catabolism and Calcium Homeostasis.' 1st edn, *Vitamins and Hormones*. 1st edn. Elsevier Inc.
- Vucenik, I., Druzijanic, A. and Druzijanic, N. (2020) 'Inositol Hexaphosphate (IP6) and Colon Cancer: From Concepts and First Experiments to Clinical Application', *Molecules (Basel, Switzerland)*, 25(24), pp. 1–13.
- Walan, P., Davidsson, S., Johansson, S., Höök, M. (2014) 'Phosphate rock

production and depletion: Regional disaggregated modeling and global implications', *Resources, Conservation and Recycling*, 93(0), pp. 178–187.

Waldroup, P.W. (1999) 'Nutritional Approaches to reducing phosphorus excretion by poultry.' *Poultry Science* 78, pp. 683-691.

Waldroup, P. W., Kersey, J.H., Saleh, E.A., Fritts, C.A., Yan, F., Stilborn, H.L., Crum, R.C. Jr., Raboy, V. (2000) 'Nonphytate phosphorus requirement and phosphorus excretion of broiler chicks fed diets composed of normal or high available phosphate corn with and without microbial phytase', *Poultry Science*. Poultry Science Association, Inc., 79(10), pp. 1451–1459.

Walk, C. L., Bedford, M.R., Santos, T.S., Paiva, D., Bradley, J.R., Wladecki, H., Honaker, C., McElroy, A.P. (2013) 'Extra-phosphoric effects of superdoses of a novel microbial phytase', *Poultry Science*. Poultry Science Association Inc., 92(3), pp. 719–725.

Walk, C. L., Bedford, M. R. and Olukosi, O. A. (2018) 'Effect of phytase on growth performance, phytate degradation and gene expression of *myo*-inositol transporters in the small intestine, liver and kidney of 21 day old broilers', *Poultry Science*. Poultry Science Association Inc., 97(4), pp. 1155–1162..

Walk, C. L. and Rama Rao, S. V. (2020) 'Increasing dietary phytate has a significant anti-nutrient effect on apparent ileal amino acid digestibility and digestible amino acid intake requiring increasing doses of phytase as evidenced by prediction equations in broilers', *Poultry Science*. The Author(s), 99(1), pp. 290–300.

Walk, C. L., Santos, T. T. and Bedford, M. R. (2014) 'Influence of superdoses of a novel microbial phytase on growth performance, tibia ash, and gizzard phytate and inositol in young broilers', *Poultry Science*. Poultry Science Association Inc., 93(5), pp. 1172–1177.

Wang, T. and Adeola, O. (2018) 'Digestibility index marker type, but not inclusion level affects apparent digestibility of energy and nitrogen and marker recovery in growing pigs regardless of added oat bran', *Journal of Animal Science*, 96(7), pp. 2817–2825.

Warren, M. F., Vu, T.C., Toomer, O.T., Fernandex, J.D., Livingston, K.A. (2020) 'Efficacy of 1- α -Hydroxycholecalciferol Supplementation in Young Broiler Feed Suggests Reducing Calcium Levels at Grower Phase', *Frontiers in Veterinary Science*, 7(June), pp. 1–11.

Warren, M. F. and Livingston, K. A. (2021) 'Implications of Vitamin D Research in Chickens can Advance Human Nutrition and Perspectives for the Future', *Current Developments in Nutrition*. Oxford University Press, 5(5), pp. 1–17.

Watson, S. P., McConnell, R. T. and Lapetina, E. G. (1984) 'The rapid formation of inositol phosphates in human platelets by thrombin is inhibited by prostacyclin', *Journal of Biological Chemistry*. © 1984 ASBMB. Currently published by Elsevier Inc; originally published by American Society for Biochemistry and Molecular Biology., 259(21), pp. 13199–13203.

Wei, H., Landgraf, D., Wang, G., McCarthy, M.J. (2018) 'Inositol polyphosphates contribute to cellular circadian rhythms: Implications for understanding lithium's molecular mechanism', *Cellular Signalling*. Elsevier, 44(June 2017), pp. 82–91.

Weinberg, S. E., Sun, L.Y., Yang, A.L., Liao, J., Yang, G.Y. (2021) 'Overview of inositol and inositol phosphates on chemoprevention of colitis-induced carcinogenesis', *Molecules*, 26(1), pp. 1–11.

Weinman, E.J., Lederer, E.D. (2012) 'PTH-mediated inhibition of the renal transport of phosphate.' *Exp. Cell Res.* May 15; 318(9):1027-32.

Werner, A. and Kinne, R. K. H. (2001) 'Evolution of the Na-Pi cotransport

systems', *American Journal of Physiology - Regulatory Integrative and Comparative Physiology*, 280(2 49-2).

White, K. E., Jonsson, K.B., Carn, G., Hampson, G., Spector, T.D., Mannstadt, M., Lorenz-Depiereux, B., Miyauchi, a., Yang, I.M., Ljunggren, O., Meitinger, T., Strom, T.M., Jüppner, H., Econs, M.J. (2001a) 'The autosomal dominant hypophosphatemic rickets (ADHR) gene is a secreted polypeptide overexpressed by tumors that cause phosphate wasting', *The Journal of Clinical Endocrinology & Metabolism*, 86(2), pp. 497–500.

White, K. E., Carn, G., Lorenz-Depiereux, B., Benet-Pages, A., Strom, T.M., Econs, M.J. (2001b) 'Autosomal-dominant hypophosphatemic rickets (ADHR) mutations stabilize FGF-23', *Kidney International*, 60(6), pp. 2079–2086.

Whiteford, C. C., Brearley, C. A. and Ulug, E. T. (1997) 'Phosphatidylinositol 3,5-bisphosphate defines a novel PI 3-kinase pathway in resting mouse fibroblasts', *Biochemical Journal*, 323(3), pp. 597–601.

Whitehead, C. C., McCormack, H.A., McTeir, L., Fleming, R.H. (2004) 'High vitamin D3 requirements in broilers for bone quality and prevention of tibial dyschondroplasia and interactions with dietary calcium, available phosphorus and vitamin A', *British Poultry Science*, 45(3), pp. 425–436.

Whitfield, H., Riley, A.M., Diogenous, S., Godage, H.Y., Potter, B.V.L., Brearley, C.A.. (2018) 'Simple synthesis of ³²P-labelled inositol hexakisphosphates for study of phosphate transformations', *Plant and Soil*. Springer International Publishing, 427(1–2), pp. 149–161.

Whitfield, H., White, G., Sprigg, C., Riley, A.M., Potter, B.V.L., Hemmings, A.M., Brearley, C.A. (2020) 'An ATP-responsive metabolic cassette comprised of inositol tris/tetrakisphosphate kinase 1 (ITPK1) and inositol pentakisphosphate 2-kinase (IPK1) buffers diphosphoinositol phosphate levels', *Biochemical Journal*, 477(14), pp. 2621–2638.

Whitfield, H., Laundon, C., Rochell, S.J., Dridi, S., Lee, S.A., Dale, T., York, T., Kühn, I., Bedford, M.R. (2022) 'Effect of phytase supplementation on plasma and organ myo-inositol content and erythrocyte inositol phosphate in chickens', *Journal of Applied Animal Nutrition*, In press.

Wideman Jr., R. F. (1984) 'Parathyroid hormone-induced phosphate excretion following preequilibration with ^{32}P ', *American Journal of Physiology*, 246(4), pp. 373–378.

Wideman Jr., R. F. and Braun, E. J. (1981) 'Stimulation of avian renal phosphate secretion by parathyroid hormone', *American Journal of Physiology*, 241(3), pp. 263–272.

Wilson, M. S. C., Bulley, S.J., Pisani, F., Irvine, R.F., Saiardi, A. (2015) 'A novel method for the purification of inositol phosphates from biological samples reveals that no phytate is present in human plasma or urine', *Open Biology*, 5(3), p. 150014.

Wilson, M. S. C., Livermore, T. M. and Saiardi, A. (2013) 'Inositol pyrophosphates: between signalling and metabolism.', *The Biochemical journal*. Portland Press Limited, 452(3), pp. 369–79.

Wilson, M. S., Jessen, H. J. and Saiardi, A. (2019) 'The inositol hexakisphosphate kinases IP6K1 and -2 regulate human cellular phosphate homeostasis, including XPR1-mediated phosphate export', *Journal of Biological Chemistry*. © 2019 Wilson et al., 294(30), pp. 11597–11608.

Winter, D., Vinegar, B., Nahal, H., Ammar, R., Wilson, G.V., Provard, N.J. (2007) 'An "Electronic Fluorescent Pictograph" Browser for Exploring and Analyzing Large-Scale Biological Data Sets', *PLoS ONE*. Edited by I. Baxter, 2(8), p. e718.

Wollenberg, E., Campbell, B.M., Vermeulen, S.J., Aggarwal, P., Corner-

Dolloff, C., Girvetz, E., Loboguerrero, A.M., Ramirez-Villegas, J., Rosenstock, T., Sebastian, L., Thornton, P.K. (2016) 'Reducing risks to food security from climate change', *Global Food Security*. Elsevier, 11, pp. 34–43.

World Bank (2022) *World Bank Commodities Price Data*.

Worley, P. F., Baraban, J. M. and Snyder, S. H. (1989) 'Inositol 1,4,5-trisphosphate receptor binding: autoradiographic localization in rat brain.', *The Journal of neuroscience : the official journal of the Society for Neuroscience*, 9(1), pp. 339–46.

Wu, Y. B., Ravindran, V. and Hendriks, W. H. (2003) 'Effects of microbial phytase, produced by solid-state fermentation, on the performance and nutrient utilisation of broilers fed maize- and wheat-based diets', *British Poultry Science*, 44(5), pp. 710–718.

Yagci, A., Werner, A., Murer, H., Biber, J. (1992) 'Effect of rabbit duodenal mRNA on phosphate transport in *Xenopus laevis* oocytes: dependence on 1,25-dihydroxy-vitamin-D3', *Pflugers Archiv European Journal of Physiology*, 422(3), pp. 211–216.

Yao, M. Z., Zhang, Y.-H., Lu, W.-H., Hu, M.-Q., Wang, W., Liang, A.-H. (2012) 'Phytases: Crystal structures, protein engineering and potential biotechnological applications', *Journal of Applied Microbiology*, 112(1), pp. 1–14.

Yi, Z., Kornegay, E.T., Ravindran, V., Denbow, D.M. (1996) 'Improving Phytate Phosphorus Availability in Corn and Soybean Meal for Broilers Using Microbial Phytase and Calculation of Phosphorus Equivalency Values for Phytase', *Poultry Science*, 75(2), pp. 240–249.

Yoon, J. H., Thompson, L. U. and Jenkins, D. J. (1983) 'The effect of phytic acid on in vitro rate of starch digestibility and blood glucose response', *The American Journal of Clinical Nutrition*, 38(6), pp. 835–842.

York, J. D. and Hatch, A. J. (2010) 'SnapShot: Inositol phosphates', *Cell*, 143(6), p. 1030.

Yu, B., Jan, Y.C., Chung, T.K., Lee, T.T., Chiou, P.W.S. (2004) 'Exogenous phytase activity in the gastrointestinal tract of broiler chickens', *Animal Feed Science and Technology*, 117(3–4), pp. 295–303.

Yu, S., Cowieson, A., Gilbert, C., Plumstead, P., Dalsgaard, S. (2012) 'Interaction of phytate and *myo*-inositol phosphate esters (IP1-5) including IP5 isomers with dietary protein and iron and inhibition of pepsin', *Journal of Animal Science*, 90, pp. 1824–1832.

Yu, W. and Greenberg, M. L. (2016) 'Inositol depletion, GSK3 inhibition and bipolar disorder', *Future Neurology*, 11(2), pp. 135–148.

Zaefarian, F., Abdollahi, M.R., Cowieson, A., Ravindran, V. (2019) 'Avian liver: The forgotten organ', *Animals*, 9(2), pp. 1–23.

Zanu, H. K., Kheravii, S.K., Morgan, N.K., Bedford, M.R., Swick, R.A. (2020) 'Interactive effect of dietary calcium and phytase on broilers challenged with subclinical necrotic enteritis: part 2. Gut permeability, phytate ester concentrations, jejunal gene expression, and intestinal morphology', *Poultry Science*. Elsevier Inc., 99(10), pp. 4914–4928.

Zeller, E., Schollenberger, M., Witzig, M., Shastak, Y., Kühn, I., Hoelzle, L.E., Rodehutschord, M. (2015a) 'Interactions between supplemented mineral phosphorus and phytase on phytate hydrolysis and inositol phosphates in the small intestine of broilers', *Poultry Science*, 94(5), pp. 1018–1029.

Zeller, E., Schollenberger, M., Kühn, I., Rodehutschord, M. (2015b) 'Hydrolysis of phytate and formation of inositol phosphate isomers without or with supplemented phytases in different segments of the digestive tract of broilers', *Journal of Nutritional Science*, 4, pp. 1–12.

Zeng, Z. K., Wang, D., Piao, X.S., Li, P.F., Zhang, H.Y., Shi, C.X., Yu, S.K. (2014) 'Effects of adding super dose phytase to the phosphorus-deficient diets of young pigs on growth performance, bone quality, minerals and amino acids digestibilities', *Asian-Australasian Journal of Animal Sciences*, 27(2), pp. 237–246.

Zhang, F. and Adeola, O. (2017) 'Techniques for evaluating digestibility of energy, amino acids, phosphorus, and calcium in feed ingredients for pigs', *Animal Nutrition*. Elsevier Taiwan LLC, 3(4), pp. 344–352.

Zhu, J., Lau, K., Puschmann, R., Harmel, R.K., Zhang, Y., Pries, V., Gaugler, P., Broger, L., Dutta, A.K., Jessen, H.J., Schaaf, G., Fernie, A.R., Hothorn, L.A., Fiedler, D., Hothorn, M. (2019) 'Two bifunctional inositol pyrophosphate kinases/phosphatases control plant phosphate homeostasis', *eLife*, 8, pp. 1–25.

Zyla, K., Mika, M., Duliński, R., Swiatkiewicz, S., Koreleski, J., Pustkowiak, H., Piironen, J. (2012) 'Effects of inositol, inositol-generating phytase B applied alone, and in combination with 6-phytase A to phosphorus-deficient diets on laying performance, eggshell quality, yolk cholesterol, and fatty acid deposition in laying hens', *Poultry Science*. Oxford University Press, 91(8), pp. 1915–1927.

Zyla, K., Dulinski, M., Pierzchalska, M., Garbacka, M., Józefiak, D., Swiatkiewicz, S. (2013) 'Phytases and myo-inositol modulate performance, bone mineralization and alter lipid fractions in the serum of broilers.' *J. Anim. Feed Sci.* 22(2013), pp. 56-62.